ZANCO Journal of Pure and Applied Sciences
The official scientific journal of Salahaddin University-Erbil
https://zancojournals.su.edu.krd/index.php/JPAS

ISSN (print):2218-0230**, ISSN (online):** 2412-3986**, DOI: http://dx.doi.org/10.21271/zjpas**

RESEARCH PAPER

Darboux and Analytic First Integrals of Kingni–Jafari System with Only One Stable Equilibrium Point.

Shno F. Muhammed1, Niazy H. Hussein2, Azad I. Amen3,*

1Department of mathematics, College of Education-Shaqlawa, Salahaddin University-Erbil, Kurdistan Region, Iraq.
2 Department of mathematics, Faculty of Science, University of Soran, Erbil, Kurdistan Region, Iraq.
3Department of mathematics, College of Basic Education, Salahaddin University-Erbil, Kurdistan Region, Iraq.
*Department of Pathological analysis, College of Science, Knowledge University.

A B S T R A C T:
In this paper, we illustrate by an evidence that the Kingni–Jafari differential system $\dot{u} = -w,\ \dot{v} = -u - w,\ \dot{w} = 3\,u - a\,v + u^2 - w^2 - v\,w + b,$ where a and b are real parameters has no Darboux and rational first integrals for any value of a, b. Furthermore, we show that this system has no global C^1 first integrals for $a \in (0,3), b > 0$ and $3b - ab > a^2$. Also, an analytic first integral for some generic condition is studied of this system at the neighborhood of the equilibrium point $\left(0, \frac{b}{a}, 0\right)$.

KEY WORDS: Invariant Algebraic Surfaces, Darboux First Integral, Exponential Factor, Analytic First Integral.
DOI: http://dx.doi.org/10.21271/ZJPAS.32.3.1
ZJPAS (2020) , 32(3);1-9 .

1.INTRODUCTION :

Kingni and Jafari in (Kingni et al., 2014) proposed the simplest electronic circuit design. This electronic circuit consists of a resistors, AD633 multiplier, capacitors and operational amplifiers. This circuit can be considered by the following three-dimensional chaotic differential system

$$\begin{aligned} \dot{u} &= -w, \\ \dot{v} &= -u - w, \\ \dot{w} &= 3\,u - a\,v + u^2 - w^2 - v\,w + b. \end{aligned} \tag{1}$$

has a rare equilibrium point $(0, \frac{b}{a}, 0)$ for $a \neq 0$. The study of chaotic System (1) is significant in physics and engineering applications, especially in circuit, control and communications.In (Wei et al., 2016), the authors proved that this system is the chaotic system with invisible attractors and that the stable equilibrium point can coexist with a strange attractor for specific parameters. Dynamics of the Kingni and Jafari system have explained via numerical simulations such as phase portraits, bifurcation diagrams and new cost function for parameter estimation. Wei et al (2016) have learned complex dynamical behaviors and topological structure of the system such as the dynamics of this system at infinity, periodic solutions, Hopf bifurcation and zero Hopf bifurcation. System (1) has been studied in the papers (Kingni et al., 2014 and Wei et al., 2016) but none of those papers mentions the integrability or non-integrability. In this paper, we investigate

* **Corresponding Author:**
Shno F. Muhammed
E-mail: shnoo.farhadd@gmail.com
Article History:
Received: 08/08/2019
Accepted: 31/10/2019
Published: 15/06 /2020

first integrals of a Darboux and an analytic type of system (1).
Solutions of a differential system can be compared with the existing behavior of a system to make if the theoretical detailing of the system is accurate. This is interesting topic in the sciences. A Darboux integrability is a method to find a solution of a differential system, for more details see (Ollagnier, 1997, Christopher et al., 2007, Llibre and Valls, 2011a, Llibre and Valls, 2011b and Hussien and Amen, 2018).

2. PRELIMINARY RESULTS.

This section is started with a short overview of the integrability problem, the Darboux method and the auxiliary results which are given (Llibre and Zhang, 2002, Llibre and Zhang, 2010, Llibre and Valls, 2011b and Llibre and Zhang, 2012). To prove our important results, firstly we give some basic definitions and theorems as a background to this study.

The associated vector field to system (1) is define by

$$\chi = -w\,\frac{\partial}{\partial u} + (-u - w)\frac{\partial}{\partial v} + (3\,u - a\,v + u^2 - w^2 - v\,w + b)\frac{\partial}{\partial w}. \qquad (2)$$

Let D be an open subset of $\mathbb{C}^3$, a non-constant function $H: D \to \mathbb{C}$ is a first integral of the polynomial vector field χ on D if it is a constant on all orbits $\big(u(t), v(t), w(t)\big)$ of χ contained in D. Obviously, that H is called a first integral of χ on D if and only if

$$\chi(H) = -w\frac{\partial H}{\partial u} + (-u - w)\frac{\partial H}{\partial v} + (3\,u - a\,v + u^2 - w^2 - v\,w + b)\frac{\partial H}{\partial w} = 0. \qquad (3)$$

A local (global) first integral H is a first integral whose domain of definition is a neighborhood of an equilibrium point (whose domain of definition is $\mathbb{R}^3$) of system (1). We recall that H is an analytic (rational) first integral if it is an analytic (rational) function.
An equilibrium point (u_0, v_0, w_0) of system (1) is said to be an attractor if all eigenvalues λ_i of the Jacobian matrix of (1) at (u_0, v_0, w_0) have negative real parts.

Theorem 2.1. Routh-Hurwitz Criterion. The zero of $\lambda^3 + a_1\lambda^2 + a_2\lambda + a_3 = 0$ have negative real parts if and only if $a_1 > 0, a_3 > 0$ and $a_1 a_2 - a_3 > 0$.

We present the following results concerning with the non-existence of first integral, that we use later on, this is due to (Llibre et al., 2015).
Theorem 2.2. If system (1) has an equilibrium point (u_0, v_0, w_0) which is either repeller or attractor, then system (1) has no C^1 first integrals defined in a neighborhood at (u_0, v_0, w_0).

A Darboux theory of integrability has a best method to determine that systems have a first integral or not. Now, we will describe its some basic nations, for more deep information look at (Christopher and Llibre, 2000 and Llibre and Valls, 2011b)). Suppose that $f = f(u, v, w) \in \mathbb{C}[u, v, w]$, then $f = 0$ is said to be an invariant algebraic surface or it is called a Darboux polynomial of χ if there exist a polynomial $K_f \in \mathbb{C}[u, v, w]$ such that

$$\chi(f) = -w\frac{\partial f}{\partial u} + (-u - w)\frac{\partial f}{\partial v} + (3\,u - a\,v + u^2 - w^2 - v\,w + b)\frac{\partial f}{\partial w} = f\,K_f, \qquad (4)$$

we recall K_f is the cofactor of f and the degree of K_f here is at most 1.
Proposition 2.3. System (1) has a rational first integral if it has two different Darboux polynomials with the match cofactors.

We denote an exponential factor of system (1) by E which defined by a non-constant function of the form $E = e^{\frac{g}{f}}$ with greatest common divisor between g and f is equal to one. That means $(g, f) = 1$, where $g, f \in \mathbb{C}[u, v, w]$ and it is satisfied

$$\chi(E) = -w\frac{\partial E}{\partial u} + (-u - w)\frac{\partial E}{\partial v} + (3\,u - a\,v + u^2 - w^2 - v\,w + b)\frac{\partial E}{\partial w} = E\,L, \qquad (5)$$

for some polynomial $L = L(u, v, w) \in \mathbb{C}[u, v, w]$ of degree at most 1 which is called the cofactor of E.

Proposition 2.4. i) The function $E = e^{\frac{g}{f}}$ is an exponential factor of polynomial differential system (1) and f is a non-constant polynomial, then $f = 0$ is an invariant algebraic surface.
ii) Finally e^{g} can be an exponential factor, getting from the multiplicity of the infinity invariant plane.

Theorem 2.5. Darboux Theorem (Christopher and Llibre, 2000). Suppose that a polynomial vector field χ of degree d in $\mathbb{C}^3$ have p irreducible invariant algebraic surfaces $f_i = 0$ such that the f_i are pairwise relatively prime with cofactors K_i for $i = 1, \dots, p$ and q exponential factors $e^{\frac{g_j}{f_j}}$ together cofactors L_j for $j = 1, \dots, q$. There exist $\lambda_i, \mu_j \in \mathbb{C}$ not all zero such that

$$\sum_{i=1}^{p} \lambda_i K_i + \sum_{j=1}^{q} \mu_j L_j = 0, \qquad (6)$$

if and only if the function

$$f_1^{\lambda_1} \dots f_p^{\lambda_p} \left(\left[e^{\frac{g_1}{f_1}} \right]^{\mu_1} \dots \left[e^{\frac{g_q}{f_q}} \right]^{\mu_q} \right), \qquad (7)$$

is the first integral of system (1).
The form (7) is called a Darboux first integral.
The following proposition is essential to prove the existence of an analytic first integral of system (1) which is due to (Llibre and Valls, 2008).
Proposition 2.6. (Llibre and Valls, 2008) . The 3-dimensioal linear differential system

$$\dot{U} = PU, \text{ where } U = \begin{pmatrix} u \\ v \\ w \end{pmatrix}, \ \dot{U} = \begin{pmatrix} \dot{u} \\ \dot{v} \\ \dot{w} \end{pmatrix},$$

has two independent first integrals which are given in the following cases

1. $F_1 = \frac{u^{\lambda_2}}{v^{\lambda_1}}$ and $F_2 = \frac{u^{\lambda_3}}{w^{\lambda_1}}$ if $P =$

$$\begin{pmatrix} \lambda_1 & 0 & 0 \\ 0 & \lambda_2 & 0 \\ 0 & 0 & \lambda_3 \end{pmatrix}, \text{ with } \lambda_i \in \mathbb{R}\backslash\{0\},$$

$i = 1,2,3.$

2. $F_1 = \frac{w^{\lambda_1}}{u^{\lambda_2}}$ and $F_2 = w \exp\left(-\frac{\lambda_2 v}{u}\right)$ if

$$P = \begin{pmatrix} \lambda_1 & 0 & 0 \\ 1 & \lambda_1 & 0 \\ 0 & 0 & \lambda_2 \end{pmatrix}, \text{ with } \lambda_i \in \mathbb{R}\backslash\{0\},$$

$i = 1,2.$

3. $F_1 = \frac{u^2}{2u\,w - v^2}$ and $F_2 = u \exp\left(-\frac{\lambda v}{u}\right)$ if

$$P = \begin{pmatrix} \lambda_1 & 0 & 0 \\ 1 & \lambda_1 & 0 \\ 0 & 1 & \lambda_1 \end{pmatrix}, \text{ with } \lambda_1 \in \mathbb{R}\backslash\{0\}.$$

4. $F_1 = \frac{(u^2+v^2)^{\lambda}}{w^{2\alpha}}$ and

$F_2 = \exp\left(-2\alpha \arctan(\frac{v}{u})\right)(u^2 + v^2)^{\beta}$ if

$$P = \begin{pmatrix} \alpha & -\beta & 0 \\ \beta & \alpha & 0 \\ 0 & 0 & \lambda \end{pmatrix}, \text{ with } \lambda,\ \alpha,\ \beta \in$$

$\mathbb{R}\backslash\{0\}$.

5. $F_1 = (u^2 + v^2)$ and

$F_2 = \exp\left(-\lambda \arctan(\frac{v}{u})\right) w^{\beta}$ if $P =$

$$\begin{pmatrix} 0 & -\beta & 0 \\ \beta & 0 & 0 \\ 0 & 0 & \lambda \end{pmatrix}, \text{ with } \lambda,\ \beta \in \mathbb{R}\backslash\{0\}.$$

3. MAIN RESULTS AND THEIR PROVING

In this part, the existence of rational first integrals (see Theorem 3.3), Darboux first integrals (see Theorem 3.5) and an analytic first integral (Theorem 3.8) are the main results of system (1) are described. Moreover, some other results relative to this topic are studied in this work such as a polynomial first integral, invariant algebraic surfaces, exponential factors and C^1 first integrals of system (1).
The following proposition is the first result in this work.
Proposition 3.1. System (1) has no polynomial first integrals.
Proof. Let $H = \sum_{i=1}^{n} H_i(u, v, w)$ be a polynomial first integral of system (1), where each H_i is a

homogeneous polynomial in its variables of degree i. By definition of first integral, we have

$$-w\,\frac{\partial}{\partial u}H+(-u-w)\frac{\partial}{\partial v}H+(3\,u-a\,v+u^2-w^2-v\,w+b)\frac{\partial}{\partial w}H=0. \quad (8)$$

Computing the terms of degree $n+1$, we obtain

$$(u^2-w^2-v\,w)\frac{\partial}{\partial w}H_n(u,v,w)=0,$$

that is

$$H_n(u,v,w)=F_1(u,v),$$

where F_1 is a polynomial of variables u and v of degree n. Also, computing the terms of degree n in equation (8), we have

$$-w\,\frac{\partial}{\partial u}F_1(u,v)+(-u-w)\frac{\partial}{\partial v}F_1(u,v)+\left(3\,u-a\,v\right)\frac{\partial}{\partial w}F_1(u,v)+(u^2-w^2-v\,w)\frac{\partial}{\partial w}H_{n-1}(u,v,w)=0,$$

this gives

$$H_{n-1}(u,v,w)=\frac{1}{\sqrt{4u^2+v^2}}\left(\left((2\,u-v)\left(\frac{\partial}{\partial v}F_1(u,v)\right)-v\,\left(\frac{\partial}{\partial u}F_1(u,v)\right)\right)\operatorname{arctanh}\left(\frac{v+2\,w}{\sqrt{4u^2+v^2}}\right)+\left(\left(-\frac{1}{2}\,\frac{\partial}{\partial u}F_1(u,v)-\frac{1}{2}\,\frac{\partial}{\partial v}F_1(u,v)\right)\ln(-u^2+w^2+v\,w)+F_2(u,v)\right)\sqrt{4u^2+v^2}\right).$$

Since $H_{n-1}(u,v,w)$ is a polynomial of degree $n-1$, then we have

$$\frac{\partial}{\partial u}F_1(u,v)+\frac{\partial}{\partial v}F_1(u,v)=0, \quad (9)$$

and

$$(2u-v)\left(\frac{\partial}{\partial v}F_1(u,v)\right)-v\,\left(\frac{\partial}{\partial u}F_1(u,v)\right)=0, \quad (10)$$

It is clear that the solution of equation (9) is

$$F_1(u,v)=F_3(v-u),$$

where F_3 is polynomial of variables u and v. Since, F_1 is the polynomial of degree n then it must be in the formula

$$F_1(u,v)=c\,(v-u)^n, \quad (11)$$

where c is arbitrary constant. Putting (11) in (10), we obtain

$$c\,n\,(v-u)^n\,u=0,$$

This gives $c\,n=0$, then $c=0$ or $n=0$. If $c=0$, this implies that $F_1=0$, then $H_n(u,v,w)=0$, in this case system (1) has no polynomial first integrals. If $n=0$ then H is a constant function, this is trivial. This means that there is no a polynomial first integral of system (1).

Proposition 3.2. System (1) does not have invariant algebraic surfaces with non-zero cofactors.

Proof. Suppose that $f=\sum_{i=1}^{n}f_i(u,v,w)$ is an invariant algebraic surfaces of system (1) with the cofactor $K=k_0+k_1u+k_2v+k_3w$, where $k_i\in\mathbb{C}$ for $i=0,\dots,3$, and each f_i is a homogeneous polynomial in its variables of degree i. Assume that $f_n\neq 0$ for $n>1$, then by definition of invariant algebraic surface, we obtain

$$-w\,\frac{\partial}{\partial u}f+(-u-w)\frac{\partial}{\partial v}f+(3\,u-a\,v+u^2-w^2-v\,w+b)\frac{\partial}{\partial w}f=Kf. \quad (12)$$

We first compute the terms of degree $n+1$ to obtain

$$(u^2-w^2-v\,w)\frac{\partial}{\partial w}f_n(u,v,w)=(k_1u+k_2v+k_3w)\,f_n(u,v,w). \quad (13)$$

This gives

$$f_n(u,v,w)=G_1(u,v)\,(-u^2+w^2+v\,w)^{-\frac{k_3}{2}}e^{\frac{arc\tanh\left(\frac{2w+v}{\sqrt{4u^2+v^2}}\right)(2k_1u+2k_2v-k_3v)}{\sqrt{4u^2+v^2}}}, \quad (14)$$

since $f_n(u,v,w)$ is a polynomial function, this implies that $k_1=0$, $k_2=-m$ and $k_3=-2m$ where $m\in\mathbb{N}\cup\{0\}$. Then equation (14) becomes

$$f_n(u,v,w)=G_1(u,v)\,(-u^2+w^2+v\,w)^m,$$

where G_1 is a polynomial of variables u and v of degree $n-2m$. Also, calculating the terms of degree n in equation (12), we take out

$$-w\left(\left(\frac{\partial}{\partial u}\,G_1(u,v)\right)(-u^2+w^2+v\,w)^m-\frac{2m\,u\,G_1(u,v)\,(-u^2+w^2+v\,w)^m}{-u^2+w^2+v\,w}\right)+(-u-w)\left(\left(\frac{\partial}{\partial v}G_1(u,v)\right)(-u^2+w^2+v\,w)^m+$$

$\frac{m\,w\,G_1(u,v)\,(-u^2+w^2+v\,w)^m}{-u^2+w^2+v\,w}\Big) + (3\,u -$
$a\,v)\left(\frac{m\,(2\,w+v)\,G_1(u,v)\,(-u^2+w^2+v\,w)^m}{-u^2+w^2+v\,w}\right) + (u^2 -$
$w^2 - v\,w)\left(\frac{\partial}{\partial w}\,f_{n-1}(u,v,w)\right)$
$= k_0 G_1(u,v)\,(-u^2 + w^2 + v\,w)^m +$
$(-mv - 2mw) f_{n-1}(u,v,w),$

this gives

$$f_{n-1}(u,v,w) = \Bigg(-\tfrac{1}{2}\ln(-u^2 + w^2 + v\,w)\left(\frac{\partial}{\partial u}\,G_1(u,v) + \frac{\partial}{\partial v}G_1(u,v)\right) + \frac{1}{(4u^2+v^2)^{\frac{3}{2}}}\Bigg(4\left(2\left(u^2+\tfrac{1}{4}v^2\right)\left(u - \tfrac{1}{2}v\right)\left(\frac{\partial}{\partial u}\,G_1(u,v)\right) + \left(-u^2v - \tfrac{1}{4}v^3\right)\left(\frac{\partial}{\partial u}\,G_1(u,v)\right) + G_1(u,v)\left((m+2\,k_0)\,u^2 - \tfrac{1}{2}m\,u\,v + \tfrac{1}{2}k_0\,v^2\right)\right)\arctan\left(\tfrac{v+2w}{\sqrt{4u^2+v^2}}\right)\Bigg) + \left(\frac{4m\,G_1(u,v)\left(-\frac{7}{2}u^3+\left(\left(-\frac{1}{4}+a\right)v+\frac{1}{2}w\right)u^2-\frac{3}{4}\left(v-\frac{1}{3}w\right)u\,v+\frac{1}{4}(av+w)\,v^2\right)}{(4u^2+v^2)(u^2-w^2-v\,w)}\right) + G_2(u,v)\Bigg)(-u^2 + w^2 + v\,w)^m.$$

Since f_{n-1} is a polynomial then we have

$$\frac{\partial}{\partial u}\,G_1(u,v) + \frac{\partial}{\partial v}G_1(u,v) = 0, \qquad (15)$$

$$\frac{1}{(4u^2+v^2)^{\frac{3}{2}}}\Bigg(4\left(2\left(u^2+\tfrac{1}{4}v^2\right)\left(u - \tfrac{1}{2}v\right)\left(\frac{\partial}{\partial u}\,G_1(u,v)\right) + \left(-u^2v - \tfrac{1}{4}v^3\right)\left(\frac{\partial}{\partial u}\,G_1(u,v)\right) + G_1(u,v)\left((m+2\,k_0)\,u^2 - \tfrac{1}{2}m\,u\,v + \tfrac{1}{2}k_0\,v^2\right)\right)\Bigg) = 0\,, \qquad (16)$$

and

$$\frac{4m\,G_1(u,v)\left(-\frac{7}{2}u^3+\left(\left(-\frac{1}{4}+a\right)v+\frac{1}{2}w\right)u^2-\frac{3}{4}\left(v-\frac{1}{3}w\right)u\,v+\frac{1}{4}(av+w)\,v^2\right)}{(4u^2+v^2)(u^2-w^2-v\,w)} = 0, \qquad (17)$$

from equation (17), if $G_1 = 0$ then $f_n(u,v,w) = 0$, this gives that system (1) has no invariant algebraic surfaces. Or, if $m = 0$, this gives $k_2 = k_3 = 0$. Then equation (12) becomes

$$-w\frac{\partial}{\partial u}f(u,v,w) + (-u-w)\frac{\partial}{\partial v}f(u,v,w) + (3\,u - av + u^2 - w^2 - v\,w + b)\frac{\partial}{\partial w}f(u,v,w) = k_0\,f(u,v,w). \qquad (18)$$

It is not essay to discover a solution of equation (18). So, the weight change of variables is used as described in (Libre & Pessoa, 2009) in order to find an invariant algebraic surfaces of system (1). Let $u = \mu U$, $v = V$, $w = W$ and $t = \mu T$, with $\mu \in \mathbb{C} \setminus \{0\}$. Then, system (1) turn into

$$\begin{aligned} \dot{U} &= -W \\ \dot{V} &= -\mu^2 U - \mu W \\ \dot{W} &= \mu^3 U^2 + 3\,\mu^2 U - a\,\mu V - \mu W^2 - \mu\,V\,W + b\mu, \end{aligned} \qquad (19)$$

where the dots denote the derivative of the variables U, V and W with respect to T. Set $F(U,V,W) = \mu^n f(\mu U, V, W) = \sum_{j=0}^{n}\mu^j F_j(U,V,W)$, where F_j is the weight homogeneous part with weight degree $n-j$ of F, and n is the weight degree of F with weight exponent $s = (1,0,0)$. And $K(U,V,W) = k_0$. Then, by invariant algebraic surfaces, we have

$$-W\sum_{j=0}^{n}\mu^j\frac{\partial}{\partial U}F_j(U,V,W) + (-\mu^2 U - \mu W)\sum_{j=0}^{n}\mu^j\frac{\partial}{\partial V}F_j(U,V,W) + (\mu^3U^2 + 3\,\mu^2 U - a\,\mu V - \mu W^2 - \mu\,V\,W + b\mu)\sum_{j=0}^{n}\mu^j\frac{\partial}{\partial W}F_j(U,V,W) = k_0\sum_{j=0}^{n}F_j(U,V,W). \qquad (20)$$

We calculate the terms which contain μ^0 to obtain

$$-\frac{\partial}{\partial U}F_0(U,V,W)Z - k_0\,F_0(U,V,W) = 0,$$

that is

$$F_0(U,V,W) = G_0(V,W)\,e^{\frac{-k_0\,U}{W}},$$

where G_0 is a polynomial function of variables V and W. Since, $F_0(U,V,W)$ is a polynomial function. Thus, we obtain $k_0 = 0$. This implies that system (1) has no invariant algebraic surfaces with non-zero cofactors.

Theorem 3.3. System (1) has no rational first integrals.

Proof. From Proposition 3.2, system (1) has no Darboux polynomials. Then by Proposition 2.3, system (1) has no proper rational first integral.

We proved that in Proposition 3.2, system (1) does not have invariant algebraic surfaces. So, by Proposition 2.4, an exponential function must be in the following

$$E = e^{g(u,v,w)},$$

for more details see (Libre & Valls, 2012).

Proposition 3.4. System (1) has only two exponential factors e^u and $e^v$with cofactors $-w$ and $-u-w$, respectively.

Proof. Let $E = e^{g(u,v,w)}$, $g(u,v,w)=\sum_{k=0}^{n} g_k(u,v,w)$ be an exponential factor with non-zero cofactor $L = L_0 + L_1u + L_2v + L_3w$, where each g_k is a homogeneous polynomial in its variables of degree k. Then, we have

$$-w\,\frac{\partial}{\partial u}e^{g(u,v,w)} + (-u-w)\frac{\partial}{\partial v}e^{g(u,v,w)} + (3\,u - a\,v + u^2 - w^2 - v\,w + b)\frac{\partial}{\partial w}e^{g(u,v,w)} = L\,e^{g(u,v,w)}. \quad (21)$$

Simplifying

$$-w\,\frac{\partial}{\partial u}g(u,v,w) + (-u-w)\frac{\partial}{\partial v}g(u,v,w) + (3\,u - a\,v + u^2 - w^2 - v\,w + b)\frac{\partial}{\partial w}g(u,v,w) = L. \quad (22)$$

Firstly, we assume that $n > 1$. calculating the terms of degree $n+1$ in equation (22), we take out

$$(u^2 - w^2 - v\,w)\frac{\partial}{\partial w}g_n(u,v,w) = 0,$$

that is

$$g_n(u,v,w) = F_1(u,v),$$

where F_1 is a polynomial of degree n. Also, computing the terms of degree n in equation (22), we obtain

$$-w\,\frac{\partial}{\partial u}F_1(u,v) + (-u-w)\frac{\partial}{\partial v}F_1(u,v) + (3\,u - a\,v)\frac{\partial}{\partial w}F_1(u,v) + (u^2 - w^2 - v\,w)\frac{\partial}{\partial w}g_{n-1}(u,v,w) = 0,$$

this gives

$$g_{n-1}(u,v,w) = \frac{1}{\sqrt{4u^2+v^2}}\left(\left((2u-v)\left(\frac{\partial}{\partial v}F_1(u,v)\right) - v\,\left(\frac{\partial}{\partial u}F_1(u,v)\right)\right)\operatorname{arctanh}\left(\frac{v+2w}{\sqrt{4u^2+v^2}}\right) + \left(\left(-\frac{1}{2}\frac{\partial}{\partial u}F_1(u,v) - \frac{1}{2}\frac{\partial}{\partial v}F_1(u,v)\right)\ln(-u^2 + w^2 + v\,w) + F_2(u,v)\right)\sqrt{4u^2+v^2}\right)$$

Since $g_{n-1}(u,v,w)$ is a polynomial of degree $n-1$, then we have

$$\frac{\partial}{\partial u}F_1(u,v) + \frac{1}{2}\frac{\partial}{\partial v}F_1(u,v) = 0 \quad (23)$$

and

$$(2u-v)\left(\frac{\partial}{\partial v}F_1(u,v)\right) - v\,\left(\frac{\partial}{\partial u}F_1(u,v)\right) = 0, \quad (24)$$

it is clearly that the solution of equation(23) is

$$F_1(u,v) = F_3(v-u),$$

where F_3 is a polynomial of the variables u and v. Since, $F_1(u,v)$ is a polynomial of degree n, then it must be in the formula

$$F_1(u,v) = c\,(v-u)^n, \quad (25)$$

where c is arbitrary constant. Putting (25) in (24) we take out

$$c\,n\,(v-u)^n = 0.$$

Since, $n > 1$ then $c = 0$, this implies that $F_1 = 0$, this gives $g_n = 0$. Thus $g = 0$, for $n > 1$. Now, we assume that $g(u,v,w)$ is a polynomial of degree $n = 1$.

Letting $g(u,v,w) = c_0 + c_1u + c_2v + c_3w$.

Then, by equation (22), we have

$$-w\,c_1 + (-u-w)\,c_2 + (3\,u - a\,v + u^2 - w^2 - v\,w + b)\,c_3 = L_0 + L_1u + L_2v + L_3w.$$

Comparing the coefficient, we obtain $c_3 = L_2 = L_0 = 0$, $c_1 = L_1 - L_3$ and $c_2 = -L_1$.

That is

$$g(u,v,w) = (L_1 - L_3)\,u - L_1\,v.$$

This implies that $e^{(L_1-L_3)\,u - L_1\,v}$ is the exponential factor with cofactor $L_1u + L_3w$. Hence, the only two independent exponential factors of system (1) are e^u and e^v with cofactors $-w$ and $-u-w$, respectively.

Now, having a Darboux first integral is illustrated in the following theorems.

Theorem 3.5. System (1) has no Darboux first integrals.

Proof. Since, e^u and e^v are the unique exponential factors with cofactors $-w$ and $-u-w$, respectively. Then by Darboux Theorem 2.5, we have

$$\mu_1(-w) + \mu_2(-u-w) = 0, \qquad (26)$$

with non-zero constants $\mu_1, \mu_2 \in \mathbb{C}$. The above equation has no non-trivial solution. Then, system (1) does not have a Darboux first integral.

The condition $ab \neq 0$ that has assumed in system (1) is an essential condition to prove the existence of C^1 and an analytic first integral.

Theorem 3.6. If $a \in (0,3), b > 0$ and $3b - ab > a^2$ then system (1) has no a global C^1 first integral.

Proof. Since $s_0 = \left(0, \frac{b}{a}, 0\right)$ is the equilibrium point of system (1), then the Jacobian matrix at s_0 of system (1) is

$$J = \begin{bmatrix} 0 & 0 & -1 \\ -1 & 0 & -1 \\ 3 & -a & -\frac{b}{a} \end{bmatrix} .$$

A characteristic equation of the above matrix is

$$P(\lambda) = \lambda^3 + \frac{b}{a}\lambda^2 + (3-a)\,\lambda + a = 0.$$

The eigenvalues are

$$\lambda_1 = \frac{A^{\frac{1}{3}}}{6\,a} + \frac{6\,a^3 - 18a^2 + 2b^2}{3a\,A^{\frac{1}{3}}} - \frac{b}{3a} \quad \text{and}$$

$$\lambda_{2,3} = -\frac{A^{\frac{1}{3}}}{12\,a} - \frac{3\,a^3 - 9a^2 + b^2}{3a\,A^{\frac{1}{3}}} - \frac{b}{3a} \pm \frac{\sqrt{3}\,i}{2}\left(\frac{A^{\frac{1}{3}}}{6a} - \frac{6\,a^3 - 18a^2 + 2b^2}{3a\,A^{\frac{1}{3}}}\right),$$

where

$$A = -108a^4 - 36\,a^3 b + 12\,a^2\sqrt{-12a^5 + 189a^4 + 54a^3 b - 3a^2 b^2 - 324a^3 - 162a^2 b + 18ab^2 + 12b^3 + 324a^2 - 27b^2} + 108a^2 b - 8b^3.$$

Then by Theorem 2.1 the eigenvalues have non-zero negative real parts if and only if $a \in (0,3), b > 0$ and $3b - ab > a^2$. Then, by Theorem 2.2 system (1) has no global C^1 first integrals in the neighborhood of s_0.

Proposition 3.7. The linear part of system (1) has no polynomial first integrals at the equilibrium point $s_0 = \left(0, \frac{b}{a}, 0\right)$, where a and b satisfy

$$27a^4 - b^3 = 0,$$
$$3a^3 - 9a^2 + b^2 = 0. \qquad (27)$$

Proof. Firstly, we use the linear transformation $(u, v, w) \to \left(u, v + \frac{b}{a}, w\right)$ to move s_0 into the origin by then system (1) becomes

$$\dot{u} = -w,$$

$$\dot{v} = -u - w\,,$$

$$\dot{w} = 3\,u - a\,v - \frac{b}{a}\,w - v\,w + u^2 - w^2. \qquad (28)$$

The linear part can be written of the above system as

$$\begin{bmatrix} \dot{u} \\ \dot{v} \\ \dot{w} \end{bmatrix} = \begin{bmatrix} 0 & 0 & -1 \\ -1 & 0 & -1 \\ 3 & -a & -\frac{b}{a} \end{bmatrix} \begin{bmatrix} u \\ v \\ w \end{bmatrix}. \qquad (29)$$

The characteristic equation at $(0,0,0)$ is

$$u^3 + \frac{b}{a}u^2 + (3-a)\,u + a = 0. \qquad (30)$$

Simply, we can see that equation (30) has a triple real root say λ if and only if it could be written as

$$(u-\lambda)^3 = u^3 - 3\,\lambda\,u^2 + 3\,\lambda^2 u - \lambda^3.$$

That is, $\lambda = \frac{-b}{3\,a}$, with

$$L_1(a,b) = \lambda^3 + a, \quad L_2(a,b) = 3 - a - 3\lambda^2.$$

Putting the value of $\lambda = -\frac{b}{3\,a}$ in L_1 and L_2. We compute the value of a and b such that $L_1 = L_2 = 0$, to obtain

$$27a^4 - b^3 = 0,$$
$$3a^3 - 9a^2 + b^2 = 0.$$

This implies that $\lambda_1 = \lambda_2 = \lambda_3 = -\frac{b}{3\,a}$, then from cases 1-3 in Proposition 2.6, we obtain the linear part of system (1) has no a polynomial first integrals.

Theorem 3.8. If a and b satisfy the condition (27), then system (1) does not have analytic first integrals at $s_0 = \left(0, \frac{b}{a}, 0\right)$.

Proof. Firstly, we move the equilibrium point $\left(0, \frac{b}{a}, 0\right)$ into the (0,0,0). Then, by the linear change of coordinates $(u, v, w) \to \left(u, v + \frac{b}{a}, w\right)$, system (1) can be transformed into system (28). Suppose that $H = \sum_{i\geq 1} H_i(x, y, z)$ is analytic first integral of system (1), where H_i is a homogeneous polynomial of degree i for all $i \geq 1$. We will illustrate by induction that

$$H_i = 0 \quad \text{for all } i \geq 1.$$

Since, H is a first integral of system (28), then by definition of first integral, we have

$$-w\,\frac{\partial H}{\partial u} + (-u - w)\frac{\partial H}{\partial v} + \left(3\,u - a\,v - \frac{b}{a}\,w - v\,w + u^2 - w^2\right)\frac{\partial H}{\partial w} = 0. \qquad (31)$$

Calculating the terms of degree 1 in equation (31), we take out

$$-w\,\frac{\partial}{\partial u}\,H_1(u, v, w) + (-u - w)\frac{\partial}{\partial v}H_1(u, v, w) + \left(3\,u - a\,v - \frac{b}{a}\,w\right)\frac{\partial}{\partial w}H_1(u, v, w) = 0. \qquad (32)$$

Then H_1 could be a zero polynomial or it could be a polynomial first integral of first degree. Since, a and b satisfy the condition (27), then, by Proposition 3.7, the linear part of system (28) has no polynomial first integral. This gives $H_1 = 0$, which proves $H_i = 0$ for $i = 1$.

Now, assume that $H_i = 0$ for $i = 1, \ldots, m-1$ with $m \geq 2$, and it will be proved for $i = m$. Using induction supposition, calculating the terms of degree m in equation (31), we obtain

$$-w\,\frac{\partial}{\partial u}\,H_m(u, v, w) + (-u - w)\frac{\partial}{\partial v}\,H_m(u, v, w) + \left(3\,u - a\,v - \frac{b}{a}\,w\right)\frac{\partial}{\partial w}\,H_m(u, v, w) = 0. \qquad (33)$$

Then, H_m could be a zero polynomial or it could be a polynomial first integral of m degree. Since, a and b satisfy the condition (27), we proceed as the case H_i for $i = 1$, and using by Proposition 3.7, we obtain that $H_m = 0$. This proves that $H_i = 0$ for all $i \geq 1$. Thus, system (28) has no analytic first integral. Going back under the change of coordinates $(u, v, w) \to \left(u, v + \frac{b}{a}, w\right)$, gives that system (1) does not have an analytic first integral at s_0.

4. CONCLUSION

In this paper, we proved that the Kingni–Jafari system has no Darboux first integrals. Also, this system has no analytic first integrals at the neighborhood of the equilibrium point and we obtained that the system has no global C^1 first integrals for $a \in (0,3), b > 0$ and $3b - ab > a^2$.

References

CHRISTOPHER, C. & LLIBRE, J. 2000. Integrability via invariant algebraic curves for planar polynomial differential systems. *Annals of Differential Equations*, 16**,** 5-19.

CHRISTOPHER, C., LLIBRE, J. & PEREIRA, J. V. 2007. Multiplicity of invariant algebraic curves in polynomial vector fields. *Pacific Journal of Mathematics*, 229**,** 63-117.

HUSSIEN, A. M. & AMEN, A. I. 2018. On Existence Inverse Integrating Factors and First Integrals for Cubic in 2D Autonomous Differential System. *ZANCO Journal of Pure and Applied Sciences*, 30**,** 56-72.

KINGNI, S., JAFARI, S., SIMO, H. & WOAFO, P. 2014. Three-dimensional chaotic autonomous system with only one stable equilibrium: Analysis, circuit design, parameter estimation, control, synchronization and its fractional-order form. *The European Physical Journal Plus*, 129**,** 76.

LLIBRE, J., OLIVEIRA, R. D. & VALLS, C. 2015. On the integrability and the zero-Hopf bifurcation of a Chen–Wang differential system. *Nonlinear Dynamics*, 80**,** 353-361.

LLIBRE, J. & VALLS, C. 2008. Analytic integrability of a Chua system. *Journal of Mathematical Physics*, 49**,** 102701.

LLIBRE, J. & VALLS, C. 2011a. On the C1 non-integrability of the Belousov–Zhabotinskii system. *Computers & Mathematics with Applications*, 62**,** 2342-2348.

LLIBRE, J. & VALLS, C. 2011b. Polynomial, rational and analytic first integrals for a family of 3-dimensional Lotka-Volterra systems. *Zeitschrift für angewandte Mathematik und Physik*, 62**,** 761-777.

LLIBRE, J. & ZHANG, X. 2002. Invariant algebraic surfaces of the Lorenz system. *Journal of Mathematical Physics*, 43**,** 1622-1645.

LLIBRE, J. & ZHANG, X. 2010. Rational first integrals in the Darboux theory of integrability in Cn. *Bulletin des sciences mathematiques,* 134**,** 189-195.

LLIBRE, J. & ZHANG, X. 2012. On the Darboux integrability of polynomial differential systems. *Qualitative theory of dynamical systems,* 11**,** 129-144.

OLLAGNIER, J. M. 1997. Polynomial first integrals of the Lotka–Volterra system. *Bull. Sci. Math,* 121**,** 463-476.

WEI, Z., MOROZ, I., WANG, Z., SPROTT, J. C. & KAPITANIAK, T. 2016. Dynamics at infinity, degenerate Hopf and zero-Hopf bifurcation for Kingni–Jafari system with hidden attractors. *International Journal of Bifurcation and Chaos,* 26**,** 1650125.

ZANCO Journal of Pure and Applied Sciences
The official scientific journal of Salahaddin University-Erbil
https://zancojournals.su.edu.krd/index.php/JPAS

ISSN (print):2218-0230**, ISSN (online):** 2412-3986**, DOI: http://dx.doi.org/10.21271/zjpas**

RESEARCH PAPER

An Investigation into the Current Situation of Implementing Building Information Modeling (BIM) in Construction Projects in Erbil City, KRG, Iraq

Khalil Ismail Wali*

Department of Civil Engineering, College of Engineering, Salahaddin University-Erbil, Kurdistan Region, Iraq.

A B S T R A C T:
Building Information Modeling (BIM) facilitates sharing all participants during the project's lifecycle management by providing shared digital resources for all stakeholders. This study carried out during 2018-2019 as an attempt to understand the current situation and to identify the potential barriers factors facing the BIM implementation in Erbil city, Kurdistan Regional Governorate (KRG)-Iraq. The results analysis of collected data revealed that only 58% of respondents had heard about the BIM against 42% had never heard about BIM. While a majority of 79% said that they had not used BIM; against only 21% said BIM used by their companies. The results of the analysis city showed that the top five significant barriers and obstacles factors encounter the implementation of BIM was the lack of conducting training courses for learning BIM techniques in Erbil city comes in the first rank. Whereas poor education syllabus and training courses in universities and governmental centers in the second rank. While, the Lack of supportive environment by the parties involved in construction and have an impact on the development of construction projects came in the third rank, and poor planning and a coordination with considerations for proper implementation and innovation management in the fourth rank, the lack of experts and technical staff in the field of BIM came in fifth ranks. The primary contribution of this study is to enhance awareness of the benefits of adopting BIM in the construction sector in Erbil city.

KEY WORDS: Building Information Modeling(BIM); Barriers; Motivation; Construction Projects
DOI: http://dx.doi.org/10.21271/ZJPAS.32.3.2
ZJPAS (2020) , 32(3);10-19 .

1. INTRODUCTION:

Building Information Modeling (BIM) is the process of developing and adopting a computer-aid model to represent the planning schedule, design, construction, and operation of a facility. BIM technique is a data-rich, object-oriented, from which views and data appropriate to various parties and users' needs can be figured out and analyzed to produce information that can be used for making decisions and to improve the process of completing the facility (America, 2005).

* **Corresponding Author:**
Khalil Ismail Wali
E-mail: khalil.wali@su.edu.krd
Article History:
Received: 22/09/2019
Accepted: 24/11/2019
Published: 15/06 /2020

Building Information Modeling (BIM) is the process of developing and adopting a computer-aid model to represent the planning schedule, design, construction, and operation of a facility. BIM technique is a data-rich, object-oriented, from which views and data appropriate to various parties and users' needs can be figured out and analyzed to produce information that can be used for making decisions and to improve the process of completing the facility (America, 2005).
The Handbook of BIM describes BIM as computer-aided modeling technology for managing and creating building information, and it helps architects, engineers, and constructor to visualize the process of constructing to be built in a simulated environment to classify any potential

design, construction, or work aspects. BIM technology represents a new approach within AEC. (Eastman et al., 2011)

The applications of BIM assists in generating the geometry, spatial relationships, geographic information, quantities and properties of building elements, cost estimation, material inventories, and preparation of project schedule. This model can be used to demonstrate the entire building life cycle (Azhar et al., 2008). On the other hand, the parties involved in adopting the BIM model uses specific software that suits with their required task, which constitutes a barrier to the exchange of data to and from the model. Moreover. Besides, poor support from senior management staff is one of the difficulties the application of BIM (Herold et al., 2008).

Regarding the legal side, the shortage of BIM standard contracts is one of the other fences for many companies and organizations (Becerik-Gerber and Kent, 2010). The government institutions require taking the leadership role in encouraging the implementation of the BIM. Also, it is necessary to cooperate with other parties who have an impact on the development of projects, such as specialists and engineers in the private sector, contractors (Hardin, 2009). BIM Model deliverables include lean construction principles, green environment policies, and entire life cycle costing. A shared interdisciplinary model is essential to provide two-way access to project stakeholders, which will eventually facilitate Integrated Project Delivery (IPD) (Kjartansdóttir et al., 2017).

The roots of BIM technique date back to the late 1970s and early 1980s in the USA and Europe through the parametric modeling researches that have been conducted in that era. However, the implementation of this technology did not practically apply in the AEC projects until the mid-2000s (Eastman et al., 2011). BIM usage is increasing across the world. In the USA and Canada, the adoption of BIM is growing throughout the states, 18% of owners used BIM in 2009, then increased to 30% in 2011 and around 44% in 2014. Recently, about 60% of owners using BIM in their projects (AUTODESK, 2014). According to the survey made by the Egyptian researcher, stated that BIM technology is being widely implemented in the Middle Eastern countries, especially in UAE and Qatar, which come at the top of the list. Only Iraq is the only country that has not implemented this technology yet (Egyptian, 2017).

2. MATERIALS AND METHODS

This study investigates the current situation and to identify the potential barriers factors of BIM implementation in the construction sector in Erbil city. To achieve the objective of this study, the field survey method conducted through a particular form of a questionnaire prepared to gather the data and information from engineers and professionals working in both the public and private construction sectors in Erbil city. The designed questionnaire comprises three main sections as follows:

Section I: This section related to general information of the respondents such as; name, nationality, age, and gender, and the educational level.

Section II: In this section, the current practices and knowledge of the respondents about the BIM were examined, which included questions about whether the respondent has heard of BIM or not.

Section III: In this section, a list of 21 barriers factors facing BIM implementation were listed together with the weight of importance by using the five- Likert scale. The scale comprises; 1: Extremely disagree, 2: Disagree, 3: Neutral, 4: Agree, 5: Highly agree (Likert, 1932).

A total of 150 forms of the questionnaire distributed, only 125 completed forms returned and accepted at a rate of 83.3%, directed to the target respondents of professional engineers and academic staff working in 25 public and private sectors of construction projects, governmental institutions, and universities academic staff in Erbil city as presented in Table 1.

Table 1. List of Projects and Organizations covered by the survey in Erbil city

Private Sectors	Public Sectors
1. Mihrabani Hospital	1. 120 m ring road
2. German Hospital	2. Erbil Municipality projects
3. Majidi Hospital	3. Ankawa Municipality projects
4. Runaky Towers	4. Erbil Municipality Engineers
5. Cristal Hotel 2	5. Ankawa Municipality Engineers
6. New US Consulate	6. Sallahadin University academic staff
7. Majidi Mall 2	7. Ministry of Municipality&Turisum
8. Justice Tower	8. Ministry of Construction & Housing
9. Empire Wing Apartments	9. Directorate of Education Projects
10. Four Towers Buildings	10. Directorate of Roads & highways
11. Greenland Residential Houses	
12.Greenland Overpass	
13. Zanyari Apartments	
14. International Tishk University	
15. Cihan University-Erbil	

3. RESULTS AND DISCUSSION

3.1. General Information for Respondents

Table 2 shows the distribution of the respondent's demographic characteristics and classifications in terms of affiliation, gender, age, category of experience, and specialization. The results analysis showed that the respondents affiliation of 44.% from the private sector, 38.% from the public sector, and 18% from both the private and public sectors. The respondents' specialization was 45% civil engineer, 30% architecture engineer, 10% electrical engineer, 10% mechanical engineer and 5% other such as (dam and water resource engineers, software engineers, and roadway and highway engineers).

Table 2. The respondent's profile.

Descriptive	Characteristic	Percentage
Work Sector	Private Public Both	44% 38% 18%
Gender	Male Female	80% 20%
Age	20-30 31-40 41-50 More than 51	17% 28% 30% 25%
Work Experience	Less than two years Two to five years Five to ten years More than ten years	0 % 12% 25% 63%
Specialization	Civil Engineer Architect Engineer Electrical Engineer Mechanical Engineer Other:	45% 30% 10% 10% 5%

3.2. Current Situation of BIM Implementation in Erbil city

To examine the respondent's knowledge of BIM technique, they questioned whether they had heard about the BIM technology or not; 58 % of them answered "yes," and 42% said "No." as shown in Figure 1. This finding indicates a critical state that means about half of the respondents yet not heard about the BIM technology application in Erbil city.

Figure 2 illustrates the respondent's source of knowledge on BIM, the majority of 85% of the respondents indicating they self-taught on BIM which comprises; (10% self-taught, 22% personal participating in conferences, 15% reading article and 12% from other sources) against only 5% got their knowledge by training course and 15% worked with companies using BIM. This finding indicates the absence of official and governmental intervention to enhance BIM adoption.

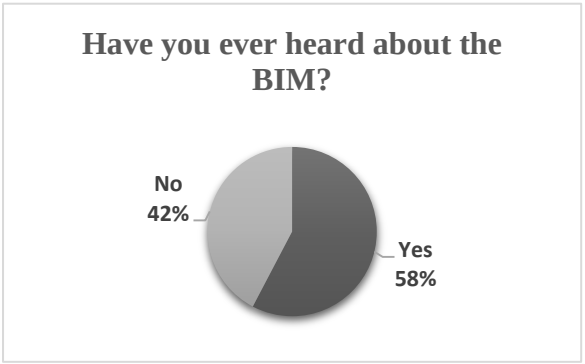

Figure 1. Percentage of hearing on BIM tool

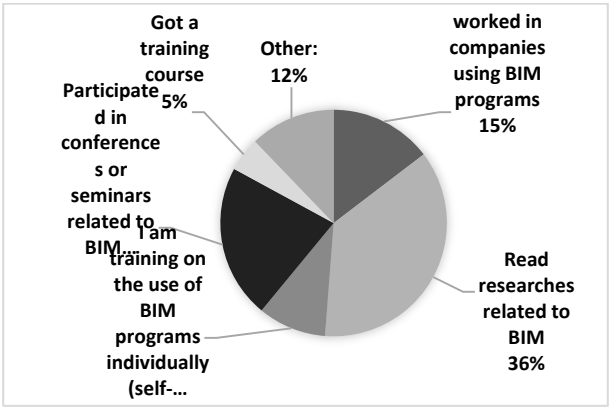

Figure 2. Respondent's sources of BIM knowledge

When respondents questioned whether their company or organization in which they employed was using BIM, the majority of 77% answered "No" against only 23% answered "Yes" as shown in Figure 3.

To examine the current level of knowledge on BIM techniques and applications, the respondents questioned to describe the current level of understanding of BIM in Architecture, Engineering and Construction industry (AEC) in Erbil city. 83% of the respondents said between low and very low level, while only 15% said medium against 2% said high, as shown in Figure 4.

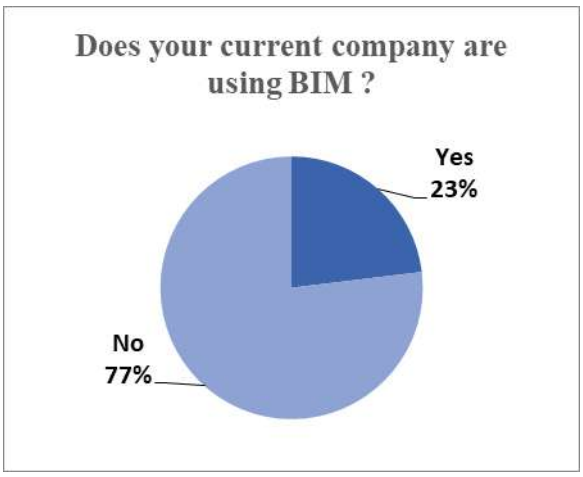

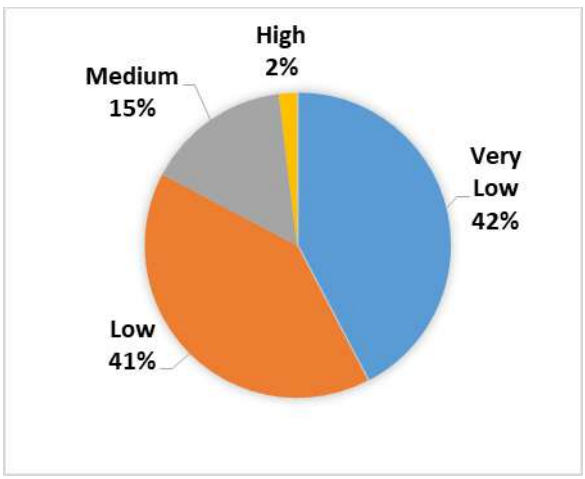

Figure 3. Respondent's Companies experience of BIM

Figure 4. Respondent's assessment of BIM Knowledge

Figure 5 represents the respondent's expectations on the development of BIM implementation in Erbil city in coming ten years (up to 2030), 60% of the respondents said "medium," 23% "low and very low", while only 17% said, "high and very high."

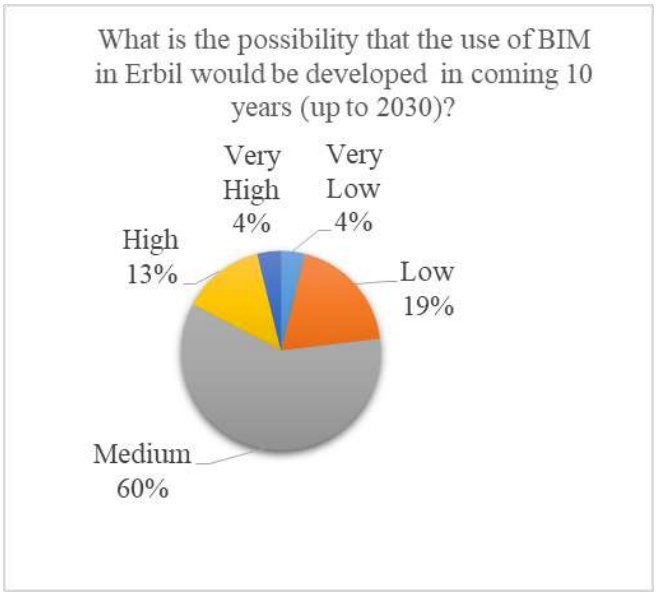

Figure 5. BIM adoption perception over the next ten years.

When the respondents asked about their opinion on the reasons behind the lack of knowledge and experience on BIM technique, the majority of 53% said the cause is due to the lack of educational courses about BIM in universities, and 18% reported that not officially being forced to use BIM in Erbil city as shown in Figure 6.

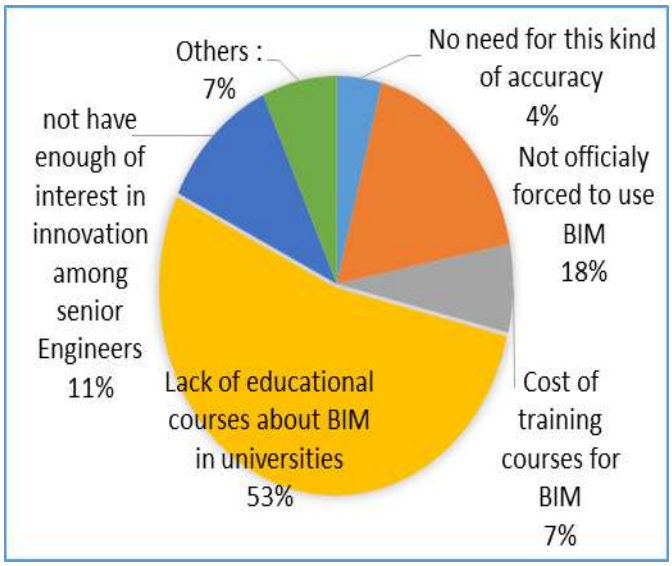

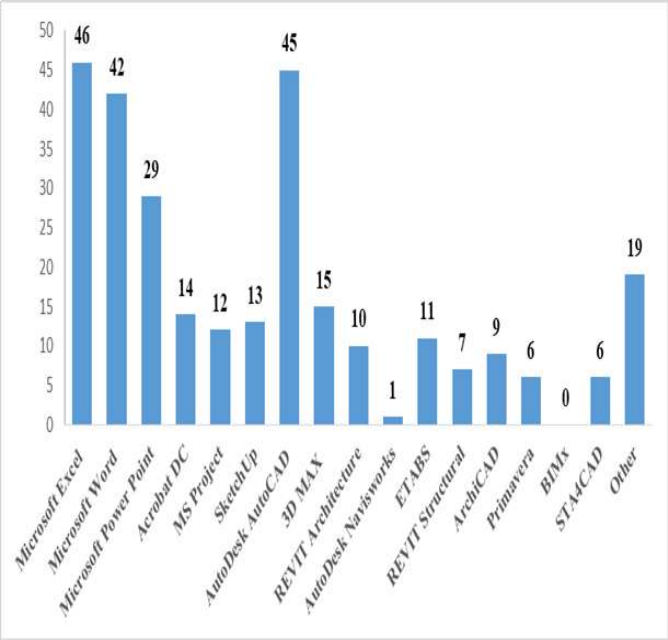

Figure 7. Software used by respondents 1

Figure 6. Reasons for lack of knowledge on BIM technique

Furthermore, Figure 7 shows the current software and project management tools used by the respondents in Erbil city, the majority of 46% indicates that the Microsoft Excel mostly used, while Autodesk CAD cames in the second rank of 45% , Revit at 10% and ArchiCAD 9%, whereas, 0% (none) of the target respondents used BIMx as an integrated tool in Erbil city

4. DATA ANALYSIS METHODS

4.1 Relative Importance Index (RII)

To analysis the collected data of this survey statistically, the relative importance index (RII) was used as a criterion to rank the importance of barriers factors facing the BIM implementation. RII calculated by using equation (1) and (2) (Krauth, 2000).

$$RII=\Sigma\frac{W}{(A*N)} \quad \text{----------(1)}$$

$$RII=\frac{5(n5)+4(n4)+3(n3)+2(n2)+1(n1)}{5(n5+n4+n3+n2+n1)} \quad \text{----------(2)}$$

Where:

W: The Likert weight ranging from 1 to 5 selected by the respondents.

A: Indicates the highest weight (which equals 5 in this survey)

N: Is refers to the total number of respondents.

4.2 Statistical reliability analysis

Calculating the value of Cronbach's alpha was used as a tool to measure the internal consistency of items related to the barriers factors facing the BIM implementation. Corbanoch's alpha ranges from 0.0 to 1.0, and the closer to 1.0 indicates the high degree of reliability range (Yockey, 2018). Table 3 shows the classification for the degree of reliability concerning the value of the Cronbach's alpha coefficient determined by using the SPSS package. For the questionnaire data collected as indicated in the part III-BIM potential barriers, the result of Cronbach's alpha evaluation was 0.992, which represents the excellent limit, and this result confirms the acceptable reliability of this part, as shown in Table 4 (Hinton et al., 2004).

Table 3. Reliability Statistics –Cronbach's Alpha

Table 4. Reliability cutoff values(Hinton et al., 2004).

Cronbach's alpha	*Degree of Reliability*
$\alpha \geq 0.9$	Excellent
$0.9 > \alpha \geq 0.8$	Good
$0.8 > \alpha \geq 0.7$	Acceptable
$0.7 > \alpha \geq 0.6$	Questionable
$0.6 > \alpha \geq 0.5$	Poor
$0.5 > \alpha$	Unacceptable

Cronbach's Alpha- Barriers	Cronbach's Alpha Based on Standardized Items	No. of Items
0.992	0.993	21

4.3 The potential barriers facing BIM implementation in Erbil city

The results of RII analysis as listed in Table 5, showed that "The lack of training courses available for learning BIM technique in Erbil city." was the most significant factor of BIM using with an essential rate of RII=0.8385 which cames in the first rank.

The second potential barrier for using BIM was "Poor education and training in universities and government centers." with RII=0.8192, cames in the second rank.

While in the third ranks cames the "Lack of supportive environment by government and other parties who have an impact on the development in Erbil city." And "lack of educational syllabus in engineering colleges in Erbil city to use such sophisticated packages and tools," both factors were with RII=0.8154.

Table 5. Potential barriers facing BIM implementation in Erbil city

No.	Barriers factors	RII	Rank
1	Absence of client demand for using BIM in their projects	0.7923	6
2	The cost of BIM and its updates.	0.7231	10
3	The cost of the hardware required with particular specifications for the operation of BIM.	0.7192	11
4	The cost needed for training courses about BIM Technique.	0.7577	8
5	The lack of training courses available for learning BIM Technique in Erbil city-KRG.	0.8385	1
6	The cost of recruitment of BIM specialists and additional staff.	0.7692	7
7	Time to apply BIM and its negative impact on current productivity.	0.5808	16
8	Lack of supportive environment by government and other parties who have an impact on the development in Erbil city.	0.8154	3
9	Lack of experts in the field of BIM.	0.8000	5
10	Insufficient BIM standards, protocols, and rules in Erbil city-KRG.	0.7577	8
11	The belief that existing techniques are adequate, BIM is not needed.	0.6269	13
12	Problems related to interoperability between BIM Technique.	0.6192	14
13	Poor education and training in universities and government centers.	0.8192	2
14	Poor planning and a coordinated approach with considerations for Implementation and innovation management	0.8038	4
15	Poor cooperation between different disciplines.	0.7692	7
16	Exposure to the risks associated with the intellectual property model and the cost of copyright and publishing.	0.6154	15

17	Lack of educational syllabus in engineering colleges in Erbil-KRG to use such sophisticated packages and tools.	0.8154	3
18	Lack of serious exposure to BIM by holding seminars and conferences about its benefits	0.7923	6
19	Insufficient skills among engineers and difficulty in learning BIM software.	0.7231	10
20	The need for uninterrupted power and a secure internet connection that can accommodate the vast amount of information.	0.6462	12
21	The strong resistance to change, especially with older ages (owners, contractors and/or engineers) and their attachment to only the software they are familiar to them.	0.7538	9

4.4 Comparison of findings with other countries

In a comparison of three top significant barriers factors of the current study in Erbil city with the researches in other countries, showing the similarity in some barriers factor to the research findings in Iran (Hosseini et al., 2015), Jordan (Matarneh and Hamed, 2017), Kuwait (Abdulfattah et al., 2017), and Qatar (Ahmed et al., 2014), as shown in Table 6.

Table 6. Comparison of three top BIM barriers between ten various countries

No.	Country[ref.]	Three top BIM barriers
1.	UK (NBS, 2015)	• Shortage of experts • Lack of training • The owner did not request the use of BIM
2.	USA (Construction, 2012)	• Cost of software • Required hardware upgrades too expensive • There is no sufficient time to evaluate it
3.	SWEDEN (Lahdou and Zetterman, 2011)	• Personal opinions towards BIM • The strong resistance to change • It is hard to find stakeholders that have the required competence to participate in the BIM project.
4.	MALAYSIA(Zahrizan et al., 2014)	• Weak knowledge of BIM • The owner did not request the use of BIM • The strong resistance to change
5.	INDIA (Kushwaha, 2016)	• Weak competition • Cost of software • The owner requests the use of BIM only at certain stage
6.	NIGERIA(Abubakar et al., 2014)	• The resistance to change • The need for BIM contracts • Cost of training
7.	QATAR (Ahmed et al., 2014)	• Shortage of experts • The need for special contracts • The strong resistance to change
8.	KUWAIT (Abdulfattah et al., 2017)	• Lack of training • Lack of Engineer's skill • Weal knowledge of BIM

9.	JORDAN (Matarneh and Hamed, 2017)	• Weak governmental efforts • Insufficient BIM standards and protocols • Weak knowledge of BIM
10.	IRAN (Hosseini et al., 2015)	• Lack of attention by policymakers and the government. • Lack of knowledge on BIM adoption process. • Lack of support from managers to accept changing current practices.
11.	ERBIL-KURDISTAN-IRAQ [current study]	• The lack of training courses for learning BIM techniques • Poor education and training in universities and government centers. • Lack of governmental support and other parties.

5.CONCLUSIONS

This study was aimed to explore the current state of BIM implementation and to find out the most probable barriers facing BIM adopting in Erbil city based on the opinions of professional staff involved in both the public and private sectors. According to the results and findings showed that 42% of the target respondents not heard on BIM, while 58% said they heard about BIM. The study also revealed that 77% of the companies involved in the construction sector not using BIM, against only 23% using BIM, whereas, 83% of the respondents believed that the current level of knowledge on BIM in Erbil city still in a range of low and very low level.

In a question of the reasons behind the lack of knowledge on BIM, 53% said due to the lack of educational courses in universities, and 18% said due to BIM still not being enforced to be used.

It was found that the majority of 46% of the respondents using Microsoft Excel, and 45% said using Autodesk CAD, whereas 0% (none) of the respondents used BIM technology.

The findings also identified the most significant barriers factors facing the BIM implementation in Erbil city, which comprises the lack of training courses available for learning BIM technique particularly in Erbil city, Poor education and training in universities and government institutions, Lack of educational syllabus in engineering colleges, Lack of supportive environment by government agencies.

The results of this study reveal that the BIM implementation in Erbil city during surveying 2018-2019 is still in the beginning phase, and it is facing several barriers and obstacles as well as ignorance from various parties involved in the construction sector. Therefore, it is recommended to initiate supporting laws and regulations to enhance the adopting of BIM in architecture, engineering, and construction industry in Erbil city. Facilitate the training courses, conducting conferences and seminars to promote BIM adoption. Finally, there is a need to improve the syllabus and curriculum of engineering colleges for undergraduate and postgraduate studies, and encouraging the researches and studies to transfer the technology and expertise in the field of BIM technology.

REFERENCES

ABDUL FATTAH, N. M., KHALAFALLAH, A. M. & KARTAM, N. A., 2017. Lack of BIM training: investigating practical solutions for the State of Kuwait. *World Academy of Science, Engineering and Technology, International Journal of Civil, Environmental, Structural, Construction and Architectural Engineering*, 11**,** 1050-1056.

ABUBAKAR, M., IBRAHIM, Y., KADO, D. & BALA, K. 2014. Contractors' perception of the factors affecting Building Information Modelling (BIM) adoption in the Nigerian Construction Industry. *Computing in civil and building engineering (2014).*

AHMED, S. M., EMAM, H. H. & FARRELL, P. Barriers to BIM/4D implementation in Qatar. The 1st international conference of cib middle east & north Africa conference, 2014. 533-547.

AMERICA, A. G. C. O. 2005. *The Contractor's Guide to BIM*, Las Vegas, NV AGC Research Foundation.

AUTODESK. 2014. *The Value of BIM for Owners: Save Time and Money During the Building Lifecycle* [Online]. Available: http://damassets.autodesk.net/content/dam/autodesk

/www/solutions/bim/BIM_for_Owners.pdf. [Accessed 23-Dec 2018].

AZHAR, S. 2011. Building information modeling (BIM): Trends, benefits, risks, and challenges for the AEC industry. *Leadership and management in engineering*, 11**,** 241-252.

AZHAR, S., NADEEM, A., MOK, J. Y. & LEUNG, B. H. Building Information Modeling (BIM): A new paradigm for visual interactive modeling and simulation for construction projects. Proc., First International Conference on Construction in Developing Countries, 2008. 435-46.

BECERIK-GERBER, B. & KENT, D. 2010. Implementation of integrated project delivery and building information modeling on a small commercial project.

CONSTRUCTION, M.-H. 2012. The business value of BIM in North America: multi-year trend analysis and user ratings (2007-2012). *Smart Market Report*.

EASTMAN, C., TEICHOLZ, P., SACKS, R. & LISTON, K. 2011. *BIM handbook: A guide to building information modeling for owners, managers, designers, engineers and contractors*, John Wiley & Sons.

EGYPTIAN, R. 2017. *Application of BIM in the Middle East* [Online]. Available: https://www.egyres.com/articles/[Accessed 20-Dec 2018].

HARDIN, B. 2009. BIM and Construction Management: proven Tools, Methods, and Workflows‖ Wiley Publishing Inc. *Indianapolis, Indiana*.

HEROLD, D. M., FEDOR, D. B., CALDWELL, S. & LIU, Y. 2008. The effects of transformational and change leadership on employees' commitment to a change: A multilevel study. *Journal of applied psychology*, 93**,** 346.

HINTON, P., BROWNLOW, C., MCMURRAY, I. & COZENS, B. 2004. Using SPSS to analyze questionnaires: Reliability. *SPSS explained***,** 356-366.

HOSSEINI, M. R., AZARI, E., TIVENDALE, L. & CHILESHE, N. Barriers to adoption of building information modeling (BIM) in Iran: Preliminary results. The 6th International Conference on Engineering, Project, and Production Management (EPPM2015), Gold Coast, Australia, 2015.

KJARTANSDÓTTIR, I. B., MORDUE, S., NOWAK, P., PHILP, D. & SNÆBJÖRNSSON, J. T. 2017. *Building Information Modelling-BIM*, Civil Engineering Faculty of Warsaw University of Technology Warsaw.

KRAUTH, J. 2000. *Experimental design: a handbook and dictionary for medical and behavioral research*, Elsevier.

KUSHWAHA, V. 2016. Contribution of building information modeling (BIM) to solve problems in architecture, engineering and construction (AEC) industry and addressing barriers to implementation of BIM. *Int. Res. J. Eng. Technol*, 3**,** 100-105.

LAHDOU, R. & ZETTERMAN, D., 2011. BIM for Project Managers How project managers can utilize BIM in construction projects.

LIKERT, R., 1932. A technique for the measurement of attitudes. *Archives of psychology*.

MATARNEH, R. & HAMED, S., 2017. Barriers to the adoption of building information modeling in the Jordanian building industry. *Open Journal of Civil Engineering*, 7**,** 325.

NBS 2015. NBS International BIM Report, UK.

YOCKEY, R. D. 2018. *SPSS Demystified: A simple guide and reference*, Routledge.

ZAHRIZAN, Z., Ali, N. M., HARON, A. T., MARSHALL-PONTING, A. & HAMID, Z. A. 2014. Exploring the barriers and driving factors in implementing building information modeling (BIM) in the Malaysian construction industry: A preliminary study. *Journal of the Institution of Engineers, Malaysia*, 75**,** 1-10.

ZANCO Journal of Pure and Applied Sciences
The official scientific journal of Salahaddin University-Erbil
https://zancojournals.su.edu.krd/index.php/JPAS

ISSN (print):2218-0230**, ISSN (online):** 2412-3986**, DOI: http://dx.doi.org/10.21271/zjpas**

RESEARCH PAPER

Midterm Load Forecasting Analysis For Erbil Governorate Based On Predictive Models

Warda Hussein Ali

Department of Electrical Power ,Engineering Technical College of Engineering, Sulaimani Polytechnic University, Sulaimani, Iraq

A B S T R A C T:

Electrical power supply is becoming more and more complex as a result of expansion, growing population, and unsuitable planning of administration and peoples. Electrical power load forecasting may be defined as the process of predicting electrical load values for future of the system with respect to current demands. This analysis is an important procedure for the power system planners and the demand controllers to ensure that the system can generate sufficient of electricity for different kinds of terms such as short, medium and long term load forecasting. The forecasting analysis allows us to manage the electrical loads with the increasing demand. For that purpose, we have used some predictive models to analyze of electrical load forecasting for Erbil Governorate in Iraq. This analysis helps us to manage our planning better, arrange system maintenance plan and enhance fuel control. This study raises an attempt for forecasting the peak (upper limit) monthly demand of electric power for one year ahead. Simple linear regression model and Auto Regressive Integrated Moving Average model were applied as forecasting models for a power consumer's dataset for the purpose of predicting forthcoming year electricity load demand. , also Forecasting models are then validated using some indicators, indicator used is Root Mean Square Error (RMSE) ,which is conceded a statistic metric that is commonly used for accuracy evaluation of LF methods, and Mean Absolute Error (MAE) both used as a forecasting accuracy criteria.

KEY WORDS: Load Forecasting Analysis, Linear Regression, Root Mean Square, ARIMA Modelling
DOI: http://dx.doi.org/10.21271/ZJPAS.32.3.3
ZJPAS (2020) , 32(3);20-29 .

1.INTRODUCTION :

Electrical loads are varying from day to day as a consequence of modern civilization and development in technology. Industrial loads, residential loads, and commercial loads are not steady, resulting mostly in the over loading of power systems. The same matter applies to Erbil governorate electric power system.

As a result, of this, there is sever need to forecast the future electrical load demands in the governorate therefore this will serve to find and evaluate the sum of the required load and prepare for the capacity of generation that would meet the electrical load demand.

The forthcoming events and situations based on earlier existing data can be defined as forecasting, the proses of making similar estimate can be called forecasting. Forecasting is important to make decisions. Load forecasting usually confused with the load prediction, however to study load forecasting, one should depend mainly on previous data that recorded. It can be said that

* **Corresponding Author:**
Warda Hussein Ali
E-mail: warda.ali@spu.edu.iq
Article History:
Received: 11/12/2019
Accepted: 23/01/2020
Published: 15/06 /2020

forecasting is more particular and it is able to cover a wide range of possible results. For now, a day's electrical load forecasting is a very important research area for electricity suppliers, financial organization, and transmission distribution, and other participants in electric power generation. It is the requirement estimation of electrical loads for a particular location depending on past-recorded data of electrical load demand (Bowerman et al., 2003).
With respect to the time period, there are three kinds of load forecasting, first long term load forecasting (LT), predicts electrical load from one year to 10 years, second if forecasting range is from one week up to a year, then it is Saied to be midterm load forecasting (MT), third, short term load forecasting (ST) relates to time period from minutes up to one day predictions.
Short-term electrical load forecasting relates to forecasting of loads from several minutes to one week ahead. A dependable (ST)forecasting supports energy suppliers and utilities to deal with the problems presented by the growth of electricity markets, and (ST)is very important as it affects strongly power system operation including estimation of variable transfer capability, power system stability margins, load elimination decisions, etc... As a result, proper load forecasting ensures more reliability in electrical power system operation while it improve the reduction of its operation coast by offering correct input day ahead scheduling.

(MT) is the second type of load forecasting, Mid-term load forecasting have period time in a week to a year and this type of forecasting rely mainly on expansion factors such as main events increment of extra loads maintenance of large consumers and seasonal change, in this term of forecasting hourly loads are used for predictions of the day peak load or weeks peak load ahead (Feinberg and Genethlion, 2005; Ismael, 2019). (LT) is third type of load forecasting which plays a basic role for both of planners and utilities in term of progression of the grid and growth planning and it relates to time frame of one to ten years and sometime up to several decades.

A number of studies and wide range of model methodologies are presented in the study for various kind of electrical load forecasting: In (Bruhns et al., 2005), researchers worked on model improvement of seasonality, and they studied midterm electrical load forecasting using nonlinear regression method.

Felly Njoku CF , Adewale A , Samuel IA . Carried out a study to calculate the medium-term electrical load forecasting using three regression models (Samuel et al., 2014).
In (Amjady, 2002), the rise of using intelligence techniques were shown, and many works have been performed using an approach of artificial neural network in long and short term electrical load forecasting. In addition, in (Nur et al., 2013), they proposed a method of exponential smoothing for forecasting of electrical load utilized of Malaysia.

A study on load forecasting in Karnataka, India has been performed using time series analysis,
Three types of ARIMA models were developed which are Auto regressive model, ARIMA, and Auto regressive moving average. Result indicated that ARIMA model is the most reliable model (N. Amral, 2007).

The main work carried out in this study is indicating results of midterm electricity load forecasting using average the load data collected from substations related Electricity Control Center (ECC) of Kurdistan region in Iraq for Erbil Governorate. Testing and proven of the accuracy for the load forecasting has been done using mean absolute percentage error (MAPE) which measures absolute variance between the actual load demand and forecasted load values and then calculates the mean and the root mean square error (RMSE) which finds the variance between the actual load demand and the forecast load, squares the variance, calculates the mean of squares and finally calculates the square root.
The time series models employed in this study involves LR and ARIMA. The research question come to mind is; How to implement the predictive models to find the forecast load? The answer of this research question is important because it helps the practitioners to make a decision in advance about increasing or decreasing the electrical load for the next year. At the same time, it helps to know which part should be increased for the next year like adding some more electrical sub-stations

or distributing the loads to the electrical network. For that reason, we have to choose the optimum model to analyze the collected data. The organization of this study is abbreviated as following; section two introduces the electrical load profile of Erbil governorate. Section three represents methodology to analyze the data obtained experimental results. Section four describes the obtained experimental results. Finally, section five gives the conclusions.

2. ERBIL GOVERNORATE LOAD PROFILE

The main resources of electricity power supply is the governed is Erbil combined gas power plant which consists of 10 units (8 simple cycle 125 MW per unit and 2 combined cycle 250 MW per unit), which is also supply Sulaimani and Duhok Governorates. In the past years, a severe shortage of electric power supply in the Erbil Governorate has been recorded. Because the available electric power supply sources mentioned above dose not meets the power consumed in the governorate. The consumers provided by electricity for a very short period time, usually ten hours per each day and that is depending on the capacity of generation. The monthly energy consuming request (Unit in MWh) data has been taking form (ECC) Kurdistan region from 2016 to September 2019. Figure 1 captures growth of energy consumption and time periods.

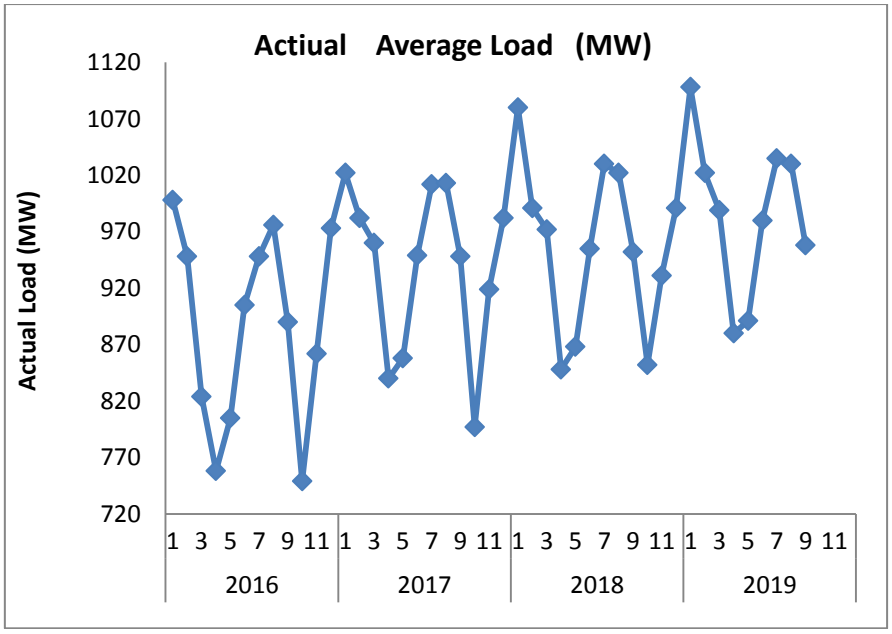

Fig.1 Monthly mean maximum demand from January 2016 to September of 2019

3.METHODOLOGY

Section bellow presents a procedure for creating an accurate model of time series that used for model electrical load forecasting in Erbil Governorate. The procedures contain selecting proper model, plotting various data, estimation of different parameter, and electrical load forecasting. The analysis is performed by using ARIMA time series modeling and linear regression method. In this research, NCSS software is used which is a Statistical Analysis Software contains a variety of tools used for statistical tasks required in research. Here, we described the necessary background and predictive models to understand what we have done.

A. The data set

To demonstrate the high and low frequency demand features using the historical electricity load demand data measured in Megawatts (MW), which were recorded as monthly from Electricity Control Center (ECC) of the Kurdistan region of Iraq in 48 months from January 2016 to September 2019 are used.

The original behavior of monthly energy consumption of the mean load can be seen in Figure1. Numbers of factors are behind the nonlinear behavior of load demand, such as country growth, weather condition during the year and ect..It is clear from the graph it grew the upward demand every year. The variation of the series is frequently stable therefore no need for logarithmic or any other transformation. Values indicated from the plot that maximum indices are reached during January, February and December, while minimum indices are reached during April, May, September and October, and this is due to various changes in temperature.

B. Forecast Modeling

In this study, the load forecasting models used are Linear Regression Analysis and ARIMA in time series model.

Time series is a numerical analysis that deals with observation of data points, or trend analysis. To yield correct statistical inferences, these data must be repeatedly measured, often over a four to five time period.
It is a set of observations xi, each value has been noticed at a particular time t, marked by {Xt}. It may show an achievement for the procedure that represented as follows:

$X_t = m\,t + S_t Y_t$…….. (1)

$t = 1, 2 \ldots n,$

Here mt represents trend component, a trend is a stable directional change in the series.

Seasonal variations are represented in time series its marked as St which is a seasonal component; and it is particularly right in series that represent climate changes. and Yt this component represents random noise which is stationary (Brockwell and Davis, 2002).

The main purpose for modeling a time series is predicting series set data that are not deterministic in normal but random component are existed in it. mt and St components must be calculated and minimized as to make time series Yt be stationary. The time series {Xt} will consider as a stationary or non-varying if the auto covariance function and mean value of {Xt} does not depend on time .A varying time series have to transfer to a stationary one. At that time only a suitable probabilistic time series model may be fined for Yt to study its characteristics and to use it for forecasting objectives. In section bellow a brief summary about each of the used models are given in this sub- section.

2.Linear Regression Model

In Linear Regression method the relation between variables are found. It could be between two variables. In this case, it is named simple linear regression. If it is found between more variables, it is named multiple linear regressions.

After the relation between variables has been found, it is assumed that parameters changing with the similar relation; therefore, the similar relationship applied to the same upcoming parameters, which will give us the value of dependent variable for the matching upcoming independent variable, Linear Regressions is very simple to match the curve and calculate the coefficients. The model takes the shape of y=mx+c, where m is the curves slope, and the intercept point is c, and the variable x is independent variable and f(x) is the dependent variable. The work is to calculate the parameters m and c with the help of variable data of x and y (Dara et al., 2013).

3.ARIMA Model

ARIMA represent auto regressive integrated moving average and is defined by three variables: (p, d, q).
Using the past values in the linear regression equation in the time series Y , refers to auto

regressive (AR(p)) component . The parameter p indicates the number of delays carried out by the model.
where φ1, φ2 are parameters for the model.
The rate of deviation in the integrated (I(d)) component represented by d. Subtracting series current values and series previous values d times is represent differencing of a series. Often, to make a series stable whenever a stationary assumption dose not met, differencing is used. Error of the time series model as a combination of prior error terms represented by moving average (MA(q)) component. The number of terms to involve in the model represents the order q.

A non-varying ARMA (p, q) time series model is shown as a sequence for random variables {Xt}, represented by:[5].

$$X_t - \phi_1 X_{t-1} - \cdots - \phi_p X_{t-p} = Z_t + \theta_1 Z_{t-1} + .. + \theta_q Z_{t-q} \quad \ldots\ldots\ldots (2)$$

Where {Zt} is defined as a series of uncorrelated random variables with zero average and unchanged variance, and the polynomials ($1-\varphi_1 z - \ldots. - \varphi_p z^p$) and ($1+\varphi_1 z + ... + \varphi_q z^q$) having no shared factors between them .
The process $\{X_t\}$ may called an ARMA (p, q) process that has mean μ if $\{X_t - \mu\}$ is an ARMA (p, q) process and easily written in the briefer form of

$$\phi(B) X_t = \theta(B) Z_t \quad \ldots\ldots\ldots\ldots\ldots (3)$$

Where θ(.) , φ(.) are respectively the qth and pth degrees of the polynomials,

$$\phi(z) = 1 - \phi_1 Z_{.} \ldots\ldots - \phi_P z^p \quad \ldots\ldots\ldots\ldots (4)$$

$$\theta(z) = 1 + \theta_1 Z_{.} + \cdots + \theta_q \; z^q \quad \ldots\ldots\ldots\ldots (5)$$

B represents backward shift carrier *($B^j X_t = X_{t-1}$,$B^j Z_t = Z_{t-j}$,$j=0,\pm1,\ldots\ldots$)*
The series $\{X_t\}$ is said to be an autoregressive procedure taking the degree p if φ (z) = 1 and having moving average procedure of degree q if θ (z) = 1 (Brockwell and Davis, 2002).

After the power load data has been pre-treated and numerically tested, the calculation of the model order and parameters are also necessary. Akaike Information Criterion (AIC) method is performed to evaluate the order of time series models that is shown in equation 6: [3]

$$AIC = Ln\ (\sigma^2) + \frac{2(P+q)}{T} \quad \ldots\ldots\ldots\ldots\ldots (6)$$

Where:

- T present numbers of non-missing values in the series.
- P represents the degree of the AR component model.
- q represents the degree MA component model
- σ represents the standard deviation of the residuals.

It is well established, at least among statisticians of some higher caliber, that models with the values of the AIC statistic within a certain threshold of the minimum value should be considered as appropriate as the model minimizing the AIC statistic. (Li et al., 2014; Charles et al, 1999).

C. Evaluation of Performance using MAE and RMSE

Time series forecasting performance measures; provide a summary of the ability of the forecast model that performs the forecasting. Two measures are used in this work to measure the performance of electrical load forecasting, they are: first is the root mean square error (RMSE) and second is the mean absolute error (MAE) (Okolobah and Ismail, 2013).
MAE is defined in equation (7) as:
E= (La- Lf)

$$\text{MAE} = \frac{1}{n}\sum_{i=1}^{n} |E_i| \quad \ldots\ldots\ldots\ldots\ldots (7)$$

Where:
E represents the error
Lf represents the forecast load
La represents the actual demand load

N represents the number of values
The RMSE is shown in equation (8) as:

$$RMSE=\sqrt{\frac{1}{n}\sum_{i=1}^{n} E_i^{\,2}} \quad \ldots\ldots\ldots\ldots\ldots\ldots (8)$$

1. THE RESULTS

In this section, we have shown our results with respect to the two predictive models:

1) Results Using the Linear Regression Model

Table I indicates the forecasted load values and actual load values, the values applying the linear regression model from 2016 to 2109 and forecasting load for 2020, in the meanwhile Figure 2 represents a comparison of the forecast and actual electric load values from January 2016 to September 2019and forecasted load for 2020.
The MAE and RMSE values are evaluated using linear regression models and the calculated values of MAE were 14.84 and RMSE value is 20.22.

Table I: forecasted and Actual load values applying regression method

Year	Months	Actual Load in MW	Forecasting load in MW
2016	1	998	993.90
	2	948	931.11
	3	824	909.00
	4	758	798.96
	5	805	813.93
	6	905	897.96
	7	948	961.46
	8	976	968.81
	9	890	896.54
	10	749	768.88
	11	862	869.60
	12	973	945.46
2017	1	1022	1026.71
	2	982	961.76
	3	960	938.84
	4	840	825.12
	5	858	840.51
	6	949	927.20
	7	1012	992.68
	8	1013	1000.19
	9	948	925.50
	10	797	793.65
	11	919	897.54
	12	982	975.76
2018	1	1080	1059.52
	2	991	992.41
	3	972	968.69
	4	848	851.28
	5	868	867.09
	6	955	956.44
	7	1030	1023.91
	8	1022	1031.56
	9	952	954.46
	10	852	818.42
	11	931	925.47
	12	991	1006.05
2019	1	1098	1092.33
	2	1022	1023.06
	3	989	998.53
	4	880	877.44
	5	891	893.66
	6	980	985.68
	7	1035	1055.13
	8	1030	1062.94
	9	958	983.42
2020	1	Predictive Value	1125.14
	2	Predictive Value	1053.72
	3	Predictive Value	1028.37
	4	Predictive Value	903.60
	5	Predictive Value	920.24
	6	Predictive Value	1014.92
	7	Predictive Value	1086.35
	8	Predictive Value	1094.32
	9	Predictive Value	1012.37
	10	Predictive Value	867.95
	11	Predictive Value	981.35
	12	Predictive Value	1066.64

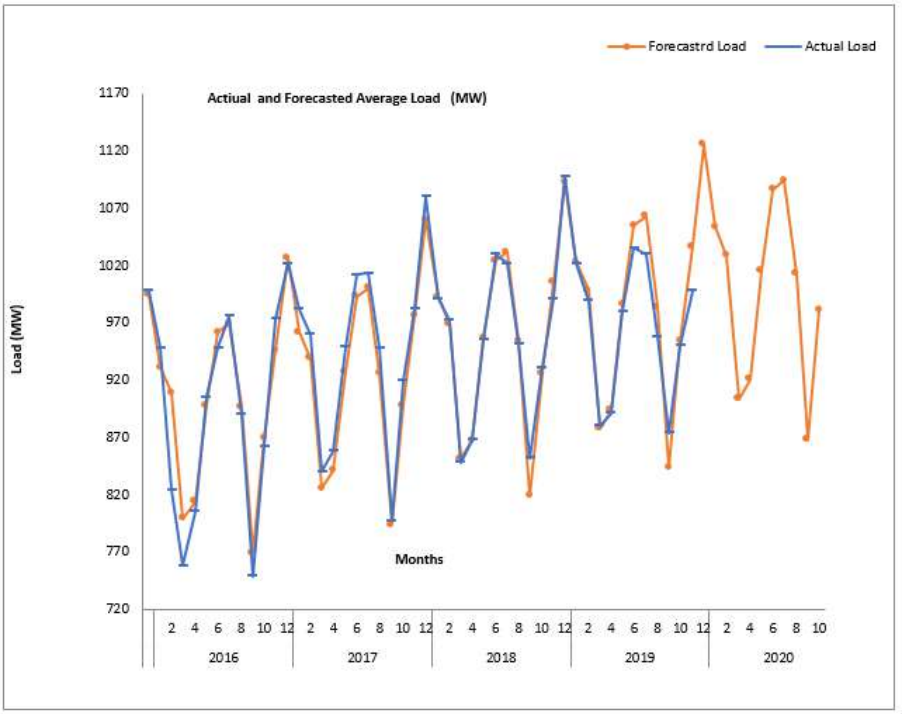

Fig.2 Comparison between the forecasted and actual load demands of Erbil from January 2016 – December 2020 using the Linear Regression Method.

2) *Results Using the auto-regressive integrated moving average ARIMA Model*

Table II indicates the computed ARIMA model for forecasting the load with their respective values of AIC.

From Table II, ARIMA (7, 1, 1) has the minimum AIC indicates that it is the most optimum model among the other ARIMA models.

The best satisfactory model for ARIMA forecasting can be proven by utilizing the accuracy criteria such as MAE and RMSE, which are given by the respective equations (7 and 8), and the result was MAE=17.05 and MASE =19.32. Table III represents the actual electrical load and the forecast average load values utilizing ARIMA model from 2016 to 2109 and forecasting load for 2020, while Figure 3 shows the forecast values from January 2016 to December 2020 and upper and lower limit of forecasted load for 2020.

Table II: The list of ARIMA potential models

ARIMA Models	(AIC)
(1,0,1)	22.74197
(1,1,1)	22.87393
(0,1,1)	22.64192
(2,1,1)	21.81226
(2,1,2)	21.46635
(1,1,3)	21.60749
(2,1,3)	21.57948
(1,1,4)	21.53301
(5,1,1)	20.36306
(7,1,1)	20.11954

Table III: shows actual and forecast load values by ARIMA.

Year	Months	Actual Load (MW)	Forecasting load (MW)
2016	1	998	980.2
	2	948	937.7
	3	824	812.9
	4	758	782.8
	5	805	803.4
	6	905	897.1
	7	948	938.6
	8	976	960.8
	9	890	885.4
	10	749	774.4
	11	862	831
	12	973	991.6
2017	1	1022	1013.8
	2	982	978.1
	3	960	889.2
	4	840	875.7
	5	858	839.7
	6	949	941.8
	7	1012	993.7
	8	1013	1026
	9	948	936.5
	10	797	833.7
	11	919	900.5
	12	982	1007.9
2018	1	1080	1019.6
	2	991	1044.1
	3	972	990.4
	4	848	885.1
	5	868	893.8
	6	955	971.1
	7	1030	1027.5
	8	1022	1018.6
	9	952	905.9
	10	852	798.1
	11	931	814.9
	12	991	882.7
2019	1	1098	963.3
	2	1022	937.1
	3	989	891
	4	880	822.7
	5	891	851.9
	6	980	933.1
	7	1035	999.3
	8	1030	943.5
	9	958	912.3
	10	874	839.8
	11	950	844.4
	12	998	908.7
2020	1	Predictive Value	939.7
	2	Predictive Value	1019
	3	Predictive Value	965.3
	4	Predictive Value	910
	5	Predictive Value	964.9
	6	Predictive Value	995.5
	7	Predictive Value	1042
	8	Predictive Value	1008.9
	9	Predictive Value	987.4
	10	Predictive Value	948.2
	11	Predictive Value	950.7
	12	Predictive Value	990.7

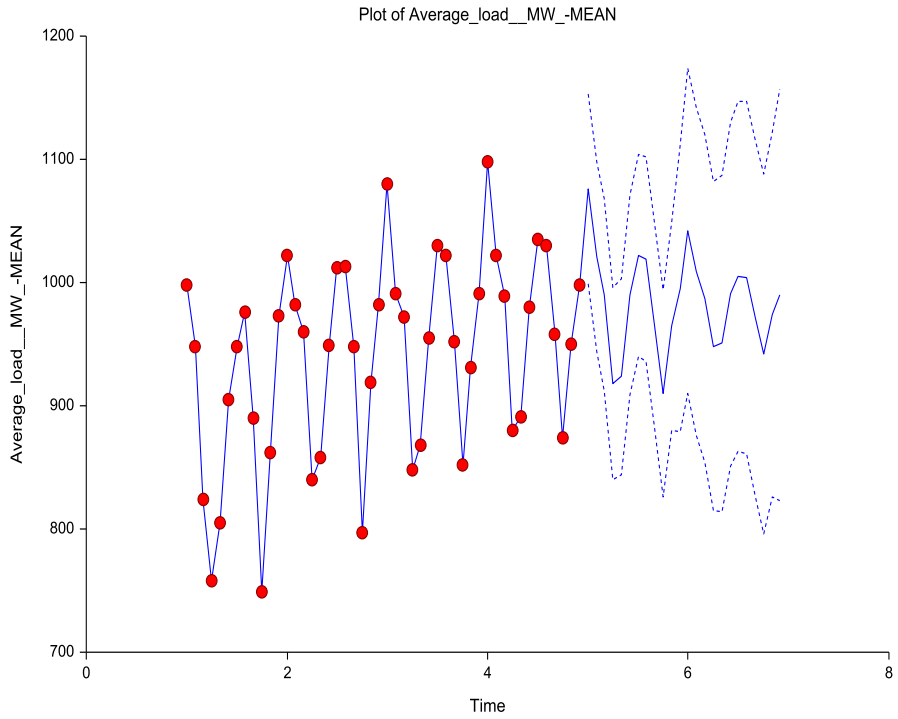

Fig.3 Forecasts data from January-2016 to Desember-2020using ARIMA (note: 1, 2, 3, 4…. Represent number of year)

5.CONCLUSION

The present research has been carried out using the peculiarity of Erbil governorate in Kurdistan, in which data was collected from the Electricity Control Center (ECC) of the Kurdistan region of Iraq to discover which type of load forecasting method between the two methods described above, has the most positively respond to the electrical load data presented. As a result, we have compared the values of MAE and the RMSE, one can conclude that ARIMA method is much better to use for the electrical load forecasting than the first method of regression analysis method because of the following reasons: First, the ARIMA was capable to forecast the electrical load data in spite of the fall (decrease) in load demands in May and April. ARIMA did not forecast electrical load only, but forecasts the future electrical load demands with a much minimized error if the results are compared to the actual electrical load demands. Second, Because of its high accuracy, and great precision, ARIMA considered being more robust to forecast electrical load demand. This will be helpful in future research studies to perform load forecasting for a long term forecasting.

Third, ARIMA method produces results much faster than regression analysis because of the direct arithmetical calculations while regression analysis needs some mathematical computations before it can begin forecasting electrical load data.

REFERENCES

Amjady N. "Short-term Hourly load Forecasting Using Time Series Modeling with Peak Load Estimation Capability"',Institute of Electrical and Electronics Engineers Transactions on Power Systems, 2002 Aug, 16(4),798–805.

Bowerman BL, O'Connell RT, Koehler AB, "Forecasting, Time Series, and Regression: an Applied Approach. 4th edition Thomson Brooks/Cole, California; 2003..

Brockwell P.J. , Davis, R.A, "Introduction to Time Series and Forecasting",Springer Texts in Statistics. Second Edition. New York, 2002, Springer-Verlag.

Bruhns A, Deurveilher G, Roy J-S, "A non-linear Regression Model for Mid-term load Forecasting and Improvements in Seasonality" 15th Power

Systems Computation Conference (PSCC), Liege; 2005,p. 1–8.

Charles A., Greenhall, A. D., et al, "Total Variance, an Estimator of Long-term Frequency Stability ", IEEE Transactions on Ultrasonic, Ferroelectrics and Frequency Control, (1999), 46(5), 1183–1191.

Dara H. Amin Mohammed, Mohammed A. Husain, and Ismael K. Saeed, "Voltage Stability Analysis and its Enhancement Using Static Shunt and Series Capacitors of KRPS" ,Zanco Journal of Pure and Applied Sciences, Salahaddin University-Erbil, Vol. 25, No. 2, 2013.

Feinberg E.A. , Genethlion, D,"Load Forecasting Applied Mathematics for Restructured Electric Power Systems: Optimization, Control, and Computational Intelligence", 2005,pp. 269-285. Springer.

Ismael Kareem Saeed, "Artificial Neural Network Based on Optimal Operation of Economic Load Dispatch in Power System", Zanco Journal of Pure and Applied Sciences, Salahaddin University-Erbil, Vol. 31, No. 4, 2019.

Li Xiaojing ,CHEN Jiabin, YONG Shangguan. "A Method to Analyse and Eliminate Stochastic Noises of Fog Based on ARMA and Kalman Filtering Method", Intelligent Human Machine Systems and Cybernetics (IHMSC),2014.

N. Amral C. S. Ozveren and D. King, "Short Term Load Forecasting using Multiple Linear Regression", 42nd Universities Power Engineering International Conference (UPEC 2007), 1192-1198 ,2007.

Nur Adilah Abd Jalil, Maizah Hura Ahmad and Norizan Mohamed, "Electricity Load Demand Forecasting Using Exponential Smoothing Methods", World Applied Sciences Journal 22, 1540-1543 ,2013

Okolobah VA, Ismail Z," New Approach to Peak load Forecasting Based on EMD and ANFIS", Indian Journal of Science and Technology, 2013 ,Dec; 6(12):5600–6.

Samuel IA, Felly-Njoku CF, Adewale AA, Awelewa AA. "Medium term load Forecasting of Covenant University Using the Regression Analysis Methods", International Journal of Energy Technologies and Policy (IISTE), 2014, 4(4):10–6.

ZANCO Journal of Pure and Applied Sciences
The official scientific journal of Salahaddin University-Erbil
https://zancojournals.su.edu.krd/index.php/JPAS

ISSN (print):2218-0230**, ISSN (online):** 2412-3986**,DOI: http://dx.doi.org/10.21271/zjpas**

RESEARCH PAPER

Daily Streamflow Prediction for Khazir River Basin Using ARIMA and ANN Models

Abdulwahd A. Kassem[1*], Adil M. Raheem[2], Khalid M. Khidir[3]

[1]Water Resources Engineering Department, College of Engineering, Salahaddin University-Erbil, Kurdistan Region, Iraq
[2]Surveying Engineering Department, College of Engineering, Alkittab University, Iraq
[3]Water Resources Engineering Department, College of Engineering, University of Dohuk, Kurdistan Region, Iraq

A B S T R A C T

The present study used both Autoregressive Integrated Moving Average (ARIMA) and Artificial Neural Network (ANN) models for Khazir river basin to simulate the daily flow at Asmawa and Khanis gauge stations. Asmawa station lies on Khazir River while Khanis lies on Gomel River as a tributary of Khazir River. In the stochastic ARIMA model, the Autocorrelation function (ACF) and partial autocorrelation function (PACF) were used to determine how robust the ARIMA model is in predicting the streamflow. In this study, the Akaike Information Criterion (AIC) formula and Bayesian information criterion (BIC) were used to evaluate which model is more accurate. The results of this study showed that models of order ARIMA are (2,0,0)(2,1,0) and (2,0,1)(2,1,0) were found much better than the other models for generating and forecasting daily flow time series for aforementioned stations. Coefficients of determination (R^2) were found 0.77 and 0.85 for both Asmawa and Khanis stations, respectively. However, two types of ANN models were used for analyzing the daily flow records of the same two aforementioned stations, Multilayer Perceptron (MLP) and Radial Basis Function (RBF). ANN-MLP model was found to be more accurate than the ANN-RBF for generating and forecasting the daily flow time series as the coefficient of determination provided by ANN-MLP for both stations were 0.83 and 0.85, respectively. In addition, the coefficients of determination produced by the ANN-RBF for both stations were 0.66 and 0.55, respectively. Based on the values of (R^2) and (RMSE) obtained in the current work, one can conclude that the ANN-MLP model is the most accurate model among the others in terms of predicting the streamflow for Asmawa station, whereas the performance of both ARIMA and ANN-MLP models for the Khanis station is the same.

KEYWORDS: Forecasting, Streamflow, ARIMA, and ANN.
DOI: http://dx.doi.org/10.21271/ZJPAS.32.3.4
ZJPAS (2020), 32(3); 30-39 .

1. INTRODUCTION

Many activities associated with the planning and operation of the water resources system, the accuracy and reliability of streamflow forecasting are significant. For the planning and management of the water resources, it is necessary to have an accurate forecasting model for river streamflow.

* **Corresponding Author:**
Abdulwahd A. Kassem
E-mail: abdulwahid.qassem@su.edu.krd
Article History:
Received: 25/06/2019
Accepted: 15/12/2019
Published: 15/06 /2020

Therefore, in the last decades, many deterministic and stochastic models have been developed, including parametric, nonparametric, linear, and nonlinear models for hydrologic time series data prediction (Marques et al., 2006). In this study, two stochastic models were applied for the Khazir basin to estimate their efficiency and ability for generating the daily streamflow data.

In 1962, Thomas and Fiering introduced a statistical model, which found wide acceptance and can be used for a different interval of time series. Box and Jenkins (1970) developed ARIMA model, which can be used to generate time series

of different time intervals. The progress in developing and finding new ones is ongoing until now. Many researchers have applied the ARIMA model for forecasting streamflow in different basins. Mohammadi et al. (2005) estimated the spring inflow by utilizing ARIMA and ANN models for Amir Kabir reservoir in Iran (Mohammadi K., 2005). Solis et al. (2008) used ARIMA model for forecasting streamflow of a Mexican river (Solis et al., 2008). Singh et al. (2011) forecasted the monthly streamflow of Kangsabati River in India by applying ARIMA and X-12-ARIMA (Singh et al., 2011). Ruqaya (2011) used ARIMA model for forecasting the inflow into Dokan reservoir in Iraq (AlMasudi, 2011). Veiga et al. (2014) developed short-term flow forecasting ARIMA and ANN models in the Bow River in Canada (Veiga et al., 2014). Ghimire (2017) used ARIMA model to predict flow for two hydrological stations in Schuylkill River at Berne and Philadelphia in the USA (Ghimire, 2017). Sameera (2017) compared the performance of both ARIMA and ARIMAX models and found that the ARIMAX model is better for predicting the flow of Balinda River in Iraq (Sameera, 2017). Khalid et al. (2018) applied SARIMA and Matalas models for forecasting the maximum and minimum daily flow of Tigris and Khabur Rivers in Iraq (Khalid et al., 2018).

Artificial Neural Network (ANN) is an empirical model, which has been widely applied to water resources system problems and was found to be a powerful tool for the prediction of streamflow time series. ANN was used for modeling the complex hydrological processes by connecting inputs and outputs through mathematical functions without the need to know the relationship between the basin characteristics (Palit and Popovic, 2006). Werbos (1974) conduct the neural networks as a tool for time series forecasting, based on observational data. Several types of neural network structures were used for forecasting and predicting time series problems such as multilayer perceptron, radial basis function, recurrent, counter propagation, and probabilistic neural networks.

The ANN model to forecast streamflow time series has been increasingly applied over the past two decades. Elena and Armando (2000) applied ANN model in two ways, conceptual type rainfall-runoff models and black-box type runoff simulation for the Sieve River basin in Italy (Toth and Brath, 2000). Sohail et al. (2006) used a new approach of training artificial neural network model (ANN) with a real coded genetic algorithm (GA) named as (GAANN) model (Sohail et al., 2006). Chowdhary and Shrivastava (2009) used the feed-forward neural network (FFNN) and radial basis function (RBF) neural network to forecast the river flow in India (Chowdhary and Shrivastava, 2009). Pandhiani and Shabri (2015) developed new hybrid models by integrating the discrete wavelet transform with an artificial neural network (WANN) model and discrete wavelet transform with least square support vector machine (WLSSVM) model to measure monthly streamflow forecasting for two rivers in Pakistan (Pandhiani and Shabri, 2015). Chu et al. (2018) forecasted runoff for the Yellow River in China by using multiple linear regressions (MLR), radial basis functions neural network (RBFNN) and supports vector regression (SVR) models (Chu et al., 2018). Zhou et al. (2018) forecasted the streamflow of the Jinsha River by using three (ANN) architectures: a radial basis function network, an extreme learning machine, and the Elman network (Zhou et al., 2018).

The main objectives of this study are to investigate the Autoregressive Integrated Moving Average (ARIMA) and Artificial Neural Network (ANN) models to forecast the daily flow time series for Khazir and Gomel rivers at Asmawa and Khanis stations respectively.

2. MATERIALS AND METHODS

2.1 Area of study and data collection

The area of this study is Khazir basin, which located in Kurdistan region - Iraq. The basin area is about 3185 km^2, with a location of 43°14'00" - 43°44'25" E longitude and 36°22'00" - 36°52'33" N latitude. The maximum elevation is 2165 meter (AMSL) at the north part of the basin, and the minimum elevation is 216 (AMSL) in the south part of the basin close to the basin outlet (Jassas et al., 2015). The main river in the basin is Khazir River, which started at Asmawa location formed from two side streams, one coming from Chamanke region and the other coming from Bakerman region, as shown in figure (1). Khazir River confluence the Gomel River at the southern part of the basin and then flow into the Greater

Zab River, which can be considers as the important tributaries of Tigris River. It is worth mentioning that Khazir River supplies the Tigris River by about 10%, that motivated the authors to select this basin as the case study in this research.

Continuous recorded daily flow time series available from the period (2004 – 2015), which were obtained from two meteorological stations, first at Asmawa location (Asmawa station) which measured daily discharge flow of Khazir river and the second at Khanis location (Khanis station) that measured the daily discharge flow of Gomel River. The statistical description of the obtained data and the location of the aforementioned stations were found in tables (1) and (2).

The first ten years (2004-2013) of the available records data were considered to analyze and calibrate both models (ARIMA and ANN) while the remaining two years (2014-2015) were used to verify both of them.

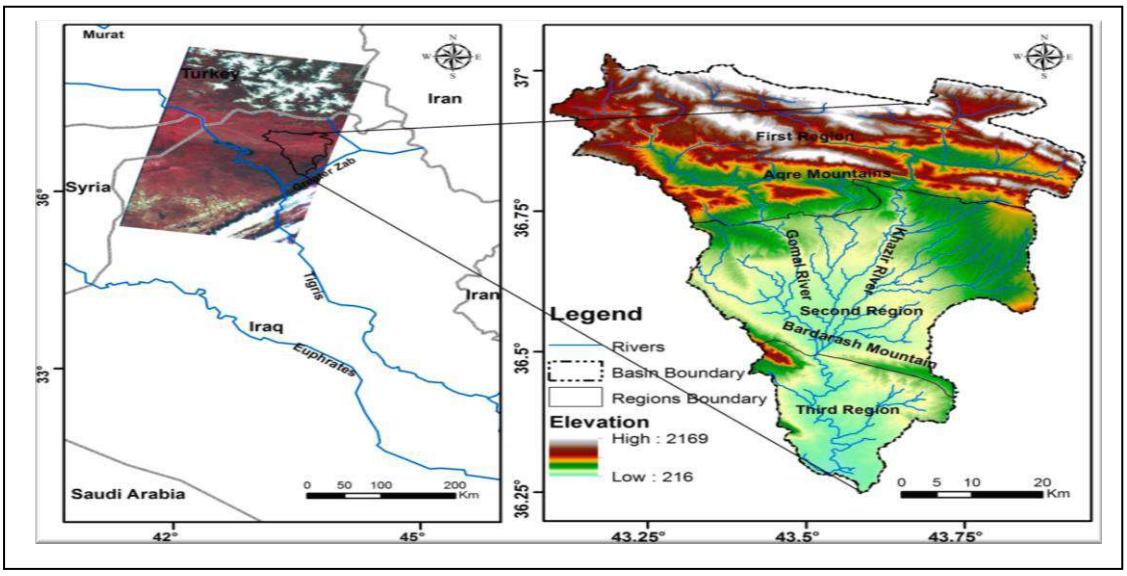

Figure 1: Khazir basin.

Table 1: The information about the Asmawa and Khanis stations location.

Station Name	River	UTM Coordinate X (m)	UTM Coordinate Y (m)	Elevation (m)	Basin area (km^2)
Asmawa	Khazir	380250	4075298	453	727
Khanis	Gomel	359037	4069587	441	537

Table 2: The statistical information of the Asmawa and Khanis stations.

Station Name	Mean (m^3/sec)	Standard deviation (m^3/sec)	Median (m^3/sec)	Skewness (m^3/sec)	Kurtosis (m^3/sec)
Asmawa	12.74	20.23	7.42	6.93	59.08
Khanis	6.10	9.19	2.67	4.32	32.12

2.2 Application of the Models:

In the current investigation, the ARIMA and ANN models were used to simulate the daily streamflow discharge for the abovementioned stations.

2.3 ARIMA model:

Autoregressive Integrated Moving Average (ARIMA) model is a generalization of an Autoregressive Moving Average (ARMA) model; both types are fitted to time series data to present generalized data and predict future points in the series. (p,d,q) refer to ARIMA parameters, which were none negative integers, (p) is referred to the autoregressive model (number of time lags), (d) is the degree of differencing (the number of times the data had past values subtracted) and (q) is the order of the moving average model. While, the seasonal ARIMA model, which is denoted by SARIMA (p, d, q) (P, D, Q), in which (S) represents the number of periods in each season, and the uppercase (P,D,Q) stands for the autoregressive, differencing, and moving average terms for the seasonal part of the ARIMA model. Seasonal Autoregressive Integrated Moving Average SARIMA $(p,d,q)(P,D,Q)_s$ can be expressed in a mathematical form expressed in equation (1) (Wang, 2006):

$$\varphi(B) * \Phi(B^S) * (W_t - \mu) = \theta(B) * \Theta(B^S) * \zeta_t \quad (1)$$

Where: φ is coefficient of autoregressive (AR), θ the coefficient of moving average (MA), Φ the coefficient of seasonal autoregressive, Θ is coefficient of the seasonal moving average, ζ is the random value at time t, B is backshift operator and S is season length.

Akaike (1974) suggested a mathematical criterion formula of building the parsimony model as Akaike Information Criterion (AIC) to select an optimal model which fits the time series data among several models. Further, the Bayesian Information Criterion (BIC) is another criterion that has been developed to select an optimal model among a finite set of models (Solis et al., 2008). Akaike mathematical formulation has the form given in equation (2).

$$AIC(p, q) = N.Ln(\sigma^2) + 2(M) \quad (2)$$

Where $M = p + q + P + Q$ (3)

While Bayesian formula described in equation (4).

$$BIC(p, q) = N.Ln(\sigma^2) + M * Ln(N) \quad (4)$$

Where σ is a standard deviation and N is the number of available data. The model which possesses least AIC and BIC values will be considered as an optimal model.

In this study, this concept was adopted to determine the more powerful model which can be used for forecasting of daily streamflow in Khazir basin.

2.4 ANN model:

Two types of the Artificial Neural Network (ANN) were applied in this research as both have been widely used in water resources engineering applications as indicated by researchers, namely; ANN-MLP and ANN-RBF. The details about both models are presented in the following:

2.4.1 Multilayer Perceptron Neural Networks (MLP)

A multilayer perceptron is a feedforward neural network architecture with uni-directional full connections between successive layers. As it is illustrated in figure (2), the structure of an MLP-ANN consists of three main layers: an input layer, a hidden layer and an output layer of neurons. These three layers were connected by strength called weight. There are two sets of weights: the input-hidden layer weights ($w_{j,i}$) and the hidden-output layer weights ($w_{k,j}$). These weights provide the network with high flexibility to freely adapt to the data.

The output results of the multilayer perceptron artificial neural networks can be obtained from equation (5):

$$\hat{y}_k = f_0\left[\sum_{j=1}^{m}\left(w_{k,j} * f_h\left(\sum_{i=1}^{n}(w_{j,i} + x_i) + b_j\right)\right) + b_k\right] \quad (5)$$

Where $\hat{y}_k$ is the output variable, x_i is the input variable, n is the number of input variables, m is

the number of neurons in the hidden layer, ($w_{j,i}$) is the weights of input-hidden and ($w_{k,j}$) is the weight

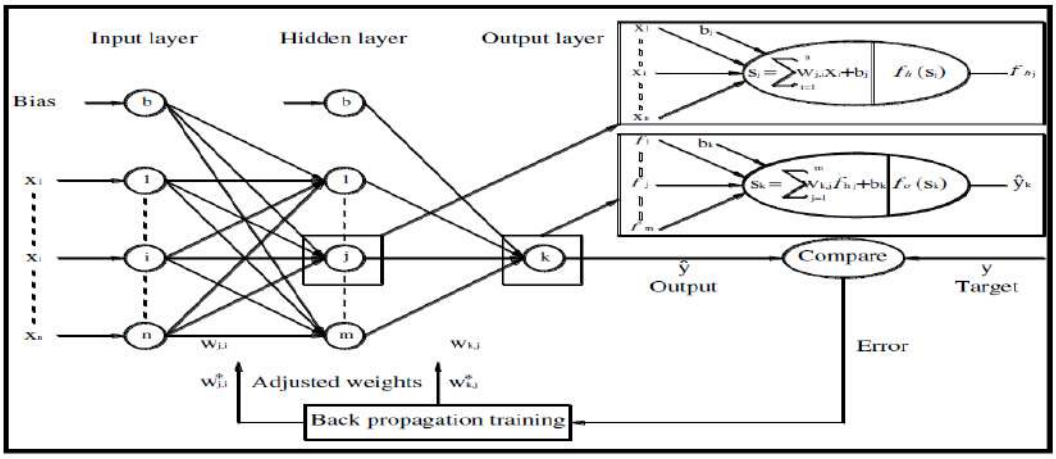

Figure 2: Structure of multilayer perceptron functions an artificial neural network.

of hidden-output layers, b_j is the bias of the hidden layer and b_k is the bias of the output layer, f_h is the activation function of the hidden layer and f_o is the activation function of the output layer (Dreyfus, 2005). A direct relationship could be obtained using an ANN model, which needs a database of the set of output variables related to the respective input variables. These variables are set in dimensionless terms to obtain a general relationship model (Al Suhaili et al., 2014).

2.4.2 Radial Basis Function Neural Networks (RBF)

The architecture of a radial basis function neural network was shown in figure (3). This type may require more neurons than standard feed-forward backpropagation networks, but often they can be designed with lesser time (Abraham, 2004). The time-series flow data have been entered the network as an input layer, and these data were transferred to the hidden layer by radial basis function. The response of the network was obtained in the output layer. The mathematical structure of Gaussian activation function is demonstrated in equation (6):

$$\hat{y}_k = \sum_{j=1}^{m}\left(w_{k,j} * f_j\left(exp\left(-\frac{\sum_{i=1}^{n}(x_i-\mu_{j,i})^2}{2\sigma_j^2}\right)\right)\right) + b_k \quad (6)$$

Where $\hat{y}_k$ is the output variable, x is the input variable, n is the number of neurons in the inputs layer, μ is the parameter which is the position of the center of the Gaussian while σ is its standard deviation. $w_{k,j}$ is the weight of the connection between the hidden neuron j and the output neuron k, b is the bias and m is the number of neurons in the hidden layer.

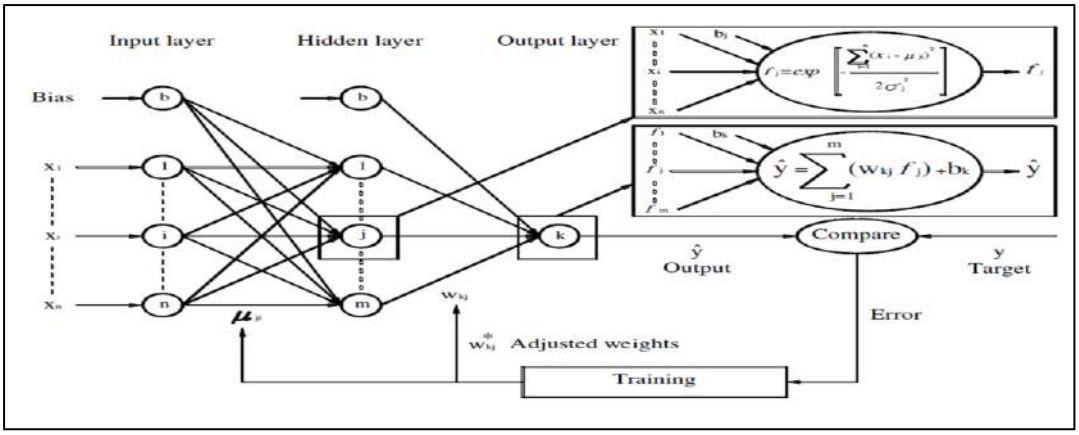

Figure 3: Structure of typical radial basis functions an artificial neural network.

In the present study, the ARIMA model was applied as a single site model by using statistical software (NCSS version 11.0), while the ANN models were applied by (Matlab version 2008) and the package of Statistical Package for the Social Sciences (SPSS version 23.0) for generating and forecasting daily flow time series. However, the linear regression method was used to predict the missing data, especially for the record data for the years 2005, 2006, and 2014 for Khanis station. The stationary test of the data was conducted because the model cannot be built for nonstationary data (Chow, 1988). The normality of the time series data should be checked using the Kolmogorov-Smirnov test by applying for the MINITAB program, which shown in figure (4) with a non-zero skewness coefficient (C_s) not equal to zero. Transformation of the data to a normal distribution was carried out by the Box-Cox method, and the coefficient (λ), was found to be (-0.4627, -0.225) for Asmawa and Khanis stations respectively. Figure (5) show the normality test of the time series data after transformation with the skewness coefficient equal to zero.

3. RESULTS AND DISCUSSION

The time series for both stations were found clear from a trend, jump and periodic. The parameters of the ARIMA model were found by applying the three stages of analysis as Identification, Parameters estimation, and Diagnostic. The order of the parameters of ARIMA models was found by applying the Autocorrelation Coefficient (ACF) and Partial Autocorrelation Coefficients (PACF).

A number of ARIMA models were tested, and the best ARIMA (p, d, q) (P, D, Q) parameters model as in equation (1) was found and shown in table (3), based on the least values of AIC and BIC for Asmawa and Khanis stations. Figure (6) shows the Autocorrelation Coefficient (ACF) and Partial Autocorrelation Coefficients (PACF) for the best models of the aforementioned stations.

Table 3: Parameters of the best models of ARIMA for Asmawa and Khanis stations.

Station Name	River	Best ARIMA model	AIC	BIC
Asmawa	Khazir	(2,0,0)(2,1,0)	2993.500	3011.872
Khanis	Gomel	(2,0,1)(2,1,0)	2962.986	2985.951

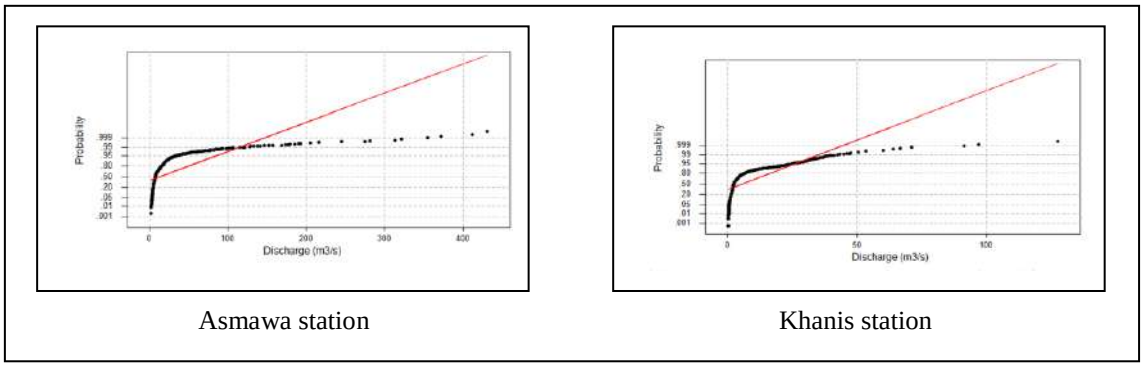

Asmawa station Khanis station

Figure 4: Testing of the normal distribution for Asmawa and Khanis stations by Kolmogorov-Smirnov test.

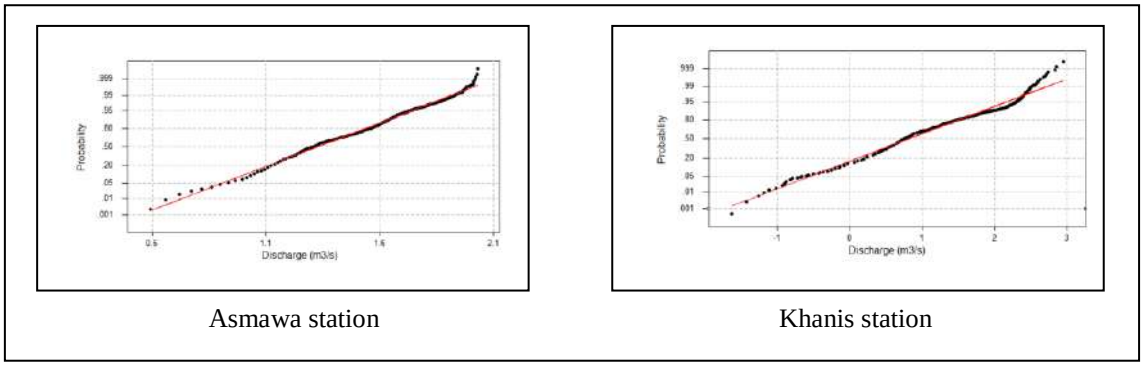

Asmawa station Khanis station

Figure 5: Testing after transforming the series to the normal distribution for Asmawa and Khanis stations.

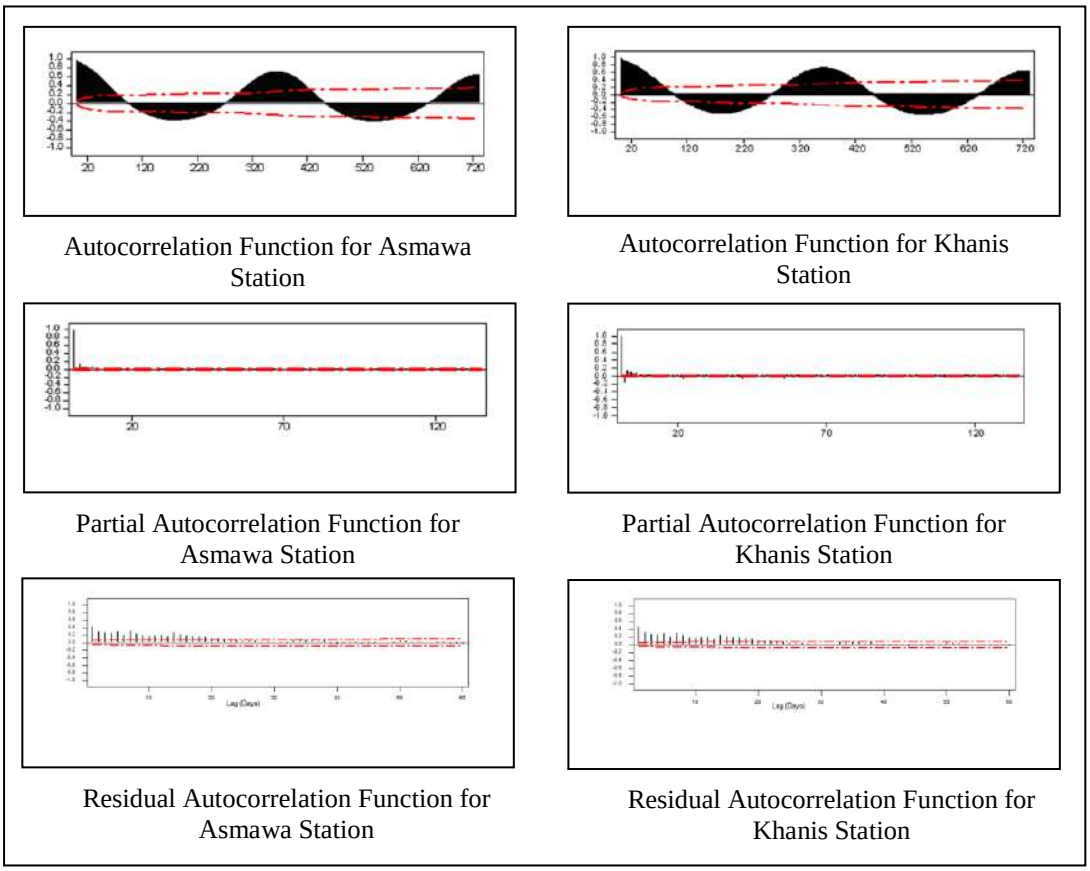

Figure 6: Autocorrelation Function, Partial Autocorrelation Function and Residual against lag for ARIMA model of Average Daily Flow Series for Asmawa and Khanis Stations.

The above ARIMA models were used in forecasting the time series of both stations, the results were demonstrated in figures (7) and (8) for the period (2014-2015) with determination coefficients (R^2) of 0.77 and 0.82 and values of the Root Mean Square Error are 3.48 and 2.19 for Asmawa and Khanis stations respectively.

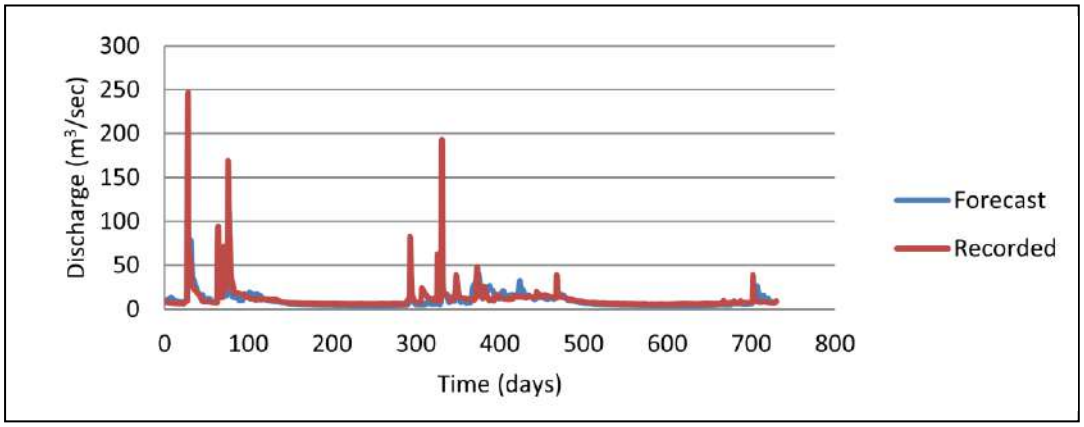

Figure 7: Hydrograph of the forecast and recorded data of daily flow series for Asmawa station using the ARIMA model.

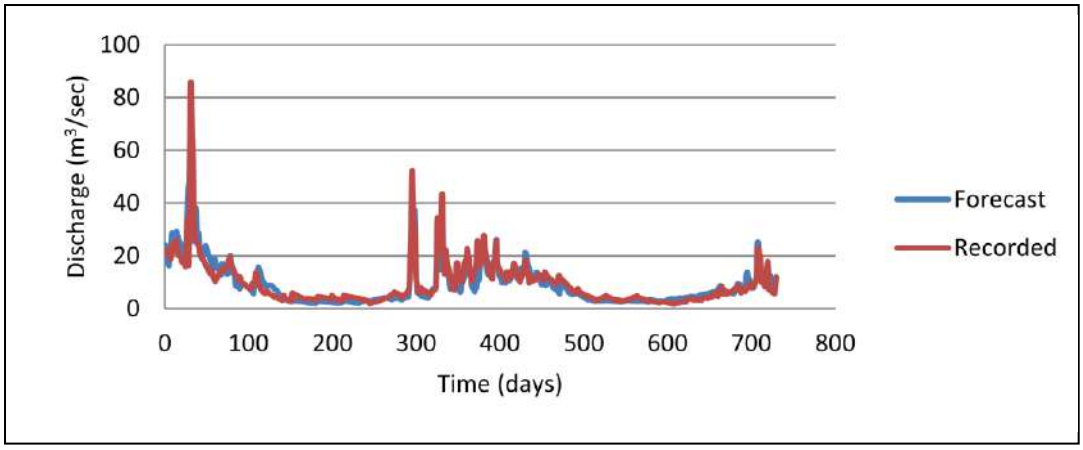

Figure 8: Hydrograph of the forecast and recorded data of daily flow series for Khanis station using the ARIMA model.

Regarding the ANN model, two types, namely, ANN-MLP and ANN-RBF models, were used in this study to forecast the daily streamflow for Khazir and Gomel rivers at Asmawa and Khanis stations, respectively. The best model was obtained by dividing the available recorded data into four seasonal groups (winter, spring, summer, and autumn), so each group was represented by its model. ANN models for Asmawa station were found to be MLP (15,6,1), MLP (15,8,1), MLP (15,6,1) and MLP (15,6,1) for aforementioned seasons, while for Khanis station the best models were found to be MLP (15,9,1), MLP (15,7,1) , MLP (15,4,1) and MLP (15,8,1) respectively.

In ANN model investigations the MLP model was found to be more efficient than the RBF model due to its high value of determination coefficients (R^2) which was (0.83, 0.85) and (0.66, 0.57) for Asmawa and Khanis stations respectively, as shown in the table (4).

The architecture structures of both types of ANN models are shown in table (5) and table (6), after several trails the best activation function for MLP type between the input and hidden layers was found to be hyperbolic tangent function, while between the hidden and output layers was found to be the identity function.

Table 4: Determination coefficient (R^2) and RMSE of ARIMA and ANN models for Asmawa and Khanis stations.

River	Station	R^2			RMSE		
		ARIMA	ANN (MLP)	ANN (RBF)	ARIMA	ANN (MLP)	ANN (RBF)
Khazir	Asmawa	0.77	0.83	0.66	9.867	6.542	9.609
Gomel	Khanis	0.851	0.85	0.55	3.449	4.055	6.778

Table 5: The architecture of (MLP) and (RBF) for Asmawa station.

Time series	ANN architecture type	Input layer nodes	Hidden layer nodes	Output layer Nodes
Average daily flow-season 1	MLP	15	6	1
	RBF		8	
Average daily flow-season 2	MLP	15	8	1
	RBF		10	
Average daily flow-season 3	MLP	15	6	1
	RBF		10	

Average daily flow-season 4	MLP RBF	15	6 10	1

Table 6: The architecture of (MLP) and (RBF) for Khanis station.

Time series	ANN architecture type	Input layer nodes	Hidden layer nodes	Output layer Nodes
Average daily flow-season 1	MLP RBF	15	9 10	1
Average daily flow-season 2	MLP RBF	15	7 10	1
Average daily flow-season 3	MLP RBF	15	4 10	1
Average daily flow-season 4	MLP RBF	15	8 10	1

The online type of training was selected, which updates the synaptic weights after every single training data record, while to avoid overtraining, maximum training epochs computed automatically, and to specify the optimization algorithm, the gradient descent method was selected.

The above ANN models were used in forecasting the time series for both Asmawa and Khanis stations, which shown in figures (9) and (10) respectively for the years (2014-2015).

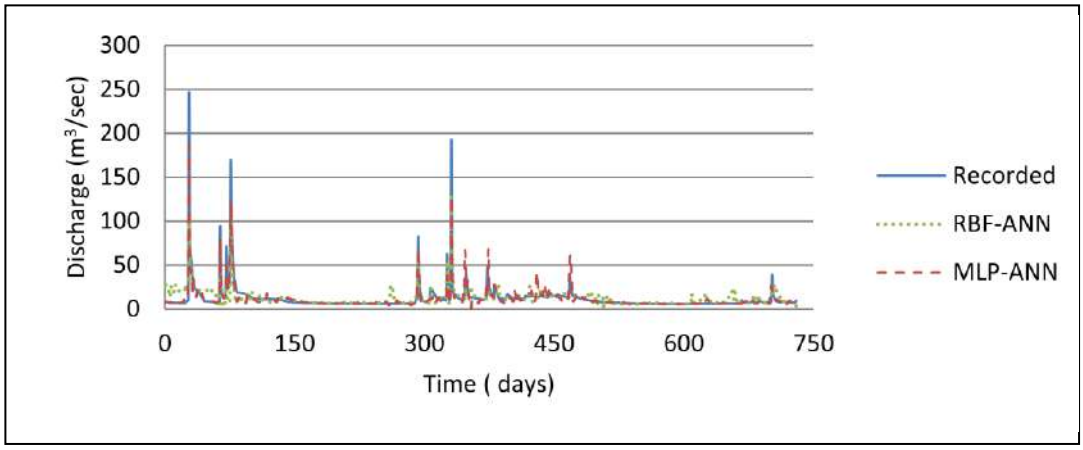

Figure 9: Hydrograph of the forecast and recorded data of daily flow series for Asmawa station using MLP-ANN and RBF-ANN Models.

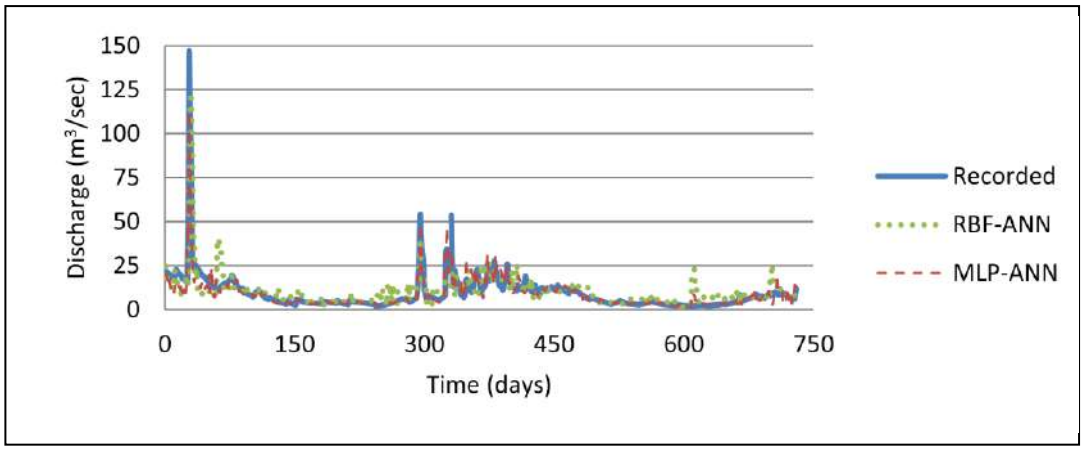

Figure 10: Hydrograph of the forecast and recorded data of daily flow series for Khanis station using MLP-ANN and RBF-ANN Models.

4. CONCLUSIONS

The ANN-MLP model was compared with the ARIMA model; the results revealed that the ANN model is more accurate than the ARIMA model in forecasting the daily time series for the years (2014-2015) for Asmawa station due to values of (R^2) and (RMSE), while the performance of both ARIMA and ANN-MLP models for the Khanis station is the same. Moreover, the ANN model can further be used to forecast for the stations' understudy, to get a more useful and accurate design of the future proposed hydraulic structures in the area of the basin.

REFERENCES

ABRAHAM, A. 2004. Artificial Neural Networks. *In:* THORN, P. H. S. A. R. (ed.) *Handbook of Measuring System Design*. John Wiley & Sons, Ltd.

AL SUHAILI, R. S. H., BAHRAINI, A. & BEHAYA, S. 2014. Artificial Neural Network Modeling for Dynamic Analysis of a Dam-Reservoir-Foundation System. *Journal of Engineering Research and Applications*, 4.

AL-MASUDI, R. K. 2011. Fitting ARIMA Models for Forecasting to inflow of Dokan Reservoir. *Journal of Babylon University*, 19.

CHOW, V. T. 1988. *Handbook of Applied Hydrology*, New York, McGraHill Book Co Inc.

CHOWDHARY, A. & SHRIVASTAVA, R. 2009. RIVER DISCHARGE PREDICTION USING ARTIFICAL NEURAL NETWORK. *Canadian Journal of Pure and Applied Sciences***,** 1275.

CHU, H., WEI, J., LI, J. & LI, T. 2018. Investigation of the relationship between runoff and atmospheric oscillations, sea surface temperature, and local-scale climate variables in the Yellow River headwaters region. *HYP Hydrological Processes*, 32**,** 1434-1448.

DREYFUS, G. 2005. *Neural networks methodology and applications*, Berlin; New York, Springer.

GHIMIRE, B. N. S. 2017. Application of ARIMA Model for River Discharges Analysis. *J. Nep. Pnys. Soc. Journal of Nepal Physical Society*, 4**,** 27.

JASSAS, H., KANOUA, W., MERKEL, B., JASSAS, H. & KANOUA, W. 2015. Actual evapotranspiration in the Al-Khazir Gomal Basin (Northern Iraq) using the surface energy balance algorithm for land (SEBAL) and water balance. *Geosciences (Switzerland)*, 5**,** 141-159.

KHALID, M. K., ADIL, M. R. & SYRAN, A. I. 2018. Stochastic Models for the Maximum and Minimum Daily Flows of Tigris and Khabur Rivers. *ZANCO Journal of Pure and Applied Sciences* 30(s1)**,** 50-61.

MARQUES, C. A. F., FERREIRA, J. A., ROCHA, A., CASTANHEIRA, J. M., MELO-GONCALVES, P., VAZ, N. & DIAS, J. M. 2006. Singular spectrum analysis and forecasting of hydrological time series. *JPCE Physics and Chemistry of the Earth*, 31**,** 1172-1179.

MOHAMMADI K., E. H. R. A. S. D. D. 2005. Comparison of Regression, ARIMA and ANN Models for Reservoir Inflow Forecasting using Snowmelt Equivalent (a Case study of Karaj). *J. Agric. Sci. Technol*, 7**,** 17-30.

PALIT, A. K. & POPOVIC, D. 2006. Computational Intelligence in Time Series Forecasting: Theory and Engineering Applications.

PANDHIANI, S. M. & SHABRI, A. B. 2015. Time series forecasting by using hybrid models for monthly streamflow data. *ams Applied Mathematical Sciences*, 9**,** 2809-2829.

SAMEERA, A. O. 2017. Comparison Between Forecasting ARIMA and ARIMAX Method. *ZANCO Journal of Pure and Applied Sciences* Vol. 28, no. 6**,** 158-65.

SINGH, M., SINGH, R. & SHINDE, V. 2011. Application of Software Packages for Monthly Stream Flow Forecasting of Kangsabati River in India. *IJCA International Journal of Computer Applications*, 20**,** 7-14.

SOHAIL, A., WATANABE, K. & TAKEUCHI, S. 2006. Streamflow forecasting by artificial neural network (ANN) model trained by real-coded genetic algorithm (GA)-A case study when the role of groundwater flow component in surface runoff is small,48**,** 233-262.

SOLIS, J. F., ESMERALDA, P. & JAVIER, L. 2008. Short-term streamflow forecasting: ARIMA vs neural networks. *AMERICAN CONFERENCE ON APPLIED MATHEMATICS (MATH '08), Harvard, Massachusetts, USA, March 24-26, 2008*.

TOTH, E. & BRATH, A. 2000 Flood Forecasting Using Artificial Neural Networks in Black-Box and Conceptual Rainfall-Runoff Modeling. *Diaksas*.

VEIGA, V., HASSAN, Q. & HE, J. 2014. Development of Flow Forecasting Models in the Bow River at Calgary, Alberta, Canada. *Water Water*, 7**,** 99-115.

WANG, W. 2006. Stochasticity, nonlinearity and forecasting of streamflow processes.

ZHOU, J., PENG, T., ZHANG, C. & SUN, N. 2018. Data Pre-Analysis and Ensemble of Various Artificial Neural Networks for Monthly Streamflow Forecasting. *Water Water*, 10**,** 628.

ZANCO Journal of Pure and Applied Sciences
The official scientific journal of Salahaddin University-Erbil
https://zancojournals.su.edu.krd/index.php/JPAS

ISSN (print):2218-0230**, ISSN (online):** 2412-3986**, DOI:**

RESEARCH PAPER

Brain Cancer Medical Diagnostic System Using Grey Scale Features and Support Vector Machine

Abdulqadir Ismail Abdullah[1]

[1]Department of Computer Science, College of Science, Knowledge University, Erbil, Kurdistan Region, Iraq

A B S T R A C T:

Automated segmentation and the classification of brain cancer based on Magnetic Resonance Imaging (MRI) is a significant medical development of the last twenty years. Based on computer systems, there are several techniques developed for diagnosis, but the automated diagnosis of cancer type is still a challenge. In this research, a cancer detection system has been proposed and tested to virtually segment the tumor and classify it based on the MRI images. To implement this, a k-mean clustering method is used in the segmentation step. In the features extraction step, each greyscale, symmetrical, and texture features are used. Then, a Principle Component Analysis (PCA) is used to minimize the number of features and Support Vector Machines (SVM) is applied to classify them. To implement the proposed methodology, a computer system was designed and simulated. A database of images was utilized to evaluate how the system is performing under testing. Finally, the test results of the experiments showed the effectiveness of the techniques used to segment and classify tumors.

KEY WORDS: Cancer detection ; Diagnostic System ; Morphological operators; Support vectors machine; Greyscale; K-mean clustering; Texture feature.
DOI: http://dx.doi.org/10.21271/ZJPAS.32.3.5
ZJPAS (2020) , 32(3);40-48 .

1. INTRODUCTION:

With the development of information technology, techniques have evolved to segment and classify different types of cancer and provide significant information for treatment and surgery. Techniques such as Screening mammography(Yaba S. P.,2015) and Magnetic Resonance Imaging (MRI) are widely used. Nonetheless, segmentation and detection of cancer are difficult due to the complex properties of a tumor such as size, shape, and location. These properties are always unique for each patient.

* **Corresponding Author:**
Abdulqadir Ismail Abdullah
E-mail:abdulqadir.abdullah@knowledge.edu.krd
abdulkhoshnaw@gmail.com

Article History:
Received: 02/10/2019
Accepted: 17/12/2019
Published: 15/06/2020

MRI is an important technique, used to study most cancer cases for many reasons.

One of these reasons is that the MRI images provide a lot of details about a tumor, and there are no significant medical side effects of this non-invasive imaging technique. The rapid development of technology led to the development of computer-aided imagery to support every medical department such as oncology, neurology, and gastroenterology (Abdulraqeb A. R. et al.,2018 and Peiet L. ,2015).

There are various kinds of techniques that can be used to extract exciting features in MRI images. A number of these techniques are simple; however, these simple techniques are not enough to give high recognition accuracy, but other methods such as grey-scale statistics give good results. A Grey-Level Co-occurrence Matrix (GLCM) is a feature extraction technique that is

widely used in medicine and other fields to process images digitally. The GLCM technique is based on statistical methods to extract textural features. Co-occurrence matrices give essential information about the textural features in an image (Bhima K. ,2016 and Akram M. U. , 2011) .

On the other hand, these diagnostic systems can improve their performance based on the system's experience; therefore, various types of machine learning methods are now applied, such as Support Vector Machine (SVM) and Artificial Neural Networks (ANN). SVM (Abdullah A. I., 2018) is a classifier that is used to solve this problem; it uses a small learning sample and provides an excellent generalization capability. SVM is already applied in several different digital image processing applications; therefore, SVM is described as being a widespread technique in the field of machine learning.

Different techniques, such as Principal Components Analysis (PCA), can be applied to reduce the data dimensionality without affecting the two quality of the image. (Arakeri M. P.,2015, Abd-Ellah M. K., 2016 and Zhang J., 2011).

In the last two decades, many of methodology have been developed to segment of the brain tumors. (Diaz I, Boulanger P, Greiner R, Hoehn B, Rowe L and Murtha A, 2013) have used four MRI modalities for segmenting Edema and Gross Tumor Volume by using automatic histogram multi-thresholding followed by morphological enhancement through geodesic dilation.(Ray N, Saha BN and Brown MR, 2007) proposed an algorithm for finding a bounding box which can enclose the abnormal brain region by symmetrical features in left and right brain structures. The algorithm works quite fast and in real time. It is also useful to provide initial estimate for other region growing algorithms(Selvakumar J, Lakshmi A and Arivoli T, 2012) implemented an algorithm using both K-Means and Fuzzy C-Means for segmenting brain tumor. Later the area and stage of tumor based on the measured area is also calculated by the algorithm. (George EB, Rosline GJ and Rajesh DG made use of optimization technique called the cuckoo search for detecting tumors and Markov Random Field for labeling the image pixels.

In (Yaba S.P. 2015), a system is proposed for detecting brain cancer using comprehensive wavelet features of mamorgram image and neural networks. In (Yaba S.P. 2015), they used an algorithm for classifying mammogram image into three categories (Norma, Benign, and Malignant). They used a test database consisting of 50 image (25 normal and 25 cancer patients).

The contribution of this research paper to the field of the brain cancer detection system is significant. The proposed methodology combines principal component analysis (PCA) and support vector machine (SVM) to obtain better results in cancer detection.

This paper is organized into the following sections: Section 2 describes the architecture of the proposed system. Section 3 introduces the results of the system experiments. The final section gives a conclusion to the presented work.

1.1 SYSTEM ARCHITECTURE

The architecture of the system consists of five steps which are applied to the MRI images to segment the tumor and classify it. Two pre-processing techniques are applied in the first step. These two techniques are histogram equalization and median filtering; both are used to enhance the quality of the images and reduce noise. Furthermore, K-mean algorithm is used for identifying different clusters to detect the tumor in the second step. To extract features of the image, each grey-level is applied to a co-occurrence matrix in the next step.

The ultimate step uses PCA to minimize the data size. Finally, in the last step, SVM is used to classify the kind of tumor in the image to either benign or malignant tumor.

Using the combination of these two methods is the focal point of the methodology used in this research paper. It combines the advantages of both methods to increase the accuracy of the system in detecting tumors.

Figure 1 shows the steps followed in the proposed system.

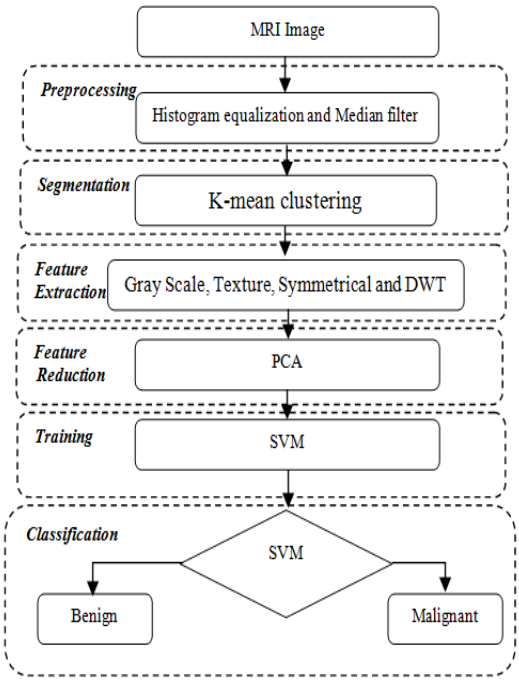

Figure (1): The steps of the System

Preprocessing

In this step, median filtering and then histogram equalization is applied to the input image to reduce the noise and improve the quality, to enhance the recognition rate.

- **Median filter**

The median filter provides excellent noise reduction capabilities. The outcome is significantly less blurry. The technique of this filter is to go over the pixels sequentially processing a small window of a fixed size. It compares the surrounding pixels to the central pixel within this window. During the scan, the surrounding pixel colors are changed with respect to the central pixel using the numerical median color value. This normalizes the image and reduces the number of sporadically colored pixels caused by noise in the imaging process. This type of filter does not affect the edge of the image, and it is possible to apply it many times (Maiti I. . 2012).

- **Histogram Equalization**

Histogram equalization is a technique, which is applied to adjust image contrast. The image intensity distribution is sometimes affected at the acquisition stage, causing poor contrast and image quality. For this reason, the image histogram is equalized to enhance the intensity of the image. The process of an equalized histogram generates an output greyscale from the input greyscale image. The equations applied to compute the histogram equalization are shown below (1):

$$k_0 = round\left(\frac{c_i(2^k - 1}{w.h}\right) \quad (1)$$

Whereby k_0 is the grey level histogram equalization value; ci is the cumulative distribution of ith greyscale in the original image; round defines a value rounding function to the nearest value; while w is the width and h is the height of the image (Natarajan P. .2011 and Gonzalez W. . 2008).

2. THEORETICAL BACKGRAOUND

2.1 SEGMENTATION

Generally segmentation techniques are used to divide an image into sections in order to detect boundries and objects for easier recognition. The segmentation step is one of the most crucial steps in the cancer detection system. This step aims to divide the image into several partitions for analysis. Initially, some basic image processing techniques are followed. Then the segmentation is done by the application of K-Means clustering" and morphological operators. K-Means clustering is applied to segment the tumor or abnormality. Morphological operators and basic image processing techniques are used to define the boundary between tumor and healthy cells further. Segmentation is implemented using the following steps:

2.1.1 Applying Threshold

The threshold technique is commonly used to determine contrast and highlight an area of the iamge. The idea of using threshold is to select a number that represents the level of greyness ina greyscale image and classify all the pixels according to that level. This uses a real number range between one and zero as a greyscale, whereby one is the darkest color and zero is the lightest. The complete image is defined as f(x, y) with x rows and y columns, a threshold grey value (T) is selected within the greyscale range, and pixels higher than this value is set to one; conversely, pixels less than this value are set to zero. (Natarajan P. , 2012) The mathematics of the operation defined below (2):

$$g(x,y) = \begin{cases} 1 & iff(X,Y)>T \\ 0 & iff(X,Y)<T \end{cases}$$

(2)

2.1.2 Watershed Transformation

Watershed transformation is another popular technique and one of the good tumor classification methods. The term watershed refers to a geological ridge between valleys, which alludes to explain this image transformation process. This technique segregates the image of different intensity portions then represents the greyscale image as a topographical map, with the lighter parts of the image being taller, and conversely, the darker elements being shorter. In a greyscale image, the intensity of the cell the tumor has contrasting intensity values, which directly relates to its topography. (Vincent L., 1999).

2.1.3 K-means Methodology

K-means algorithm is an efficient unsupervised methodology. It is applied in various computer applications. In this method; basically, the data is clustered into similar clusters based on the similar characteristics of the data points to discover patterns. In this algorithm, similar data points are grouped into clusters, so there are multiple clusters each representing data points with the same features. To explain this method, let's say that, X = {x1, x2,……,xN} is a group of data points and these must be split into a number of clusters C = {c1, c2,……,ck}. K-means method works by selecting several centroids and compute repetitively to optimize them. The center of all clusters is computed by using the equation below:

$$J = \sum_{n=1}^{N} \sum_{k=1}^{K} ||X_N - C_K||^2 \qquad (3)$$

Where $||\boldsymbol{X_N} - \boldsymbol{C_K}||^2$ Indicates the distance between data point XN, which relates to the centroid of cluster CK. J is the distance of n points from their related centroid (Shanker R., 2017)

2.1.4 Morphological Operators

Morphological operations are tools applied to extract image features to determine region shape, such as boundaries. Some of the basic morphological techniques are erosion and dilation. These are done in both opening and closing operations. First, in the opening operation erosion is executed, to remove any undesirable pixels and then dilation is applied to concentrate on the required region. Secondly, in the closing operation, a dilation process is followed by an erosion process, in order to fill the gaps. The opening of image A by image B is denoted by $A \circ B$ and is defined as a composition of erosion and dilation. The dual operation to opening is closing, which is defined as a dilation followed by an erosion. The closing of A by B is denoted by $\cdot B$. The followings are the mathematical representations of closing and opening:

$$A \circ B = (A \ominus B) \oplus B$$
$$A \bullet B = (A \oplus B) \ominus B \qquad (4)$$

After these techniques are applied, clusters with high-intensity value pixels will form. The result of this is shown in Figure 2.

Input Image **After Segmentation**

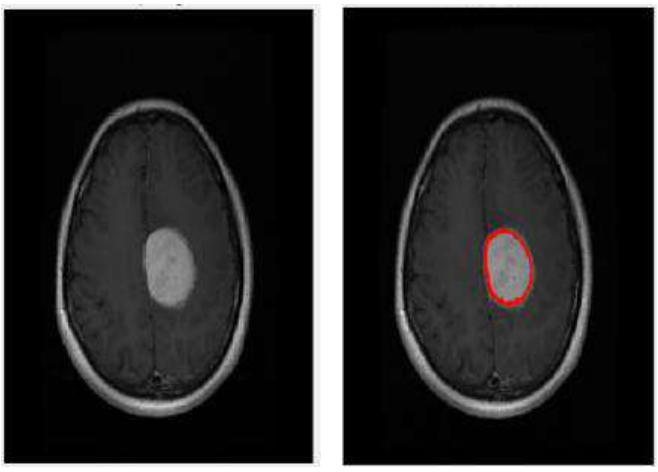

Figure (2): The segmentation stage output.

2.2 FEATURE EXTRACTION

Feature extraction represents one of the major parts of this system. It is used to obtain new sets of features from an image to apply in the following steps. The ultimate goal of this step is to define a wide range of data features as recognized features. Many methods can be used to extract these features. In this stage, greyscale, texture and symmetrical methods are used.

2.2.1 Grey Scale features

In this step, five types of features from a greyscale image are extracted including mean-variance, standard deviation, skew and kurtosis (Abo-Zahhad M. ,2015) These are explained as

follows:

Variance: defines the sum of the squared difference of pixels from the mean pixel value.

$$Variance = \frac{1}{N}\sum_{i=1}^{N}(|x_i - \mu|^2) \qquad (5)$$

Where x refers to the value of an individual grey pixel, $\boldsymbol{\mu}$ represents the grey pixel value, and N indicates the total number of pixels.

Standard Deviation: defines the square root of the variance.

$$SD = \sqrt{\text{Variance}} \qquad (6)$$

Skew: Is a measure of the symmetry in the grey level.

$$Skewness = Variance^{-3}\sum_{x=1}^{m}\sum_{y=1}^{n}(f(x,y) - \mu)^{-3} \qquad (7)$$

Kurtosis: is a measure of the flatness of the histogram grey level.

$$Kurtosis = (Variance^{-4})\sum_{x=1}^{m}\sum_{y=1}^{n}(f(x,y) - \mu)^{-4} \qquad (8)$$

2.2.2 Texture Features

The second type of feature extraction method is applied to the co-occurrence distribution matrix. Thirteen features are extracted for each input image which they are outlined in the equations below (Hossam M. M., 2010):

$$Entropy = -\sum_{s=1}^{n}\sum_{k=1}^{n} q(s,k)\, log(q(s,k)) \qquad (9)$$

$$Dissimalrity = \sum_{s=1}^{n}\sum_{k=1}^{n} q(s,k) * |(s-k)| \qquad (10)$$

$$Inverse = \sum_{s,k=1}^{n}\frac{q(s,k)}{(s-k)^2} \qquad (11)$$

$$Energy = \sum_{s=1}^{n}\sum_{k=1}^{n}(q(s,k))^2 \qquad (12)$$

$$Contrast = \sum_{s=1}^{n}\sum_{k=1}^{n} q(s,k) * (s-k)^2 \qquad (13)$$

$$IDM = \sum_{i=1}^{n}\sum_{j=1}^{n}\frac{q(s,k)}{1+(s-k)^2} \qquad (14)$$

Where IDM refers to Inverse Difference Moment.

2.2.3 Symmetrical feature

In images we can determine the symmetry between two regions. Symmetry is useful in detecting objects and boundries as it is known in human vision. Symmetry could be determined using:

$$Exterior\ Symmetry = \frac{\sum_{l=1}^{t}(s-s')^2}{t} \qquad (15)$$

Where s and s' represent the sample vectors

2.2.4 Feature Reduction

The ultimate goal of the feature reduction step is to reduce the computer processing time of mathematic operations by minimizing repeated operations on the dataset. For this reason, feature reduction is a significant step and Principal Component Analysis (PCA) aims to extract standard features, from high-dimensional feature space to a low-dimensional feature spac(Kaya I. E. ,2017).

3 TRAINING AND CLASSIFICATION

The goal of these stages is to classify the features extracted using an SVM method(ABDULLAH, A. I., 2019). SVM is a supervised learning binary classification method. It is applied to recognize a tumor and to classify its abnormality. The accuracy of the SVM classifier depends on its kernel functions. There are various kinds of functions that can be applied to calculate accuracy. The function types are linear, polynomial or radial functions (Abdul Qayyumet al., 2016 and Zhang Y., 2012).

A brief description of SVM is made here and more details can be found in [C. G. J. Schotten, W. W. L. Van Rooy, and L. L. F. Janssen,1995].

1- Linear case: We should now consider the case of two classes' problem with N training samples. Each samples are described by a Support Vector (SV) Xi composed by the different "band" with n dimensions. The label of a sample is Yi. For a two classes case we consider the label - 1 for the first class and +1 for the other. The SVM classifier consists in defining the function

$$f(x) = \text{sign}(\langle\omega, X\rangle + b) \qquad (16)$$

which finds the optimum separating hyperplane as presented in Figure below , where ω is normal to

the hyperplane, and $\frac{|b|}{\|w\|}\|$ is the perpendicular distance from hyperplane to the origin.

The sign of f(x) gives the label of the sample. The goal of the SVM is to maximize the margin between the optimal hyperplane and the support vector. So we search the min $\frac{\|w\|}{2}\|$.

To do this, it is easier to use the Lagrange multiplier. The problem comes to solve:

$$f(x) = \text{sign}\left(\sum_{i=1}^{N_S} y_i . \alpha_i \langle x . x_i \rangle + b\right) \quad (17)$$

where αi is the Lagrange multiplier.

2- Nonlinear case: If the case is nonlinear as the Figure 2 the first solution is to make soft margin that is particularly adapted to noised data. The second solution that is the particularity of SVM is to use a kernel. The kernel is a function that simulates the projection of the initial data in a feature space with higher dimension Φ: Kn → H. In this new space the data are considered as linearly separable. To apply this, the dot product ⟨xi , xj ⟩ is replaced by the function:

$$K(x, x_i) = \langle \emptyset(x), \emptyset(x_i) \rangle \quad (18)$$

Then the new function to classify the data are:

$$f(x) = \text{sign}\left(\sum_{i=1}^{N_S} y_i . \alpha_i . K(x, x_i) + b\right) \quad (19)$$

Three kernels are commonly used:

The mathematical equations of these functions are shown below:

Linear kernel:

$$f_k = f(s, s') \quad (20)$$

Where s and s' represent the sample vectors and $\mathbf{f_k}$ is the linear kernel.

Polynomial kernel:

$$k(s, s') = (1 + s . s')^2 \quad (21)$$

RBF kernel

$$k(s, s') = e^{(-||s - s'||)^2} \quad (22)$$

3.1 System Performance Parameters

In order to evaluate the performance of the system we employeed three parameters (Sensitivity, Specificity, and Accuracy). The sensitivity parameter measured the percent of correct positive cases identified. The specificity parameter measured the percent of correct negative cases identified. The accuracy parameter is the percent of the true positives and true negatives. The followings are the parameter equations (Sumithra M. G., 2016).

$$Sensitivity = \frac{TP}{(TP + FN)} * 100\% \quad (23)$$

$$Specificity = \frac{TN}{(TN + FP)} * 100\% \quad (24)$$

$$Accuracy = \frac{(TP + TN)}{(TP + TN + FP + FN)} * 100\% \quad (25)$$

The database (Cheng. J., et al., 2015 and Cheng. J., et al., 2016) used to evaluate the performance of the system consists of 114 cases; 60 cases are benign cancers, and the others are malignant cancers

4 EXPERIMENTS AND RESULTS

The system discussed in this paper was implemented using MATLAB® 2018a software. The database used to evaluate the performance of the system contained images of 114 cases; 60 cases are benign cancers, and the others are malignant cancers.

The images were used as input to the system and all the steps were impelented on the data starting from preprocessing to prepare the data, then feature extraction, then an importan step was the segmentation and detection of the tumors in the images. Finally the most important step of classification of the brain tumors to benign or malignant.

Some of the results which it was obtained from the step of segmentation are shown in the figure 3.

Input Image **Segmentation Result**

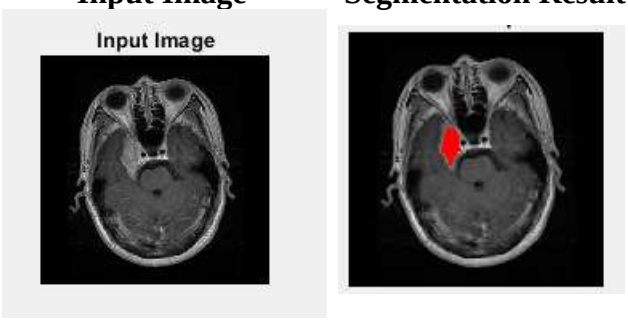

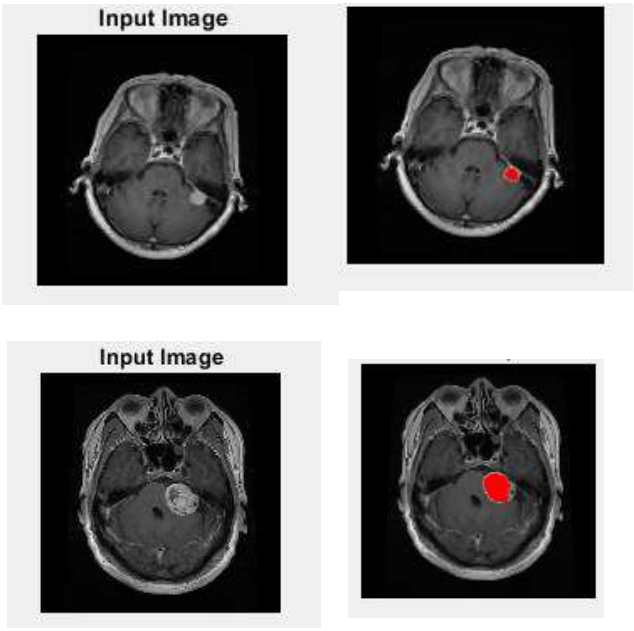

Figure (3): Segmentation Results.

After this step, the system carries out feature reduction and then classification. From this step all the results are recorded in terms of the accuracy, sensitivity, and specifity of the classification.

The performance of the system using parameters such as sensitivity, specificity, and accuracy are shown in table 1. As we see the system performed well considering all the parameters used to evaluate. The sensitivity parameter was at (%92.7), the specifity parameter was at (%99.7), and the accuracy was at (%99.6).

From this experimentation, it is noticed that a polynomial kernel function presents the best results from all the SVM methods used.

Table 1. The parameter results of the system.

Seq.	Parameters	Value
1	Sensitivity	%92.7190
2	Specificity	%99.7452
3	Accuracy	%99.6312

From the results obtained above we can analyze and say that the designed system can be a an accurate and very good tool for cancer detection that can be used by medical staff in determining the cancer cases. The system was able to carry out the process and all the required steps with a high percent of sensitivity, specifity, and accuracy. We can say that the system can be trusted in doing its function.

5 CONCLUSION

In this paper, a medical diagnostic system is designed to segment imaged brain tumors and then succefully classify it. The system contains five steps: pre-processing, segmentation, feature extraction, feature reduction, and classification. The segmentation step is executed by using each of k-mean clustering techniques and additionally uses morphological operator methods to successfully detect most tumors within a sample image database. The system database images came from 114 patients, 60 of these patients are diagnosed with benign tumors, while the other 54 are diagnosed with malignant tumors. Feature extraction methods such as "each of greyscale", texture and symmetry features, are applied. In the classification stage, the SVM method used four types of kernels for recognition; these are Linear, Quadratic, polynomial and RBF.

In conclusion, the system designed in this research work and its methodology proved to be succefull in carrying out a difficult process of identifying brain tumor. From the data used and its results we can say that the system was able to detect brain cancer with high level of sensitivity, specifity, and accuracy. Future work can include applying this system to detect breast cancer in women from mammogram images.

In order to determine the effectivitiy of the system by comparison, the system used in this research was compared to the system suggested by (Yaba S. P. 2015). In the system suggested by (Yaba S. P. 2015) they used the methodology of comprehensive wavelet features and neural netwroks. The test data used by (Yaba S. P. 2015) was 50 MRI images (25 for normal patients and 25 for cancer patients), while database images we used were from 114 patients, 60 of these patients are diagnosed with benign tumors, while the other 54 are diagnosed with malignant tumors. Higher level of the data will give the system and advantage in the results obtained.

In the performance evaluation of the system in (Yaba S. P. 2015), they used only two parameters (Specifity and Sensitivity) while in our study we used three parameters (Sensitivity, Specifity, and Accuracy). This is another advantage of the system of our study.

From the results obtained by the two systems we can determine that the system proposed by (Yaba S. P. 2015) was slightly more sensitive but it lacked in the specifity, and the data for accuracy were not available for comparison.

REFERENCES

Abdulraqeb A. R., Al-haidri W. A. and Sushkova L.T. 2018. "A novel segmentation algorithm for MRI brain tumor images," 2018 Ural Symposium on Biomedical Engineering, Radioelectronics and Information Technology (USBEREIT), Yekaterinburg, pp. 1-4.

Abd-Ellah M. K., Awad A. I., Khalaf A. A. M. and Hamed H. F. A. 2016. "Design and implementation of a computer-aided diagnosis system for brain tumor classification," 2016 28th International Conference on Microelectronics (ICM), Giza, pp. 73-76.

ABDULLAH, A. I., "Facial Expression Identification System Using Fisher Linear Discriminant Analysis and K- Nearest Neighbor Methods.". ZANCO Journal of Pure and Applied Sciences, Vol. 31, no. 2, Apr. 2019, pp. 9-13,

ABDULLAH, A. I., AL-DABAGH, M. Z. N. & ALHABIB, M.H.. 2018. Independent Component Analysis and Support Vector Neural Network for Face Recognition. International Journal of Applied Engineering Research, pp. 4802-4806.

Abo-Zahhad M., Gharieb R. R., Ahmed S. M., and Abd Ellah M. K. 2015."Huffman image compression incorporating DPCM and DWT," Journal of Signal and Information Processing, vol. 6, pp. 123–135.

Akram M. U. and Usman A.. 2011. "Computer aided system for brain tumor detection and segmentation," International Conference on Computer Networks and Information Technology, Abbottabad, pp. 299-302.

Arakeri M. P. and Reddy G. R. M. 2015. "Computer-aided diagnosis system for tissue characterization of brain tumor on magnetic resonance images," Signal, Image and Video Processing, vol. 9, no. 2, pp. 409–425.

Bhima K. and Jagan A. . 2016. "Analysis of MRI based brain tumor identification using segmentation technique," 2016 International Conference on Communication and Signal Processing (ICCSP), Melmaruvathur, pp. 2109-2113.

Gonzalez W. 2008. "Digital Image Processing", 2nd ed. Prentice Hall, Year of Publication.

Halder A., Pradhan A., Dutta S. K. and Bhattacharya P. 2016. "Tumor extraction from MRI images using dynamic genetic algorithm based image segmentation and morphological operation," 2016 International Conference on Communication and Signal Processing (ICCSP), Melmaruvathur, pp. 1845-1849.

Hossam M. M., Hassanien A. E. and Shoman M. . 2010. "3D brain tumor segmentation scheme using K-mean clustering and connected component labeling algorithms," 2010 10th International Conference on Intelligent Systems Design and Applications, Cairo, pp. 320-324.

Cheng. J. 2015. "Enhanced Performance of Brain Tumor Classification via Tumor Region Augmentation and Partition." PLOS one 10.8. Available online at [https://journals.plos.org/plosone/article?id=10.1371/journal.pone.0140381]

Cheng. J. . 2016. "Retrieval of Brain Tumors by Adaptive Spatial Pooling and Fisher Vector Representation." PLOS one 6.6.2016. Available online at [https://journals.plos.org/plosone/article?id=10.1371/journal.pone.0157112]

Kaya I. E., Pehlivanlı A. Ç., Sekizkardeş E. G., Turgay I. . 2017. PCA based clustering for brain tumor segmentation of T1w MRI images, Computer Methods and Programs in Biomedicine, vol. 140, Pages 19-28.

Maiti I. and Chakraborty M. 2012. "A new method for brain tumor segmentation based on watershed and edge detection algorithms in HSV colour model," 2012 NATIONAL CONFERENCE ON COMPUTING AND COMMUNICATION SYSTEMS, Durgapu, pp. 1-5.

Natarajan P., Krishnan N. , KenkreN. S. , Nancyand S. et.al., 2012. " Tumor detection using threshold operation in MRI brain images", 2012 IEEE International Conference on Computational Intelligence and Computing Research, pp. 18-20.

Natarajan P., Krishnan N. .2011. "MRI Brain Image Edge Detection with Windowing and Morphological Erosion", IEEE International Conference on Computational Intelligence and computing Research, pp. 94-97.

Pei L., Reza S. M. S. and Iftekharuddin K. M.. 2015. "Improved brain tumor growth prediction and segmentation in longitudinal brain MRI," 2015 IEEE International Conference on Bioinformatics and Biomedicine (BIBM), Washington, DC, pp. 421-424.

Qayyum A. and Basit A. 2012." Automatic breast segmentation and cancer detection via SVM in mammograms", 2016 International Conference on Emerging Technologies (ICET), 18-19.

Shanker R., Singh R. and Bhattacharya M. 2017, "Segmentation of tumor and edema based on K-mean clustering and hierarchical centroid shape descriptor," 2017 IEEE International Conference on Bioinformatics and Biomedicine (BIBM), Kansas City, MO, pp. 1105-1109.

Sumithra M. G. and Deepa B. .2016." Performance analysis of various segmentation techniques for detection ofbrain abnormality", 2016 IEEE Region 10 Conference (TENCON), pp. 2056-2061.

Tajudin A. S. et al. 2017. "An improved watershed segmentation technique for microbleeds detection in MRI images," 2017 International Conference on Electrical, Electronics and System Engineering (ICEESE), Kanazawa, pp. 11-16.

Tuo J. Z., Yuan Z., Liao W. and Chen H.. 2011. "Analysis of fMRI Data Using an Integrated Principal Component Analysis and Supervised Affinity Propagation Clustering Approach," in IEEE Transactions on Biomedical Engineering, vol. 58, no. 11, pp. 3184-3196.

Vincent L. and Soille P. .1999. "Watersheds in digital spaces: an efficient algorithm based on immersion simulations," IEEE Trans. Pattern and Machine Intelligence. vol. 13, no. 6, pp. 583-598.

Xuan X. and Liao Q. 2007. "Statistical Structure Analysis in MRI Brain Tumor Segmentation", Fourth International Conference on Image and Graphics, pp.421-426.

Yaba S. P. 2015. Breast Cancer detection System based onComprehensive Wavelet Features of Mammogram Images and Neural Network. ZANCO Journal of Pure and Applied Sciences Vol. 27 No. 6.

Zhang Y. and Wu L. .2012. An MR brain images classifier via principal component analysis and kernel supportvector machine, Progress In Electromagnetics Research, Vol. 130, pp. 369-388.

Diaz I, Boulanger P, Greiner R, Hoehn B, Rowe L and Murtha A, "An Automatic Brain Tumor Segmentation Tool, " 35th Annual Intl. Conf. IEEE Eng. In Med. And Bio. Soc. (EMBC), pp. 3339-3342, 2013

Ray N, Saha BN and Brown MR, "Locating Brain Tumors from MR Imagery Using Symmetry," IEEE Conf. on Signals, Systems and Computers, pp. 224-228, Nov. 2007

Selvakumar J, Lakshmi A and Arivoli T, "Brain tumor segmentation and its area calculation in brain MR images using K-Means clustering and Fuzzy C-Means Algorithm," IEEE Intl. Conf. on Advances in Engineering, Science and Management (ICAESM), pp. 186-190, March 2012

George EB, Rosline GJ and Rajesh DG, "Brain Tumor Segmentation using Cuckoo Search Optimization for Magnetic Resonance Images," Proceedings of the 8th IEEE GCC Conference and Exhibition, pp. 1-6, Feb. 2015

ZANCO Journal of Pure and Applied Sciences
The official scientific journal of Salahaddin University-Erbil
https://zancojournals.su.edu.krd/index.php/JPAS

ISSN (print):2218-0230**, ISSN (online):** 2412-3986**, DOI:**

RESEARCH PAPER

Semi Solid Casting of Aluminum Alloy Using a Cooling Slope Technic.

Hawzheen Abdulwahid Ibrahim[1], Mohammadtaher M. Saeed Mulapeer[2]
Department of Mechanical and Mechatronics Engineering, College of Engineering, Salahaddin University-Erbil, Kurdistan Region, Iraq.

A B S T R A C T:

In this study, semi-solid metal casting technology has been used to make castings from Al alloy 6063 scrap using different casting temperatures and a cooling slope of 30cm long. The purpose of the cooling slope was to cool down the liquid metal into a semi-solid state of about 60% liquid before entering the mold. The results showed that the semi-solid metal cast samples that pass over a cooling slope had higher strength and ductility as compared to the traditional direct casted samples due to the evolution of microstructure from dendritic into globular morphology. A ductility increase over 38%, 100%, and 34% is recorded for semi-solid casting over a cooling slope compared to direct casting for liquid metal at 750^{o}C, 800^{o}C, and 900^{o}C respectively. Strength is improved by about 8% for semi-solid casting at 750 and 900^{o}C compared to direct casting. For 800^{o}C no improvement is recorded in terms of the tensile strength for cooling slope over direct casting

KEY WORDS: Al alloy 6063, Semi-solid casting, Cooling slope, Mechanical properties, Structure morphology.
DOI: http://dx.doi.org/10.21271/ZJPAS.32.3.6
ZJPAS (2020) , 32(3);49-56 .

1. Introduction

Through the last fifty years, a lot of casting techniques have been used which allowed engineers to make the most complex shapes and parts from any metals or their alloys. Semi-solid metal (SSM) is a new metal casting technology that is different from the traditional metal casting technologies that use liquid metals as starting materials. Semi-solid metal (SSM) processing is the process of creating near net complex shape from feedstock's that are a non-dendritic in microstructure in a liquid state.

* **Corresponding Author:**
Hawzheen Abdulwahid Ibrahim
E-mail: hawzheen.mech@gmail.com
Article History:
Received: 11/12/2019
Accepted: 23/01/2020
Published: 15/06 /2020

Prof. Fleming and his Ph.D. student Spencer was the first who discovered the first idea of a semi-solid process in the 1970s during work on the hot tearing of lead-tin (Sn - 15% Pb) alloy. They discovered that the materials that continuously stirred had spherical microstructure compared to non-stirred material which has a dendritic microstructure (Spencer 1971). There are two main technologies for the casting of semi-solid metal (SSM) parts; rheocasting and thixocasting. Rheocasting includes melting the metal of dendritic structure and cooling it to its semi-solid state to change the microstructures from dendritic to a spherical and non-dendritic shape by using a suitable technic then injecting the resulting slurry into a die (Pola, Tocci et al. 2018) (Kirkwood 1994). In the thixocasting process, a solid feedstock of non-dendritic microstructure is used and re-

heating to its semisolid temperature then formed into a die. The most implemented routes that have been used for producing non-dendritic grains are: Mechanical Stirring, Magneto Hydrodynamic (MHD) stirring, Cooling slope process, Stress-Induced and Melt-Activated (SIMA) Process, Direct Partial Re-melting (DPRM), Swirled Enthalpy Equilibration Device Process (SEED), Ultrasonic Vibration method, Shearing-Cooling Roll method, Gas-Induced method (GISS) and Continuous Rheoconversion method (CRP) (Mohammed, Omar et al. 2013) (Hirt and Kopp 2008) (Kirkwood, Suéry et al. 2010). Semi-solid metal forming has many advantages over traditional direct casting such as increasing the die life because of decreasing the thermal shock, lower porosity and macrosegregation and it has lower processing cost with better mechanical properties such as higher ductility and higher strength (Nafisi and Ghomashchi 2005). Among all the techniques used to produce semisolid feedstock, the cooling slope is the easiest process and the most cost-effective. This is why it attracted research works worldwide. (Gencalp and Saklakoglu 2010) have presented that when vibrate the cooling slope channel during semisolid casting of A380 alloy, the nucleation of the particles increased and as a result, a large number of dendritic arms have been broken into spherical grains when comparing with without vibrating the cooling slope. (HAGA, R et al. 2010) have improved the cooling slope by using a cooling roll having a V-shaped groove that continuously rotated at 5 and 10 meter/minute providing a cool and new flow path for the molten liquid and they found that this method has prevented the adhesion of the liquid metal to the cooling slope especially when the cooling path was rotating at 10m/minute in which the adhesion of the solidifying metal to the cooling path is totally eliminated. (Prosenjit, Ray et al. 2012) studied the effect of the tilt angle of the cooling slope and grain refiners on grain morphology and tensile properties of the semi-solid Al A356 alloy. They presented that the grains had more spherical shapes when the cooling slope has been tilted at 60^o while it had some degenerated dendrites at 40^o. They also found that tensile properties were generally improved by using cooling slope compared to direct casting but the best improved occurred when small amounts of Al-5Ti-1B as grain refiner were added to the molten metal passing over a cooling slope tilted at 60^o. (Abdull-Rasoul and Hassan 2015) also investigated the effect of cooling slope tilt angle and grain refiner on mechanical properties of casted 6063 aluminum alloy. They presented that a cooling slope mounted at 30^o, 40^o and 50^o tilt angle of the semi-solid metal casting for both 0.46% Mg and 1.6% Mg had high strength and more spherical grains as compared to 60^o tilt angle.

The authors of this study found that there are a lot of scraps Al alloy 6063 in the Erbil market resulted from local factories that make door and window frames that are normally wasted into landfills and cause a lot of environmental problems. Recycling of this scrap will result in restoring huge amounts of valuable material and reducing environmental issues and on the other hand using new techniques of recycling such as semi-solid metal casting can result in the production of high-quality feedstock for a local and global market. So, the aim of this study is to produce high-quality feedstock from Al alloy 6063 scrap gathered from local factories using a cooling slope technique instead of direct casting.

2. Experimental equipment and procedures:

In this work scraps of Al alloy 6063 have been used as the starting material with the chemical composition shown in table (1). A single-phase electrical furnace of 3500W and graphite crucibles was used to melt down the scrap and superheat it to 750^oC, 800^oC, and 900^oC. A water-cooled cooling slope made from L shaped carbon steel section as shown in figure (1) has been used with an active length of 300mm and tilted at 45^o to produce the semi-solid slurry. The mold to which the semi-solid slurry flow into was made from carbon steel with a mold cavity of 35mm diameter and 240mm length as shown in figure (2). Each time 500g of the scrap was fed into the furnace and melted and superheated to the desired temperature then poured the molten metal into the cooling slope plate running down into the mold cavity and left in the air to be cooled to room temperature. Three different procedures were used for comparison, one is by direct pouring the molten metal into the mold cavity, the second was by pouring the molten metal onto the cooling slope cooled with circulating water, and the third was by

pouring the molten metal onto cooling slope with no water circulation. The resulted feedstocks from the three different procedures were then sectioned according to ASTM E3 and E112 for microscopical examination to study grain structure morphology and to investigate tensile properties according to ASTM B557.

Table (1) chemical composition of 6063 aluminum alloy

Al %	Mg %	Si %	Fe %	Cu %	Cr %	Zn %	Ti %	Mn %
98.88	0.434	0.387	0.16	0.0117	0.0038	0.0265	0.004	0.0443

Figure (1): The cooling slope device.

Figure (2): the Mold.

3 Results and Discussions

3.1 Grain Morphology:

From the microstructure evaluation, we found that the samples have dendritic structures when direct cast from 750°C, 800°C and 900°C as presented in figure (3). The average grain size according to the Linear intercepts method as per ASTM E112; was found to be 60µm at 750°C. Increasing the casting temperature to 800°C the average grain size increased to 75µm and 80µm at 900°C with a clearer dendritic grain texture. While the samples that passed over the cooling slope had shown a different in grain morphology and nearly spherical shape with a smaller size. Using a cooling slope produced a very fine globular non-dendritic and more homogenous grain. When the molten alloy poured onto the cooling slope it will solidify during flowing down along the cooling plate as the result the temperature of the slurry is decreased to below its liquidus temperature usually near 550^{o}C in which only about 60% is still liquid and solid nuclei start forming. The primary particles of the solidus will be nucleated and grow over the wall of the plate and detached because of the shear stress of the incoming molten alloy flow. They flowed to the mold and before becoming dendritic in structure they will be solidified as a result the average size of the grains will be reduced dramatically. Comparing the grain texture from the figure (3) and figure (4); it can be seen that grain texture has greatly evolved and totally turned into a globular morphology for different pouring temperatures. Figure (5) shows

that the average grain size lays between 29 and 40µm when using a cooling slope while it was between 60 and 80µm for direct casting from the same temperature. Using water cooling within the cooling slope does not have a great effect on the grain size and morphology.

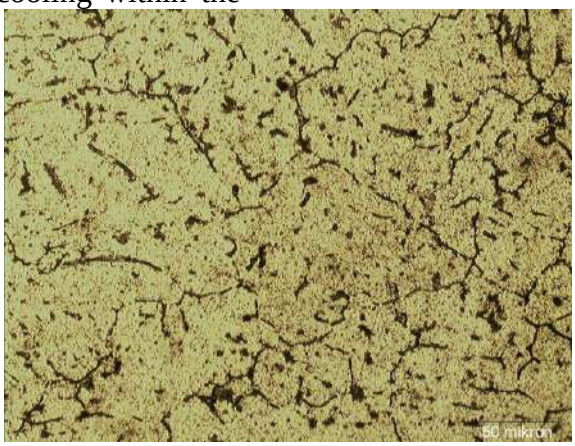

(a) Casting at 750°C.

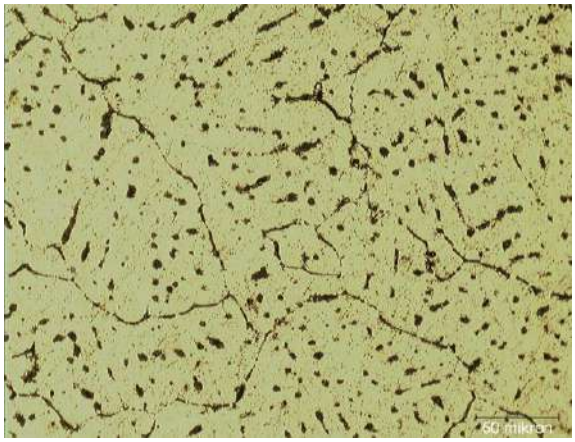

(b) Casting at 800°C.

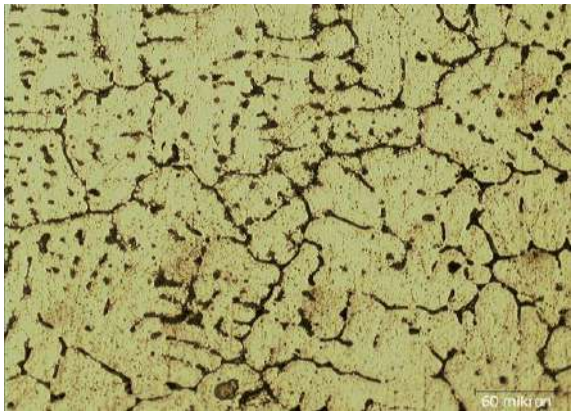

(c) Casting at 900°C.

Figure (3) Grain texture and morphology of direct casted samples at different casting temperature. X150

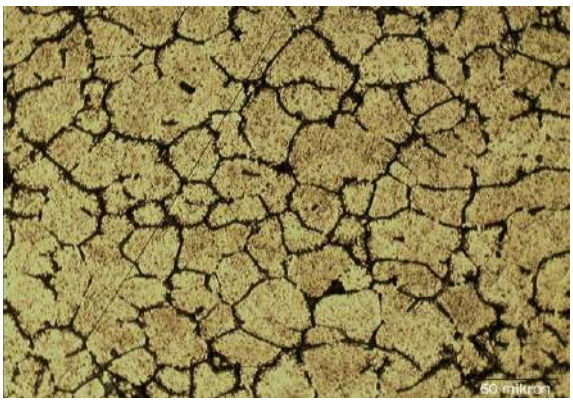

(a) Cooling slope rheocasting with water cooling at 750°C. X150.

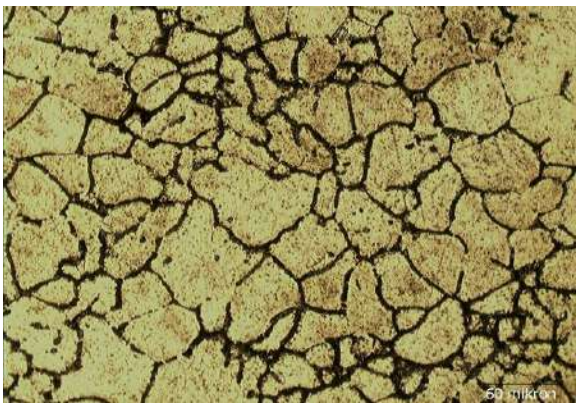

(d) Cooling slope rheocasting without water cooling at 800°C. X150.

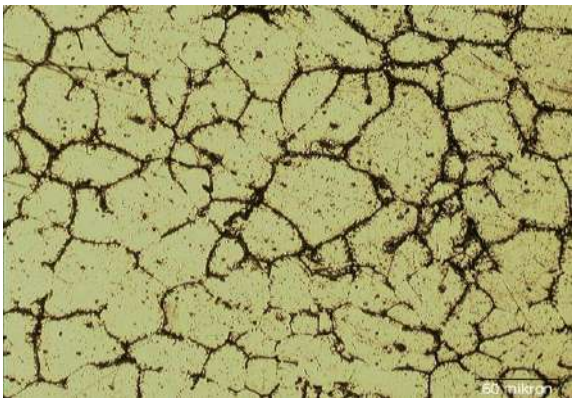

(b) Cooling slope rheocasting without water cooling at 750°C. X150.

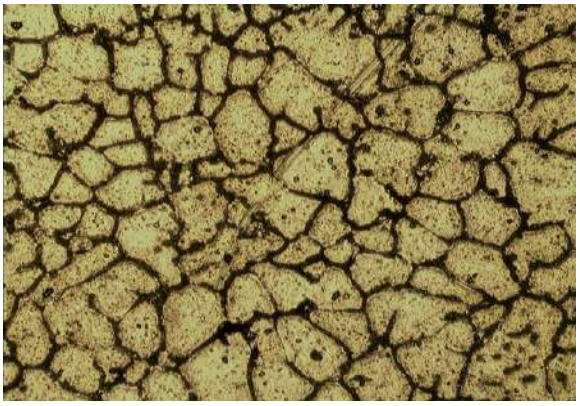

(e) Cooling slope rheocasting with water cooling at 900°C. X150.

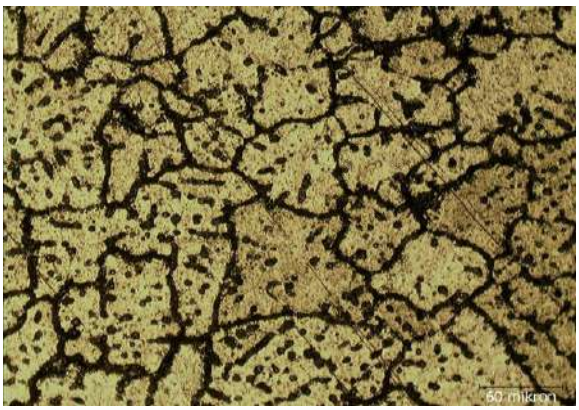

(c) Cooling slope rheocasting with water cooling at 800°C. X150.

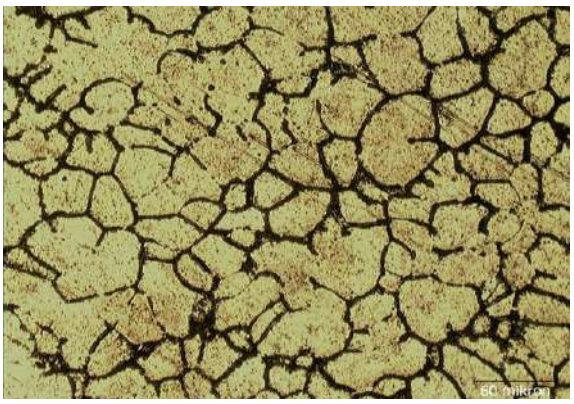

(f) Cooling slope rheocasting without water cooling at 900°C. X150.

Figure (4): semi-solid casted samples microstructure at different conditions.

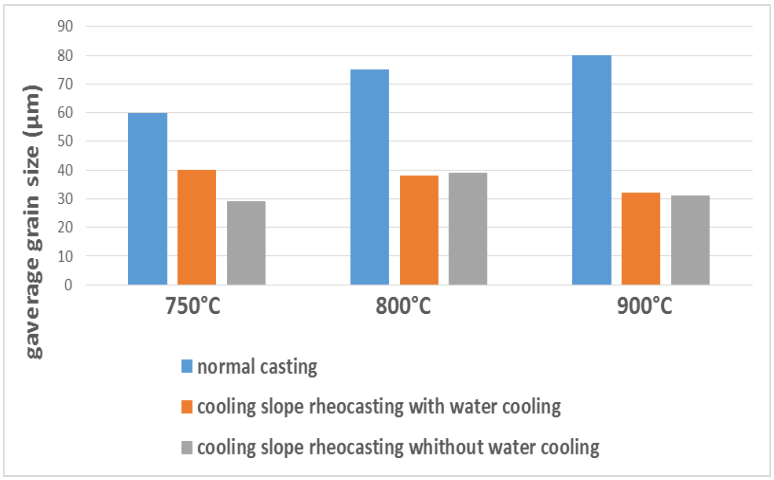

Figure (5) Relation between grain size and casting temperature at different casting conditions.

3.2 Tensile Test:

A universal computerized tensile testing machine of the capacity of 600KN was used to determine the strength and ductility of the casted samples. Tensile strength and ductility of metals and alloys are usually a reflection of its grain structure and morphology. Table (3) illustrate tensile properties of the direct casting of Al alloy 6063 at three different casting temperature of 750°C, 800°C and 900°C while table (4) shows the tensile properties of the same alloy when casting over a cooling slope from the same temperatures. The improvement in tensile properties is quite clear and is attributed to the changes have seen in the microstructure morphology. Figure (6) presents a tensile test result of three samples one obtained from direct casting from 800^{o}C and the other two samples obtained from the cooling slope casting at the same temperature with and without water circulation. There can be observed an improvement of both the ductility and the tensile strength and the highest improvement was recorded in terms of ductility of about 100% when using a cooling slope with no water circulation. It can be seen from figures (7) and (8) that there is a general improvement in mechanical properties by increasing the strength and ductility as a result of replacing the primary phase structures from dendritic to a globular and non-dendritic shape and by reducing grain size and morphology using a cooling slope semisolid casting process. Ductility increased to about 38%, 100% and 34% for semi-solid casting over a cooling slope compared to direct casting for liquid metal at 750^{o}C, 800^{o}C, and 900^{o}C respectively. Strength is improved by about 8% for semi-solid casting at 750^{o}C and 900^{o}C compared to direct casting. A very little or it can be said that there was no improvement in strength for samples cast from 800^{o}C for cooling slope over direct casting. It was also observed that using water circulation with the cooling slope has no or very little effect on grain texture, morphology and tensile properties of the casted samples.

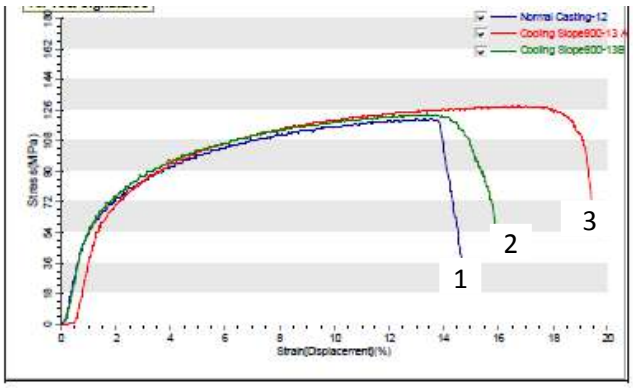

Figure (6): One stress-strain diagram of the tensile tests for three different samples**;**

1- Direct casting from 800^{o}C

2- Casting over cooling slope from 800^{o}C with water circulation.

3- Casting over cooling slope from 800^{o}C without water circulation.

Table (2) Tensile strength and ductility of direct cast samples.

Sample No	Casting temperature (°C)	Ultimate strength(MPa)	Ductility (%)
1	750°C	118	18%
2	800°C	126	15%
3	900°C	115	24%

Table (3) Tensile strength and ductility of semi-solid casted samples using a cooling slope.

Sample No	Casting temperature (°C)	condition	Ultimate strength(MPa)	Ductility (%)
4	750°C	Using cooling water circulation	127	22%
5	750°C	No cooling water circulation.	121	25%
6	800°C	Using cooling water circulation	127	22%
7	800°C	No cooling water circulation.	128	32%
8	900°C	Using cooling water circulation	124	32%
9	900°C	No cooling water circulation.	124	27%

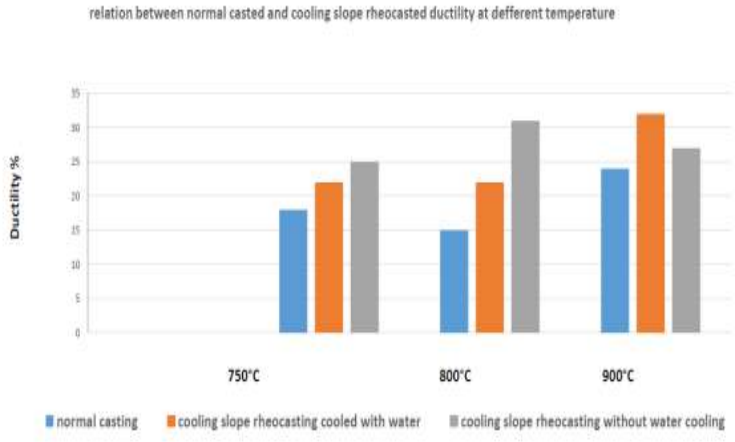

Figure (7): Relationship between casting condition and ductility at different temperatures

.

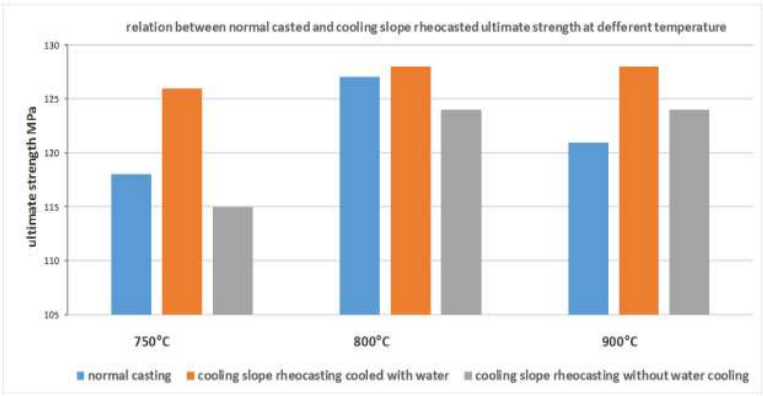

Figure (8): Relationship between casting condition and tensile strength at different temperatures.

3. Conclusions:

1- Semi-solid casting of Al alloy 6063 resulted in the evolution of the microstructure that was changed from dendritic to globular grain texture with a reduced grain size down to about 29um.

2-Ductility is greatly improved to an extent of 100% using a cooling slope when pouring temperature was 800^{o}C reduced to about 34% for higher temperatures.

3- Strength is improved to about 8% for semi-solid casting using a cooling slope and pouring temperature of 750^{o}C and 900^{o}C. Very little improvement was recorded in terms of tensile strength for pouring temperature of 800^{o}C.

4- Water circulation within the cooling slope has been found to have no or very little effect on grain morphology and tensile properties of the casted samples.

4. Acknowledgments:

These moments allow me to express my deepest thanks and gratitude to Mr. Mowafaq Izzadin; the expert and senior technicians at the mechanical engineering department who tirelessly helped us in the preparation and machining of the samples for the mechanical tests. Thank you so much, we appreciate it.

References:

Abdull-Rasoul, A. and Z. K. Hassan (2015). ". Mechanical Properties of Aluminum-Magnesium Alloy Prepared by Slope Plate Casting Process." Engineering and Technology Journal **33**(1 part (B)): 85-98.

Gencalp, S. and N. Saklakoglu (2010). "Semisolid Microstructure Evolution during Cooling Slope Casting under Vibration of A380 Aluminum Alloy." Materials and Manufacturing Processes **25**(9): 943-947.

HAGA, T., et al. (2010). "Effects of casting factors of cooling slope on semisolid condition." Transactions of Nonferrous Metal Sociaty of China **20**: 968−972.

Hirt, G. and R. Kopp (2008). Thixoforming: Semi-solid Metal Processing
Chichester, John Wiley and Sons.

Kirkwood, D. H. (1994). "Semisolid metal processing." International Materials Reviews **39**: 173-189.

Kirkwood, D. H., et al. (2010). Semi-solid Processing of Alloys. Berlin, Heidelberg, Materials Science-Springer.

Mohammed, M. N., et al. (2013). "Semisolid metal processing techniques for nondendritic feedstock production." ScientificWorldJournal **2013**: 752175.

Nafisi, S. and R. Ghomashchi (2005). "Semi-solid metal processing routes: An overview." Canadian Metallurgical Quarterl **44**(3): 289–304.

Pola, A., et al. (2018). "Microstructure and Properties of Semi-Solid Aluminum Alloys: A Literature Review." Metals **8**(3): 181.

Prosenjit, D., et al. (2012). "Mechanical properties and Tensile fracture mechanism of Rheocast A356 Al alloy using Cooling Slope." Advanced Materials Research **585**: 354-358.

Spencer, D. (1971). Rheology of liquid–solid metallic alloys, Ph. D Thesis,/MIT & Cambridge Univ.

ZANCO Journal of Pure and Applied Sciences
The official scientific journal of Salahaddin University-Erbil
https://zancojournals.su.edu.krd/index.php/JPAS

ISSN (print):2218-0230**, ISSN (online):** 2412-3986**, DOI: http://dx.doi.org/10.21271/zjpas**

RESEARCH PAPER

Some results on S-numerical range of operator matrices

Berivan Faris Azeez [1], Ahmed Muhammad [2]

[1] Department of Mathematics, Faculty of Science and Health, Koya University, Koya، KOY45, Kurdistan Region- F.R. Iraq.
[2] Department of Mathematics, College of Science, Salahaddin University-Erbil, Kurdistan Region, Iraq

A B S T R A C T:
A linear operator on a Hilbert space may be approximated with finite matrices by choosing an orthonormal basis of the Hilbert space. In this paper, we found an approximation of the S-numerical range of bounded and unbounded operator matrices by variation methods. Applications to Hain-L*ü*st operator and Stokes operator are given.

KEY WORDS: S-numerical range; projection method; Schr*ö*dinger operator; Hain-L*ü*st operator; Stokes operator.
DOI: http://dx.doi.org/10.21271/ZJPAS.32.3.7
ZJPAS (2020) , 32(3);57-63 .

1.INTRODUCTION :

Suppose $\mathcal{H}$ is a Hilbert space, with a scalar product $\langle\ ,\ \rangle$ and let S be a bounded self-adjoint operators. For an (possibly) unbounded linear operators $A: D(A) \subset \mathcal{H} \longrightarrow \mathcal{H}$ we define

$$W_S^{\pm}(A) = \left\{ \frac{\langle SAx, x\rangle}{\langle Sx, x\rangle} : x \in D(A), \langle Sx, x\rangle = \mp 1 \right\}, \qquad (1)$$

where $D(\,.\,)$ denotes the domain. The sets $W_S^{\pm}(A)$ generalize the well-known and widely used notation of classical numerical range

$$W(A) = \{\langle Ax, x\rangle : x \in D(A), ||x|| = 1\}. \qquad (2)$$

By the well-known Toeplitz-Hausdorff Theorem (Hausdorff, 1919, Toeplitz, 1918). The set *W(A)* is convex. This set has been examined extensively see(Gustafson and Rao, 1997, R.A.Horn and C.R.Johnson, 1991) and has a lot of applications in functional analysis, operator theory, numerical analysis, perturbation theory, quantum mechanics see(Bebiano and Providência, 1998, Gustafson and Rao, 1997, Halmos, 2012), and the references therein.

There are many results concerning the interplay between the algebraic and analytic properties of an operator and the geometrical properties of its numerical range. Likewise, the indefinite numerical range motivated the interest of researchers see(Bebiano et al., 2008, Gustafson and Rao, 1997, Halmos, 2012, Li et al., 1996, Muhammad, 2005b, Muhammad, 2005a, N.Bebiano et al., 2004)): which in particular have investigated these relations in the Krein space setting. Although sharing some analogous properties with the classical numerical range, has a quite different behavior. Unlike the numerical range $W_S(A)$
is not convex. On the other hand it is neither closed nor bounded (Li et al., 1996).

We also define the related sets

$$W_S^{+}(A) = \left\{ \frac{\langle SAx, x\rangle}{\langle Sx, x\rangle} : x \in D(A), \langle Sx, x\rangle = 1 \right\}, \qquad (3)$$

And

$$W_S^{-}(A) = \left\{ \frac{\langle SAx, x\rangle}{\langle Sx, x\rangle} : x \in D(A), \langle Sx, x\rangle = -1 \right\}, \qquad (4)$$

* **Corresponding Author:**
Berivan Faris Azeez
E-mail: berivan.faris@koyauniversity.org
Article History:
Received: 02/12/2019
Accepted: 20/01/2020
Published: 15/06 /2020

It is well-known that each of the sets $W_S^+(A)$ and $W_S^-(A)$ is convex set and, as $W_S(A) = W_S^+(A) \cup W_S^-(A)$, $W_S(A)$ decomposes into at most two convex subsets. In (Bebiano et al., 2004) boundary generating curves, corners and computer generation of the Krein space numerical range are investigated, in (Bebiano et al., 2005, Li et al., 1996, Nakazato et al., 2011)relations between the sets $W_S^+(A)$ and $W_S^-(A)$ are discussed.

The set $W_S(A)$ and $W_S^{\pm}(A)$ have been investigated. When S is a nonsingular indefinite Hermitian matrix, some authors use $W_S(A)$ or $W_S^+(A)$ as the definition for a numerical range of A associated with the indefinite inner product $\langle u,u\rangle_S = \langle Su,u\rangle$. We list some basic properties of the S-numerical range that follows easily from the definition.

In this note we see how to compute $W_S(A)$ by projection methods, which reduce the problem to that of computing the S-numerical range of a (finite) matrix and block matrix.

The paper is organized as follows. In Section 2.1 and 2.2 some theoretical results are investigated dealing with the approximation of S-numerical range for a (possibly) unbounded operators using projection method. In Section 3, applying these results to compute the S-numerical range of operators.

1.1 Definition and Results

We initiate this subsection with a basic concept in functional analysis, the core of an operator, which will be utilized further in the remainder. For this reason and also for the sake of completeness, we remind the reader of the following well-known definitions.

Definition 1.1. [(Kato, 2013), p.166] Let A be an operator on a Hilbert space H. The set $C \subseteq D(A)$ is a core of A if for any $x \in D(A)$ there exist $x_k \in C$ such that $||x_k - x|| \longrightarrow 0$ and $||Ax_k - Ax|| \longrightarrow 0$.

The following easy observation will be useful, and its proof is similar to the proof of [(Tahiri, 2015),Theorem 2.4.12].

Theorem 1.2. If A is positive (negative) definite and S is indefinite, then $W_S(A)$ is the union of two disjoint unbounded intervals.

Lemma 1.3. [(Kato, 2013), Problem 5.16] If A is a bounded and closed operator, then any linear submanifold C of $D(A)$ dense in $D(A)$ is a core of A.

Proof Suppose that $\alpha = (\alpha_1, \alpha_2, \dots, \alpha_k, \dots)^t \in \mathcal{D}(A)$, then there exist a sequence $\alpha = (\alpha_1, \alpha_2, \dots, \alpha_k, 0,0,0)^t \in C$ such that $\big||\alpha - \alpha_k|\big| = \sum_{j=k+1}^{\infty} |\alpha_j|^2 \longrightarrow 0$, and $\big||A\alpha - A\alpha_k|\big| \leq \big||A|\big|\big||\alpha - \alpha_k|\big| \longrightarrow 0$.Thus C is a core of A.

2 S-numerical range approximation using projection methods

We use the following conventions. For any closed subspace $V \subset H$ we denote by P_V the orthogonal projection in H onto V. For a linear operator A, if $V \subset D(A)$ then $A_V \coloneqq P_V A|_V$ denotes the compression of A to V.

Projection methods for accomplish a subset of the S-numerical range, under hypotheses. Only when one wishes to be sure of generating the whole of $W_S(A)$ it is important to make some extra assumptions. This section is devoted to the major results of the paper and it is divided into two subsections, since we distinguish between the estimation of the S-numerical range of a bounded and an unbounded operator.

2.1 Bounded linear operator

In the beginning of this section, we consider a bounded (linear) operator A on a complex Hilbert space H. We start with the following definitions.

Definition 2.1. Let A be an operator and $\{\emptyset_k : k \in \mathbb{N}\}$ be an orthonormal sequence of vectors H. For a fixed integer $k \geq 2$, the kxk matrices that arise from the operator A and the orthonormal vectors and $\{\emptyset_k : k \in \mathbb{N}\}$ are

$$\mathbb{A}_k = \begin{pmatrix} \langle A\phi_1,\phi_1\rangle\langle A\phi_1,\phi_2\rangle\cdots\langle A\phi_1,\phi_k\rangle \\ \langle A\phi_2,\phi_1\rangle\langle A\phi_2,\phi_2\rangle\cdots\langle A\phi_2,\phi_k\rangle \\ \vdots \quad\quad \vdots \quad \vdots \quad \vdots \\ \langle A\phi_k,\phi_1\rangle\langle A\phi_k,\phi_2\rangle\cdots\langle A\phi_k,\phi_k\rangle \end{pmatrix}, \quad (5)$$

that is the (p,r)-element of $\mathbb{A}_k$matrix is equal to $\langle A\phi_p,\phi_r\rangle$, for $p = 1,2,\dots,k$.

Definition 2.2. let S be a self-adjoint operator, and $\{\emptyset_k : k \in \mathbb{N}\}$ be an orthonormal sequence of vectors H. For a fixed integer $k \geq 2$, the kxk matrices that arise from the operators S and the orthonormal vectors $\{\emptyset_k : k \in \mathbb{N}\}$ are

$$\mathbb{S}_k = \begin{pmatrix} \langle S\phi_1,\phi_1\rangle\langle S\phi_1,\phi_2\rangle\cdots\langle S\phi_1,\phi_k\rangle \\ \langle S\phi_2,\phi_1\rangle\langle S\phi_2,\phi_2\rangle\cdots\langle S\phi_2,\phi_k\rangle \\ \vdots \quad\quad \vdots \quad \vdots \quad \vdots \\ \langle S\phi_k,\phi_1\rangle\langle S\phi_k,\phi_2\rangle\cdots\langle S\phi_k,\phi_k\rangle \end{pmatrix}, \quad (6)$$

that is the (p,r)-element of $\mathbb{S}_k$ matrix is equal to $\langle S\phi_p,\phi_r\rangle$, for $p = 1,2,\dots,k$.

Theorem 2.3. Let A be a bounded operator in a Hilbert space *H* and *S* be self-adjoint operator. Let $\{l_k : k \in \mathbb{N}\}$ be a nested family of subspaces in *H*, given by $k = span\{\phi_1, \phi_2, \dots, \phi_k\}$, where $\{\phi_k : k \in \mathbb{N}\}$ is an orthonormal basis of *H*. Consider kxk matrices $\mathbb{A}_k$ and $\mathbb{S}_k$in Eq. (5) and Eq. (6) respectively. Then $W_{\mathbb{S}_k}(\mathbb{A}_k) \subseteq W_s(A)$.

Proof Define an isometry $i: l_k \longrightarrow \mathbb{C}^k$ by $i(\alpha_1\phi_1, \alpha_2\phi_2, \dots, \alpha_k\phi_k) \coloneqq (\alpha_1, \alpha_2, \dots, \alpha_k)$.
Suppose that $\lambda \in W_{\mathbb{S}_k}(\mathbb{A}_k)$, then there exist an S-unit vector $\alpha \in \mathbb{C}^k$, with $\big|\big|x\big|\big| = 1$ such that $\lambda = \langle S\mathbb{A}_k\alpha, \alpha\rangle$. Choose $\xi \in l_k$, such that $i(\xi) = \alpha$ and $\big|\big|\xi\big|\big| = 1$. Then a direct computation shows that $\lambda = \langle A\xi, \xi\rangle_s$ where $= \sum_{j=1}^{k} \alpha_j\phi_j$. Thus $\lambda \in W_s(A)$.

Proposition 2.4. Let $\{l_k : k \in \mathbb{N}\}$ and $\mathbb{A}_k$be as in Theorem 2.3 and let S be a self-adjoint operator. Given $r = 1,2, \dots$ then $W_{\mathbb{S}_k}(\mathbb{A}_k) \subseteq W_{\mathbb{S}_k}(\mathbb{A}_{k+r})$.

Proof This is an instant consequence of the fact that $\mathbb{C}^k$ is a subspace of $\mathbb{C}^{k+1}$. In detail
If λ is in $W_{\mathbb{S}_k}(\mathbb{A}_k)$ then there exist an S-unit vector $\alpha \in \mathbb{C}^k, \big|\big|\alpha\big|\big| = 1$ such that $\lambda = \langle S\mathbb{A}_k\alpha, \alpha\rangle$ where α can be extended to vectors in $\mathbb{C}^{k+1}$ say $\hat{\alpha}$ whose (k+1)th-components are zero. It is easy to see that $\langle S\mathbb{A}_k\alpha, \alpha\rangle = \langle S\mathbb{A}_{k+1}\alpha, \alpha\rangle$ and the result follows.

The following theorem stands as both a generalization and application of Theorem 2.3 and estimates the S-numerical range of a bounded operator by infinite union of S-numerical ranges of its suitable projection.

Theorem 2.5. Let A be a bounded operator on a Hilbert space H. Let S be a self-adjoint operator.
Also $\{l_k : k \in \mathbb{N}\}$, $\mathbb{A}_k$ and $\mathbb{S}_k$ be as in Theorem 2.3, then $W_S(A) = \overline{\bigcup_{l=2}^{\infty} W_{\mathbb{S}_k}(\mathbb{A}_k)}$.
Before proving this theorem, we require the following lemma.

Lemma 2.6. Let A be a bounded operator on the Hilbert space H. Let $(l_k)_{k\in\mathbb{N}}$ be a family of spaces in H with $l_k = span\{\phi_1, \phi_2, \dots, \phi_k\}$, where $\langle\phi_i, \phi_j\rangle = \delta_{jk}$. Then $\langle A_k\underline{\tilde{\alpha}}_k, \underline{\tilde{\alpha}}_k\rangle_{S,\mathbb{C}^k} = \langle A_k\underline{\tilde{\alpha}}_k, \underline{\tilde{\alpha}}_k\rangle_{S,H}$, where A_k is the sub matrix of the finite matrix of inner products $\langle\phi_i, \phi_j\rangle, 1 \le i, j < \infty, \underline{\tilde{\alpha}}_k = \alpha_1\emptyset_1, \alpha_2\emptyset_2, \dots, \alpha_k\emptyset_k$ and $\alpha_k = (\alpha_1, \alpha_2, \dots, \alpha_k) \in \mathbb{C}^k$.

Proof Since we know $(A_k)_{pq} \coloneqq \langle A\phi_p, \phi_q\rangle_S$, for each p, q. Then a simple computation shows that $\langle A_k\underline{\tilde{\alpha}}_k, \underline{\tilde{\alpha}}_k\rangle_{S,\mathbb{C}^k} = \sum_{q=1}^{k}\sum_{q=1}^{k}(SA_k)_{pq}\,\alpha_p\bar{\alpha}_q = \langle A\underline{\tilde{\alpha}}_k, \underline{\tilde{\alpha}}_k\rangle_{S,H}$

Proof [Proof of Theorem 2.5.] Using the preceding theorem it suffices to show that $W_S(A) \subseteq \overline{\bigcup_{l=2}^{\infty} W_{\mathbb{S}_k}(\mathbb{A}_k)}$. Let $\lambda \in W_S(A)$, then there exist an S-unit vector α∈H, with $\big|\big|x\big|\big| = 1$ and $< \alpha, \alpha >_S = 1$ such that $\lambda = \frac{<A\alpha,\alpha>_S}{<\alpha,\alpha>_S}$. Suppose that $\mathcal{C} = \text{Span}\{\emptyset_1, \dots, \emptyset_k, \dots\}$ is a linear span of a countable of infinity orthonormal elements of H by Problem 1.1, $\mathcal{C}$ is a core of A. Thus by Definition 1.1 there exists a sequence $\alpha_1, \alpha_2, \dots$ with each $\alpha_k \in \mathbb{C}^k$given by $\alpha_k = P_k\alpha$, where $P_k : H \to l_k$ is orthogonal projection such that $||\alpha - \alpha_k|| \to 0$ and $||A\alpha - A\alpha_k|| \le ||A||||\alpha - \alpha_k|| \to 0$, Then for each $k \in \mathbb{N}$ choose $\lambda_k = \frac{<A_k\tilde{\alpha}_k,\tilde{\alpha}_k>_{\mathbb{S}_k}}{<\tilde{\alpha}_k,\tilde{\alpha}_k>_{\mathbb{S}_k}}$. Lemma 2.6 shows that there exists $\lambda_k \in W_{\mathbb{S}_k}(\mathbb{A}_k)$ such that $|\lambda_k - \lambda| \to 0$ as $k \to \infty$; hence $\overline{W_S(A)} \subseteq \overline{\bigcup_{k=1}^{\infty} W_{\mathbb{S}_k}(\mathbb{A}_k)}$.

2.2 Unbounded linear operators

We investigate the S-numerical range of an unbounded linear operator $A : \mathcal{D}(A) \subset H \to H$ where $\mathcal{D}(A)$ is the domain of A extending the result of the first subsection.

Theorem 2.7. Let $A : \mathcal{D}(A) \subset H \to H$ be an unbounded operator a on a Hilbert space H.
Let S be a self-adjoint operator. Let $\{l_k : k \in \mathbb{N}\}$ be a nested family space of $\mathcal{D}(A)$ given by $l_k = span\{\phi_1, \phi_2, \dots, \phi_k\}$, where $\{\emptyset_k : k \in \mathbb{N}\}$ is an orthonormal basis of H. Consider k x k matrices $\mathbb{A}_k$ and $\mathbb{S}_k$ in Eq. (5) and Eq. (6) respectively in Theorem 2.3. then $W_{\mathbb{S}_k}(\mathbb{A}_k) \subseteq W_S(A)$.

Proof Define an isometry $i : l_k \to \mathbb{C}^k$ by $i(\alpha_1\emptyset_1 + \alpha_2\emptyset_2 + \cdots + \alpha_k\emptyset_k) \coloneqq (\alpha_1, \alpha_2, \dots, \alpha_k)$. Suppose that $\lambda \in W_S(\mathbb{A}_k)$. Then there exist an S-unit vector α∈$\mathbb{C}^k$, with $< \alpha, \alpha >_S = 1$, and λ is an eigenvalue of $(\mathbb{A}_j)_{\alpha,\alpha} \coloneqq < \mathbb{A}_k\alpha, \alpha >_S$. Choose $x \in l_k$, such that i(x) = α and $\big|\big|x\big|\big| = 1$. In a good view of Lemma 2.6 this immediately gives $(\mathbb{A}_k)_{\alpha,\alpha} \coloneqq < \mathbb{A}_k\alpha, \alpha >_S$, so $\lambda \in W_S(A)$.

Proposition 2.8. In notation of Theorem 2.3, $(W_S(\mathbb{A}_k))_{k=1}^{\infty}$is a nested sequence, and let S be a self-adjoint operator. Then $W_{\mathbb{S}_k}(\mathbb{A}_k) \subseteq W_{\mathbb{S}_{k+1}}(\mathbb{A}_{k+1})$ for $k = 1,2, \dots$

Proof This is an instant sequence of the fact that $\mathbb{C}^k$ is the subspace of $\mathbb{C}^{k+1}$. In detail: if $\lambda\, is\, in\, W_{\mathbb{S}_k}(\mathbb{A}_k)$ then there exist an S-unit vector

$\alpha \in \mathbb{C}^k$, with $||\alpha|| = 1$ and $< \alpha, \alpha >_S = 1$ such that $\lambda =< \mathbb{A}_k\alpha, \alpha >_{\mathbb{S}_k}$ and α can be extended to vectors in $\mathbb{C}^{k+1}$, say $\hat{\alpha}$ whose $(k+1)-^{th}$ components are zero. It is easy to see that$< \mathbb{A}_k\alpha, \alpha >_{\mathbb{S}_k} =< \mathbb{A}_{k+1}\alpha, \alpha >_{\mathbb{S}_{k+1}}$and the result follows.

Theorem 2.9. Let A, S, $\mathbb{A}_k$, and $\mathbb{S}_k$ be as in Theorem 2.7. Let $\mathcal{C} = \text{Span}\{\emptyset_1, \ldots, \emptyset_k, \ldots\}$ be a core of A. Then $W_S(A) = \overline{\cup_{k=1}^{\infty} W_{\mathbb{S}_k}(\mathbb{A}_k)}$.

Proof In the view of Theorem 2.7 it therefore now suffices to show that $W_S(A) = \overline{\cup_{k=1}^{\infty} W_{\mathbb{S}_k}(\mathbb{A}_k)}$. Let $\lambda \in W_S(A)$, then there exist an S-unit vector $x \in \mathcal{D}(A)$, with $||x|| = 1$ and $< x, x >_S = 1$ such that $\lambda = \frac{<Ax,x>_S}{<x,x>_S}$, since $\mathcal{C}$ is a core of A. There exist a sequence $(x_k)_{k=1}^{\infty}$with each $x_k \in \text{Span}\{\emptyset_1, \ldots, \emptyset_{S,k}\}$ for some $S_k > 0$, such that $||x - x_k|| \to 0$ and $||Ax - Ax_k|| \to 0$. Fix $k > 0$. Let i: $\text{Span}\{\emptyset_1, \ldots, \emptyset_{S,k}\} \to \mathbb{C}^{S,k}$, be the standard isometrics as in the proof of theorem (2.3). Define $\hat{\alpha}_k \in \mathbb{C}^{S,k}$ by $\hat{\alpha}_k = i(x_k)$). Consider the $S_k \times S_k$ matrix $\mathbb{A}_{S,k}$ that is the *(p,r)*-element of $\mathbb{A}_{S,k}$ matrix is equal to $< A\emptyset_p, \emptyset_r >_S$ for $p, r = 1,2, \ldots, k$. Then for each $k \in \mathbb{N}$ choose $\lambda_k =< A\hat{\alpha}_k, \hat{\alpha}_k >_{\mathbb{S}_k}$, Lemma 2.6 shows that there exists $\lambda \in W_{\mathbb{S}_k}(\mathbb{A}_k)$ such that $||\lambda - \lambda_k|| \to 0$ as $k \to \infty$. In view of Proposition 2.8 this immediately gives that $\lambda \in \overline{\cup_{k=1}^{\infty} W_{\mathbb{S}_k}(\mathbb{A}_k)}$.

3 Numerical experiments on a matrix differential operator

In this section, we will give and illustrate some examples based on a Schr*ö*dinger operator, multiplication operator, Hain-L*ü*st operator and Stocks operator to illustrate the theorems proved. The computations were performed in MATLAB.

3.1 S-numerical range of Schr*ö*dinger operator

3.2 Example 1

In the Hilbert space $H := L_2(0,1)$, we introduce the Schr*ö*dinger operator

$$L = -\frac{d^2}{dx^2} + q, \qquad (7)$$

(with bounded potential q) and the domain of L is given by

$$D(L) = \{u \in H^2(0,1): u(0) = 0 = u(1)\},$$

and let $S: L_2(0,1) \to L_2(0,1)$be a multiplication operator defined on $L_2(0,1)$ by

$$(Sf)(t) = u(t)f(t), \qquad (8)$$

where $u(t) = 20t - 25$, $u \in C[0,1]$ and $f \in L_2(0,1)$, and the domain of S is given by $D(S) = L_2(0,1)$.

Remark 1.

(i) For this example, because L is self-adjoint and bounded below with purely discrete spectrum, the eigenvalues of L are given by

$$\lambda_n := \inf \quad \sup g(y)$$
$$L \subset D(L) y_1 \in L$$
$$dim\, L = n\; y \neq 0$$

where g is the Rayleigh functional (Murnaghan, 1932),

$$g(y) := \frac{\langle Ly, y\rangle}{\langle y, y\rangle}, \qquad y \in D(L), y \neq 0.$$

Hence

$$\pi^2 = \lambda_1 := \inf\, g(y)$$
$$y \in D(L) \qquad (9)$$
$$y \neq 0$$

(ii) We assume that the real valued potential q = 0, because if the operator L included a potential, for instance, then its eigenfunctions would not generally be explicitly computable. So still $-\frac{d^2}{dx^2}$ is equipped with Dirichlet boundary conditions on [0, 1]. It is obvious the eigenvalues and normalized eigenfunctions for the operator L in $L^2[0,1]$ are

$$\lambda_j = j^2\pi^2, \phi_j(x) = \sqrt{2}\sin(j\pi x), \; j = 1,2,3, \ldots \qquad (10)$$

under the setting $p(x) = 0$.

(iii) In Eq.(7), and Eq.(8) it is not difficult to see that, the linear span $C = \{\phi_1, \phi_2, \ldots\}$ is a core of each L, and S respectively. Where $\{\phi_k : k \in \mathbb{N}\}$ is an orthonormal basis in $L^2(0,1)$.

(iv) We may use the eigenfunctions in Eq. (10) as basis elements for discretization of the type discussed in section 2.1, forming the matrix elements $\langle L\phi_k, \phi_j\rangle$, and $\langle S\phi_k, \phi_j\rangle$ and consider the infinite operator matrices $\mathcal{Q} = \langle L\phi_k, \phi_j\rangle$ and $\hat{\mathcal{Q}} = \langle S\phi_k, \phi_j\rangle$. The matrices $\mathbb{A}_k$ and $\mathbb{S}_k$defined in Eq .(5) and Eq. (6) are obtained by leading sub-matrices of the $\mathcal{Q}$, and $\hat{\mathcal{Q}}$with the appropriate dimensions. Observe that

$$\langle L\phi_k, \phi_j\rangle_S = diag\{\pi^2, 4\pi^2, 9\pi^2, \ldots\}, \qquad (11)$$

and

$$\langle S\phi_k, \phi_j\rangle = 20\int_0^1 2t\sin(j\pi x)\sin(j\pi x) - 25\delta_{jk}dx \quad (12)$$

(v) If we assume that the Hermitian matrix $\mathbb{S}_k \in M_n$ is non-singular, then it is not a restriction to consider the matrix $J = I_k \oplus -I_k$ instead of $\mathbb{S}_k$, in the definition of the S-numerical range, where I_k is the identity matrix.

Figure (1) shows attempts to compute $W_{\mathbb{S}_k}(\mathbb{A}_k)$ for various k and also some attempts to estimate these sets by qualitative means, using existing theorems from the literature as well as the theorems proved above.

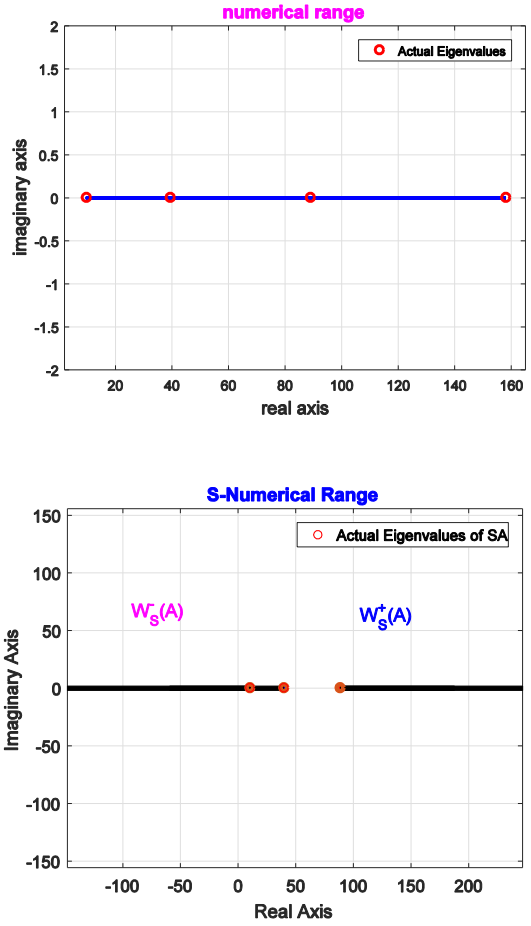

Figure 1: On the left-hand side, estimation of numerical range of $\mathbb{A}_k$ for k = 4. While for the right-hand side, estimation of $W_{\mathbb{S}_k}(\mathbb{A}_k)$ for $k = 4$.

Remark 2.

(i) It is clear the numerical range of $\mathbb{A}_k$ for $k = 4$ is equal to $[\pi^2, 16\pi^2]$.

(ii) In this example $\mathbb{A}_k$ is positive definite and $\mathbb{S}_k$ is indefinite, then according to Theorem 1.2 $W_{\mathbb{S}_k}(\mathbb{A}_k)$ is the union of two disjoint unbounded intervals $(-\infty, 9\pi^2] \cup [16\pi^2, \infty)$.

3.4 S-numerical range of Hain-Lüst operator

Example 2

In the Hilbert space $L_2^2(0,1) := L^2(0,1) \oplus L^2(0,1)$ we introduce the matrix differential operator

$$A := \begin{pmatrix} \tilde{L} & w(x) \\ \tilde{w}(x) & u(x) \end{pmatrix}, \quad (13)$$

on the domain

$$\mathcal{D}(A) := \left\{ \begin{pmatrix} y_1 \\ y_2 \end{pmatrix} : y_1 \in (H_0^1(0,1) \cup H^2(0,1)) \right\}$$
$$and\ y_2 \in L_2(0,1)$$

Where $\tilde{L}$ is the Sturm-Liouville operator $\tilde{L}y = -y''$ with a Dirichlet boundary conditions, $w = \tilde{w} = 1$ and $u = 20x - 25$. This operator was introduced by Hain and L¨ust in application to problems of magneto hydrodynamics (Hain and Lust, 1958), and the problems of this type were studied in (Langer et al., 1990), (Adamjan and Langer, 1995) and (Langer and Tretter, 1998).

Now from the matrix elements $< \tilde{L}\phi_k, \phi_j >$, $< \tilde{w}\phi_k, \phi_j >$, $< w\phi_k, \phi_j >$, $< u\phi_k, \phi_j >$. With respect orthonormal basis in Eq. (10) and consider the infinite block operator matrix.

$$\mathcal{Q} = \begin{pmatrix} < \tilde{L}\phi_k, \phi_j >, & < \tilde{w}\phi_k, \phi_j > \\ < w\phi_k, \phi_j > & < u\phi_k, \phi_j > \end{pmatrix}.$$

The matrix $\mathbb{A}$ defined in (5) is obtained by taking leading sub-matrix of the block of $\mathcal{Q}$, with appropriate dimensions. Observe that

$< \tilde{L}\phi_k, \phi_j >= \text{diag}\{\pi^2, 4\pi^2, 9\pi^2, \dots\}$,

$< \tilde{w}\phi_k, \phi_j >= diag\{1, 1, 1, \dots\}$,

$< w\phi_k, \phi_j >= diag\{1, 1, 1, \dots\}$,

$< u\phi_k, \phi_j >= 20\int_0^1 xsin(k\pi x)\sin(j\pi x)\,dx - 25\delta_{k,j}$.

Let S be a self-adjoint operator

$$S = \begin{pmatrix} \tilde{L} & \tilde{w} \\ w & u \end{pmatrix}.$$

Where $\tilde{L}$ is the Sturm-Liouville operator $\tilde{L}y = -y''$ with Dirichlet boundary conditions, $w = \tilde{w} = 1$ and $z = e^x$.

The domain of S in this case is given by

$$\mathcal{D}(A) := \left\{ \begin{pmatrix} y_1 \\ y_2 \end{pmatrix} : y_1 \in (H_0^1(0,1) \cup H^2(0,1)) \right\}.$$
$$and\ y_2 \in L_2(0,1)$$

By the same argument the matrix elements $< \tilde{L}\phi_k, \phi_j >$, $< \tilde{w}\phi_k, \phi_j >$, $< w\phi_k, \phi_j >$,

$< u\phi_k, \phi_j >$. With respect orthonormal basis in Eq. (10) and consider the infinite block operator matrix.

$$\tilde{\mathcal{Q}} = \begin{pmatrix} < \tilde{L}\phi_k, \phi_j >, & < \tilde{w}\phi_k, \phi_j > \\ < w\phi_k, \phi_j > & < z\phi_k, \phi_j > \end{pmatrix}.$$

The matrix $\mathbb{S}_k$ defined in Eq. (6) are obtained by taking sub-matrix of the block of $\mathcal{Q}$, with appropriate dimensions. Observe that

$\widetilde{< \tilde{L}\phi_k, \phi_j >} = \text{diag}\{\pi^2, 4\pi^2, 9\pi^2, \dots\}$,

$< \tilde{w}\phi_k, \phi_j >= diag\{1, 1, 1, \dots\}$,

$< w\phi_k, \phi_j \geq diag\{1, 1, 1, \dots\}$,

$< u\phi_k, \phi_j >= \int_0^1 \sin(k\pi x) \sin(j\pi x)\, dx$.

Remark 3. It is not difficult to see that the subspace $\mathcal{C}_1 := \mathcal{C}_{\tilde{L}} \oplus \mathcal{C}_u \subset \mathcal{D}(A) = \left(D(\tilde{L}) \cap D(\tilde{w})\right) \oplus \left(D(w) \cap D(u)\right)$, is a core of A also.

$\mathcal{C}_1 := \mathcal{C}_{\tilde{L}} \oplus \mathcal{C}_z \subset \mathcal{D}(S) = \left(D(\tilde{L}) \cap D(\tilde{w})\right) \oplus \left(D(w) \cap D(z)\right)$, is a core of S.

Figure (2) shows attempts to compute $W_{\mathbb{S}_k}(\mathbb{A}_k)$ for various k and also some attempts to estimate these sets by qualitative means, using existing theorems from the literature as well as the theorems proved above.

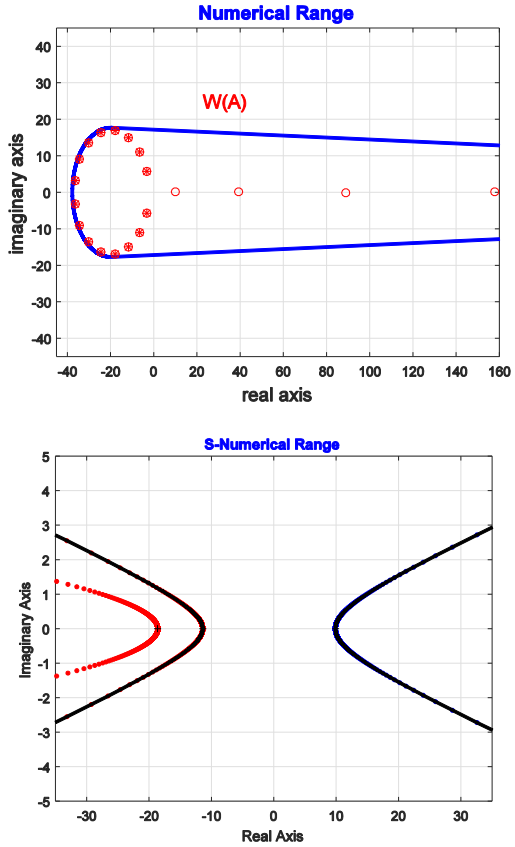

Figure 2: On the left-hand side, estimation of numerical range of $\mathbb{A}_k$ for k = 18. While for the right-hand side, estimation of $W_{\mathbb{S}_k}(\mathbb{A}_k)$ for $k = 4$.

Remark 4.

(i) In order to understand the right-hand side result in Figure 2 it is helpful to find an analytical. Estimate for *W(A)*. Let $\vec{y} = \begin{pmatrix} y_1 \\ y_2 \end{pmatrix} \in \mathcal{D}(A)$, $||\vec{y}|| = 1$, and let $\lambda =< A\vec{y}, \vec{y} >=< -D^2 y_1, y_1 > +< y_2, y_1 > +< y_1, y_2 > +< zy_2, y_2 >= \int_0^1 |y_1'|^2 + 2\Re\left(\int_0^1 y_1 \overline{y_2}\right) + \int_0^1 z|y_2|^2\, dx$ (14)

Equation (14) gives us an estimate for the first term on the right hand side of (14),

$$\int_0^1 |y_1'|^2 \geq \pi^2 \int_0^1 |y_1|^2 \quad (15)$$

For the second term on the right hand side of (14), the Cauchy Schwarz inequality and Youngs inequality yield

$$2\Re\left(\int_0^1 y_1 \overline{y_2}\right) \geq -\left(\int_0^1 |y_1|^2 + |y_2|^2\right) dx. \quad (16)$$

Also third term of the right hand side of equation (14) satisfies

$$\Re\left(\int_0^1 z|y_2|^2\, dx\right) \geq \inf \Re(z) \left(\int_0^1 |y_2|^2\, dx\right). \quad (17)$$

Hence from Equations (15), (16), (17) we get that

$\Re(\lambda) \geq \pi^2 \int_0^1 |y_1|^2\, dx - 1 +$
$\inf \Re(z) \int_0^1 |y_2|^2\, dx.$ (18)

This simplifies to

$\Re(\lambda) \geq \pi^2 ||y_1||^2 - 1 + \left(1 - ||y_1||^2\right) inf\ \Re(z)$
$= \pi^2 - \inf \Re(z) ||y_1||^2 + \inf \Re(z) - 1.$

This yields

$$\Re(\lambda) = \begin{cases} \inf \Re(z) - 1, & if\ \pi^2 - \inf \Re(z) \geq 0; \\ \pi^2 - 1, & if\ \pi^2 - \inf \Re(z) < 0. \end{cases}$$

For our example these yield $\Re(\lambda) \geq -39$.

To estimate $Im(\lambda)$ observe that

$$Im(\lambda) = \int_0^1 \big(Im(z)\big)|y_2|^2 \leq \sup_{x\in[0,1]} \big(Im(z)\big) \int_0^1 |y_2|^2 dx \leq 18, \quad (19)$$

and

$$Im(\lambda) = \int_0^1 \big(Im(z)\big)|y_2|^2 \leq \sup_{x\in[0,1]} \big(Im(z)\big) \int_0^1 |y_2|^2 dx \geqslant -18, \quad (20)$$

This completes the estimates on *W(A)*.

(ii) On the other hand for the right-hand side, since the S-numerical range is in general neither bounded nor closed, it is difficult to generate an accurate computer plot of this set. For $\mathbb{A}_k \in M_k$ and $k > 2$, the description of $\mathbb{A}_k$ is complicated, so in our example

$W_{\mathbb{S}_k}(\mathbb{A}_k)$ is bounded by the hyperbola centered at (0,1) and The foci of the hyperbolas are the eigenvalues of $\mathbb{A}_k$.

4 Conclusions

Our results describes the practical difficulties that related with the S-numerical ranges of operator matrices and block operator matrices of differential operators, even so good theoretical outcomes are available to underpin the approximation procedure. Completely analytic approaches are important to understand while the numerical results are deceptive, and apparently numerical results should be deal with skepticism.

References:

ADAMJAN, V. M. & LANGER, H. 1995. Spectral properties of a class of rational operator valued functions. *Journal of Operator Theory***,** 259-277.

BEBIANO, N., LEMOS, R., DA PROVIDENCIA, J. & SOARES, G. 2004. On generalized numerical ranges of operators on an indefinite inner product space. *Linear and Multilinear Algebra,* 52**,** 203-233.

BEBIANO, N., LEMOS, R., DA PROVIDÊNCIA, J. & SOARES, G. 2005. On the geometry of numerical ranges in spaces with an indefinite inner product. *Linear algebra and its applications,* 399**,** 17-34.

BEBIANO, N. & PROVIDÊNCIA, J. O. D. 1998. Numerical ranges in physics. *Linear and Multilinear Algebra,* 43**,** 327-337.

BEBIANO, N., PROVIDIA, J. D., NATA, A. & SOARES, G. 2008. *Krein Spaces Numerical Ranges and their Computer Generation*, Electron. J. Linear Algebra,.

GUSTAFSON, K. E. & RAO, D. K. 1997. Numerical range. *Numerical Range.* Springer.

HAIN, K. & LUST, R. 1958. Zur Stabilität zylindersymmetrischer Plasmakonfigurationen mit Volumenströmen. *Zeitschrift für Naturforschung A,* 13**,** 936-940.

HALMOS, P. R. 2012. *A Hilbert space problem book*, Springer Science & Business Media.

HAUSDORFF, F. 1919. Der wertvorrat einer bilinearform. *Mathematische Zeitschrift,* 3**,** 314-316.

KATO, T. 2013. *Perturbation theory for linear operators*, Springer Science & Business Media.

LANGER, H., MENNICKEN, R. & MÖLLER, M. 1990. A second order differential operator depending nonlinearly on the eigenvalue parameter. *Oper. Theory Adv. Appl,* 48**,** 319-332.

LANGER, H. & TRETTER, C. 1998. Spectral decomposition of some nonselfadjoint block operator matrices. *Journal of Operator Theory***,** 339-359.

LI, C.-K., TSING, N.-K. & UHLIG, F. 1996. Numerical ranges of an operator on an indefinite inner product space. *Electronic Journal of Linear Algebra*.

MURNAGHAN, F. D. 1932. On the field of values of a square matrix. *Proceedings of the National Academy of Sciences of the United States of America,* 18**,** 246.

NAKAZATO, H., BEBIANO, N. & DA PROVIDÊNCIA, J. 2011. THE NUMERICAL RANGE OF LINEAR OPERATORS ON THE 2-DIMENTIONAL KREIN SPACE. *ELECTRONIC JOURNAL OF LINEAR ALGEBRA,* 22**,** 430-442.

R.A.HORN & C.R.JOHNSON 1991. *"Topics in matrix analysis"*, Cambridge University Press, New York.

TAHIRI, F. E. 2015. *Numerical Ranges of Linear Pencils. PhD thesis,* University of Coimbra.

TOEPLITZ, O. 1918. *Das algebraische analogon zu einem salze you fient*, Math. Z. Vol.2, (1918),187-197.

BEBIANO, N., PROVIDIA, J. D., NATA, A. & SOARES, G. 2008. *Krein Spaces Numerical Ranges and theirComputer Generation*, Electron. J. Linear Algebra,.

GUSTAFSON, K. E. & RAO, D. K. 1997. Numerical range. *Numerical Range.* Springer.

HALMOS, P. R. 2012. *A Hilbert space problem book*, Springer Science & Business Media.

LI, C.-K., TSING, N.-K. & UHLIG, F. 1996. Numerical ranges of an operator on an indefinite inner product space. *Electronic Journal of Linear Algebra*.

MUHAMMAD, A. M. S. 2005a. *Elliptical range of n-tuple operators on a complex Hilbert space,* Zanko Journal for Pure and Applied Science.

MUHAMMAD, A. M. S. 2005b. *Line segments of the boundary of numerical range,* Zanko Journal for Pure and Applied Science.

N.BEBIANO, LEMOS, R., PROVIDENCIA, J. D. & SOARES, G. 2004. On generalized numerical ranges of operators on an indenite inner product space, Linear and Multilinear Algebra, 52:203233. *Mathematische Annalen*.

ZANCO Journal of Pure and Applied Sciences
The official scientific journal of Salahaddin University-Erbil
https://zancojournals.su.edu.krd/index.php/JPAS

ISSN (print):2218-0230**, ISSN (online):** 2412-3986**, DOI: http://dx.doi.org/10.21271/zjpas**

RESEARCH PAPER

Molecular basis of ciprofloxacin (fluoroquinolone)-resistant in clinical isolates of *Escherichia coli*

Ahmed Mohammed Tofiq[1]

[1]Department of Biology, College of Education, University of Garmian, Kalar-Sulaimani, Kurdistan Region, Iraq

A B S T R A C T:

It has recently been shown that antibiotic resistance is considered as one of the extremely imperative worrisome in medicine, with tremendously resistant pathogens of numerous species of bacteria demonstrating difficult to treat. The aim of this study was to determine mutations in DNA gyrase subunits GyrA and GyrB, and topoisomerase IV subunits ParC and ParE in clinical isolates of *Escherichia coli*, which are important determining factors for paramount levels of fluoroquinolone (ciprofloxacin) resistance. This article was achieved through five months survey for the occurrence of ciprofloxacin resistant *E. coli* in clinical samples from outpatient clinics in Kalar city. Fifty seven samples were collected included (4) wound swabs, (1) conjunctiva, (2) vaginal and (2) otitis media swabs, as well as (48) urine samples from the period March to August, 2018. The collected samples were cultivated on selective and differential media for *E. coli* isolation. Classical biochemical tests and molecular basis (16SrRNA) were performed for the identification of 14 isolates of *E. coli*. These isolates were tested for antibiotic sensitivity (17 different antimicrobials agents were tested, included ciprofloxacin). The isolates showed ciprofloxacin resistance and were checked for mutations in the quinolone resistance-determining regions (QRDR) of *gyrA*, *gyrB*, *parC*, and *parE* genes by polymerase chain reaction and DNA sequencing. Subsequently, amino acid substitutions were detected by Clustal Omega. Two main mutations in *gyrA*, in addition to a range of extra mutations, were identified in resistant isolates. There were no mutations in the QRDR of each of *gyrB*, and *parC* of CIP-resistant isolates, except a single mutation in *gyrB* out of QRDR, and only in one isolate. However, one main mutation in *parE*, as well as two extra mutations were identified in two resistant isolates. The current study has demonstrated the occurrence of CIP-resistant *E. coli* in clinical specimens, with half of them being unsusceptible to ciprofloxacin, among those, 85.7% were also resistant to at least three antibacterial classes.

KEY WORDS: CIP (fluoroquinolone)-resistant *E .coli*, 16SrRNA, chromosomal mutations, *gyrA*, *gyrB*, *parC*, and *parE* genes
DOI: http://dx.doi.org/10.21271/ZJPAS.32.3.8
ZJPAS (2020) , 32(3);64-74 .

1.INTRODUCTION :

One of the most urgent universal troubles in medicine is antimicrobial resistance, with the evolving of pathogenic species that are extensively drug- resistance demonstrating obstacle to management (Redgrave *et al.*, 2014). Broad-spectrum antibiotics quinolones and fluoroquinolones (FQs) are powerful inhibitors of DNA gyrase and topoisomerase IV, that are two bacterial type II topoisomerases, and are essential enzymes engaged in numerous important and key cellular activities comprising DNA replication (Drlica, 1990; Hooper and Wolfson, 1993; Hooper, 2001; Hoshino *et al.*, 1994; Pruss *et al.*, 1986); have entered the clinics since the end of 1980s for the eradication of extreme or resistive infections (Redgrave *et al.*, 2014). FQs have been extensively used in human and animal medicine (Aldred *et al.*, 2013), and ciprofloxacin (CIP) is the predominant one in human medicine (Hopkins *et al.*, 2005). In spite of the widely and optimistic treatment of *Escherichia coli* infections with fluoroquinolones, resistance to these antibiotics developed and increased

* **Corresponding Author:**
Ahmed Mohammed Tofiq
E-mail: ahmed.mohammed@garmian.edu.krd
Article History:
Received: 06/08/2019
Accepted: 08/11/2019
Published: 15/06 /2020

significantly from an early stage of their initiation in medicine (Jiménez Gómez *et al.*, 2004).

Both of DNA gyrase and topoisomerase IV are heterotetramers, comprising of two A (GyrA) subunits and two B (GyrB) subunits, encoded by the *gyrA* and *gyrB* genes for the former, and two C (ParC) and E (ParE) subunits encoded by *parC* and *parE* genes for the two laters, respectively (Ruiz *et al.*, 1997). When either of these enzymes stimulates impermanent double-stranded breaks, from the beginning, they adhere covalently to the DNA double helix to construct enzyme-DNA complexes prior of breaking the bound DNA, then passing another piece of DNA via this break, and reconnecting the proper DNA (Drlica *et al.*, 2008). On the other hand, neither DNA gyrase nor topoisomerase IV will be able to re-ligate the DNA substrate when FQs bind to either; in this case the broken pieces of DNA bound to the enzyme are described as cleaved complexes (Drlica *et al.*, 2008). This binding of FQs takes place within the enzyme at the target site of helix-4 of either GyrA or ParC (Redgrave *et al.*, 2014).

Different mechanisms of resistance to FQs were discovered over the time in various species of bacteria, especially in *Salmonella* and *E. coli*. The two main genetic mechanisms of resistance were included chromosomal mutations and plasmid-mediated, which only the plasmid one is interchangeable (Hopkins *et al.*, 2008). Moreover, the most popular and well-known mechanism of resistance that confer highest level of resistance to FQs is the mutations in one or more of the genes (*gyrA*, *gyrB*, *parC*, and *parE*) of topoisomerases II, the primary and secondary target of these antibiotics (Redgrave *et al.*, 2014). A short DNA sequence in these genes known as quinolone resistance-determining region (QRDR) is the region where mutations arise from (Yoshida *et al.*, 1990; Yoshida *et al.*, 1991). Mutations in the QRDR of these genes lead to substitution in the amino acid in this region which in turn alter the structure and configuration of the target protein and ultimately changes the binding affinity of FQs to the target enzyme, resulting in drug resistance (Hooper, 2000; Piddock, 1999).

Earlier research studies have concluded that the occurrence of mutations in *parC* gene in addition to both of *gyrA* and *gyrB* genes have been attributed to the attainment of fluoroquinolone resistance (Nakamura *et al.*, 1989; Hooper and Wolfson, 1993; Ouabdesselam *et al.*, 1995; Vila *et al.*, 1996; Vila *et al.*, 1994). (Jiménez Gómez *et al.*), in 2004 mentioned that the mechanism of resistance to FQs has been mainly ascribed to mutations in both of *gyrA* and *parC* genes, but with lesser frequency in *gyrB* and *parE* genes. More precisely, mutations in the QRDR of *gyrA* and *parC* or in the associated genes for instance *gyrB* and *parE*, or in all of those genes together may also be engaged in increased levels of resistance to FQs (Hopkins *et al.*, 2005).

The aim of this study was to explore the presence of CIP-resistant *E. coli* in clinical specimens and to characterize representative resistant isolates with respect to the susceptibility to antimicrobials, and the presence of chromosomal mutations in the QRDR of *gyrA*, *gyrB*, *parC*, and *parE* genes.

2. MATERIALS AND METHODS

2.1 Sampling and Bacterial Identification

From March to August 2018 fifty-seven (57) clinical samples were gathered from patients who visited the private outpatient clinic in Kalar city. The clinical specimens included; (4) wound swabs (4), (1) from conjunctiva, (2) vaginal swabs, (2) otitis media, and (48) urine. Fresh swabs transferred to the laboratory of microbiology from the private clinic, and they had been cultured directly onto MacConkey agar plates. Urine samples were collected in sterile disposable container and labeled properly, then by the use of platinum microbiological loop 1µl of non-centrifuged urine samples were streaked onto plates of MacConkey agar. Cultured plates incubated at 37ºC for 18 to 48 hours. Lactose fermenter (LF) isolates were sub-cultured to prepare pure cultures. Initially, Gram reaction and colonial characteristics of the bacterial isolates were studied, then traditional biochemical tests (Cheesebrough, 2006; Willey *et al.*, 2008) included catalase, oxidase, indole, methyl red, Voges Proskauer, citrate, urease, nitrate reduction, H_2S, gas, heamolysis on blood agar and coagulase, applied on the presumptive *E. coli* colonies (isolates). PCR primers (Table. 1) designed by Tawfeeq *et al.* (2017) for the amplification of 16S rRNA was used for the confirmation of *E. coli* colonies.

2.2 Antimicrobial susceptibility testing

Kirby-Bauer disk diffusion method (Bauer *et al.*, 1966) was performed to test 17 different

antibiotics against *E. coli* isolates. Antibiotic discs included Piperacillin (100µg) Amikacin (30µg), Meropenem (10µg), Trimethoprim (10µg), Ciprofloxacin (10µg), Nitrofurantoin (300µg), Levofloxacin (5µg), Cephalexin (30µg), Moxifloxacin (5µg), Ofloxacin (5µg), Norfloxacin (10µg), Doxycycline (10µg), Cefixime (5µg), Cefpirome (30µg), Cefpodoxime (10µg), Cefotaxime (30µg), Amoxicillin/Clavulanic acid (30µg) were distributed on plates of Mueller-Hinton agar according to the newest version of the guidelines justified in the Clinical Laboratory Standards Institute (CLSI) by Patel *et al.* (2016) for the purpose of initial detection of ciprofloxacin-resistant *E. coli.*

2.3 Genomic DNA extraction

Colonies from fresh cultures of the presumptive *E. coli* isolates were utilised for the extraction of genomic DNA. Boil preparation (a single colony from each isolate was carefully suspended in 50µl of deionized water, then heated for 10 min at 95°C and spun down at 10,000 × g for 5 min. supernatant was used directly as a DNA template for PCR) or methodology described in *AccuPrep* Genomic DNA Extraction Kit (Bionner) was followed precisely.

2.4 Primers

All the primers that were used in the current study synthesized by Humanizing Genomics (Macrogen) are available in (Table. 1) For the molecular identification of *Escherichia coli* primers designed (Tawfeeq *et al.*, 2017) for the amplification of *Escherichia coli* 16SrRNA based on the complete annotation sequence of *E. coli* obtained from National Centre for Biotechnology Information (Accession No. J01859.1) and *E .coli* ATCC25922 as a reference strain.

In order to identify mutations in QRDR of *gyrA*, *gyrB*, *parC*, and *parE* genes in CIP resistance isolates of *Escherichia coli*, they were amplified by PCR using oligonucleotide primers (Table. 1). These primers were designed based on *gyrA*, *gyrB*, *parC*, and *parE* sequences of *E. coli* K-12, GeneBank accession numbers; X57174.1, D87842, M58408.1, and M58409.1, respectively.

2.5 PCR amplification (16SrRNA and QRDR of *gyrA*, *gyrB*, *parC*, and *parE* genes)

All the PCR assays were carried out in 25µl final reaction volume, composed of 2µl of DNA template (genomic DNA), 0.5µl of each primer (forward and reverse) for 16SrRNA, 12.5µl of One PCRTM master mix (GeneDirex), consisted of Taq DNA polymerase, dNTPs, PCR buffer, enhancer, gel loading dye, and fluorescence dye. Total volume of the reaction mixture was completed through the addition of the required amount of nuclease free water. Prepared PCR mixtures were spun down shortly for 5-10 seconds in a micro-refrigerated centrifuge, then placed in thermal cycler (TCY, Crealcon, NL) and exposed to the following cycling parameters: initial denaturation at 94°C for 4minutes, followed by 35 cycle of denaturation at 94°C for 30 seconds, annealing at 55°C for 1minute and extension at 72°C for 2minutes and a final extension step at 72°C for 5minutes.

Same procedure and PCR parameters were followed for the amplification of QRDR of *gyrA*, *gyrB*, *parC*, and *parE* genes, except that specific primers (Table. 1) for each of these genes were used, and the annealing temperature was at 51.5°C/1minute, and 54°C/minute for the multiplication of *gyrA* and *parC*, and *gyrB* and *parE* genes, respectively.

2.6 DNA analysis by agarose gel electrophoresis

To visualize the amplified DNA fragments, 1.5% agarose gel electrophoresis either containing ethidium bromide or prime safe dye (GeneAid) at 100 volts for 90 minutes, and at room temperature was used. Amplicon size determined by comparison with 100 bp DNA ladder (GeneDirex). This form of DNA analysis uncovered amplification of the expected 648-bp fragment for the *gyrA* gene, 447-bp fragment for the *gyrB*, 395-bp for the *parC*, and 266-bp for the *parE* gene, sequentially. All these fragments were contained the quinolone resistance-determining region of *gyrA*, *gyrB*, *parC*, and *parE* genes, respectively.

2.7 Gel purification

PCR products (fragments) in section 2.6 were gel purified using *PrimPrep* Gel Purification kit to remove primers, free nucleotides, and any unrelated bands (in case if there is any), in order to avoid their interaction with the subsequent steps, according to the manufacturer instructions.

2.8 DNA sequencing

Samples of the gel purified PCR products were processed as early as possible for DNA sequencing in South Korea.

2.9 Blast alignment and Clustal Omega (Clustal W)

Sequenced DNA fragments of the QRDR of *gyrA, gyrB, parC,* and *parE* genes were aligned using blast alignment with their sequences in the original DNA template. ExPASy program was used for the translation of DNA sequences of these genes into protein sequences. Then mutations in the amino acid sequences of each of their correspondence proteins revealed by Clustal Omega when compared with original (non-mutated) proteins of these genes.

3. RESULTS AND DISCUSSION

Out of 57 clinical samples collected for this study, 48 (84.21%) of them were urine samples, 4 (7.01%) wound swabs, 2 (3.5%) for each of otitis media and vaginal swabs, and the rest was 1 (1.75%) for the case of conjunctivitis (Table. 2). Since this work was about *Escherichia coli*, in particular, those resistant to ciprofloxacin with the detection of the expected mutations in the target enzymes, gyrase and topoisomerase, that confers *Escherichia coli* isolates un-susceptibility towards ciprofloxacin, a fluoroquinolone antibiotic, the focus was only on *E. coli* strains isolated from the tested clinical samples.

Out of the 47 samples that were collected, only 14 *E. coli* isolates were obtained, and they were all from the 48 samples of urine, while there was no any *E .coli* in the other samples (Table. 2). As usual, classical biochemical tests recommended in the diagnostic text books were performed for the identification of the isolates. Later on, isolates confirmed in terms of molecular biology via PCR amplification of 627bp of 16SrRNA (Table. 1 and Figure. 1).

Data from an agar diffusion technique which was performed for studying the susceptibility testing of *E .coli* isolates toward 17 antibiotics from different antimicrobial classes displayed that 12(85.7%) *E .coli* isolates were multidrug resistant. Gosling *et al.* (2012) stated that 88.1% of *E .coli* strains were multidrug resistant as well. However, in the current study only 7(50%) isolates were CIP resistant.

PCR amplification was performed on the 14 isolates of *E .coli*, however, gel purification of PCR products and sequencing were applied on all the 7 isolates of *E .coli* which were CIP-resistant in order to identify mutations in *gyrA, gyrB, parC*, and *parE* genes (Figures 2a, and 2b). According to a procedure described by Oram and Fisher (1991), a DNA fragment of 648 bp, covered a sequence of nucleotides from 24 to 671 of the QRDR of *gyrA* was amplified. For the amplification of nucleotide sequence from 995 and up to 1442 of QRDR of *gyrB* to obtain a piece of DNA with 447 bp a procedure described previously by Vila *et al.* (1994) was followed. Moreover, to amplify DNA fragments of 395 bp and 266 bp of QRDR of each of *parC* and *parE,* methodology described by Vila *et al.*, (1996), and Sorlozano *et al.*, (2007), respectively, were followed. However, it should be mentioned that although the primers that were used in this study were constructed by previous researchers, due to the fact of the confirmation that they are undoubtedly covering the QRDRs of the genes under investigation, but they all were checked to confirm that they have been constructed based on the *E .coli* K-12 genes sequences database, as described precisely in section 2.4.

DNA sequences (FASTA) of *gyrA, gyrB, parC*, and *parE* genes for the each of the 7 isolates of CIP-resistant *E .coli* were obtained from South Korea after a period of time. The sequence of each of the genes in each of the 7 isolates was blast aligned and compared with the corresponding sequence of QRDR of the reference strain, *E .coli* K-12. Then, ExPASy program was used to translate DNA sequences into amino acid sequences, which utilized in Clustal Omega program to reveal and identify the places where mutations in the amino acids sequences of GyrA, GyrB, ParC, and ParE proteins occurred that confers resistance to FQs (CIP).

One main mutation, encoding Ser83Leu was detected in the QRDR of *gyrA* in one of *E. coli* isolates that has been studied. This result is similar to those observed by Sorlozano *et al*., (2007) and Gosling *et al.*, (2012) to some extent. They have displayed the second main mutation as Asp87Asn, but in the current study this mutation was Asp87Val, which agreed with observations reported by (Oram and Fisher), in 1991, as they detected similar change. Vila *et al.*, in 1994 mentioned that amino acid changes observed in

eight mutants of *E. coli* isolates at amino acid 87 was Asp to Asn, while it was Asp to Tyr in other three mutants. Amino acid mutations Asp_{87}→Asn, or Gly or Tyr in *gyrA* were found in 7, 2, and 1 clinical isolates of isolates *E. coli*, respectively (Bachoual *et al.*, 1998). Other researchers clarified that the first main mutation, Ser83Leu, is responsible for conferring low level of resistant to FQs (Chapman and Georgopapadakou, 1988); (Oram and Fisher, 1991; Yoshida *et al.*, 1988). Furthermore, the second main mutation, the Asp87 codon of *gyrA* is associated with a significant increase in the resistance to FQs (Vila *et al.*, 1994). More precisely, Vila *et al.* (1994) concluded that Ser83Leu change fosters a high level of resistance toward nalidixic acid but a low level of resistance against ciprofloxacin, and Asp87Asn change possibly act a complementary role in developing high levels of resistance to ciprofloxacin in the strains. Gosling *et al.*, (2012) showed that 90% of CIP-resistant isolates had the two main mutations (Ser_{83}→Leu + Asp_{87}→Asn), while the rest of the strains (10%) had single mutation (Ser_{83}→Leu). They also showed that half of their strains had silent mutations, as extra mutations. In the current study, Ala85Val, Arg98Threo, Ile117Arg, Pro118Lys, and Pro120Val were observed as additional mutations that were located the quinolone resistant determining region of *gyrA* in two of the isolates (Figure. 3). Similar results were observed by Yoshida *et al.*, (1990), as they described additional mutations such as Ala67, Gly81, Ala84, and Gln106 for the QRDR of *gyrA*. Randall *et al.*, (2005) explained these extra mutations as they probably representing the variation in strains of *E. coli*, the condition which has also been seen in *Salmonella*.

Within the *gyrB* gene of *E. coli* two quinolone resistance-determining sites, Asp426 and Lys447 are present where mutations occured (Ruiz *et al.*, 1997; Yamagishi *et al.*, 1986; Yoshida *et al.*, 1991). Mutation in the first point Asp_{426}→Asn confers resistance to either the old quinolones (nalidixic acid) or to the new fluoroquinolones (ciprofloxacin), whereas mutation in the second point Lys_{447}→Glu increased the susceptibility to the new fluoroquinolones while confers resistance to nalidixic acid (Yoshida *et al.*, 1991); Hooper and Wolfson, 1993). This study did not detect any single or double mutations in the QRDR of *gyrB*, which is consistent with the results of (Jiménez Gómez *et al.*, 2004), while it contradicts the results presented by (Vila *et al.*, 1994), as they determined only a single amino acid change, Lys447Glu at the GyrB protein in one of the clinical isolates of *E. coli* out of 27. Concomitantly, Vila *et al.*, (1994) and Quabdesselam *et al.*, (1995) added that this is clearly and strongly indicating the predominance of mutations in *gyrA* over *gyrB*. However, a single amino acid change from Glycine to Arginine was determined out of QRDR (Figure 3), and in one of the strains, which has not been previously described.

Although Gosling *et al.*, (2012) mentioned that FQ- resistant in clinical strains of *E. coli* has often been attributed to the presence of two mutations in *gyrA* and one mutation in *parC*, in this study, none of the 7 strains of CIP-resistant *E. coli* possessed single or double mutations in the DNA sequence of *parC* that acquired detectable amino acid substitutions in the QRDR of ParC. The current observations were in agreement with conclusions reported by (Jiménez Gómez *et al.*, 2004). In contrast to the present study, Chen *et al.*, in 2001 showed that (63%) of the clinical isolates of *E. coli* exhibited a single mutation Ser80Ile of ParC. Moreover, Bachoual *et al.*, (1998) showed that all the clinical strains of *E. coli* were carried one amino acid substitution in ParC; either Ser80Ile, or Ser80Arg, or Glu84Lys in 8, 2, and 1 of the isolates. Mutations in the QRDR of *parC* in the *E. coli* isolates observed by Sorlozano *et al*., (2007) encoded Ser80Ile, Ser80Arg, Glu84Lys, Glu84Gly, and Glu84Val, respectively. Interestingly, Vila *et al.*, (1996), proved that feasible amino acid changes in both of ParC and GyrA prompt an increased level of FQ resistance.

With regard to *parE*, present study showed the presence of a single mutation in the QRDR of *parE*, encoding Ser458Ala in one of the isolates, in addition to two other mutations outside the QRDR, which they are Serine to Phenylalanine and Leucine to Proline in another isolate of *E. coli*. This result is suggesting that *parE* gene mediate or contribute to the development of fluoroquinolone resistance. Sorlozano *et al*. (2007) found a single mutation in the QRDR of *parE* gene of 10 isolates of *E. coli*, encoding Sr458Ala. However, Lindgren *et al.* (2003) reported a different mutation located outside the quinolone resistant determining region, occurred in the identical codon as that for Ser458Thr. In the contrary, each of Ruiz *et al.* (1997) and Jiménez Gómez *et al.* (2004), independently, did not find

any changes in the QRDR of *parE*. However, the last group of researchers did not eliminate the possibility of the occurrence of other substitutions outside QRDR. This is due to the fact that they have investigated the presence of homology between QRDR of *gyrB* gene in the B subunit of DNA gyrase represented by Asp426 and Lys447 with the residues Asp420 and Lys441 of ParE, which would be the most significant candidate for study in *parE* gene in case if it plays a role in the evolution of quinolone resistance. Therefore, based on this assumption, Sorlozano *et al*. (2007) concluded that mutations in *parE* may be linked to quinolone resistance. As the current study detected mutations outside the QRDR of *parE*, which is concomitant with the observations of other researchers, Hopkins *et al.* (2005) recommended the performance of further investigation to confirm their contribution to quinolone resistance.

Table 1. Sequences, symbols, and product size of reference primers

Primers	Primer Sequence (5'--------3')	Product Size (bp)	Reference
16SrRNA-F	GAAGACTGACGCTCAGGTGCGAA	627	(Tawfeeq *et al.*, 2017)
16SrRNA-R	CCGTGGCATTCTGATCCACGATTA		
gyrA-F	TACACCGGTCAACATTGAGG	648	(Oram and Fisher, 1991)
gyrA-R	TTAATGATTGCCGCCGTCGG		
gyrB-F	CTCCTCCCAGACCAAAGACA	447	(Vila *et al.*, 1994)
gyrB-R	TCACGACCGATACCACAGCC		
parC-F	AAACCTGTTCAGCGCCGCATT	395	(Vila *et al.*, 1996)
parC-R	GTGGTGCCGTTAAGCAAA		
parE-F	TACCGAGCTGTTCCTTGTGG	266	(Sorlozano *et al.*, 2007)
parE-R	GGCAATGTGCAGACCATCAG		

Table 2. Percentage of clinical specimens, and the prevalence of (CIP-resistant and CIP-sensitive) *E. coli*

Specimen	No. (% of clinical specimen)	Total no. of *E. coli*	CIP-resistant *E. coli*	CIP-sensitive *E. coli*
Urine	48 (84.21%)	14(100 %)	7(50%)	7(50 %)
Wound swab	4 (7.01)	0	0	0
Otitis media	2 (3.50%)	0	0	0
Vaginal swab	2 (3.50%)	0	0	0
Conjunctiva	1 (1.75%)	0	0	0
Total	57	14	7	7

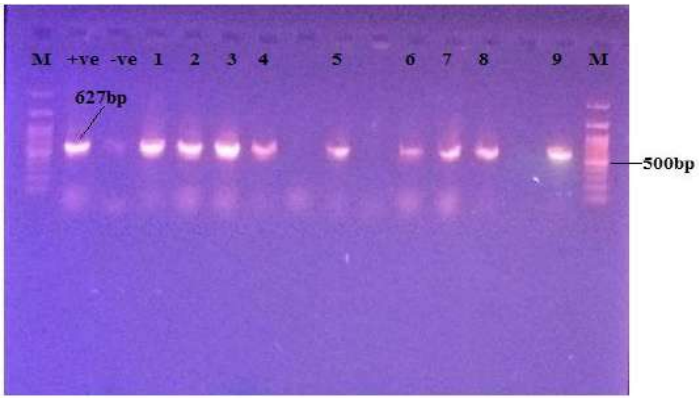

Figure 1. Identification of *E. coli* isolates in terms of molecular biology. M: 100bp DNA marker, +ve; positive control (16SrRNA of *E .coli* ATCC25922), -ve; negative control. Lanes 1 – 9; PCR amplification of 627bp of 16SrRNA of *E. coli* strains.

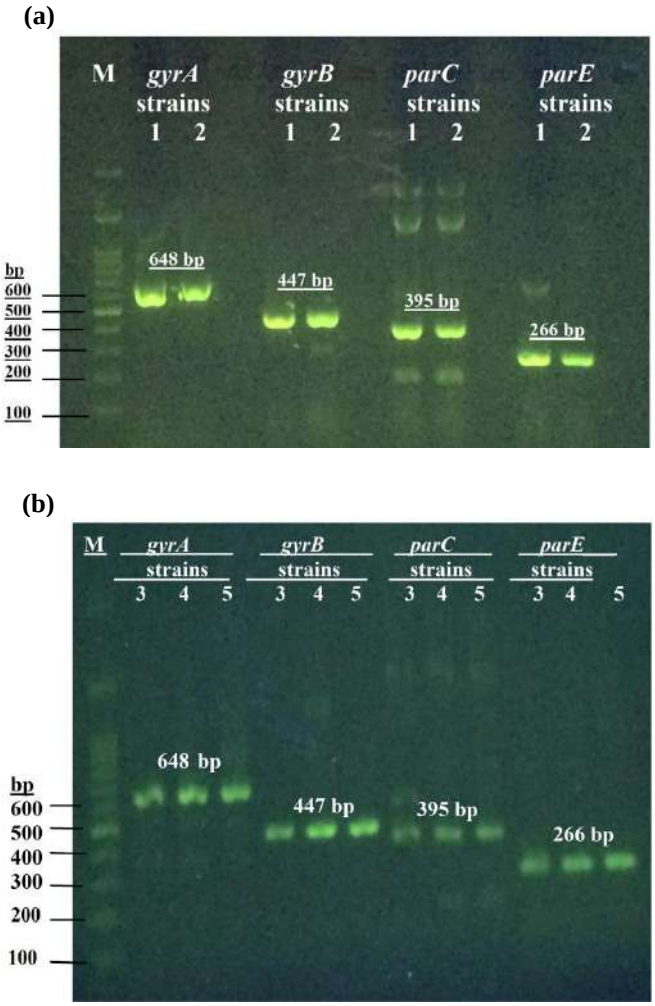

Figure 2. PCR fragments of QRDR of *gyrA*, *gyrB*, *parC*, and *parE* from CIP-resistant *E. coli* isolates 1, and 2 in **(a)**, and isolates 3, 4, and 5 in **(b)**. M: 100bp DNA marker, from left to right; lanes 1 & 2 are PCR products (648 bp) of *gyrA*, lanes 4 & 5 are PCR products (447 bp) of *gyrB*, lanes 7 & 8 are PCR products (395 bp) of *parC*, lanes 10 & 11 are PCR products of *parE*, lanes 3, 6, and 9 left blanks in **(a)**.

```
gyrA        YTGQHStopGRAEELLSGLCDVGHCWPCAARCPRWPEAGTPSRTLRHERTRQStop----     56
A-Ref.      --------PLTPIWIMetRCRSLLAVRCRMetSEMetAStopSRYTVAYFTPStopTYSt     52
A-A         --------PIILSWIAMetSG--HCWPCAARCPEMetAStopSRYTVAYFTPStopTYSt     50
A-M         ---------------------------------------------------TPStopTYSt     10
                                    ****

gyrA        ----------------LEQSLS--------------------------topKICPCRWSt     74
A-Ref.      opAMetTGTKPIKNLPVSLVTStopSVNTIPMetVTWRFMetTRSSAWRSHSRCVTCWSt     112
A-A         opAMetTGTKPIKNLPVSLVTStopSVNTIPMetVTWRSMetTRSSAWRSHSRCVICWSt     110
A-M         opAMetTGTKPIKNLPVSLVTStopSVNTIPMetVTRRSMetTRLSVWRSHSRCVICWSt     70
                 :.   *                              . *   ***

gyrA        opRNRStop------------IPSPWStopLGGLStopHDRPHGAAILAALYAGRRSGSt     122
A-Ref.      opTVRVTSVLSTATLRRQCVIRKSVWRKLPMetNStopWPISKKRRSISLITMe------     166
A-A         opTVRVTSVLSTATLRRQCVIRKSVWRKLPMetNStopWPISKKRRSISLITMe------     164
A-M         opTVRVTSVPSTATLRRQCVIRKSVWRKLPMetNStopWPISKK----------------     114
                  **  * *                * * . *:   ****    :
        ********************************************************************************

B-A         AFSEStopSAVDSRStopTNCWRNTCWKTQPTRKSWSAKLSMetLPVPVKLRVARVKSto      60
gyrB        ------------------------------------SSQTKDKLVSSEVKSAVEQQM--e      22
B-M         ---------------------------------------VLStopVISGStopQQM--e      18
                                  .          :

B-A         pPAVKVRWIStopLACRAN------WQTARNAIRRFPNCTLWKGTPRAALRSRGVTARTR      114
gyrB        tNELLAEYLLENPTDAKIVVGKIIDAARAREAARRAREMe--tTRRKGALDLAGLPGK-L      79
B-M         tNELLAEYLLENPTDAKIVVGKIIDAARAREAARRAREMe--tTRRKGALDLAGLPGK-L      75
              : ..::   *  .:           **:* **  :    .   :.**   *: .:

B-A         RFCRStopRVKSSTLRKRASIRCS------------------LLR----KWRR-StopS-      150
gyrB        ADCQERDPALSELYLVEGDSAGGSAKQGGNRKNQAILPLKGKILNVEKARFDKMetLSSQ      139
B-M         ADCQERDPALSELYLVEGDSAGGSAKQGRNRKNQAILPLKGKILNVEKARFDKMetLSSQ      135
             *:.  * :..  * :  *   *                  :*.    :: : .*  *

                        B-A       ------PRLAVVAGRE   160
                        gyrB      EVATLITALGCGIGR-   154
                        B-M       EVATLITALGCGPGRE   151
        ********************************************************************************

A-C         ------------GSVStopLGStopCQRQIStop-----KIGPYRRStopR---TGS---      37
parC        KPVQRRIVYAMetSE------LGLNASAKFKKSARTVGDVLGKYHPHGDSACYEAMetVL      54
M-C         ---------RMetStopSDWAStopCQRQFKKSARTVGDVLGKYHPHGDSACYEAMetVL      51
                   *           .. ::..        :* *:         : .

A-C         -topIPSARRYRLLStopSD-GPDGA-------------------TVLLPLSAGStopWS      76
parC        MetAQPFSYRYPLVDGQGNWGAPDDPKSFAAMetRYTESRLSKYSELLLSELGQGTADWV      114
M-C         MetAQPFSYRYPLVDGQGNWGAPDDPKSFAAMetRYTESRLSKYSELLLSELGQGTADWV      111
              * : ** *:.   .  .**.                      :**   . .*  *

A-C         GELGRAGRSEIVRGNALHRIPVVEIFRAAIERAGAGDGStopLGAKLRRHFAGAENATCP      136
parC        PNFDGTLQEPKM-etLPARLPNILLN-----------------GT---------------      141
M-C         PNFDGTLQEPKM-etLPARLPNILLN-----------------GTTKRRStopILN----      149
                  ::. : :.  :  .   *:* : :                  *:

                        A-C       SAKHFAStopQGTTK    151
                        parC      ---------------    141
                        M-C       ----VSAPSPPGKGK    160
        ********************************************************************************

 A-E        ------------------------------------------------------------Stop       4
 parE       LNCWRRWRFPAPSAVCVRPKKWCVKSStopPAARRCLANWLIVPRRTLTVPSCSLWKVTP       60
 M-E        ------------------------------------------------------------R       1


A-E          RADLPAGARSRI-----SGDHATERStopDPStop-------HLGSLFRRSA----GF--       46
parE        QADLPSRRAIANIRRSCHStopKVRSLTPGKSLPTKCWLRRKC--TIFRStopRSVSILT       118
M-E         RRGSASRRAIANIRRSCHStopKVRSLTPGKFLPTKCWPRRKCMetIFRStopRSVSILT       61
            : .  :            .   . **  *.              ::** :     .:

A-E         ---AGSARYFGSDRYRSStopQRRSEPASLWQNLYPRGCGL-------------------       84
parE        ATIStopASFVMetAKS---VSSRMetR----TLMetVCTLPRCSALCSStopNISARWS       171
M-E        ATIStopASFVMetAKS---VSSRMetR----TLMetVGTLP------------------       96
                    :     *  :  :*    . * *      .*      *

                         A-E       ---StopWLAHC--     93
                         parE      topNTVTFTSHCHR     185
```

M-E ---------- 96

Figure 3. CLUSTAL OMEGA. Alignment of multiple amino acid sequences derived from the nucleotide sequences of *gyrA*, *gyrB*, *parC*, and *parE* genes of CIP-resistant *E. coli* isolates in comparison to the original amino acid sequences of GyrA, GyrB, ParC, and ParE of *E. coli* K-12.

4. CONCLUSIONS

In summary, we have demonstrated the role of mutations in *gyrA* gene of DNA gyrase, and *parE* gene of the topoisomerase IV in the resistance of *E. coli* isolates against fluoroquinolones, especially ciprofloxacin. This illustrates the conclusion that the mechanism of targeting of either DNA gyrase or topoisomerase by fluoroquinolones depends on both of the bacterial species and specific FQ, in a manner that DNA gyrase is targeted by FQs in Gram-negative bacteria, while topoisomerase IV is preferentially targeted in Gram-positive bacteria (Drlica *et al.*, 2008). Although of this preference, if the primary target of FQs has been substituted to resistant allele, they will bind to the secondary target and exhibit antibacterial action (Redgrave *et al.*, 2014).

In addition to the target-site mutations in DNA gyrase, in case if it is accompanied by mutations in topoisomerase IV or not, is considered an important factor for determining high levels of resistance to fluoroquinolones, there are extra mechanisms implicated in conferring resistance to FQs that were not been included in the present study. Mutations that results in downregulation of the outer membrane porin proteins that are present in the cell wall of Gram-negative bacteria, and works like a barrier for hydrophilic molecule (Chenia *et al.*, 2006; Strahilevitz *et al.*, 2009) are known in the isolates of diverse species with quinolone resistance (Danilchanka *et al.*, 2008; Everett *et al.*, 1996). Chromosomal multidrug efflux pump that are actively expels the antibiotics out of the bacterial cells, and, to a lesser degree, the occurrence of plasmid-mediated quinolone resistance (PMQR) genes (Redgrave *et al.*, 2014), are regarded as complementary mechanisms that cannot be ruled out and possibly enhance the emergence of resistance and associate to the selection of isolates with FQ resistant during the term of management with these group of antibiotics.

Acknowledgments

Thanks, and gratitude to Dr. Rahman Faraj for his kindness and assistance during specimen collection and Mr. Abas Salih for linguistic proofreading.

Conflict of Interest

There is no conflict of interest.

References

Aldred, K.J., McPherson, S.A., Turnbough, C.L., Jr., Kerns, R.J., Osheroff, N., 2013. Topoisomerase IV-quinolone interactions are mediated through a water-metal ion bridge: mechanistic basis of quinolone resistance. Nucleic Acids Res 41, 4628-4639.

Bachoual, R., Tankovic, J., Soussy, C.J., 1998. Analysis of the mutations involved in fluoroquinolone resistance of in vivo and in vitro mutants of *Escherichia coli*. Microbial drug resistance (Larchmont, N.Y.) 4, 271-276.

Bauer, A.W., Kirby, W.M.M., Sherris, J.C., Turck, M., 1966. Antibiotic Susceptibility Testing by a Standardized Single Disk Method. American Journal of Clinical Pathology 45, 493-496.

Chapman, J.S., Georgopapadakou, N.H., 1988. Routes of quinolone permeation in *Escherichia coli*. Antimicrobial agents and chemotherapy 32, 438-442.

Cheesebrough, M., 2006. District laboratory practice in tropical countries, Part2, 2 ed. Cambridge University Press.

Chen, J.Y., Siu, L.K., Chen, Y.H., Lu, P.L., Ho, M., Peng, C.F., 2001. Molecular epidemiology and mutations at *gyrA* and *parC* genes of ciprofloxacin-resistant Escherichia coli isolates from a Taiwan medical center. Microbial drug resistance (Larchmont, N.Y.) 7, 47-53.

Chenia, H.Y., Pillay, B., Pillay, D., 2006. Analysis of the mechanisms of fluoroquinolone resistance in urinary tract pathogens. Journal of Antimicrobial Chemotherapy 58, 1274-1278.

Danilchanka, O., Pavlenok, M., Niederweis, M., 2008. Role of porins for uptake of antibiotics by *Mycobacterium smegmatis*. Antimicrob Agents Chemother 52, 3127-3134.

Drlica, K., 1990. Bacterial topoisomerases and the control of DNA supercoiling. Trends in genetics: TIG 6, 433-437.

Drlica, K., Malik, M., Kerns, R.J., Zhao, X., 2008. Quinolone-Mediated Bacterial Death. Antimicrobial Agents and Chemotherapy 52, 385-392.

Everett, M.J., Jin, Y.F., Ricci, V., Piddock, L.J., 1996. Contributions of individual mechanisms to fluoroquinolone resistance in 36 *Escherichia coli* strains isolated from humans and animals. Antimicrobial agents and chemotherapy 40, 2380-2386.

Gosling, R.J., Clouting, C.S., Randall, L.P., Horton, R.A., Davies, R.H., 2012. Ciprofloxacin resistance in *E. coli* isolated from turkeys in Great Britain. Avian pathology: journal of the W.V.P.A 41, 83-89.

Hooper, D., Wolfson, J., 1993. Mechanisms of bacterial resistance to quinolones, in: Hooper, D., Wolfson, J. (Eds.), Quinolone Antimicrobial Agents, 2nd ed. American Society for Microbiology, Washington, DC., pp. 97-119.

Hooper, D.C., 2000. Mechanisms of action and resistance of older and newer fluoroquinolones. Clinical Infectious Diseases 31, S24-S28.

Hooper, D.C., 2001. Mechanisms of action of antimicrobials: focus on fluoroquinolones. Clinical infectious diseases: an official publication of the Infectious Diseases Society of America 32 Suppl 1, S9-s15.

Hopkins, K.L., Davies, R.H., Threlfall, E.J., 2005. Mechanisms of quinolone resistance in *Escherichia coli* and *Salmonella*: recent developments. International journal of antimicrobial agents 25, 358-373.

Hopkins, K.L., Day, M., Threlfall, E.J., 2008. Plasmid-mediated quinolone resistance in *Salmonella enterica*, United Kingdom. Emerging infectious diseases 14, 340.

Hoshino, K., Kitamura, A., Morrissey, I., Sato, K., Kato, J., Ikeda, H., 1994. Comparison of inhibition of *Escherichia coli* topoisomerase IV by quinolones with DNA gyrase inhibition. Antimicrobial agents and chemotherapy 38, 2623-2627.

Jiménez Gómez, P.A., García de los Rios, J.E., Rojas Mendoza, A., de Pedro Ramonet, P., García Albiach, R., Reche Sainz, M.P., 2004. Molecular basis of quinolone resistance in *Escherichia coli* from wild birds. Can J Vet Res 68, 229-231.

Lindgren, P.K., Karlsson, Å., Hughes, D., 2003. Mutation rate and evolution of fluoroquinolone resistance in *Escherichia coli* isolates from patients with urinary tract infections. Antimicrobial agents and chemotherapy 47, 3222-3232.

Nakamura, S., Nakamura, M., Kojima, T., Yoshida, H., 1989. gyrA and gyrB mutations in quinolone-resistant strains of *Escherichia coli*. Antimicrobial Agents and Chemotherapy 33, 254-255.

Oram, M., Fisher, L.M., 1991. 4-Quinolone resistance mutations in the DNA gyrase of *Escherichia coli* clinical isolates identified by using the polymerase chain reaction. Antimicrob Agents Chemother 35, 387-389.

Ouabdesselam, S., Hooper, D.C., Tankovic, J., Soussy, C.J., 1995. Detection of gyrA and gyrB mutations in quinolone-resistant clinical isolates of *Escherichia coli* by single-strand conformational polymorphism analysis and determination of levels of resistance conferred by two different single gyrA mutations. Antimicrobial Agents and Chemotherapy 39, 1667-1670.

Patel, J., Franklin, R., George, M., Stephen, G., James, S., David, P., Robin, P., Mair, P., Sandra, S., Jana, M., Maria, M., John, D., Melvin, P., Barbara, L., 2016. Clinical Laboratory Standards Institute (CLSI); Performance standards for antimicrobial susceptibility testing; M100S, 26th ed, Pennsylvania 19087 USA.

Piddock, L.J., 1999. Mechanisms of fluoroquinolone resistance: an update 1994–1998. Drugs 58, 11-18.

Pruss, G.J., Franco, R.J., Chevalier, S., Manes, S., Drlica, K., 1986. Effects of DNA gyrase inhibitors in *Escherichia coli* topoisomerase I mutants. Journal of bacteriology 168, 276-282.

Randall, L.P., Coldham, N.G., Woodward, M.J., 2005. Detection of mutations in *Salmonella enterica gyrA*, *gyrB*, *parC* and *parE* genes by denaturing high performance liquid chromatography (DHPLC) using standard HPLC instrumentation. The Journal of antimicrobial chemotherapy 56, 619-623.

Redgrave, L.S., Sutton, S.B., Webber, M.A., Piddock, L.J., 2014. Fluoroquinolone resistance: mechanisms, impact on bacteria, and role in evolutionary success. Trends in microbiology 22, 438-445.

Ruiz, J., Casellas, S., Jimenez de Anta, M.T., Vila, J., 1997. The region of the *parE* gene, homologous to the quinolone-resistant determining region of the *gyrB* gene, is not linked with the acquisition of quinolone resistance in *Escherichia coli* clinical isolates. The Journal of antimicrobial chemotherapy 39, 839-840.

Sorlozano, A., Gutierrez, J., Jimenez, A., de Dios Luna, J., Martínez, J.L., 2007. Contribution of a new mutation in parE to quinolone resistance in extended-spectrum-beta-lactamase-producing *Escherichia coli* isolates. Journal of clinical microbiology 45, 2740-2742.

Strahilevitz, J., Jacoby, G.A., Hooper, D.C., Robicsek, A., 2009. Plasmid-mediated quinolone resistance: a multifaceted threat. Clinical microbiology reviews 22, 664-689.

Tawfeeq, H., Toufiq, A., M Ali, K., 2017. Incidence and Molecular Identification of *Escherichia coli* Harbouring Gentamicin Resistant Gene among Pregnant Women. Eurasian Journal of Science and Engineering 3.

Vila, J., Ruiz, J., Goni, P., De Anta, M., 1996. Detection of mutations in parC in quinolone-resistant clinical isolates of *Escherichia coli*. Antimicrobial Agents and Chemotherapy 40, 491-493.

Vila, J., Ruiz, J., Marco, F., Barcelo, A., Goni, P., Giralt, E., De Anta, T.J., 1994. Association between double mutation in *gyrA* gene of ciprofloxacin-resistant clinical isolates of *Escherichia coli* and MICs. Antimicrobial Agents and Chemotherapy 38, 2477-2479.

Willey, J., Sherwood, L., Woolverton, C.J., 2008. PRESCOTT, HARLEY, AND KLEIN'S MICROBIOLOGY, 7th ed. Colin Wheatley/Janice Roerig-Blong, New York.

Yamagishi, J.-i., Yoshida, H., Yamayoshi, M., Nakamura, S., 1986. Nalidixic acid-resistant mutations of the *gyrB* gene of *Escherichia coli*. Molecular and General Genetics MGG 204, 367-373.

Yoshida, H., Bogaki, M., Nakamura, M., Nakamura, S., 1990. Quinolone resistance-determining region in the DNA gyrase *gyrA* gene of *Escherichia coli*. Antimicrobial agents and chemotherapy 34, 1271-1272.

Yoshida, H., Bogaki, M., Nakamura, M., Yamanaka, L.M., Nakamura, S., 1991. Quinolone resistance-determining region in the DNA gyrase *gyrB* gene of *Escherichia coli*. Antimicrobial agents and chemotherapy 35, 1647-1650.

Yoshida, H., Kojima, T., Yamagishi, J.-i., Nakamura, S., 1988. Quinolone-resistant mutations of the *gyrA* gene of *Escherichia coli*. Molecular and General Genetics MGG 211, 1-7.

ZANCO Journal of Pure and Applied Sciences
The official scientific journal of Salahaddin University-Erbil
https://zancojournals.su.edu.krd/index.php/JPAS

ISSN (print):2218-0230**, ISSN (online):** 2412-3986**, DOI: http://dx.doi.org/10.21271/zjpas**

RESEARCH PAPER

Seroprevalence of anti-*Toxoplasma gondii* antibodies among women of childbearing age in Zakho City, Kurdistan Region/Iraq

[1]Sarwin Sultan Muhamad Mizuri , [2]Wijdan Mohammed Salih Mero
[1,2].Department of Biology, College of Science University of Zaxo, Kurdistan Region, Iraq.

A B S T R A C T:

Toxoplasma gondii is the causative agent of toxoplasmosis. That makes serious health problems among immunocompromised patients which comprise pregnant women as well. The present study aimed to investigate the seroprevalence of anti-*Toxoplasma gondii* Antibodies among women of childbearing age and their associations to some demographic factors in Zakho City, Kurdistan Region/Iraq. Blood samples were collected randomly from 630 women aged 15-45 which were divided into subgroups (15-20), (21-26), (27-32), (33-38) and (39-45) years after taking their consent for the detection of anti-*Toxoplasma* IgG and IgM antibodies. A special questioner sheet was designed for the study containing full information about each participant. The diagnoses were done using ELISA-IgG and IgM kits and Rapid Test (RT) method. The prevalence of anti-*Toxoplasma* antibodies was 78/630 (12.38 %), including 73 (11.58 %) for ELISA IgG, 4 (0.63 %) for ELISA IgM and 1 (0.15 %) for RT method. The age group 33-38 years and married females showed the highest seroprevalence of 19/93 (20.43 %), 67/535 (12.52 %), respectively using ELISA IgG. Statically there were significant relations regarding ages, educational status, contact with cats and consumption of undercooked meat. This investigation indicated that the seroprevalence of anti-*Toxoplasma* antibodies among women at childbearing age is still a high rate. Furthermore, the association of some risk factors must be taken into consideration and this requires the introduction of health education programs to the community.

KEY WORDS: *Toxoplasma gondii*; Seroprevalence; ELISA IgG/IgM; Zakho
DOI: http://dx.doi.org/10.21271/ZJPAS.32.3.9
ZJPAS (2020) , 32(3);75-84 .

1. INTRODUCTION:

Toxoplasma gondii, is an obligatory intracellular protozoan parasite with a cosmopolitan distribution, infecting human and other warm blooded animals and causing community health problems (Al-Kadassy *et al*., 2018). It is suggested that one-third of the global population is infected with this parasite, even though it is a latent form of a disease and is non-fatal (Dubey, 2010; Tenter *et al*., 2000).

* **Corresponding Author:**
Sarwin S.M. Mizuri
E-mail: sarwin.sultan@yahoo.com
Article History:
Received: 01/10/2019
Accepted: 04/12/2019
Published: 15/06 /2020

A high frequency of this disease has been reported between pregnant women and women of childbearing age from different parts of the world (Pappas *et al*., 2009). Many techniques have been used for detecting toxoplasmosis such as serological, histological, and molecular or their recombination. The serological tests include, indirect fluorescent antibody assay (IFA), the latex agglutination test (LAT), the indirect haemaglutination assay, Sabin–Feldman dye test, immunosorbent agglutination assay test (ISAAT), but the more common and accurate serological test is the enzyme linked immunosorbent assay (ELISA) (Frenkel, 1970; Remington *et al*., 1995; Mawlood, 2017). The seroprevalence rate of toxoplasmosis among women of childbearing age

in Zakho City, Kurdistan Region of Iraq was poorly studied, consequently, the purpose of this study was to estimate the seroprevalence of anti-*Toxoplasm gondii* antibodies among Women of childbearing age and their relation with some demographic factors (age, marital status, educational status, occupation, contact with cats, application of hygienic habit, and consumption of undercooked meat in Zakho city, Kurdistan Region/Iraq.

2. MATERIALS AND METHODS

2.1 Sample collection and processing

Six hundred and thirty blood samples were taken randomly from women at childbearing age, who visited Zakho Maternity Hospital after taking their consent and permission from health authority, during the period from July 2018 to July 2019, the women were divided into subgroups (15-20), (21-26), (27-32), (33-38) and (39-45) years. From each patient, 5 ml of blood was withdrawn, using a sterile disposable syringe; the collected blood was transferred to a clean tube, without anticoagulant, each tube was labeled clearly. From each participant full information was taken, included: age, occupation, residency, marital status, educational status, time of gestation in pregnant women, history of abortion, cat in neighbor, application of hygiene, and method of cooking meat. Each of the collected blood samples was transferred to centrifuge tube and centrifuged at 4000 rpm for 4 minutes, and then the separated serum was dispensed into two Eppendorf tubes using micropipette and stored at -20^{o}c until to be used. The seroprevalence of anti-toxoplasma IgG and IgM antibodies was determined using ELISA and RT techniques. The ELISA kits used were from Bioactiva diagnostica (Germany), The RT test cassette was from Bio Tina GmbH (Germany). The procedures were done according to the instructions supplied with the kit. The serological tests were performed in Zakho General Hospital/ Zakho City. Regarding ELISA test the sample was considered Positive: if the ratio >1.1, and it was considered Negative: if the ratio <0.9 for both IgG and IgM antibodies.

2.2 Statistical analysis of the data

The data were statistically treated using computer program (IBM-SPSS Static) version 19, besides, (Open-Epi) version (3.01) program achieved to detect chi-square and any significant differences of *T. gondii* seroprevalence in the tested groups. *P*-value 0.05 (5 %) demonstrated statistically significant (Sokel and Rohlf, 2009).

3. RESULTS

3.1 Seroprevalence of anti-*Toxoplasma gondii* antibodies using ELISA and RT

The overall seroprevalence of anti-*T. gondii* IgG and IgM antibodies were 78/630 (12.38 %) of the tested blood samples, using Enzyme-Linked Immunosorbent Assay (ELISA) and Rapid Test (RT). The maximum rate 73/78 (11.58 %) was recorded by ELISA for Anti- IgG Abs. Regarding IgM only 5/78 (0.79 %) sera samples were positive, 4 by ELISA and only one by RT that is why this result unnoticed in the tables. Statistically the difference between ELISA IgG/IgM and Rapid test was highly significant (*P-value*=<0.0000001) as presented in table (1).

Table 1. The overall seroprevalence of anti-*Toxoplasma gondii* antibodies by using ELISA and RT (No. =630).

Type of Test	No: of positive sample	% of positive
ELISA IgG	73	11.58
ELISA IgM	4	0.63
RT IgG	0	-
RT IgM	1	0.15

Total	78	12.38

X^2 =180.6 df=3 *P*-value= <0.0000001 Significant*

3.2 Seroprevalence of anti-*T. gondii* antibodies according to age:

Table (2) shows the seroprevalence of anti-*Toxoplasma* antibodies among women of different age groups. The maximum seroprevalence (20.43 %) was recorded for anti-IgG among the age group 33-38 years. The seroprevalence rate increased with age until the age of 38 years and then declined after age 39 yrs. Regarding IgM only 5 positive cases were recorded, four by ELISA and one by RT as indicated in Table (2). Furthermore, the maximum rate of ELISA IgM was found among age groups 15-20 and 33-34 years, which were (1.08 %) and (1.07 %), respectively. Whereas, the minimum rate (0.53 %) was recorded between the age group 21-26 years. statistically there were significant relationships among different age groups related to ELISA tests (P>0.05).

Table 2. The relation between seropositivity of anti-*T. gondii* antibodies and age by using ELISA

Age (years)	No: Tested	ELISA IgG+ No:	%	ELISA IgM+ No:	%
15-20	92	2	2.17	1	1.08
21-26	188	20	10.63	1	0.53
27-32	174	21	12.06	1	0.57
33-38	93	19	20.43	1	1.07
39-45	83	11	13.25	0	0
Total	630	73	-	4	-

X^2=16.63 df=8 *P*-value=0.03418 Significant*

3.3 Association between anti-*Toxoplasma gondii* Abs and marital status:

The maximum seroprevalence rate (12.52 %) for anti-*Toxoplasma* IgG a ntibodies was recorded among married women, followed by single women (6.31 %). Regarding ELISA IgM, the recorded cases (0.74 %) were among married women only as shown in Table (3).

Table 3. Seroprevalence of anti-*T. gondii* antibody marital status by using ELISA.

Marital status	No: tested	ELISA IgG+ No:	%	ELISA IgM+ No:	%
Married	535	67	12.52	4	0.74
Single	95	6	6.31	0	0

Total	630	73	11.58	4	-

X^2=3.838 df=2 *P*-value=0.1468 Non-Significant

3.4 The relation between anti-*Toxoplasma gondii* antibodies and educational status:

Concerning the educational status, the highest seroprevalence (17.75 %) was observed among illiterate, then decreased among women who studied until different school levels (11.98 %). On the other hand, the rate decreased among women who completed their university education (7.18 %). Regarding IgM antibodies, they were recorded at a rate of (1.16 %) among women with school education. Statistically, significant differences were observed among different educational level groups (*P*-value=0.02779) as revealed in table (4).

Table 4. Seropositivity of anti-*T. gondii* antibody and educational status by using ELISA.

Educational status	No:	ELISA IgG+		ELISA IgM+	
		No:	%	No:	%
Illiterate	107	19	17.75	0	0
High school	342	41	11.98	4	1.16
University level	181	13	7.18	0	0
Total	630	73	-	4	-

X^2=10.89 df=4 *P*-value=0.02779 Significant*

3.5 The Relation between seroprevalence of anti-*T .gondii* antibodies and occupation:

The seroprevalence of anti-*Toxoplasma* antibodies according to occupation, showed the maximum seroprevalence (16.66 %) of IgG among employed women, followed by students (12.90 %). On the other hand, the lowest seroprevalence (11.02 %) was observed among housewives. While IgM antibodies were recorded only among housewives (0.78 %). There was non-significant relation between the prevalence of the parasite and the occupation (P>0.05) as revealed in table (5).

Table 5. Seropositivity of anti-*T. gondii* Abs according to occupation by using ELISA

Occupation	No:	ELISA IgG+		ELISA IgM+	
		No:	%	No:	%
Housewife	526	58	11.02	4	0.76
Student	62	8	12.90	0	0
Employed	42	7	16.66	0	0
Total	630	73	11.58	4	-

X^2=2.071 df=4 *P*-value=0.7228 Non-Significant

3.6 The relation between seroprevalence rates of anti-*T. gondii* Abs and contact with cats

Table (6) shows the relationship between seroprevalence of anti-*T. gondii* antibodies and contact with cats. The results indicate that the highest rate of IgG was 39/237 (16.45 %) in women who had contacts with cats. While regarding ELISA IgM 3/237 (1.26 %) had a history of contact with cats. A significant difference noticed among both groups (*P-value*=0.003244).

Table 6. Seropositivity of anti-*T. gondii* Abs and contacts with cats by using ELISA

Cat Contact	No:	ELISA IgG+		ELISA IgM+	
		No:	%	No:	%
Yes	237	39	16.45	3	1.26
No	393	34	8.65	1	0.25
Total	630	73	-	4	-
X^2=11.46	**df=2**	***P*-value=0.003244**		**Significant***	

3.7 Association between seropositivity of anti-*T. gondii* Abs and consumption of undercooked meat

The seroprevalence rate of anti-*Toxoplasma* IgG antibodies was the highest (100 %) among women who consumed undercooked meat than others as shown in Table (7). While the IgM cases (0.64 %) were recorded among those who do not consume undercooked meat.

Statistically this difference was highly significant (*P*-value<0.0000001).

Table 7. Association between seropositivity of anti-*T. gondii* Abs and consumption of undercooked meat by using ELISA

Consumption Of undercooked Meat	No:	ELISA IgG+		ELISA IgM+	
		No:	%	No:	%
Yes	5	5	100	0	0
No	625	68	10.88	4	0.64
Total	630	74	-	4	-
X^2=38.46	**df=2**	***P*-value=0.0000001**		**Highly Significant***	

3.8 Association between prevalence of anti-*T. gondii* Abs and application of hygienic habit.

Table (8) shows the relationship between prevalence of anti-*Toxoplasma* and application of hygienic habit. The rate of ELISA IgG Abs was (3.84 %) among women who applied the hygienic habit, while the rate increased (11.92 %) among women who did not apply hygienic habit. In contrast, the ELISA IgM Abs only present among

women who do not apply hygienic habits (0.66 %). Statistically these differences were statistically non-significant between both groups (*P*-value=0.4083).

Table 8. The relation between seropositivity of anti-*T. gondii* Abs and application of hygienic habit

Application of hygienic habit	No:	ELISA IgG+		ELISA IgM+	
		No:	%	No:	%
Yes	26	1	3.84	0	0
No	604	72	11.92	4	0.66
Total	630	73	-	4	-

X^2=1.719 df=2 *P*-value=0.4083 Non-Significant

4. DISCUSSION

Nowadays, the importance of toxoplasmosis extended as opportunistic pathogens particularly in immunocompromised persons, which include; pregnant women, AIDS patients, immunosuppression organ transplant patients and malignant patients (James, 1989; Koltas *et al*., 1992; Breecher, 2004). Toxoplasmosis detection is very important particularly throughout pregnancy, for the reason that if a woman infected with toxoplasmosis for the first time during her pregnancy, the infection can pass to her fetus, and this leads to numerous severe consequences and damage of the fetus (Kadhim and Mohammed, 2011).

In the present study, the total prevalence of anti-*Toxoplasma* antibodies was 12.38 % which was lower than that reported by Al-Atroshi (2011) in Duhok City, she reported a rate of 37.8 % by using LAT, (27.7%) by using ELISA IgG and 0nly (0.4 %) by ELISA IgM. On the other hand, using the same test much higher rates of anti-*T. gondii* Abs were recorded by Akreyi (2008) and Hamad (2009) in Erbil City and Al-Ubaydi (2004) in Mosul City which was 8 (54.46 %) and 79 %, respectively. The result of anti IgG in the current study was 11.58 % this result is lower than that reported by Kadhim and Mohammed (2013) in Babylon province, as they reported a rate of 18.9 %. In the present study only 4 (0.63 %) samples were seropositive for anti-IgM among 630 samples; this rate was close to the study performed in the United Arab Emirates in which 3 IgM were detected among patients with fetal loss (Singh, 1998).

On the other hand, Al-Khafajy (2004) in Baghdad reported a very high rate (43.7 %) for IgM, in spontaneously aborted women. This high result could be due to the sources of the samples because in the present instruction the samples were collected randomly not only from spontaneously aborted women. The higher seroprevalence rates of anti-*Toxoplasma* Abs in women might be due to warmer and more humid weather in these parts of the country (Al-Doski, 2000). Regarding age, the highest percentage was seen among age group (33-38) which was 20.43 % for ELISA IgG. The maximum rate among this age group may be due to more exposure of these ages to the risk of infection sources that leads to chronic infection with this agent (Srirup *et al.*, 2011). Much higher rate (45.3 %) among nearly same ages (30-35) years and the minimum rate (14.6 %) among 16-20 years were reported by Al-Atroshi (2011) in Duhok city. The difference in both studies might be due to change in population as both were performed in the same province but during different periods.

On the other hand in a study carried out in Sanandaj City/ Iran, Fatollahpour (2016) reported the highest seroprevalence rate (68.5 %) of anti-*Toxoplasma* IgG Abs among women under the age of 25 years. Illiterate women showed the highest (17.75 %) seroprevalence rate of anti-*Toxoplasma* IgG Abs as compared to women with high school and university levels which were 11.98 % and 7.18 %, respectively. Similarly,

Jones *et al*. (2001) in United State of America and Hashemi and Saraei (2010) in Iran, both of them reported higher seroprevalence of toxoplasmosis in illiterate women and stated that lower levels of education were associated with an increased risk for toxoplasmosis. On the other hand, women with high level of education may have more awareness to adopt appropriate hygienic measures (Jones *et al*., 2001).

While, the present results contradict with many studies, such as Al-Atroshi and Mero (2013) in Duhok; Hamad and Kadir (2013) and Mawlood (2018) in Erbil; Fatollahpour (2016) in Iran, they did not find any significant association among different educational levels. In this study, the prevalence of anti-toxoplasmosis IgG Abs increased among employed women (16.66 %) followed by students and housewives which was 12.90 % and 11.02 %, respectively. This may be due to the type of jobs and poor application of hygienic habits. Additionally, not all housewives are illiterate and live in low socioeconomic levels besides not all employed women are educated. This outcome was highly contradicted with previous studies in Duhok, United State of America and in Erbil (Al-Atroshi, 2011; Jones *et al*., 2013; Mawlood, 2018), respectively they reported that housewives had greater proportion of anti-*Toxoplasma* Abs than students and employed women as they were exposed more to risk factors (handling contaminated raw meat, drinking raw milk, direct contact with oocysts through farming or gardening as well as the ingestion of the oocysts with inadequate washing of vegetables) than other women (Alvarado-Esquivel *et al*.,2009). Saida and Nooraldeen (2014) reported that vegetables had major epidemiological role for transmission of protozoan cyst and oocyst, toxoplasma oocyst revealed (18.3 %) in Erbil city. A significant relation was observed among seroprevalence rate and cat contacts since presences of felines increases the risk of this infection (Avelino *et al*., 2004). This consequence is similar to studies carried out by Al-Khaffaf (2001); Al-Delamy (2002); and Al-Ubaydi (2004) in Mosul City, (Hatam *et al.,* 2005) in Fasa/Iran, (Ayi *et al*., 2009) in Ghana, all of them observed significant relations between exposure to cat and prevalence rate of this disease. On the other hand, the present finding disagrees with the study of Cook *et al*. (2000) in Europe, Al-Atroshi (2011) and Al-Doski (2000) in Duhok; Al-Najjar (2005) and Al-Harbi (2009) in Mosul, they did not report any significant association between contacts with cats and infections. This could be attributed to the fact that now cats are not used for hunting mice, and they spend most of their time outside houses and are not allowed to enter kitchens (Al-Doski, 2000). In the present study the seroprevalence rate of anti-*Toxoplasma* IgG Abs was significantly higher (*p*-value=0.0000001) among women who eat undercooked meat than those who eat well cooked meat (100 %) and (10.88 %), respectively. While IgM Abs were reported at a low rate (0.64 %) only among women who did not consume undercooked meat, these women may be acquired the infection through another route. This result contradict with studies performed in Duhok City in Iraq, Brazil, Iran, Makkahcity in Saudia Arabia, Venezuela and in Ghana, in all of these studies they did not find any significant differences related to consuming uncooked meat (Al-Doski, 2000; Avelino *et al*., 2004; Hatam *et al*., 2005; Al-Harthi *et al*., 2006; Diaz-Suarez and Estevez, 2009; Ayi *et al*., 2009), respectively.

Correspondingly, this outcome agrees with the studies of some researchers in which they found significant association between consumption of raw meat and infection with toxoplasmosis by Al-Delamy, (2002) in Mosul; Studenicova *et al*. (2006) in Slovakia; Spalding *et al.* (2005) in Brazil; Baril *et al*. (1999) and Wilson and McAuley (1999) in France and Mead *et al.* (1999) in United State of America. They stated that in most of these countries the habit of eating undercooked meat is common especially in developed countries.

However, Al-Doski, (2000) in Duhok City in Iraq; Diaz-Suarez and Estevez, (2009) in Venezuela; Ayi *et al*. (2009) in Chana; Al-Harthi *et al*. (2006) in Makkah City in Saudia Arabia; Hatam, *et al*. (2005) in Iran, they stated that the habit of eating undercooked meat is rare in their community as compared with other countries like Europe and may be restricted to those who eat outdoors in restaurants. Regarding to the application of hygienic habits in this study, the seroprevalence of anti-toxoplasmosis IgG Abs among women who use appropriate hygienic measures such as using different cutting board for meats and vegetables and practicing recurrent washing of kitchen utensils and hands during cooking, washing fruits

and vegetables by using antiseptics and salt was 3.84 % lower than those who did not apply most of these measures (11.92 %) for IgG even though this difference was statistically non-significant (P>0.05), while IgM Abs were only present among women who did not apply hygienic methods, but it was at low rate (0.66 %). There is a strong relation between toxoplasmosis and the application of hygienic habit because sometimes the parasite infects women during cleaning the vegetables (Norouzi *et al*., 2017). This is in agreement with the study of Al-Atroshi (2011) in Duhok city in Iraq, she also reported higher seroprevalence rate of anti-toxoplasma Abs among women with poor application of hygienic methods. Also Fouladvand *et al*. (2010) in Iran reported that there was strong and significant relationship between seropositivity of anti-*Toxoplasma* Abs and washing the vegetables.

5.CONCLUSIONS

The present study showed that the total seroprevalence of anti-*Toxoplasma* Abs among women at childbearing age was 12.38) in Zakho City, the majority were seropositive for anti-*Toxoplasma* Abs by ELISA while only one IgM case was recorded by RT, indicating the high specificity of ELISA for diagnosis. Married women showed higher prevalence. The high risk factors contributed to infection with age (33-38 years), education (illiterate's status), occupation (employed group), and most contact with cats eating more undercooked meat and poor application of hygienic measures. Therefore, the community requires an introduction to health education program by health authority, especially for pregnant women.

ACKNOWLEDGMENTS

I wish to record my deep sense of gratitude and profound thanks to my supervisor Prof. Dr. Wijdan M.S. Mero for her keen interest and her inspiring guidance. I also wish to express my gratitude to the staff members of Zakho Maternity Hospital and Zakho General Hospital for their help during the study.

REFERENCES

Akreyi, R.S. (2008). Comparative pathological study of toxoplasmosis in placentae of women, ewes and does in Hawler (Erbil) area (Doctoral dissertation, M. Sc. Thesis, College of Veterinary Medicine, University of Dohuk).

Al- Atroshi, A.M. (2011). Seroprevalence of Toxoplasmosis among women of child- bearing age from different socioeconomic classes in Duhok city and some nearby villages. M.Sc. Thesis College of Education, University of Zakho.

Al-Atroshi, A.A.M and Mero, W.M.S. (2013). Seroprevalence of Anti -*Toxoplasma* Antibodies Among Women of Child Bearing Age in Duhok Province. Science Journal of University of Zakho. 1(1); 44-49.

Al-Delamy, L.H.A.M. (2002). Epidemiological, immunological and pathological study on the parasite casing toxoplasmosis in females of Ninevah Governorate and follow up study on the effect of some drugs on patients. M.Sc.Thesis, College of Science, University of Mosul.

Al-Doski, B (2000). Seroepidemiological study of Toxoplasmosis among different groups of population in Duhok city by using latex agglutination test and indirect hemagglutination test .M.Sc. Thesis. College of Medicine, University of Duhok.

Al-Harbi, A.A. (2009). Detection of anti-*Toxoplasma gondii* antibodies among patients with type 2 Diabetes Mellitus .M.Sc. Thesis, College of Medicine, University of Mosul.

Al-Harthi, S.A., Jamjoom, M.B., Ghazi, H.O. (2006). Seroprevalence of *Toxoplasma gondii* among pregnant women in Makkah, Saudi Arabia. Umm Al-Qura Univ. *J. Sci. Med. Eng*, 18(2): 217 -227.

Al-Kadassy, M.A., Baraheem, H.O., Bashanfer, S.A. (2018). Prevalence of *Toxoplasma gondii* infection in women of child-bearing age in faculty of Medicine and health sciences Hodeida City, Yemen. *The Pharma Innovation Journal*, 7(9): 256-261.

Al-Khafajy, A.H.M. (2004). Cytogenetic, Immunological and Biochemical Studies on Women Infected with *Toxoplasma gondii* with a history of abortion. M.Sc. Thesis. College of Medicine, Al-Nahrain University, Baghdad, Iraq.

Al-Khaffaf, F.H. (2001). Isolation and seroepidemiological study of toxoplasmosis among women in child-bearing age in Neneva- governorate. M.Sc. Thesis, College of Science, University of Mosul.

Al-Najjar, S.A. (2005). Detection of anti-*Toxoplasma* antibodies among patients with acute leukaemia or lymphoma using latex agglutination test and ELISA. M.Sc. Thesis, College of Medicine, University of Mosul, Iraq.

Al-Ubaydi, G. T. (2004).Toxoplasmosis in pregnant women and its relation with some parameters. M. Sc. Thesis. College of Science. University of Mosul.

Avelino, M.M., Júnior, D.C., Parada, J.B., Castro, M.A. (2004). Risk factors for *Toxoplasma gondii* infection in women of childbearing age. *Braz. J. Infect. Dis*., 8 (2).

Ayi, I., Edu, S.A.A., Apea-Kubi, K.A., Boamah, D., Bosompem, K.M., EDOH, D. (2009). Seroepidemiology of toxoplasmosis amongst pregnant women in the greater Accra Region of Ghana. *Ghana Med J*, 43(3): 107- 114.

Baril, L., Ancelle, T., Goulet, V., Thulliez, P., Tirard-Fleury, V., Carme, B. (1999). Risk factors for *Toxoplasma* infection in pregnancy: a case–control study in France. *Scand. J. Infect. Dis*, 31(3):305–309.

Breecher, M. (2004). Toxoplasmosis, www.helthatoz.com. https://docu.tips/documents/blood-bank-and-transfusion-5c1308fc614d4. {Visited on 27/11/2019}.

Cook, A.J.C., Gilbert, R.E., Buffolano, W., Zufferey, J., Petersen, E., Jenum, P.A. (2000). Sources of *Toxoplasma* infection in pregnant women: European multicentre casecontrol study. *B.M.J*, 321:142147.

Diaz-Suarez, O., Estevez, J. (2009). Seroepidemiology of toxoplasmosis in women of child-bearing age from a marginal community of Maracaibo, Venezuela .Rev. Inst. Med. trop. S. Paulo, 51(1):13-17.

Dubey, J.P. (2010). Toxoplasmosis of animals and humans. 2nd edition. Beltsville, Maryland: U.S.A. CRC Press, 3:112.

Fatollahpour, A.,Karbassi, G., Roshani, D., Ramezany, P., Mohammadbeigi, R. (2016). Sero- epidemiological study of TORCH infection in women of Childbearing age in West of Iran. Research Journal of Pharmaceutical, Biological and Chemical Sciences, 7(6): 1460-1465.

Fouladvand, M., Barazesh, A., Naeimi, B., Zandi, K., Tajbakhs, S. (2010). Seroprevalence of toxoplasmosis in high school girls in Bushehr city, South-west of Iran. *Afr. J. Microbiol. Res*, 4 (11): 1117-1121.

Frenkel, J.K. (1970). Pursuing Toxoplasma. *The Journal of Infectious Diseases*, 122 (6): 553–559.

Hamad, N.R. (2009). Epidemiology and comparison between the efficacy of different techniques for diagnosis of *Trichomonas vaginalis* and *Toxoplasma gondii* among women in Erbil Province-Iraqi Kurdistan. PhD. Thesis, Collage of Science, University of Salahaddin.

Hamad, N.R., Kadir, M.A. (2013). Prevalence and comparison between the efficacy of different techniques for diagnosis of *Toxoplasma gondii* among women in Erbil Province-Iraqi Kurdistan. *AIIC*, 901-908.

Hashemi, H. J. and Saraei, M. (2010). Seroprevalence of *Toxoplasma gondii* in unmarried women in Qazvin, Islamic Republic of Iran. *E Mediterr Health J*; 16 (1): 24-28.

Hatam, G.R., Shamseddin, A., Nikouee, F. (2005). Seroprevalence of toxoplasmosis in High School Girls in Fasa District, Iran. *Iran J. Immunol*, 2:177-81.

James, J.S. (1989). Toxoplasmosis, Cryptosporidiosis experimental treatments (not in USA), www.aids.org.

Jones, J. L.; Kruszon-Moran, D. and Wilson, M. (2003).*Toxoplasma gondii* infection in the United States, 1999–2000. *Emerg Infect Dis*, 9: 1371–1374.

Jones, J. L; Kruzon-Moran, D.; Wilson, M.; McQuillan, G.; Navin, T.; McAuley, J.B. (2001). *Toxoplasma gondii* in the United States seroprevalence and risk factors. *Am. J. Epidemiol;* 154: 357–365.

Kadhim, R. (2013). Seroprevalence of *Toxoplasma gondii* antibodies among pregnant women in Babylon Province, Iraq. *kufa Journal for Nursing sciences*. *Available at*: https://www.researchgate.net/publication/308984182.{visited on 28/11/2019}

Koltas, I.S., Tanrıverdi, S., Kara, H., Ozcan, K. and Yıldızer, K. (1992). The Investigation of *Toxoplasma gondii* antibodies using IFA and IHA. *Ann Med Sci*, 8:98-101.

Mawlood, H.H. (2018). A Comparative serological study and moleculer characterization of *Toxoplasma gondii* between Erbil city, Kurdistan region/ Iraq and Nashville city. State of Tennessee/USA. Ph.D. Thesis, Faculty of Science, University of Zakho.

Mawlood, H.H., Mero, W. M. S., Ismael, R. A. and Isa, A. M. (2017). Sero-prevalence of TORCH infections among pregnant and non-pregnant women using different Immunological techniques in Erbil city, Kurdistan region/Iraq. *ZANCO Journal of Pure and Applied Sciences*, 29(2).

Mead, P.S., Slutsker, L., Dietz, V., McCaig, L.F., Bresee, J.S., Shapiro, C., Griffin, P.M., Tauxe, R.V. (1999). Food-related illness and death in the United States. *Emerg. Infect. Dis*, 5: 607-624.

Norouzi, L.Y., Sarkari, B., Asgari, Q., Abdolahi, K.S. (2017). Molecular Evaluation and Seroprevalence of Toxoplasmosis in Pregnant Women in Fars province, Southern Iran. *Ann Med Health Sci Res*, 7 (1): 16-19.

Pappas, G., Roussos, N., Falagas, M.E. (2009). Toxoplasmosis snapshots: global status of *Toxoplasma gondii* seroprevalence and implications for pregnancy and congenital toxoplasmosis. *Int J Parasitol;* 39:1385-1394.

Remington, J.S., McLeod, R, Desmonts, G. (1995). Toxoplasmosis. In: JS Remington, JO Klein, eds. Infectious Disease of the Fetus and Newborn Infant. Philadelphia: W.B. Saunders Company, 140–267.

Saida, L.A and Nooraldeen, K.N. (2014). Prevalence of parasitic stages in six Leafy Vegetables in Markets of Erbil City, Kurdistan Region-Iraq. *Zanco Journal of Pure and Applied Sciences*, 26 (2): 25-30.

Singh, N. (1998). Status of *Toxoplasma* antibodies in recurrent fetal loss in U.A.E. women. *Indian J. Pediatr,* 65(6):891–897.

Sokal, R. R. and Rohlf, F. J. (2009). Introduction to Biostatistics. 2nd ed. Dover edition. pp: 366.

Spalding, S.M., Amendoeira, M.R., Klein, C.H., Ribeiro, L.C. (2005). Serological screening and toxoplasmosis exposure factors among pregnant women in South of Brazil. *Rev. Soc. Bras. Med. Trop*, 38(2):173-177.

Srirup, A.; Nibedita, D. and Pal, D. (2011). Seroprevalence and risk factors of *T. gondii* in pregnant women in Kolkata, India. *Journal of Recent Advance in Applied Science*, 26: 27-33.

Studenicova, C., Bencaiova, G., Holkova, R. (2006). Seroprevalence of *Toxoplasma gondii* antibodies in a healthy population from Slovakia. *E.J.I.M*, 17:470–473.

Tenter, A.M., Heckeroth, A.R., Weiss, L.M. (2000). *Toxoplasma gondii*: from animals to humans. *Int J Parasitol;* 30:1217–1258.

Wilson, M., McAuley, J.B. (1999). *Toxoplasma*. In: Murray, P.R.; Baron, E.J.; Pfaller, M.A.; Tenover, F.C. and Yolker, R.H. "Manual of clinical microbiology". 7th edition. American society for Microbiology, Washington, pp. 1374 – 1382.

ZANCO Journal of Pure and Applied Sciences
The official scientific journal of Salahaddin University-Erbil
https://zancojournals.su.edu.krd/index.php/JPAS

ISSN (print):2218-0230**, ISSN (online):** 2412-3986**, DOI: http://dx.doi.org/10.21271/zjpas**

RESEARCH PAPER

Nutritional Status of Children Under Five Years in Hassan Sham Camp in Mosul City in Iraq

Ayad Abdullah Rasheed[1],Salih Ahmid Abdullah[2], Nasih Abdulla Hossain Gardi[3]

1M.Sc.in community health nursing, Ministry of Health / Khabat health directorate.
2Ph.D. in community health nursing, College of Nursing / Hawler Medical University.
3Ph.D. in in internal medicine, College of Medicine / Hawler Medical University.

A B S T R A C T:

Background and objective: Adequate nutrition is essential in early childhood to ensure healthy growth, proper organ formation and function, a strong immune system, and neurological and cognitive development. Economic growth and human development require well-nourished populations who can learn new skills, think critically and contribute to their communities (WHO, 2010). The aim of study was to identify nutritional status of children under five years old in Hasan Sham camps in Mosul City in Iraq.

Methods: Quantitative design, cross-sectional descriptive study has been conducted to assess the health status of children under five years in Hasan sham camps Mosul City. The data were collected in July, 2017. So 322 children were chosen randomly out of 1300 children under five years old age. For the purpose of data collection, a questioner was designed according the needs of study that contained three part. Part one included questioner related to demographic characteristics, Part two included type of feeding, Part three contain Anthropometric measurement, Data were collected through using modified questionnaires was designed through extensive review of relevant literature.

Results: the study revealed that percentage of health problems was as followings: Chronic underweight 4%, Chronic stunting8%, Acute stunting 22%, Chronic wasting 1%, Acute wasting 7%.

Conclusion: study revealed that theirs not association between age groups and underweight, stunting, and wasting among children. And there is not association between gender and underweight, stunting, and wasting among children.

Keywords: Nutritional status, Hassan Sham Camp.

KEY WORDS: Fritillaria zagrica,Tulipa kurdica,Antioxidant,Antimicrobial Activity,TPC,TFC.
DOI: http://dx.doi.org/10.21271/ZJPAS.32.3.10
ZJPAS (2020) , 32(3);85-94 .

1.INTRODUCTION

The World Health Organization (WHO) defines malnutrition as "the cellular imbalance between supply of nutrients and energy and the body's demand for them to ensure growth, maintenance, and specific function (WHO, 2010)

* **Corresponding Author:**
Ayad Abdullah Rashid
E-mail: ayadabdulla1999@gmail.com
Article History:
Received: 11/11/2019
Accepted: 15/12/2019
Published: 15/06 /2020

Malnutrition serious health problems caused by a continuing or the body's poor absorption or use of nutrients. Malnutrition is often a result of food shortages or poverty (Roberta, 2000). Overweight and obesity are serious problems related to growth in U.S. children population (Clark, 2008). The prevalence of obesity in some developing countries has reached even higher levels than in many industrialized nations (WHO, 2000). Stunting is low height for age (Doak, et al., 2005). In the line of coexistence of stunting and overweight in children, these are risk factors for chronic diseases in adulthood (Frenk, et al., 1991; Moore, 2004).

Management of many chronic diseases that may develop due to the increased incidence of obesity would be beyond the capacity of many nations (Moore, 2004). It is equally important to identify the coexistence of both under nutrition and over nutrition, as an intervention that is designed to prevent only one problem could exacerbate the other (Uauy, and Kain, 2002). Growth indices in the form of length/height for age, weight for age, weight for height, and body mass index (BMI) for age are important tools for the assessment of nutritional status of children. The prevalence of nutritional indicators in the form of stunting, underweight, wasting, risk of overweight, overweight, and obesity in children under 5 years of age is one of the ways of assessment of nutritional status of the population and used as a nutritional surveillance indictors among this age group (De Onvs, et al., 1993) Concerning length/height for age; it can help identify children who are stunted or severely stunted due to prolonged under nutrition or repeated illness (chronic malnutrition). While weight for age; it is used to assess whether a child is underweight or severely underweight. On the other hand weight for length/height is especially useful in situations where children's ages are unknown (e.g. refugee situations). It helps identify children with low weight for height who may be wasted or severely wasted (acute malnutrition). Beside that, BMI for age is an indicator that is especially useful for screening for risk of overweight (WHO, 2008). overweight and obesity. weight gain and obesity are two common manifestation of hypothyroidism. (Baban, et al., 2017). fruit has a nutritional, industrial, pharmaceutical values (Majeed, et al., 2019).

General objective

To assess the nutritional status of children under 5 years in Syrian camps of Mosul City

Specific objectives are:

1-To provide a data base for nutritional assessment indicators among children under five years in Hassan Sham Camps.

2-To identify relationship between Anthropometric measurements and gender of Children.

3-To identify relationship between Anthropometric measurements and age of Children.

Research questionnaires and data:

1-Demographical data include (name of camp, Childs name, Gender, date of birth)

2-weight kg measurement.

3- Height Measurement.

4-Body mass index (BMI)

5- z-score

MATERIALS AND METHODS

2.1. Research design

Quantitative design, cross-sectional descriptive study was conducted to assess the nutritional status of children under 5 years in Hasan Sham camp in Mosul city.

2.2. Setting of the study

The study was conducted in Hasan Sham camp in Mosul City in Iraq.

2.3. Ethical consideration

Ethical consideration was a main principle of data collection. Permission has been take from ethical committee of nursing college Hawler Medical University, permission also taken for including the parents of children participate in the study.

2.4. Administrative arrangement

For the purpose of this study, a written of an official permission obtained from the scientific committee/College of Nursing/Hawler Medical University. The data collection and permission to conduct this study has been secured from General Directorate of Erbil Asaish,

2.5. Sample of the Study

(322) children were chosen randomly out of (1300) children under five years old age was calculated according to the formula .

2.6. Inclusion criteria

Children under 5 years old, and both gender male and female, parents who refused to participate and some children has chronic illness like congenital malformation which they cannot included the study.

2.7. Exclusion criteria

Children above 5 years old, parents who refused to participate their children in the study and some children has chronic illness like congenital malformation which they cannot included the study.

2.8 Sample size estimation

The sample size was calculated using the level of significance 95%, 5% degree of precision Population size of children under five years old age was 1300. Therefore, estimated sample size

was 322 and it was calculated according to the following formula.

Sample

$$n = \frac{\left(\frac{z}{d}\right)^2 \times (0.50)^2}{1 + \frac{1}{N}\left[\left(\frac{z}{d}\right)^2 \times (0.50)^2 - 1\right]}$$

z = confident interval 95% (1.96)
d = sampling error (0.05)
N = population size (1300)
n = Sample size = (322)
(Polit, and Hunger, 1999).

2.9. Distribution of samples by camps

1- *Hassan Sham* children 1day to 5 years old age = 322.

2.10. Duration of conducting the study

The study was conducted during the period of July, 2017. The data were collected during the period of 1st July, 2017 to 15th July, 2017.

2.11. Tools, Instrument and methods of data collection

A questionnaire was developed after extensive review of relevant literature, which consisted of:

2.11.1. Part one: Socio demographic data:

This part is concerned with socio demographic characteristics of children which include items such as age and sex.

2.11.2. Part two: anthropometric measurements

This part concerned with measurement of body height, weight to find out the cases of underweight, stunting, wasting, by using WHO schedule growth standard (WHO, 2007). There are two schedule one special for males and another for females formed by WHO growth standard to calculate Z score. The prevalence of moderate and severe underweight was defined as the number of children whose weight for age was below -2 and -3, respectively. Also, the prevalence of moderate and severe wasting and stunting was well-defined as the total of children with weight for height (wasting) or height for age (stunting) who were below -2 and -3.in present study used scale of body weight measurement, and wood scale

Weight in Kg, length/height in cm, age and sex data was used to calculate z-scores i.e. standard deviation score of the different nutritional indicators. Age was determined by months (exact age). Baby was weighted with minimum amount of clothing and the result was rounded to the nearest 50 grams. Measurements were carried out using WHO/Seca scale for infants and children scales were checked for zero error daily. Length/ Height was taken without shoes using wooden board for height measurements and wood board for length measurement, both of them are of WHO/Seca, and the figures was rounded to the nearest centimeter.

2.12. Pilot study

A pilot study was conducted from 1st July, 2017 to 15th July, 2017on 35 children under five years in Hassan sham camp from the samples of pilot study were excluded from the original study. Pre-test and post-test method was used to determine the readability of the questionnaire. The analysis of data was done via using correlation coefficient test this test revealed that there is no significant differences between both results (r = 0.88).

2.13. Pilot study were to:

1. Identify the reliability of questionnaire.
2. Determine the clarity and content acceptability of questionnaire
3. Identify the barriers and complication during data collection.
4. Identify the average time require for data collection.

2.13.1. Person coefficient correlation r-test

It was making to evaluate the reliability of questionnaire as following

r = correlation coefficient for variable x and y, if r = (± 1) =Perfect, (± 0.75–± 1) =Strong, (± 0.5–± 0.75) =Moderate (< 0.5) =Weak, (0) =no association.
n = number of cases (sample)
x = an individual score for variable x (test)
y = an individual score for variable y (retest)
∑ = summation of variables (test and retest), (Polit, and Hunger, 1999).

2.14. Validity

The questionnaire has been validated by panel of (25) experts in different specialty of nursing, medicine and statistics to investigate the content of questionnaire for clarity, relevancy and adequacy. A copy of the questionnaire was referred to each expert. The result had indicated that the common of the experts agreed upon the items of the study with few comments and suggestions which were all taken into attention. Modifications were employed and the final draft

of the instrument was complete to be suitable for conducting the study.

2.15. Statistical data analysis

Data was prepared, organized and entered into the computer. A statistical package for social sciences (SPSS, version 19) for windows was used to analyze the data categorical variable were described through frequency and percentages. The data were analyzed through the application of two approaches which are:

2.16.1. Descriptive data analysis approach

This approach is employed through:

Frequency and percentage

(Polit, and Hunger, 1999).

2.16.2 Inferential data analysis approach

This approach was presented through

Chi-square Test (X^2):

Chi-square test (X^2) was used to determine the significance association between socio demographic data (age and gender) with health condition results of children.

$$r = \frac{n(\sum xy) - (\sum x)(\sum y)}{\sqrt{[n\sum x^2 - (\sum x)^2][n\sum y^2 - (\sum y)^2]}}$$

(Polit, and Hunger, 1999).

P-value: the exact significance level of a statistical test that is the probability of obtaining a value of the test statistic that is at least as extreme as that observed when the null hypothesis is true. All statistical produces were tested on a probability of P. value were considered in following:

≤ 0.01 High significant (HS)
≤ 0.05 Significant (S)
>0.05 Non Significant (NS)
(Polit, and Hunger, 1999).

RESULTS AND DISCUSSION

3.1 Socio Demographical Characteristics of sample study:

3.1.1 Age group of children

Concerning Age group of children, table 1 shows that the highest percentage of age group was 1-14 which represent 39.5%, and the lowest age group was 43-56 which represent 13.6%.

3.1.2 Gender

Table 2 shows that the majority of the study sample was female which represent 51.7%. while the male group represent 48.3%.

3.1.1 Type of feeding of children

Concerning type of feeding of children, table 1 shows that the highest percentage of children was with breast feeding which represent 56.8%, and the lowest was food eating which represent 0.8%.

3.3 Anthropometric measurements

3.3.1 Underweight

Table 2 show the children with chronic underweight were represent 4%. While the number of children with acute moderate underweight was represented (10%).and representation of normal weight for age among children was 88%.

3.3.2 Stunting

Table 3 show the children with chronic stunting were represent (8%). While the While the number of children with acute stunting was represented (22%).and representation of normal weight for age among children was 67%.

3.3.3 Wasting

Table 4 show the children with chronic wasting were represents 1%. While the number of children with acute wasting was represented (7 %).and representation of normal height for weight among children was 87%.

3.4.1 Association between Anthropometric measurements of children and their weight for age group

Finding of the study show that there is not significant statistical association between weight for age of children and their age groups (P- value =0.444), This finding shown in table 29

3.4.2 Association between Anthropometric measurements of children and their Height for age group

Table 5 shows that was there is not significant statistical association between height for age of children and their age groups (P- value =0.470)

3.4.3 Association between anthropometric measurements of children and their Height for age group

Table 6 shows that was no significant statistical association between height for weight of children and their age groups (P- value =0.205).

3.5 Association between Anthropometric measurements of children and their gender

Finding of the study show that there is not significant statistical association between weight for age of children and their gender (P- value =0.893). No significant statistical association between height for age of children and their age gender (P- value =0.914), and no significant

statistical association between height for weight of children and their age groups (P- value =0.457). This finding shown in table 7. **DISCUSSION**

4.1 Socio-Demographic Characteristic of sample study:

4.1.1Age group

The highest age groups of Children were (1-14) which represent 39.5%

4.1.2 Gender

Concerning gender group of female children was represent 51.7%. While the male group represent 48.3%.

		F	%
Age group	1-14	102	39.5%
	15-28	73	28.3%
	19-42	48	18.6%
	43-56	35	13.6%
Gender	Male	125	48.3%
	Female	134	51.7%
Feeding	Breast feeding	147	56.8%
	Botol feeding	73	28.2%
	Breast and botol feeding	37	14.3%
	Only food eating	2	0.8%

Table 1: Distributions of the sample by age in months, gender and feeding type Socio-demographic characteristics

4.3 Anthropometric measurement

4.3.1 Underweight

In current study the finding reveals that children who had moderate underweight were 10%, and 4 % of children were had chronic underweight. This result is agreement the finding of another study that conducted in Erbil City which found that significant association between underweight and age group of Syrian refugee in Erbil city (Rasheed and Aziz, 2017). Additionally, the present study finding is Agree with finding of the Rapid Nutritional Assessment of under five children months in Syrian refugee camp located in Al-Anbar governorate/Al-Qa'im district in Iraq (UNICEF, 2012). The survey was carried out by the Nutritional Research Institute (NRI) / Ministry of Health-Iraq with the supported provided by UNICEF Iraq (UNICEF, 2012) who find the children with acute underweight which represented 7.6% and1.9% of children had chronic underweight (UNICEF, 2012).

			Age groups				
	1-14		15-28		19-42	43-56	Total
	F	%	F	%	F %	F %	F %
-3 chronic under weight	6	2	0	0	2 1	2 1	10 4
-2 acut modera te under weight	11	4	4	2	5 2	7 3	27 10
-1 normal weight	30	12	27	10	18 7	14 5	89 34
1 normal weight	5	2	3	2	1 0	1 0	10 4
Total	52	20	34	13	26 10	24 9	136 52

Table 3: Frequency and percentage of 259 children regarding their weight for age

4.3.2 Stunting.

In present study, the children who had acute stunting were 9%.and 4.5 % of children were had chronic stunting. Agree with report summarize the results of the Rapid Nutritional Assessment of under five children in Syrian refugee camp located in Al-Anbar governorate/Al-Qa'im district in Iraq. The survey was carried out by the Nutritional Research Institute (NRI) / Ministry of Health-Iraq with the supported provided by UNICEF Iraq, who find the children with acute stunting which represented 15.1% and5.3% of children had chronic stunting (UNICEF, 2012).

			age groups						
	1-14		15-28		19-42		43-56		
	F	%	F	%	F	%	F	%	Total
-3 chronic stuning	8	3	5	2	5	2	4	2	22 8
-2 Acute stuning	19	7	18	7	13	5	8	3	58 22

1 normal weight	38 15	31	12	16	6	12	5	97	37
0 Normal height	32 12	12	5	10	4	11	4	65	25
1 Normal height	3 1	3	1	3	1	0	0	9	3
2 normal height	1 0	4	2	1	0	0	0	6	2
Total	101 39	73	28	48	18	35	13	257	99

Table 4: Frequency and percentage of 363 children regarding their height for weight

4.3.3 Wasting

In current study the children who had acute wasting were 4.4%.and 1.1 % of children were had chronic wasting. Agree with report summarize the results of the Rapid Nutritional Assessment of under five children in Syrian refugee camp located in Al-Anbar governorate/Al-Qa'im district in Iraq. The survey was carried out by the Nutritional Research Institute (NRI) / Ministry of Health-Iraq with the supported provided by UNICEF Iraq (UNICEF, 2012). who find the children with acute wasting which represented 4.8% and2.2% of children had chronic wasting (UNICEF, 2012).

			Age groups					
	1-14		15-28		19-42	43-56		
	F	%	F	%	F %	F	%	Total
-3chronic wasting	2	1	0	0	0 0	0	0	2 1
-2 acute wasting	11	4	2	1	1 0	3	1	17 7
-1 normal height for weight	15	6	7	3	7 3	5	2	34 13
0 normal height for weight	67	26	60	23	40 15	25	10	192 74
Total	95	37	69	27	48 18	33	13	245 94

Table 4: Frequency and percentage of 363 children regarding their height for weight

4.9 Association between age and Anthropometric measurements

There is different factor affecting underweight ,stunting and wasting in children in camps which included poverty ,nutritional supplement in camps by polices ,organization like UN ,WHO, And perception, Religion ,culture ,diet habit of parents which affect significantly on children .

		Age group				Total	P-value
		1-14	15-28	19-42	43-56		
weight for age group	-3 under weight	6	0	2	2	10	0.444
	-2 acut under weight	11	4	5	7	27	
	-1normal weight	30	27	18	14	89	
	1normal weight	5	3	1	1	10	
Total		52	34	26	24	136	

Table 4: Association between Anthropometric measurements of children and their weight for age group

4.10 Association between age group and underweight

The finding of present study showed significant association between age group and underweight in children in camps. This finding agree with s report study summarize the results of the Rapid Nutritional Assessment of under five children in Syrian refugee camp located in Al-Anbar governorate/Al-Qa'im district in Iraq. The survey was carried out by the Nutritional Research Institute (NRI) / Ministry of Health-Iraq with the supported provided by UNICEF Iraq (UNICEF, 2012). which showed that there was statistical significant association between age group and underweight (UNICEF, 2012). This finding of the study agree with study done in Kenya by Badake, *et al.,* which showed that there was significant association between age group and underweight (Badake, *et al.,* 2014). Also agree with study of Nutritional Status and the Characteristics Related to Malnutrition in Children Under Five Years of Age in Nghean, Vietnam by Hien and Kam (2008) which showed that there was significant

association between age group and underweight (Hien, and Kam, 2008).

4.11 Association between stunting and age group

The finding in this reveals that there were significant association between age group and stunting in children in camps. This finding agree with study report study summarize the results of the Rapid Nutritional Assessment of under five children in Syrian refugee camp located in Al-Anbar governorate/Al-Qa'im district in Iraq. The survey was carried out by the Nutritional Research Institute (NRI) / Ministry of Health-Iraq with the supported provided by UNICEF Iraq (UNICEF, 2012). which showed that there was statistical significant association between age group and stunting. Also agree with study done in Kenya by Badake, *et al.,* which showed that there was significant association between age group and stunting (Badake, *et al.,* 2014). Also agree with study of Nutritional Status and the Characteristics Related to Malnutrition in Children Under Five Years of Age in Nghean, Vietnam by Hien and Kam (2008) which showed that there was significant association between age group and stunting (Hien, and Kam, 2008).

		Age group				Total	P-value
		1-14	15-28	19-42	43-56		
Height for age group	-3 chronic stunting	8	5	5	4	22	0.470
	-2 Acute stunting	19	18	13	8	58	
	1 normal weight	38	31	16	12	97	
	0 Normal height	32	12	10	11	65	
	1 Normal height	3	3	3	0	9	
	2 normal height	1	4	1	0	6	
Total		101	73	48	35	257	

Table 5: Association between age groups of children and their height for age group

4.12 Association between wasting and age group

The finding of present study showed significant association between age group and wasting in children in camps. This finding agree with s report study summarize the results of the Rapid Nutritional Assessment of under five children in Syrian refugee camp located in Al-Anbar governorate/Al-Qa'im district in Iraq. The survey was carried out by the Nutritional Research Institute (NRI) / Ministry of Health-Iraq with the supported provided by UNICEF Iraq, (2012) which showed that there was statistical significant association between age group and wasting prevalence (UNICEF, 2012). Agree with study done in Kenya by Badake, *et al.,* which showed that there was significant association between age group and wasting (Badake, *et al.,* 2014). Also agree with study of Nutritional Status and the Characteristics Related to Malnutrition in Children Under Five Years of Age in Nghean, Vietnam by Hien and Kam (2008) which showed that there was significant association between age group and wasting (Hien, and Kam, 2008).

		Age group				Total	P-value
		1-14	15-28	19-42	43-56		
Height for weight	3chronic wasting	2	0	0	0	2	0.205
	-2 acute wasting	11	2	1	3	17	
	-1 normal height for weight	15	7	7	5	34	
	0 normal height for weight	67	60	40	25	192	
Total		95	69	48	33	245	

Table 6: Association between age groups of children and their height for weight group

4.13 Association between age and Anthropometric measurements:

Thiers different factor affecting underweight ,stunting and wasting in children in camps which included poverty ,nutritional supplement in camps by polices ,organization like UN ,WHO, And perception, Religion ,culture ,diet habit of parents which affect significantly on children

4.14 Association between gender and underweight:

In presence study showed that there significant associated between gender and underweight females was significant more than males. This finding disagree with report study summarize the results of the Rapid Nutritional Assessment of under five children in Syrian refugee camp located in Al-Anbar governorate/Al-Qa'im district in Iraq. The survey was carried out by the Nutritional Research Institute (NRI) / Ministry of Health-Iraq with the supported provided by UNICEF Iraq (UNICEF, 2012). which showed that there was no statistical significant association between gender and underweight (UNICEF, 2012). Disagree with study done in Kenya by Badake, *et al.,* which showed that there was no significant association between gender and underweight (Badake, *et al.*, 2014). Agree with study of Nutritional Status and the Characteristics Related to Malnutrition in Children Under Five Years of Age in Nghean, Vietnam by Hien and Kam (2008) which showed that there was significant association between gender and underweight (Hien, and Kam, 2008).

4.15 Association between gender and stunting

In current study showed that there are no significant associated between gender and stunting. This finding agree with study report summarize the results of the Rapid Nutritional Assessment of under five children in Syrian refugee camp located in Al-Anbar governorate/Al-Qa'im district in Iraq. The survey was carried out by the Nutritional Research Institute (NRI) / Ministry of Health-Iraq with the supported provided by UNICEF Iraq (UNICEF, 2012) which showed that there was no statistical significant association between gender and stunting (UNICEF, 2012). Our study disagrees with study done in Kenya by Badake, *et al.,* which showed that there was significant association between gender and stunting who find that the prevalence of boys more than girls (Badake, *et al.,* 2014). Agree with study of Nutritional Status and the Characteristics Related to Malnutrition in Children Under Five Years of Age in Nghean, Vietnam by Hien and Kam (2008) which showed that there was no significant association between gender and stunting (Hien, and Kam, 2008).

		Gender		
		Male	Female	P-value
		Count	Count	
weight for age group	-3 under weight	4	6	0.893
	-2 acute under weight	14	13	
	-1normal weight	40	49	
	1normal weight	5	5	
Height for age group	-3 chronic stunting	12	10	0.914

	-2 Acute stunting	29	30	
	1 normal weight	48	49	
	0 Normal height	29	36	
	1 Normal height	5	4	
	2 normal height	2	4	
Height for weight	-3chronic	0	2	0.457
	-2 acute wasting	7	10	
	-1 normal height for weight	15	19	
	0 normal height for weight	96	97	

Table 7: Association between Anthropometric measurements of children and their gender

4.16 Association between gender and wasting

In our study showed that there are no significant associated between gender and wasting in children. This finding disagree with report study summarize the results of the Rapid Nutritional Assessment of under five children in Syrian refugee camp located in Al-Anbar governorate/Al-Qa'im district in Iraq. The survey was carried out by the Nutritional Research Institute (NRI) / Ministry of Health-Iraq with the supported provided by UNICEF Iraq, (2012) which showed that there was no statistical significant association between gender and wasting with higher prevalence in girls (UNICEF, 2012). Disagree with study done in Kenya by Badake, *et al.,* which showed that there was significant association between gender and wasting. who found that the prevalence of boys more than girls (Badake, *et al.,* 2014). Agree with study of Nutritional Status and the Characteristics Related to Malnutrition in Children Under Five Years of Age in Nghean, Vietnam by Hien and Kam (2008) which showed that there was no significant association gender and wasting (Hien, and Kam, 2008).

CONCLUSIONS

Through the course of data analysis and discussion of the health status of Children under five years in Syrian refugee camps, the study concluded that:

Concerning Age group of children, table 1 shows that the highest percentage of age group was 1-14 which represent 39.5%, and the lowest age group was 43-56 which represent 13.6%

1- The highest percentage of age group was 1-14 month which represents 39.5%, and the lowest age group was 43-56 month which represents 13.6%.

2-The majority of sample study was female.

3-The highest percentage of children was with breast feeding which represent 56.8%

4- Findings of the study show that the no significant statistical association between weight,

height, and height for weight for age of children and their age groups

5- Findings of the study show that the no significant statistical association between weight, height, and height for weight for age of children and their age groups.

Acknowledgements

Before all "great thank to God" the most glorious, most merciful, most Compassionate.

I would like to appreciate my grateful thanks to Ministry of Higher Education and Scientific Research, Hawler Medical University and College of Nursing for supporting this thesis. Grateful thanks are presented to all experts who have enriched the study questionnaire through their review and scientific recommendations. I am pleased to thank all my colleagues who assisted to finish this study especially Mr. Dara Al-BAnna,Mr.Sangar Al-gaff, Mr. Mohammed Hatam,and Mr. Jawdat Mamand Al-Hagbaker

References

Baban, A.A., Ahmed, S.A., Ahmed, B.S. and Hameed, S.A. (2017). Correlation between thyroid hormones and body weight in hypothyroid females in Erbil city. *Zanco Journal of Pure and Applied Sciences*, 29(5): 186-191.

Badake, Q.D., Maina, I., Mboganie, M.A., Muchemi, G., Kihoro, E.M., Chelimo, E. and Mutea, K., (2014). Nutritional status of children under five years and associated factors in Mbeere South District, Kenya. *African Crop Science Journal*, Vol. 22, Issue Supplement s4, pp. 799–806.

Clark, M J. (2008). Community Health Nursing Advocacy for population Health. 5th edition. p384.

De Onvs, M., Monteiro, C., Akrı, J. and Glugston, G. (1993). The worldwide magnitude of protein energy malnutrition: An overview from the WHO Global Database on Child Growth. *Bull World Health Organ*; 71(6):703-12.

Doak, C.M., Adair, L.S., Bentle, M., Monteiro, C. and Popkin, B.M. (2005). The dual burden household and the nutrition transition paradox. *Int J Obes*; 29(1):129-136

Frenk, J., Bobadilla, J., Stern, C., Frejka, T. and Lozano R. (1991). Elements for a theory of the health transition. *Health Transit Rev*. 1(1):21-38.

Hien, N.N. and Kam, S. (2008). Nutritional Status and the Characteristics Related to Malnutrition in Children Under Five Years of Age in Nghean, *Vietnam. J Prev Med Public Health*. 41(4):232-240.

Majeed, Z.R., Qasim, F.K. and Hassan, H.A. (2019). Hypotensive Action of Pomegranate Seed Extract and Zinc Chloride in Hypertensive Rats. *ZANCO Journal of Pure and Applied Sciences*, 31(5):44-52.

Moore, T.R, (2004). Adolescent and adult obesity in women: a tidal wave just beginning. *Clin Obstet Gynecol*. 47(4):884 -889, 980-981.

Polit, O. and Hunger, B. (1999), Nursing Research, Principle Methods 6th Edition. Philadelphia, Lippincott: 354-698

Rasheed, A.A. and Aziz, K.F. (2017). Health status of children under five years old age in Syrian refugee camps in Erbil city. The Second International Conference College of Medicine, HMU, 22nd - 24th November, 2017, Divan Hotel - Erbil - Kurdistan, Iraq .[Internet],Available.from http: https:/ /hmu.edu.krd/images/Medicine/Conference/2-11.pdf

Roberta, L.D., (2000). Nutrition and Wellness. Teacher's Annotated Edition. p81.

Uauy, R. and Kain, J., (2002). The epidemiological transition: need to incorporate obesity prevention into nutrition programmes. *Public Health Nutr*; 5(1A):223-229.

UNICEF, (2012). Rapid Nutritional Assessment of under five children in Syrian refugee camp located in Al-Anbar governorate/Al-Qa'im district in Iraq.[Internet], Available from file:///C:/Users/Future/Downloads/RapidNutritionalAssessmentforChildren6_59months%20(1).pdf

United Nations Refugee Agency, (2013). UNHCR Registration Trends for Syrians (02 April). Available at http://data.unhcr.org/syrianrefugees/country.php?id=103 (accessed 10 March 2013).

United Nations Refugee Agency, (2014a). UNHCR Registration Trends for Syrians (28 February). Available at http://data.unhcr.org/syrianrefugees/country.php?id=103 (accessed 1 March 2014).

United Nations Refugee Agency, (2014b). UNHCR Registration Trends for Syrians (05 March). Available at http://data.unhcr.org/syrianrefugees/country.php?id=103 (accessed 10 March 2014)

World Health Organization (WHO), (2007). Child Growth Standards and the National Center for Health Statistics/WHO international growth reference: implications. for. child. Healthprogrammes. www.ncbi.nlm. nih.gov/pmc/ articles /pmc3225111/#b18

World Health Organization, (2000). Obesity: Preventing and Managing the Global Epidemic. Report No.894; 23-28.

World Health Organization, (2002). Reducing risk, Promoting Healthy Life. The World Health Report: Geneva: WHO; 98-122.

World Health Organization, (2008). Training Course on Child Growth, WHO Child Growth Standards, Interpreting Growth Indicators. WHO, Geneva; 13-14.

World Health Organization, (2010). Malnutrition the Global Picture. WHO. http://www.who. int/home-page/. [cited 2010 Dec 10].

ZANCO Journal of Pure and Applied Sciences
The official scientific journal of Salahaddin University-Erbil
https://zancojournals.su.edu.krd/index.php/JPAS

ISSN (print):2218-0230**, ISSN (online):** 2412-3986**, DOI: http://dx.doi.org/10.21271/zjpas**

RESEARCH PAPER

Prevalence of infections with antibiotic-resistant Acinetobacter baumannii in different clinical samples from hospitals in Erbil

Sakar B. Smai[1] and Aryan R. Ganjo[2]

[1]Par Private hospital, Erbil, Kurdistan Region, Iraq

[2]Department of Pharmacognosy, College of Pharmacy, Hawler Medical University, Erbil, Kurdistan Region, Iraq.

A B S T R A C T:

Drug-resistant *Acinetobacter baumannii* is one of the important pathogen causing nosocomial infections. This pathogen is becoming resistant to a large group of antimicrobial agents, leading to a high rate of mortality and morbidity. The aim of the study was to determine the prevalence of *Acinetobacter baumannii* isolates from different clinical samples and analyze its antibiotic susceptibility profiles, and pathogenic perspective. During the period of study from November 2016 to December 2017, different clinical specimens including (urine, wound swab, burn, sputum and blood) obtained from patients hospitalized in Par private hospital and Rizgari teaching hospital in Erbil city. Conventional microbiological methods were used for identification of *A. baumannii*. Antibiotic susceptibility testing was performed by the method commended by the Clinical Laboratory and Standards Institute (CLSI). *A. baumannii* nosocomial infection was increasing especially in patients with risk factors, the current study showed that sputum isolates are the most frequently encountered 20 (51.3%) followed by others. The prevalence of *A. baumannii* according to person's gender among the 39 positive growth 25(17.1%) were from males and 14(12.3%) from females. The study revealed that there was an increase in antimicrobial resistance, most of the isolates even non susceptible to carbapenems with the exception of colistin that had an effective rule in comparison with the others. The study showed that the incidence of multi-drug resistance *A. baumannii* was high and the rate of resistance in A. baumannii to carbapenems was rising. Most isolates of *A. baumannii* were multi-resistance against antibiotics.

KEY WORDS: *Acinetobacter baumannii*, Carbapenems, Multi-drug resistance, Nosocomial infections
DOI: http://dx.doi.org/10.21271/ZJPAS.32.3.11
ZJPAS (2020) , 32(3);95-100 .

1. INTRODUCTION

Acinetobacter baumannii has emerged as a prominent cause of nosocomial infections, particularly in intensive care units (ICUs), initiating a variety of infections including respiratory tract infection, septicemia, urinary tract infections and wound infections (Al-Dabaibah *et al*., 2012, Aljindan *et al*., 2015)

The nosocomial infection is the infection that happens after 48 hours of admission of patients in the hospital, shortly after hospitalization, and on entrance moment the patient did not have such an infection (Amini *et al*., 2012, Khaledi *et al*., 2017). Hospital-acquired infections can cause increased patient morbidity and mortality, affect the achievement of initial illness treatment, prolonged hospital stay which then causes additional budgets for the health care system (Ozdemir *et al*., 2011, Armin et al., 2015). The opportunity of *A. baumannii* isolation from hospitalized patients is related to some essential factors, such as colonization of bacteria in the environment, medical staff-to-patient and patient-to-patient proportion (Almaghrabi *et al*., 2018).

* **Corresponding Author:**
Aryan R. Ganjo
E-mail: aryan.ganjo@hmu.edu.krd
Article History:
Received: 30/12/2018
Accepted: 16/12/2019
Published: 15/06 /2020

Acinetobacter spp. has been everywhere especially in healthcare set up. This microorganism inhabits mucous membranes and human soft tissues and can infect the patient's skin, nervous system, respiratory tract, blood, and urinary tract (Begum *et al*., 2013, Sarhaddi *et al*., 2017). Over recent decades *Acinetobacter* spp. acquired resistance to multiple antimicrobial agents and displayed extraordinary capability to develop different mechanisms of resistance that lead to multidrug resistance (MDR) and cause extended outbreaks (Farshadzadeh *et al*., 2015). The resistant to multiple classes of antibiotics becoming unsuccessful in the treatment of numerous *A. baumannii* isolates (Xie *et al*., 2018). The aim of the current study was to estimate the occurrence of in *A. baumannii* isolated from the patients at two hospitals in the Erbil city. In addition, we also aimed to characterize to antibiotic resistance patterns of *A. baumannii*.

1. MATERIALS AND METHODS

A total of 260 consecutive clinical specimens were recovered during November 2016 to December 2017 from different specimens including sputum, wound swab, burn, urine, blood and body fluids submitted to the microbiology laboratory in Rizgari teaching hospital and Par private hospital. All isolates were identified to the species level by conventional biochemical and microbiological methods and confirmed using Vitek II techniques. Patients who were hospitalized with signs and symptoms of infection were involved in the study. The demographic data of patients concerning gender, signs, and symptoms were collected (Dhabaan *et al*., 2011, Lusignani *et al*., 2017). The antimicrobial susceptibility testing was accomplished by the Kirby–Bauer disc diffusion method on Mueller–Hinton agar with colistin (10µg), imipenem (10µg), amikacin (30µg), ciprofloxacin (5µg), meropenem (10µg), ceftazidime (30µg), gentamicin (10µg), tobramycin (10µg), cefepime (30µg), and piperacillin/tazobactam (TZP) (100/10µg), according to the Clinical and Laboratory Standards Institute CLSI, 2017 guidelines (CLSI, 2017).

Statistical Analysis:

The statistical analysis was performed using the SPSS Statistics [version22]. The data were presented as percentages; Chi-square was used to calculate significance for frequencies. A *p* value of less than 0.05 was regarded as statistically significant.

2. RESULTS AND DISCUSSION

Among 260 patients with a nosocomial infection which were detected during this period 39 patients were infected by *A. baumannii*. In the current study, patients who received aggressive antimicrobial agents were more disposed to infection with *A. baumannii* than other patients. This study showed that sputum isolates are the most frequently encountered 20 (7.7%), burn 7(2.7%), wound swab 5(1.9%), blood 4(1.5%), 2(0.8%) for urine finally 1(0.4%) was for pus.

Out of (260) isolates the proportion of male were (146) and females were (114) There is no significant difference between male and female among all (260) isolates *p* 0.182. After the interpretation of the data we found that the prevalence of *A. baumannii* according to person's gender among the 39 positives, 25(17.1%) were from males and 14(12.3%) from females. In the present study, the higher rate of *A. baumannii* was found in male compared to females.

Table 1: The Prevalence of *A. baumannii* in different clinical specimens

Patient	No and % *A. baumannii* isolates						Total
	Sputum	Burn	Wound swab	Blood	Urine	Pus	
Infected	20	7	5	4	2	1	39
	7.7%	2.7%	1.9%	1.5%	0.8%	0.4%	15 %
Uninfected	39	30	40	31	48	33	221
	15%	11.5%	15.4%	11.9%	18.4%	12.7%	85 %
Total	59	37	45	35	50	34	260

Table 2: Distribution of *A. baumannii* in relation with gender in different clinical specimens among infected and uninfected specimens:

	Infected	Uninfected	Total	*P* Value
Male	25 9.6%	121 46.5%	146 56.1%	0.182
Female	14 5.4%	100 38.5%	114 43.9%	
Total	39 15%	221 85%	260 100%	

Table 3: Distribution of *A. baumannii* isolates from different samples, by patient's gender

Patient	No. and % *A. baumannii* isolates						Total	*P* value
	Sputum	Burn	Wound swab	Blood	Urine	Pus		
Male	15	3	3	3	1	0	25	0.431
	5.75%	1.15%	1.15%	1.15%	0.4%	0%	9.6%	
Female	5	4	2	1	1	1	14	
	1.9%	1.5%	0.8%	0.4%	0.4%	0.4%	5.4%	
Total	20	7	5	4	2	1	39	
	7.7%	2.7%	1.9%	1.5%	0.8%	0.4%	15%	

The results of the susceptibility profile of 39 *A. baumannii* clinical isolates to the examined antibiotics were obtained. In the present study, most isolates of *A. baumannii* showed nonsusceptible against routine antimicrobial agents, although colistin was more effective. Interestingly carbapenem presents as the non-effective antibiotics during the study. It is obvious that *A. baumannii* isolates showed high resistance (97.4%) to ciprofloxacin, (89.74%) to amikacin and (87.17%) to imipenem

The resistance pattern differed across samples of different sources. In addition, antibiotic resistance was lowest with colistin 100% susceptible Table 4.

Table 4: Resistance pattern of *Acinetobacter baumannii isolates* from different clinical samples

Antibiotics	Sputum (*n*=20)	Burn (*n*=7)	Wound (*n*=5)	Blood (*n*=4)	Urine (*n*=2)	Pus (*n*=1)	Total (*n*=39)
Piperacillin /tazobuctum	20 (100 %)	7 (100%)	5 (100%)	4 (100 %)	2 (100 %)	1(100 %)	39 (100%)
ceftazidime	20 (100 %)	7 (100%)	5 (100%)	4 (100 %)	2 (100 %)	1(100 %)	39 (100%)
imepinem	17(85 %)	6 (85.8 %)	5(100 %)	3(75 %)	2(100 %)	1(100 %)	34(87.1 %)
meropenem	19(95 %)	7 (100%)	5 (100%)	4 (100 %)	2 (100 %)	1(100 %)	38(97.5 %)
amikacin	18(90 %)	6(85.8 %)	5(100 %)	3(75 %)	2(100 %)	1(100 %)	35(89.8 %)
tobramycine	20 (100 %)	7 (100%)	5 (100%)	4 (100 %)	2 (100 %)	1(100 %)	39 (100%)
trimeth/sulfa	20 (100 %)	7 (100%)	5 (100%)	4 (100 %)	2 (100 %)	1(100 %)	39 (100%)
colistin	0%	0%	0%	0%	0%	0%	0 %
cefepeme	20 (100 %)	7 (100%)	5 (100%)	4 (100 %)	2 (100 %)	1(100 %)	39 (100%)
gentamicin	20 (100 %)	7 (100%)	5 (100%)	4 (100 %)	2 (100 %)	1(100 %)	39 (100%)
ciprofloxacin	19(90 %)	7(100 %)	5(100 %)	4(100 %)	2(100 %)	1(100 %)	38(97.5 %)

The increase in global reports of *A. baumannii* and antimicrobial resistance accompanying, particularly in the health-care-associated infections and the majority of hospital infections has elevated an alarm (Pourhajibagher *et al*., 2016, Odsbu *et al*., 2018), specifically in critical care areas, which are responsible for the most severe nosocomial outbreaks (Moradi *et al*., 2015) Many studies have revealed that *A. baumannii* which has emerged worldwide as a pathogen causing serious infections in the hospital has the capability to persist in the hospital milieu for a long period of time, colonize subjects and can progress into a true pathogen at any time (Uwingabiye *et al*., 2016). Infections caused by *A. baumannii* have an undesirable impression on clinical consequences and treatment expenses. *A. baumannii* creates many health problems in hospitals (Armin *et al*., 2015). Results of our study indicated that respiratory tract infections were the most common type of clinical isolates of *A. baumannii*, which has also been observed in earlier studies (Saed *et al*., 2015). Frequently of respiratory infection associated with mechanical ventilation, endotracheal intubation, and intra vascular catheter (Raka *et al*., 2009).

Developing of multi-drug resistant *A. baumannii* in the hospital could be due to lack of proper infection-control performance, the patient's normal bacterial flora under the aggressive antibiotics, or contaminated instruments, and overcrowding situations in the hospitals. In the present study, the higher rate of *A. baumannii* was found in male compared to females as in Table 2, 3, which is in agreement with observations in previous studies due to their exposing to the bacteria in environments (Oncul *et al*., 2009, Batarseh *et al*., 2015, Hatami, 2018). The predominance of male patients infected with *Acinetobacter* has been confirmed in other studies but the cause is not justified (Uwingabiye *et al*., 2016).

Our Laboratory results displayed isolates of *A. baumannii* have become resistant against most of frequently prescribe antimicrobial agents including aminoglycosides, cephalosporins, quinolones, and extended-spectrum penicillins Figure 1. As described by other researchers (Begum *et al*., 2013, Xie *et al*., 2018). These findings which are in general similar to the results of studies in Jordan, Iran, and China (Dhabaan *et al*., 2011, Sarhaddi *et al*., 2017, Jiang *et al*., 2014). In our study, according to antimicrobial susceptibility test results, a considerable amount of *A. baumannii* isolates over (85%) were resistant to imipenem and meropenem suggesting that carbapenems are inappropriate for the treatment of *A. baumannii* infections anymore.

Over the decades, carbapenems have been measured as the best therapeutic choice for infections caused by drug-resistant *A. baumannii*. In this research, 87.1 % and 97.4% of the isolates were resistant to imipenem and meropenem respectively, which was the great resistance rate compared with other studies. Many researchers described Carbapenems (imipenem, meropenem) remain one of the most important therapeutic options for these infections despite carbapenem-resistant *A. baumannii* reaching an alarmingly high level in some countries (Uwingabiye *et al*., 2016), such as China (97.6%%), Islamic Republic of Iran (97.7%), and Morocco (87.7%) (Jiang *et al*., 2014, Amini *et al*., 2012, Uwingabiye *et al*., 2016). However, *A. baumannii* resistance to imipenem and meropenem is still low in other investigations as Turkey 53.3% and 46.7% respectively (Ozdemir *et al*., 2011). Jordan (70.1 and 71.6%, respectively) (Dhabaan *et al*., 2011) for imipenem and meropenem.

In general, the resistance rate usually varies over time, even in countries. Further studies are needed to elucidate the cause of these differences. The resistant of *A. baumannii* to carbapenem in clinical isolates is a serious threat, suggesting that if carbapenem is overused, early interruption of treatment, lead to rapid increase in resistance and treatment failure are likely to happen (Ganjo *et al*., 2016). For carbapenem-resistant *A. baumannii*, colistin is one of the most persistently used alternative agents according to the Behera (Behera *et al*., 2017). Colistin is still considered to be the most effective single antimicrobial agents against multi-drug resistant *A. baumannii*, and is always reserved as a last resort of antibiotic (Hatami, 2018).

In the present study, the resistance rate of isolates to colistin was (0%), studies in Turkey and Iran (Ozdemir *et al*., 2011, Sarhaddi *et al*., 2017), reported the antibiotics with the highest *in vitro* susceptibility was colistin, 100 % susceptible against *A. baumannii* other data reported from Jordan (1.7%), and (0.5%) in Saudi Arabia (Batarseh *et al*., 2015, Al-Mously, 2013). In contrast, a study from Iran (Sepahvand *et al*., 2015) reported that 6% of the isolates were resistant to colistin which was a higher rate of resistance when compared with our result.

Resistance pattern of each antimicrobial agent (except for colistin) for *A. baumannii* in different clinical specimens was all above 50% (Table 4). The sensitivity of all clinical isolates was 100% for colistin. Indiscriminate use of antibiotics in the hospitalized patients, delay in hospital discharge, prolonged use of catheters, organ implants lead to extent resistant bacteria that colonized in susceptible patients (Amini *et al*., 2012).

An appropriate strategy required to manage protocols of infection control or encourage medical staffs to use the best therapeutic choices, that resulting in short hospitalization, increase survival rate, reduced financial cost, and control the spread of multi- drug resistant *A. baumannii*.

3. CONCLUSIONS

This study highlights the extraordinary incidence of drug resistance among clinical *A. baumannii* isolates in our hospitals. The occurrence of drug resistance *A. baumannii* is a serious worldwide threat to community and

healthcare settings that indications to increased length of hospitalization, mortality and medical costs. The surveillance data, as well as strict control of infection in the hospital environment, are necessary to struggle infections caused by resistance strains of *A. baumannii*.

Conflict of interest

None declared conflicts of interest.

References

AL-DABAIBAH, N., OBEIDAT, N. M. & SHEHABI, A. A. 2012. Epidemiology features of Acinetobacter baumannii colonizing respiratory tracts of ICU patients. *The International Arabic Journal of Antimicrobial Agents*, 2.

AL-MOUSLY, N. 2013. Acinetobacter baumannii bloodstream infections in a tertiary hospital: Antimicrobial resistance surveillance. *International Journal of Infection Control*, 9.

ALJINDAN, R., BUKHARIE, H., ALOMAR, A. & ABDALHAMID, B. 2015. Prevalence of digestive tract colonization of carbapenem-resistant Acinetobacter baumannii in hospitals in Saudi Arabia. *Journal of medical microbiology*, 64**,** 400-406.

ALMAGHRABI, M. K., JOSEPH, M. R., ASSIRY, M. M. & HAMID, M. E. 2018. Multidrug-Resistant Acinetobacter baumannii: An Emerging Health Threat in Aseer Region, Kingdom of Saudi Arabia. *Canadian Journal of Infectious Diseases and Medical Microbiology*, 2018.

AMINI, M., DAVATI, A. & GOLESTANIFARD, M. 2012. Frequency of nosocomial infections with antibiotic resistant strains of acinetobacterspp. In icu patient. *Iranian Journal of Pathology*, 7**,** 241-245.

ARMIN, S., KARIMI, A., FALLAH, F., TABATABAII, S. R., ALFATEMI, S. M. H., KHIABANIRAD, P., SHIVA, F., FAHIMZAD, A., RAHBAR, M. & MANSOORGHANAII, R. 2015. Antimicrobial resistance patterns of Acinetobacter baumannii, Pseudomonas aeruginosa and Staphylococcus aureus isolated from patients with nosocomial infections admitted to tehran hospitals. *Archives of Pediatric Infectious Diseases*, 3.

BATARSEH, A., AL-SARHAN, A., MAAYTEH, M., AL-KHATIREI, S. & ALARMOUTI, M. 2015. Antibiogram of multidrug resistant Acinetobacter baumannii isolated from clinical specimens at King Hussein Medical Centre, Jordan: a retrospective analysis. *Eastern Mediterranean Health Journal*, 21.

BEGUM, S., HASAN, F., HUSSAIN, S. & SHAH, A. A. 2013. Prevalence of multi drug resistant Acinetobacter baumannii in the clinical samples from Tertiary Care Hospital in Islamabad, Pakistan. *Pakistan journal of medical sciences*, 29**,** 1253.

BEHERA, I. C., SWAIN, S. K. & CHANDRA, M. 2017. Incidence of colistin-resistant Acinetobacter baumannii in an Indian tertiary care teaching hospital. *IJAR*, 3**,** 283-286.

CLINICAL AND LABORATORY STANDARDS INSTITUTE (2017). *Methods for dilution antimicrobial susceptibility tests for bacteria that grow aerobically. Approved standard M07-A10, Wayne, PA*.

DHABAAN, G. N., HAMIMAH, H. & SHORMAN, M. 2011. Emergence of extensive drug-resistant Acinetobacter baumannii in North of Jordan. *African Journal of Microbiology Research*, 5**,** 1070-1074.

FARSHADZADEH, Z., HASHEMI, F. B., RAHIMI, S., POURAKBARI, B., ESMAEILI, D., HAGHIGHI, M. A., MAJIDPOUR, A., SHOJAA, S., RAHMANI, M. & GHARESI, S. 2015. Wide distribution of carbapenem resistant Acinetobacter baumannii in burns patients in Iran. *Frontiers in microbiology*, 6**,** 1146.

GANJO, A. R., MAGHDID, D. M., MANSOOR, I. Y., KOK, D. J., SEVERIN, J. A., VERBRUGH, H. A., KREFT, D., FATAH, M., ALNAKSHABANDI, A. & DLNYA, A. 2016. OXA-carbapenemases present in clinical acinetobacter baumannii-calcoaceticus complex isolates from patients in kurdistan region, Iraq. *Microbial Drug Resistance*, 22**,** 627-637.

HATAMI, R. 2018. The frequency of multidrug-resistance and extensively drug-resistant Acinetobacter baumannii in west of Iran. *Journal of Clinical Microbiology and Infectious Diseases*, 1.

JIANG, M., ZHANG, Z. & ZHAO, S. 2014. Epidemiological characteristics and drug resistance analysis of multidrug-resistant Acinetobacter baumannii in a China hospital at a certain time. *Pol J Microbiol*, 63**,** 275-81.

KHALEDI, A., ELAHIFAR, O., VAZINI, H., ALIKHANI, M. Y., BAHRAMI, A., ESMAEILI, D. & GHAZVINI, K. 2017. Increasing Trend of Imipenem-Resistance Among Acinetobacter baumannii Isolated From Hospital Acquired Pneumonia in Northeast of Iran. *Avicenna Journal of Clinical Microbiology and Infection*, 4.

LUSIGNANI, L. S., STARZENGRUBER, P., DOSCH, V., ASSADIAN, O., PRESTERL, E. & DIAB-ELSCHAHAWI, M. 2017. Molecular epidemiology of multidrug-resistant clinical isolates of Acinetobacter baumannii. *Wiener klinische Wochenschrift*, 129**,** 816-822.

MORADI, J., HASHEMI, F. B. & BAHADOR, A. 2015. Antibiotic resistance of Acinetobacter baumannii in Iran: a systemic review of the published literature. *Osong public health and research perspectives*, 6**,** 79-86.

ODSBU, I., KHEDKAR, S., KHEDKAR, U., NERKAR, S. S., TAMHANKAR, A. J. & STÅLSBY LUNDBORG, C. 2018. High Proportions of Multidrug-Resistant Acinetobacter spp. Isolates in a District in Western India: A Four-Year Antibiotic Susceptibility Study of Clinical Isolates.

International journal of environmental research and public health, 15**,** 153.

ONCUL, O., ULKUR, E., ACAR, A., TURHAN, V., YENIZ, E., KARACAER, Z. & YILDIZ, F. 2009. Prospective analysis of nosocomial infections in a burn care unit, Turkey. *Indian J Med Res*, 130**,** 758-64.

OZDEMIR, H., KENDIRLI, T., ERGUN, H., ÇIFTÇI, E., TAPISIZ, A., GURIZ, H., AYSEV, D., İNCE, E. & DOGRU, U. 2011. Nosocomial infections due to Acinetobacter baumannii in a pediatric intensive care unit in Turkey. *Turk J Pediatr*, 53**,** 255-60.

POURHAJIBAGHER, M., HASHEMI, F. B., POURAKBARI, B., AZIEMZADEH, M. & BAHADOR, A. 2016. Antimicrobial resistance of Acinetobacter baumannii to imipenem in Iran: a systematic review and meta-analysis. *The open microbiology journal*, 10**,** 32.

RAKA, L., KALENC, S., BUDIMIR, A., KATIĆ, S., MULLIQI-OSMANI, G., ZOUTMAN, D. & JAKA, A. 2009. Molecular epidemiology of Acinetobacter baumannii in central intensive care unit in Kosova teaching hospital. *Brazilian Journal of Infectious Diseases*, 13**,** 408-413.

SAED, S., YAZDANPANAH, M., LAL-DEHGHANI, M., KHALIGHI, A., HONARMAND, M., AFROUGH, P. & GHAZVINI, K. 2015. Emerging Trend of Acinetobacter Nosocomial Infection in Northeast of Iran. *Journal of Medical Bacteriology*, 2**,** 56-61.

SARHADDI, N., SOLEIMANPOUR, S., FARSIANI, H., MOSAVAT, A., DOLATABADI, S., SALIMIZAND, H. & JAMEHDAR, S. A. 2017. Elevated prevalence of multidrug-resistant Acinetobacter baumannii with extensive genetic diversity in the largest burn centre of northeast Iran. *Journal of global antimicrobial resistance*, 8**,** 60-66.

SEPAHVAND, V., DAVARPANAH, M. A. & HEJAZI, S. H. 2015. Epidemiology of colistin-resistant Acinetobacter baumannii in Shiraz, Iran. *J. Appl. Environ. Biol. Sci.*, 5**,** 45-48.

UWINGABIYE, J., FRIKH, M., LEMNOUER, A., BSSAIBIS, F., BELEFQUIH, B., MALEB, A., DAHRAOUI, S., BELYAMANI, L., BAIT, A. & HAIMEUR, C. 2016. Acinetobacter infections prevalence and frequency of the antibiotics resistance: comparative study of intensive care units versus other hospital units. *Pan African Medical Journal*, 23.

XIE, R., ZHANG, X. D., ZHAO, Q., PENG, B. & ZHENG, J. 2018. Analysis of global prevalence of antibiotic resistance in Acinetobacter baumannii infections disclosed a faster increase in OECD countries. *Emerging microbes & infections*, 7**,** 31.

ZANCO Journal of Pure and Applied Sciences
The official scientific journal of Salahaddin University-Erbil
https://zancojournals.su.edu.krd/index.php/JPAS

ISSN (print):2218-0230**, ISSN (online):** 2412-3986**, DOI: http://dx.doi.org/10.21271/zjpas**

RESEARCH PAPER

Synthesis, Characterization and Biological Evaluation of Some New Heterocyclic Compounds Derived from 2-Naphthol

Trifa Khalaf Mohammed[1], Media Noori Abdullah[2], Rostam Rasul Braiem [3]

1Chamchamal Technical institute/ Sulaimani Polytechnic University, Iraq
[2]Department of Chemistry, College of Science, Salahaddin University-Erbil, Kurdistan Region, Iraq
[2]Department of Chemistry, College of Science, Salahaddin University-Erbil, Kurdistan Region, Iraq

A B S T R A C T:

The present study deals with the synthesis, spectroscopic characterization, antibacterial and antifungal activities of novel series five-membered ring heterocyclic compounds containing nitrogen and sulfur heteroatoms. The synthetic routes have been divided into two parts: The first one includes synthesis of compounds (**4a-c**) through one pot operation three component reaction of 2-naphthol **(1)**, substituted benzaldehyde **(2a-c)** and thiourea **(3)** in 1,2-dichloromethane, using a catalytic amount of $ZrOCl_2.8H_2O$ and compound (**6**) was synthesized using semicarbazide (**5)** in absolute ethanol and indium (III) chloride as catalyst. The second part is the hetero-cyclization reactions of the compounds (**4a-c** and **6)** to obtain the heterocyclic compounds (**7a-c, 8**, and **9)**. The structures of the synthesized products are verified on the basis of (FT-IR, ^{1}H-NMR and ^{13}C-NMR) spectroscopy. The synthesized compounds antibacterial activities were screened against *Staphylococcus aureus* (Gram positive) and *Escherichia coli* (Gram negative) bacteria as compared to standard amikacin and antifungal activity against *Candida albicans* fungi as compared to standard Nystatin, well diffusion method is used. The antibacterial and antifungal activities of synthesized compounds **(7a-c, 8** and **9)** were higher than the antibacterial and antifungal activities of synthesized compounds **(4a-c** and **6)**.

KEY WORDS: Three component reaction, Heterocyclic compound, Thiazole, Thiazolidin-4-one, 1,2-dihydro-3*H*-1,2,4-triazol-3-one, antibacterial and antifungal activities.
DOI: http://dx.doi.org/10.21271/ZJPAS.32.3.12
ZJPAS (2020) , 32(3);101-115 .

1.INTRODUCTION :

Heterocyclic compounds are considered one of the important type of organic compounds due to their applications in industrial and drug design (Taylor et al., 2016). Nitrogen, sulfur and oxygen atoms are the most common heteroatoms because of their important biologically activity (Al-Mulla, 2017).

Three component reactions have gained a special place and vital field of chemistry because they are a process for the achievement of high levels of diversity and brevity, as they allow to be combined as three compounds in a single event to form a single product by one pot operations in a very fast, efficient and time-saving manner without isolation of the intermediates or modification of the reaction conditions (Chunduru and Rao, 2010).

Thiazoles are five membered heterocyclic ring compounds containing sulfur and nitrogen atoms (Toche and Deshmukh, 2017), which have a wide spectrum of biological activities (Ayati *et al*., 2015, Rouf and Tanyeli, 2015). Thiazoledin-4-

* **Corresponding Author:**
Trifa Khalaf Mohammed
E-mail: trya.mohamed@yahoo.com
Article History:
Received: 11/11/2019
Accepted: 18/12/2019
Published: 15/06 /2020

ones are saturated form of thiazole with carbonyl group on the fourth carbon (Kumar and Patil, 2017). The chemistry of thiazolidinones have drawn scientific interest through the years because this particular ring system is the core structure in a variety of synthetic compounds (Abdullah, 2014), an important scaffold known to be associated with a broad spectrum of biological activities (Kapoor *et al*., 2016, Nirwan *et al*., 2019).

1,2-dihydro-3*H*-1,2,4-triazol-3-ones are unsaturated five-membered heterogeneous aromatic rings containing three nitrogen atoms, which possessed a broad spectrum of biological activities (Shneine and Alaraji, 2016, Kaur and Chawla, 2017). Due to the importance of five-membered heterocyclic ring with two hetero atoms, this study achieved the synthesis of some novel heterocyclic compounds with their antibacterial and antifungal activities.

2. Experimental section

2.1. Instruments

Melting points were determined by Stuart Scientific capillary melting point apparatus. The completeness of the reactions are monitored by thin layer chromatography (TLC) on pre-coated silica gel aluminum plates, n-hexane: methanol: chloroform (5:2:3) are used as eluent. Sonication was implemented in ultrasonic cleaner (frequency 40-KHz, normal ultrasonic power 240W). Fourier transform infrared spectroscopy (FT-IR) ranges have been documented on spectrometer (Thermo Fisher FT-IR Model: Nicolet^{TM} iS^{TM}10) were recorded in Raparin University. ^{1}H-NMR and ^{13}C-NMR spectra recorded on a Bruckner (400 MHZ, in Zanjan University/ Iran) using TMS as internal standard and (DMSO-d_6) as solvent, chemical shift are assessed in parts per million (δ ppm), and the abbreviations used were s =singlet, *d*= doublet, *t*= triplet, *m* =multiplet and br =broad.

2.2. Methods

2.2.1. General method of the synthesis of 1-thiocarbamidoalkyl-2-naphthol (4a-c)

(Nagawade and Shinde, 2007, Younis et al., 2012)

In round bottom flask a mixture of 2-naphthol **(1)** (1.44g, 0.01mol), substituted benzaldehyde **(2a-c)** ((1.02 mL) benzaldehyde, (1.51g) 3-nitro benzaldehyde and 4-nitro benzaldehyde, 0.01mol)), thiourea **(3)** (0.91g, 0.012mol), $ZrOCl_2.8H_2O$ (0.032g, 0.1mol) as catalyst in 1,2-dichloromethane (15 mL) were irradiated in an ultrasonic cleaner bath at room temperature for (12-20 min.), the progress of the reactions monitored by TLC. Afterward, the reaction mixture was cooled to the room temperature, H_2O (20 mL) was added and stirred for about (3 min.), the precipitate was filtered off, recrystallized from ethanol. The chemical reactions are shown in the (**Scheme 1**).

Physical properties and Spectral data of ((2-hydroxynaphthalen-1-yl)(phenyl)methyl)thiourea (**4a**)

Chemical formula ($C_{18}H_{16}N_2OS$), m.p: (178-180 ^{o}C), yield: (2.65g, 85.8 %), color: off-white; FT-IR (cm^{-1}): 3338 and 3278 ($NH_{2str.}$), 3175 (N-$H_{str.}$), 3105 (O-$H_{str.}$), 3030 (C-$H_{Ar.\ str.}$), l580 (C=$C_{str.}$), 1235 (C-$O_{str.}$). ^{1}H-NMR (δ ppm) (DMSO-d_6): 10.06 (s, 1H, OH), 9.25 (br. s,1H, NH), 8.16 (br. s, 2H, NH_2), 7.88-7.13 (m, 11$H_{Ar.}$), 5.79 (s, 1H, CH). ^{13}C-NMR (δ ppm) (DMSO-d_6): 183.67 (C=S), 153.70 (C_2), 143.45 (C_1^-), 133.5 (C_{10}), 129.8 (C_3^-, C_5^-), 129.04 (C_5), 128.64 (C_4, C_6), 128.04 (C_2^-, C_6^-), 127.23 (C_8), 126.58 (C_4^-), 126.24 (C_9), 123.21 (C_7), 119.66 (C_3), 119.01 (C_1), 54.26 (CH).

Physical properties and Spectral data of ((2-hydroxynaphthalen-1-yl)(3-nitrophenyl)methyl)thiourea (**4b**)

Chemical formula: ($C_{18}H_{15}N_3O_3S$), m.p: (165-167C^{o}), yield: (3.15g, 89.3 %), color: yellow; FT-IR (cm^{-1}): 3384 and 3362 ($NH_{2str.}$), 3281 (N-$H_{str.}$), 3184 (O-$H_{str.}$), 3027 (C-$H_{Ar.\ str.}$), l590 (C=$C_{str.}$), 1498 ($NO_{2asym.\ str.}$), 1337 ($NO_{2sym.\ str.}$), 1271 (C-$O_{str.}$). ^{1} H-NMR (δ ppm) (DMSO-d_6): 10.26 (s, 1H, OH), 10.1 (br. s, 1H, NH), 9.18 (br. s, 2H, NH_2), 8.14-7.19 (m, 10$H_{Ar.}$), 4.40 (s, 1H, CH). ^{13}C-NMR (δ ppm) (DMSO-d_6): 184.26 (C=S), 153.91 (C_2), 148.22 (C_3^-), 146.34 (C_1^-), 133.06 (C_6^-), 132.83 (C_{10}), 130.60 (C_5^-), 130.11 (C_5), 129.21 (C_4,C_6), 128.74 (C_8), 127.55 (C_2^-), 123.2 (C_9), 121.75 (C_7), 120.71 (C_4^-), 118.84 (C_3), 118.34 (C_1), 53.56 (CH)

Physical properties and Spectral data of ((2-hydroxynaphthalen-1-yl)(4-nitrophenyl)methyl)thiourea (**4c**)

Chemical formula: ($C_{18}H_{15}N_3O_3S$), m.p: (174-176C^{o}), yield (3.3g, 93 %), color: yellow;

FT-IR (cm^{-1}): 3445 and 3414 ($NH_{2str.}$), 3331 (N-$H_{str.}$), 3211 (O-$H_{str.}$), 3051 (C-$H_{Ar.\ str.}$), 1582 (C=$C_{str.}$), 1487 ($NO_{2asym.\ str.}$), 1330 ($NO_{2sym.\ str.}$), 1254 (C-O). ^{1}H-NMR (δ ppm) (DMSO-d_6): 10.17(s, 1H, OH), 10.09 (br. s, 1H, NH), 9.13 (br. s, 2H, NH_2), 8.74-7.18 (m, 10$H_{Ar.}$), 4.77 (s, 1H, CH). ^{13}C-NMR (δ ppm) (DMSO-d_6): 153.85 (C=S), 152.21 (C_2), 146.37 (C_1^-), 146.25 (C_4^-), 132.8 (C_{10}), 130.52 (C_2^-,C_6^-), 129.18 (C_5), 128.75 ($C_{4,6}$), 127.41 (C_8), 123.87 (C_3^-,C_5^-), 123.66 (C_9), 123.14 (C_7), 118.97 (C_3), 118.64 (C_1), 56.53 (CH).

2.2.2. General method of the synthesis of 2-((2-hydroxynaphthalen-1-yl)(4-nitrophenyl) methyl)hydrazine-1-carboxamide (6) (Pouramiri and Kermani, 2017)

A solution of 2-naphthol **(1)** (1.44g, 0.01mol), 4-nitrobenzaldehyde **(2)** (1.51g, 0.01mol), semicarbazide **(5)** (1.226g, 0.011mole) and indium (III) chloride (0.022g, 0.1 mol) in absolute ethanol (15mL) with chloroacetic acid (1.89g, 0.02mol) were irradiated in ultrasonic bath at room temperature for about 15min.. The progress of the reaction was checked by thin layer chromatography, after completion of the reaction, the crude product was filtered off, washed and recrystallized from ethanol. The chemical reaction is shown in the **Scheme (2).**

Physical properties and Spectral data of 2-((2-hydroxynaphthalen-1-yl)(4-nitrophenyl)methyl) hydrazine-1-carboxamide (**6**)

Chemical Formula: ($C_{18}H_{16}N_4O_4$), m.p: (234-236C^o), yield (3.23g, 91.6 %), color: yellow; FT-IR (cm^{-1}): 3445 (N-$H_{str.}$), 3281 and 3169 ($NH_{2str.}$), 3105 (O-$H_{str.}$), 3058 (C-$H_{Ar.\ str.}$), 1681 (C=$O_{str.}$), 1602 (C=$C_{str.}$), 1543 ($NO_{2asym.\ str.}$), 1359 ($NO_{2sym.\ str.}$), 1258 (C-O). ^{1}H-NMR (δ ppm) (DMSO-d_6): 11.29 (br. s, 1H, CH-NH), 10.88 (s, 1H, OH), 10.65 (br. s, 1H, NH-C=O), 8.57-7.65 (m, 10$H_{Ar.}$), 5.16 (s, 1H, CH); ^{13}C-NMR (δ ppm) (DMSO-d_6): 162.25 (C=O), 159.08 (C_2), 143.16 (C_1^-), 138.9 (C_4^-), 133.9 (C_{10}), 132.9 (C_2^-, C_6^-), 132.43 (C_5), 132.37 (C_4, C_6), 122.27 (C_8), 120.16 (C_3^-, C_5^-), 119.84 (C_9), 119.67 (C_7), 119.56 (C_3), 117.14 (C_1), 57.64 (CH).

2.2.3. General method for the synthesis of thaizoles (7a-c) (Kubba and Rahim, 2018)

Phenacyl bromide (0.398g, 0.002 mol) added slowly to solution of compound **(4a-c)** ((0.616g of 4a and 0.706g of 4b, 4c), 0.002 mol) in ethanol in a round bottom flask and refluxed for about (4-6 h). The progress of the reactions monitored by TLC, the mixture was cooled at room temperature then poured into cold water. The precipitate was filtered off and recrystallized from toluene: ethanol (25:75) to afford the pure product. The reactions are shown in the (**Scheme 3**).

Physical properties and Spectral data of (phenyl((5-phenylthiazol-2-yl)amino)methyl)naphthalen-2-ol (**7a**)

Chemical Formula: ($C_{26}H_{20}N_2OS$), m.p: (199-201C^o), yield (0.611g, 74.8 %), color: dark brown; FT-IR (cm^{-1}): 3479 (N-$H_{str.}$), 3350 (O-$H_{str.}$), 3058 (C-$H_{Ar.\ str.}$), l627 (C=$N_{str.}$), 1578 and 1574 (C=$C_{str.}$), 1251 (C-$O_{str.}$). ^{1}H-NMR (δ ppm) (DMSO-d_6): 9.94 (s, 1H, OH), 7.38-6.48 (m, 16H_{Ar} &1H, $CH_{thiazole}$), 5.51 (br. s, 1H, NH), 5.0 (s, 1H, CH); ^{13}C-NMR (δ ppm) (DMSO-d_6): 166.02 (C=$N_{thiazole}$), 158.8 (C_2), 157.36 (C-$N_{thiazole}$), 153.55 (C_1^-), 152.51 (C_{10}), 150.95 ($C_1^=$), 148.4 (C_3^-, C_5^-, $C_3^=$, $C_5^=$), 138.48 (C_5), 130.36 ($C_4^=$), 129.61 (C_4, C_6), 124.29 (C_2^-, C_6^-), 122.94 ($C_2^=$, $C_6^=$), 122.21 (C_8), 120.61 (C_4^-) 119.69 (C_9), 119.34 (C_7), 117.97 (C-$S_{thiazole}$), 116.24 (C_3), 112.65 (C_1), 56.32 (CH).

Physical properties and Spectral data for1-((3-nitrophenyl)((5-phenylthiazol-2yl)amino)methyl) naphthalene-2-ol (**7b**)

Chemical Formula: ($C_{26}H_{19}N_3O_3S$), m.p: (186-188C^o), yield (0.721g, 80 %), color: dark brown; FT-IR (cm^{-1}): 3403 (N-$H_{str.}$), 3271 ($OH_{str.}$), 3056 (C-$H_{Ar.\ str.}$), l600 (C=$N_{str.}$), 1557 (C=$C_{str.}$), 1505 ($NO_{2asym.\ str.}$), 1380 ($NO_{2sym.\ str.}$), 1251 (C-$O_{str.}$); ^{1}H-NMR (δ ppm) (DMSO-d_6): 10.31(s, 1H, OH), 8.75-6.60 (m, 15H_{Ar}), 6.75 (s, 1H $CH_{thiazole}$), 5.45 (br. s, 1H, NH), 5.0(s, 1H, CH). ^{13}C-NMR (δ ppm) (DMSO-d_6): 166.66 (C=$N_{thiazole}$), 166.47 (C_2), 162.90 (C-$N_{thiazole}$), 162.68 (C_3^-), 158.85 (C_1^-), 157.36 (C_6^-), 143.0 (C_{10}), 142.89 ($C_1^=$), 137.08 (C_5^-), 135.36 ($C_3^=$, $C_5^=$), 135.29 (C_5), 135.17 ($C_4^=$), 134.76 (C_4, C_6), 134.47 ($C_2^=$, $C_6^=$) 132.82 (C_8), 131.97 (C_2^-), 129.45 (C_9), 126.79 (C_7), 119.39 (C_4^-), 119.36 (C-$S_{thiazole}$), 118.93 (C_3), 116.28 (C_1), 52.70 (CH).

Physical properties and Spectral data of 1-((4-nitrophenyl)((5-phenylthiazol-2-yl)amino)methyl) naphthalene-2-ol (**7c**)

Chemical Formula: ($C_{26}H_{19}N_3O_3S$), m.p: (193-195C^o), yield (0.76g, 84 %), color: dark brown; FT-IR (cm^{-1}): 3359 (N-$H_{str.}$), 3228 ($OH_{str.}$), 3033 (C-$H_{Ar.\ str.}$), l622 (C=$N_{str.}$), 1597 (C=$C_{str.}$), 1573 ($NO_{2asym.\ str.}$), 1308 ($NO_{2sym.\ str.}$), 1284 (C-$O_{str.}$). ^{1}H-NMR (δ ppm) (DMSO-d_6): 9.90 (s, 1H, OH), 7.91-6.87 (m, 15$H_{Ar.}$), 6.78 (s, 1H, $CH_{thiazole}$), 5.75 (br. s, 1H, NH), 5.15 (s, 1H, CH). ^{13}C-NMR (δ ppm) (DMSO-d_6): 169.41 (C=$N_{thiazole}$), 165.7 (C_2), 152.74 (C-$N_{thiazole}$), 151.47 (C_1^-), 150.95 (C_4^-), 148.61 (C_{10}), 147.92 ($C_1^=$), 144.14 ($C_3^=$, $C_5^=$), 140.59 (C_2^-, C_6^-), 128.24 (C_5), 127.49 ($C_4^=$), 147.75 (C_4, C_6), 125.03 ($C_2^=$, $C_6^=$), 124.30 (C_8), 122.32 (C_3^-, C_5^-), 120.58 (C_9), 119.52 (C_7), 118.02 (C-$S_{thiazole}$), 116.43 (C_3), 112.68 (C_1), 56.21 (CH).

2.2.4. General method for the synthesis of 2-(2-(((2-hydroxynaphthalen-1-yl)(phenyl)methyl) imino)-4-oxothiazolidin-5-yl)acetic acid (8)

(Sushilkumar and Devanand, 2003)

In a 100 mL round bottom flask fitted with reflux condenser, compound **(4a)** (0.616g, 0.002mol) and maleic anhydride (0.196g, 0.002mol) in glacial acetic acid (20 mL) were refluxed with stirring for 12h. The progress of the reactions monitored by TLC, the reaction mixture was minimized to half under reduced pressure, cooled at room temperature and poured on cold water. The precipitate was filtered off, dried and recrystallized from ethanol. The reaction is shown in the (**Scheme 4**).

Physical properties and Spectral data of 2-(2-(((2-hydroxynaphthalen-1-yl)(phenyl)methyl) imino)-4-oxothiazolidin-5-yl)acetic acid **(8)**

Chemical Formula: ($C_{22}H_{18}N_2O_4S$), m.p: (206-208C^o), yield (0.63g, 78 %), color: gray; FT-IR (cm^{-1}): 3276 ($NH_{str.}$), 3083 ($OH_{str.}$), 3042 (C-$H_{Ar.\ str.}$), 1766 (C=$O_{str.\ carboxylic\ acid}$), 1666 (C=$O_{str.\ thiazoledin\text{-}4\text{-}one}$), l581 (C=$N_{str.}$), 1538 (C=$C_{str.}$), 1274 (C-$O_{str.}$). ^{1}H-NMR (δ ppm) (DMSO-d_6): 12.51 (s, 1H, $OH_{carboxylic\ acid}$), 10.98 (br. s, 1H, NH), 9.88 (s, 1H, $OH_{2\text{-}naphthol}$), 7.89-6.78 (m, 11$H_{Ar.}$), 4.14 (t, 1H, CH $_{thizoledin\text{-}4\text{-}one}$), 3.49 (s, 1H, CH), 2.39 (d, 2H, CH_2). ^{13}C-NMR (δ ppm) (DMSO-d_6): 177.95 (C=$O_{carboxylic\ acid}$), 169.57 (C =$O_{thizoledin\text{-}4\text{-}one}$), 148.62 ($C_2$), 145.78 (C-N $_{thiazoledin\text{-}4\text{-}one}$), 143.95 ($C_1^-$), 142.77 ($C_{10}$), 140.08 ($C_3$, C_5^-), 137.20 (C_5), 130.11 (C_2, C_6), 129.50 (C_2^-, C_6^-), 127.51 (C_8), 126.90 (C_4^-), 124.67 (C_9), 121.61 (C_7), 119.69 (C_3), 112.09 (C_1), 60.72 (CH) , 56.55 ($CH_{thiazoledin\text{-}4\text{-}one}$), 48.10 ($CH_2$).

2.2.5. General method of the synthesis of 1-((2-hydroxynaphthalen-1-yl)(4-nitrophenyl) methyl)-5-phenyl-1,2-dihydro-3*H*-1,2,4-triazol-3-one (9) (Shalini et al., 2009)

Benzoyl chloride (0.28g, 0.002mol) and compound (**6**) (0.704g, 0.002mol) were dissolved in ethanol, Potassium carbonate (0.42g, 0.003mol) added , the mixture was refluxed for 6 h. Then heated on water bath on slightly alkaline medium 4% NaOH (20 mL) for around 4 h. the result was neutralized by dilute HCl. The solvent was evaporated and the product was recrystallized from ethanol. The reaction is illustrated in the (**Scheme 5**).

Physical properties and Spectral data of 1-((2-hydroxynaphthalen-1-yl)(4-nitrophenyl) methyl)-5-phenyl-1,2-dihydro-3*H*-1,2,4-triazol-3-one **(9)**

Chemical Formula: ($C_{25}H_{19}N_3O_2$), m.p: (278-280C^o), yield (0.63g, 71.9 %), color: brown; FT-IR (cm^{-1}): 3236 (N-$H_{str.}$), 3137 ($OH_{str.}$), 3035 (C-$H_{Ar.\ str.}$), 1664 (C=$O_{str.}$), l611 (C=$N_{str.}$), 1541 (C=$C_{str.}$), 1509 ($NO_{2asym.\ str.}$), 1342 ($NO_{2sym.\ str.}$), 1245(C-$O_{str.}$). ^{1}H-NMR (δ ppm) (DMSO-d_6): 9.48 (s, 1H, OH), 8.81 (br. s, $NH_{1,2\text{-}dihydro\text{-}3H\text{-}1,2,4\text{-}triazol\text{-}3\text{-}one}$), 8.01-6.72 (m, 15$H_{Ar.}$), 4.54 (s, 1H, CH). ^{13}C-NMR (δ ppm) (DMSO-d_6): 169.56 (C=$O_{1,2\text{-}dihydro\text{-}3H\text{-}1,2,4\text{-}triazol\text{-}3\text{-}one}$), 164.71 (C=$N_{1,2\text{-}dihydro\text{-}3H\text{-}1,2,4\text{-}triazol\text{-}3\text{-}one}$), 144.52 ($C_2$), 142.79 ($C_1^-$), 137.19 ($C_4^-$), 132.51 ($C_{10}$), 130.11 ($C_4^=$), 129.51 ($C_2^-$, C_6^-), 128.80 (C_5, $C_5^=$, $C_3^=$), 127.30 ($C_1^=$), 126.91 (C_4, C_6), 124.65 ($C_2^=$, $C_6^=$), 121.64 (C_8), 119.47 (C_3, C_5^-), 118.90 (C_9), 118.04 (C_7), 115.00 (C_3), 112.07 (C_1^-), 59.00 (CH).

2.2.6. General method of antibacterial activity

(Landage et al., 2019)

An antibacterial activity of synthesized compounds was determined *in vitro* against two bacterial strains Gram-positive (*Staphylococcus aureus*), Gram-negative (*Escherichia coli*) by agar well diffusion method. 20ml of Muller Hinton agar was poured in to sterile petri dish and spread with 100 µl of culture. The well was made in the agar by sterile cork borer of width (6 mm) then 100 µl of synthesized compounds (500ppm and 1000ppm) were loaded in the well along with amikacin as positive control and DMSO as negative control. The plates incubated at 37°C for 24 hours, the zone of inhibition produced by each compound was measured in mm.

2.2.7. General method of antifungal activity
(Pejchal et al., 2015)

Antifungal activity was screened against *Candida albicans* in Muller Hinton agar medium, preparation of nutrient broth, dilution and application were carried out using the same procedure as for antimicrobial testing. The standard antibiotic Nystatin was used as control positive and the plates were incubated at 30 °C for 48 h. The diameters of zone of inhibition observed were measured.

3. RESULTS AND DISCUSSION:

In this study, five membered heterocyclic compounds thaizole, 4-thiazolidinone were synthesized from the reaction of 1-thiocarbamidoalkyl-2-naphthol derivatives **(4a-c)** with phenacyl bromide in ethanol and maleic anhydride in glacial acetic acid, respectively and 1,2-dihydro-3H-1,2,4-triazol-3-one with benzoyl chloride in ethanol. Scheme **(3, 4and 5)**

The FT-IR spectra of the starting materials are changed, when the compounds of (**4a-c**) are cyclized to the compounds (**7a-c** and **8**), two peaks of ($NH_{2str.}$) groups are disappeared, while different new peaks are appeared for ($C=N_{str.}$) functional groups at (1600-1627 cm^{-1}). In compound (**8**) two peaks are appeared for each of the carbonyl group of carboxylic acid and amide (thiazolidin-4-one) at 1766 cm^{-1} and 1666 cm^{-1}, respectively (de Aquino et al., 2008). When compound (**6**) is converted to the compound (**9**) two peaks of ($NH_{2str.}$) at 3169 and 3281 cm^{-1} are disappeared, while ($C=N_{str.}$) peak are appeared at 1611 cm^{-1}, peak of Carbonyl group is shifted from 1681 cm^{-1} to 1664 cm^{-1}.

^{1}H-NMR spectra of the compounds (**4a-c** and **6**) are changed when cyclization occurred and compounds (**7a-c**, **8** and **9**) are obtained. The protons of NH_2 groups are disappeared in the cyclization products, while these two protons are present in the compounds **4a, 4b, 4c** and **6** at 8.16 , 9.18, 9.13 and 6.71 ppm respectively. Singlet band of ($CH_{thiazole}$) are appeared for the compounds **4a, 4b** and **4c** at 6.48, 6.75 and 6.78 ppm, respectively (Bhosale et al., 2012). A singlet band of (OH), doublet bands of (CH_2) and triplet bands of ($CH_{thiazoledin-4-one}$) are appeared at 12.51, 2.39 and 4.14 ppm in compound **8** (Gurumurthi et al., 2009). As described before the two protons of NH_2 group, which appeared at 6.71 ppm are disappeared when compound **6** is cyclized, one proton of the NH-CH that appeared at 11.29 ppm disappeared, while the NH-CO proton band shifted and appeared as a singlet at 8.81 ppm (Ali et al., 2018). Five aromatic protons increased when compounds (**7a-c** and **9**) were formed.

^{13}C-NMR spectra of the synthesized compounds support the formation of new products when the compounds (**4a-c** and **6**) are cyclized to yield (**7a-c**, **8** and **9**). The chemical shifts for carbon of (C=S) group in compound (**4a-c**) are disappeared and the carbon of ($C=N_{thiazole}$) group are formed at 166.02-169.41 ppm, while carbon of ($\underline{C}$-N $_{thiazole}$) and ($\underline{C}$-S $_{thiazole}$) are appeared at 152.74-162.90 ppm and 117.97-119.36 ppm, respectively. This showed that the number of carbons are increased when the compound **4a** is converted to the compound **8**, because of the presence of the carbon $\underline{C}$ =O $_{thizoledin-4-one}$, $\underline{C}$-N $_{thiazoledin-4-one}$, $\underline{C}$-S $_{thiazoledin-4-one,}$ and CH_2 and $C=O_{carboxylic\ acid}$ at 169.57, 145.78, 56.55, 48.10 and 177.95 ppm, respectively. Also, the carbon of (C=S) at 183.67 ppm are disappeared. When the compound **9** is formed from the compound **6** and the chemical shifts for carbon of C=O is shifted from 162.25 to 169.56 ppm and the chemical shift for carbon of ($\underline{C}$=N $_{dihydro\text{-}3\textit{H}\text{-}1,2,4\text{-}triazol\text{-}3\text{-}one}$) group is appeared at 164.71 ppm. Six aromatic carbons are increased in the compounds (**7a-c** and **9**).

All synthesized compounds showed the difference ability for stopping or destroying the growth of bacteria or fungi. Commonly the antibacterial and antifungal activities of the compounds **(4a-c and 6)** are increased when they converted to the heterocyclic compounds **(7a-c, 8 and 9)** and the ability of the synthesized compounds against *Staphylococcus aureus* bacteria, *Escherichia coli* bacteria and *Candida albicans* fungi are increased by increasing their concentrations as shown in the (**Table 1 and Table 2**). The compound **(7a)** was highly active while prepared as 1000 µg/ml.

4. CONCLUSION

As concluded, the useful and simple methods are used for the synthesis of some new heterocyclic compounds in good yields. Nitro group needed less reaction time than Hydrogen. Ultrasound technique is used to save time. The suitable solvent that used for recrystallization of

the products was ethanol. Heterocyclic compounds **(7a-c**, **8** and **9)** are exhibited higher growth inhibition than synthesized compounds (**4a-c** and **6)** against *Staphylococcus aureus*, *Escherichia coli* and *Candida albicans*, increasing the concentration of synthesized compound the growth inhibition are increased.

ACKNOWLEDGEMENT

We are indebted of Chemistry Department/College of Science/ Salahaddin University -Erbil for providing the facilities and financial support during the investigation.

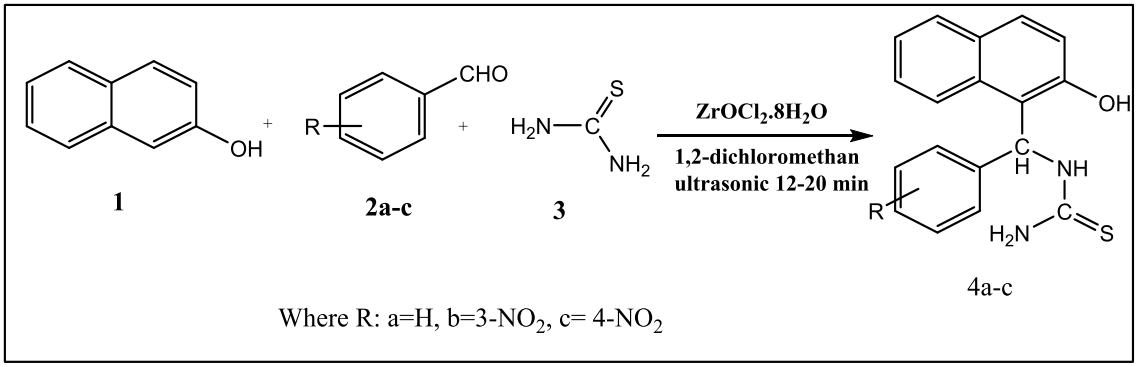

Scheme 1: Synthesis of compounds **(4a-c)**

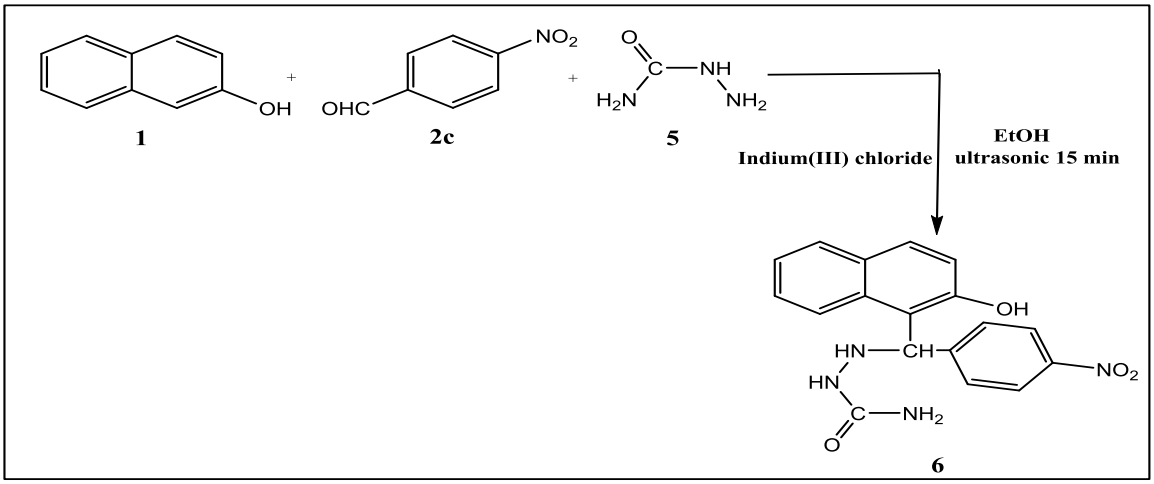

Scheme 2: Synthesis of compounds **(6)**

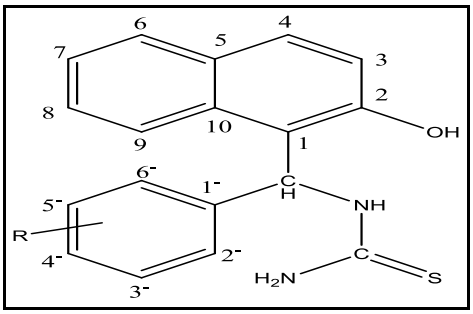

Fig.1: Numbering of compounds (**4a-c**)

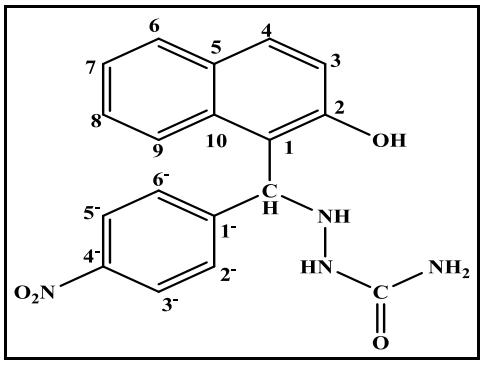

Fig. 2: Numbering of compound (**6**)

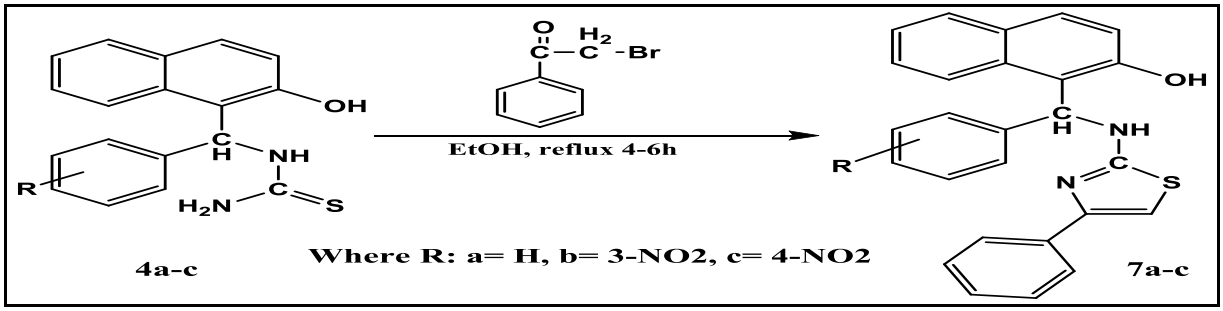

Scheme 3: Synthesis of compounds **(7a-c)**

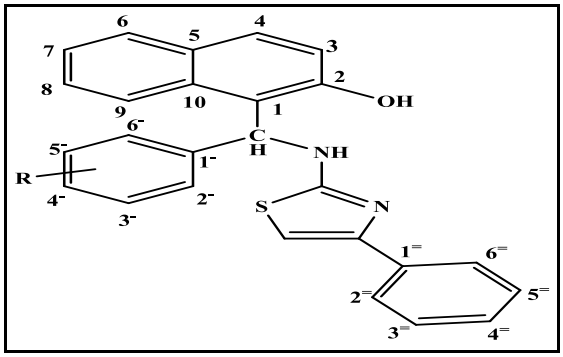

Fig. 3: Numbering compounds (**7a-c**)

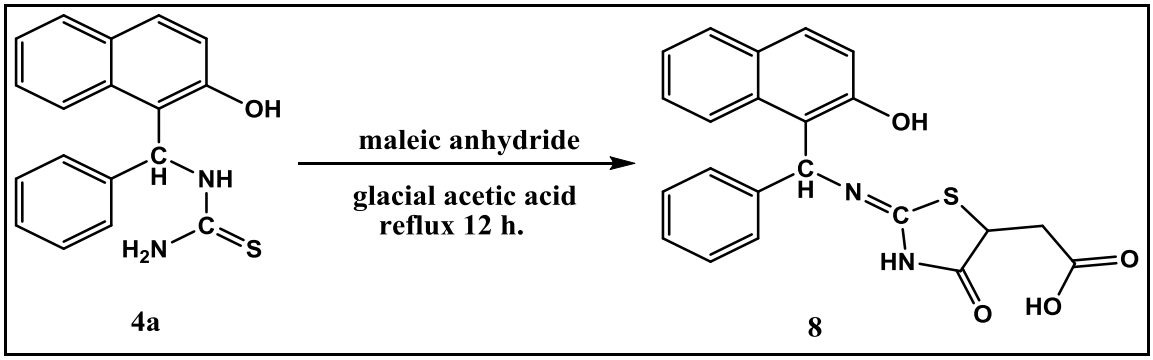

Scheme 4: Synthesis of compound **(8)**

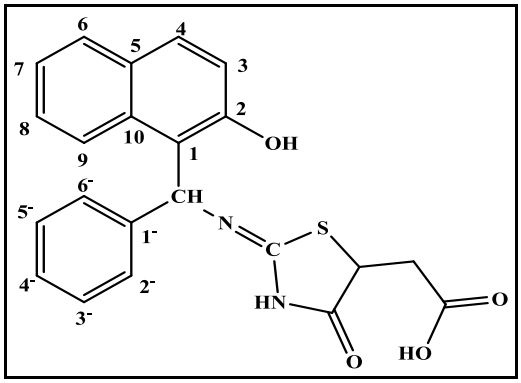

Fig. 4: Numbering of compound (**8**)

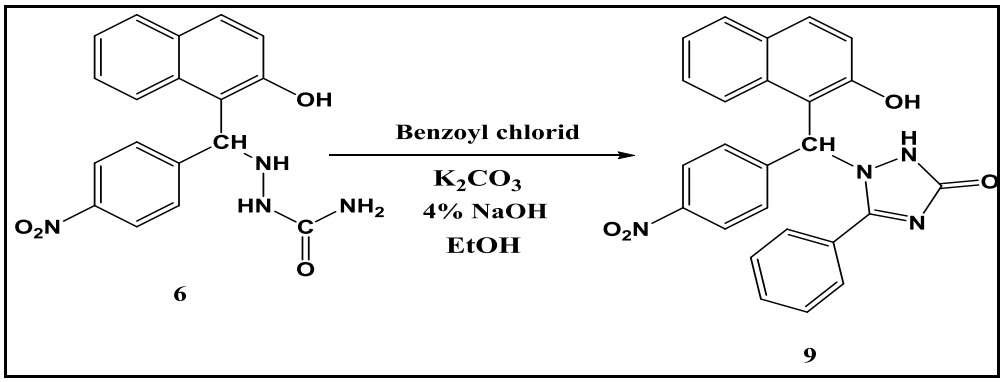

Scheme 5: Synthesis of compound **(9)**

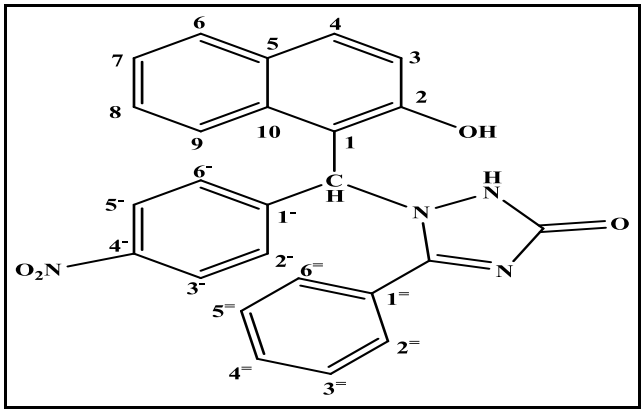

Fig. 5: Numbering of compound **(9)**

Table 1: The antibacterial and antifungal activities of compounds (**4a-c** and **6**)

Variables		Antibacterial Activity			Fig.
		Gram positive	Gram negative	Antifungal	
Compound	Conc.	S. aureus	E. coli	C. albicans	
4a	500ppm	11	11	7	
	1000 ppm	13	12	9	
4b	500 ppm	12	9	9	
	1000 ppm	13	12	11	
4c	500ppm	11	9	9	9
	1000 ppm	12	12	12	10
6	500ppm	13	11	11	11
	1000 ppm	14	12	13	
Amikacin	33			NT	9 and 10
Nystatin	NT			23	11

Table 2. The antibacterial and antifungal activities of compounds (**7a-c** and **9**)

Variables		Antibacterial Activity			Fig.
		Gram positive	Gram negative	Antifungal	
Compound	Conc.	S. aureus	E. coli	C. albicans	
7a	500ppm	25	24	11	9
	1000 ppm	31	29	16	10
7b	500ppm	25	25	13	
	1000 ppm	28	27	17	
7c	500ppm	24	23	15	
	1000 ppm	30	27	20	
8	500ppm	23	24	12	
	1000 ppm	27	28	15	
9	500ppm	26	24	14	11
	1000 ppm	30	29	18	
Amikacin		33		NT	9 and 10
Nystatin		NT		23	11

S. aureus= *Staphylococcus aureus*, E. coli= *Escherichia coli*, C. albicans= *Candida albicans*
NT: not test
For antibacterial:
Highly active (inhibition zone > 30 mm); active (inhibition zone 23-30 mm); moderately active (inhibition Zone 16--23 mm); slightly active (inhibition zone 9-16 mm); inactive (inhibition zone < 9 mm)
For antifungal:
Highly active (inhibition zone > 20 mm); active (inhibition zone 15-20 mm); moderately active (inhibition Zone 10-15 mm); slightly active (inhibition zone 5-10 mm); inactive (inhibition zone < 5 mm)

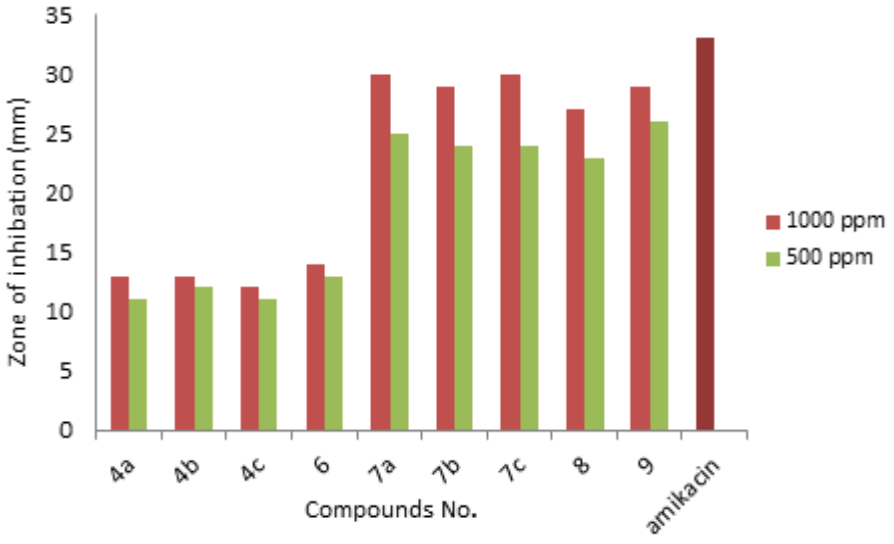

Fig. 6: Antibacterial activity of the synthesized compounds against *Staphylococcus aureus* bacteria.

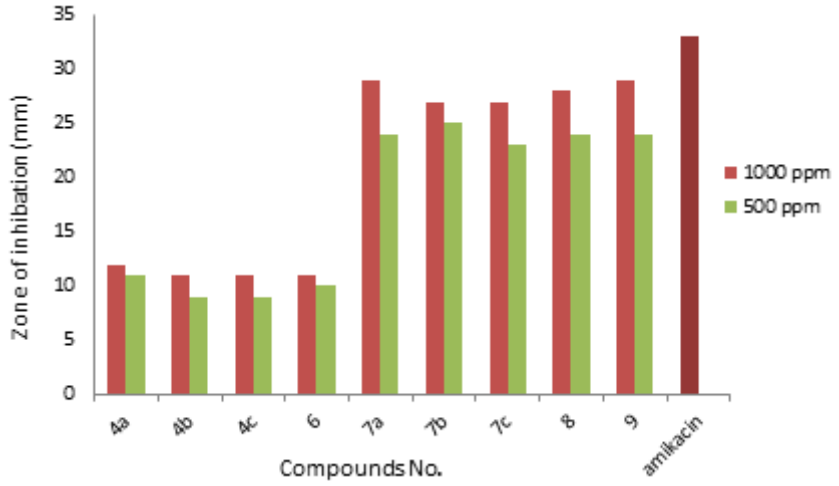

Fig. 7: Antibacterial activity of the all synthesized compounds against *Escherichia coli* bacteria.

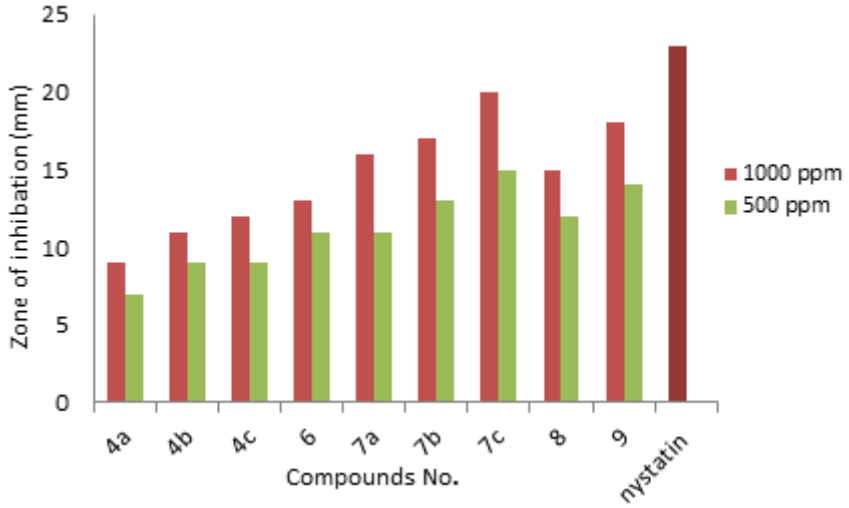

Fig. 8: Antifungal activity of the synthesized compounds against *Candida albicans* fungi

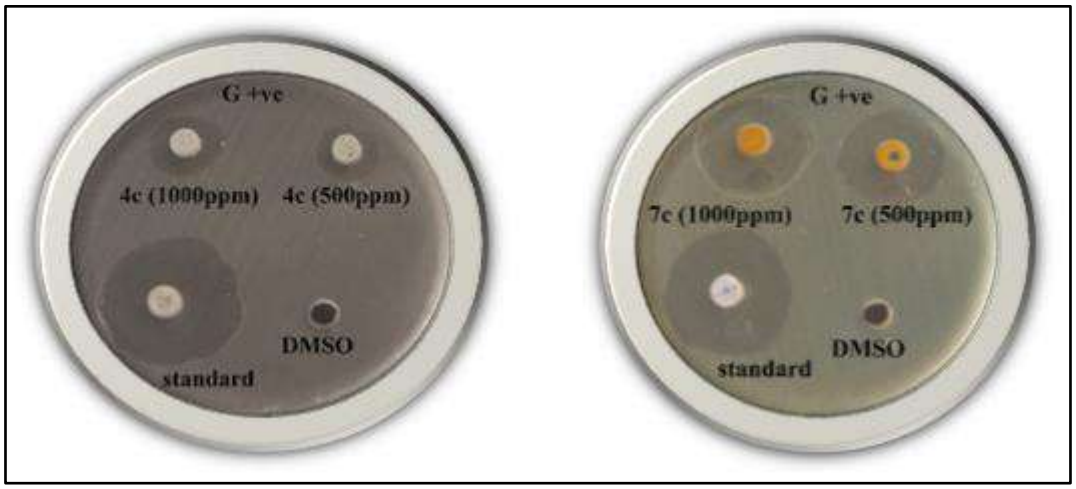

Fig. 9: Anti-bacterial activities of synthesized compounds (**4c** and **7c**) against *Staphylococcus aureus*

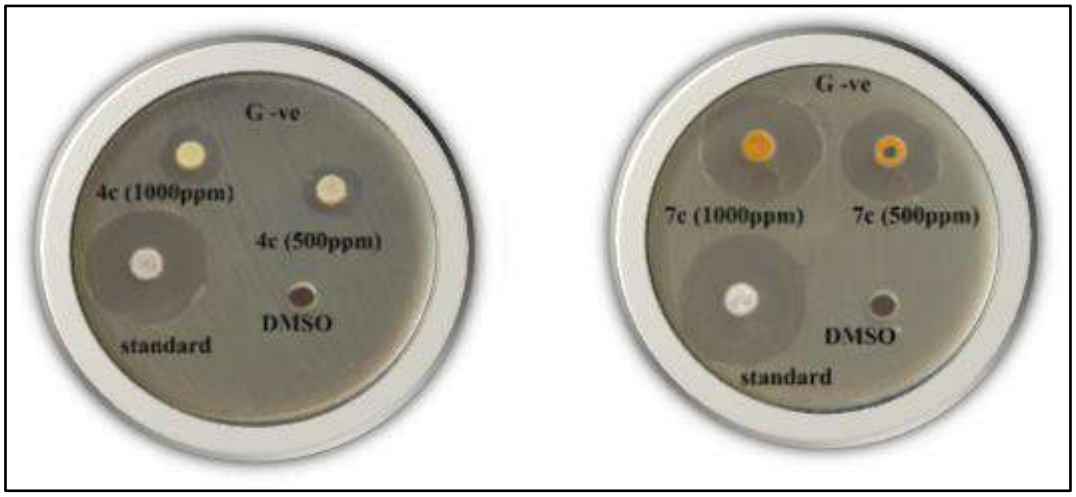

Fig. 10: Anti-bacterial activities of synthesized compound **(4c** and **7c)** against *Escherichia coli*

Fig. 11: Antifungal activities of synthesized products **(6** and **9)** against *Candida albicans*

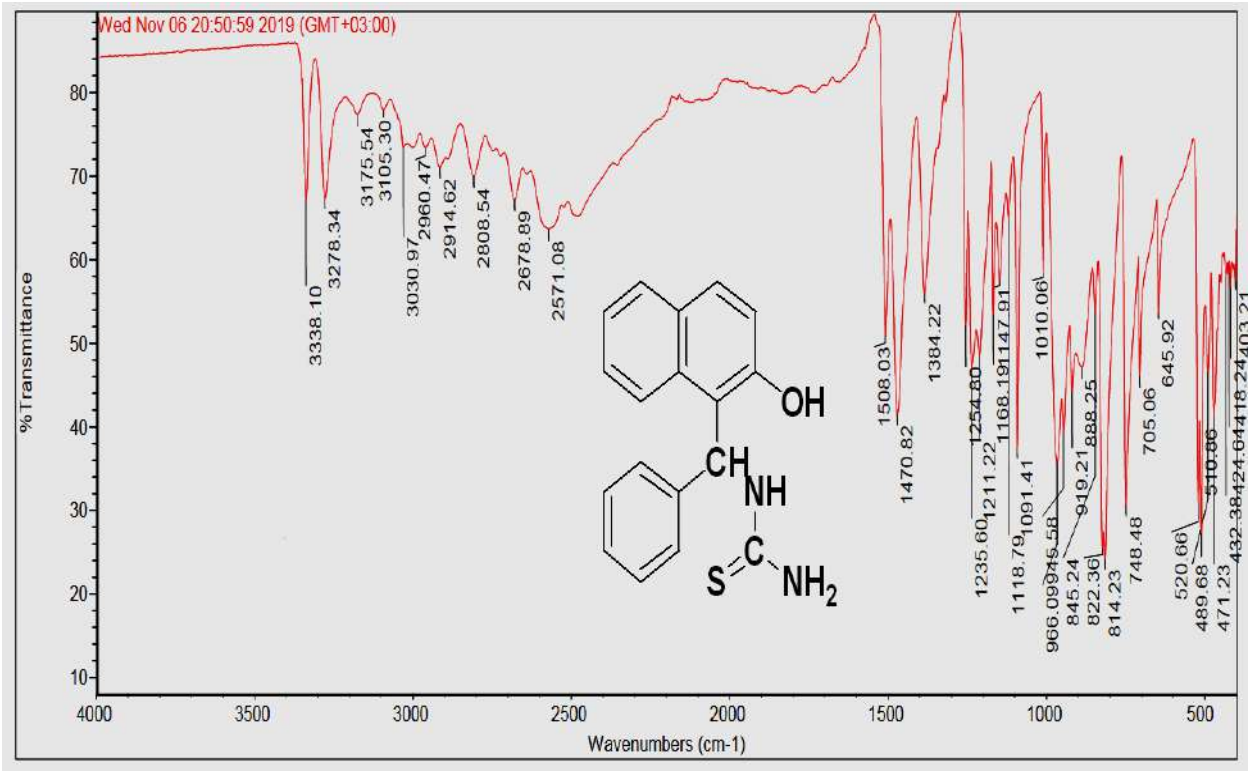

Fig. 12: FT-IR spectrum of ((2-hydroxynaphthalen-1-yl)(phenyl)methyl)thiourea **(4a)**

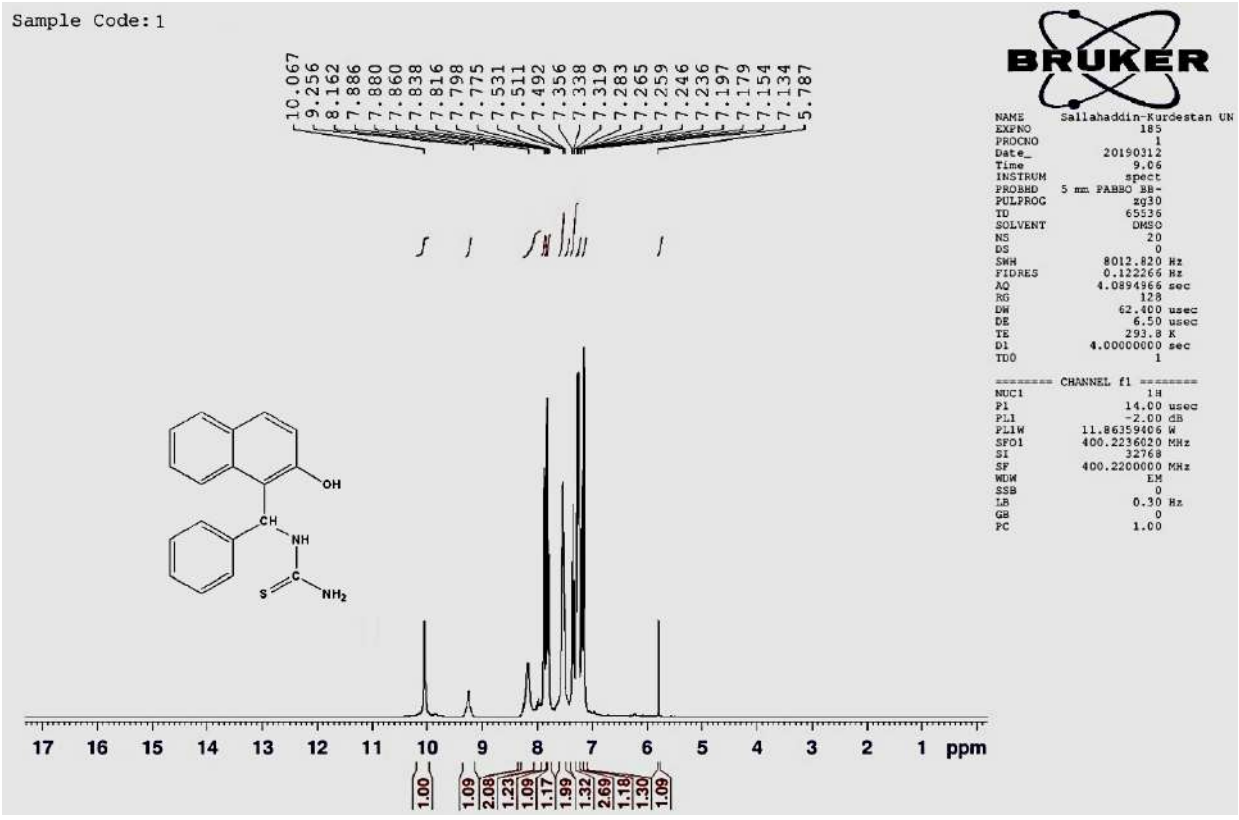

Fig. 13: ^{1}H-NMR Spectrum of ((2-hydroxynaphthalen-1-yl)(phenyl)methyl)thiourea **(4a)**

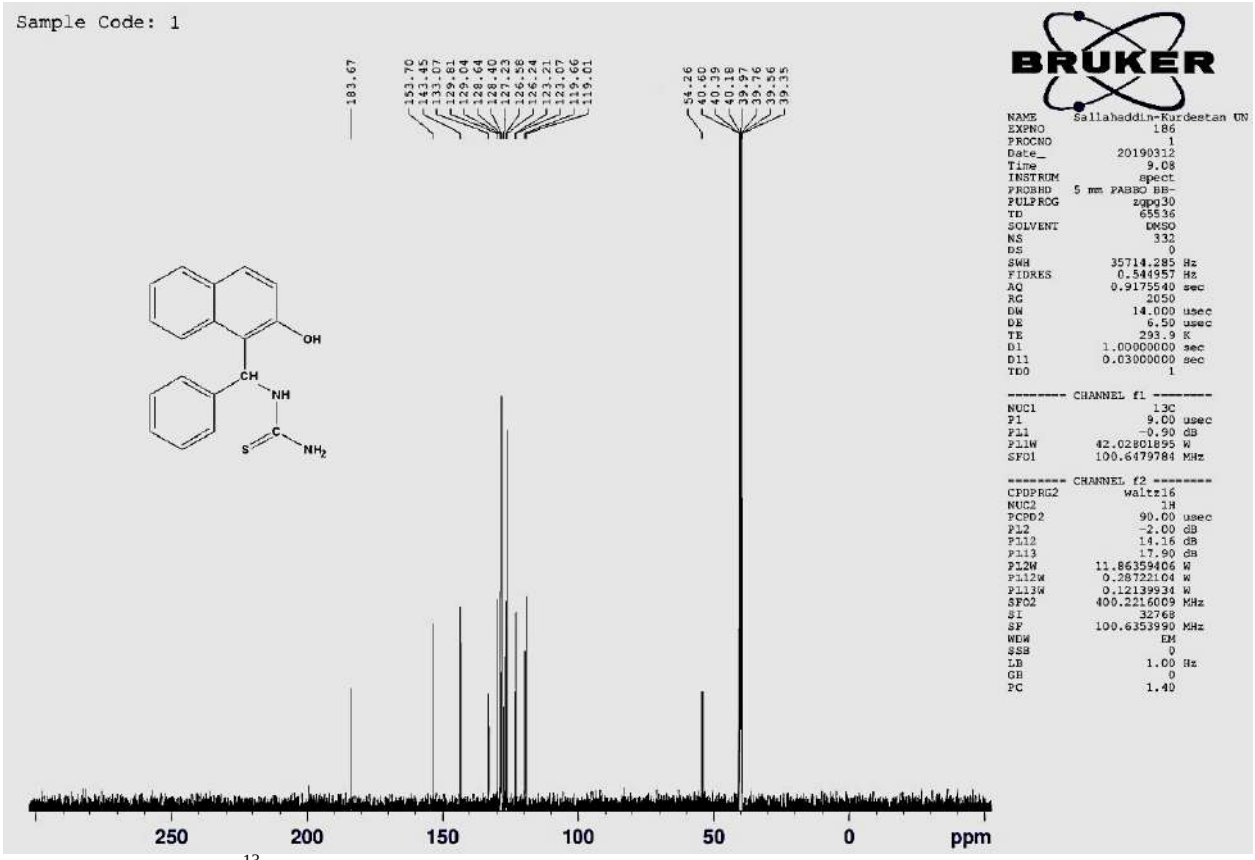

Fig. 14: ^{13}C-NMR spectrum of ((2-hydroxynaphthalen-1-yl)(phenyl)methyl)thiourea **(4a)**

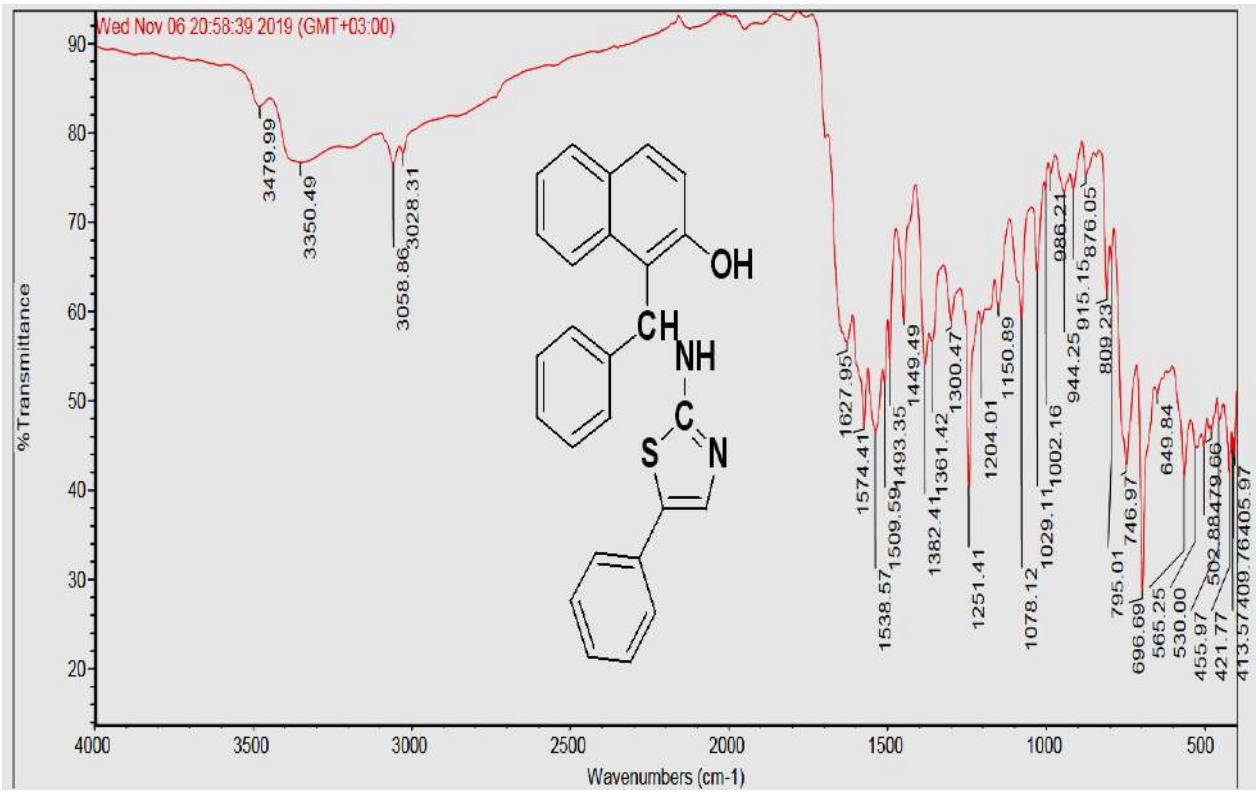

Fig. 15: FT-IR spectrum of (phenyl((5-phenylthiazol-2-yl)amino)methyl)naphthalen-2-ol **(7a)**

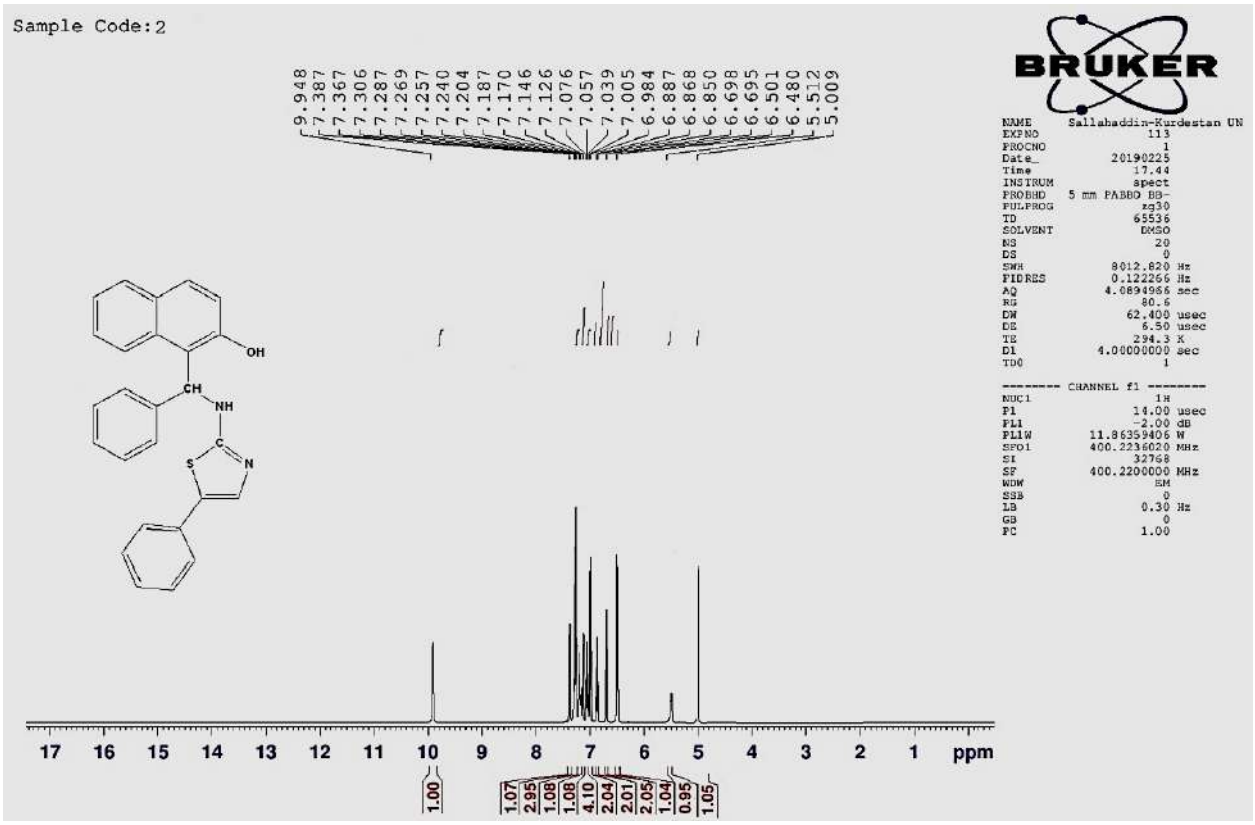

Fig. 16: ^{1}H-NMR Spectrum of (phenyl((5-phenylthiazol-2-yl)amino)methyl)naphthalen-2-ol **(7a)**

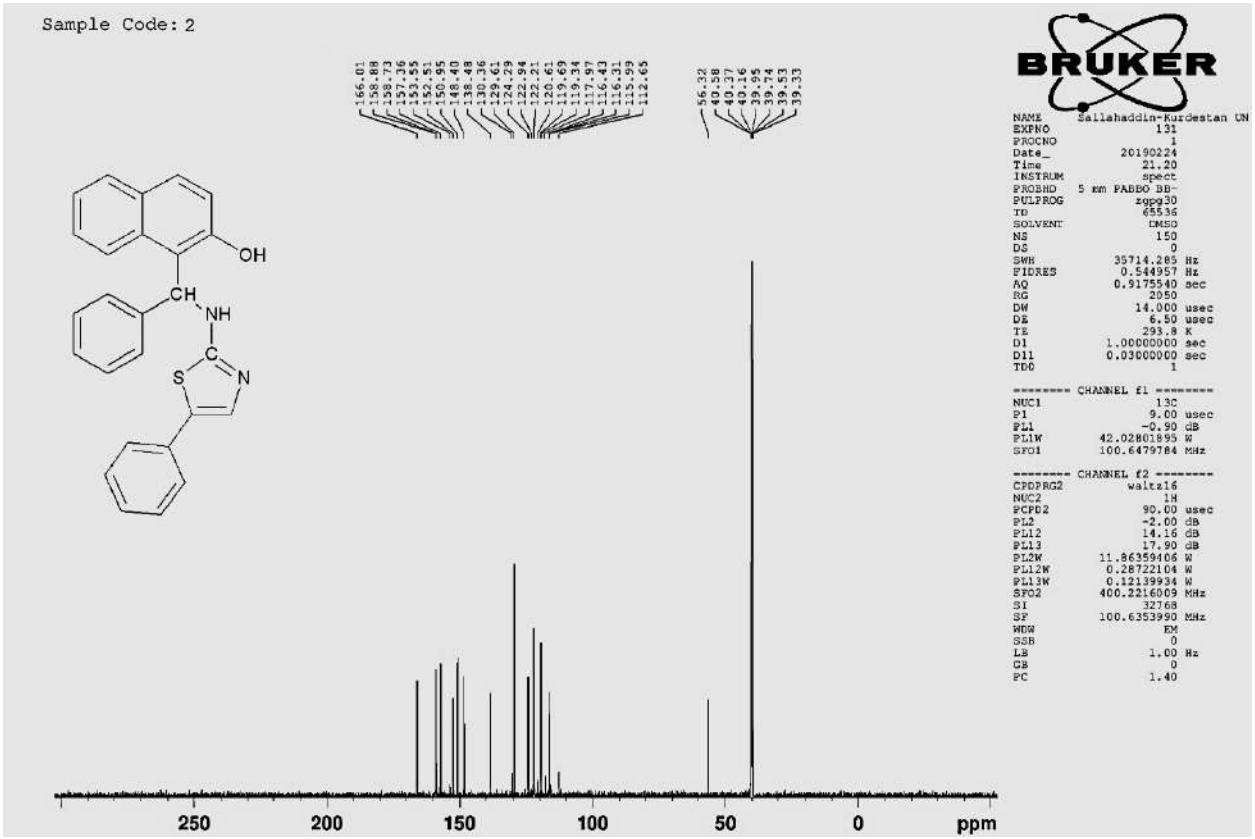

Fig. 17: ^{13}C-NMR spectrum of (phenyl((5-phenylthiazol-2-yl)amino)methyl)naphthalen-2-ol **(7a)**

REFERENCES

ABDULLAH, M. N. 2014. Environmentally Benign Approach to the Synthesis of Some New Thiazolidinone Derivatives. *Zanco Journal of Pure and Applied Sciences* 26**,** 1-12.

AL-MULLA, A. 2017. A review: biological importance of heterocyclic compounds. *Der Pharma Chemica*, 9(13)**,** 141-1472.

ALI, R. A., AMER, Z. & AL-TAMIMI, E. O. 2018. Synthesis and characterization of substituted 1, 2, 4-triazole and their derivatives on poly ethylene. *Journal of Pharmaceutical Sciences and Research*, 10**,** 1079-1084.

AYATI, A., EMAMI, S., ASADIPOUR, A., SHAFIEE, A. & FOROUMADI, A. 2015. Recent applications of 1, 3-thiazole core structure in the identification of new lead compounds and drug discovery. *European journal of medicinal chemistry*, 97**,** 699-718.

BHOSALE, P., CHAVAN, R. & BHOSALE, A. 2012. Design, synthesis, biological evaluation of thiazolyl Schiff base derivatives as novel anti-inflammatory agents. *Indian Journal of Chemistry*, 51B, 1649-1654.

CHUNDURU, V. S. & RAO, V. R. 2010. Synthesis of coumarin-substituted thiazolyl-pyrazolone derivatives via one-pot reaction. *Journal of Sulfur Chemistry*, 31**,** 545-550.

DE AQUINO, T. M., LIESEN, A. P., DA SILVA, R. E., LIMA, V. T., CARVALHO, C. S., DE FARIA, A. N. R., DE ARAUJO, J. M., DE LIMA, J. G., ALVES, A. J. & DE MELO, E. J. 2008. Synthesis, anti-Toxoplasma gondii and antimicrobial activities of benzaldehyde 4-phenyl-3-thiosemicarbazones and 2-[(phenylmethylene) hydrazono]-4-oxo-3-phenyl-5-thiazolidineacetic acids. *Bioorganic & medicinal chemistry*, 16**,** 446-456.

GURUMURTHI, S., SUNDARI, V. & VALLIAPPAN, R. 2009. Synthesis and biological evalution of some thiazolidinone derivatives of acyclic and cyclic ketones as antibacterial agents. *Oriental Journal of Chemistry*, 25(3)**,** 615-619.

KAPOOR, G., PATHAK, D. P., BHUTANI, R. & KANT, R. 2016. Thiazolidinone as a pharmacologically active molecule. *J Chem Pharm Res*, 8(4)**,** 151-68.

KAUR, P. & CHAWLA, A. 2017. 1, 2, 4-Triazole: a review of pharmacological activities. *International Research Journal of Pharmacy*, 8(7)**,** 10-29.

KUBBA, A. A. M. & RAHIM, N. A. 2018. Synthesis, Characterization and Antimicrobial Evaluation with DFT Study of New Two-Amino-4-(4-Chlorophenyl) Thiazole Derivatives. *Iraqi Journal of Pharmaceutical Sciences (P-ISSN: 1683-3597, E-ISSN: 2521-3512)*, 27**,** 79-88.

KUMAR, R. & PATIL, S. 2017. Biological prospective of 4-thiazolidinone: a review. *Hygeia Journal for drugs and medicines, 9, 80-97.*

LANDAGE, V., THUBE, D. & KARALE, B. 2019. Synthesis, characterisation and antimicrobial screening of some new thiazolyl chromones and pyrazoles. *Indian journal of chemistry*, 58B, 916-920.

NAGAWADE, R. R. & SHINDE, D. B. 2007. Zirconyl (IV) Chloride--Catalyzed Multicomponent Reaction of β-Naphthols: An Expeditious Synthesis of Amidoalkyl Naphthols. *Acta Chimica Slovenica*, 54, 642-646.

NIRWAN, S., CHAHAL, V. & KAKKAR, R. 2019. Thiazolidinones: Synthesis, Reactivity, and Their Biological Applications. *Journal of Heterocyclic Chemistry*, 56**,** 1239-1253.

PEJCHAL, V., PEJCHALOVÁ, M. & RŮŽIČKOVÁ, Z. 2015. Synthesis, structural characterization, antimicrobial and antifungal activity of substituted 6-fluorobenzo [d] thiazole amides. *Medicinal Chemistry Research*, 24**,** 3660-3670.

POURAMIRI, B. & KERMANI, E. T. 2017. Lanthanum (III) chloride/chloroacetic acid as an efficient and reusable catalytic system for the synthesis of new 1-((2-hydroxynaphthalen-1-yl)(phenyl) methyl) semicarbazides/thiosemicarbazides. *Arabian Journal of Chemistry*, 10**,** S730-S734.

ROUF, A. & TANYELI, C. 2015. Bioactive thiazole and benzothiazole derivatives. *European journal of medicinal chemistry*, 97**,** 911-927.

SHALINI, M., YOGEESWARI, P., SRIRAM, D. & STABLES, J. 2009. Cyclization of the semicarbazone template of aryl semicarbazones: synthesis and anticonvulsant activity of 4, 5-diphenyl-2H-1, 2, 4-triazol-3 (4H)-one. *Biomedicine & pharmacotherapy*, 63**,** 187-193.

SHNEINE, J. K. & ALARAJI, Y. H. 2016. Chemistry of 1, 2, 4-triazole: A review article. *International Journal of Science and Research (IJSR)*, 5, 1411-1423.

SUSHILKUMAR, S. B. & DEVANAND, B. S. 2003. Synthesis and Anti-inflammatory Activity of [2-(Benzothiazol-2-ylimino)-4-oxo-3-phenylthiazolidin-5-yl]-acetic acid derivatives. *Journal of the Korean Chemical Society*, 47**,** 237-240.

TAYLOR, A. P., ROBINSON, R. P., FOBIAN, Y. M., BLAKEMORE, D. C., JONES, L. H. & FADEYI, O. 2016. Modern advances in heterocyclic chemistry in drug discovery. *Organic & biomolecular chemistry*, 14**,** 6611-6637.

TOCHE, R. & DESHMUKH, S. U. 2017. A Review on some Thiazole Containing Heterocyclic Compounds and their Biological Activity. *International Journal of Science and Research in Science and Technology*, 3, 20-25

YOUNIS, M. N., ZIWAR G. B., ABDULLA, M. N. 2012.. Green Approach: Multi component Reaction of alpha and beta-Naphthols Using Zirconyl(IV) Chlorid Catalyst. *Zanco Journal of Pure and Applied Science*, 24**,** 67-76.

ZANCO Journal of Pure and Applied Sciences
The official scientific journal of Salahaddin University-Erbil
https://zancojournals.su.edu.krd/index.php/JPAS

ISSN (print):2218-0230**, ISSN (online):** 2412-3986**, DOI: http://dx.doi.org/10.21271/zjpas**

RESEARCH PAPER

A Study of Zooplankton Community in Alwand River and Dam- Iraq

Nargs A.Akbar, Luay A. Ali.

Dept. of biology, College of Education, Salahaddin University-Erbil, Kurdistan region, Iraq

A B S T R A C T:

This study was conduct on the zooplankton community from eight selected sites in the Alwand Rivers and Alwand Dam .Monthly samples of water, zooplankton and phytoplankton were collected for the period from June 2018 to February 2019 .The results of physico-chemical properties of water showed that the Air temperature ranged from 9-47 °C while water temperature ranged from 8-35.7 °C, hydrogen ion concentration in most of studied period was alkaline side above 7 , it was ranged between 7.6 -8.26, Turbidity ranged from 5.98 to 317.6 NTU, dissolved oxygen from 1.5 mg.l^{-1} to 3.13 mg.l^{-1} and electrical onductivity from 918 to 1782 µs.cm-¹. Regarding to zooplankton, 81 species belonging to Rotifera (70 species), Cladocera (6 species) and zcopopoda (4 species). Also total count of phytoplankton was ranged from 60000 to 145000 cells.l^{-1} while total count of zooplankton from 4566.758 to 32433.98 ind.m^{-3}.

KEY WORDS: Zooplankton, Alwand river, Alwand Dam, Iraq.
DOI: http://dx.doi.org/10.21271/ZJPAS.32.3.13
ZJPAS (2020) , 32(3);116-126 .

INTRODUCTION

Zooplankton is the floating and microscopic animal found in all the water bodies, especially the pelagic and littoral zones in the ocean, also in ponds, lakes, and rivers, scientists have found that all of the zooplankton descent into one of two categories, the first group is called holoplankton these zooplankton spend their entire lives drifting through the epi- and meso- pelagic zones. While the second group is called meroplankton are organisms lives plankton one part of life cycle (Dede and Deshmukh, 2015).

Zooplankton communities that inhabit different water bodies in diversity and density as well as in the physicochemical properties of water. Moreover, zooplankton has been considered are one of the most important components in fresh water ecosystems, they perform several vital functions with in lake ecosystems including the transference of energy and nutrients from producers to secondary consumers, the sequestration of nutrients, and the removal of phytoplankton from the water column, also used as one of the bioindicators for accessing aquatic ecosystem health (Apaydın Yağcı,et al ,2017)
Numerous studies on Strong relation exist between phytoplankton and zooplankton in different parts of the world, Lonsdale, et al. (1996) made a study on effects of zooplankton grazing on phytoplankton communities in Lower Hudson River. However, Gołdyn et al. (2008) studied

* **Corresponding Author:**
Nargs, A, Akbar
E-mail: nargsali88@Yhaoo.com
Article History:
Received: 13/11/2019
Accepted: 12/01/2019
Published: 15/06 /2020

seasonal variability in phytoplankton formation and grazing effect on phytoplankton at the Swarzędzkie Lake in western Poland, In Greater Zab River Ali (2010) conducted a study on Seasonal variation in physico-chemical properties and zooplankton biomass. While, Dorche et al. (2018) studied the Seasonal variations of plankton structure as bioindicators in Zayandehrud Dam Lake in Iran.

The aim of this study is to survey and study the zooplankton community and its relations to phytoplankton in Alwand River and Dam-Iraq, and some physicochemical and factors of the rivers have also been measured.

MATERIALS AND METHODS

The Alwand River originates from Iranian territory, and enters Iraq Southeast of the city of Khanaqin, in 2013 the Alwand Dam was built about 7 km south-east of the Khanaqin City. The length of Alwand dam about 1342m. Then high of the dam about 24 meters, while the usual storage capacity reached to up to 37.924 million cubic meters, Khanaqin city is located on the coordinates of 34 ° 20′00 ″ N 45 ° 23′00 ″ E (Hassan, 2013; Saed ,2015).

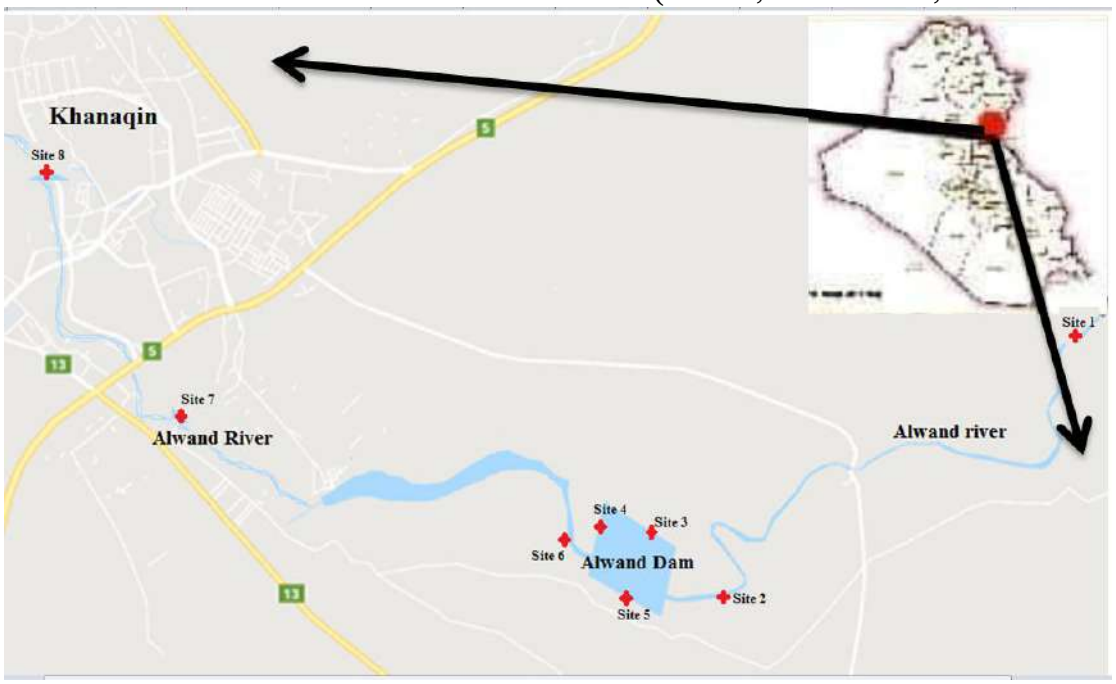

Fig. (1) Map of Iraq showing the studying sites on Alwand River and Dam-Iraq.

Water Samples for physical, chemical and biological variables in eight sites from of Alwand river and Alwand Dam were collected by using a polyethylene bottle washed them with a river sample twice before using during period from June 2018 to the February 2019 (Fig.1). The measurements of physico-chemical parameters were conducted including: Air temperature by using precise mercury thermometer, pH using pH-meter model HI 2210, Electrical conductivity by using EC-meter model (Senz μSiemen conductivity tester), and Turbidity monred by using Turbidity meter model TB, 210 IR, while Dissolved Oxygen and BOD_5 measured by Azide modification method (A.P.H.A.1998). The zooplankton samples were collected by passing 30 liters of River and Dam water using a network of plankton (55 mash pore in diameter), then concentrated samples were fixed with 5% formalin and subsequently stored in 70% ethanol (APHA 2012). As for the phytoplankton Enumeration, was conducted on the basis of modified membrane filtration technique (Hinton and Maulood, 1979).

Statistical analysis was conducted for the data using IBM spss program version 22. One way Analysis of Viriance (ANOVA) without replication to determine the effect of different sites and sampling date, the comparison between the means of studied factors data were conducted using least significant differences (LSD) value (P<0.05). Duncan was also used to determine whether the mean results of sites and date are significantly different or not.

RESULTS AND DISCUSSION

In the present study, table (1) showing the results of physical and chemical properties of the Alwand River and Dam at eight studied sites, from the table appear that the air temperature was ranged from 9 to 47 C°, the lowest value was recorded at site 7 during December 2018, while the highest value was recorded at site 6 during July 2018. The similar results were reported by (Saadalla, 1998) in Diyala River. On the other hand, the measurements of water temperature ranged from 8 to 35.7 C°. The minimum water temperature was recorded at two site (7,1) during December 2018 and January 2019 respectively. While, the maximum water temperature observed in site 4 during July 2018. The statistical analysis showed that the air and temperature value was significantly different (P< 0.05) between studied sites and date of sampling. The fluctuations in air and water temperature are close with that reported and explained by (Bello et al., 2017).

Hydrogen ion concentration in Alwand river and Dam during of most of studied period was at alkaline side above 7, the higher value was 8.26 recorded in site 2 during December 2018, while, the lower value was 7.6 recorded in site 6 during November 2018 with high significant differences (p<0.005) between date of sampling and studied sites. Such results is normal condition for Iraqi Inland water and as a result of geological formation of the area (Ganjo, 1997), also the same results were reported by (Dhahir, 2016) in Dukan Lak and (Ali, 2010) in Lesser Zab River.

The level of electrical conductivity at the studied river and Dam water was ranged from 918 to 1782 µs. cm-¹. The higher level of EC was recorded in site 4 during Octoper 2018, while the lower level of EC was recorded in site 6 during February 2019. Statistical analysis observed that the EC value was significantly different (P< 0.05) between studied sites and date of sampling. The variability may be associated with the presence of chloride ions and dissolved ions that form the main constituents of water and directly affect EC values and similar results have been reported by (Moyel and Aboud, 2015) in Shatt al-Arab River.

The level of turbidity ranged from 5.98 to 317.6 NTU. The maximum value was 317.6 recorded at Site 8 during November 2018. While, the minimum value was 5.98 recorded at site 7 during February 2019 with significant differences (P<0.005) between study sites and date of sampling. This may be due to several factors such as discharging of many contaminants or due to heighten of phytoplankton growth (Ali, 2010). These recorded results were close to that reported by (Saadalla, 1998) in Diyala River.

Dissolved oxygen concentration of studied river was ranged from 1.5 to 2.93 $mg.l^{-1}$. The higher level of dissolved oxygen was 2.93 recorded at Site 1 during January 2019. While, the minimum value was observed in site 8 during September 2018. Statistically the results showed significant differences (p< 0.05) between both study sites and dates of sample, this may be attributed to a high organic matter which escort by increase in action of anaerobic bacteria and decreasing of dissolved oxygen in water (Toma, 2011). In addition to, BOD_5 values were ranged between 0.01 to 1.43 $mg.l^{-1}$, the lower value was recorded at two sites (6,7) during June 2018, whereas the higher value was recorded at site 2 during September 2018, and statistically analysis showed significant differences (p< 0.05) between study sites and dates of sample. The fluctuation in BOD_5 value may be related to the several causes such as human activities pollution caused by throwing pollutants directly into the river and high decomposition of organic matters in the lake during summer due to high water temperature, and low water level (Ali and Dhahir, 2017).

Concerning to zooplankton community study, 80 species of zooplankton were identified (Table 2) represented by three groups; Cladocera was dominant group (68.889%). Copepoda was second ranked in order of zooplankton abundance in the study site with (41.463%). The third ranked order of zooplankton in studied river and Dam was Rotifera with (17.607%).

Regarding to Cladocera, 6 species (*Bosmina coregoni* (Baird, 1857), *Bosmina longirostris* ((Muller 1785) *Eubosmina tubicen* (Brehm, 1953), *Alona rectangular(Sars 1861), Cerodaphnia reticulate* (Jurine ,1820) and *Scapholeberis kingi* (Sars ,1903)) were recorded they belonged to four families; Bosminidae Chydoridae, and Daphinidae. The lowest value of Cladocera was observed in the winter months. The high density of Cladocera was 833.35 ind.m^{-3} recorded at site 5 during June 2018, this may be due to agreeable environmental conditions, including temperature, dissolved oxygen and the availability Bumper food in the form of bacteria, waste disposal and also abundance of food resources (aquatic plants and phytoplankton) as organic matter on this site (Salve and Hiware, 2010).

However, Copopoda represented by 4 species (*Diacyclops thomasi* (Forbes 1882), *Megacyclops viridis* (Kiefer,1927), *Orthocyclops modestus* (Herrick,1883) and *Microcyclops rubellus* (Lilljeborg, 1901)) belonged to one family (Cyclopoidea), the higher population density of it was in summer season with 566.678 ind.m^{-3} reported at site 5 during June and July 2018, while lower number of copepoda was recorded in winters seasons with significant differences ($p< 0.05$) between study sites and dates of sample. The current results are consistent with the result of (Saadalla, 1998) in Himreen impoundment and (Sontakke and Mokashe, 2014) in Dekhu reservoir in India.

Rotifera come in third ranked in this study, during the sampling date 70 species of it were observed belonged to 12 families; Philodinidae, Branchionidae, Lecanidae, Lepadellidae, Scaridiidae, Asplanchnidae, Trichotriidae, Notommatidae, Trochosphaeridae, Testudinellidae, Synchaetidae and Euchlanidae. The total recorded Rotifera in the present study was ranged between 33.334 to 11900.238 ind.m^{-3}, with significant differences ($p< 0.05$) for both study sites and dates of sample. The maximum value was recorded in site 3 during December 2018, while the minimum value were recorded in sites 1 during January 2019, and this may be due to decrease of phytoplankton number in which zooplankton grazing on it, in addition to low temperature during cold winter months. The current results were agreed with those reported by (Ali, 2010) in Greater Zab River.

It is worth to mention that the total number of phytoplankton was ranged from 60000 to 145000 cells.l^{-1}. Maximum number of phytoplankton was observed at site 3 during September 2018, while a minimum number was recorded at Site 2 during November 2018. The lower densities of phytoplankton was recorded in cold months and this may be related to low temperatures in addition to other factors such as light, nutrients and primary consumers that acts as growth limit. Concerning to zooplanktonic communities the results showed that the total zooplankton number was ranged from 4566.758 to 32433.98 ind.m^{-3}, the maximum and minimum number were observed in December and July 2018 respectively. The variations in the population densities may be due to many factors such as water temperature, dissolved oxygen, hydrogen ion concentration and electrical conductivity. From the statistical analysis appear that there are positive correlations between each of Rotifera and Copepoda and phytoplankton with r=0.101 and 0.022 respectively, while a negative correlation was observed between Cladocera and phytoplankton with r=-0.002. These results are close with the results reported by Haque (2015) in Tidal Sangue River in Bangladesh. Generally, decrease of the number of zooplankton during November 2018 may be due to decrease of phytoplankton number in which zooplankton grazing on it, in addition to

low temperature during cold winter months. These results are consistent with those reported by Saadalla (1998) in Diyala River and El-Sherbiny, et al (2011) in Timsah Lake in Egypt.

Table (1) Physico-chemical properties of ALwand River and Dam, data represented as minimum and maximum value from June 2018 to February 2019

Physico-chemical Parameters	Site1	Site2	Site3	Site4	Site5	Site 6	Site7	Site8
Air temperature(˚C)	15-43	15-42	20-43	20-44.33	15-45	13-47	9-41	12-42
Water temperature(˚C)	8-32.33	12.33-33.33	13-33.33	12-35.7	14-31	12-31.7	8-30.7	11-32.33
Hydrogen ion con. (pH)	7.8-8.12	7.59-8.26	7.80-8.19	7.72-8.21	7.65-8.24	7.6-8.16	7.73-8.22	7.52-8.21
Electrical conductivity (EC) (µs.cm-¹)	921-1685	932-1701	944-1759	937-1782	941-1702	918-1691	971-1699	962-1708
Turbidity (NTU)	18.66-113	13.6-79.4	9.03-36.03	7-29.1	6.48-23.7	9.85-39.7	5.98-42.43	10.74-317.6
Dissolved oxygen (mg $.l^{-1}$)	1.47-2.93	1.98-2.37	1.33-2.67	1.7-3.1	1.6-3.13	1.8-3.13	2.1-2.73	1.5-3
Biochemical oxygen demand (BOD_5) (mg $.l^{-1}$)	0.04-1.13	0.03-1.43	0.03-1.3	0.05-1.16	0.04-1.13	0.01-1.1	0.01-1.1	0.03-0.83

Table (2) list of Zooplankton recorded during studied period in ALwand River and ALwand Dam.

ZOOPLANKTON	**Site1**	**Site2**	**Site3**	**Site4**	**Site5**	**Site6**	**Site7**	**Site8**
Phylum: Rotifera (17.607%)								
Class: Bdelloidea								
Order: Bdelloidae								
Family: Philodinidae								
Bdelloidae sp (Ehrenberg)	+	+	+	+	+	+	+	+
Bdelloidae sp (Ehrenberg)		+	+		+			
Class: Monogonata								
Order: Ploima								
Family: Branchionidae								
Anuraeopsis fissa (Gosse 1851)	+	+	+					
Anuraeopsis ovalis (Bergendal)					+			

Keratella tecta (Gosse,1851)	+	+	+	+		+	+	+
Keratella tropica (Apstein 1907)	+	+	+	+	+	+	+	+
Keratella Cochalaris (Gosse,1851)	+	+	+	+	+	+	+	+
Brachionus forficula (Wierzejski,1891)	+	+	+	+	+	+	+	+
Brachionus falcatus (Zacharias ,1898*)*	+	+	+	+	+	+	+	+
Brachionus angularis (Gosse,1851)	+	+	+	+	+	+	+	+
Brachionus rotundiformis (Tschugunoff,1921)	+	+	+	+	+	+	+	+
Brachionus dimidiatus (Bryce,1931)		+	+	+		+	+	+
Brachionus calyciflorus (Pallas,1766)		+	+	+	+	+	+	+
Brachionus quadridentatus (Hermann1783)		+			+	+	+	+
Brachionus Plicatilis (Muller,1786)			+	+	+	+	+	+
Brachionus Rubens (Ehrenberg,1838)				+				
Brachionus variabilis (Hempel,1896)			+	+	+		+	
Brachionus Diversicornis (Daday,1883)		+					+	
Platyias quadricornis (Ehrenberg,1832)		+	+					
Notholca acuminate (Ehrenberg, 1832)			+	+	+			+
Notholca Squamula (Muller 1786)					+	+	+	+
Family: Scaridiidae								
Scaridium longicaudum (Muller 1786)			+					
Family:*Asplanchnidae*								

Asplanchna priodonta (Gosse,1850)		+	+	+	+	+	+	+
Asplanchna Herriki (Guerne ,1888)			+	+		+	+	+
Family: Synchaetidae								
Synchaeta sp (Ehrenberg,1832)	+	+	+	+	+	+	+	+
Polyarthra vulgaris (Carlin 1956)			+		+	+	+	+
Polyarthra dolichoptera(Idelson,1925)		+	+		+	+		+
Family:trichotriidae Harring (1913)								
Trichotria tetractis (Ehrenberg.1830)	+	+	+	+	+	+		
Trichotria Pocillum (O.F.M. ,1776)			+	+	+			
Trichocerca porcellus (Gosse,1886)						+		
Trichocerca pusilla (Jennings, 1903)								+
Family: Notommatidae								
Cephalodella gibba (Ehrenberg 1830)	+	+	+	+	+	+	+	+
Cephalodella remanni(Donner, 1950)		+	+	+	+			+
Cephalodella Tantilloides (Hauer,1935)		+			+			
Cephalodella spp					+	+		
Cephalodella hoodia (Gosse ,1886)	+	+	+		+			+
Family: Lecanidae								
Lecane bulla (Gosse, 1851)	+	+	+	+	+	+	+	+
Lecane elasma (Harring & Myers, 1926)	+	+	+		+		+	+
Lecane thienemanni (Hauer,1938)	+							

Lecane stenroosi (Meissner,1908)	+				+	+	+	+
Lecane undulate(Hauer ,1938)		+			+			+
Lecane crepida (Harring,1914)		+	+		+			+
Lecane luna (Muller,1776)		+	+	+	+		+	+
Lecane hornemanni (Ehrenberg,1833)		+		+			+	
Lecane lunaris (Ehrenberg,1832)		+	+	+	+		+	+
Lecane tenuiseta (Harring ,1914)		+			+			
Lecane hamate (Stokes,1896)					+			+
Lecane scutata(Harring &Myers1926)					+			
Lecane punctate (Murray,1913)		+	+	+				
Lecane cornuta (Muller,1786)		+						
Lecane Donneri (Chengalath &Mulamoottil ,1974)							+	
Lecane Pyriforms (Daday,1905)		+						
Family: Lepadellidae								
Lepadella ovalis (Muller, 1896)		+	+	+	+			
Lepadella patella (Muller ,1773)	+			+	+			
Lapadella salpina (Ehrenberg, 1834)	+	+	+		+			+
Squatinella longispinata (Tatem,1867)		+			+			
Colurella obtuse (Gosse ,1886)	+	+	+	+	+		+	+
Colurella uncinata (Muller,1773)		+						
Colurella colurus (Ehrenberg ,1830)		+	+		+			
Colurella Adriatica(Ehrenberg ,1831)	+			+				
Family: Euchlanidae								
Euchlanis lyra (Hudson,1886)		+	+	+				

Euchlanis dilatate (Ehrenberg 1832)			+		+		+	+
Euchlanis triquetra (Ehrenberg 1838)	+	+	+	+	+		+	
Euchlanis tetractis (Ehrenberg)					+			
Euchlanis sp								+
Dipleuchlanis propatula (Gosse,1886)						+		
Order:Flosculariaceae								
Family:Trochosphaeridae								
Filinia longiseta (Ehrenberg,1834)							+	+
Family:Testudinellidae								
Testudenila patina (Hermann,1783)		+						
Phylum: Arthropoda								
Subphylum: Maxillopoda								
Class: Crustacea								
Order: Copepoda (41.463%)								
Family: Cyclopida								
Diacyclops thomasi (Forbes 1882)		+		+	+	+		
Megacyclops viridis (Kiefer,1927)					+			
Orthocyclops modestus (Herrick,1883)					+	+		
Microcyclops rubellus (Lilljeborg, 1901)		+	+	+	+	+	+	+
Class: Branchiopoda								
Order: Cladocera (68.889%)								
Family: Bosminidae								
Bosmina coregoni (Baird, 1857)	+	+		+	+	+	+	

Bosmina longirostris (Muller 1785)	+	+		+	+	+	+	+
Eubosmina tubicen (Brehm, 1953)	+	+		+	+	+		
Family: Chydoridae								
Alona rectangular (Sars 1861)			+					+
Family: Daphniidae								
Cerodaphnia reticulate (Jurine ,1820)		+						
Scapholeberis kingi (Sars ,1903)			+					

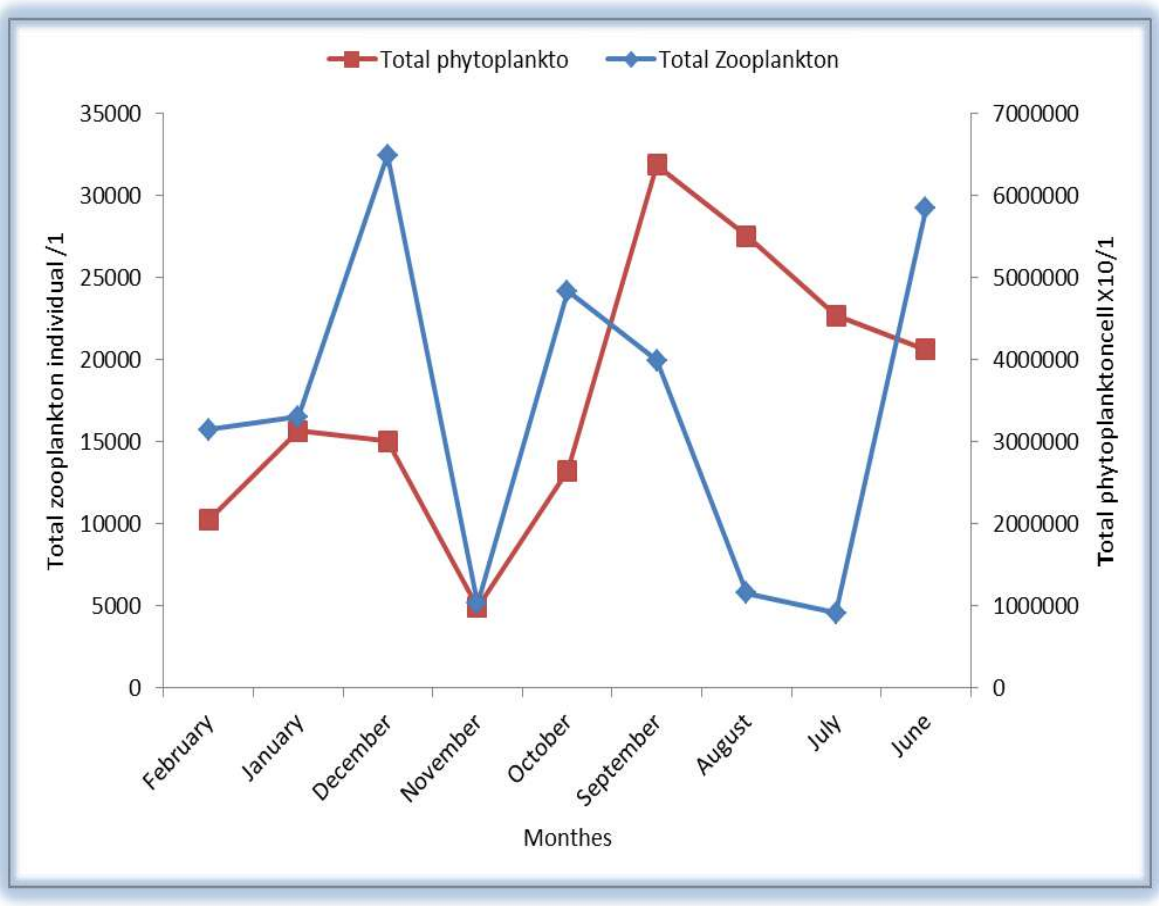

Fig. (2) Relationship between total zooplankton and total phytoplankton in ALwand river and Dam.

REFERENCES

Abdel Aziz , N. E. & Gharib, S. M. 2006. The Interaction Between Phytoplankton And Zooplankton In A Lake-Sea Connection, Alexandria, Egypt. International Journa Of Oceans And Oceanography, 1(1).p. 151-165.

Ali , L. A. & Dhahir, S. F. 2017. A Study Of Zooplankton Community In Dukan Lake, Kurdistan Region-Iraq, With A New Record Of Craspedacusta Sowerbii Lankester (1880) Medusa (Cnidaria: Hydrozoa). Baghdad Science Journal , 14(4) .

Ali, L. A. 2010. Seasonal Variation In Physico-Chemical Properties And Zooplankton Biomass In Greater

Zab River –Iraq. Jordan Journal of Biological Sciences , 3(3). P. 115 – 120.

American Public Health Association (A.P.H.A.). 1998. Standard Methods For The Examination of water And wastewater, 20th Edition. A.P.H.A., 1015 Fifteenth Street, NW, Washington, DC.

Apaydın Yağcı, M.; Yeğen, V.; Yağcı, A. & Uysal, R. 2017. A Preliminary Study On Zooplankton Species In Different Aquatic Habitats Of Anatolia (Turkey). Limnofish, 3(1).p. 45-50.

AMERICAN PUBLIC HEALTH ASSOCIATION (A.P.H.A.) 2012. Standard methods for the examination of water and wastewater. 20th. Ed. A.P.H.A., 1015 Fifteenth Street, NW, Washington, DC. 20005-2605.

Bello, A. D.; Hashim, N. B. & Mohd Haniffah , M. R. 2017. Predicting Impact Of Climate Change On Water Temperature And Dissolved Oxygen In Tropical Rivers. Climate, 5(58).

Dede, A. N. & Deshmukh, A. L. 2015. Study On Zooplankton Composition And Seasonal Variation In Bhima River Near Ramwadi Village, Solapur District (Maharashtra), India . Int.J.Curr.Microbiol.App.Sci ,4(3). p. 297-306.

Dhahir, S. F. 2016. A Study Of The Shore Zooplankton Community In The Small Part Of Dukan Lake, Kurdistan Region/ Iraq. Msc. Thesis. University Of Salahaddin.

Dorche, E. E.; Shahraki, M. Z.; Farhadian,O. &Keivany,Y. 2018 . Seasonal Variations Of Plankton Structure As Bioindicators In Zayandehrud Dam Lake, Iran. Limnol. Rev. , 18(4).p. 157–165.

El-Sherbiny, M.; Gab-Alla, A. & Al-Aidaroos, A. M. 2011. Seasonal Composition And Population Density of Zooplankton In Lake Timsah, Suez Canal, Egypt. OCEANOLOGIA ,53(3).p. 837-859.

Ganjo, D. 1997. A Limnological Study On Ruwandiz River Path Within Arbil Province, Iraq. Ph.D. Thesis. University Of Salahaddin.

Gołdyn, R. & Kowalczewska-Madura, K. 2007. Interactions Between Phytoplankton And Zooplankton In The Hypertrophic Swarzędzkie Lake In Western Poland . Journal Of Plankton Research, 30(1).p. 33–42.

Haque, A K M F. ; Begum , N. & Islam , M. S. 2015. Seasonal Variations In Phytoplankton And Zooplankton Population In Relation To Some Environmental Factors In The Tidal Sangu River In Chittagong In Bangladesh. J. Sylhet Agril. Univ. , 2(2).p. 209-219.

Hassan, M. H. 2013. The Project Of Alwand Dam And Its Impact On Sustainable Agricultural Development In Khanaqin Spand . Journal Of Garmyan University , 2 . p. 233-248.

Hinton, G. C. F. & Maulood, B. K. 1979. Fresh Water Diatoms From Suliamanyah, Iraq. Nova. Hedwigia, 31.p. 449-466 .

Lonsdale, D. J.; Cosper, E. M. & Doall, M. 1996. Effects Of Zooplankton Grazing On Phytoplankton Size-Structure And Biomass In The (Lower Hudson River Estuary). 19(4).p. 874-889.

Moyel, M. & Aboud, H. N. 2015. Water Quality Assessment Of The Shatt Al-Arab River, Southern Iraq . Journal Of Coastal Life Medicine .3(6) .p.465-459.

Saadalla ,H. A. 1998.Ecological Study On The Effect Of Himreen Impoundment On The Benthic And Planktonic Invertebrates Of River Diyala. Ph.D. Thesis. University Of Baghdad.

Saed, E. H. 2015 .Visual Pollution And Its Effects On The Contemporary Urban Environment Of Khanaqin City (A Thesis About Environmental Geography) . Msc. Thesis .University Of Garmyan Faculty Of Humanity..

Salve, B. & Hiware, C. 2010. Zooplankton Diversity Of Wan Reservoir, Nagpur (MS) India, J. Of Trends Res. Sci. And Tech., 2 (1). p. 39-48.

Sontakke, G.; Mokashe , S. 2014. Diversity Of Zooplankton In Dekhu Reservoir From Aurangabad, Maharashtra. Journal Of Applied And Natural Science ,6 (1).p. 131-133.

Toma , J. J. 2011. Limnological Study In Dokan Lake, Kurdistan Region Of Iraq. Journal Of Environmental Studies, 6.p.1-12.

ZANCO Journal of Pure and Applied Sciences
The official scientific journal of Salahaddin University-Erbil
https://zancojournals.su.edu.krd/index.php/JPAS

ISSN (print):2218-0230**, ISSN (online):** 2412-3986**, DOI: http://dx.doi.org/10.21271/zjpas**

RESEARCH PAPER

Effect of Vitamin C Against Lead Acetate Toxicity on Sperm Count, Sperm Morphology and Testis Tissue in the Rat Before and in Recovery Period

Gulzar Star Hama amin [1], Karim Rahman Hamad[2]

[1&2] Department of Biology, College of Education, Salahaddin University-Erbil, Kurdistan Region, Iraq.

A B S T R A C T

The present study was conducted to investigate the effect of lead acetate (LA) (30 mg/Kg B.wt/day), and vitamin C (Vit.C) (100 mg/Kg B.wt/day) against LA toxicity in adult male rats. The design of study included two experiments (exp.). In exp-I rats were divided into 3 groups. Group I: control, group II: received LA, and group III: received LA coadministrated with Vit.C, for 6 weeks. In exp-II rats were divided into 4 groups. Group I: control, group II: received LA, group III: received LA coadministrated with Vit.C, and group IV: received LA. The groups were treated for 6 weeks, then groups II, &III in order to be recover were left without treatment (as control) for additional 6 weeks. While group IV after cessation of LA received Vit.C within recovery period (for 6 weeks). At the end of each experiment rats were sacrificed. Blood samples were collected and used for determination of serum MDA. Histological sections were made from testis. Sperm characteristics included sperm count was determined from caudal epididymis and sperm abnormalities from left vas deferens. In exp-I, LA group showed significantly decreased sperm count, significant increase in sperm abnormalities and MDA, and testicular tissue damage. While in group III Vit.C against LA significantly improved sperm characteristics and testicular tissue as well. In exp-II, Group II showed almost no improvement in sperm characteristics and testicular tissue, whereas MDA was increased non-significantly from control. In group III the coadministrated Vit.C with LA, markedly improved sperm characteristics, and testicular tissue similar to Vit.C against LA in exp-I. Meanwhile, the improvement by Vit.C in group IV was occurred in lesser extent. In conclusions, Vit.C had a protective effect against LA toxicity, and it was markedly more effective when coadministrated along with LA rather than its administration after cessation of LA.

KEY WORDS: Lead acetate, Vitamin C, Testis, Sperm count, Sperm abnormality.
DOI: http://dx.doi.org/10.21271/ZJPAS.32.3.14
ZJPAS (2020) , 32(3);127-138. .

1. INTRODUCTION

Lead is a heavy metal of wide occupational and environmental contamination. Lead toxicity is associated with an increased risk of adverse effect on a variety of target organs (Abd-El-Reheem and Zaahkcuk, 2007).

It causes serious health effects which might be permanent and lead to fatality (Assi *et al.*, 2016). The reproductive system of both males and females is affected by lead (Wani *et al.*, 2015). Several surveys have linked exposure to lead with decreased sperm count and other signs of male reproductive toxicity (Bonde *et al.*, 2002). The study of (Liu *et al.*, 2008) showed toxic effect of LA on male offspring rats which exhibited disordered arrangement of germ cells and Leydig cells, a decreased spermatogenic cell layer in the seminiferous tubules, and giant cells in the

* **Corresponding Author:**
Gulzar Star Hama amin
E-mail: Gulzarstar91@gmail.com
Article History:
Received: 03/12/2019
Accepted: 15/01/2020
Published: 15 /06 /2020

lumen, however the diameter of seminiferous tubules significantly decreased. Other study demonstrated that the histopathological examination of testes obtained from rats treated with lead, showed mild degenerative changes (Hari Priya and Reddy, 2012). In another study, rats exposed to LA, revealed that lead can induce pronounced alterations on germ cells in the testis (Haouas *et al*., 2015). Previously it has been shown that lead caused significant reduction in epididymal sperm count in mice (Wadi and Ahmad, 1999). In addition, it was reported that LA significantly decreased total testicular sperm and total cauda epididymal sperm in rats (Ait Hamadouche, 2009). Furthermore, the reduction in epididymal sperm count in rats was confirmed by (Hari Priya and Reddy, 2012; Anjum and Reddy, 2014). Clinical and animal studies also indicate that abnormalities of spermatogenesis result from toxic lead exposure (Sokol *et al*., 1985), and higher percentages of immature and abnormal sperm in lead exposed workers have been reported (Telišman *et al.*, 2007). Besides that, researchers revealed the significant increase in sperm abnormality in lead acetate intoxicated rats (Allouche *et al*., 2009; Elgawish and Abdelrazek, 2014; Ramah *et al.*, 2015).

Vitamin C is a water-soluble substance (Bendich *et al.*, 1986), It has a low-molecular weight that protects the cell from oxygen-nitrogen radicals (Ogutcu *et al*., 2008). Vitamin C (ascorbic acid), has been used in the treatment of lead toxicity. It has importance in maintaining the testes physiological integrity (El-Tohamy and El-Nattat, 2010). Previous study indicated that vitamin C at a concentration (10 mg/kg body weight) which is equivalent to the human therapeutic dose significantly minimize the testicular malondialdehyde content, and a companied by increase in sperm count and significant decrease in the percentage of abnormal sperm morphology in the mice exposed to lead acetate for 5-8 weeks (Mishra and Acharya, 2004). (Ayinde *et al.*, 2012) reported that vitamin C coadministrated with lead acetate significantly increased sperm count in lead treated rats, and decreased the percentage of abnormal sperm morphology. In view of our reviewing and observations, there is little information deals with the study of protective effect of vitamin C against lead acetate toxicity on male reproductive system, therefore the present research plan aimed to study the effects of lead acetate and vitamin C against lead acetate toxicity on sperm count, sperm abnormalities and testis section before and in recovery period in the rat.

2. MATERIALS AND METHODS

2.1. Animals and housing

The male rats (*Rattus norvegicus)* of this study were obtained from inbreeding in animal house of Department of biology, College of Education, Salahaddin university-Erbil. During the entire period of experiments the rats were kept in special cages with a steel stainless wire mesh top to hold standard rodent diet (Pico Lab. Rodent Diet 20) and tap water *ad libitum*. The room temperature was kept at about 22±4 ^{o}C and the light dark cycle was 12/12 hours.

2.2. Chemicals

lead acetate trihydrate Pb $(CH_3COO)_2$ .3H2O (LA) and ascorbic acid ($C_6H_8O_6$) (Vit.C) were manufactured by (Scharlab S.L. SPAIN).

2.3. Design of the experiments

2.3.1. Experiment I

Twenty-one adult male rats were divided randomly into three equal groups, each group contains seven rats. Treatments were given for six weeks as the following:

Group I (control): Rats received 0.6 ml distilled water (D.W)/ day orally by gavage.

Group II {lead acetate (LA) group}: Rats received LA 30 mg/kg B.wt in 0.6 ml D.W/ day orally by gavage.

Group III {lead acetate + Vitamin C (LAV) group}: Rats received LA 30 mg/kg B.wt in 0.3 ml D.W/ day and Vit.C 100 mg/kg B.wt in 0.3 ml D.W/ day orally by gavage.

2.3.2. Experiment II

Twenty-eight adult male rats were divided randomly into four equal groups as the following:

Group I (control): Rats received 0.6 ml D.W/ day orally by gavage.
Group II {lead acetate- Recovery (LAR) group}: Rats received LA 30 mg/kg B.wt/ day in 0.6 ml D.W orally by gavage.
Group III {lead acetate + Vit.C- Recovery (LAVR) group}: Rats received LA 30 mg/kg B.wt in 0.3 ml D.W/ day and Vit.C 100 mg/kg B.wt in 0.3 ml D.W/ day orally by gavage.
Group IV {lead acetate- Recovery+ Vit.C (LARV) group}: Rats received LA 30 mg/kg B.wt/ day in 0.6 ml D.W orally by gavage. At the end of six weeks of treatment, in groups (II, III & IV) of the experiment the treatments were stopped. The groups II & III were remained (as control) without treatment, while group IV received Vit.C (100 mg/kg B.wt in 0.3 ml D.W/ day orally by gavage), in order to be recover for additional six weeks.

2.4. Collection of blood samples

At the end of both experiments (I&II), after fasting for 24 hours, rats were anaesthetized by ether (Kempinas *et al*., 1994). Blood samples were collected by a syringe 5 ml through cardiac puncture, and immediately placed into gel tube. The samples were centrifuged, (Sorvall RC-5B Refrigerated Super speed Centrifuge), then the sera in Eppendorf tube were stored in deep freeze.

2.5. Dissection and removal organs

After withdrawal of blood samples, animals were dissected. The left testis and left caudal epididymis (epid.) were removed, and testis was preserved in 10% formal saline for fixation. The left caudal epididymis was used in sperm counting.

2.6. Sperm count

Left caudal epididymis of each rat was cut and homogenized in 5 ml of normal saline (0.9% NaCl) by manual homogenizer. Homogenates were kept in refrigerator at $4^{o}C$ for 24 hours to allow sperm to be released from the walls. Then 1 ml of the refrigerated homogenate was added to 7 ml of Eosin (0.2 %) and the samples were placed in a Neubauer hemocytometer, using light microscope. Head of the sperms were counted in 25 squares (Yucra *et al*., 2008).

2.7. Sperm morphology

Sperms were prepared from left vas deferens according to *(*Wyrobek *et al.,* 1983), the suspensions were smeared and dried. Then stained with 1% Eosin for 5 minutes. The slides were washed by distilled water and left to dry. Then sperm morphology (normal sperms, head defect sperms and tail defect sperms) were identified under microscope (1000X).

2.8. Histological sectioning

Preserved testes samples in 10% formal saline exposed to serial processes. Then embedded in paraffin wax and cooled (Drury and Wallington, 1980). Paraffin sections were cut by rotary microtome, then stained with hematoxylin (H) and eosin (E) (Bancroft and Gamble, 2008).

2.9. Malondialdehyde

Serum malondialdehyde (MDA) level was measured spectrophotometrically, by (APEL PD-303 SPECTROPHOTOMETER, 100~240V AC 50/60Hz 15W. APEL CO., LTD. JAPAN) at 532 nm. Thiobarbituric acid reaction (TBAR) method was used, and lipid peroxidation was expressed as MDA in μmol/L.

2.10. Statistical analysis

All data were expressed as mean ± S.E and statistical analysis carried out by GraphPad Prism Eight, version 6. Data analysis was made using one-way ANOVA. Results compared by ANOVA and Tukey's multiple comparisons test to determine significance among groups. Values were considered to be significantly different when $P<0.05$.

3. RESULTS

3.1. Experiment I

3.1.1. Effect of vitamin C against lead acetate toxicity on sperm count

The sperm count in groups of control (127.1± 11.61 x10^6 sperm/epid.), LA (28.94± 7.628 x10^6 sperm /epid.) and LAV (115.5± 9.538 x10^6 sperm /epid.) are shown in table 1 and figure 1-A. The sperm count was decreased significantly (P<0.01) in LA group and non-significantly in LAV group as compared to control, while in LAV group it was increased significantly (P<0.01) as compared to LA group.

3.1.2. Effect of vitamin C against lead acetate toxicity on sperm morphology

The value of sperm morphology (including normal sperm, sperm with head defect, and sperm with tail defect) in groups of control (84.22± 3.080 %; 3.088± 0.650 %; 12.69± 2.618 %), LA (34.34± 1.678 %; 11.24± 1.896%; 54.42± 1.232%), and LAV (72.72± 2.994%; 4.577± 0.178%; 22.70± 2.851%) are shown in table 1 and figure 1-B, C&D.

The percentage of normal sperms was decreased significantly (P<0.01) in LA group as compared to control. Also, in LAV group the percentage of normal sperms significantly (P<0.05) decreased from control, while it was increased significantly (P<0.01) as compared to LA group. Sperm with head defect and tail defect sperm in LA group significantly (P<0.01) increased as compared to control, while the comparison of head defect sperm of LAV group with that of control was non-significant. Also, in LAV group the percentage of head defect sperms significantly (P<0.01) decreased as compared to LA group. The percentage of tail defect sperm in LAV group was significantly (P<0.05) increased as compared to control, while it was decreased significantly (P<0.01) as compared to LA group.

Table 1: Effect of vitamin C against lead acetate toxicity on sperm count and sperm morphology in the rats.

In each group n=7

Parameters / Groups	Sperm Count x10^6 / epid.	Normal sperm (%)	Head defect sperm (%)	Tail defect sperm (%)
Control	127.1± 11.61[a]	84.22± 3.080[a]	3.088± 0.650[a]	12.69± 2.618[a]
LA	28.94± 7.628[b]	34.34± 1.678[b]	11.24± 1.896[b]	54.42± 1.232[b]
LAV	115.5± 9.538[a]	72.72± 2.994[c]	4.577± 0.178[a]	22.70± 2.851[c]

Data presented as mean ± S.E. The same letters mean non-significant differences while the different letters mean significant differences.

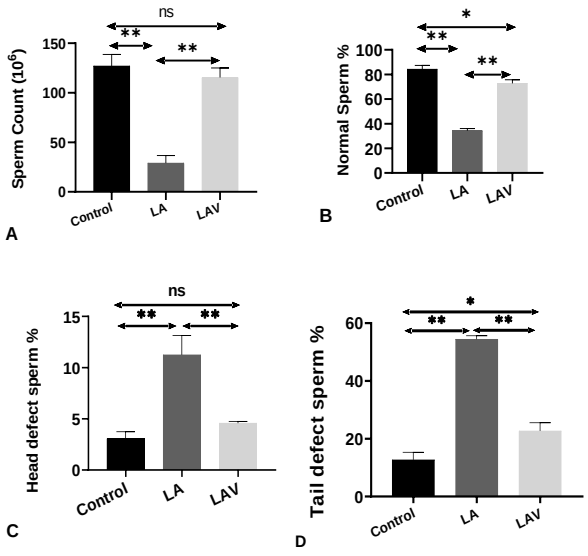

Figure 1: Effect of vitamin C against lead acetate toxicity on: A- Sperm count, B- Percentage of normal sperms, C- Percentage of head defect sperm and D- Percentage of tail defect sperm in the rats *=P<0.05 **=P<0.01.

3.1.3. Effect of vitamin C against lead acetate toxicity on serum MDA level

The serum MDA level in groups of control (4.344± 0.364 µmol/L), LA (6.706± 0.757 µmol/L), and LAV (4.865± 0.718 µmol/L) are shown in table 2 and figure 2. In LA group it was increased significantly (P<0.05) as compared to control. While non-significant change was observed in LAV group as compared to control and LA group.

Table 2: Effect of vitamin C against lead acetate toxicity on serum MDA level in the rats.

In each group n=7

Groups / Parameter	control	LA	LAV
MDA (µmol/L)	4.344± 0.364[a]	6.706± 0.757[b]	4.865± 0.718[ab]

Data presented as mean ± S.E. The same letters mean non-significant differences while the different letters mean significant differences.

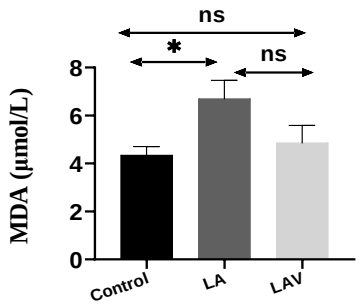

Figure 2: Effect of vitamin C against lead acetate toxicity on serum MDA level in the rats *=P<0.05.

3.1.4. Effect of vitamin C against lead acetate toxicity on histological sections of testis

The histological section of testis of control rat (figure 3) shows normal architecture of seminiferous tubules, organization of germ cells, active spermatogenesis, large number of spermatozoa in the lumen of seminiferous tubules, and large number of Leydig cells in the interstitial tissue.

The histological section of testis of rat treated with LA (figure 4) shows deformities in testicular architecture, atrophied seminiferous tubules and decline in their diameters. Degeneration in Sertoli cells and germ cell layers including all types of germ cells, indicating sever disruption in spermatogenesis. The lumen of seminiferous tubule free of spermatozoa and contains cell debris. Few spermatogonia appear shrunk with pyknotic nuclei. Depletion of Leydig cells, congested blood vessel in edematous interstium.

The histological section in testis of rat of LAV group (figure 5) shows improvement in tissue architecture of seminiferous tubules, with active spermatogenesis and organization in germ cell layers. Improvement in degenerated interstitium and Leydig cell, but still the section obviously shows reduced diameter in seminiferous tubule, and degeneration as in Leydig cells, and edema in interstitum.

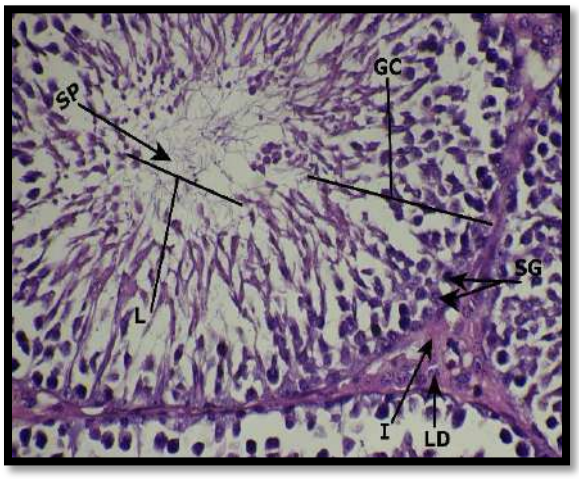

Figure 3: Section from testis of control rat, showing normal testicular architecture, seminiferous tubules, normal germ cell layers (GC) with active spermatogenesis and large amount of spermatozoa (SP) in lumen (L), and normal Leydig cells in interstitial tissue (I). (Stain: H&E. 400x).

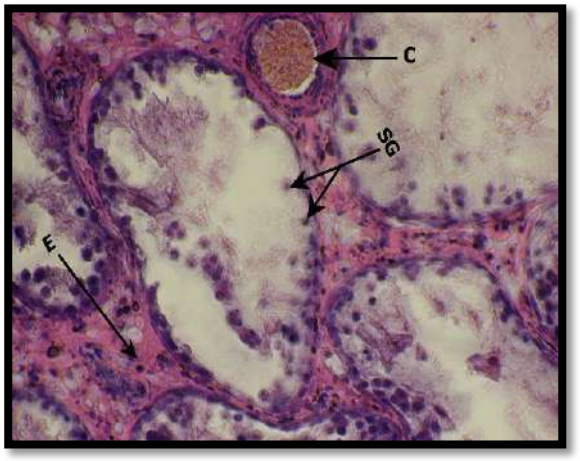

Figure 4: Section from testis of rat treated with LA, showing deformities in testicular architecture. Atrophied shrunk seminiferous tubules. With exception of irregular layer of spermatogonia (SG), almost seminiferous tubule contains no spermatogenic cells and spermatozoa. Sever edema (E) and congested blood vessel (C) in interstitial space. (Stain: H&E. 400x).

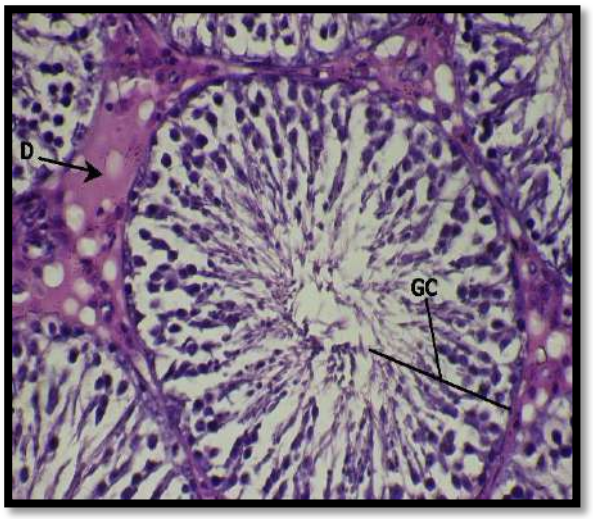

Figure 5: Section from testis of rat treated with Vit.C in coadministration with LA, showing improved seminiferous tubule with normal germ cell layers (GC) and active spermatogenesis. But still degeneration in Leydig cells (D) and mild edema are seen between seminiferous tubules (Stain: H&E. 400x).

3.2. Experiment II

3.2.1. Effect of vitamin C against lead acetate toxicity on sperm count in recovery period

Sperm counts in groups of control (112.700± 15.850 $x10^6$ sperm /epid.), LAR (29.070± 7.460 $x10^6$ sperm /epid.), LAVR (87.570± 11.520 $x10^6$ sperm /epid.), and LARV (67.760± 14.77 $x10^6$ sperm /epid.) are shown in table 3 and figure 6-A. Sperm count in LAR group was significantly ($P<0.01$) decreased as compared to control group. Both Vit.C supplemented groups (LAVR & LARV) showed non-significant reduction as compared to control. While sperm count in LAVR group was increased significantly ($P<0.05$) as compared to LAR group, and non-significantly increased as compared to LARV group. In spite of the observation of higher sperm count in LARV group compared to LAR group the difference was non-significant between them.

3.2.2. Effect of vitamin C against lead acetate toxicity on sperm morphology in recovery period

Sperm morphology (including normal sperm, sperm with head defect and sperm with tail defect) in groups of control (88.110± 3.019 %; 3.135± 0.625 %; 8.752± 2.552 %), LAR (41.070± 1.487%; 10.010± 1.133 %; 48.920± 1.837 %), LAVR (76.100± 2.375 %; 4.517± 0.288 %; 19.380± 2.241%) and LARV (57.730± 5.141 %; 7.807± 1.027 %; 34.460± 4.444 %) are shown in table 3 and figure 6- B, C & D.

The percentage of normal sperm in LAR and LARV groups were decreased significantly ($P<0.01$) as compared to control. While the percentage of normal sperm in LAVR group showed non-significant reduction as compared to control, and significantly ($P<0.01$) increased as compared to LAR and LARV. Also, in LARV group the percentage of normal sperms was significantly ($P<0.01$) increased as compared to LAR group. The percentage of head defect sperm significantly ($P<0.01$) increased in groups LAR and LARV as compared to control. While in LAVR the percentage of head defect sperm was increased non-significantly as compared to control, and significantly decreased as compared to LAR ($P<0.01$), and LARV ($P<0.05$). In addition, the percentage of head defect sperm in LARV group slightly decreased from LAR group. The percentage of tail defect sperms in LAR and LARV groups were increased significantly ($P<0.01$) as compared to control group, while LAVR group showed non-significant increase as compared to control,

and significantly (P<0.01) decreased as compared to LAR and LARV groups. Also, in LARV group the percentage of tail defect sperm was significantly (P<0.01) decreased as compared to LAR group.

Table 3: Effect of vitamin C against lead acetate toxicity on sperm count and sperm morphology in the rat in recovery period.

In each group n=7

Parameters / Groups	Sperm Count x 10^6/ epid.	Normal sperm (%)	Head defect sperm (%)	Tail defect sperm (%)
Control	112.700± 15.850[a]	88.110± 3.019[a]	3.135± 0.625[a]	8.752± 2.552[a]
LAR	29.070± 7.460[b]	41.070± 1.487[b]	10.010 ± 1.133[b]	48.920± 1.837[b]
LAVR	87.570± 11.520[a]	76.100± 2.375[a]	4.517± 0.288[a]	19.380± 2.241[a]
LARV	67.760± 14.77[ab]	57.730± 5.141[c]	7.807± 1.027[b]	34.460± 4.444[c]

Data presented as mean ± S.E. The same letters mean non-significant differences while the different letters mean significant differences.

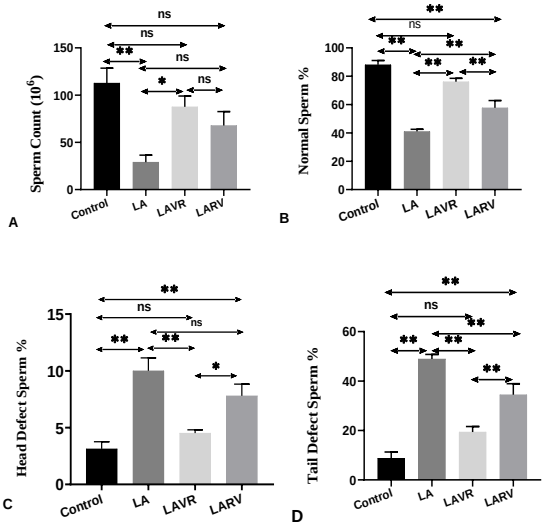

Figure 6: Effect of vitamin C against lead acetate toxicity on: A- sperm count, B- percentage of normal sperms, C- percentage of head defect sperm and D- percentage of tail defect sperm in the rat in recovery period *=P<0.05 **=P<0.01.

3.2.3. Effect of vitamin C against lead acetate toxicity on serum MDA level in recovery period

The serum MDA level in groups of control (4.350± 0.222 µmol/L), LAR (5.025± 0.438 µmol/L), LAVR (4.368± 0.367 µmol/L), and LARV (4.994± 0.485 µmol/L) are shown in table 4. Non-significant differences were observed in serum MDA level among all groups.

Table 4: Effect of vitamin C against lead acetate toxicity on serum MDA level in the rat in recovery period.

In each group n=7

Parameter / Groups	control	LAR	LAVR	LARV
MDA(µmol/L)	4.350± 0.222[a]	5.025± 0.438[a]	4.368± 0.367[a]	4.994± 0.485[a]

Data presented as mean ± S.E. The same letters mean non-significant differences while the different letters mean significant differences.

3.2.4. Effect of vitamin C against lead acetate toxicity on histological sections of testis in recovery period

The histological section of testis of control rat (figure 7) shows normal architecture of seminiferous tubules, organization of germ cells, active spermatogenesis, large number of spermatozoa in the lumen of seminiferous tubules, and large number of Leydig cells in the interstitial tissue.

Most of the testis section's area of LAR group (figure 8) shows severe degeneration and deformities in atrophied seminiferous tubule. Also, un improvement seen in degenerated germ cell layers, and interstitial tissue as well.

The histological section of testis of LAVR group (figure 9) shows that Vit.C prevented lead degenerative effect on tissue architecture, prevented damage in seminiferous tubules to a remarkable extent, decreased degeneration in germ cell layers, and increased activity in spermatogenesis, hence increased the spermatozoa in the lumen. Also improved Leydig cells, and interstium. While the histological section of

testis of LARV group (figure 10). Vit.C administration throughout the period of withdrawal treatment of LA slightly reduced testicular tissue degeneration. The section shows shrunken seminiferous tubule, lost testicular architecture, degeneration in germ cell layer, irregular layer of spermatogonia, absence of spermatocytes and spermatids in germinal epithelium, indicating loss of spermatogenesis, and the lumen contains cell debris. Also showed edematous interstitial tissue, with degeneration in Leydig cells.

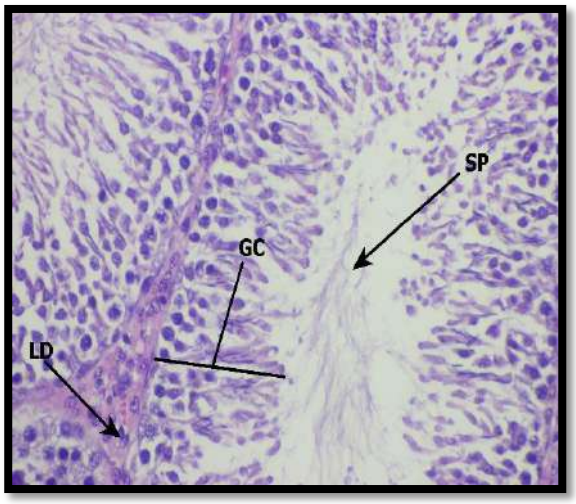

Figure 7: Section from testis of control rat, showing normal testicular architecture, seminiferous tubule, with normal germ cell layers (GC) with active spermatogenesis and large amount of spermatozoa (SP) in lumen (L). And normal Leydig cells in interstitial tissue (I). (Stain: H&E. 400x).

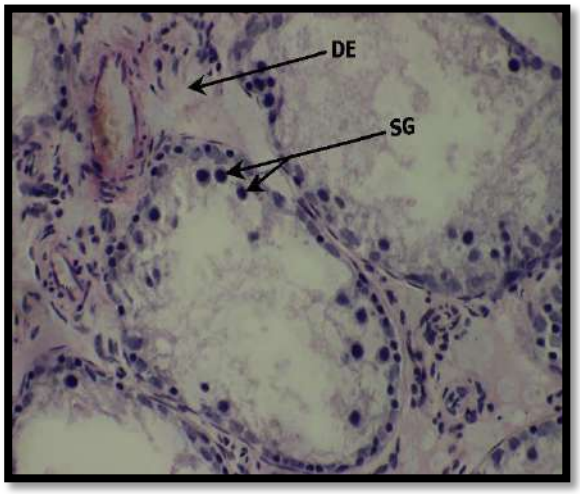

Figure 8: Section from testis of rat treated with LA left to be recovery, still showing deformities in testicular architecture. Atrophied shrunken seminiferous tubules with exception of irregular layer of spermatogonia (SG), almost seminiferous tubule contains no spermatogenic cells and spermatozoa. Sever edema (E) in interstitial space. (Stain: H&E. 400x).

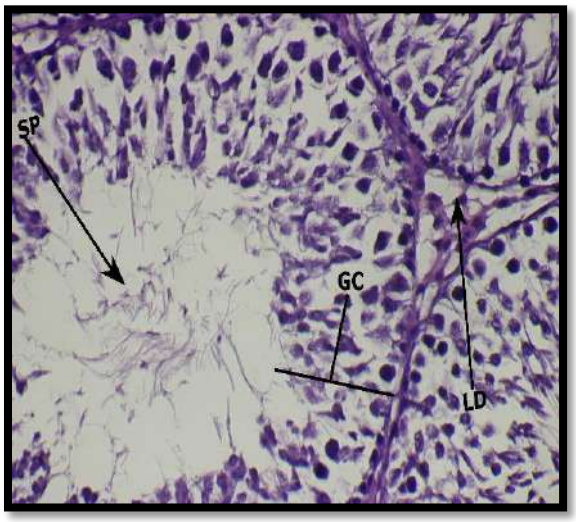

Figure 9: Section from testis of rat treated with Vit.C in coadministration with LA left to be recovery, showing improvement in testicular architecture, improved seminiferous tubule with germ cell layers (GC). The lumen contains spermatozoa. Leydig cells (D) are seen between seminiferous tubules (Stain: H&E. 400x).

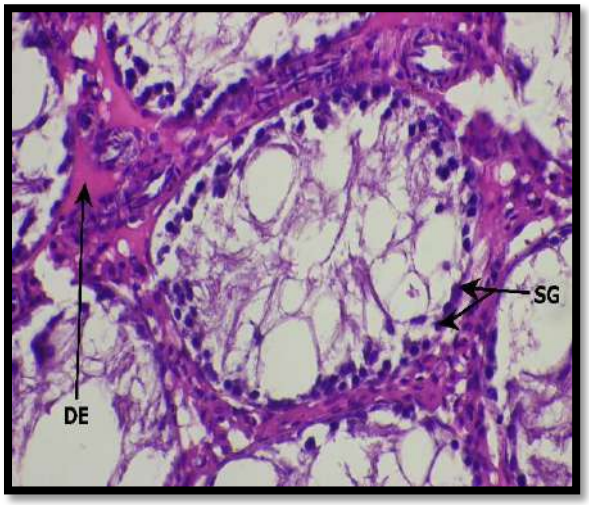

Figure 10: Section from testis of rat of LARV group, showing slightly improvement in atrophied seminiferous tubule. Seminiferous tubule contains irregular layer of spermatogonia (SG), and cell debris in lumen. Also, edema and degeneration in interstitial tissue (DE) are seen in the section (Stain: H&E. 400x).

4. DISCUSSION

In experiment I, the significant decrease of sperm count and significant increase in percentage of sperm abnormality in LA group is supported by (Pasha *et al.*, 2016) who reported significantly decreased epididymal sperm count and significantly increased sperm abnormality in rats exposed to LA. Which is confirmed by (Nasr *et al*., 2017). (Anjum *et al.*, 2016) reported that the increased oxidative stress induced by lead could damage the sperm membrane, DNA, and protein. This may explain the reduced sperm reserves and sperm membrane integrity in rats.

The damaged testis tissue in LA group is supported by (Al-Omair *et al*., 2017) who showed degenerations, and deformities in the testis architecture. Also, testis damage by LA was confirmed in the rat by (Mabrouk, 2018; Ali and Al-Derawi, 2018).

The protection of sperm count, sperm morphology and improvement of testicular architecture by Vit.C against lead acetate toxicity in LAV group is supported by (Sharma, 2013) who showed higher sperm count, lower percentage of abnormal sperm and improvement of testis in mice treated with Vit.C against lead acetate toxicity. The testis improvement might be due to inhibition of lead absorption in intestine (Dawson *et al*., 1999), early chelation of lead upon the first stages poisoning (Raafat *et al.*, 2009), of course such mechanism minimize lead storage to low extent. Also, might be due to scavenging the reactive oxygen and nitrogen species before they induce damage in the organ (Ambali *et al.*, 2011). In addition, Vit.C increase antioxidant content, and reduce lipid peroxidation product in the lead treated rats (Ayinde *et al*., 2012)**.**

In the present work the significantly increased serum MDA level in LA group in agreement with the study of (El-Nekeety *et al*., 2009) who showed that rats treated with LA, revealed significant increase in MDA level. Also, the present study is supported by (Ahmad Nisar *et al.*, 2013; Ali and Al-Derawi, 2018) who confirmed that LA caused a significant increase in lipid peroxidation level in rat. The reduction in MDA of LAV group, indicating improvement towards the normal, and supported by the study of (Ahmad Nisar *et al.*, 2013) who demonstrated the protective effect of Vit.C against oxidative stress induced by lead in rat. Also accordance with the present work (El-Tantawy, 2016) showed that treatment with Vit.C along with LA resulted a significant decrease in MDA in rats.

In experiment II, the significant decrease of sperm count and significant increase in percentage of sperm abnormality in LAR group most probably is attributed to limited ability of rats in repairing of damaged testis tissue (figure 8) which is indicating the impairment of testis in supplying the epididymis by spermatozoa. In addition, the ability of lead to accumulate in the testis and epididymis (Fahim *et al*., 2013), which is slowly released from body compartment (Flora and Agrawal, 2017), make the organ in which lead is accumulated even in recovery period continuously affected by LA toxicity.

The significant increase of sperm counts and significant decrease in percentage of sperm abnormality in LAVR group from LAR group indicating improvement by Vit.C most probably occur through elimination of lead by chelation of lead ions as reported by (Raafat *et al*., 2009), and scavenging the reactive oxygen and nitrogen species before they could cause damage to the organs as reported by (Ambali *et al*., 2011). It was reported that, the increased oxidative stress induced by lead could damage the sperm membrane, DNA, and protein. This may explain the reduced sperm reserves and sperm membrane integrity in rats (Anjum *et al*., 2016). So, removing of lead by Vit.C decreasing oxidative stress, hence increasing sperm reserves and sperm membrane integrity.

Since the recovery in sperm count and sperm abnormalities by Vit.C in LAVR group markedly is more than in LARV group. So, the present study displays the limited ability of Vit.C in LARV group to remove the degenerative effect of lead toxicity which left behind before administration of Vit.C.

The MDA level was improved toward normal in recovery period in LAR group. While (Omobowale *et al*., 2014) reported that given 0.5 and 1.0 mg/ml of LA for 6 weeks resulted in significantly increased MDA level in the liver of rats, and after withdrawn of LA for another 6 weeks rats exposed to 1.0 mg/ml LA did not recover.

The alteration in serum MDA level in all experimental groups (LAR, LAVR, & LARV) was non-significant as compared to control. However, in LAVR group its value reduced more than in other two groups and reached to control. This may be due to early chelation of lead ions (Raafat *et al*., 2009). And also, may be partly due to the antioxidant role of the vitamin resulted in scavenging the reactive oxygen and nitrogen species before they could induce damage in the organs (Ambali *et al*., 2011).

The damaged testis tissue in LAR group proportionally similar to that of LA treated group in exp-I. Unchange in testis tissue damage after stoppage of lead administration in recovery period most probably is attributed to limited ability of rat in repairing of damaged testis tissue. In addition, the tissue degeneration may be in part is attributed to stored lead in the testis as reported by (Mudipalli, 2007) that absorbed lead stored in soft tissue. Also (Ali and Al-Derawi, 2018) reported that lead accumulation in testicular tissue leads to oxidation and damage.

In LAVR group, Vit.C protected testicular tissue against LA most probably due to inhibition of lead absorption in intestine (Dawson *et al*., 1999), early chelation of lead (Raafat *et al*., 2009), and scavenging the reactive oxygen and nitrogen species before they could induce damage in the organs (Ambali *et al*., 2011). It seems that, the interstitial tissue involving Leydig cells was improved in LAVR group better than in LAV group-exp.I, may be due to self-recovery in interstitial tissue of testis after Vit.C treatment in recovery period. In contrast to LAVR group, the damaged tissue in LARV group was slightly improved, and indicating that Vit.C protect testis tissue through chelation of lead and scavenging radicals before lead inducing damage, and limitedly it repairs the damaged testis tissue induced by lead toxicity.

CONCLUSIONS

In the present study**,** the coadministration of Vit.C with LA left to recovery (exp.II) showed improvement in sperm counting, sperm abnormality, and in testicular tissue, similar to that of coadministration Vit.C with LA of (exp.I). Whereas, the improvement by Vit.C provided after cessation of LA treatment (exp.II), markedly was less than that of coadministration of Vit.C with LA left to be recover. On the other hand, almost there is no improvement in all measurements in LA group of recovery (exp.II) other-than MDA which is proportionally related to oxidative stress and indicates to lowering of LA in these animals.

References

ABD-EL-REHEEM, A. & ZAAHKCUK, S. 2007. Protective effect of Vitamin C and selenium against the toxicity induced by lead acetate on some physiological parameters in blood of male albino rats. *Bulletin of the Physiological Society of Egypt,* 27**,** 59-76.

AHMAD NISAR, N., SULTANA, M., ASHRAF WAIZ, H., AHMAD PARA, P., AHMAD BABA, N., AHMAD ZARGAR, F. & HUSSAIN RAJA, W. 2013. Experimental study on the effect of vitamin C administration on lipid peroxidation and antioxidant enzyme activity in rats exposed to chlorpyriphos and lead acetate. *Veterinary World,* 6.

AIT HAMADOUCHE, N. 2009. Reproductive toxicity of lead acetate in adult male rats. *Am. J. Sci. Res.,* 3**,** 38-50.

AL-OMAIR, M. A., SEDKY, A., ALI, A. & ELSAWY, H. 2017. Ameliorative Potentials of Quercetin against Lead-Induced Hematological and Testicular Alterations in Albino Rats. *Chin J Physiol,* 60**,** 54-61.

ALI, S. & AL-DERAWI, K. 2018. Al monsour NAA "Testicular toxic effect of lead acetate on adult male rats and the potential protective role of alcoholic extract of ginseng (histological, histomorphometrical and physiological)". *Sci. J. Med. Res,* 2**,** 87-92.

ALLOUCHE, L., HAMADOUCHE, M. & TOUABTI, A. 2009. Chronic effects of low lead levels on sperm quality, gonadotropins and testosterone

in albino rats. *Experimental and Toxicologic Pathology,* 61**,** 503-510.

AMBALI, S., ANGANI, M., ADOLE, A., KAWU, M., SHITTU, M., AKANDE, M. & OLADIPO, O. 2011. Protective effect of vitamin C on biochemical alterations induced by subchronic co-administration of chlorpyrifos and lead in Wistar rats. *Journal Environment Analytic Toxicol,* 1**,** 108.

ANJUM, M. R. & REDDY, P. S. 2014. Recovery of lead- induced suppressed reproduction in male rats by testosterone. *Andrologia,* 47**,** 560-567.

ANJUM, M. R., MADHU, P., REDDY, K. P. & REDDY, P. S. 2016. The protective effects of zinc in lead-induced testicular and epididymal toxicity in Wistar rats. *Toxicology and industrial health,* 33**,** 265-276.

ASSI, M. A., HEZMEE, M. N. M., HARON, A. W., SABRI, M. Y. M. & RAJION, M. A. 2016. The detrimental effects of lead on human and animal health. *Veterinary world,* 9**,** 660.

AYINDE, O. C., OGUNNOWO, S. & OGEDEGBE, R. A. 2012. Influence of Vitamin C and Vitamin E on testicular zinc content and testicular toxicity in lead exposed albino rats. *BMC Pharmacology and Toxicology,* 13**,** 17.

BANCROFT, J. D. & GAMBLE, M. 2008. *Theory and practice of histological techniques,* Elsevier Health Sciences.

BENDICH, A., MACHLIN, L., SCANDURRA, O., BURTON, G. & WAYNER, D. 1986. The antioxidant role of vitamin C. *Advances in Free Radical Biology & Medicine,* 2**,** 419-444.

BONDE, J. P., JOFFE, M., APOSTOLI, P., DALE, A., KISS, P., SPANO, M., CARUSO, F., GIWERCMAN, A., BISANTI, L. & PORRU, S. 2002. Sperm count and chromatin structure in men exposed to inorganic lead: lowest adverse effect levels. *Occupational and environmental medicine,* 59**,** 234-242.

DAWSON, E. B., EVANS, D. R., HARRIS, W. A., TETER, M. C. & MCGANITY, W. J. 1999. The effect of ascorbic acid supplementation on the blood lead levels of smokers. *Journal of the American College of Nutrition,* 18**,** 166-170.

DRURY, R. & WALLINGTON, E. 1980. Preparation and fixation of tissues. *Carleton's histological technique,* 5**,** 41-54.

ELGAWISH, R. A. R. & ABDELRAZEK, H. M. 2014. Effects of lead acetate on testicular function and caspase-3 expression with respect to the protective effect of cinnamon in albino rats. *Toxicology Reports,* 1**,** 795-801.

EL-NEKEETY, A. A., EL-KADY, A. A., SOLIMAN, M. S., HASSAN, N. S. & ABDEL-WAHHAB, M. A. 2009. Protective effect of Aquilegia vulgaris (L.) against lead acetate-induced oxidative stress in rats. *Food and chemical toxicology,* 47**,** 2209-2215.

EL-TANTAWY, W. H. 2016. Antioxidant effects of Spirulina supplement against lead acetate-induced hepatic injury in rats. *Journal of traditional and complementary medicine,* 6**,** 327-331.

EL-TOHAMY, M. & EL-NATTAT, W. 2010. Effect of antioxidant on lead-induced oxidative damage and reproductive dysfunction in male rabbits. *J Am Sci,* 6**,** 613-622.

FAHIM, M. A., TARIQ, S. & ADEGHATE, E. 2013. Vitamin E modifies the ultrastructure of testis and epididymis in mice exposed to lead intoxication. *Annals of Anatomy-Anatomischer Anzeiger,* 195**,** 272-277.

FLORA, S. J. & AGRAWAL, S. 2017. Arsenic, cadmium, and lead. *Reproductive and developmental toxicology.* Elsevier.

HAOUAS, Z., ZIDI, I., SALLEM, A., BHOURI, R., AJINA, T., ZAOUALI, M. & MEHDI, M. 2015. Reproductive toxicity of lead acetate in adult male rats: Histopathological and cytotoxic studies. *Journal of Cytology & Histology,* 6**,** 1.

HARI PRIYA, P. & REDDY, P. S. 2012. Effect of restraint stress on lead- induced male reproductive toxicity in rats. *Journal of Experimental Zoology Part A: Ecological Genetics and Physiology,* 317**,** 455-465.

KEMPINAS, W., FAVARETTO, A., MELO, V., CARVALHO, T. L., PETENUSCI, S. & OLIVEIRA- FILHO, R. 1994. Time-dependent effects of lead on rat reproductive functions. *Journal of Applied Toxicology,* 14**,** 427-433.

LIU, H., NIU, R., WANG, J., HE, Y. & WANG, J. 2008. Changes caused by fluoride and lead in energy metabolic enzyme activities in the reproductive system of male offspring rats. *Fluoride,* 41**,** 184-191.

MABROUK, A. 2018. Therapeutic effect of thymoquinone against lead- induced testicular histological damage in male Wistar rats. *Andrologia,* 50**,** e13014.

MISHRA, M. & ACHARYA, U. R. 2004. Protective action of vitamins on the spermatogenesis in lead-treated Swiss mice. *Journal of Trace Elements in Medicine and Biology,* 18**,** 173-178.

MUDIPALLI, A. 2007. Lead hepatotoxicity & potential health effects. *Indian Journal of Medical Research,* 126**,** 518-528.

NASR, N. E., ELMADAWY, M. A., ALMADALY, E. A., ABDO, W. & ZAMEL, M. M. 2017. Garlic Powder Attenuates Apoptosis Associated with Lead Acetate-Induced Testicular Damage in Adult Male Rats. *Alexandria Journal for Veterinary Sciences,* 54.

OGUTCU, A., SULUDERE, Z. & KALENDER, Y. 2008. Dichlorvos-induced hepatotoxicity in

rats and the protective effects of vitamins C and E. *Environmental Toxicology and Pharmacology,* 26**,** 355-361.

OMOBOWALE, T. O., OYAGBEMI, A. A., AKINRINDE, A. S., SABA, A. B., DARAMOLA, O. T., OGUNPOLU, B. S. & OLOPADE, J. O. 2014. Failure of recovery from lead induced hepatoxicity and disruption of erythrocyte antioxidant defence system in Wistar rats. *Environmental toxicology and pharmacology,* 37**,** 1202-1211.

PASHA, H. F., REZK, N. A., SELIM, S. A. & EL MOTTELEB, D. M. A. 2016. Therapeutic effect of spermatogonial stem cell on testicular damage caused by lead in rats. *Gene,* 592**,** 148-153.

RAAFAT, B. M., SHAFAA, M. W., RIZK, R. A., ELGOHARY, A. A. & SALEH, A. 2009. Ameliorating effects of vitamin C against acute lead toxicity in albino rabbits. *Australian J. Basic Appl. Sci,* 3**,** 3597-3608.

RAMAH, A., EL-SHWARBY, R. M., NABILA, M. & EL-SHEWEY, E. A. 2015. The effect of lead toxicity on male albino rats reproduction with ameliorate by vitamin E and pumpkin seeds oil. *Benha Veterinary Medical Journal,* 28**,** 43-52.

SHARMA, D. N. 2013. Ascorbic Protects Testicular Oxidative Stress and Spermatozoa Deformationsin Male Swiss Mice Exposedto Lead Acetate. *Universal Journal of Environmental Research & Technology,* 3.

SOKOL, R. Z., MADDING, C. E. & SWERDLOFF, R. S. 1985. Lead toxicity and the hypothalamic-pituitary-testicular axis. *Biology of reproduction,* 33**,** 722-728.

TELIŠMAN, S., ČOLAK, B., PIZENT, A., JURASOVIĆ, J. & CVITKOVIĆ, P. 2007. Reproductive toxicity of low-level lead exposure in men. *Environmental research,* 105**,** 256-266.

YUCRA, S., GASCO, M., RUBIO, J., NIETO, J. & GONZALES, G. F. 2008. Effect of different fractions from hydroalcoholic extract of Black Maca (Lepidium meyenii) on testicular function in adult male rats. *Fertility and sterility,* 89**,** 1461-1467.

WADI, S. A. & AHMAD, G. 1999. Effects of lead on the male reproductive system in mice. *Journal of Toxicology and Environmental Health Part A,* 56**,** 513-521.

WANI, A. L., ARA, A. & USMANI, J. A. 2015. Lead toxicity: a review. *Interdisciplinary toxicology,* 8**,** 55-64.

WYROBEK, A. J., GORDON, L. A., BURKHART, J. G., FRANCIS, M. W., KAPP, R. W., LETZ, G., MALLING, H. V., TOPHAM, J. C. & WHORTON, M. D. 1983. An evaluation of the mouse sperm morphology test and other sperm tests in nonhuman mammals: A report of the US Environmental Protection Agency Gene-Tox Program. *Mutation Research/Reviews in Genetic Toxicology,* 115**,** 1-72.

ZANCO Journal of Pure and Applied Sciences
The official scientific journal of Salahaddin University-Erbil
https://zancojournals.su.edu.krd/index.php/JPAS

ISSN (print):2218-0230**, ISSN (online):** 2412-3986**, DOI: http://dx.doi.org/10.21271/zjpas**

RESEARCH PAPER

Synthesis, computational study, and antibacterial activity of rhodanine and thiazolidine-2,4-dione scaffolds

Rozh Qasim Amin[1], Hiwa Omer Ahmad[1*]
1Department of Pharmaceutical Chemistry, College of Pharmacy, Hawler Medical University. Hawler, Kurdistan Region, Iraq

A B S T R A C T:

In this research, different thiazolidine-2,4-dione and 2-thioxothiazolidin-4-one derivatives (**1-13)** have been synthesized by Knoevenagel Condensation (**1-13**). Thiazolidine-2,4-dione and 2-thioxothiazolidin-4-one derivatives have an important role in medicinal chemistry and drug design. All synthesized compounds (**1-13**) have been confirmed by IR, ^{1}H and ^{13}C-NMR spectral data. A computational study was used to determine values of the lowest unoccupied molecular orbital and highest occupied molecular orbital energy gap to show the chemical stability, and reactivity of compounds (**1-13**). Small values of energy between a lowest unoccupied molecular orbital and a highest occupied molecular orbital energy gap indicate chemical stability and reactivity of synthesized compounds. $E_{LUMO-HOMO}$ ranged between 0.004-0.306 eV indicated high reactivity of the prepared molecule. Thermodynamic energies have been calculated for synthesized compounds including Enthalpy, Entropy, and Gibbs free energy, negative values have been detected for all synthesized compounds (**1-13**).
Antibacterial activity has done for all synthesized compounds (**1-13**) against Gram-positive *Staphylococcus aureus* and Gram-negative *Escherichia coli* by the method of disc diffusion show that all synthesized compounds except **7**, **8**, **11** and **13** have antibacterial effect for both or one type of bacteria. Antibacterial activity is observed as a clear circular **zone of inhibition** for selected synthesized compounds by disc Inhibition zones of *Staphylococcus aureus*, and *Escherichia coli bacteria.* The range for *Staphylococcus aureus* were between (6-24)mm and for *Escherichia coli* were between (6-18)mm, the measuring of the zones were with the discs.

KEY WORDS:Synthesis, computational study, 2-thioxothiazolidin-4-one, antibacterial activity, and thiazolidine-2,4-dione.
DOI: http://dx.doi.org/10.21271/ZJPAS.32.3.15
ZJPAS (2020) , 32(3);139-156 .

INTRODUCTION

Five-membered multi-heterocyclic rings like hydanoin derivatives play important roles in medicinal chemistry and biological activity (Syldatk et al., 1990, Faghihi and Hagibeygi, 2003, Yu et al., 2004, Jawhar et al., 2018). Drugs based on five-membered heterocyclic include thiohydantoins, thiazolidine-2, 4-dione and 2-thioxothiazolidin-4-one, are used in drug discovery (Sun et al., 2001, Murugan et al., 2009, Bhatti et al., 2013).

*** Corresponding Author:**
Hiwa Omer Ahmad
E-mail: Hiwa.omar@hmu.edu.krd
Article History:
Received: 03/12/2019
Accepted: 04/02/2020
Published: 15/06 /2020

5-substituted 2-thioxothiazolidin-4-one and thiazolidine-2, 4-dione were synthesized by Knoevenagel condensation reaction with different substituted aldehydes (Scheme 1) (Sandhu, 2013, Ahn et al., 2006, Murugan et al., 2009, Veisi et al., 2015).
Potential (*IP*) and electron affinity (*EA*) have been obtained by orbital energies calculation to obtain ionization values for neutral molecules. Ionization potential and electron affinity are the negative values of the highest occupied molecular orbital energy (-*E*HOMO) and the lowest unoccupied molecular orbital energy (-*E*LUMO), respectively (i.e., IP =-*E*HOMO and *EA* =-*E*LUMO) (Yadav et al., 2015, Wang et al., 2017, Rajamanikandan et al., 2017).

We aimed to synthesize, and computational study of several thiazolidine-2,4-dione and 2-thioxothiazolidin-4-one derivatives. The reactivity and polarity of prepared compounds will be changed by various substituents on benzylidine at position 5. Therefore, computational study has been used to show their reactivity based on substituents. The computational study gives information about hardness, softness, and electronegativity of our synthesized compounds. We tried to give details about the effect of substituent's differences on the antibacterial activity. We imply to obtain difference between more polar compounds with less polar compounds to have antibacterial activities.

2. Experimental

2.1. Chemistry experimental section

2.1.1. Material and methods

All starting compounds obtained from Fisher Scientific, Sigma-Aldrich, Acemec Biochemical, CHEM-LAB and Scharlau. ^{1}H-NMR and ^{13}C-NMR spectra were recorded on 500 MHZ spectrometer and FT-IR instrument was used for identification. ^{1}H-NMR and ^{13}C-NMR spectra were recorded on Brukeravance (500 MHz) spectrometer. Parts per million is a unit of chemical shift and tetra-methylsilane expressed as a standard. NMR spectram were recorded in solutions in the deuterated solvent mentioned in the method section.

2.1.2. General procedure

Method 1: Commercially available Thiazolidine-2,4-dione with corresponding aldehydes, piperidine were dissolved in ethanol in a round bottom flask. The mixture was stirred at 150 ℃. The solid product was filtered and washed several times by ethanol. All pure compounds were collected. Recrystallization was done by ethanol (Ghosh et al., 2011).

Method 2: Commercially available 2-thioxothiazolidin-4-one was placed with corresponding aldehydes, piperidine was dissolved in ethanol in a round bottom flask using a magnetic stirrer and reflux condenser. The mixture was stirred at 150 ℃. The solid product was filtered off and washed with ethanol. The pure compounds were collected. Recrystallization was done by ethanol (McNulty et al., 1998).

2.2. Antibacterial activity

The antibacterial activity was performed by method disc diffusion. All synthesized compounds were screened in against two types of bacterial strains namely *Staphylococcus aureus*, and *Escherichia coli* prepared by our self. The comparison was used with known antibiotics such as Amikacin, Amoxcillin-clavulanic acid, Ampicillin, and cefotaxime. The inhibition zone was measured for each synthesized compound in millimeters (Chaudhari et al., 2012).

The clinical sample was taken from urinary catheterized patients in Rizgari hospital. Bacteria identification were by VITEK II compact system, and molecular approach using 16S rRNA, nuc and coa gen. Bacterial strains Identified according to conventional test such as gram stain, and cultural characteristics like colony properties on bacterial culture media. Biochemical tests analysis like detection of different and special enzymes. Molecular approach using 16S rRNA, nuc and coa genes (Jonas et al., 1999).

3. Discussion

3.1. Chemistry

Different 5-substituted 2-thioxothiazolidin-4-one and thiazolidine-2,4-dione were synthesized by the reaction of Knoevenagel condensation reaction, 2-thioxothiazolidin-4-one or thiazolidine-2,4-dione were dissolved in ethanol with corresponding aldehydes in the base medium (by using piperidine) based on the process previously (Scheme 2) (Ahn et al., 2006, Murugan et al., 2009, Sandhu, 2013, Veisi et al., 2015).

Identification of functional groups were done by using FTIR spectroscopy. Obtained NH stretching vibrations were lower value for carbonyl (X=O) in compounds (1-**8**) than thiocarbonyl group (X=S) in compounds (**9-13)** (Katritzky et al., 1988, Martínez-Mayorga et al., 2004), respectively. The NH stretching vibrations are calculated at (2971-3239) cm^{-1}, and (3012-3409) cm^{-1} in the spectra for compounds 1-**8** and **9-13**. Compounds (**1-8**) show appearance of (1715-1750)) cm^{-1} belong to ν(C=O) carbonyl group and appear at (1671-1691) cm^{-1} due to the second (C=O) of carbonyl group, (1500-1672) cm^{-1} due to the ν(C=C) and (3012-3409) cm^{-1} belong to ν(NH) group. While, compounds (**9-13**) show appearance of (1677-1725) cm^{-1} belong to ν(C=O) carbonyl group and appear absorption at (1475-1598) cm^{-1} because of the (C=S) group, (1428-1598) cm^{-1} for the

presence of the ν(C=C) group and (2971-3239) cm^{-1} belong to (NH) group. ^{1}H-NMR spectrum for hydrogen (NH) peak for 2-thioxothiazolidin-4-one derivatives are higher values than thiazolidine-2,4-dione derivatives, Chemical shift for hydrogen NH are (12.61, 12.61, 12.48, 12.30, 12.39,12.45, 12.58, 12.30, 13.82, 13.96, 13.54, 13.83, 13.78) for (**1-13**), respectively. Compound **12** has a CH_2 peak at 5.22, compound **11** has $2CH_3$ (6H) at 3.02, and compound **6** has an OH peak at 10.32. In ^{13}C –NMR, there is (C-F) peak in 164.29, (C-O) at 167.94, (CH_3) at 40.15 for compounds **2**, **3**, and **8**, respectively(Alizadeh et al., 2009, Barakat et al., 2014)

3.2. Computational study

The LUMO-HOMO energy gap is the most important parameter for the chemical reactivity (Jalbout and Fernandez, 2002). The shorter LUMO-HUMO energy gap is considered as the high reactivity (Johansson et al., 2004), The LUMO-HOMO energy gap for all synthesized compounds were calculated by Gaussian using HF- 6-31G (Abdullah et al., 2016, Abdallah, 2019) (Figure 1).

Values of 0.00418 and 0.00391are the ΔE for compounds **5** and **10** respectively, small values of **5**, and **11** indicated that the presence of electron attracting group (NO_2) attached to the benzyl ring on the 5-position could affect the energy gap (Vikneshvaran and Velmathi, 2017, Ahmad, 2015). The highest energy gap value compared with the other synthesized compounds is 0.306 for compound **3** indicated low reactivity. Hydroxyl group attached to benzyl ring as an electronic donating group expected to have an effect on the reactivity. While, the lowest energy differences for compound **5**, and **10** are 0.00418 eV , and 0.00391 eV indicated more reactive than compound **6** with energy gap difference 0.0276 eV and the other synthesized compounds. The reactivity of synthesized compounds indicated as follow **10 >5 > 2 > 1, 9 > 11 > 8 > 4 > 6 > 12 > 13> 7 > 3**. (Table 1).

Ionization potential was calculated by Koopmans's theory (Chong et al., 2002) using orbital energies which is equal to a negative value of HOMO energy. Electron affinity is a negative value of LUMO energy(Shankar et al., 2009, Rocha et al., 2015). The chemical hardness η of the molecule based on the molecular orbital can be calculated by the following equation (equation 1) (Pearson and Pearson, 2005, Galván et al., 2015).

(Pearson and Pearson, 2005, Galván et al., 2015).

$\eta = \frac{ELUMO-EHOMO}{2}$	…….(Equation 1)

While electro negativity χ can be obtained by equation 2

$x = \frac{ELUMO+E\ HOMO}{2}$	……..(Equation 2)

Chemical hardness η for compound **1** is equal to the energy gap between LUMO-HOMO and LUMO-HOMO divided by two and the half between the HOMO and LUMO corresponds to electro negativity χ of the molecule. Hardness η and softness η values give information about the molecule about reactivity and stability. Therefore, Other chemical properties were calculated by using HOMO and LUMO energy values such as; hardness which is equal to η = IP-EA/2, electrophilicity index ω = μ2 /2η, electro-negativity χ = IP+EA/2, chemical potential μ=-χ, and softness s = 1/2η (Table 2) (Rocha et al., 2015).

Hardness of compound **1** is equal to 0.13196 which is a measure of the resistance of a chemical species to changes in it is electronic configuration, stability and reactivity (Makov, 1995). It has also been claimed that the interaction between hard species is predominantly electrostatic, while between soft species (3.789) it is predominantly covalent (Pearson and Pearson, 2005).

Thermodynamic parameters

Thermodynamic parameters for all synthesized compounds have been calculated by using B3LYP/6-31G level in Gaussian 09 W. Molar heat capacity constant volume (Cv), Gibbs free energy (ΔG), enthalpies (ΔH), entropies (S) and energy (E), have been calculated for compounds

(**1-13)** (Table 3). In all reactions the values of ΔG are negative and S > 0 that's mean the reactions occur spontaneously (Romero-Gonzalez et al., 2005), energy is released during an exothermic process because of the negative value of ΔH (ΔH < 0) (Kuhlman and Raleigh, 1998).

3.3.Antibacterial activity

All synthesized compounds (**1-13**) were used against *Staphylococcus aureus,* a Gram-positive and *Escherichia coli* as Gram-negative bacterial strains by the process of diffusion. Discs for all (**1-13**) were formed for the study by mixing 10 mg of each compound with 490 mg of KBr under pressure, because the synthesized compounds were powder and we needed to make it as a disc (Figure 2) (Samad and Hawaiz, 2019).

Antibacterial activity is observed as a clear circular **zone of inhibition** around selected synthesized compounds disc Inhibition zones of *Staphylococcus aureus,* and *Escherichia coli* **(Table 4)**. ANOVA (turkeys multiple comparisons) were used for statistical analysis in the study (Oses et al., 2016).

Compounds (**7**, **8**, **11** and **13)** have no antibacterial activity neither with *S. aureus as* or *E. coli* ,because of the presence of tertiary amine and chlorine atoms in compound attached in the benzyl ring inhibit the response of synthesized compound against Gram positive and Gram negative bacteria. Previously studies showed that tertiary amine alone has a high antibacterial activity, because of covalent bonds between polystyrene and fiber (TAF) with tertiary amines (Endo et al., 1987).

No substituents on benzyl ring attached to 5-position in both thiazolidine-2,4-dione and rhodanine (**1** and **9**) have potent against *S. aureus as* and *E. coli*, while presence of hydroxyl and fluorine atoms (**3** and**12**) have a power of positive and Gram negative bacteria. Compare with the other compounds have higher inhibition zone in both type of bacteria. In previous study showed that compounds containing fluoro group show a higher antibacterial activity than the other compounds against *E. coli,* and *S. aureus* (Naeem, 2010).

Substituents attached on compound **2** and 4 are fluorine and methoxy which give a potency against gram negative bacteria while, fluorine in compound **12** has a response for both type of bacteria.

Nitro substituent attache to compound **10** and **5** has a different effect. In compound **10** has the inhibition of Gram negative. While in compound **5** which is thiazolidine-2,4-dione (C=O) might has inhibition zone against Gram positive.

Conclusions

Several compounds (**1-13**) have been prepared by the Knoevenagel condensation with different substituents on the position 5. We found that 5-substituents of thiazolidine-2,4-dione and rhodanine have different rate constant and time duration of the reaction . Therefore, the approximately rate constant of reactions were different from compounds to other. The precipitation of compound (**10**) after mixing of starting materials was produced in 25 minutes, while the slowest precipitation has been identified for compounds (**2** and **3**). All synthesized compounds (**1-13**) have been confirmed via the spectrum of IR, ^{1}H and ^{13}C-NMR. The small values of $\Delta E_{LUMO-HOMO}$ gap are 0.00418 eV and 0.00391 eV for compounds **10** and **5** respectively, small values of **5**, and **10** indicated that the presence of electron attracting group (NO_2) substituted to the benzyl ring on the 5-position can affect the energy gap. While compound **1** and **9** have the same ΔE (0.263 eV) because both have not substituent on the Benzaldehyde. The reactivity of synthesized compounds indicated as follow **10 >5 > 2 > 1, 9 > 11 > 8 > 4 > 6 > 12 > 13> 7 > 3**. The synthesized compounds (**1-13**) were objected to *Staphylococcus aureus* as a Gram positive and *Escherichia coli* as Gram negative bacteria. We identified that different functional groups have different potent against Gram positive *S. aureus* and Gram negative *E. coli*. 5-subistitited of thiazolidine-2,4-dione and rhodanine has a good inhibition zone against both type of bacteria, and with their substituents showed different inhibition zone, in 5-subistituated thiazolidine-2,4-dione presence of hydroxyl group and in rhodanine derivatives presence of flouro group has a inhibition zone with both type of bacteria. Attaching of (F and OCH_3) in the benzyl ring at position 5 of thiazolidine-2,4-dione and rhodanine with (NO_2) as a substituent has inhibition zone only with Gram positive bacteria, while thiazolidine-2,4-dione with (NO_2) has antibacterial activity only with Gram negative bacteria *Escherichia coli*.

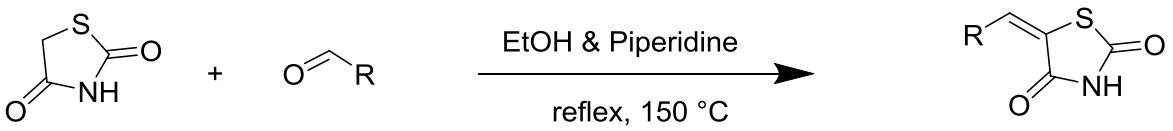

Scheme 1: Knoevenagel condensation reaction for thiazolidine-2,4-dione derivates

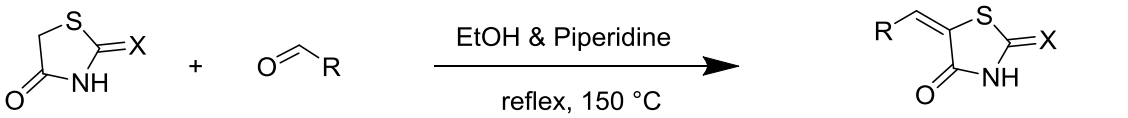

Compounds (**1-9**): X=O
Compounds (**10-13**):X=S

R=

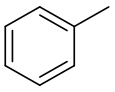

1, 9

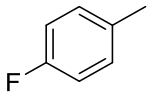

2, 12

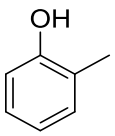

3

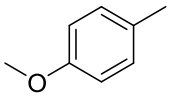

4

R=

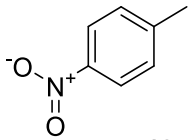

5, 10

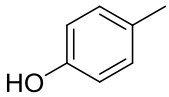

6

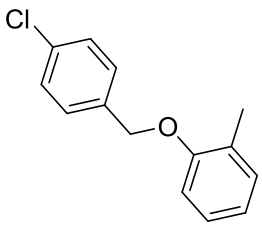

7, 13

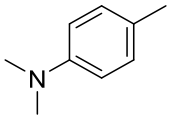

8, 11

Scheme 2: Synthesis of thiazolidine-2,4-dione (X=O) and 2-thioxothiazolidin-4-one (X=S) derivative

Synthesize of 5-benzylidenethiazolidine-2,4-dione

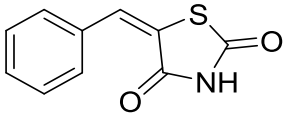

1

Method 1: Thiazolidine-2,4-dione (1.0 g, 8.6 mmol), piperidine (0.3 ml, 0.3 mmol), and benzaldehyde (2. 0 ml, 19.7 mmol) were dissolved in 20 ml of ethanol, reflex for 6 hrs at 150 °C.

M.P.=244-245 ℃, ^{1}H NMR (500 MHz, d_6-DMSO) δ 12.61 (s, 1H, N**H**), 7.77 (s, 1H, **H**CCS), 7.58 (d, *J* = 7.3 Hz, 2H, Ar), 7.55 – 7.49 (m, 2H, Ar), 7.49 – 7.44 (m, 1H, Ar). ^{13}C- NMR (126 MHz, d_6-DMSO). δ 168.3 (**C**OS), 167.7 (**C**ON), 133.5 (**C**-CH), 132.3 (**C**H-C), 130.4 (Ar), 129.7 (Ar) , 123.9 (**C**-S). IR (neat): vmax=1736 cm^{-1} (C=O), 1684 cm^{-1} (C=O), 3120 cm^{-1} (NH), 1662 cm^{-1} (C=C).

Synthesis of (E)-5-((4-fluorocyclohexa-2,4-dien-1-yl)methylene)thiazolidine-2,4-dione

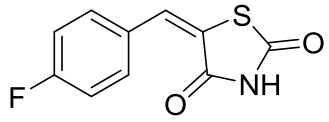

2

Method 1: Thiazolidine-2,4-dione (1.0 g, 8.6 mmol), piperidine (0.3 ml, 0.3 mmol), and 4-Flurobenzaldehyde (2.0 ml, 18.7 mmol) were dissolved to 20 ml of ethanol, reflex overnight at 150 °C.

(500 MHz, d6-dmso):

M.P.= 219-220 ℃. ^{1}H -NMR (500 MHz, d_6-DMSO): δ 12.61 (s, 1H, N**H**), 7.79 (s, 1H, C**H**CS), 7.68 – 7.63 (m, 2H, Ar), 7.38 (d, *J* = 8.6 Hz, 2H, Ar).^{13}C-NMR (126 MHz, d_6-DMSO): δ 168.2 (**C**OS), 167.8 (**C**ON), 164.3 (**C**F), 162.3 (**C**HCS), 132.9 (**C**CH), 131.1 (Ar), 130.2 (**C**S), 123.8 (Ar), 117.0(Ar). IR (neat): vmax =1725 cm^{-1} (C=O), 16

86 cm^{-1} (C=O), 3118 cm^{-1} (NH), 1606 cm^{-1} (C=C).

Scheme (2.3). Synthesis of (E)-5-(2-hydroxybenzylidene)thiazolidine-2,4-dione

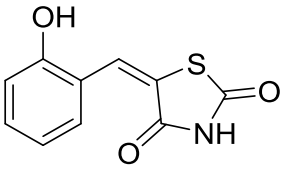

3

Method 1: Thiazolidine-2,4-dione (1.0 g, 8.5 mmol), piperidine (0.3 ml, 0.3 mmol), and 2-hydroxy benzaldehyde (0.91 gm, 7.45 mmol) were dissolved to 20 ml of ethanol, reflex overnight at 150 °C.

M.P.=274-276 ℃. ^{1}H- NMR (500 MHz, d_6-DMSO δ 12.48 (s, 1H, N**H**), 10.48 (s, 1H, O**H**), 8.01 (d, *J* = 19.7 Hz, 1H, C**H**CS), 7.29 (dd, *J* = 16.0, 7.6 Hz, 2H, Ar), 6.98 – 6.86 (m, 2H, Ar). ^{13}C- NMR (126 MHz, d_6-DMSO): δ 168.6(**C**OS), 167.9 (**C**O), 132.6 (**C**OH), 128.7 (H**C**CS), 127.5 (Ar), 122.3 (Ar),, 120.1 (Ar),, 116.6 (C-S). IR (neat): vmax=1721 cm^{-1} (C=O), 1680 cm^{-1} (C=O), 3409 cm^{-1} (NH), 3172 cm^{-1} (OH), 1662 cm^{-1} (C=C).

Synthesis of (E)-5-(4-methoxybenzylidene)thiazolidine-2,4-dione

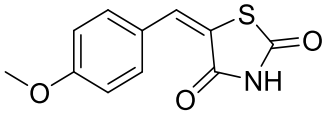

4

Method 1: Thiazolidine-2,4-dione (1.0 g, 8.6 mmol), piperidine (0.3 ml, 0.3 mmol), and 4-methoxy benzaldehyde (2.0 ml, 17.0 mmol) were dissolved to 20 ml of ethanol, reflex for 4 hrs. at 150 °C**.**

M.P.= 260-261℃. ^{1}H -NMR (500 MHz, d_6-DMSO): δ 12.79 (s, 1H, N**H**), 8.32 (d, *J* = 8.6 Hz, 3H, C**H**CS), 8.04 – 7.63 (m, 4H, Ar), 3.38 (d, *J* = 46.7 Hz, 3H, C**H**$_3$). ^{13}C- NMR (126 MHz, d_6-DMSO): δ 167.6 (**C**O), 166.9 (**C**O), 147.2 (**C**OCH3), 139.7 (**C**HCS), 131.5 (Ar), 129.4 (Ar), 125.0 (**C**-S), 39.4 (**C**H$_3$). IR (neat): vmax=1750 cm^{-1} (C=O), 1714 cm^{-1} (C=O), 3186 cm^{-1} (NH), 1161cm^{-1} (C-O), 1672 cm^{-1} (C=C).

Synthesis of (E)-5-(4-nitrobenzylidene)thiazolidine-2,4-dione

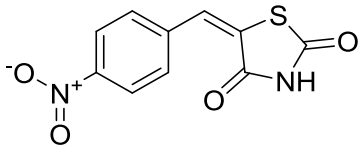

5

Method 1: Thiazolidine-2,4-dione (1.0 g, 8.5 mmol), piperidine (0.3 ml, 0.3 mmol), and 4-nitro benzaldehyde (1.0 gm, 8.6 mmol) were dissolved to 20 ml of ethanol, reflex for 2 hrs at 150 ℃

M.P.=297-298 ℃. ^{1}H- NMR (500 MHz, d_6-DMSO): δ 12.30 (s, 1H, N**H**), 8.06 – 7.45 (m, 1H, C**H**CS), 7.41 (d, *J* = 8.6 Hz, 2H, Ar), 6.80 (d, *J* = 8.6 Hz, 2H,Ar). ^{13}C- NMR (126 MHz, d_6-DMSO): δ 168.7 (**C**OS), 167.9 (CO), 151.9 (**C**N), 133.7 (**C**H), 132.0 (**C**CH), 120.5 (Ar), 116.6 (Ar), 112.2 (**C**S). IR (neat): vmax=1720 cm^{-1} (C=O), 1677 cm^{-1} (C=O), 3090 cm^{-1} (NH), 1326 cm^{-1} (C-N), 1611$cm1^{-1}$ (C=C).

Synthesis of (E)-5-(4-hydroxybenzylidene)thiazolidine-2,4-dione

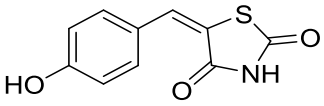

6

Method 1: Thiazolidine-2,4-dione (1.0 g, 8.6 mmol), piperidine (0.3 ml, 0.3 mmol), and 3-nitro benzaldehyde (1.0 gm, 8.6 mmol) were dissolved to 20 ml of ethanol, reflex for 2 hrs. at 150 ℃

M.P.= 296-297 ℃. ^{1}H NMR (500 MHz, d_6-DMSO): δ 12.39 (s, 1H, N**H**), 10.32 (s, 1H, O**H**), 7.67 (s, 1H, C**H**CS), 7.42 (d, *J* = 8.2 Hz, 2H), 6.90 (d, *J* = 8.3 Hz, 2H). ^{13}C NMR (126 MHz, d_6-DMSO) δ 168.7 (**C**=O), 168.4 (**C**=O), 160.5 (**C**-O), 133.0m (**C**H-C), 124.1 (Ar), 116.6 (Ar). IR (neat): vmax=1719 cm^{-1} (C=O), 1671cm^{-1} (C=O), 3110 cm^{-1} (NH), 3399 cm^{-1} (OH), 1570 $cm1^{-1}$ (C=C).

Synthesis of (E)-5-(2-((4-chlorobenzyl)oxy)benzylidene)thiazolidine-2,4-dione

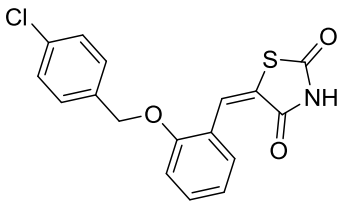

7

Method 1: Thiazolidine-2,4-dione (1.0 g, 8.6 mmol), piperidine (0.3` ml, 0.3 mmol), and 4-chloro benzaldehyde (1.7 gm, 6.9 mmol) were dissolved to 20 ml of ethanol, reflex for 4 hrs. at 150 ℃.

M.P.=197-198 ℃. ^{1}H- NMR (500 MHz, d_6-DMSO): δ 12.58 (s, 1H, N**H**), 8.01 (s, 1H, C**H**CS), 7.48 (s, 4H, Ar), 7.45 (d, *J* = 8.1 Hz, 1H, C**H**CCH), 7.42 (s, 2H,C**H**Cl), 7.11 (t, *J* = 7.5 Hz, 1H C**H**CO), 5.24 (s, 2H, CH_2). ^{13}C -NMR (126 MHz, d_6-DMSO): δ 168.5 (**C**=O), 167.9 (**C**=O), 157.4 (C-O), 136.0 (**C**-H), 133.2 (**C**-H), 132.7 (**C**-Cl), 130.1 (**C**-CH_2), 129.1 (Ar), 128.8 (Ar), 126.5 (**C**-S), 124.2 (Ar), 122.4 (Ar), 121.8 (**C**HCO), 69.4 (**C**H_2). IR (neat): vmax=1759. cm^{-1} (C=O), 1691 cm^{-1} (C=O), 3012 cm^{-1} (NH), 805 cm^{-1} (C-Cl), 1588 $cm1^{-1}$ (C=C), 1250 cm^{-1} (C-O).

Synthesis of (E)-5-(4-(dimethylamino)benzylidene)thiazolidine-2,4-dione

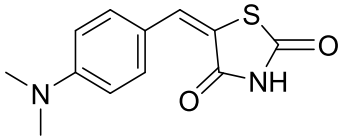

8

Method 1: Thiazolidine-2,4-dione (1.0 g, 8.6 mmol), piperidine (0.3 ml, 0.3 mmol), and 4-(dimethylamino) benzaldehyde (1.3 gm, 8.7 mmol) were dissolved to 20 ml of ethanol, reflex for 2 hrs. at 150 ℃.

M.P.= 295-298 ℃. ^{1}H- NMR (500 MHz, d_6-DMSO): δ 12.30 (s, 1H, N**H**), 7.65 (s, 1H, C**H**CS), 7.41 (d, *J* = 8.7 Hz, 2H, Ar), 6.80 (d, *J* = 8.7 Hz, 2H, Ar), 3.00 (s, 6H, C**H**$_3$). ^{13}C- NMR (126 MHz, d_6-DMSO) δ 168.7 (**C**=O), 167.6

(**C**=O), 151.6 (**C**NCH$_3$), 134.0 (**C**H), 120.0 (Ar), 115.5 (Ar), 113.3 (**C**-S), 40.2 (**C**H$_3$). IR (neat): vmax= 1720 cm^{-1} (C=O), 1677 cm^{-1} (C=O), 3089 cm^{-1} (NH), 1500 cm1^{-1} (C=C), 1100 cm^{-1} (C-N), 2760 cm^{-1} (C-H).

Synthesis of (E)-5-benzylidene-2-thioxothiazolidin-4-one

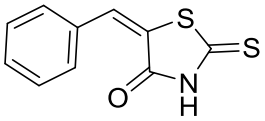

9

Method 2: 2-thioxothiazolidin-4-one (1.0 g, 7.5 mmol), piperidine (0.3 ml, 0.3 mmol), and benzaldehyde (2.0 ml, 18.7 mmol) were dissolved to 20 ml of ethanol at 150 ℃ for 6 hrs.

M.P.= 198-200 ℃. ^{1}H -NMR (500 MHz, d$_6$-DMSO): δ 13.82 (s, 1H, N**H**), 7.63 (s, 1H, C**H**CS), 7.58 (d, *J* = 7.1 Hz, 3H Ar,), 7.50 (ddd, *J* = 9.7, 3.7 Hz, 2H, Ar). ^{13}C -NMR (126 MHz, d$_6$-DMSO): δ 195.83 (**C**=S), 169.44 (**C**=O), 133.40 (**C**H), 132.08, (**C**CH), 131.17 (Ar), 130.91(Ar), 129.88(**C**-S). IR (neat): vmax= 2971cm^{-1} (NH), 1698 cm^{-1} (C=O), 1475 cm^{-1} (C=S), 1598 cm^{-1} (C=C).

Synthesis of (E)-5-(4-nitrobenzylidene)-2-thioxothiazolidin-4-one

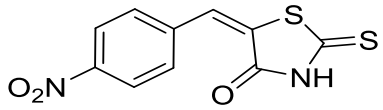

10

Method 2: 2-thioxothiazolidin-4-one (1.0 g, 7.5 mmol), piperidine (0.3 ml, 0.3 mmol), and 4-nitro benzaldehyde (1.3 gm, 8.6 mmol) were dissolved to 20 ml of ethanol, reflex for 25 mines at 150 ℃.

M.P.= 269-270 ℃. ^{1}H- NMR (500 MHz, d$_6$-DMSO): δ 13.96 (s, 1H, N**H**), 8.43 (s, 1H, C**H**CS), 8.30 (d, *J* = 8.2 Hz, 2H, Ar), 7.99 (d, *J* = 7.8 Hz, 2H, Ar). ^{13}C NMR (126 MHz, d$_6$-DMSO): δ 195.8 (**C**=S), 170.2 (**C**=O), 148.3 (**C**-N), 136.6 (**C**-H), 134.8 (**C**CH), 131.2 (Ar), 130.8 (Ar), 125.1 (**C**-N). IR (neat): vmax= 3239 cm^{-1} (NH), 1725 cm^{-1} (C=O), 1598 cm^{-1} (C=S), 1428 cm^{-1} (C=C), 1222 cm^{-1} (C-N).

Synthesis of (Z)-5-(4-(dimethylamino)benzylidene)-3-thioxoisothiazolidin-4-one

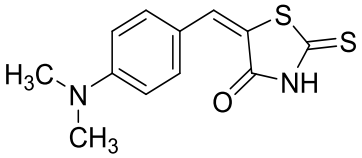

11

Method 2: 2-thioxothiazolidin-4-one (1.0 g, 7.5 mmol), piperidine (0.3` ml, 0.3 mmol), and 4-(dimethylamino) benzaldehyde (1.3 gm, 8.7 mmol) were dissolved to 20 ml, reflex for 3 hrs. at 150℃.

M.P.=197-198℃. ^{1}H- NMR (500 MHz, d$_6$-DMSO): δ 13.54 (s, 1H, N**H**), 7.50 (s, 1H, C**H**CS), 7.40 (d, *J* = 8.7 Hz, 2H, Ar), 6.80 (d, *J* = 8.7 Hz, 2H, Ar), 3.02 (s, 6H, C**H**$_3$). ^{13}C -NMR (126 MHz, d$_6$-DMSO) δ 195.5 (**C**=S), 170.4 (**C**=O), 151.6 (**C**NCH$_3$), 133.3 (**C**HCS), 120.1 (Ar), 117.6 (Ar), 111.9 (C-S) 43.4 (**C**H$_3$) . IR (neat): vmax= 3150 cm^{-1} (NH), 1677 cm^{-1} (C=O), 1561 cm^{-1} (C=S), 1519 cm^{-1} C=C), 1250 cm^{-1} (C-N).

Synthesis of (E)-5-(4-fluorobenzylidene)-2-thioxothiazolidin-4-one

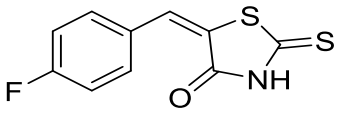

12

Method 2: 2-thioxothiazolidin-4-one (1.0 g, 7.5mmol), piperidine (0.3 ml, 0.3 mmol), and 4-floro benzaldehyde (2.0 ml, 18.7 mmol) were dissolved to 20ml of ethanol, reflex for 3 hrs. at 150 ℃.

^{1}H NMR (500 MHz, dmso) δ 13.83 (s, 1H), 7.66 (dd, *J* = 7.8, 5.6 Hz, 1H), 7.37 (t, *J* = 8.4 Hz, 1H).

^{1}H NMR (500 MHz, dmso)

M.P.=224-225 ℃, ^{1}H NMR (500 MHz, d$_6$-DMSO) δ 13.83 (s, 1H, N**H**), 7.70 – 7.65 (m, 1H, C**H**CS), 7.66 (s, *J* = 7.8, 5.6 Hz, 2H), 7.36 (s, 2H). ^{13}C NMR (126 MHz, d$_6$-DMSO) δ 195.8 (**C**=S),

169.4 (**C**=O), 164.8 (**C**-F), 162.3 (**C**H), 133.7 (Ar), 130.8 (**C**-S), 117.3 (Ar). IR (neat): vmax= 3015cm-1 (NH), 1699 cm-1 (C=O), 1584 cm^{-1} (C=S), 1482 cm^{-1} (C=C), 534 cm^{-1} (C-F).

Synthesis of (E)-5-(2-((4-chlorobenzyl)oxy)benzylidene)-2-thioxothiazolidin-4-one

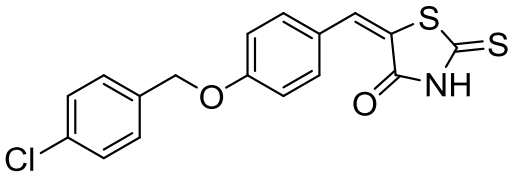

13

Method 2: 2-thioxothiazolidin-4-one (1.0 g, 7.5mmol), piperidine (0.3` ml, 0.3 mmol), and 1-((4-chlorobenzyl)oxy)-2-vinylbenzene (1.7 gm, 12.09 mmol) were dissolved to 20 ml of ethanol reflex for 4hrs at 150℃.

M.P.=239-240℃, ^{1}H NMR (500 MHz, d_6-DMSO) δ 13.78 (s, 1H, N**H**), 7.84 (s, 1H, C**H**CS), 7.47 (d, *J* = 11.5 Hz, 4H, Ar), 7.39 (d, *J* = 7.6 Hz, 2H, Ar), 7.21 (d, *J* = 8.3 Hz, 2H, Ar), 7.12 (t, *J* = 7.5 Hz, 1H), 5.25 (s, 2H, C**H**$_2$). ^{13}C NMR (126 MHz, d_6-DMSO) δ 196.5 (**C**=S), 170.1 (**C**=O), 157.6 (**C**-O), 136.2 (**C**-H), 133.0 (**C**CH_2), 129.7 (**C**Cl), 128.7 (2***C**H), 126.2 (**C**-CH), 121.9 (C-S), 114.0 (2X**C**H), 69.4 (**C**H_2). IR (neat): vmax= 3036 cm^{-1} (NH), 1699 cm^{-1} (C=O), 1584 cm^{-1} (C=S), 1482 cm^{-1} (C=C), 800 cm^{-1} (C-Cl).

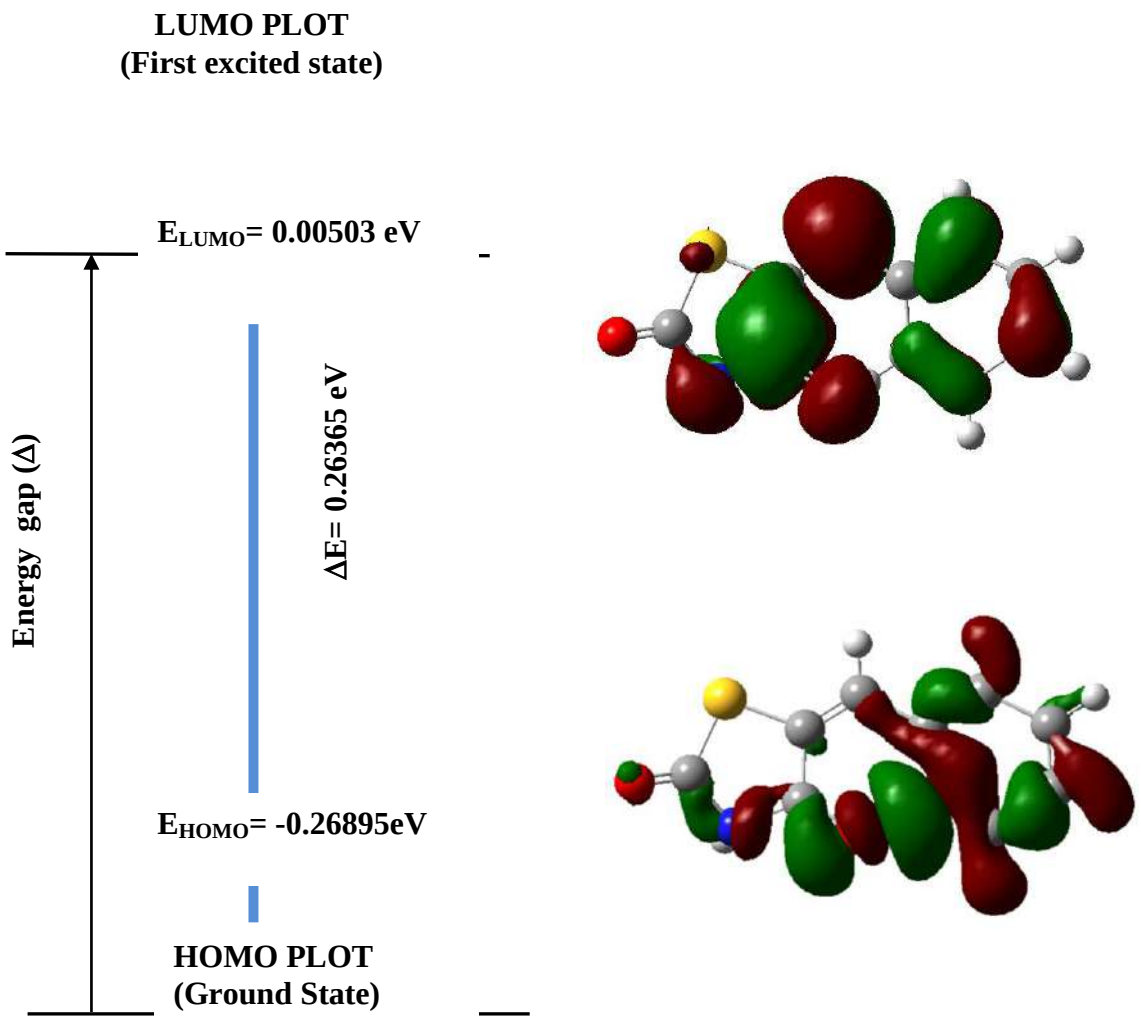

Figure 1.Molecular orbitals and LUMO and HOMO energy gap of compound **1**

Table 1: Data for HOMO, LUMO, and LUMO- HOMO gap (ΔE) for compounds **1-13**

No.	Compounds	HOMO/eV	LUMO/eV	ΔE, (LUMO-HOMO)
1.	5-benzylidenethiazolidine-2,4-dione (**1**)	-0.26895	0.00503	0.26365
2.	5-((4-fluorocyclohexa-2,4-dien-1-yl)methylene)thiazolidine-2,4-dione (**2**)	-0.29539	0.03306	0.26233
3.	5-(2-hydroxybenzylidene)thiazolidine-2,4-dione (**3**)	-0.31383	0.00768	0.30615
4.	5-(4-methoxybenzylidene)thiazolidine-2,4-dione (**4**)	-0.27636	0.00314	0.27322

5.	)-5-(4-nitrobenzylidene)thiazolidine-2,4-dione (**5**)	-0.28395	-0.28786	0.00391
6.	5-(4-hydroxybenzylidene)thiazolidine-2,4-dione (**6**)	-0.2771	0.00081	0.27629
7.	5-(2-((4-chlorobenzyl)oxy)benzylidene)thiazolidine-2,4-dione (**7**)	-0.31564	0.01359	0.30205
8.	5-(4-(dimethylamino)benzylidene)thiazolidine-2,4-dione (**8**)	0.02120	-0.29169	-0.27049
9.	5-benzylidene-2-thioxothiazolidin-4-one (**9**)	-0.26389	0.01121	0.26389
10.	5-(4-nitrobenzylidene)-2-thioxothiazolidin-4-one (**10**)	-0.27706	-0.28124	0.00418
11.	(E)-5-(4-(dimethylamino)benzylidene)-2-thioxothiazolidin-4-one (**11**)	-0.29483	0.02493	0.2699
12.	(E)-5-((4-fluorocyclohexa-2,4-dien-1-yl)methylene)-2-thioxothiazolidin-4-one (**12**)	-0.28119	-0.00279	0.2784
13.	(E)-5-(2-((4-chlorobenzyl)oxy)benzylidene)-2-thioxothiazolidin-4-one (**13**)	-0.30933	0.01967	0.28966

Table 2: Reactivity properties, HOMO and LUMO energies, LUMO-HOMOenergy gap of compound **1**.

Molecular parameters	**B3LYP/6-31G(d,p)**
EHOMO (eV)	**-0.26895**

ELUMO (eV)	**0.00503**
ΔE LUMO-HOMO (eV)	**0.26365**
Ionization potential, IP (eV)	**0.26895**
Electron affinity, EA (eV)	**-0.00503**
Electronegativity, χ (eV)	**0.27398**
Chemical potential, μ (eV)	**-0.27398**
Chemical hardness, η (eV)	**0.13196**
Chemical softness, s (eV-1)	**3.789**
Global electrophilicity index ω	**2.84177**

Table 3: Thermodynamic parameters of **1-13**

Compounds	**E(Kcal/mol)**	**ΔG(Kcal/mol)**	**ΔH(Kcal/mol)**	**S(Kcal/mol)**	**CV(Kcal/mol)**
1	-619887.329	-619915.6718	-619886.737	0.097046	0.039226
2	-682879.094	-682910.954	-682878.501	0.044261	0.108848
3	-664154.296	-664182.5245	-664153.703	0.097444	0.039904
4	-691698.407	-691728.458	-691697.814	0.102778	0.044273
5	-745110.057	-745140.6766	-745109.465	0.106307	0.043715
6	-469732165.8	-748597.067	-748565.1032	0.107209	0.044823
7	-664092.506	-664121.686	-664091.913	0.099859	0.040958
8	-1120477.18	-1120513.987	-1120476.594	0.125417	0.063167
9	-819607.569	-819634.802	-819606.977	0.093325	0.035416
10	-951220.205	-951251.196	-951219.613	0.105931	0.043889
11	-903082.448	-903113.669	-903081.855	0.106706	0.04577
12	-881627.256	-881655.96	-881626.663	0.098266	0.038311
13	-1322938.49	-1322975.165	-1322937.897	0.124995	0.062528

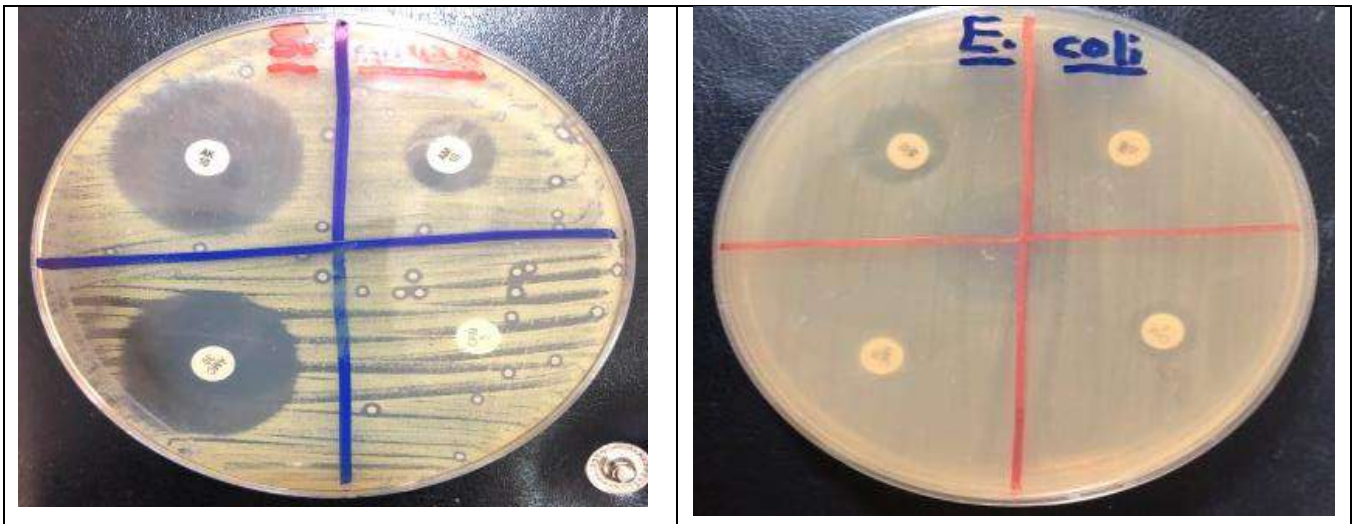

Figure 2-a : Antibacterial activities of Amikacin, Amoxcillinclavulanic acid, Ampicillin, and Cefotaxime with *Staphylococcus aureus*, and *Escherichia coli* by disc diffusion method

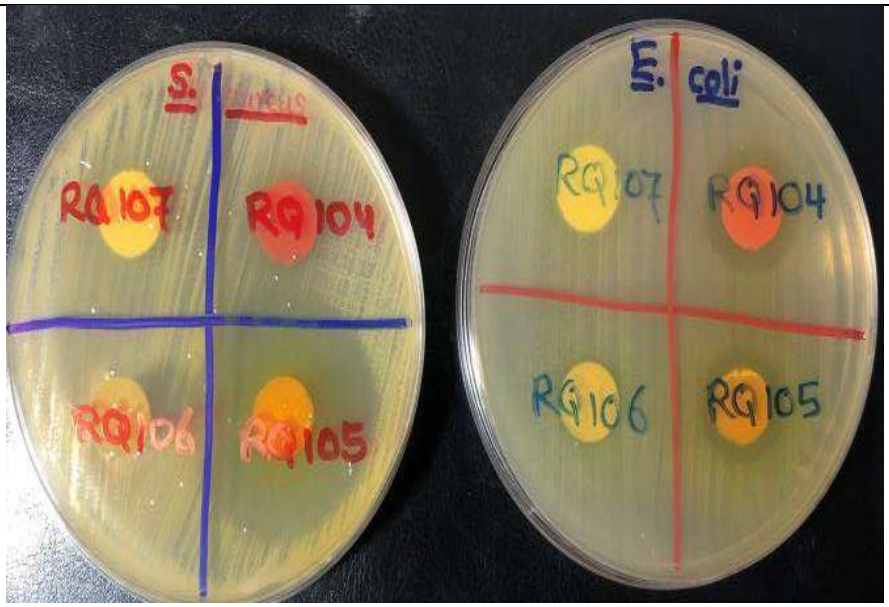

Figure 2-b : Antibacterial activities of synthesized compounds (R.Q.104 = comp **11**and R.Q.106 = Comp **12**) with *Staphylococcus aureus*, and *Escherichia coli* by disc diffusion method

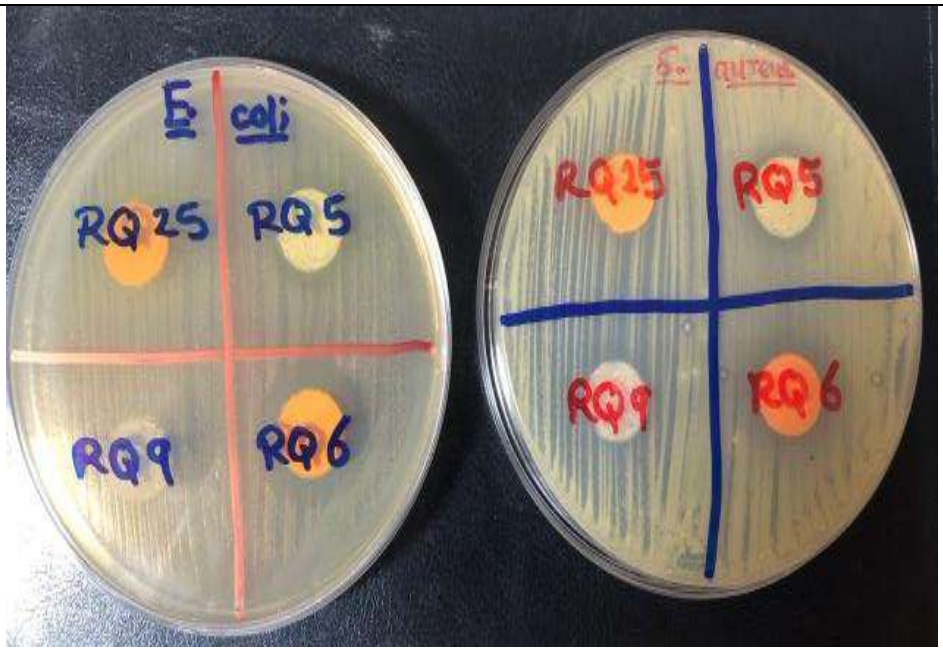

Figure 2-c : Antibacterial activities of synthesized compounds (R.Q.5 = comp **4,** R.Q.6 = comp. **5**, R.Q.9 = comp **7**, and R.Q.25 = comp. **8** with *Staphylococcus aureus*, and *Escherichia coli* by disc diffusion method

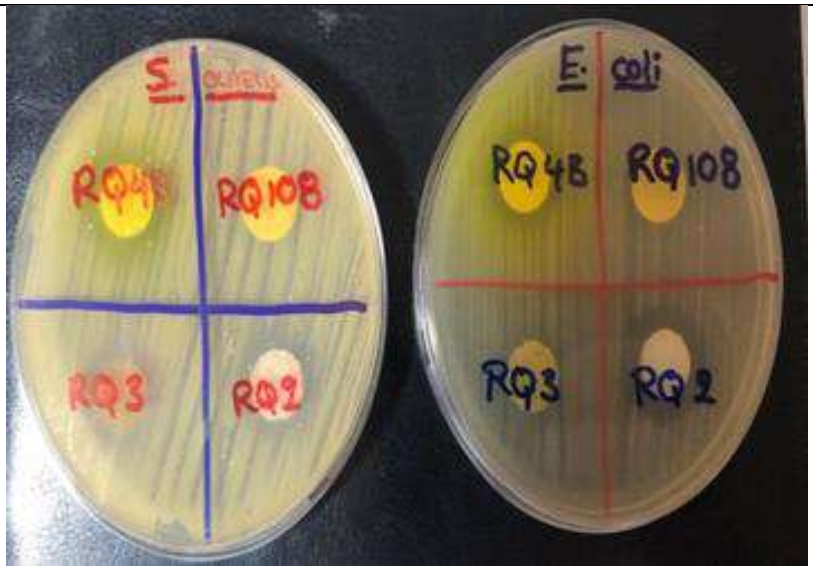

Figure 2-d : Antibacterial activities of synthesized compound (R.Q.2= comp **1**, R.Q.3= comp **2**, R.Q.4-B= comp **3** and R.Q.108= comp **13**) with *Staphylococcus aureus*, and *Escherichia coli* by disc diffusion method

Table 4: Inhibition zone of the tested compounds against *Staphylococcus aureus*, and *Escherichia coli*		
Compounds	Inhibition zones of *S. aureus* and *E. coli* for the tested compound (mm)	
	E-coli	***S. aureus***
1	18	15
2	6	13
3	15	14
4	6	14
5	18	6
7	6	6
8	6	6
9	12	22
10	6	24
11	6	6
12	12	17
13	6	6

References

ABDALLAH, H. 2019. Theoretical study for the inhibition ability of some bioactive imidazole derivatives against the Middle-East respiratory syndrome corona virus (MERS-Co). *ZANCO Journal of Pure and Applied Sciences,* 31**,** 71-78.

ABDULLAH, B. J., OMAR, M. S. & JIANG, Q. J. 2016. Grüneisen Parameter and Its Related Thermodynamic Parameters Dependence on Size of Si Nanoparticles. *ZANCO Journal of Pure and Applied Sciences,* 28**,** 126-132.

AHMAD, H. O. 2015. *Kinetics and mechanism of racemisation reactions of configurationally labile stereogenic centres in drug-like molecules in aqueous solutions; thiohydantoins and related compounds.* Cardiff University.

AHN, J. H., KIM, S. J., PARK, W. S., CHO, S. Y., DU HA, J., KIM, S. S., KANG, S. K., JEONG, D. G., JUNG, S.-K. & LEE, S.-H. 2006. Synthesis and biological evaluation of rhodanine derivatives as PRL-3 inhibitors. *Bioorganic & medicinal chemistry letters,* 16**,** 2996-2999.

ALIZADEH, A., ROSTAMNIA, S., ZOHREH, N. & HOSSEINPOUR, R. 2009. A simple and effective approach to the synthesis of rhodanine derivatives via three-component reactions in water. *Tetrahedron Letters,* 50**,** 1533-1535.

BARAKAT, A., AL-MAJID, A. M., AL-NAJJAR, H. J., MABKHOT, Y. N., GHABBOUR, H. A. & FUN, H.-K. 2014. An efficient and green procedure for synthesis of rhodanine derivatives by aldol-thia-Michael protocol using aqueous diethylamine medium. *RSC Advances,* 4**,** 4909-4916.

BHATTI, R. S., SHAH, S., KRISHAN, P. & SANDHU, J. S. 2013. Recent pharmacological developments on rhodanines and 2, 4-thiazolidinediones. *International journal of medicinal chemistry,* 2013.

CHAUDHARI, L., JAWALE, B. A., SHARMA, S., SHARMA, H., KUMAR, C. & KULKARNI, P. A. 2012. Antimicrobial activity of commercially available essential oils against Streptococcus mutans. *J Contemp Dent Pract,* 13**,** 71-74.

CHONG, D. P., GRITSENKO, O. V. & BAERENDS, E. J. 2002. Interpretation of the Kohn–Sham orbital energies as approximate vertical ionization potentials. *The Journal of Chemical Physics,* 116**,** 1760-1772.

ENDO, Y., TANI, T. & KODAMA, M. 1987. Antimicrobial activity of tertiary amine covalently bonded to a polystyrene fiber. *Appl. Environ. Microbiol.,* 53**,** 2050-2055.

FAGHIHI, K. & HAGIBEYGI, M. 2003. New polyamides containing azobenzene unites and hydantoin derivatives in main chain: synthesis and characterization. *European polymer journal,* 39**,** 2307-2314.

GALVÁN, J. E., GIL, D. M., LANÚS, H. E. & ALTABEF, A. B. 2015. Theoretical study on the molecular structure and vibrational properties, NBO and HOMO–LUMO analysis of the POX3 (X= F, Cl, Br, I) series of molecules. *Journal of Molecular Structure,* 1081**,** 536-542.

GHOSH, S., DAS, J. & CHATTOPADHYAY, S. 2011. A novel light induced Knoevenagel condensation of Meldrum's acid with aromatic aldehydes in aqueous ethanol. *Tetrahedron letters,* 52**,** 2869-2872.

JALBOUT, A. & FERNANDEZ, S. 2002. Part II. Gaussian, complete basis set and density functional theory stability evaluation of the singlet states of Cn (n= 1–6): energy differences, HOMO–LUMO band gaps, and aromaticity. *Journal of Molecular Structure: THEOCHEM,* 584**,** 169-182.

JAWHAR, Z. S., AHMAD, H. O., HAYDAR, A. A., ABDULLAH, H. A. & MAHAMAD, S. A. 2018. One-Pot Synthesis, Pharmacological Evaluation, Docking Study, and DFT Calculations for Selected Imidazolidine-2, 4-Diones. *Science Journal of University of Zakho,* 6**,** 150-154.

JOHANSSON, P., NILSSON, H., JACOBSSON, P. & ARMAND, M. 2004. Novel Hückel stabilised azole ring-based lithium salts studied by ab initio Gaussian-3 theory. *Physical Chemistry Chemical Physics,* 6**,** 895-899.

JONAS, D., GRUNDMANN, H., HARTUNG, D., DASCHNER, F. & TOWNER, K. 1999. Evaluation of the mecA femB duplex polymerase chain reaction for detection of methicillin-resistant Staphylococcus aureus. *European Journal of Clinical Microbiology and Infectious Diseases,* 18**,** 643-647.

KATRITZKY, A. R., SOBIAK, S. & MARSON, C. M. 1988. Comparative study of the 13C nuclear magnetic resonance shifts of carbonyl and thiocarbonyl compounds. *Magnetic resonance in chemistry,* 26**,** 665-670.

KUHLMAN, B. & RALEIGH, D. P. 1998. Global analysis of the thermal and chemical denaturation of the N-terminal domain of the ribosomal protein L9 in H2O and D2O. Determination of the thermodynamic parameters, ΔH°, ΔS°, and ΔC° p, and evaluation of solvent isotope effects. *Protein science,* 7**,** 2405-2412.

MAKOV, G. 1995. Chemical hardness in density functional theory. *The Journal of Physical Chemistry,* 99**,** 9337-9339.

MARTÍNEZ-MAYORGA, K., JUARISTI, E. & CUEVAS, G. 2004. Manifestation of Stereoelectronic Effects on the Calculated Carbon− Hydrogen Bond Lengths and One-Bond 1 J CH NMR Coupling Constants. Relative Acceptor Ability of the Carbonyl (CO), Thiocarbonyl (CS), and Methylidene (C CH2) Groups toward C− H Donor Bonds. *The Journal of organic chemistry,* 69**,** 7266-7276.

MCNULTY, J., STEERE, J. A. & WOLF, S. 1998. The ultrasound promoted Knoevenagel condensation of aromatic aldehydes. *Tetrahedron Letters,* 39**,** 8013-8016.

MURUGAN, R., ANBAZHAGAN, S. & NARAYANAN, S. S. 2009. Synthesis and in vivo antidiabetic activity of novel dispiropyrrolidines through [3+ 2] cycloaddition reactions with thiazolidinedione and rhodanine derivatives. *European journal of medicinal chemistry,* 44**,** 3272-3279.

NAEEM, M. 2010. *Eco-friendly synthesis of thiazolidinone derivatives and their biological studies.* University of the Punjab, Lahore.

OSES, S. M., PASCUAL-MATE, A., DE LA FUENTE, D., DE PABLO, A., FERNANDEZ-MUINO, M. A. & SANCHO, M. T. 2016. Comparison of methods to determine antibacterial activity of honeys against Staphylococcus aureus. *NJAS-Wageningen Journal of Life Sciences,* 78**,** 29-33.

PEARSON, R. G. & PEARSON, R. G. 2005. Chemical hardness and density functional theory. *Journal of Chemical Sciences,* 117.

RAJAMANIKANDAN, S., JEYAKANTHAN, J. & SRINIVASAN, P. 2017. Binding mode exploration of LuxR-thiazolidinedione analogues, e-pharmacophore-based virtual screening in the designing of LuxR inhibitors and its biological evaluation. *Journal of Biomolecular Structure and Dynamics,* 35**,** 897-916.

ROCHA, M., DI SANTO, A., ARIAS, J. M., GIL, D. M. & ALTABEF, A. B. 2015. Ab-initio and DFT calculations on molecular structure, NBO, HOMO–LUMO study and a new vibrational analysis of 4-(dimethylamino) benzaldehyde. *Spectrochimica Acta Part A: Molecular and Biomolecular Spectroscopy,* 136**,** 635-643.

ROMERO-GONZALEZ, J., PERALTA-VIDEA, J., RODRıGUEZ, E., RAMIREZ, S. & GARDEA-TORRESDEY, J. 2005. Determination of thermodynamic parameters of Cr (VI) adsorption from aqueous solution onto Agave lechuguilla biomass. *The Journal of chemical thermodynamics,* 37**,** 343-347.

SAMAD, M. K. & HAWAIZ, F. E. 2019. Synthesis, characterization, antioxidant power and acute toxicity of some new azo-benzamide and azo-imidazolone derivatives with in vivo and in vitro antimicrobial evaluation. *Bioorganic chemistry,* 85**,** 431-444.

SANDHU, J. S. 2013. Ultrasound-assisted synthesis of 2, 4-thiazolidinedione and rhodanine derivatives catalyzed by task-specific ionic liquid:[TMG][Lac]. *Organic and medicinal chemistry letters,* 3**,** 2.

SHANKAR, R., SENTHILKUMAR, K. & KOLANDAIVEL, P. 2009. Calculation of ionization potential and chemical hardness: a comparative study of different methods. *International Journal of Quantum Chemistry,* 109**,** 764-771.

SUN, G., XU, X., BICKETT, J. R. & WILLIAMS, J. F. 2001. Durable and regenerable antibacterial finishing of fabrics with a new hydantoin derivative. *Industrial & engineering chemistry research,* 40**,** 1016-1021.

SYLDATK, C., LÄUFER, A., MÜLLER, R. & HÖKE, H. 1990. Production of optically pure d-and l-α-amino acids by bioconversion of d, l-5-monosubstituted hydantoin derivatives. *Microbial Bioproducts.* Springer.

VEISI, H., NAEIMI, A., MALEKI, B., ASHRAFI, S. S. & SEDRPOUSHAN, A. 2015. Synthesis of 5-Alkylidene-2, 4-thiazolidinediones and Rhodanines Promoted by Propylamino-functionalized Nano-structured SBA-15. *Organic Preparations and Procedures International,* 47**,** 309-315.

VIKNESHVARAN, S. & VELMATHI, S. 2017. Interfacial properties of electron-donating and electron-withdrawing group-substituted chiral Schiff bases

on mild steel corrosion in 1 M hydrochloric acid solution. *Journal of Bio-and Tribo-Corrosion,* 3**,** 19.

WANG, W., ZHOU, Y., PENG, H., HE, H.-W. & LU, X.-T. 2017. Synthesis and herbicidal activity of α-[(substituted phenoxybutyryloxy or valeryoxy)] alkylphosphonates and 2-(substituted phenoxybutyryloxy) alkyl-5, 5-dimethyl-1, 3, 2-dioxaphosphinan-2-one containing fluorine. *Journal of Fluorine Chemistry,* 193**,** 8-16.

YADAV, M., BEHERA, D., KUMAR, S. & YADAV, P. 2015. Experimental and quantum chemical studies on corrosion inhibition performance of thiazolidinedione derivatives for mild steel in hydrochloric acid solution. *Chemical Engineering Communications,* 202**,** 303-315.

YU, F.-L., SCHWALBE, C. H. & WATKIN, D. J. 2004. Hydantoin and hydrogen-bonding patterns in hydantoin derivatives. *Acta Crystallographica Section C: Crystal Structure Communications,* 60**,** o714-o717.

ABDALLAH, H. 2019. Theoretical study for the inhibition ability of some bioactive imidazole derivatives against the Middle-East respiratory syndrome corona virus (MERS-Co). *ZANCO Journal of Pure and Applied Sciences,* 31**,** 71-78.

ABDULLAH, B. J., OMAR, M. S. & JIANG, Q. J. 2016. Grüneisen Parameter and Its Related Thermodynamic Parameters Dependence on Size of Si Nanoparticles. *ZANCO Journal of Pure and Applied Sciences,* 28**,** 126-132.

AHMAD, H. O. 2015. *Kinetics and mechanism of racemisation reactions of configurationally labile stereogenic centres in drug-like molecules in aqueous solutions; thiohydantoins and related compounds.* Cardiff University.

AHN, J. H., KIM, S. J., PARK, W. S., CHO, S. Y., DU HA, J., KIM, S. S., KANG, S. K., JEONG, D. G., JUNG, S.-K. & LEE, S.-H. 2006. Synthesis and biological evaluation of rhodanine derivatives as PRL-3 inhibitors. *Bioorganic & medicinal chemistry letters,* 16**,** 2996-2999.

BHATTI, R. S., SHAH, S., KRISHAN, P. & SANDHU, J. S. 2013. Recent pharmacological developments on rhodanines and 2, 4-thiazolidinediones. *International journal of medicinal chemistry,* 2013.

CHONG, D. P., GRITSENKO, O. V. & BAERENDS, E. J. 2002. Interpretation of the Kohn–Sham orbital energies as approximate vertical ionization potentials. *The Journal of Chemical Physics,* 116**,** 1760-1772.

FAGHIHI, K. & HAGIBEYGI, M. 2003. New polyamides containing azobenzene unites and hydantoin derivatives in main chain: synthesis and characterization. *European polymer journal,* 39**,** 2307-2314.

GALVÁN, J. E., GIL, D. M., LANÚS, H. E. & ALTABEF, A. B. 2015. Theoretical study on the molecular structure and vibrational properties, NBO and HOMO–LUMO analysis of the POX3 (X= F, Cl, Br, I) series of molecules. *Journal of Molecular Structure,* 1081**,** 536-542.

JALBOUT, A. & FERNANDEZ, S. 2002. Part II. Gaussian, complete basis set and density functional theory stability evaluation of the singlet states of Cn (n= 1–6): energy differences, HOMO–LUMO band gaps, and aromaticity. *Journal of Molecular Structure: THEOCHEM,* 584**,** 169-182.

JAWHAR, Z. S., AHMAD, H. O., HAYDAR, A. A., ABDULLAH, H. A. & MAHAMAD, S. A. 2018. One-Pot Synthesis, Pharmacological Evaluation, Docking Study, and DFT Calculations for Selected Imidazolidine-2, 4-Diones. *Science Journal of University of Zakho,* 6**,** 150-154.

JOHANSSON, P., NILSSON, H., JACOBSSON, P. & ARMAND, M. 2004. Novel Hückel stabilised azole ring-based lithium salts studied by ab initio Gaussian-3 theory. *Physical Chemistry Chemical Physics,* 6**,** 895-899.

KUHLMAN, B. & RALEIGH, D. P. 1998. Global analysis of the thermal and chemical denaturation of the N-terminal domain of the ribosomal protein L9 in H2O and D2O. Determination of the thermodynamic parameters, ΔH°, ΔS°, and ΔC° p, and evaluation of solvent isotope effects. *Protein science,* 7**,** 2405-2412.

MURUGAN, R., ANBAZHAGAN, S. & NARAYANAN, S. S. 2009. Synthesis and in vivo antidiabetic activity of novel dispiropyrrolidines through [3+ 2] cycloaddition reactions with thiazolidinedione and rhodanine derivatives. *European journal of medicinal chemistry,* 44**,** 3272-3279.

PEARSON, R. G. & PEARSON, R. G. 2005. Chemical hardness and density functional theory. *Journal of Chemical Sciences,* 117.

RAJAMANIKANDAN, S., JEYAKANTHAN, J. & SRINIVASAN, P. 2017. Binding mode exploration of LuxR-thiazolidinedione analogues, e-pharmacophore-based virtual screening in the designing of LuxR inhibitors and its biological evaluation. *Journal of Biomolecular Structure and Dynamics,* 35**,** 897-916.

ROCHA, M., DI SANTO, A., ARIAS, J. M., GIL, D. M. & ALTABEF, A. B. 2015. Ab-initio and DFT calculations on molecular structure, NBO, HOMO–LUMO study and a new vibrational analysis of 4-(dimethylamino) benzaldehyde. *Spectrochimica Acta Part A: Molecular and Biomolecular Spectroscopy,* 136**,** 635-643.

ROMERO-GONZALEZ, J., PERALTA-VIDEA, J., RODRıGUEZ, E., RAMIREZ, S. & GARDEA-TORRESDEY, J. 2005. Determination of thermodynamic parameters of Cr (VI) adsorption from aqueous solution onto Agave lechuguilla biomass. *The Journal of chemical thermodynamics,* 37**,** 343-347.

SANDHU, J. S. 2013. Ultrasound-assisted synthesis of 2, 4-thiazolidinedione and rhodanine derivatives catalyzed by task-specific ionic liquid:[TMG][Lac]. *Organic and medicinal chemistry letters,* 3**,** 2.

SHANKAR, R., SENTHILKUMAR, K. & KOLANDAIVEL, P. 2009. Calculation of

ionization potential and chemical hardness: a comparative study of different methods. *International Journal of Quantum Chemistry,* 109**,** 764-771.

SUN, G., XU, X., BICKETT, J. R. & WILLIAMS, J. F. 2001. Durable and regenerable antibacterial finishing of fabrics with a new hydantoin derivative. *Industrial & engineering chemistry research,* 40**,** 1016-1021.

SYLDATK, C., LÄUFER, A., MÜLLER, R. & HÖKE, H. 1990. Production of optically pure d-and l-α-amino acids by bioconversion of d, l-5-monosubstituted hydantoin derivatives. *Microbial Bioproducts.* Springer.

VEISI, H., NAEIMI, A., MALEKI, B., ASHRAFI, S. S. & SEDRPOUSHAN, A. 2015. Synthesis of 5-Alkylidene-2, 4-thiazolidinediones and Rhodanines Promoted by Propylamino-functionalized Nano-structured SBA-15. *Organic Preparations and Procedures International,* 47**,** 309-315.

VIKNESHVARAN, S. & VELMATHI, S. 2017. Interfacial properties of electron-donating and electron-withdrawing group-substituted chiral Schiff bases on mild steel corrosion in 1 M hydrochloric acid solution. *Journal of Bio-and Tribo-Corrosion,* 3**,** 19.

WANG, W., ZHOU, Y., PENG, H., HE, H.-W. & LU, X.-T. 2017. Synthesis and herbicidal activity of α-[(substituted phenoxybutyryloxy or valeryoxy)] alkylphosphonates and 2-(substituted phenoxybutyryloxy) alkyl-5, 5-dimethyl-1, 3, 2-dioxaphosphinan-2-one containing fluorine. *Journal of Fluorine Chemistry,* 193**,** 8-16.

YADAV, M., BEHERA, D., KUMAR, S. & YADAV, P. 2015. Experimental and quantum chemical studies on corrosion inhibition performance of thiazolidinedione derivatives for mild steel in hydrochloric acid solution. *Chemical Engineering Communications,* 202**,** 303-315.

YU, F.-L., SCHWALBE, C. H. & WATKIN, D. J. 2004. Hydantoin and hydrogen-bonding patterns in hydantoin derivatives. *Acta Crystallographica Section C: Crystal Structure Communications,* 60**,** o714-o717.

ZANCO Journal of Pure and Applied Sciences
The official scientific journal of Salahaddin University-Erbil
https://zancojournals.su.edu.krd/index.php/JPAS

ISSN (print):2218-0230**, ISSN (online):** 2412-3986**, DOI: http://dx.doi.org/10.21271/zjpas**

RESEARCH PAPER

Molecular Marker Study for *Hyles euphorbiae* (Lepidoptera: Sphingidae) Based on Mitochondrial DNA Genes in Erbil Province

Govand M. Qader[1], Mukhlis H. Aali[1], Hana H. Mohammad[1]

[1]Department of Biology, College of Science, Salahaddin University-Erbil, Kurdistan Region, Iraq

A B S T R A C T:

The Hawkmoths consisting more than 1,500 species over worldwide in 200 genera. The family sphingidae is splitted into two taxonomic categories which is sub-family sphinginae and macroglossinae. The mitochondrial genes sequence commonly used for taxonomic phylogeny due to maternal inheritance and less degradation. The aim of the present study was the taxon identification of *Hyles euphorbia* among other level species of this genus. Sixteen *Hyles* (eight males and eight females) were use and then DNA was extracted from insect anterior abdomen. Multiplex PCR was performed for amplification of specific targeted sequence DNA in mitochondrial cytochrome oxidase I and II genes. The *Hyles euphorbiae* was successfully identified and this corresponds to the amplification of sixteen specimens of targeted DNA fragment with using a group specific primers that covering the targeted sequence between 277 bp and 280 bp. The present study was concluded that the *Hyles euphorbiae* exists in Kurdistan region and Multiplex PCR can be done for this reason.

KEY WORDS: COI, COII, mtDNA, *Hyles euphorbiae*, Multiplex PCR.
DOI: http://dx.doi.org/10.21271/ZJPAS.32.3.16
ZJPAS (2020) , 32(3);157-162.

1. INTRODUCTION

he Hawkmoths (Lepidoptera: Sphingidae) consisting more than 1,500 species over worldwide in 200 genera and appear on every continent exclude Antarctica are one of the most obvious and widely studied insects (Kawahara and Barber, 2015, Kawahara et al., 2009, Duarte et al., 2008). Hawk moth is a successful genus that evolved in Neotropics depending on molecular data (Hundsdoerfer et al., 2019, Ernst et al., 2018).

* **Corresponding Author:**
Govand Musa Qader
E-mail: govand.qader@su.edu.krd
Article History:
Received: 27/11/2019
Accepted: 06/02/2020
Published: 15/06 /2020

The sphingidae name was formulated by Samouelle in 1819. The family sphingidae is splitted into two taxonomic category, first one sub-family sphinginae that consist of 116 genera, second one sub-family macroglossinae that contain 89 genera (Messenger, 1997) and sub-family Smerinthinae (Li et al., 2018).

Sphingidae is one of the nocturnal recognizable family belong to abundant size and prevalence which is appeal to light sources (Moré et al., 2005). Mating behaviour occurred at night (Kilaso and Tigvattananont, 2018). The new island *Hyles* was collected during the day and without light (Tennent and Russell, 2015). The spurge hawk moth *Hyles euphorbiae L.* (Lepidoptera: sphingidae) are from moderate to large size and the body weight between 0.1 to 7 gram. Hawkmoth species distributed in Central/Southern Europe and Western Asia (Hundsdoerfer et al., 2005b). The mysterious biogeographic pattern in *Hyles* during speciation

stage is belong to cosmopolitan distribution, polymorphic also disapproval classification species (Mende et al., 2016, Halloway et al., 2018).

Hawkmoth has role in balance ecosystem through floral pollination, the floral member advertises and signal got to pollinator by olfactory neurons in terminal of proboscis which strongly have role in floral diversity by transferring pollen grains (Haverkamp et al., 2016, Heywood et al., 2017). The long tongued moths are adapted for pollination (Suetsugu et al., 2015).

Classification in the past was done depended on superficially phenotype body characters like pattern and of wing and abdomen in mature stage, color in larval immature stage and genital feature (Hundsdoerfer and Kitching, 2017). Species identification requires data from more sources such behavior phenotype and DNA markers so only a very little variation in molecular level is enough also quite efficient to detect unknown insect (Funk and Omland, 2003, Dayrat, 2005).

The DNA sequence of mitochondrial genes commonly used for taxonomic phylogeny due to maternal inheritance, sequence conservation, little modification, quick development and less degradation (Avise et al., 1987). The sequence data comprise about 2300 bp of the mitochondrial genes cytochrome c oxidase subunit I (COX I), cytochrome c oxidase subunit II (COX II), and the gene of the ribosomal transfer RNA for leucine (tRNA-leu). In the mitochondrial genome of *Hyles*, this ribosomal region lies between the two COX genes (Hundsdoerfer et al., 2005a). The primers were designed depending on the various marker sequence of commonly used mitochondrial genes like cytochrome oxidase I, II and 16S rRNA genes for species level classification (Folmer et al., 1994, Caterino et al., 2000). *Hyles* can be used as a model organism for biological and environmental studies like species development and role of genetic factor in ecology adaptation (Barth et al., 2018, Cock, 2018).

Deoxyribonucleic acid (DNA) barcode sequence generated for Sphingidae through which compare with global DNA insects that can find the exact geographical distribution (Haxaire et al., 2015). The various projects of insect taxonomy really realize to use specific primer not universal primers to gain accurate and success PCR (Hebert et al., 2004, Penton et al., 2004). Molecular techniques is the quick method used to develop biology fields and till now our knowledge of molecular feature evolution remains relatively limit and understanding on phylogenetic relationship depend on the analysis of molecular data (Blair and Hedges, 2005, C Regier et al., 2005). The aim of the present study was taxon identification of *Hyles euphorbia* among other level species of this genus.

2. MATERIALS AND METHODS

2.1. Sample Collection:

The larvae of *H. euphorbiae* were collected on Euphorbia macrocalda at the periods from March – April from the villages Hanara at Shaqlawa, in Iraqi Kurdistan region. The food plants restricted to the genus *Euphorbia* (Euphorbiaceae). The captured larvae were taken from field to laboratory in appropriate box. The fresh leafy spruge leaves were provided as food for developing larvae. The larvae were kept in the room temperature during the experiment. Cotton wad dipped in 10 per cent honey solution was provided as food for the moths. Sixteen *Hyles* (eight males and eight females) were collected manually using entomological net and then ethyl acetate was used as an injection solution ventrally between thorax and abdomen to kill the sphingidae. The specimens preserved in 100% ethanol or store at -20°C until DNA extraction (Hundsdoerfer et al., 2005a, Primo et al., 2013, Singh and Kaur, 2017a, Santos et al., 2015, Sondhi et al., 2017). Sex differentiation were carried out by phenotypic character of wing frenulum, male with one large and female with a brush like bristle (Primo et al., 2013).

2.2 Genomic DNA Extraction from Insect Sample

The piece of the anterior abdomen was separated from sphingidae and followed by DNA isolation from sixteen of Hyles member depend on protocol of geneaid DNA isolation kit manufacturers' instructions. Weight 10-20 mg of anterior abdomen tissue and transfer to 1.5 ml Eppendorf tube. Micropestle and mortal was used to squash the tissue, suspend in 600 µl cell lysis buffer, homogenize the sample by continue grinding (Mende and Hundsdoerfer, 2013).

Digest the tissue by adding 12 µl of Proteinase K to the tube and mix by vortex then incubate at 60ºC for 30-60 minutes, during incubation, invert the tube periodically. Add 200 µl of Protein Removal Buffer to the sample lysate then vortex immediately for 10 seconds. Centrifuge at 14-16,000 x g for 3 minutes to form a tight pellet. Transfer the supernatant to a clean 1.5 ml microcentrifuge tube then add 600 µl of isopropanol and mix well by gently inverting 20 times. Centrifuge at 14-16,000 x g for 5 minutes then carefully discard the supernatant and add 600 µl of 70% ethanol to wash the pellet. Centrifuge at 14-16,000 x g for 3 minutes then carefully discard the supernatant and air-dry the pellet for 10 minutes. Add 100 µl of DNA Hydration Buffer then gently vortex for 10 seconds. Incubate at 60ºC for 30-60 minutes to dissolve the DNA pellet. During incubation, tap the bottom of the tube to promote DNA rehydration. Then the concentration and purity of genomic DNA extracts from each insect samples were determined using Nano-Drop nd-1000 spectrophotometer by recording the concentration from (110.1 - 177.89 ng/µl) and purity (1.15 – 1.88) for each sample.

2.3. Molecular Technique Analysis

The mitogenome study can be used for phylogenetic of Lepidoptera including Bombycidae, Saturniidae and Sphingidae. Molecular technique was performed for amplification of specific targeted sequence DNA in mitochondrial cytochrome oxidase I, II genes and t-RNA gene for leucine (Hundsdoerfer et al., 2009, Kim et al., 2016, Gu et al., 2016). Multiplex PCR was carried out to amplify three fragments covering 794 bp in total (B: 277 bp, H: 280 bp and L: 237 bp), the primers that used in the study were designed specifically for *Hyles* or *Hylex euphorbiae* complex (HEC) (Mende and Hundsdoerfer, 2013).

Amplification was conducted in polymerase chain reactions in total volume 25 µl containing 3.4 µl of nuclease free water, 0.6 µl for each primer *Hyles* COIca100f:5-TAAGATTAYTAATTCGAGCAG-3, MLepR1": 5-CCTGTTCCAGCTCCATTTTC-3, HEC-COIca1110f: 5-ATGATACATATTATGTTGTAGC-3, HEC-COIca1350r: 5-GAGATATATGACCCTAATGATGA-3, HylesMCOIIf: 5-GATACTGAAGATATGAATATTC-3, HylesCOIIca2125r: 5-TTGTTTGGTTTAAACGTCCAGG-3) respectively (10 pmol/µl) (Simon et al., 1994) and 15µl of master mix (Promega, USA). Three microliters genomic DNA as a template was used. The program file condition consisted of an initial 5 min denaturation at 95º C followed by 35 cycles of 95º C for 30 s, 57º C for 1 min 30 s and 72°C for 45 s and final elongation at 60°C for 30 min and was performed on a thermal Cycler (Techne, UK). After PCR amplification,10µl PCR product was loaded on to 2% agarose then the separated bands were stained with ethidium bromide and visualized under UV light (Brown, 2016).

3. RESULTS AND DISCUSSION

3.1. Extraction Yield

The grouping and identifying of Lepidoptera is applicable depending on phenotypic characters while insect speciation in this genus cannot be used therefore PCR target amplifications of COX I, COX II and t-RNA were conducted and used as standard tool for molecular taxonomy of *Hyles* classification (Hundsdoerfer et al., 2005a, Singh and Kaur, 2017b).

The *Hyles* can be classify according to Cytochrome C oxidase *in vitro* replication (Hundsdoerfer et al., 2009, Mende and Hundsdoerfer, 2013, Mende and Hundsdoerfer, 2014). Species communities can be rapidly identify via a group of specific primers (Sint et al., 2014). The set of taxon specific primers of Multiplex PCR were created specifically that bind accurately only with complementary DNA target sequence to classify Lepidoptera (Mende and Hundsdoerfer, 2013, Sint et al., 2014).

In the present study the *Hyles euphorbiae* was successfully identified amplified two just targeted fragments 277 and 280 bp in length of the CO I/II genes. This corresponds to the amplification of sixteen specimens of targeted DNA fragment with using a group specific primers in multiplex PCR that covering targeted sequence between 277 bp and 280 bp in length. The findings of the present study are in agreement with previous investigation of Mende and Hundsdoerfer, who reported that successfully PCR

amplified targeted fragments 277 and 280 bp in length of the CO I/II genes from 143 specimens by using these specific primers (Mende and Hundsdoerfer, 2013). Among the total specimens, ten haplotypes male and female of *Hyles euphorbiae* were detected successfully as elucidated in (Figure 1). Additionally, our work was confirmed by using the same primer in Uniplex PCR and they indicated the same results (Figure 2). While the DNA amplicons 237 bp had not offered and obtained from sixteen specimens of targeted DNA fragment with using a specific primer in Uniplex PCR might be due to the lack of suitable targeted and priming sites of PCR primer in the insect's genomic DNA to amplify of the gene of the ribosomal transfer RNA of *H. euphorbiae* collected in Kurdistan Region as illustrated in (Figure 3). Hundsdoerfer et al. was found that the there is a close relation between mtDNA of *H. euphorbiae* and *H. tithymali* lineage it means the remaining specimen have different DNA loci may belong *H. tithymali* (Hundsdoerfer et al., 2005a).

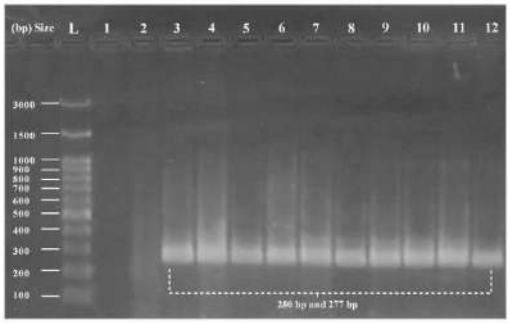

Figure 1. Agarose gel electrophoresis (2%) showing 277bp and 280 bp Multiplex PCR fragments corresponding to amplification of mitochondrial genes. Lane L: 100 bp DNA ladder. Lane 1: Negative control (H_2O was used as a template). Lane 2: *Hyles euphorbiae* not amplified with the specific primers. Lane 3-12: *Hyles euphorbiae* target DNA sequence amplified (B and H fragments) with the specific primers.

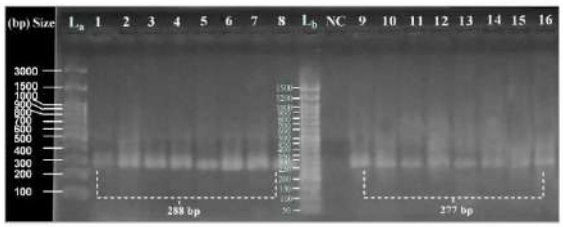

Figure 2: Agarose gel electrophoresis (2%) representing 277 bp and 280 bp Uniplex PCR products corresponding to amplification of mitochondrial genes. Lane La: 100 bp DNA ladder. Lane 1-8: 288 bp PCR DNA amplicons (H fragments) with the specific primer correspond to *Hyles euphorbiae* species. Lane Lb: 50 bp DNA ladder. Lane NC: Negative control (H2O was used as a template). Lane 9-16: 288 bp PCR DNA product sizes (B fragments) with the specific primer correspond to *Hyles euphorbiae* species.

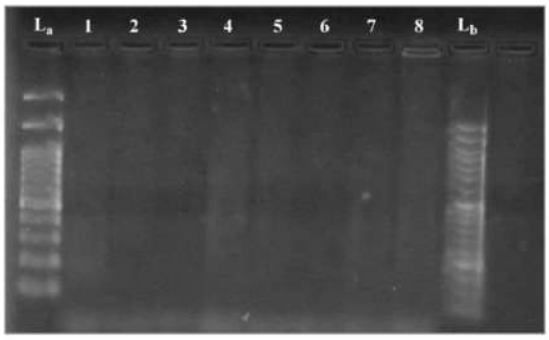

Figure 3: Illustrates failure of PCR amplification results obtained with specific primer corresponding to amplification (L fragments) of mitochondrial genes by (2%) agarose gel electrophoresis. Lane La: 100 bp DNA ladder. Lane 1-8: No PCR DNA amplicons with the specific primer correspond to *Hyles euphorbiae* species. Lane Lb: 50 bp DNA ladder.

4. CONCLUSIONS

The present study concluded that *Hyles euphorbiae* exists in Kurdistan region and Multiplex PCR can be used for this purpose. With regard to our findings of the present study, future DNA sequence analyses by recent molecular taxonomical study should examine the mitochondrial genes sequences in more detail to revealed the geographical distribution of mitochondrial lineages for *Hyles euphorbia* species with other hawkmoths species.

Acknowledgements

We would like to thank University of Salahaddin-College of Science/Biology Department, for helping us and providing facilities.

References

AVISE, J. C., ARNOLD, J., BALL, R. M., BERMINGHAM, E., LAMB, T., NEIGEL, J. E., REEB, C. A. & SAUNDERS, N. C. 1987. Intraspecific phylogeography: the mitochondrial DNA bridge between population genetics and systematics. *Annual review of ecology and systematics*, 18**,** 489-522.

BARTH, M. B., BUCHWALDER, K., KAWAHARA, A. Y., ZHOU, X., LIU, S., KREZDORN, N., ROTTER, B., HORRES, R. & HUNDSDOERFER, A. K. 2018. Functional characterization of the Hyles euphorbiae hawkmoth transcriptome reveals strong expression of phorbol ester detoxification and seasonal cold hardiness genes. *Frontiers in zoology,* 15**,** 20.

BLAIR, J. E. & HEDGES, S. B. 2005. Molecular phylogeny and divergence times of deuterostome animals. *Mol Biol Evol,* 22**,** 2275-84.

BROWN, T. A. 2016. *Gene cloning and DNA analysis: an introduction*, John Wiley & Sons.

C REGIER, J., SHULTZ, J. & KAMBIC, R. 2005. *Regier JC, Shultz JW, Kambic RE. Pancrustacean phylogeny: hexapods are terrestrial crustaceans and maxillopods are not monophyletic. Proc Biol Sci 2005;272:395-401*.

CATERINO, M. S., CHO, S. & SPERLING, F. A. 2000. The current state of insect molecular systematics: a thriving Tower of Babel. *Annu Rev Entomol,* 45**,** 1-54.

COCK, M. J. 2018. Hawk-moths (Lepidoptera: Sphingidae) of Trinidad, West Indies: an illustrated and annotated list. *Living World, Journal of the Trinidad and Tobago Field Naturalists' Club***,** 10-81.

DAYRAT, B. 2005. Towards integrative taxonomy. *Biological Journal of the Linnean Society,* 85**,** 407-415.

DUARTE, M., CARLIN, L. F. & MARCONATO, G. 2008. Light-attracted hawkmoths (Lepidoptera: Sphingidae) of Boracéia, municipality of Salesópolis, state of São Paulo, Brazil. *Check List,* 4.

ERNST, M., NOTHIAS-SCAGLIA, L.-F., VAN DER HOOFT, J., SILVA, R. R., SASLIS-LAGOUDAKIS, C. H., GRACE, O. M., MARTINEZ-SWATSON, K., HASSEMER, G., FUNEZ, L. & SIMONSEN, H. T. 2018. Did a plant-herbivore arms race drive chemical diversity in Euphorbia? *bioRxiv***,** 323014.

FOLMER, O., BLACK, M., HOEH, W., LUTZ, R. & VRIJENHOEK, R. 1994. DNA primers for amplification of mitochondrial cytochrome c oxidase subunit I from diverse metazoan invertebrates. *Mol Mar Biol Biotechnol,* 3**,** 294-9.

FUNK, D. J. & OMLAND, K. E. 2003. Species-Level Paraphyly and Polyphyly: Frequency, Causes, and Consequences, with Insights from Animal Mitochondrial DNA. *Annual Review of Ecology, Evolution, and Systematics,* 34**,** 397-423.

GU, X.-S., MA, L., WANG, X. & HUANG, G.-H. 2016. Analysis on the complete mitochondrial genome of Andraca theae (Lepidoptera: Bombycoidea). *Journal of Insect Science,* 16**,** 105.

HALLOWAY, A., WHELAN, C. J. & BROWN, J. S. 2018. The hummingbird and the hawk-moth: Species distribution, geographical partitioning, and macrocompetition across the United States. *bioRxiv***,** 212894.

HAVERKAMP, A., YON, F., KEESEY, I. W., MIßBACH, C., KOENIG, C., HANSSON, B. S., BALDWIN, I. T., KNADEN, M. & KESSLER, D. 2016. Hawkmoths evaluate scenting flowers with the tip of their proboscis. *Elife,* 5**,** e15039.

HAXAIRE, J., ROUGERIE, R., MIELKE, C. G. & KITCHING, I. J. 2015. Manduca exiguus (Gehlen, 1942): a valid species from southern and south-eastern Brazil, Uruguay and north-eastern Argentina (Lepidoptera: Sphingidae).

HEBERT, P. D., PENTON, E. H., BURNS, J. M., JANZEN, D. H. & HALLWACHS, W. 2004. Ten species in one: DNA barcoding reveals cryptic species in the neotropical skipper butterfly Astraptes fulgerator. *Proc Natl Acad Sci U S A,* 101**,** 14812-7.

HEYWOOD, J. S., MICHALSKI, J. S., MCCANN, B. K., RUSSO, A. D., ANDRES, K. J., HALL, A. R. & MIDDLETON, T. C. 2017. Genetic and environmental integration of the hawkmoth pollination syndrome in Ruellia humilis (Acanthaceae). *Annals of botany,* 119**,** 1143-1155.

HUNDSDOERFER, A. K., BUCHWALDER, K., O'NEILL, M. A. & DOBLER, S. 2019. Chemical ecology traits in an adaptive radiation: TPA-sensitivity and detoxification in Hyles and Hippotion (Sphingidae, Lepidoptera) larvae. *Chemoecology,* 29**,** 35-47.

HUNDSDOERFER, A. K. & KITCHING, I. J. 2017. Historic DNA for taxonomy and conservation: A case-study of a century-old Hawaiian hawkmoth type (Lepidoptera: Sphingidae). *PloS one,* 12**,** e0173255.

HUNDSDOERFER, A. K., KITCHING, I. J. & WINK, M. 2005a. A molecular phylogeny of the hawkmoth genus Hyles (Lepidoptera: Sphingidae, Macroglossinae). *Mol Phylogenet Evol,* 35**,** 442-58.

HUNDSDOERFER, A. K., KITCHING, I. J. & WINK, M. 2005b. The phylogeny of the Hyles euphorbiae complex (Lepidoptera: Sphingidae): Molecular evidence from sequence data and ISSR-PCR fingerprints. *Organisms Diversity & Evolution,* 5**,** 173-198.

HUNDSDOERFER, A. K., RUBINOFF, D., ATTIE, M., WINK, M. & KITCHING, I. J. 2009. A revised molecular phylogeny of the globally distributed

hawkmoth genus Hyles (Lepidoptera: Sphingidae), based on mitochondrial and nuclear DNA sequences. *Mol Phylogenet Evol,* 52**,** 852-65.

KAWAHARA, A. Y. & BARBER, J. R. 2015. Tempo and mode of antibat ultrasound production and sonar jamming in the diverse hawkmoth radiation. *Proceedings of the National Academy of Sciences,* 112**,** 6407-6412.

KAWAHARA, A. Y., MIGNAULT, A. A., REGIER, J. C., KITCHING, I. J. & MITTER, C. 2009. Phylogeny and biogeography of hawkmoths (Lepidoptera: Sphingidae): evidence from five nuclear genes. *PLoS One,* 4**,** e5719.

KILASO, M. & TIGVATTANANONT, S. 2018. Bionomics of the Australian hawk moth, Theretra laterillii lucasii (Walker)(Lepidoptera: Sphingidae). *International Journal of Agricultural Technology,* 14**,** 535-542.

KIM, M. J., KIM, J. S. & KIM, I. 2016. Complete mitochondrial genome of the hawkmoth Notonagemia analis scribae (Lepidoptera: Sphingidae). *Mitochondrial DNA Part B,* 1**,** 416-418.

LI, J., LIN, R.-R., ZHANG, Y.-Y., HU, K.-J., ZHAO, Y.-Q., LI, Y., HUANG, Z.-R., ZHANG, X., GENG, X.-X. & DING, J.-H. 2018. Characterization of the complete mitochondrial DNA of Theretra japonica and its phylogenetic position within the Sphingidae (Lepidoptera, Sphingidae). *ZooKeys***,** 127.

MALLET, J., WYNNE, I. R. & THOMAS, C. D. 2011. Hybridisation and climate change: brown argus butterflies in Britain (Polyommatus subgenus Aricia). *Insect Conservation and Diversity,* 4**,** 192-199.

MENDE, M. & HUNDSDOERFER, A. 2014. *More evidence for an admixture of the Hyles euphorbiae complex's main lineages in Mediterranean Europe (Lepidoptera: Sphingidae)*.

MENDE, M. B., BARTEL, M. & HUNDSDOERFER, A. K. 2016. A comprehensive phylogeography of the Hyles euphorbiae complex (Lepidoptera: Sphingidae) indicates a 'glacial refuge belt'. *Scientific Reports,* 6**,** 29527.

MENDE, M. B. & HUNDSDOERFER, A. K. 2013. Mitochondrial lineage sorting in action – historical biogeography of the Hyles euphorbiae complex (Sphingidae, Lepidoptera) in Italy. *BMC Evolutionary Biology,* 13**,** 83.

MESSENGER, C. 1997. *The Sphinx Moths (Lepidoptera: Sphingidae) of Nebraska*.

MORÉ, M., KITCHING, I. & COCUCCI, A. 2005. *Sphingidae: Esfíngidos de Argentina. Hawkmoths of Argentina*.

PARMESAN, C., RYRHOLM, N., STEFANESCU, C., HILL, J. K., THOMAS, C. D., DESCIMON, H., HUNTLEY, B., KAILA, L., KULLBERG, J., TAMMARU, T., TENNENT, W. J., THOMAS, J. A. & WARREN, M. 1999. Poleward shifts in geographical ranges of butterfly species associated with regional warming. *Nature,* 399**,** 579.

PENTON, E. H., HEBERT, P. D. N. & CREASE, T. J. 2004. Mitochondrial DNA variation in North American populations of Daphnia obtusa: continentalism or cryptic endemism? *Molecular Ecology,* 13**,** 97-107.

PITTAWAY, A. R. 1993. *The Hawkmoths of the Western Palaearctic,* Leiden, The Netherlands, Brill.

PRIMO, L. M., DUARTE, J. A. & MACHADO, I. C. 2013. Hawkmoth fauna (Sphingidae, Lepidoptera) in a semi-deciduous rainforest remnant: composition, temporal fluctuations, and new records for Northeastern Brazil. *An Acad Bras Cienc,* 85**,** 1177-88.

SANTOS, F. L., CASAGRANDE, M. M. & MIELKE, O. H. 2015. Saturniidae and Sphingidae (Lepidoptera, Bombycoidea) assemblage in Vossoroca, Tijucas do Sul, Paraná, Brazil. *Anais da Academia Brasileira de Ciências,* 87**,** 843-860.

SIMON, C., FRATI, F., BECKENBACH, A., CRESPI, B., LIU, H. & FLOOK, P. 1994. Evolution, Weighting, and Phylogenetic Utility of Mitochondrial Gene Sequences and a Compilation of Conserved Polymerase Chain Reaction Primers. *Annals of the Entomological Society of America,* 87**,** 651-701.

SINGH, D. & KAUR, N. 2017a. *DNA barcoding of some Indian species of hawk moths based on COI gene (Lepidoptera : Sphingidae)*.

SINGH, D. & KAUR, N. 2017b. DNA barcoding of some Indian species of hawk moths based on COI gene (Lepidoptera: Sphingidae).

SINT, D., NIEDERKLAPFER, B., KAUFMANN, R. & TRAUGOTT, M. 2014. Group-Specific Multiplex PCR Detection Systems for the Identification of Flying Insect Prey. *PLOS ONE,* 9**,** e115501.

SONDHI, Y., KITCHING, I., BASU, D. N. & KUNTE, K. 2017. A new species of Theretra Hübner (Lepidoptera: Sphingidae) from the southern Western Ghats, India. *Zootaxa,* 4323**,** 185-196.

SUETSUGU, K., TANAKA, K., OKUYAMA, Y. & YUKAWA, T. 2015. Potential pollinator of Vanda falcata (Orchidaceae): Theretra (Lepidoptera: Sphingidae) hawkmoths are visitors of long spurred orchid. *European Journal of Entomology,* 112.

TENNENT, W. J. & RUSSELL, P. J. 2015. Notes on some hawk-moths (Lepidoptera: Sphingidae) from the Cape Verde Islands. *Zoologia Caboverdiana,* 5**,** 105-110.

ZANCO Journal of Pure and Applied Sciences
The official scientific journal of Salahaddin University-Erbil
https://zancojournals.su.edu.krd/index.php/JPAS

ISSN (print):2218-0230**, ISSN (online):** 2412-3986**, DOI: http://dx.doi.org/10.21271/zjpas**

RESEARCH PAPER

Curcumin oil and Grapeseed oil can antagonize the Effect of All-Trans-Retinoic Acid (ATRA) on Rat's Kidney

Khabat A. ALI

Department of Biology, College of Education, Salahaddin University-Erbil, Kurdistan Region, Iraq

A B S T R A C T:

Tretinoin chemically is all-trans retinoic acid associated with retinol groups. It is yellow to light orange crystalline powder that urges the cytodifferentiation and diminish proliferation of acute promyelocytic leukemia (APL) cells in culture and in vivo. The accurate mechanism operation of tretinoin is uncharted. Researchers have shown that tretinoin has potentially teratogenic and toxic side influences in mice, rats, hamster rabbits and patients. The most frequent adverse events in kidney were renal insufficiency, dysuria, acute renal failure, micturition recurrence and renal tubular necrosis and also it causes enlargement of prostate .

There were no adequate and well-controlled studies in animal models. So, monitoring of kidney functions with its texture had to be done. In recent years herbal extract treatment showed capability of ameliorative role for the disturbance of organs functions with toxic and injuries in different tissues especially kidney tissue.

Current research was conducted in 28 days and 49 rats were included and they were divided into seven groups each group containing 7 rats: the first was negative control group gavageed with olive oil at dose (2ml/kg/bw) , while the second and third were positive control groups administrated at dose (15&30 mg/kg/bw) respectively with ATRA ,indeed the others treated groups combinations between the two ATRA concentrations with curcumin oil at dose (50 mg /kg/bw) were included the fourth and fifth groups respectively, and the last two groups administrated grape oil at dose (50 mg /kg/bw) were included the sixth and seventh group respectively .

From this study, we discovered that treating the rats by extracted grapeseed oil with ATRA recovered the damaged kidney architecture near to normal as well as improved their renal functions.

KEY WORDS: All-trans Retinoic acid, curcumin oil, grape seed, antioxidant, nephrotoxicity
DOI: http://dx.doi.org/10.21271/ZJPAS.32.3.17
ZJPAS (2020) , 32(3);163-175 .

INTRODUCTION

Retinoic acid is one of the pro-vitamin A, relevant composites that extend their impact throughout activation of receptors (Elsayed et al., 2014). Retinoic acid has various effects on physiological means, like; cell growth, differentiation, apoptosis, and inflammation (Zhou et al., 2013).

* **Corresponding Author:**
Khabat A. ALI
E-mail: khabat.ali@su.edu.krd
Article History:
Received: 20/11/2019
Accepted: 13/02/2020
Published: 15/06 /2020

The anti-proliferative effects of retinoid are attributable to modulation of gene receptors transcription (Wagner et al., 2000). ATRA is assimilated in the small intestine and esterified as retinyl esters to be transported by blood stream and then it's chiefly conveyed to the liver as a storing house, principally in the hepatic stellate cell. As well as hydrolysis of retinyl esters results in retinol which, then joins to retinol-binding protein (RBP), (Dai et al., 2017). The mechanical effect of this acid on the kidney is not known but retinoid had an indication of kidney dysfunction and is also a risk agent for the progression of

chronic kidney infection (Cravide & Remuzzi, 2013).

Various plant seeds had shown to exhibit medical properties such as antidiabetic, anti-allergic, anti-inflammatory, antibacterial, antioxidant activity (Aggarwal, et al., 2016, Hassan et al., 2017).
Curcumin is one of the medical herbs which are well known for thousands of years and have many useful features. The vital element existing in Curcuma longa of the family Zingiberaceae has a complex of pharmacological impressions inclusive potent anti-inflammatory activity (Nasri et al., 2014, Aggarwal, et al., 2016). Curcumin oil extract (CEO) is gathered from C.Longa which manifest powerful anti-inflammatory and anti-arthritic exploits (Maheshwari et al .,2006).In addition, the oil is utilized for a broad spectrum of dysfunctions, including biliary malady, anorexia, coryza, cough, wound, hepatic dysfunctions, rheumatic diseases, sprains and swellings created by damage and sinusitis (Sukandar et al., 2010). Besides that, curcumin oil improves renal distractions and tissue normalization nearly to the normal state (Nonose et al 2014).
Grapeseed oil (GSO) is an extract of the grape seeds which has been used recently for cosmetics and treating various disorders and wound curing (Shivananda et al., 2011). In addition to cooking, GSO has a variety of health advantages and is admitted as a good and powerful antioxidant mixture for its content of polyphenol, flavonoids, saturated fatty acids and vitamin E (El-Ashmawy et al., 2007, Freitas et al 2008). Many studies refer to the effect of GSO in anti-inflammatory, anti-carcinogenic, platelet aggregation inhibiting and metal chelating properties (Nagib, 2014).

The study was conducted to examine the effect of two natural products curcumin and grapeseed oils against the nephrotoxic effect of all Trans retinoic acid in rats.

1. MATERIALS AND METHODS

1.1. MATERIALS

1.2. Plant Material Collection:

A- Olive oil extract, Curcumin seed oil extract (CEO) and Grapeseed oil extract (GSO) were purchased from local markets in Erbil city, Iraq.
B-Tretinoin Capsules are all-trans retinoic acid (ATRA) supplied as (10mg), two-tone (longitudinally) with reddish-brown opaque and yellow gelatin crust, imprinted with TR" with black paint on the yellow side., American Health packaging. Par Pharmaceuticals (10mg/30UD) NDC68084-075-21packaded from NDC, Columbus, OH 10370-268.

1.3. Animals model

The experiments were conducted at the animal house of the University of Sallahaddin, college of Education, Department of Biology, Erbil, Iraq. Adult Sprague Dawley strain albino rats at 9-10 months' age and 250-350 body weighing were obtained from an upbringing colonist kept on a usual rodent chow and water ad libitum and a 12 h artificial light/dark cycle, were kept in well–ventilated cage at room temperature under controlled condition of ambient temperature 250C. The animals were given standard rat pellets and tap water ad libitum.
The experiments were conducted over 49 rats, divided into seven groups and each group contained 7 rats for 28 days: control group: The rats were given olive oil (2ml/kg/bw) with standard chow and tap water ad libitum, ATRA given at dosage of (15&30 mg/kg/bw) in second and third groups respectively, CEO treated dosage (50 mg /kg/bw) + ATRA at dosage of (15&30 mg/kg/bw) in fourth and fifth groups respectively, GSO treated at dosage (50 mg /kg/bw) + ATRA at a dosage of (15&30 mg/kg/bw) in sixth and seventh groups respectively ,The rats in all groups were receiving materials orally by gavage.
The experiments were completed within 28 days. At the end, animals were sacrificed and dissected and their kidneys were taken for histological examinations.

1.4. Blood sampling

Blood samples were taken from peripheral veins by 5 ml syringe. Put into gel and clot-activator tubes for serum separation. Their sera were separated by 3000 round per minute centrifugation for 20 min. They were frozen at −80°C for chemical assays of renal function tests (blood urea, serum creatinine and uric acid) for all study groups (Cheng et al., 2005).

.

1.5. Histopathological examinations

Kidney tissues were preserved in neutral buffered formalin 10% solution and were processed to obtain Formalin Fixed Paraffin Embedded (FFBE) blocks. Changes were assessed in histopathological sections at 5-micron cuts stained with hematoxylins and eosin (H&E) stains (Murice-Lambert et al., 1989).

1.6. Statistical analysis

The data was coded and entered using the statistical analysis, Graph Pad Prism 8 was used to analyze the data wich was done by Shapiro-wilk test and Kolmogorov-Smirnov test.

2. RESULTS

The persistence project was programmed for and conducted over 49 rats, divided into seven groups each group contained 7 rats for 28 days: the first group was negative control group gavageed with olive oil at dose (2ml/kg/bw) , while the second and third were positive control groups administrated at dose of (15&30 mg/kg/bw) respectively with ATRA, and for the fourth and fifth treated groups; combinations between the two ATRA concentrations with curcumin oil at dose of (50 mg /kg/bw) were used consequently, also the last two groups administrated grape oil at dose of (50 mg /kg/bw) which included the sixth and seventh group consequently.

The outline treatise of kidney function values were revealed considerable effects. Blood urea values in combinations groups include ATRA2+CEO, and ATRA2+GSO affected significantly *$p<0.05$ and **$P<0.01$ in comparison with the ATRA1 and ATRA2 respectively, while other treated groups had no significant effects showed in Figure 1. In additions, the values of serum creatinine were significantly influences *$p<0.05$ and **$P<0.01$ among treated groups ATRA1 and ATRA2 with ATRA2+COE and ATRA2 + GSO respectively, as it is manifest in Figure 2. The last examinations involved serum uric acid values were showed an effect *$p<0.05$ between ATRA2 with all treated groups as obvious in Figure 3.

The rats' renal tissue sections were investigated for changes in all study groups. ATRA2 (high dose) showed more histologic alteration Figures 6 and 7, than ATRA1 (low dose) Figure 5, including the inflammatory cells infiltration, necrosis of renal tubules, blood vessels wall thickenings, blood vessel congestion, interstitial hyperplasia, haemorrhage, hydropic degeneration, fibroblast hyperplasia, glomerular congestions and glomerular necrosis. In ATRA1 and ATRA2 with curcumin oil Figures 8, 9 and 10 respectively, no frank changes appear in the renal sections in comparison with the spun clique of grape oil especially ATRA1 +GSO Figure 11 and 12 which is upkeep the section more than ATRA2+GSO Figure 13 and 14 for recovered nephrotoxicity nearly to the normal state Figure 1.

3. DISCUSSION

Tretinoin persuaded toxicities in lab animals and human was recognized when retinoid is given repeatedly. So, collectively known as hypervitaminosis was now standard therapy for acute myelocytic leukaemia (Tallman et al., 2000, Saadedin et al, 2004). All-Trans retinoic acid (ATRA) cased nephritic disorder, dysuria, sever renal failure, micturition frequency and renal tubular necrosis. Also, documented enlarged prostate (Thomas et al., 2000). The outcomes of the research obviously indicated the impact of ATRA1 and ATRA2 on rats' kidney functional test values which interpret the difference among the study groups' data. Furthermore, the disturbance of kidney's physiological test improved as seen in the significant reduction of renal function test values blood urea, serum creatinine and uric acid which elevated significantly *$p<0.05$ and **$P<0.01$ in comparison with the treated groups CEO and GSO in the present data by dependent two different doses of ATRA .

Studies in human have demonstrated a complex behavior of ATRA, concluded that its elimination was dependent and capacity-limited (Camacho, 2003). Recently, recorded that an ATRA inducible side effects are increased to nearly 10-fold above normal after 3 hours of ATRA administration in rats (Lampen, et al., 2001, Ozpolat et al., 2003). As well as retinoid performs a critical role in various physiological and disordered processes such as proliferation, differentiation, apoptosis and visibility (Gudas, 2012). The influence of various nephritic disorders is ATRA dose-dependent which boost the danger of prolonged

renal disease and secondary kidney complications (Xu et al., 2004). Indeed, researchers recorded similar outcomes of renal histopathological identifications which improved the present results of renal sections, including that higher dose of ATRA (30%), caused additional infarctions in renal textures; like glomerular congestion ,glomerular necrosis, macrophage cell, necrosis in interstitial space, vascular wall thickening and inflammatory cells infiltrations, as well as interstitial hyperplasia , cells infiltrations , haemorrhage and necrosis in renal tubules.

Meanwhile, some histological changes which were induced by low dose of ATRA (15%), caused blood vessels congestion, degeneration of convoluted tubules and inflammatory cells infiltrations.

In fact, retinoid receptors in the improvement of diverse renal destructions were not quite realized (Kavukcu et al., 2001). The researcher recorded that retinoid receptors induced nephrotoxicity and injury , also it developed many complications in its function (Miller et al., 2010, Zhou et al., 2012).

In recent years, the sizable emphasis has been focused on the greatness of the naturally accessible botanicals that can be employed in individuals with everyday diet because of their components' anti-oxidant and anti-inflammatory properties (Ugur et al., 2015).

Curcumin was the main turmeric component and in addition to its anti-inflammatory and anti-oxidant effects, it has chemo preventive properties (Ugur et al., 2015, Ramazan, et al., 2016). It also has different biological and pharmacological effects like anti-ischemic, anti-bacterial, anti-fungal and anti-carcinogenic effects. These effects are due to different methoxy substance in the chemical composition of this compound (Chiagoziem et al., 2014, Kumar et al., 2017).

Curcumin extracts oil is a curcumin formulation exhibit bioavailability (Antony et al., 2008). (Chiagoziem et al., 2014, Aggarwal et al., 2016), investigated that the CEO has no noxious consequences and it was used safely in the treated animals. Also, no significant influence was induced in the first 48 hours compared to the control group. As no considerable differences were seen in the CEO used animals, it was resolved that CEO doesn't have any mutagenic potential.

(Kizhakkedath, 2013, Parasuraman, 2011) Researchers also agreed with the present findings, as the sections of tow isolated compartment rats with high dose of ATRA and low dose of ATRA which were treated with CEO respectively showed blood vessels congestion, vaculation of convoluted tubules and necrosis. As well as, showed glomerular congestion, hydropic degeneration of convoluted tubules, fibroblast hyperplasia, reduced bowman spaces and inflammatory cells infiltrations. From these findings we conclude that more time was needed for curcumin to recover low dose of ATRA and high dose of ATRA tissue damage.

Present results indicated that's no real recovering change occurs in renal rats' sections affected by ATRA. That might be related to the short duration which is 28 days, for evaluated protective and therapeutics role to exert its actions and against ATRA toxicity. Further evaluations need to be done on the CEO in order to explore and impact their practical applications, which can be used in different doses and durations on varying animals' models.

Grapeseed oil has been investigated to possess many characteristics, including antioxidant, anti-inflammatory, anti-carcinogenic, platelet aggregations inhibiting and metal chelating properties (Al-Attar et al., 2015, Alawi, et al., 2018). So GSO has a high level of anti-oxidant vitamin E, which makes the oil very stable and cures lesions (Shi, and Pohorly , 2003, Stojiljkovic et al.,2008, Mohsen et al., 2019).

Nephrotoxicity is a dilemma property by functional alterations which are generated by difficulties of protein formations, glutathione deficiency, lipid peroxidation and mitochondrial impairment. Besides, oxidative destruction is speculated to be one of the principal mechanisms initiated in approximately all chronic renal diagnostic methods (Gutin et al., 2008, Shinagawa et al., 2015, Erisir et al .,2018 , Rasheed et al .,2018).

Further, the rat groups treated with GSO showed significant improvements in renal function test values of blood urea, creatinine and uric acid.

Moreover, treatment of rats with GSO for 28 days after intoxication with ATRA at both doses, serum kidney biochemical alteration were returned significantly $*p<0.05$ and $**P<0.01$ to normal levels with the improvement of renal tissue changes (Xia et al., 2010).

Finally, treated rats with GSO + high dose of ATRA showed slight changes in the renal tissues

when compared with GSO + low dose of ATRA which is against the nephrotoxicity and the tissues appeared nearly within normal. The protective effects of GSO are referred to its powerful antioxidant mixture for its content of polyphenol, flavonoids, saturated fatty acids and vitamin E which contains free radical scavenging properties (Garavaglia et al., 2016,Yousefaetal,2018). On top of that, vitamin E has a great role in anti-inflammatory, anti-carcinogenic, platelet aggregation inhibiting and metal chelating properties (Nagib, 2014) .

4. CONCLUSION

Grapeseed oil succeeded in reducing the nephrotoxicity induced by all-trans retinoic acid in rats.

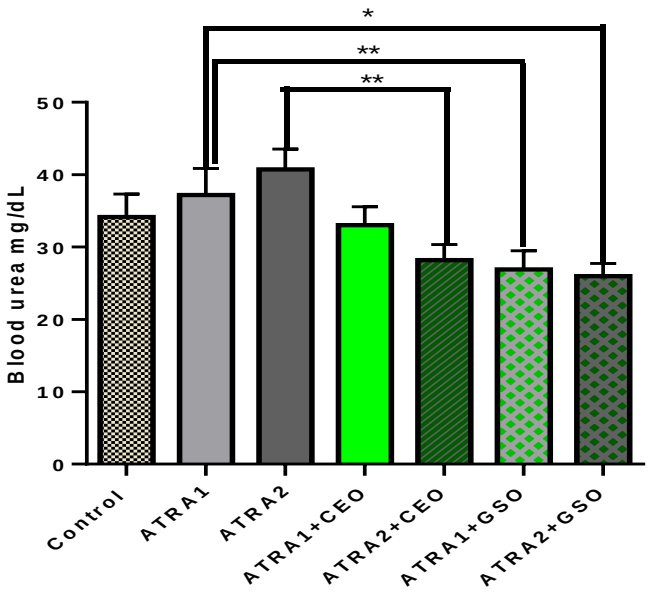

Figure1. Blood urea in the treated groups, n=7(values are Mean ± SE) mg/dl.

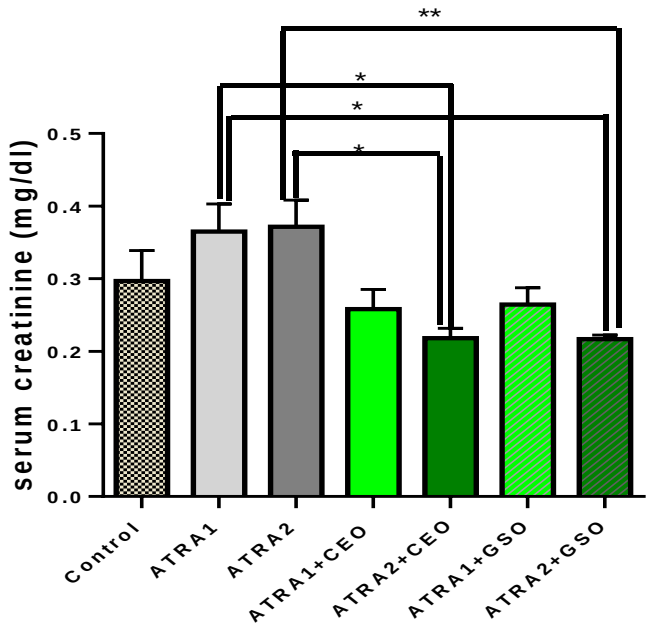

Figure 2. Serum creatinine in the treated groups, n=7 (values are Mean ± SE) mg/dl.

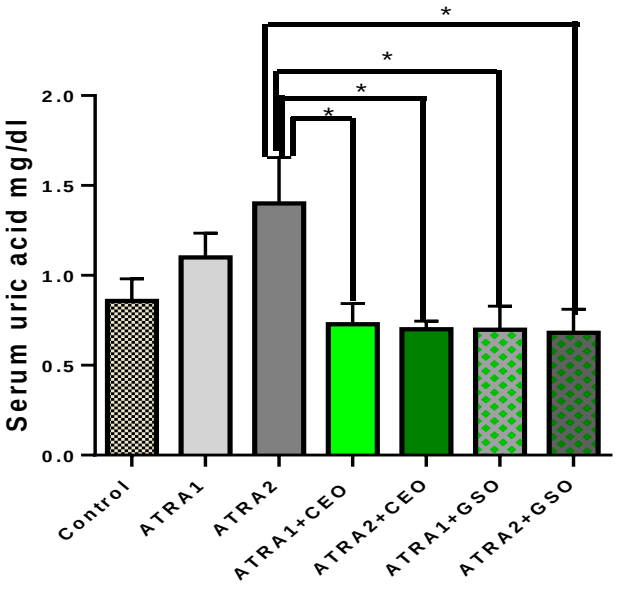

Figure 3. Serum uric acid in the treated groups, n=7 (values are Mean ± SE) mg/dl.

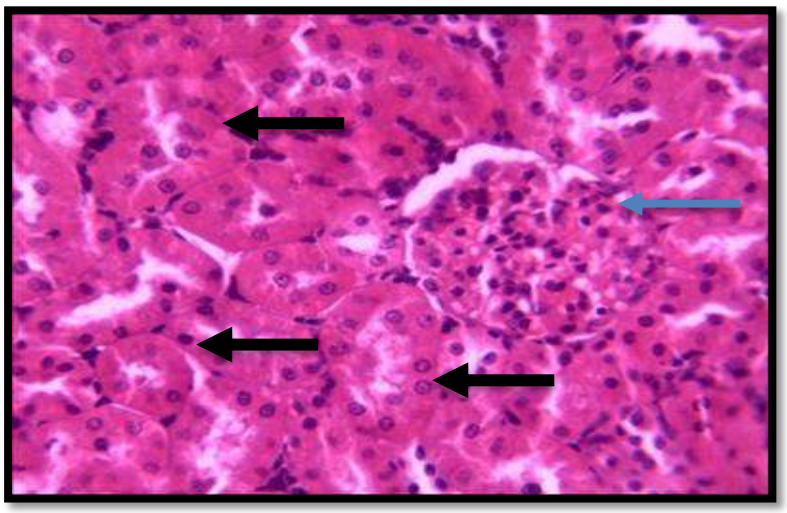

Figure 4. Kidney tissue section of normal rat treated with olive oil (2%) showed normal looking glomeruli (blue arrow) and tubules (black arrows) H&E 400 xs.

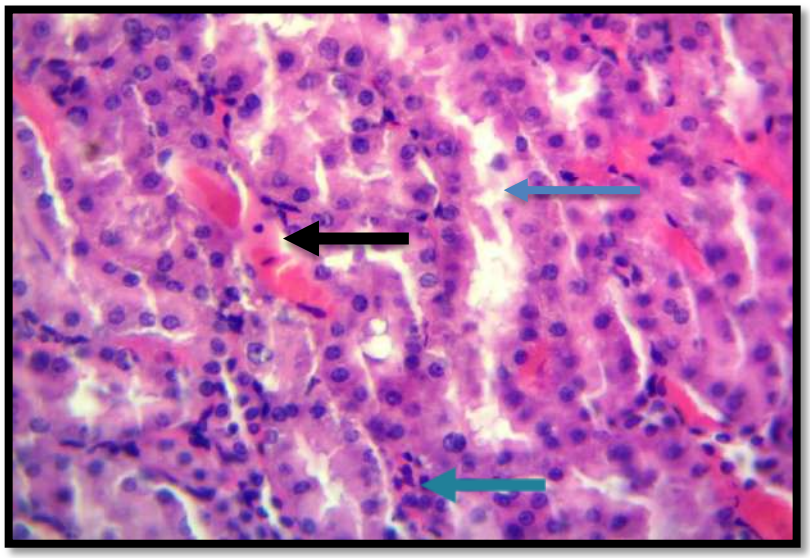

Figure5. Kidney tissue section administrated rats with ATRA (15%), showed blood vessels congestion (black arrow), degeneration of convoluted tubules (gray arrow), and inflammatory cells infiltrations (blue arrow), H&E 400x.

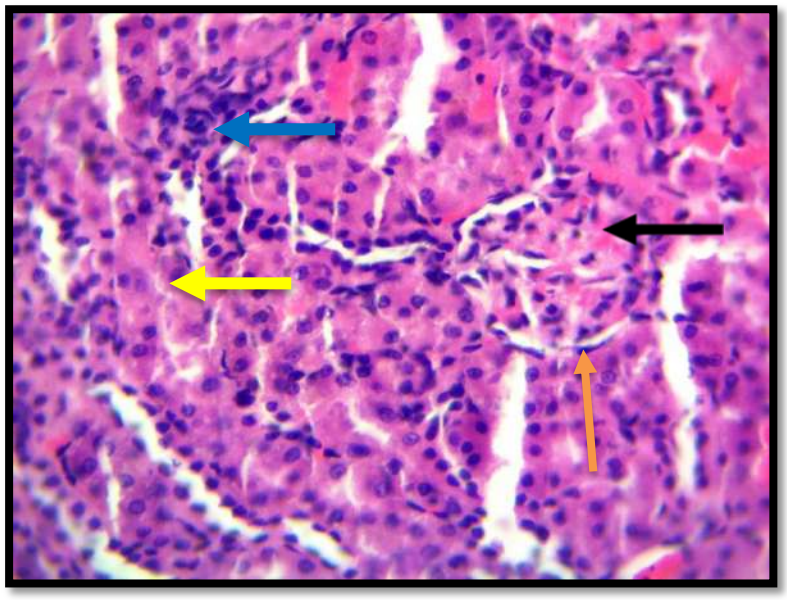

Figure 6.Kidney tissue section administrated rats with ATRA (30%), showed glomerular congestion (black arrow), hydropic degeneration of convoluted tubules (yellow arrow), fibroblast hyperplasia (orang arrow), and inflammatory cells infiltrations (blue arrow), H&E 400x.

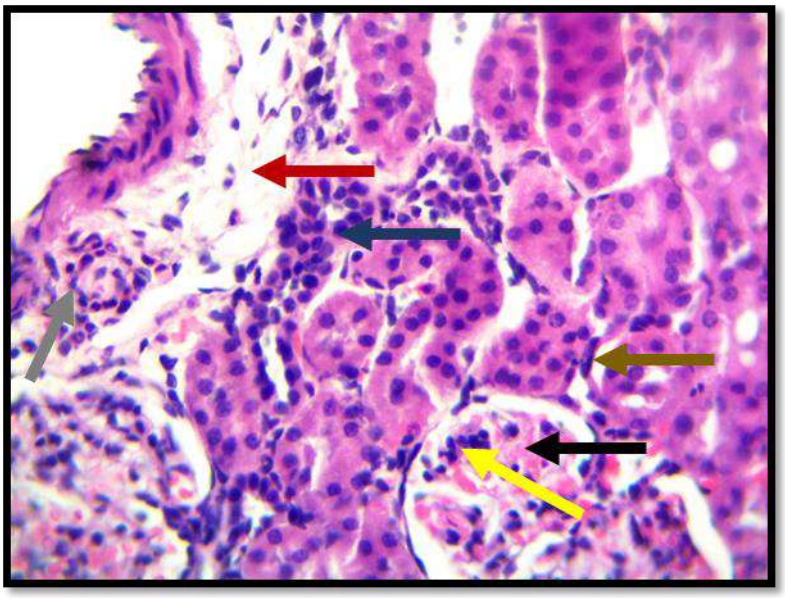

Figure 7. Kidney tissue section administrated rats with ATRA (30%), showed glomerular congestion (black arrow), and necrosis (yellow arrow), macrophage cell (brawn arrow), necrosis in interstitial space (red arrow), vascular wall thickening (gray arrow), and inflammatory cells infiltrations (blue arrow), H&E 400x.

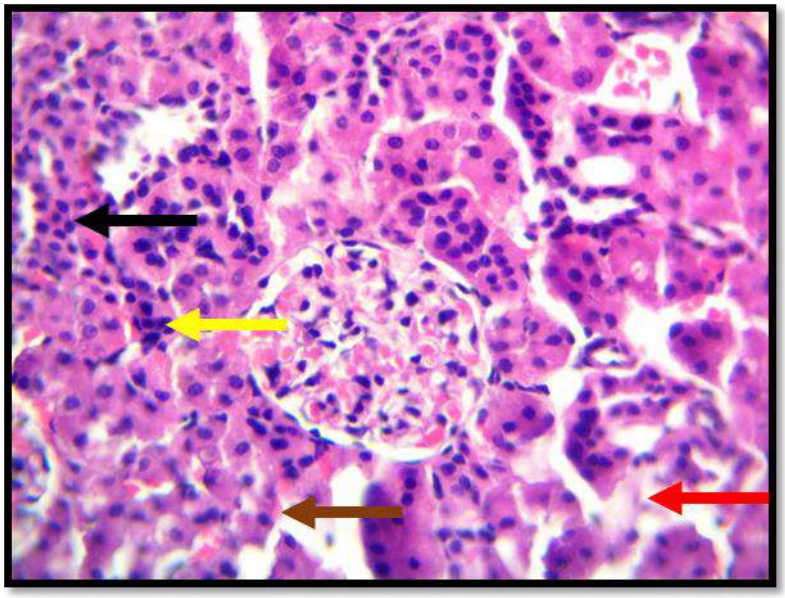

Figure 8.Kidney tissue section administrated rats with ATRA (15%) + CEO (50%), showed interstitial hyperplasia (black arrow), inflammatory cells infiltrations (yellow arrow), haemorrhage (brawn arrow), and necrosis in renal tubules (red arrow), H&E 400x.

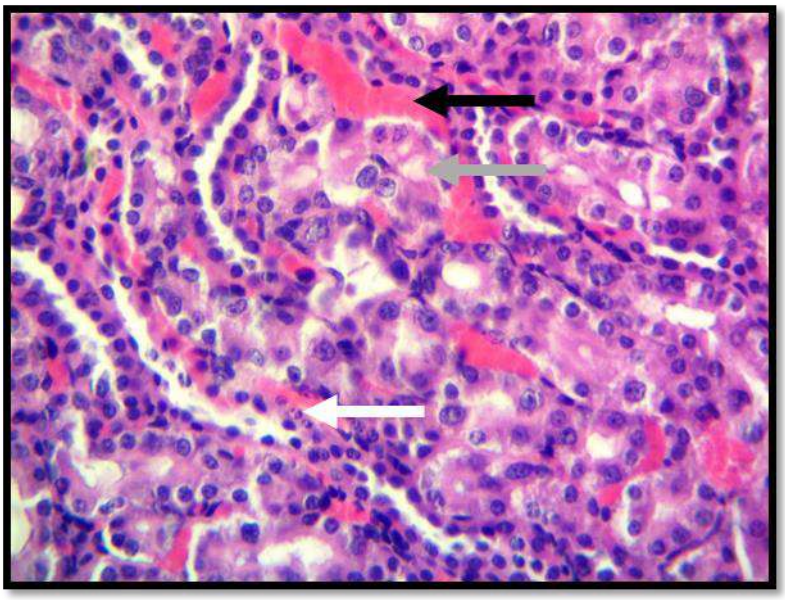

Figure 9. Kidney tissue section treated rats with ATRA (30%) + CEO (50%), showed blood vessels congestion (black arrow), vaculation of convoluted tubules (grey arrow), and necrosis (white arrow), H&E 400x.

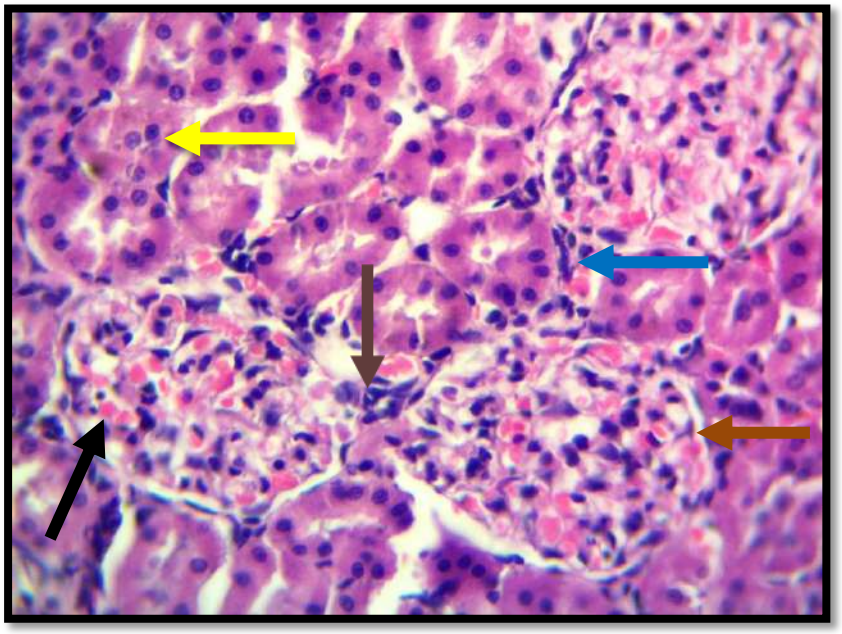

Figure 10. Kidney treated rats with ATRA (30 %) + CEO (50%), showed glomerular congestion (black arrow), hydropic degeneration of convoluted tubules (yellow arrow), fibroblast hyperplasia (brawn arrow), reduced bowman spaces (green arrow), and inflammatory cells infiltrations (blue arrow), H&E 400x.

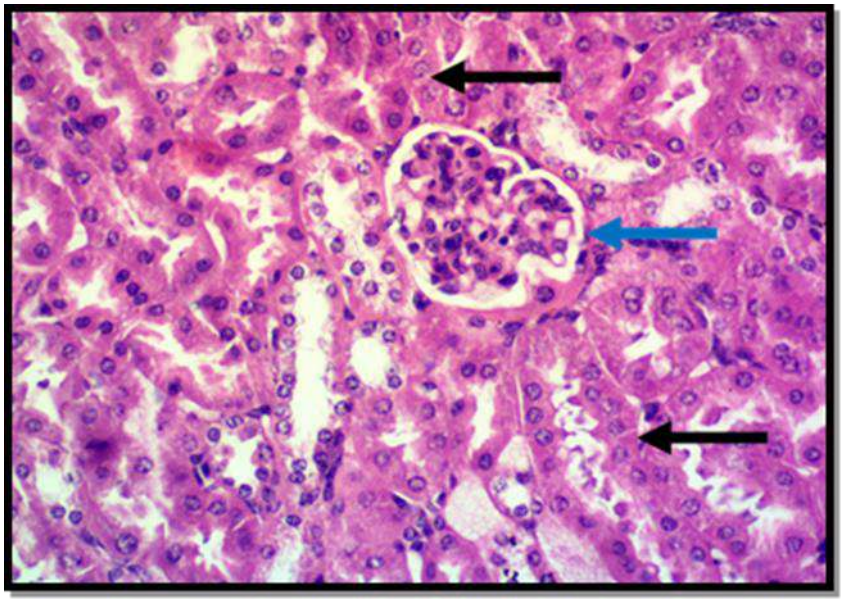

Figure 11. Kidney tissue section administrated rats with ATRA (30%) + GOE (50%), showed nearly appearance in comparison to the normal tissue, convoluted tubules (black arrow), glomerular (blue arrow), H&E 400x.

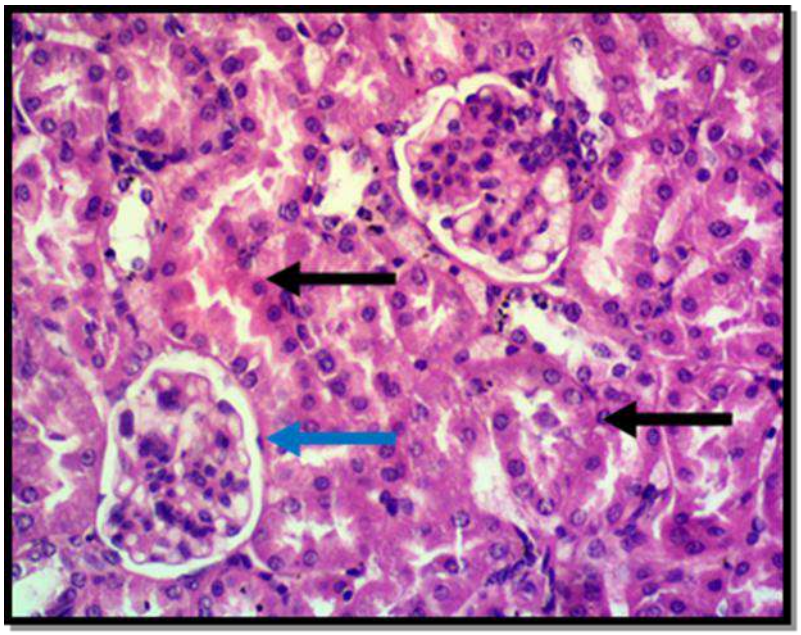

Figure 12. Kidney tissue section administrated rats with ATRA (30%) + GOE (50%), showed nearly appearance in comparison within normal tissue, convoluted tubules (black arrow), glomerulus (blue arrow), H&E 400x.

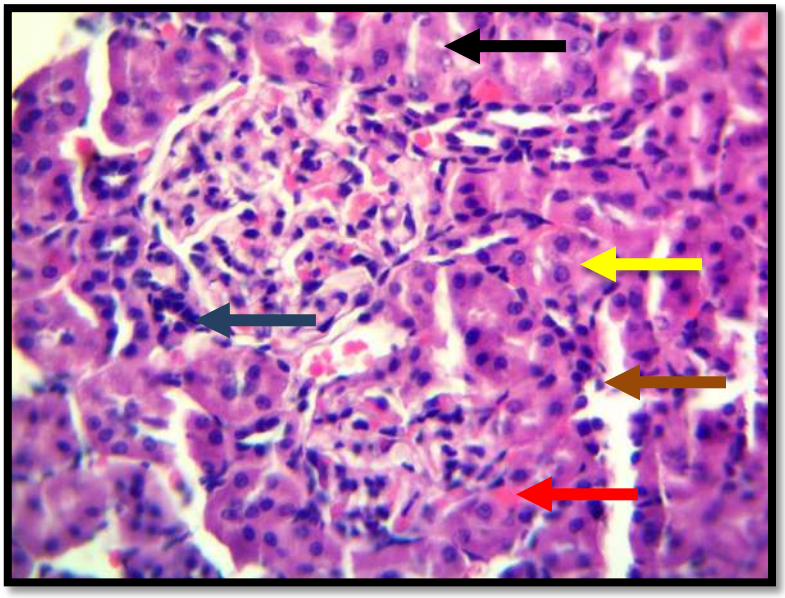

Figure 13. Kidney tissue section administrated rats with ATRA (15%) + GOE (50%), showed vaculation (black arrow), hydropic degeneration of convoluted tubules (yellow arrow), necrosis (green arrow), hemorrhage (red arrow), and inflammatory cells infiltrations (blue arrow), H&E 400x.

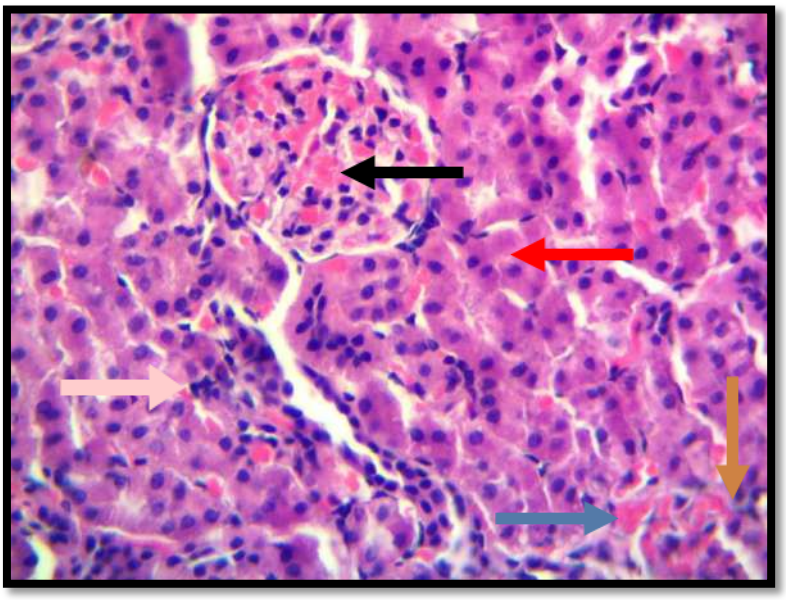

Figure 14. Kidney tissue section administrated rats with ATRA (15%) + GOE (50), showed glomerulus congestion (black arrow), hydropic degeneration of convoluted tubules (red arrow), interstitial hyperplasia (green arrow) hemorrhage (blue arrow) and inflammatory cells infiltrations (pink arrow) H&E 400x.

References

AGGARWAL, M. L., KARAMPENDETHU, M. C. & BINU, T. K.2016.Systematic and comprehensive investigation of the toxicity of curcuminoid-essential oil complex: A bioavailable turmeric formulation. *Molecular Medicine Reports.* 13: 592-604.

Al-ATTAR, A.M. 2015.Effect of grapeseed oil on diazinon-induced physiological and histopathological alterationsin rats.*Saudi Journal of Biological Sciences* ,22:284–292.

ALAWI, N.A., ELHag, G.A., RABAH,S.O. , Al-BAQAMI, N.M., FAHMY, N.S., Al-ATTAR, A.M. & ABUZEID, I.M.2018. The protective effect of grape (*Vitis vinifera*) seed oil ontesticular structure of male rats exposed to lead.*Advances in Biological Research* ,12 (1): 16-25.

ANTONY, B., MERINA, B., IYER, V.S., JUDY, N., LENNERTZ, K. & JOYAL, S.2008. A pilot cross-over study to evaluate human oral bioavailability of BCM-95CG (Biocurcumax), a novel bioenhanced preparation of Curcumin. *Indian Journal Pharmcology Science* 70: 445-449.

CAMACHO, L.H. 2003. Clinical applications of retinoids in cancer medicine.*Journal of Biology Regultion Homeostatic Agents*, 17(1):98-114.

CHENG, Z. J., VAPAATALO, H. and MERVAALA, E. (2005) Angiotensin Ii and Vascular Inflammation. *Med Sci Monit.* 11. p.194-205.

CHIAGOZIEM, A.O., SUNNY, O. A., VICTORIA. I.O., AZEEZAT, L. A. & OLUWAFEMI, E. K. 2014.Protective Effect of Curcumin against the liver toxicity causedby propanil in rats.*International Scholarly Research Notices*, 1-8.

CRAVIDE, P. & REMUZZI, G. 2013.Pathophysiology of proteinuria and its value as an outcome measure in chronic kidney disease. *British Journal of Clinical Pharmacology*. 76(4):516-23.

DAI, Y. ,ANQUN, C.,RUIJIE, L., LEYI, G.,SHUCHITAE, S.,WEIJING, C., FADI, S.,DAVID, J. S., JEFFREY,W. P.,STUART, J. S.,MARCUS, J. M.,NORBERT, B. G.,XIAOQIANG, D.,PETER Y., CHUANG, K. L.&JOHAN, C.H. 2017. Retinoic acid improves nephrotoxic serum–induced glomerulonephritis through activation of podocyte retinoic acid receptor α.92, *Kidney International*,(6): 1444-1457.

El-ASHMAWY, I.M.,SALEH, A. &SALMA, O.M. 2007. Effects of marjoram volatile oil and grape seed extract on ethanol toxicity in male rats. *Basic Clinical Pharmacology Toxicology*, 101(5):320-327.

Elsayed, A. M. ,TAMER, M.A. ,EL-SAYED,A. ABDEL-AZIZ ,H.AA.& MOHAMED, S. AB. 2016. All-trans retinoic acid potentiates cisplatin-induced kidney injury in rats: impact of retinoic acid signaling pathway. *Naunyn-Schmiedebergs Arch Pharmacol*, 389(3):327-337.

ERISIR, Z., ULKU, G. S., MEHTAP, O., YASIN, B, SEDA, I. M.& MEHMET, C. 2018. Effects of

dietary grape seed on performance and some metabolicassessments in Japanese quail with different plumage colors exposed toheat stress.*Revista Brasileriera de Zootecnia*,ISSN 1806-9290,47

FREITAS, D. S., JACQUES, R.A., RICHTER, M.F., SILVA, A.L. & CARAMAO ,E.B. 2008. Pressurized liquid extraction of vitamin E from Braziliangrape seed oil. *JournalChromatography*, 1200(1): 80-83.

GARAVAGLIA, J. , MARKOSKI,M. , OLIVEIRA, A. ,, MARCADENTI,A. 2016.Grape seed oil compounds: biological and chemical actions for health.*Nutrtion Metabolism Insights*. 16(9):59-64.

GETIN,A., KAYNAR,L., KOCYIGIT, I., HACIOGLU ,S.K., SARAYMEN ,R., ORTUURK ,A., ORHAN, O.and SAGDIG, O. 2008.The effect of grape seed extract on radiation-induced oxidative stress in the rat liver. *Turkish Journalof Gastroenterology*. 19(2): 92-98.

GUDAS, L.J. 2012. Emerging roles for retinoids in regeneration and differentiation in normal and disease states. *iochemica et Biophysia Acta*. 1821(1):213-321.

HASSAN, D. H.&FALAH. M.A.2017. Histological and ultrastructural study on the effect of celery juice on ethylene glycol induced urolithiasis in male albino rats . *Journal of Pure and Applied Sciences,* 29 (s4) :s1-s12.

JULIANO, G., MELISSA M. M., ALINE, O. & ALINE M.2016. Grape Seed Oil Compounds: Biological and Chemical Actions for Health.*Nutrition and Metabolic Insights*:9(59): 59–64.

KAVUKCU, S., TURKMEN, M.A.& SOYLU, A. 2001. Could the effective mechanismsof retinoids on nephrogenesis be also operative on the ameliorationof injury in acquired renal lesion*Pediatric Nephrology*, 16:689-690.

KIZHAKKEDATH, R. 2013. Clinical evaluation of a formulation containing *Curcuma longa* and *Boswellia serrata* extracts in the management of knee osteoarthritis. *Molecular Medicine Reports* 8: 1542-1548.

KUCCMAR, P., BARUA,C., SULAKHIYA,K., SHARMA,R. 2017. Curcumin Ameliorates Cisplatin-Induced Nephrotoxicity and Potentiates Its Anticancer Activity in SD Rats: Potential Role of Curcumin in Breast Cancer Chemotherapy. *Frontiers in Pharmacology*, 8(132): 8373-8383.

LAMPEN, A., MEYER, S. & NAU, H. . 2001.Effects of receptor-selective retinoids on cyp26 gene expression and metabolism of all-trans-retinoic acid in intestinal cells. *Drug Metabolism and Disposition*, 29(5):742-7.

MAHESHWARI, R.K., SINGH, A.K., GADDIPATI, J. & SRIMAL, R.C. 2006. Multiple biological effects of curcumin: A short review.*Journal of Life Science*, 78: 2081-2087.

MILLER, R.P., TADAGAVADI, R.K., RAMESH, G.& REEVES, W.B. 2010.Mechanisms of cisplatin nephrotoxicity. *Toxins*. 2(11):2490-2518.

MOHSEN,E.M., , NADA, M. E. , AMEER, A.S., AZZA, S. A., EMAN, A. A., ESRAA, A.A., MOHAMED, A. E., OMNIA, N.B., SHIMAA, R. A., AHMED, A.M., AHMED, M. S., ESRAA, A.E., MOHAMED, A.E., El BADR, E. B. & NERMEEN, B. E.2019. Protective effects of vitamin E and grape seed oil against acute hepatorenal ivermectin toxicity in mice: biochemical and histopathological studies. *GSC Biological and Pharmaceutical Sciences*, 7(02): 087–094.

MURICE-LAMBERT, E.,BANFORD, A. and. Folger, R. (1989). Histological preparation of implanted biomaterials for light microscopic evaluation of the implant-tissue interaction. *Biotechnology Histochemestry*, 64(1):19-24.

NAGIB, R. M. 2014. Inhibitory effects of grape seeds powder, extract and oil on Gentamicin Induced nephrotoxicity in rats.*Egypt Journal of Nutrition and Health*, 9 (1): 1-20.

NASRI, H., NAJMEH, S., MORTAZA, R., SAMERA, R., MARYAM, S. & MAHMOUD, Rk. 2014. Turmeric: A Spice with Multifunctional Medicinal Properties. *Journal of Herbal Medicine Pharmacology*. 3(1): 5-8.

NONOSE, N., JOSE, A. P., PAULO, R. M., MURILO, R.R., DANIELA, T. S., CARLOS, A.R.*2014*. Oral administration of curcumin (Curcuma longa) can attenuate the neutrophil inflammatory response in zymosan-induced arthritis in rats. *Acta Cirurgica Brasileira*,29(11):727-734.

OZPOLAT, B., LOPEZ, B.G., ADMSON, P., FU, C.J.& WILLIAMS, A.H. 2003. Pharmacokinetics of ntravenouslyadministered liposomal all-transretinoicacid (ATRA) and orally administered ATRA in healthy volunteers.*Journal Pharm Pharmacology Scinice*, 6(2):292-301

PARASURAMAN, S.2011. Toxicological screening. *Journalof Pharmacology Pharmacother* 2: 74-79, 2011.

RAMAZAN, U., OZGUR, A., AYHAN, D., NEVZAT, G., MEHMET, T., HASAN, G., IREM, P., IBRAHIM, H., NECIP, I.& KAZIM, S.2016. Effects of curcumin on anion/cation transporters and multidrug response proteins in cisplatin induced nephrotoxicity. *International Journal Clinical Exp erment Medicine*,9(10):19623-19633.

RASHEED, N.Sh., HASSAN,D. H.&FALAH,M. A.2018. Hepatotoxicity and nephrotoxicity of lead nitrate in toad bufo viridis. *Journal of Pure and Applied Sciences,* 30 (6) :37-45.

SAADEDDIN, A. ,FRANCISCA, T. M., JAIME, C.T., AMPARO, A. & JOSE, E. P.

2004.Pharmacokinetics of the time-dependent elimination of all-trans-retinoic acid in rats.*American Association of Pharmaceutical Scientists*, 6(1): 1–9.

SHI, J., YU,K. and POHORLY, J.Y. 2003. Polyphenolics in grape seeds-biochemistry and functionality. *Journal of Medicinal Foods.*, 6(4):291-299.

SHINAGAWA, F. B., FERNANDA, C. D., LUCILLIA, R. O. & JORGE, M. F. 2015. Grape seed oil: a potential functional food.*Food Science and Technology*,35(3), 399-406.

SHIVANAND, N.B., DAN, R., D. MARSHALL, G.R.,ISITOR, G. XUE, S. & SHI, J. 2011. Wound-healing properties of the oils of vitis viniferaand vaccinium macrocarpon. *PhytotherapyResearch*, 25(8): 1201-1208.

STOJILJKOVIC, N, D., MIHAILOVIC, S., VELJKOVIC, M., STOILJKOVI, C. and JOVANOVIC,I. 2008. Glomerular basement membrane alterations induced by gentamicin administration in rats. *Expremnt of Toxicology and Patholology*. 60:69-75.

SUKANDAR, E.Y. , PERMAN, H. A, ADNYANA, I.K. SIGIT, J.I. , ILYAS,HASIMUN, R.A.&MARDIYAH, D. 2010.Clinical study of turmeric (*Curcuma longa* L.) and garlic (*Allium sativum* L.) extracts as antihyperglycemic and antihyperlipidemic agent in type-2 Diabetes-Dyslipidemia. Patient. .*International journal of farmacolog*, 6 (4): 456-463.

TALLMAN, M.S., ANDERSEN, J.W., SCHIFFER, CA, APPELBAUM, F.R., FEUSNER,J.H., OGDEN, A., SHEPHERD,L., ROWE,J.M., FRANCOIS, C., LARSON,R.S. & WIERNIK, P.H. 2000. Clinical description of 44 patients with acutepromyelocytic leukemia who developed retinoic acid syndrome. *Blood*.2000; 95(1): 90-95.

THOMAS L. W., JEFFREY L. L., SCOTT, A. B., CHRIS, W. W. & PAUL, A. C. 2000.The nonclinical safety evaluation of the anticancer drug atragen (liposomal all-trans-retinoic acid). *International Journal of Toxicology*, 19:33–42.

Ugur S, Ulu R, Dogukan A, Gurel A, Yigit IP, Gozel N, Aygen B, Ilhan N.2015.The renoprotective effect of curcumin in cisplatin-induced nephrotoxicity.*Renal Failair*. 37(2):332-406.

WAGNER, U. , CLAUDIUS D., CHRISTIAN, M., INGO, L., KERSTIN, A., RUDIGER W., JURGEN, F. & EBERHARD, R. 2000.Retinoic Acid Reduces Glomerular Injury in a Rat Model of Glomerular Damage. *Juornal of The American Society Nephrology August*, 11 (8): 1479-1487.

XIA, E.Q., DENG, G.F., GUO, Y.J.& LI, H.B. 2010.Biological activities of polyphenols from grapes. *International Journal of Molecular Scinice*.;11(2):622–646.

XU, Q., LUCIO,C. J., KITAMURA,M., RUAN, X., FINE, L.G.& NORMAN, T. 2004.Retinoids in nephrology: promises and pitfalls. *Kidney Internationaljournal*, 66(6):2119-2131.

YOUSEFA, M. I., Dina K.A.& HEBA, M. A.2018.Neuro- and nephroprotective effect of grape seed proanthocyanidin extractagainst carboplatin and thalidomide through modulation of inflammation,tumor suppressor protein p53, neurotransmitters, oxidative stress and histology*Toxicology Reports*,5 : 568–578.

ZHOU, T.B., DRUMMEN, G.P., QIN,Y.H. 2012. The controversial role of retinoicacid in fibrotic diseases: analysis of involved signaling pathways. *International Journal of Molecular Scinice*, 14(1):226-243.

ZHOU,T.B. , WEI,F.W., YUAN,H.Q. & SHENG,S.Y.,2013.Assosiation of all trans retinoic acid treatment with therenin angiotensin aldosteron systemexpression in glomerulosclerosis rats. *Journal of The Renin-Angiotensin-Aldosteron System.*14(4):299-307.

ZANCO Journal of Pure and Applied Sciences
The official scientific journal of Salahaddin University-Erbil
https://zancojournals.su.edu.krd/index.php/JPAS

ISSN (print):2218-0230**, ISSN (online):** 2412-3986**, DOI: http://dx.doi.org/10.21271/zjpas**

RESEARCH PAPER

Determination of Some Heavy Metals in Environment of Bakery and Samoon Furnaces at Erbil City, Kurdistan Region, Iraq

Hawraz Sami Khalid*, Aveen Faidhalla Jalal, Khaled Wale Khdr, Maylan Omar Ahmad

Department of Chemistry, College of Education, Salahaddin University-Erbil, Kurdistan Region, Iraq.

A B S T R A C T:

This study was investigated for the assessment of dust contamination with some heavy metals in Naans bakery and Samoon furnace environment and to indicate their potential sources of origin. Fifteen locally Naans bakery and Samoons furnace places were chosen for sampling of accumulated residue dust and heating fuel in Erbil city, Kurdistan Region, Iraq. Naan bakeries used liquefied gas (NGB) for heating while Samoon furnaces used liquefied kerosene (OSF) or liquefied gas (GSF) as heating source. The wet acid digestion method was applied for the sample treatment using a mixture of concentrated perchloric acid ($HClO_4$ 70%), hydrochloric acid (HCl 37%), and nitric acid (HNO_3 65%) with a volume ratio (1:1:2). The analyses were carried out using flame atomic absorption spectrometer to determine some selected heavy metals (Cu, Cr, Cd, and Ni). The results showed that the recorded percentage for observed metals (OM) from the entire of the investigated dust samples (n=15) were different and individually equal to 20%, 60%, 93.3%, and 100% for each of Cd, Cr, Ni, and Cu respectively. The level of metals content in most of dust samples exceeded standard permissible limits for metals in dust environment. The recorded level for total selected metal load (TSML) in dust samples of NGB environment (392.23 $\mu g \cdot g^{-1}$) was approximately twice times more than each of the OSF (207.45 $\mu g \cdot g^{-1}$) and GSF (211.31 $\mu g \cdot g^{-1}$) environment. Results data showed that the environment of most bakery Naan and Samoon furnace was unsafe for baking and contaminated with these heavy metals.

KEY WORDS: Heavy Metals; Dust; Samoon Furnace; Naan Bakery; FAAS; Erbil City
DOI: http://dx.doi.org/10.21271/ZJPAS.32.3.18
ZJPAS (2020) , 32(3);176-186 .

1. INTRODUCTION

Heavy metals are among noteworthy pollutants in municipal environment, and getting to be an intensive public health problem due to their extreme toxicity and carcinogenicity (Wei and Yang, 2010). Humans are exposed to the threat of metals throughout numerous pathways because these metals are widely distributed in the environment and originated from both human activities and natural sources (Abd-Alhameed, 2019, Darwesh, 2019).

There are several distribution sources of heavy metals in the environment including natural weather conditions of the earth's crust, soil erosion, industrial effluents, sewage discharge, mining, urban runoff, applying control agents on crops disease or insects, heating sources and many others. The wide distribution of heavy metals in the human environment can also be referred from extensively chemical applications in industries, agriculture, medicine, homes, and more others (Morais et al., 2012, Yang and Massey, 2019, Abd-Alhameed, 2019, Darwesh, 2019)

Most heavy metals have confirmed to be a toxic and major health risk linked with them because they tend to be bioaccumulated inside organ

* **Corresponding Author:**
Hawraz Sami Khalid
E-mail: hawraz.khalid@su.edu.krd
Article History:
Received: 07/03/2020
Accepted: 19/05/2020
Published: 15/06 /2020

tissues (Al-Attar, 2016, Bazzaz and Muhammad, 2018). They sometimes act as interfere with the human metabolic processes and are harmful to their body. The absorbed dose, exposure duration and the way of exposure of metals by the human body are the main factors to be metal toxicity. Human inhalation, ingestion, and dermal absorption are known as main exposure routes for heavy metals contact (Jaishankar et al., 2014). Some metals are harmful, get accumulated in the body and have several health risks. Metals toxicity can cause a variety of disorders and damage human organs throughout oxidative stress produced by free radical formation. Some chronic problems linked with long-term heavy metal exposures are metal lapse caused by lead exposure. Besides, cadmium has effects on the liver, kidney and gastrointestinal tract (Lu et al., 2010). The implications of metals toxicity consequences on children's health have been distinguished to be more severe compared to adults. The consequence risks of these elements' toxicity on children's health include behavioral disorders, neurocognitive disorders, mental retardation, respiratory problems, cardiovascular and cancer diseases (Jaishankar et al., 2014, Yang and Massey, 2019).

One of the imperative pathways of insinuation to heavy metal for humans is through suspended or residue dust in the environment. Dust is generally defined as a solid matter composed of soil, natural biogenic and anthropogenic metallic constituent materials (Ferreira-Baptista and De Miguel, 2005). Assessment of Cd, Cu, Cr, Pb, Ni, and Zn heavy metals' level and distribution in dust samples around our environment such as indoors, outdoors, streets, schools, markets, agricultural fields, and working places have recently received much attention. Thus, researchers have extensively concerned this issue through analysis of various environmental samples to assess their characteristics and health risk assessment exposure to the human (Abd-Alhameed, 2019, Amin et al., 2017, Cheng et al., 2018, Darwesh, 2019, Jin et al., 2019, Khudhur et al., 2016, Zgłobicki et al., 2018, Zhou et al., 2019).

Crude oils are generally defined as a complex mixture of inorganic and organic matter. Presenting heavy metals in crude oils can be categorized as inorganic compounds (Sainbayar et al., 2011). The presence of trace metals level can be used to classify the quality of crude oils in terms of residual, light, medium, and heavy fraction (Barbooti et al., 1986). The refining treatment of heavy crude oil is a constable in comparison to light crude oil due to the high content of metals content (Reynolds, 2003). Investigation of heavy metals content in crude oils, products and their environment has been widely conducted by researchers. The uses of inappropriate crude oil as heating sources can be selected as polluted sources with heavy metals ongoing to spreading and pre-concentration of their residue dust in the environment (Barbooti, 2015, Jadoon et al., 2016, Roldan et al., 2004, Darwesh, 2019).

Refractory bricks which are the most important type of bricks, also called fire brick or firebrick (FB) can withstand to the elevated temperature (Edwards, 2019). Firebricks play an important role as materials of heat/energy storage and resistance which have also been used with kerosene fuel in the waste heat recovery by bakers in Erbil city. Many recent studies verified that brick kilns and manufactures are commonly known as one of the most main sources of soil, air, and water pollutants with heavy metals (Issa et al., 2019, Proshad et al., 2017, Sikder et al., 2016)

According to many studies investigation, main anthropogenic sources including industrial, traffic and domestic emission, atmospheric deposited, weathering of pavement, and more others are the main pollution sources of heavy metals for municipal dusts in the environment (Abd-Alhameed, 2019, Amin et al., 2017, Darwesh, 2019, Khudhur et al., 2016, Sezgin et al., 2004). According to Fabis (1987), world permissible limits for some heavy metals such as Hg, Cd, Cu, Ni, Co, Pb, Cr and Zn in soil and dust samples are 2, 3, 50, 50, 50, 100, 100 and 300 $\mu g \cdot g^{-1}$ respectively. It is known that, based on income, availability and waste heat recovery, firebricks and low quality kerosene fuel have been randomly used as a heating source by some bakers and furnaces owner in Erbil city, Kurdistan Region, Iraq. Considering the above and based on human health safety, the main objective of this study is to determine some heavy metals in the Naan bakery and Samoon furnace environment for the first time. Besides, the content of the selected metals in the used heating sources is investigated to know sources of pollutants.

2. MATERIALS AND METHODS

2.1. Chemicals

All the used chemicals were of analytical grades including nitric acid (HNO_3 65%), hydrochloric acid (HCl 37%), and perchloric acid ($HClO_4$ 70%). According to AAS manufacturer guideline (Whiteside and Milner, 1984) chromium nitrate [$Cr(NO_3)_3.9H_2O$] and nickel nitrate [$Ni(NO_3)_2.6H_2O$] were used and dissolved in distilled water throughout the experiments for the preparation of 1000 mg/kg of Cr and Ni stock solutions respectively. Chemicals such as CdO (dissolved in 5M diluted HCl) and Cu metal (dissolved in 5M HNO_3) were also used to prepare 1000 mg/kg of Cd and Cu stock solutions respectively. Then, serious working solutions for the selected of the metals ion were individually prepared from the stock solutions using distilled water.

2.2. Instruments

Sensitive Balance (KERN & Sohn GmbH), Box Furnace (Gallenkamp Size 1), Classic Digestion-Heater (Gerhardt) and digestion Kjeldal's flask were used for weighting and the sample digestion process. Flame atomic absorption spectrometer (FAAS) (Pye-Unicam SP9 model flame AAS, Cambridge, CB, UK) accoutered with a hollow cathode lamp as the light source and acetylene-air flame burner was used to determine selected metal ions in whole sample solutions. The instrumental parameters and optimum conditions were those suggested by the manufacturer guideline (Whiteside and Milner, 1984). The wavelengths (nm) selected for the determination of the metals ion were as follows: Cd, 228.8 nm; Cr, 357.9 nm; Cu, 324.8 nm; and Ni, 232.0 nm. Acetylene (C_2H_2) flow rate was 0.8-1.4 $mL{\cdot}min^{-1}$ and air flow rate was 18-28 $mL{\cdot}min^{-1}$. The nebulizer uptake rate was 6 $mL{\cdot}min^{-1}$. The hallow cathode lamp currents were 5, 8, 12, and 15 mA for Cu, Cd, Cr, and Ni respectively.

2.3. Study Area and Sample Collection

During sample collection, fifteen locally Naan bakery, and Samoon furnace environments were selected from different places in Erbil city, Kurdistan Region, Iraq (**Figure 1**) during January 2018. Naan bakeries used liquefied gas (NGB) with assisting firebricks for heating but Samoon furnaces used liquefied kerosene (OSF) or liquefied gas (GSF) as heating source. In the five (NGB1-5) places, dust residues and firebricks (FB) were collected as a sample. Dust residues and kerosene fuel sample in the six (OSF1-6) places were collected, while only dust residue sample was collected inside the four (GSF1-4) places. Three different samples of commercial kerosene from filling stations as reference kerosene (RK) and two samples of unused firebricks as reference firebrick (RFB) were collected and used to compare with other samples. During the period of sampling, thirteen of the bakers and Samoon furnaces owner did not allow sampling (NA1-13). Dusts residue sample was collected by using a clean brush, placed in clean plastic bags, labeled and kept from the laboratory till the analysis day.

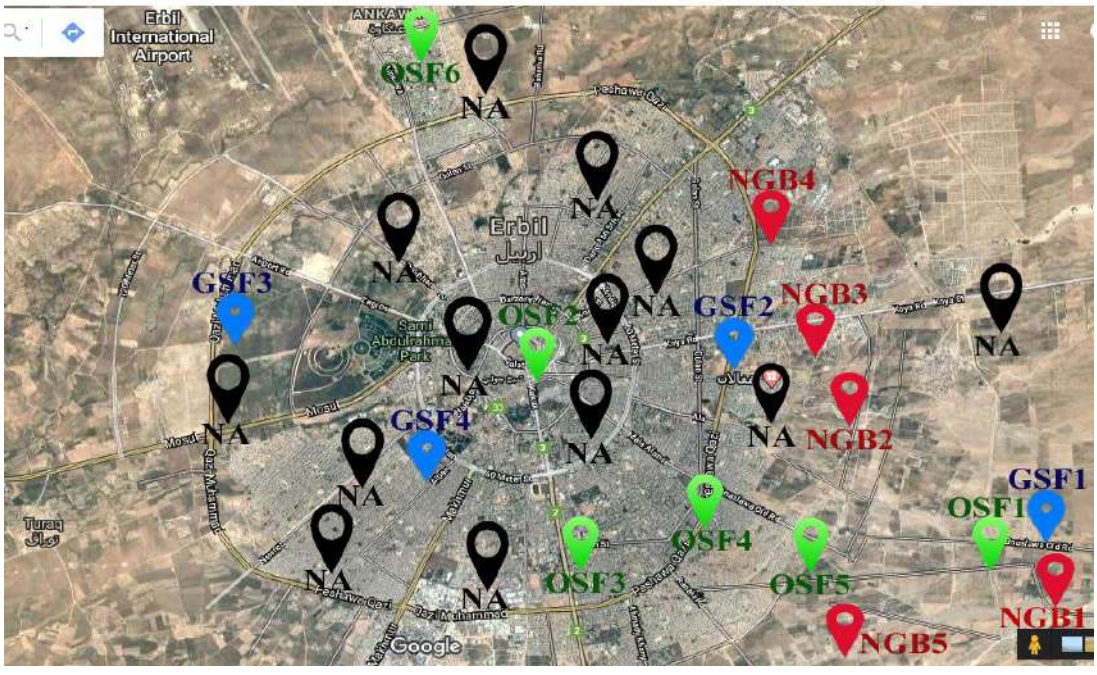

Figure 1: Study area and sampling location inside Erbil city center, NGB1-5; five Naan bakeries used liquefied gas, GSF1-4; four Samoon furnaces used liquefied gas, OSF1-6: Six Samoon furnaces used liquefied kerosene and NA1-13: thirteen places not allow sampling.

2.4. Sample Preparation and Digestion

Prior to analysis, a strong wet digestion method was applied to the residue dust and firebricks (FB) samples (Latif et al., 2014, Srithawirat and Latif, 2015). During sample digestion, 1.0 g of residue dust sample was treated and heated with 20 ml of a mixture of perchloric acid ($HClO_4$ 70%), hydrochloric acid (HCl 37%), and nitric acid (HNO_3 65%) with a volume ratio (1:1:2) to digest the sample completely. The digestion process was conducted in digestive Kjeldal's flask by using classic digestion-heater. Next, the solution was allowed to cool, filtrated, transferred and diluted with distilled water to 50 mL volumetric flask. The above steps were also applied to digest the collected FB samples.

For the kerosene digestion, combined suggested methods were applied with few modifications (Tekie et al., 2015). 10 mL of kerosene sample was added to the crucible and covered with a cap. Then, the sample was heated at 350℃ for about one hour using Box Furnace. Next, the temperature was increased until 450℃ for an extra one hour to destroy most of the organic material. After that, remained residue was quantitatively transferred to digestive Kjeldal's flask. Subsequently, 20 ml of the same acid mixture was used to complete digestion. Finally, the solution was transferred and diluted with distilled water to 50 ml volumetric flask. The above steps were repeated for blank and each type of the collected samples. Blank solution which contains only the digested acids or the reagents used to dissolve or digest the analyzed samples were individually prepared and repeated three times for each of the samples. Blank solution is mainly used for calibration purposes or zeroed the absorbance of all the other presented components in the sample solution except the component of interest.

2.5. Metal Analysis

During sample analysis, flame atomic absorption spectrometer (FAAS) was used to determine the level of chromium (Cr), cadmium (Cd), copper (Cu), and nickel (Ni) heavy metals in all the digestive samples. Optimum operating instrumental conditions were conducted based on the instruments guideline (Whiteside and Milner, 1984). Finally, the estimated level of each metal in each sample was calculated and presented as parts per million ($\mu g \cdot g^{-1}$ for solid samples) and ($\mu g \cdot mL^{-1}$ for liquid samples).

2.6. Country permissible limit for heavy metals in dust/soil

In the last decades, maximum permissible level for heavy metals in dust and soil environment have been regulated and announced by many countries based on many researches and the safety of human's health. List of the declared maximum permissible limits for metals content which are shown in **Table 1** were used to assess the recorded level of heavy metals in investigated samples.

2.7. Statistical analysis

The results of the study were subjected to statistical significance using both Microsoft Excel 2010 and GraphPad Prism 6 program software. One-sample t test was employed to assess comparison of levels mean of heavy metals to the maximum permissible limits. One-way ANOVA analysis was performed to examine the difference of heavy metal levels between studied samples. Significance level was set to 0.05. Results are shown in various tabulated form in tables and figures. This research was performed on fifteen collected samples from vary Naan bakeries and Samoon furnaces environment.

3. RESULTS AND DISCUSSIONS

All results data for the level of selected heavy metals including Cr, Cd, Cu, and Ni in the fifteen locally Naans bakery and Samoons furnace samples are presented in Figures 2, 3, and 4 in detail. According to results, the recorded percentage for observed metal (OM) from the entire of the investigated dust samples (n=15) were different and individually equal to 20%, 60%, 93.3%, and 100% for each of Cd, Cr, Ni, and Cu respectively. Thus, the percentage of OM value for Cu metal was the highest (100%) because copper metal was presented and detected in a whole ($\frac{15}{15} \times 100$) of the analyzed dust samples.

3.1. OSF Environment

In **Figure 2 (a)**, results data for the content of the selected metals are shown for the collected residue dust samples from the six OSF environments. The levels of Ni and Cu were recorded in a high amount and ranged from < d.l. $\mu g \cdot g^{-1}$ (OSF6) to 157.83 $\mu g \cdot g^{-1}$ (OSF2), and 38.463 $\mu g \cdot g^{-1}$ (OSF3) to 117.76 $\mu g \cdot g^{-1}$ (OSF4), respectively. Besides, the level of Cr metal was present only in the last three samples (OSF4-6) and ranged from 56.25 $\mu g \cdot g^{-1}$ to 66.66 $\mu g \cdot g^{-1}$. The cadmium level for two of the samples was only present and equal to 0.2066 $\mu g \cdot g^{-1}$ (OSF1) and 1.2396 $\mu g \cdot g^{-1}$ (OSF4). Thus, the highest recorded heavy metals level was Ni in the OSF2 sample and was 157.83 $\mu g \cdot g^{-1}$.

Results data in **Figure 2 (b)** show the content of the metals in kerosene samples from the six OSF places and RK from commercial filling stations. The kerosene fuel which is mainly used by OSF owners as main heating source was used for the metal analysis in order to know the source of heavy metals in the collected residue dust samples in OSF environment. In order to evaluate the levels of the targeted metals (Figure 2 (b)), the recorded data of RK was also compared with the data of kerosene fuel from OSF places. Thus, the levels of Cr and Cd in all of the collected OSF samples were present as below the detection limit. The concentration of the Cu metal was only detected in the first two samples including 5.769 $\mu g \cdot mL^{-1}$ (OSF1) and 3.245 $\mu g \cdot mL^{-1}$ (OSF2). However, the Ni concentration was not detectable in all of the collected kerosene samples except the OSF4 sample (2.83 $\mu g \cdot mL^{-1}$).

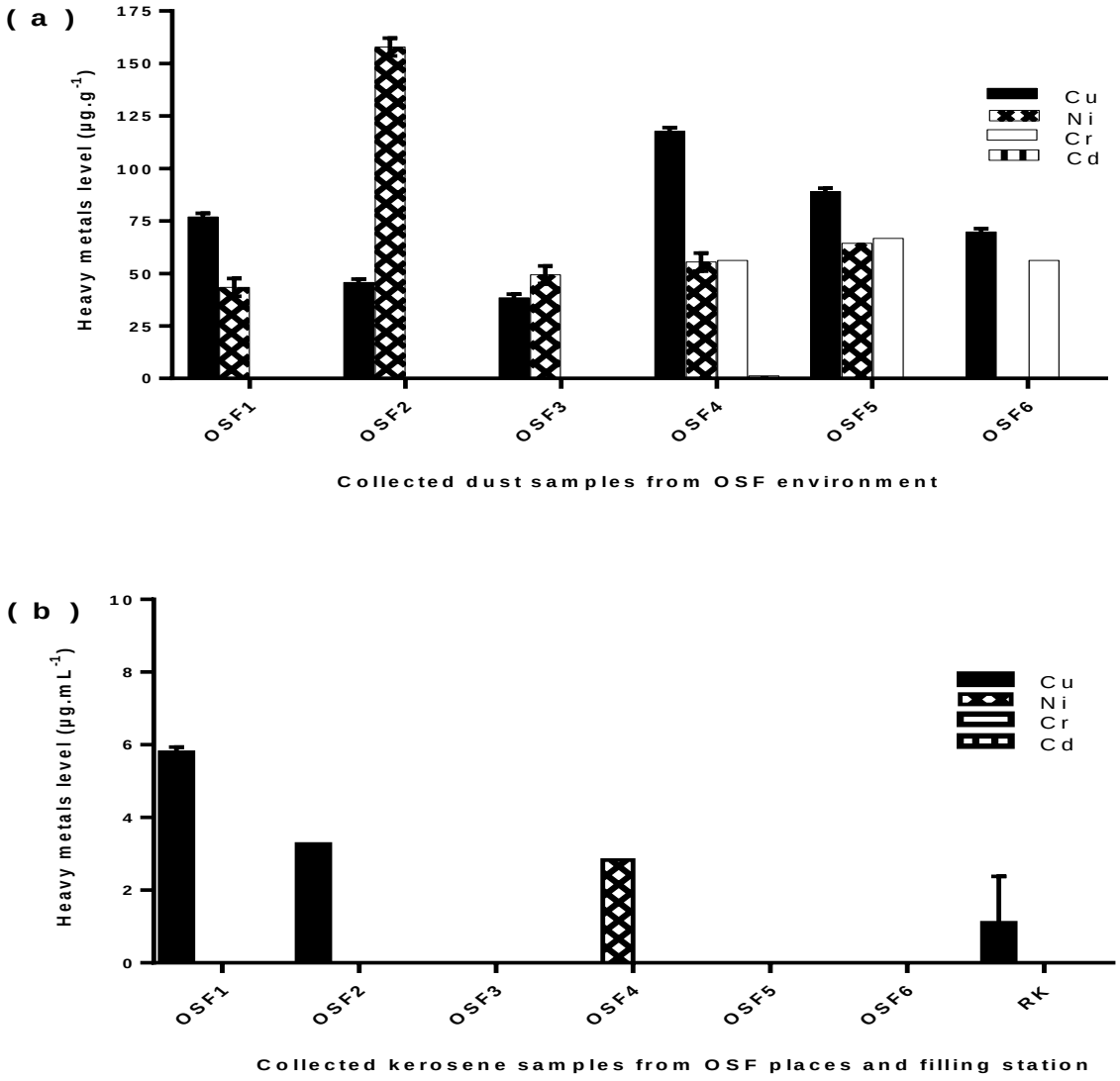

Figure 2: Shows the content of metals in collected (a) residue dust samples from six OSF environment, and (b) kerosene samples from the six OSF1-6 places compared with mean level of reference kerosene samples (RK) from filling station.

According to result in **Figure 2 (b),** the mean content of the selected metals in the RK sample is present as a below detectable excepting 1.08 ± 1.29 $\mu g \cdot mL^{-1}$ for Cu metal. Due to comparing the level of the selected metals in **Figure 2 (b),** the samples of RK which given by filling stations can be seen as a purer than some kerosene samples collected from OSF places. In addition, the presence of the targeted metals in the collected residue dust samples of OSF places can come from the environment and preconcentration stepwise of residue dust of the kerosene fuel consumption.

3.2. GSF Environment

The investigated metals levels in the collected dust samples are shown in **Figure 3** for the four GSF places. The content of investigated metals in GSF samples were in the ranges of 58.89–91.35 $\mu g \cdot g^{-1}$ for Cu, 40.361–117.65 $\mu g \cdot g^{-1}$ for Ni, < d.l.–87.5 $\mu g \cdot g^{-1}$ for Cr and < d.l.–1.24 $\mu g \cdot g^{-1}$ for Cd, respectively.

The result data in **Figure 3** confirmed that the level of the selected metals in all the samples recorded in a high amount excepting Cd level was present as a minimum amount or below the detection limit. Thus, all of the GSF environments are contaminated and included a high present amount of these metals. The presence of the selected heavy metals in the collected residue dust samples of OSF places can come from the environment atmosphere and may come from preconcentration stepwise of residue dust of the used fuel consumption.

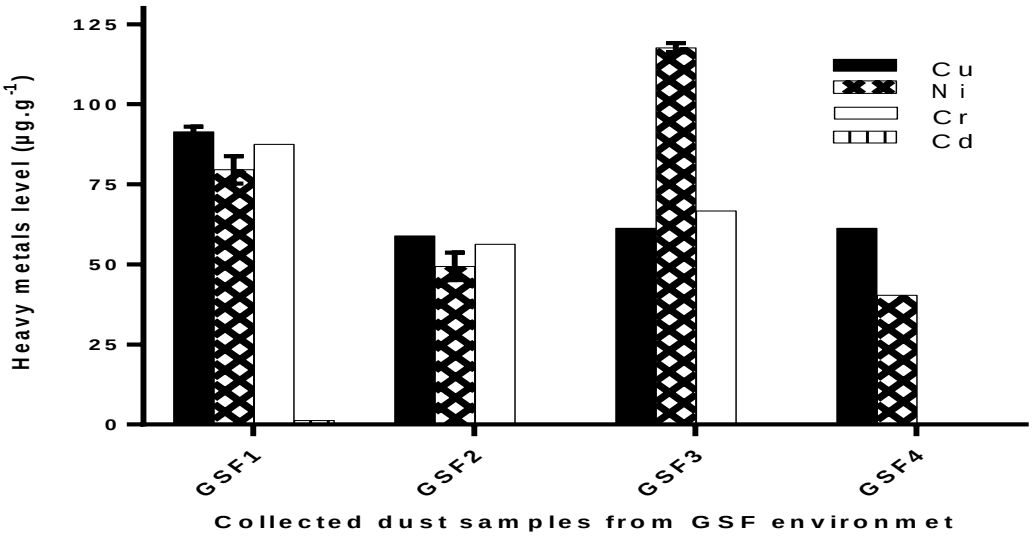

Figure 3: Shows the selected metals level in collected residue dust samples from GSF environment

3.3. NGB Environment

The determined level for the selected heavy metals is illustrated in **Figure 4** for the collected residue dust and firebrick (FB) samples from five NGB environments. Firebricks play an important role as assisted materials of heat/energy storage or in the waste heat recovery which have also been used with kerosene fuel by bakers in Erbil city. Results data on reference firebricks (RFB) were also used to compare with the collected firebrick samples from NGB places.

According to results data in **Figure 4 (a-b),** both Cu and Ni metals recorded at a high level in the entire collected samples of the NGB environment. The Cu and Ni levels range in the NGB samples

are equal to (67.3 - 328.12 $\mu g \cdot g^{-1}$ in dust, 36.05 - 308.89 $\mu g \cdot g^{-1}$ in FB), and (67.465 - 166.86 $\mu g \cdot g^{-1}$ in dust, 61.442-209.04 $\mu g \cdot g^{-1}$ in FB), respectively. The content of investigated Cr metal in the dust and FB samples were in the range (<d.l. – 178.54 $\mu g \cdot g^{-1}$) and (<d.l. – 619.96 $\mu g \cdot g^{-1}$), respectively. Also, the highest Cr metal level recorded inside NGB4 (619.96 $\mu g \cdot g^{-1}$ in FB) environment. The level of Cd in all of the NGB samples exhibited below detection limit excepting FB sample from NGB1 including 0.2066 $\mu g \cdot g^{-1}$.

The content of the investigated metals inside the RFB demonstrated at a minimum level or below the detection limit. However, a high amount of the selected heavy metals present in the collected FB in NGB samples. In NGB environment, the main sources of targeted heavy metals could come from the polluted atmosphere, fuel consumption and the decay of the FB components during heating.

Considering comparing all the above result data, the highest levels for the determined heavy metals in the residue dust environment recorded as follows concentration ($\mu g \cdot g^{-1}$): NGB (328.12) > OSF (117.76) > GSF (91.35) for Cu, NGB (166.86) > GSF (117.65) > OSF (64.45) for Ni, NGB (178.54) > GSF (87.5) > OSF (66.66) for Cr, and GSF (1.24) > OSF (1.23) > NGB (<d.l.) for Cd. The highest amount of Cu, Ni, and Cr were recorded inside the NGB environment due to comparing with finding results from GSF and OSF places. It verifies that most of the bakeries' Naan environment contaminated with a high amount of these heavy metals because the recorded level for total selected metals load (TSML) in NGB environment (392.23 $\mu g \cdot g^{-1}$) was approximately twice times higher than both OSF (207.45 $\mu g \cdot g^{-1}$) and GSF (211.31 $\mu g \cdot g^{-1}$) environment respectively (**Table 1**).

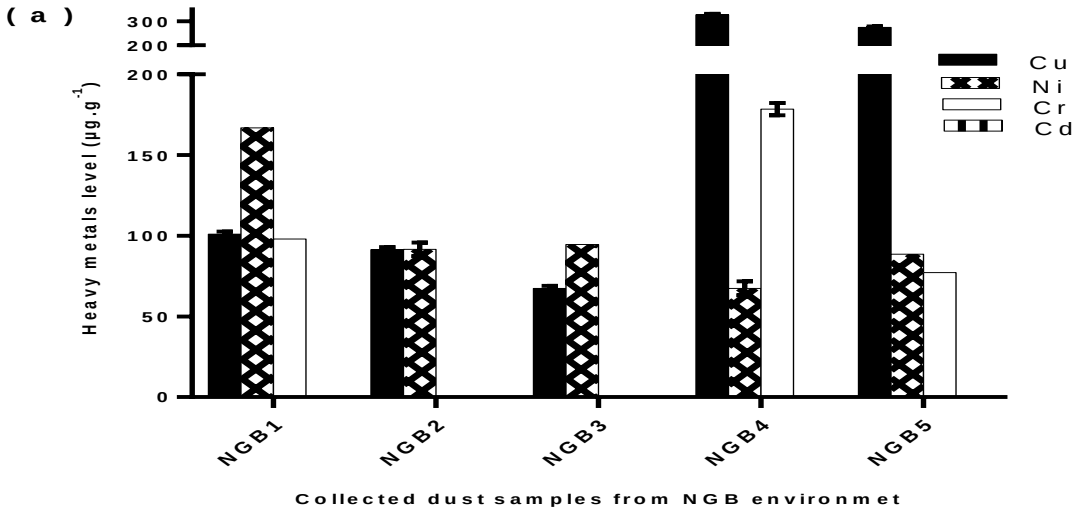

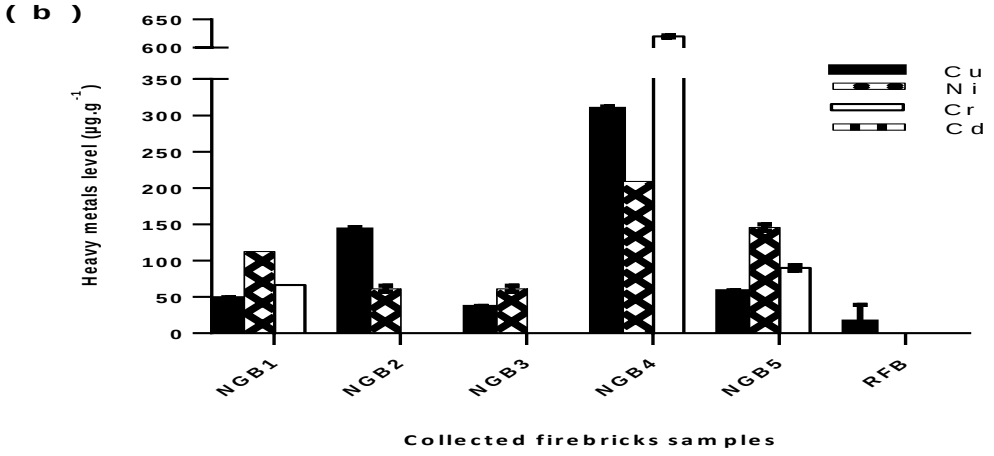

Figure 4: Shows the level of some heavy metals in collected (a) residue dust samples from five NGB environment, and (b) firebrick samples from five NGB environment compared with unused reference firebricks (RFB).

Collected residue dust for the most of the samples in this study included different amount of the investigated heavy metals. Summarized results in this study are shown and compared with different country standard allowable limitation guidelines for heavy metals in dust/soil in **Table 1** (Al-Fatlawi and Al-Alwani, 2012, ECDGE, 2004, Okedeyi et al., 2014, Sezgin et al., 2004, Fabis, 1987).

In the **Table 1**, Fabis (1987) allowable standard for heavy metals permission limit in dust was selected and used to evaluate finding results in this study. Of note, the means content of Cu and Ni in all investigated dust samples exceeded the permissible limit specified by Fabis (1987) (**Table 1**). However, mean concentration of cadmium (Cd) in all dust samples was lower than the selected permissible limit. Indeed, the mean concentrations of all elements in NGB environment were higher than selected maximum permissible limit excepting Cd metal. There was no significant difference between OSF, GSF, and NGB samples in terms of mean content of targeted heavy metals in dust ($p= 0.43$) due to performing One-way ANOVA analysis.

For the dust samples in NGB environment, only 20% of samples exceeded the permissible limit for Cr, while all samples (100%) significantly exceeded the permissible limit for Cu and Ni. In terms of the documented exceeding permissible limit for Cu and Ni metals, 66.66% and 50% in the dust OSF samples and 100% and 50% in the dust GSF samples were documented respectively. None Findings over permissible limit were presented in the entire (15) of the samples for Cd metal. In terms of mean content for Cr in dust samples, only NGB samples environment exceeded the permissible limit specified by Fabis (1987) with 20%.

Based on many recent studies, sources of metals accumulation in dust environment were mainly derived from industrial emissions including weathering and combusting of coal and fuel combustion from traffic activities (Cai and Li, 2019, Tang et al., 2017, Wan et al., 2016, Dalton et al., 2018). Thus, it can be seen that the accumulated residue dust from bakeries and furnaces environment contaminated with polluted metals ongoing to accumulation and pre-concentration stepwise of the polluted atmosphere, the decay of firebricks and fuel consumption. Thus, results in this study show that the environment of most bakeries and furnaces inside Erbil city can be seen as unsafe for baking and impure place for working and human health ongoing to including above permissible limits for heavy metals.

Table 1: shows heavy metals level (µg·g^{-1}) in residue dust samples and country allowable guidelines for some metal limits in soil/dust

No.	Sample code			Cu	Cd	Cr	Ni	Total selected metals load (TSML) (µg·g^{-1})
1	This study Iraq-Erbil City	(OSF1-6)	Range (µg·g^{-1})	38.46 – 117.76	<d.l. – 1.23	<d.l. – 66.66	<d.l. – 157.83	207.45
			Mean (µg·g^{-1})	**72.92**	**0.723**	**59.7**	**74.09**	
			SD (µg·g^{-1})	29.10	0.73	6.0	47.45	
			%OM	100%	33.3%	50%	83.3	
			%EPL	66.66%	0.0%	0.0%	50%	
2		(GSF1-4)	Range (µg·g^{-1})	58.89 – 91.35	<d.l. – 1.24	<d.l. – 87.5	40.36 – 117.65	211.31
			Mean (µg·g^{-1})	**68.21***	**1.24**	**70.14**	**71.73**	
			SD (µg·g^{-1})	15.5	0.0	19.9	34.9	
			%OM	100%	25%	75%	100%	
			%EPL	100%	0.0%	0.0%	50%	
3		(NGB1-5)	Range (µg·g^{-1})	67.3 – 328.12	<d.l.	<d.l. – 178.54	<d.l. – 166.86	392.23
			Mean (µg·g^{-1})	**172.6***	**<d.l.**	**117.8**	**101.8***	
			SD (µg·g^{-1})	119.9	<d.l.	53.6	37.9	
			%OM	100%	0.0%	60%	100%	
			%EPL	100%	0.0%	20%	100%	
Permissible limit (PL) guidelines for dust/soil								
No.	**World standard countries**			**Cu (µg·g^{-1})**	**Cd (µg·g^{-1})**	**Cr (µg·g^{-1})**	**Ni (µg·g^{-1})**	**References**
1	**Germany**			40.0	1.0	60.0	50.0	(Okedeyi et al., 2014)
2	**Netherlands**			40.0	0.5	30.0	15.0	
3	**Sweden**			40.0	0.4	60.0	30.0	(ECDGE, 2004)
4	**USA**			75.0	1.9	150.0	21.0	
5	**Ireland**			50.0	1.0	--	30.0	
6	**Fabis 1987**			**50**	**3**	**100**	**50**	(Sezgin et al., 2004) (Fabis, 1987, Al-Fatlawi and Al-Alwani, 2012)

%EPL: means the percentage of analyzed samples which were exceeding permissible limit (EPL) or above mentioned permissible limit for each metal, SD: Standard Deviation. <d.l: below detection limit. *: Significantly higher than maximum permissible limit, %OM: represents the percentage of observed or presented for each individual metal in the entire of sample, NGB1-5; five Naan bakeries used liquefied gas, GSF1-4; four Samoon furnaces used liquefied gas, OSF1-6: Six Samoon furnaces used liquefied kerosene. TSML: represents the summation calculation of the means level of all selected metals (Cu, Cd, Cr, and Ni) for each of the analyzed sample, n; number of collected samples.

4. CONCLUSIONS

According to result data, most of the collected dust samples inside the bakeries and furnaces environment in Erbil city included a high amount of the investigated heavy metals and exceeded standard permissible limits. The polluted atmosphere, fuel consumption and firebricks decay during heating can be selected as main sources for metals contamination due to pre-concentration and accumulation process of dust residue. The recorded metals content in most bakeries and furnaces environment were higher than most country guidelines for standard allowable metals in soil and dust environment. The assessment comparison of results proved that the environment of bakeries' Naan is unsafe for baking or working and more contaminated than Samoon furnaces environment.

5. RECOMMENDATION

Results data show that more attention should be paid to heavy metal contamination of the foods environment in the future because of their high toxicity potential, widespread use, and prevalence. It is recommended that the government should prevent the use of low quality kerosene consumption as heating sources by the local bakery and furnace owner. Additionally, bakery and furnace owners must clean their entire working area daily from accumulated residue dust especially inside the heating environment chamber due to more attention to health safety.

ACKNOWLEDGMENT

I would like deeply thank to Naan's bakery and Samoon's furnace owner who allowed us for the sampling during this research project.

REFERENCES

ABD-ALHAMEED, M. M. 2019. Spatial Distribution of Heavy Metals in Surface Soil Horizons Surrounding Erbil Steel Company (ESC) Areas. *ZANCO Journal of Pure and Applied Sciences,* 31**,** 32-38.

AL-ATTAR, M. S. 2016. Effects of Nickel and Cadmium Contaminated Fish Meat on Chromosomal Aberrations and Sperm Morphology of Swiss Albino Mice. *ZANCO Journal of Pure and Applied Sciences,* 28.

AL-FATLAWI, S. & AL-ALWANI, M. 2012. Heavy metal pollution of roadside dust samples with different traffic volumes at Hilla city, . *The Iraqi J For Mech. & Material Eng,* 12**,** 660-672.

AMIN, J. K. M., JALAL, S. S. & JARJEES, F. Z. 2017. The Elemental Composition of Atmospheric Particles and Dust Fall Rate in Erbil Governorate. *ZANCO Journal of Pure and Applied Sciences,* 29**,** 38-48.

BARBOOTI, M. M. 2015. Evaluation of analytical procedures in the determination of trace metals in heavy crude oils by flame atomic absorption spectrophotometry. *American Journal of Analytical Chemistry,* 6**,** 325.

BARBOOTI, M. M., AL-MADFAI, S. & AL-SAMMERRAI, D. 1986. Thermogravimetric characterization of Quayarah heavy crude oils. *Journal of thermal analysis,* 31**,** 253-260.

BAZZAZ, J. N. & MUHAMMAD, G. R. 2018. Some heavy metals assessment in frozen chicken meat sold in Erbil local markets. *ZANCO Journal of Pure and Applied Sciences,* 30**,** 96-101.

CAI, K. & LI, C. 2019. Street dust heavy metal pollution source apportionment and sustainable management in a typical city—Shijiazhuang, China. *International journal of environmental research and public health,* 16**,** 1-15.

CHENG, Z., CHEN, L.-J., LI, H.-H., LIN, J.-Q., YANG, Z.-B., YANG, Y.-X., XU, X.-X., XIAN, J.-R., SHAO, J.-R. & ZHU, X.-M. 2018. Characteristics and health risk assessment of heavy metals exposure via household dust from urban area in Chengdu, China. *Science of The Total Environment,* 619**,** 621-629.

DALTON, A., FEIG, G. T. & BARBER, K. 2018. Trace metal enrichment observed in soils around a coal fired power plant in South Africa. *Clean Air Journal,* 28**,** 1-9.

DARWESH, D. A. 2019. Heavy metals evaluation in soil of agricultural field around a pond of gas plant in the Kurdistan Region of Iraq. *ZANCO Journal of Pure and Applied Sciences,* 31**,** 28-35.

ECDGE 2004. Heavy metals and organic compounds from wastes used as organic fertilisers. *Study on behalf of the European Commission, Directorate-General Environment, ENV. A,* 2**,** 73-74.

EDWARDS, H. G. 2019. *Porcelain to Silica Bricks: The Extreme Ceramics of William Weston Young (1776-1847)*, Springer.

FABIS, W. 1987. Schadstoftbelastung Von Böden-Auswirkurgen auf Böden-und Wassergalitat Allg Farstzeitsehr. *BLV Verlaggesellshaft, Munich***,** 128-131.

FERREIRA-BAPTISTA, L. & DE MIGUEL, E. 2005. Geochemistry and risk assessment of street dust in Luanda, Angola: a tropical urban environment. *Atmospheric environment,* 39**,** 4501-4512.

ISSA, M. J., HUSSAIN, H. M. & SHAKER, I. H. 2019. Assessment of the Toxic Elements Resulting from the Manufacture of Bricks on Air and Soil at Abu Smeache Area-Southwest Babylon governorate-Iraq. *Iraqi Journal of Science***,** 2443-2456.

JADOON, S., AMIN, A. A., MAHMOOD, H. K., HAMOODI, D. A. & SABIR, M. F. M. 2016. Determination of Trace Metals in Crude Oils by Atomic Absorption Spectrophotometry in Khurmala and Guwayar Oil Fields of Kurdistan

Region, Iraq. *American Scientific Research Journal for Engineering, Technology, and Sciences (ASRJETS)*, 20**,** 213-223.

JAISHANKAR, M., TSETEN, T., ANBALAGAN, N., MATHEW, B. B. & BEEREGOWDA, K. N. 2014. Toxicity, mechanism and health effects of some heavy metals. *Interdisciplinary toxicology*, 7**,** 60-72.

JIN, Y., O'CONNOR, D., OK, Y. S., TSANG, D. C., LIU, A. & HOU, D. 2019. Assessment of sources of heavy metals in soil and dust at children's playgrounds in Beijing using GIS and multivariate statistical analysis. *Environment international*, 124**,** 320-328.

KHUDHUR, N. S., KHUDHUR, S. M. & AMEEN, N. O. H. 2016. A Study on soil bacterial population in steel company and some related area in Erbil city in relation to heavy metal pollution. *ZANCO Journal of Pure and Applied Sciences*, 28**,** 101-116.

LATIF, M. T., YONG, S. M., SAAD, A., MOHAMAD, N., BAHARUDIN, N. H., MOKHTAR, M. B. & TAHIR, N. M. 2014. Composition of heavy metals in indoor dust and their possible exposure: a case study of preschool children in Malaysia. *Air Quality, Atmosphere & Health*, 7**,** 181-193.

LU, X., WANG, L., LI, L. Y., LEI, K., HUANG, L. & KANG, D. 2010. Multivariate statistical analysis of heavy metals in street dust of Baoji, NW China. *Journal of hazardous materials*, 173**,** 744-749.

MORAIS, S., COSTA, F. G. & PEREIRA, M. D. L. 2012. Heavy metals and human health. *Environmental health–emerging issues and practice*, 10**,** 227-246.

OKEDEYI, O. O., DUBE, S., AWOFOLU, O. R. & NINDI, M. M. 2014. Assessing the enrichment of heavy metals in surface soil and plant (Digitaria eriantha) around coal-fired power plants in South Africa. *Environmental Science and Pollution Research*, 21**,** 4686-4696.

PROSHAD, R., AHMED, S., RAHMAN, M. & KUMAR, T. 2017. Apportionment of hazardous elements in agricultural soils around the vicinity of brick kiln in Bangladesh. *Journal of Environmental and Analytical Toxicology*, 7**,** 2161-0525.1000439.

REYNOLDS, J. G. 2003. Removal of nickel and vanadium from heavy crude oils by exchange reactions. Lawrence Livermore National Lab.(LLNL), Livermore, CA (United States).

ROLDAN, P., ALCÂNTARA, I., ROCHA, J. C., PADILHA, C. & PADILHA, P. 2004. Determination of Copper, Iron, Nickel and Zinc in fuel kerosene by FAAS after adsorption and pre-concentration on 2-aminothiazole-modified silica gel. *Eclética Química*, 29**,** 33-40.

SAINBAYAR, J., MONKHOOBOR, D. & AVID, B. 2011. Determination of trace elements in the Tamsagbulag and Tagaan Els crude oils and their distillation fractions using by ICP-OES. *Advances in Chemical Engineering and Science*, 2**,** 113-117.

SEZGIN, N., OZCAN, H. K., DEMIR, G., NEMLIOGLU, S. & BAYAT, C. 2004. Determination of heavy metal concentrations in street dusts in Istanbul E-5 highway. *Environment international*, 29**,** 979-985.

SIKDER, A. H. F., KHANOM, S., HOSSAIN, M. F. & PARVEEN, Z. 2016. Accumulation of Zn, Cu, Fe, Mn and Pb due to brick manufacturing in agricultutral soils and plants. *Dhaka University Journal of Biological Sciences*, 25**,** 75-81.

SRITHAWIRAT, T. & LATIF, M. T. 2015. Concentration of selected heavy metals in the surface dust of residential buildings in Phitsanulok, Thailand. *Environmental earth sciences*, 74**,** 2701-2706.

TANG, Z., CHAI, M., CHENG, J., JIN, J., YANG, Y., NIE, Z., HUANG, Q. & LI, Y. 2017. Contamination and health risks of heavy metals in street dust from a coal-mining city in eastern China. *Ecotoxicology and Environmental Safety*, 138**,** 83-91.

TEKIE, H. A., MCCRINDLE, R. I., MARAIS, P. J. & AMBUSHE, A. A. 2015. Evaluation of six sample preparation methods for determination of trace metals in lubricating oils using inductively coupled plasma-optical emission spectrometry. *South African Journal of Chemistry*, 68**,** 76-84.

WAN, D., HAN, Z., YANG, J., YANG, G. & LIU, X. 2016. Heavy metal pollution in settled dust associated with different urban functional areas in a heavily air-polluted city in North China. *International journal of environmental research and public health*, 13**,** 1119.

WEI, B. & YANG, L. 2010. A review of heavy metal contaminations in urban soils, urban road dusts and agricultural soils from China. *Microchemical journal*, 94**,** 99-107.

WHITESIDE, P. J. & MILNER, B. A. 1984. *Pye Unicam atomic absorption data book*, England, Pye Unicam Ltd.

YANG, F. & MASSEY, I. Y. 2019. Exposure routes and health effects of heavy metals on children. *BioMetals*, 32**,** 563-573.

ZGŁOBICKI, W., TELECKA, M., SKUPIŃSKI, S., PASIERBIŃSKA, A. & KOZIEŁ, M. 2018. Assessment of heavy metal contamination levels of street dust in the city of Lublin, E Poland. *Environmental earth sciences*, 77**,** 774.

ZHOU, L., LIU, G., SHEN, M., HU, R., SUN, M. & LIU, Y. 2019. Characteristics and health risk assessment of heavy metals in indoor dust from different functional areas in Hefei, China. *Environmental Pollution*, 251**,** 839-849.

ZANCO Journal of Pure and Applied Sciences
The official scientific journal of Salahaddin University-Erbil
https://zancojournals.su.edu.krd/index.php/JPAS

ISSN (print):2218-0230**, ISSN (online):** 2412-3986**, DOI: http://dx.doi.org/10.21271/zjpas**

RESEARCH PAPER

Evaluation the Nutritional Status of Imported Tea Brands in Erbil City.

[1]Dalshad Azeez Darwesh and, [2]Snowber Muhamad Ahmed

[1]Department of Environmental sciences, College of science, Salahaddin University-Erbil, Kurdistan Region, Iraq

[2] Department of General science, College of Basic Education, Salahaddin University-Erbil, Kurdistan Region, Iraq

A B S T R A C T:

A laboratory study was conducted to determine the nutritional composition of the various tea brands that were imported into Erbil city. The tea samples included 12 most popular tea brands purchased in various local market and tea shopping with five replications. The design of experimental based on a CRD. The results were indicated that the concentration of (P, N, K and Ca%) in all tea samples were ranged between (0.0350-0.1288, 1.0127-5.8086, 0.0028-0.0275 and 0.1306-0.8891) respectively. The concentration of Mn in tea brands were ranged between (0.0075-0.0325%), the higher concentration recorded in brand2. The loading rotation with Principal axis factoring was conducted to assess the underlying structure for the thirteen variables on the quality and quantity of tea brands. Two factors were selected, based on the validity that the variables were designed to index two constructs quality and quantity. The result of factor analysis revealed that the first factor responsible on 23.38% of the variance, the second factor accounted for 15.56% of the variance. The recorded eigenvalues were 3.040 and 2.035 for F_1 and F_2 respectively.

KEY WORDS: Tea; Nutrients composition; Essential elements; Caffeine.
DOI: http://dx.doi.org/10.21271/ZJPAS.32.3.19
ZJPAS (2020) , 32(3);187-192 .

1.INTRODUCTION :

The very common most popular drinking in several countries around the world is tea and it is increasing in demand due to the increase in consumption, the widespread consumption of tea around the world due to its aromatic, taste, smell and, above all, its beneficial effects on health, Moreover, it's a cheap drink, so tea is considered a second drink after water and has been expanded worldwide, thus tea becomes a part of the human lifestyle. The quantity and quality of tea production are related to a range of environmental factors, including soil fertility, soil management and climate conditions. The chemical components of tea are the object of extensive scientific studies, so the appropriate estimation of the nutrient components of teas is very important in limiting the quality of tea which health depended. (Hollman et al., 1996). The composition of tea leaves were studied methodically. The polyphenol group was the main constituents of tea leaves which involved 25±35% on a dry weight basis (Balentine et al., 1997 and Hara et al., 1995). In addition to phenol compounds the tea also contains protein, caffeine, and various kinds of vitamins like A, B and vitamin C. Tea also provides large amounts of nutrients like potassium, manganese, calcium, iron and fluoride ions to the drinking. A round the world different papers were published internationally on the organic and inorganic composition of teas, specially the nutrition status of tea by (Ferrara et al., 2001; Christiane and Edward 2001; Alberti et al.,2003; Shu et al., 2003; Mokgalaka et al., 2004; Kumar et al., 2005 ; Mehmet et al., 2008; Seenivasan et al., 2008 and Czernicka et al.,2017). The concentration of elements Ca, Na, K, Mg, and

* **Corresponding Author:**
Dalshad Azeez Darwesh
E-mail: dalshas.darwesh@su.edu.krd
Received: 01/10/2019
Accepted: 10/12/2019
Published: 15/06 /2020

N, expressed by mg/g level, while the concentration of elements Cr, Fe, Co, Ni, Cu, Zn, and Cd expressed by µg/g (Cao et al., 1998). A large quantity and quality of tea are consumed by the Kurdish population, thus a huge and different tea brands imported from several countries to meet the growing demand, with out assessment the nutritional status, in particular, the essential composition of imported tea plants. Therefore, it is necessary to assess the level of essential elements of imported tea with regard to their permissible limit. Thus this study aimed to assess the nutritional status of some common brands of tea imported to Kurdistan region.

2. MATERIALS AND METHODS

2.1 Experimental design

The tea samples included 12 most common tea brands purchased in different local market and tea shopping with five replications. The experimental designed in a completely randomized (CRD). Oven drier at 65°C was used for drying the samples, then dried samples were digested using acid digestion mixture H_2O_2 and H_2SO_4 acid (1/1 , v/v). The N percentage was measured by the Distillation, and the P concentration was determined by the by spectrophotometric method while the flame photometric method of Allen (1974) were used to determined K and Ca. The digested samples were used to determine the concentration of Fe, Cu, Mn and Zn by atomic absorption flame emission spectrophotometry. (Michael et al., 2008). The caffeine concentration was estimated by using high-performance liquid chromatography (HPLC). The determination, pure caffeine was used for preparation standards curve (Hollman et al.,1996). The total carbohydrate and volatile and ash were determinate according to methods described in (Allen ,1974).

2.2 Statistical analysis

Data were statistically analyzed using SPSS version 24. All data expressed as a mean value. The difference among the means of tea brands was compared by applying Duncan multiple comparison tests at (5%) level of significance, the results were subject to the factor analysis (principal component analysis and discriminate measure). (Steele and Torrie, 1969 and Cirocka et al., 2016).

3. RESULTS AND DISCUSSION

The data analysis revealed that the mean values described large difference among selected brands of tea. Table 1 present mean finding related to the nutrients in the selected tea brands, the statistical analysis show a significant differences of nutrients among tea brands accept the Zn show no significant differences. The content of macroelements (P, N, K and Ca%) in all tea samples were ranged between (0.0350-0.1288, 1.0127-5.8086, 0.0028-0.0275 and 0.1306-0.8891) respectively. The highest contents of P, N, K and Ca were found in tea brands (7, 11, 3 and 4), while the lowest contents of the same macroelements were recorded in brands (5, 3, 11 and 3) respectively. This discrepancies of minerals content among tea brands may be related to the variation among the tea kinds, harvesting time, soil types and climate properties. Michael et al., (2005) revealed that the concentrations of K and Ca were ranged between (1.77-2.48) and (0.062-0.182) respectively in the black teas. The studied tea brands were showed large ranges values of K and lower range value of Ca compared to the ranges obtained in the study was carried out by (Michael et al.,2005) . This variation in Ca content may be related to soils properties, climate condition of the cultivation tea farms. The high concentration of Ca is important because of its role in the formation of teeth, bone and muscles. The higher levels of N and P in the studied tea plants explained on the ground that these elements are greatly translocated from old leaves to young leaves due to their higher mobility Marschner (1995). Also Kumar et al., (2005) estimated a higher concentration of K in tea leaves and they interpreted their result on the bases that the K able to binding with some organic compound which facilitate its translocation in the tea leaves. The concentration of Mn in tea brands were ranged between (0.0075-0.0325), the higher concentration recorded in tea brand 2 this result is lower than that reported by Micheal et al., (2008) in black tea , while higher than the range has been reported by Czernicka et al., (2017) in China black tea . The concentration of iron in teas under study

was located within the range of (0.0121-0.024%) being highest in brand 6 (0.0182%) lower range of iron has been reported by Micheal et al., (2008) in black tea. While the concentration of Cu ranged between (0.002-0.0085%). Wang et al., (1993) indicate that the concentration of Cu was ranged from 9.6 to 20.9 mg/kg, (0.00096-0.0020%) in Chinese tea brands, which are lower than the values obtained for the studied tea brands. The result of many studies indicated that essential elements play a vital role in human metabolisms, particularly in growth, development, preventing healing the disease. Iron is an important element of the human body, because of participation in oxygen and electron transport, and it is necessary for the formation of the hemoglobin.

Table 1. Range and mean value of essential elements in different tea brands

Tea brands	Essential elements %							
	P	**N**	**K**	**Ca**	**Mn**	**Fe**	**Cu**	**Zn**
1	0.053d	3.122bc	0.0059cd	0.714ab	0.0128de	0.0177a	0.0023c	0.00730a
2	0.076bc	2.074de	0.0052cd	0.718ab	0.0245a	0.0161abc	0.0032c	0.00660a
3	0.113a	1.446e	0.0193a	0.144e	0.0127de	0.0128c	0.0024c	0.00683a
4	0.073c	4.177b	0.0083c	0.822a	0.0225ab	0.0155abc	0.0035c	0.00660a
5	0.052d	3.630bc	0.0065cd	0.595bc	0.0222ab	0.0145abc	0.0030c	0.00683a
6	0.087bc	4.141b	0.0142b	0.273de	0.0229ab	0.0182a	0.0035c	0.00587a
7	0.119a	2.658cd	0.0157b	0.385d	0.0147c	0.0168ab	0.0056b	0.00697a
8	0.087bc	3.908b	0.0082c	0.177de	0.0192abc	0.0171ab	0.0055b	0.00563a
9	0.089b	3.711bc	0.0063cd	0.606bc	0.0208ab	0.0149abc	0.0026c	0.00677a
10	0.076bc	3.409bc	0.0042d	0.565c	0.0091e	0.0165abc	0.0037c	0.00673a
11	0.045d	5.209a	0.0033d	0.244de	0.0082e	0.0168ab	0.0059ab	0.00773a
12	0.080bc	3.856b	0.0048cd	0.574c	0.0188bc	0.0134bc	0.0072a	0.00660a
Grand Mean	**0.079**	**3.445**	**0.0085**	**0.485**	**0.0174**	**0.0158**	**0.0040**	**0.00671**
Sd	**0.0229**	**1.0915**	**0.0053**	**0.2316**	**0.00596**	**0.0023**	**0.0017**	**0.0012**
Minimum	0.0350	1.0127	0.0028	0.1306	0.00750	0.0121	0.0020	0.0043
Maximum	**0.1288**	**5.8086**	**0.0275**	**0.8891**	**0.03250**	**0.0240**	**0.0085**	**0.0095**

The data analysis in table 2 refers to the significant differences among tea brands for protein, volatile, caffeine, ash and total carbohydrate ($P<0.05$). Among the chemical composition, the caffeine and total carbohydrate are most abundances, their concentration ranged between (12.00-45.44% and 13.735-53.492%) respectively, the high content of caffeine and total carbohydrate (38.037% and 49.764%) recorded in tea brands (7 and 3) respectively. Czernicka et al., (2017) has reported that the caffeine concentration in China black tea was ranged between (31.5-43.42), which are lower than the value of most studied tea brands. The value of (protein =31.063, volatile=3.357 and ash=6.723) were recorded in tea 9,12 and 4 respectively, The concentration of protein, volatile and ash were higher compared to those were reported by Czernicka et al., (2017) in China black tea. The discrepancy in the nutrients content of different brand teas may be related to the variation in the soil characteristics and the environmental condition of the countries tea production, in addition to the genetic and physiological variation among the tea brands.

The loading rotation with principal axis factoring was conducted to evaluate the influence of the thirteen variables on the quality and quantity of tea brands. Two factors were selected, based on the validity that the variables were designed to index two constructs quality and quantity. The result of factor analysis figure.1 revealed that the first factor responsible on 23.38% of the variance, the second factor accounted for 15.56% of the

variance. The recorded eigenvalues were 3.040 and 2.035 for F1 and F2 respectively.

Table 2. Range and mean value of chemical composition in different tea brands

Tea brands	%				
	Protein	**Volatile**	**Caffeine**	**Ash**	**Total Carbohydrate**
1	10.360f	2.504bc	29.177ab	5.173bcd	38.784ab
2	12.720e	2.520bc	35.275ab	3.297e	33.737b
3	6.773h	2.840bc	23.247c	6.277b	49.764a
4	9.743gf	2.593bc	33.203ab	6.723a	33.027bc
5	8.007gf	2.443bc	37.550a	5.953abc	32.207bc
6	13.542e	2.947ab	33.813ab	4.753cd	32.413bc
7	17.667d	2.401c	38.037a	4.757cd	26.038c
8	30.320a	2.353c	29.670ab	5.277bcd	20.989c
9	31.063a	2.533bc	26.833bc	4.790cd	21.519c
10	26.700b	2.429c	23.240c	6.413ab	30.107bc
11	26.277b	2.363c	28.443ab	4.387de	24.284c
12	22.930c	3.357a	24.373c	5.790c	29.316bc
Grand Mean	**18.008**	**2.607**	**30.238**	**5.299**	**31.849**
Sd	**8.788**	**0.364**	**7.541**	**1.108**	**9.667**
Minimum	14.720	2.080	12.000	2.880	13.735
Maximum	**32.000**	**3.650**	**45.440**	**7.650**	**53.492**

The results in figure.1 revealed that the samples of tea lower values of F1 are obviously prominent from teas characterized by higher values of F1. The data analysis in figure 2 show the parameters and factor variation for the rotated factors, with value less than 0.4 omitted to enhance simplicity. The first factor, which seems to index quality, loads most strongly on the concentration of (K, P, N and Ca), with loadings in the first column. The N and Ca contents indexed low quality of tea brands and have negative effect. The second factor, which seemed index quantity, was involved the protein and Cu strongly positive effect on quantity, while the carbohydrate shows negative loading. Moreover, the nitrogen has its highest negative loading from the quantity index but also had a positive loading from the quality index. (Cirockaetal.,2016).

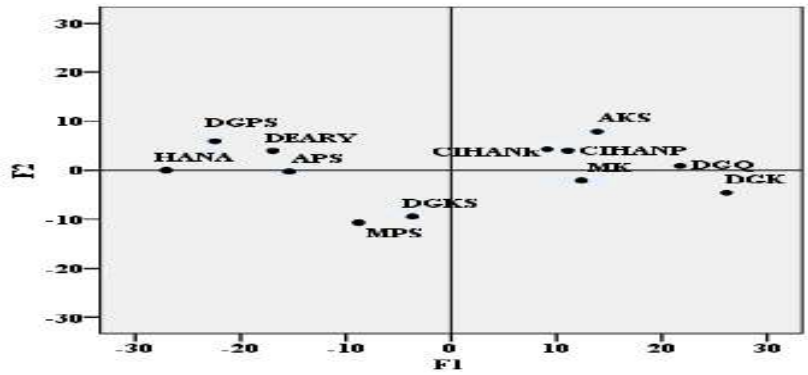

Figure 1. Scatter plot of object of two discriminate function of the all analyses tea samples

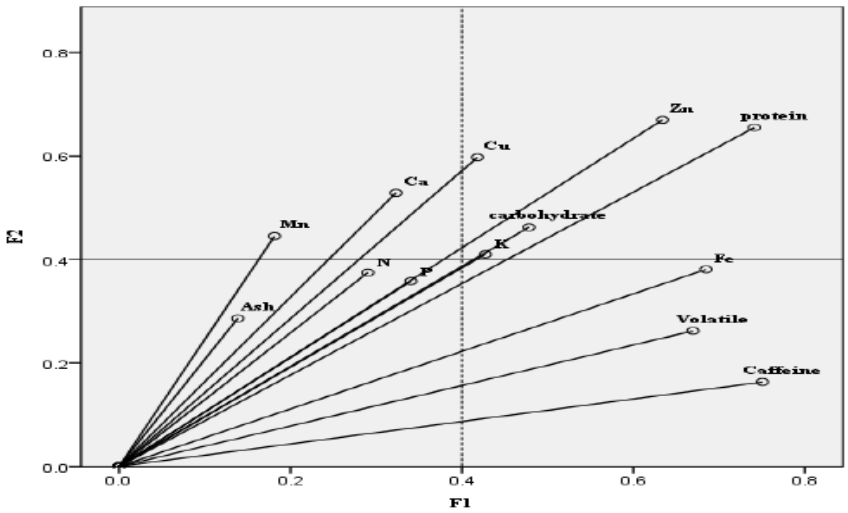

Figure2. Scatter plot of loading for 13 variables of the all analyses tea samples

4. CONCLUSIONS

The statistical analyses show a significant differences of nutrients among tea brands except the Zn show no significant differences. The concentration of Mn in tea brands were ranged between (0.0075-0.0325), the higher concentration was recorded in tea brand 2, while the levels of microelements and macro elements were within the ranged in comparisons with the previous studies except the level of Iron. The concentration of Cu and protein in all tea brands is great importance in respect of quantity, while the carbohydrate shows negative loading. Moreover, the nitrogen has its highest negative loading from the quantity index but also had a positive loading from the quality index. The tea brands 10, 11 and 12 characterized by excellent quality particularly brand 10 .

Acknowledgements

The authors would like to thanks every bodies, for their great assistance and providing all requirements to complete this research.

Conflict of Interest

There is no conflict of interest

References

ALBERTI, G. RAFFAELA B., ANTONELLA P., and MARIA P .2003. Determination of the total concentration and speciation of Al(III) in tea infusions. Journal of Inorganic Biochemistry 97 , 79–88

ALLEN, S. E. 1974. Chemical analysis of ecological materials. Black well scientific publication Osney Mead, Oxford. pp: 64-214

BALENTINE, D. A., WISEMAN, S. A., and BOUWENS, L. C. 1997. The chemistry of tea flavonoids. Critical Reviews in Food Science and Nutrition. 37, 693-704.

CAO, X., ZHAO, G., YIN, M., and LI, J. 1998. Determination of ultratrace rare earth elements by inductively coupled plasma mass spectrometry with microwave digestion and AG50W-X8 cation exchange chromatography. Analyst, 123, 1115–1119.

CHRISTIANE J. D. and EDWARD R. F .2001.A review of latest research findings on the health promotion properties of tea. Journal of Nutritional Biochemistry. 12, 404–421

CIROCKA J. B., MAŁGORZATA. G and PIOTR S .2016. Analytical Assessment of Bio-and Toxic Elements Distribution in Puerh and Fruit Teas in View of Chemometric Approach Biol Trace Elem Res 174,240–250

CZERNICKA M. GRZEGORZ Z., MARCIN B., BOGDAN S., and CZESŁAW P .2017. Study of nutritional value of dried tea leaves and infusions of black, green and white teas from chinese plantations Rocz Panstw. Zakl Hig 68(3),237-245

FERRARA, L., MONTESANOA, D., and SENATORE, A. 2001. The distribution of minerals and flavonoids in the tea plant (Camellia sinensis). II Farmaco, 56, 397–401.

HARA, Y., LUO, S J., WICKREMASHINGHE, R. L., and YAMANISHI, T. 1995. Chemical composition of tea. Food Reviews International, 11, 435-456.

HOLLMAN, P. C. H., HERTOG, M. G. L., and KATAN, M. B. (1996). Analysis and health effects of flavonoids. Food Chemistry, 57, 4-46.

KUMAR, A., NAIR, A. G. C., REDDY, A. V. R., and GARG, A. N. 2005.Availability of essential elements in Indian and US tea brands. Food Chemistry, 89, 441–448.

MARSCHNER, H. 1995. Mineral nutrient of higher plants (2nded.). London: Academic Press.

MEHMET M., O ZCAN A., AHMET U., NVER A., TOLGAUCAR B, and DERYA A. 2008. Mineral content of some herbs and herbal teas by infusion and decoction. Food Chemistry 106 , 1120–1127

MICHAEL YEMANE A B.S. CHANDRAVANSHI B.,AND TADDESE WONDIMU C. 2008. Levels of essential and non essential metals in leaves of the tea plant (Camellia sinensis L.) and soil of Wush farms, Ethiopia. Food Chemistry 107, 1236–1243

MOKGALAKA, N. S., MCCRINDLE, R. I., and BOTHA, B. M. 2004. Multielement analysis of tea leaves by inductively coupled plasma optical emission spectrometry using slurry nebulization. Journal of Analytical Atomic Spectrometry, 19, 1375–1378.

SEENIVASAN S, MANIKANDAN N, MURALEE DHARAN NN,and SELVASUNDARAM R. 2008.Heavy metal content of black teas from South India. Food Control 19,746–749.

STEEL, R.G.D. and TORRIE, J.H. 1969. Principle and Procedures of Statistics. McGraw Hill, New York.481pp

W.S. SHU, Z.Q. ZHANG, C.Y. LAN and, M.H. Wong .2003. Fluoride and aluminium concentrations of tea plants and tea products from Sichuan Province, PR China Chemosphere 52, 1475–1482AKTER, M.

ZANCO Journal of Pure and Applied Sciences
The official scientific journal of Salahaddin University-Erbil
https://zancojournals.su.edu.krd/index.php/JPAS

ISSN (print):2218-0230**, ISSN (online):** 2412-3986**, DOI: http://dx.doi.org/10.21271/zjpas**

RESEARCH PAPER

The influence of plant growth regulators on phytochemical components in the leaves and calyxes of Roselle (*Hibiscus sabdariffa* L.)

Media I. MuhammedAmin[1], Sawsan M. S. Ali Kanimarani[2]

[1]Horticulture department, College of Agricultural Science and Engineering, Salahaddin University-Erbil, Kurdistan Region, Iraq
[2]Horticulture department, College of Agricultural Science and Engineering, Salahaddin University-Erbil, Kurdistan Region, Iraq

A B S T R A C T:
A study was conducted at the open field of Zanco Village, Erbil-Iraq in 2018 to determine the effect of foliar application of some plant growth regulators (IAA, BA and GA_3) on phytochemical components in the leaves and calyxes of Roselle. The investigation was performed as factorial experiment under randomized complete block design with three replications, growth regulators were foliar applied alone or combined treatments as: control, IAA (100 $mg.l^{-1}$) , BA (150 $mg.l^{-1}$), GA_3 (150 $mg.l^{-1}$), IAA (100 $mg.l^{-1}$) + BA (150 $mg.l^{-1}$) , IAA (100 $mg.l^{-1}$) + GA_3 (150 $mg.l^{-1}$), BA (150 $mg.l^{-1}$)+GA_3 (150 $mg.l^{-1}$) and IAA (100 $mg.l^{-1}$) + BA (150 $mg.l^{-1}$) + GA_3 (150 $mg.l^{-1}$). Parameters under study were: Moisture content (%) in the stem and Chlorophyll (spad) (%), Protein (%), Total soluble solid (%), Total flavonoids (mg. g^{-1}), Anthocyanin ($mg.kg^{-1}$), Ascorbic acid (vitamin C) $mg.kg^{-1}$, Genistein ($mg.kg^{-1}$), Hesperetin ($mg.kg^{-1}$) and Myrecetin ($mg.kg^{-1}$), were recorded in the leaves and calyxes of Roselle. Results showed that the highest levels of plant growth regulators in single and combined forms give the highest values of the above-mentioned parameters except treatment 100 $mg.l^{-1}$ IAA caused significant difference only in total flavonoids ($mg.g^{-1}$).

KEY WORDS: *Hibiscus sabdariffa* L., plant growth regulators; phytochemical components; Leaves and Calyxes.
DOI: http://dx.doi.org/10.21271/ZJPAS.32.3.20
ZJPAS (2020) , 32(3);193-199

1.INTRODUCTION

Roselle *Hibiscus sabdariffa* L. is an annual herb belongs to Malvaceae family and cultivated mainly for its leaves, stems, seeds and fruits (Fasoyiro *et al*. 2005). It is an important medicinal plant which is used for curing various degenerative diseases like hypertensions, cancer and inflammatory of liver and kidney (Riaz and Chopra,2018). The bright red and fleshy cup-shaped fruits are the most important part of Roselle plants that can be managed into food and beverages, pharmaceuticals and cosmetic products (Mohamad *et al*. 2011). Plant growth regulators considered as a new generation of agrochemicals
that affects plant growth physiology and influences a plant's natural rhythm when added in small quant-ities, as stated earlier, in certain physiological processes pursuit in plant systems, growth regulators contribute in dynamic utilization of metabolites (Antony *et al.*, 2003).

* **Corresponding Author:**
Media I. MohammedAmin
E-mail: media.mohammedamin@su.edu.krd or sussan_ms@yahoo.com
Article History:
Received: 22/10/2019
Accepted: 15/12/2019
Published:15/06/2020

Among the plant growth regulators, Auxins are primary regulators of plant form. The auxin Indole 3-acetic acid (IAA) is a natural auxin found in the plants and present in a synthetic form, while the cytokinin Benzyladenine (BA) is a synthetic plant regulator (Bidwell, 1979 and Friml, 2003). BA is used to promote branching and increase flower set. Gibberellic acid (GA_3) is known as growth stimulators which mediate many reactions in plants, from germination of seeds to senescence (Mostafa and Abou Al-Hamd, 2011). Moreover, Kadiri *et al.* (1997) show that single and combined growth regulator treatments of 100 $mg.l^{-1}$ IAA, 100 $mg.l^{-1}$ GA3 and 10% and 15% coconut milk significantly increased chlorophyll and vitamin C contents of Okra (*Abelmoschus esculetus* L.) and Roselle (*Hibiscus sabdariffa* L.) Also, Aycock *et al.* (1999) stated that the treatment with cytokinin for Gossypium plants showed a significant yield increases. However, Hassanein *et al.* (2005) noticed that the maximum increase of anthocyanin ($mg.g^{-1}$) in Roselle sepals had been registered in response to 100 $mg.l^{-1}$ of both GA_3 + BA. Mukhtar (2008) noticed that foliar application treatments with 100 $mg.l^{-1}$ IAA, 100 $mg.l^{-1}$ GA3 and 15% coconut milk significantly increased total chlorophyll contents ($mg.g^{-1}$), vitamin C (µg/g) and protein (%) of Roselle. Hayssam *et al.* (2012) discovered that using of GA_3 (10^{-6} M) improve relative water content, Chlorophyll a, b, total Chlorophyll and anthocyanin by comparing to control, when they elaborated the influence of GA_3 on the growth and photosynthetic pigments of Roselle under salt stress in Saudi Arabia. Ramtin *et al.* (2015) showed that by spraying plants via benzyl adenine 50 µM (8.973%) on standard Carnation (*Dianthus caryophyllus* L.), it had more water content which is about two folds more than control (4.426%). Khandaker *et al.* (2018) showed that foliar spray of 60 $mg.l^{-1}$ GA_3 increased chlorophyll (spad) content (47.5) in Okra var. Singa 979, and the highest total soluble solids (TSS) content (2.47% Brix) were recorded for the 90 $mg.l^{-1}$ IAA treatment. Because of the few studies in Iraqi Kurdistan region about the effect of plant growth regulators on the phytochemical components of Roselle (*H. sabdariffa* L.) this study was conducted to theorize the impacts of some plant growth regulators (PGR) on the leaves and calyxes on this of Roselle in Kurdistan environment.

2.MATERIALS AND METHODS

The experiment was carried out during May 22th to December 31th 2018 at Zanco Village open field, Erbil-Iraq to study the effect of foliar spraying of different growth regulators (Indole acetic acid, Benzyle adenine and Gibberillic acid) on chemical constituents of Roselle (*H. sabdariffa* L.). Several soil samples were taken from different locations of field depending on the depth of 0-30 cm (Estefan *et al*., 2013), the soil analysis findings are shown in table (1). Table (2) displays the metrological data analyzed during the experimental phase.

Table (10) Some physical and chemical properties of the soil used in the study*

Properties	Field soil
pH	7.78
Electro conductivity (EC)	0.2 $dS.m^{-1}$
Organic matter	0.01%
Total potassium (K_2O)	176 $mg.l^{-1}$
Clay	25.4%
Silt	25.9%
Sand	48.7%
Soil Texture	Sandy Clay Loam

*Laboratory of Directorate of Research in Erbil/Soil and Laboratories Department.

Table (2) The metrological data during the study periods*

Months	Average Temperature C°		Average Relative Humidity %	Sum of Rain /mm
	Minimum	Maximum		
May	12.25	39.59	43.28	27.60
June	21.60	46.4	21.00	0.00
July	20.43	46.15	15.60	0.00
August	19.69	43.73	17.55	0.00
September	14.91	42.80	18.40	0.0
October	7.07	37.41	37.62	31.3
November	4.95	28.32	70.28	118.6
December	1.16	18.73	80.67	174.2

*Agriculture research center Erbil, Ministry of Kurdistan region.

2.1 Seed sowing and cultivation

The seeds of (*H. sabdariffa* L.) were gained from the research centre of agriculture, Ministry of Agriculture, Erbil- Iraq.

The seeds were dressed by Raxil fungicide (1.5 kg.ton^{-1}) three days before sowing; seeds were sown on May, 22th 2018 (3 seeds. hole^{-1}) with spacing of 40cm between holes and 50 cm between rows. The seedlings at the stage of 3 true leaves were thinned to one plant. hole^{-1}, leaving healthy and uniform seedlings, each plot contains 6 seedlings (Castro *et al*., 2004, Ahmed *et al*., 2011 and Gebremedin, 2015).

2.2 Plant growth regulators treatments

The Plant growth regulators(PGRs) IAA, BA (99.9% supplied by, Transhuman Technologies LTD, London, UK) and GA_3 (90% supplied by, dephyte, Germany). These two levels of each of PGRs (0 and 100 mg.l^{-1}) IAA and (0 and 150 mg.l^{-1}) were dissolved in a few drops of 1N sodium hydroxide (NaOH), (0 and 150 mg.l^{-1}) BA was dissolved in a few drops of 1N hydrochloric acid (HCl) (Pullaiah *et al*., 2017).

2.3 The experiment's description

The experiment was considered a factorial in Randomized Complete Block Design with 3 blocks of 8 experimental units each (120×50 cm) representing single and combined growth regulator treatments, each unit contain 6 plants. The treatments were:

1- control (only distilled water)
2- IAA 100 mg.l^{-1}
3- BA 150 mg.l^{-1}
4- $GA_3$150 mg.l^{-1}
5- IAA (100 mg.l^{-1}) + BA (150 mg.l^{-1})
6- IAA (100 mg.l^{-1}) + GA_3 (150 mg.l^{-1})
7- BA (150 mg.l^{-1}) + GA_3 (150 mg.l^{-1})
8- IAA (100 mg.l^{-1}) + BA (150 mg.l^{-1}) + GA_3 (150 mg.l^{-1}).

The plants were sprayed until they were run – off according to their treatments during evening hours, three spraying times were performed with 15 day intervals, first spraying was 60 days after seed sowing.

The obtained results were analyzed statistically, the means of single effects of plant growth regulators compared by t-test according to "Levene's Test for Equality of Variances", the means of combined effects of plant growth regulators compared by Duncan's Multiple Range Test at 5% probability level (Al-Rawi and Khalaf-Allah,1980). The statistical analysis was carried out using SPSS (Statistical Package for Social Sciences) program (Casanova *et al*., 2004).

2.4 Determination of chemical composition

2.4.1 Moisture content (%):

Moisture content in the stems was determined by moisture meter L606 Wagner (Rev, 2004).

2.4.2 Chlorophyll content (%):

The total content of chlorophyll was measured by SPAD-502 chlorophyll meter, for each data three fully expanded leaves were used before harvesting (Shekhany, 2014).

2.4.3 Protein content (%):

The amount of protein was calculated by multiplying the value of nitrogen by 6.25. Micro kjeldahl was used to determine the nitrogen content of the leaves and calyxes when 300 mg of dried oven sample powder was digested with 5 ml sulfuric acid (98%) and 5 ml hydrogen peroxide (36%) and sodium hydroxide (40%) and boric acid distillation (Guebel *et al.,* 1991).

2.4.4 Total soluble solids (TSS%):

Total soluble solids of leaves and calyxes was measured by using hand refractometer (Atago 8469) as described by (Kim *et al*., 2003).

2.4.5 Total flavonoids (mg.g^{-1}):

The maximum amount of flavonoids in the leaves and calyxes was determined by colorimetric aluminum chloride, using spectrophotometer at the absorbancy of 510 nm, the calculation of flavonoid amounts was computed from calibration curve as total flavonoid equivalent (mg)/ dry weight (g) (Kim *et al*., 2003).

2.4.6 Total anthocyanin content (TAC) (mg.kg^{-1}):

TAC has been calculated by pH-differential anthocyanin pigments undergoing reversible

structural transformations with a change in pH evidenced by markedly different absorption spectra, this method was described by (Sutharut and Sudarat, 2012).

2.4.7 Ascorbic acid (mg.kg^{-1}):

The amount of ascorbic acid in the leaves and calyxes was calculated by the 2,6 dichlorophenol indophenols method as explained (Shintani, 2013).

2.4.8 Genistein, Hesperetin and Myricetin (mg.kg^{-1}):

The active substances (Genistein, Hesperetin and Myricetin) were extracted using the described method by (Obouayeba *et al.*, 2014) and measured the content of the oxidative leaves of the antioxidants through the duration of their retention by HPLC (High-Performance Liquid Chromatography) system by using column C18-ODS (25 cm×4.6 mm).

All chemical analysis was done in laboratory of department of the environment and water, Ministry of Science and Technology, Baghdad-Iraq.

3. RESULTS AND DISCUSSION

3.1 Effect of IAA

The results of table (3) shows that spraying of 100 mg.l^{-1} IAA caused significant difference only in total flavonoids in the leaves of *H. sabdariffa* L. and the highest value was (43.25 mg.g^{-1}). Whereas, no significant differences obtained on moisture contents in the stem and other chemical contents in the leaves and calyxes. There is an agreement in result between the current experiment with those obtained by (Cui *et al*., 2010) they found significant increases in total flavonoids of adventitious *Hypericum perforatum* roots by 0.5 and 1.0 mg.l^{-1} IAA exogenous supplies. Flavonoids are also reasonable candidates for endogenous auxin transport regulators (Jacobs and Rubery, 1988).

Table (3) Effect of IAA on studied components of *H. sabdariffa* L.

Chemical contents	IAA mg.l^{-1}						p-Values		
	0			100					
	stem	leaves	calyxes	Stem	leaves	calyxes	Stem	leaves	calyxes
Moisture content (%)	17.43	-	-	18.79	-	-	0.312	-	-
Chlorophyll (Spad) (%)	-	56.06	-	-	60.97	-	-	0.361	-
Protein (%)	-	28.19	17.48	-	23.24	20.78	-	0.190	0.038
TSS (%)	-	13.35	14.29	-	14.52	15.26	-	0.101	0.053
Total flavonoids (mg.g^{-1})	-	33.74	18.01	-	43.25	20.04	-	0.034	0.114
Anthocyanin (mg.kg^{-1})	-	103.55	716.65	-	111.59	782.24	-	0.125	0.104
Ascorbic acid (mg.kg^{-1})	-	80.38	15.22	-	89.64	16.74	-	0.100	0.050
Genistein (mg.kg^{-1})	-	16.98	29.08	-	19.82	31.32	-	0.052	0.068
Hesperetin (mg.kg^{-1})	-	2.35	4.03	-	3.31	5.22	-	0.060	0.055
Myricetin (mg.kg^{-1})	-	10.35	11.23	-	11.39	13.05	-	0.068	0.054

* Means a statistically significant difference of $P<0.05$ according to "Levene's Test for Equality of Variances"

3.2 Effect of BA

Table (4) presents the effect of BA on water content in the stem and chemical contents in the leaves and calyxes of *Hibiscus sabdariffa* L. it can be seen that BA had significant effects on water content in the stem and all chemical components in the leaves and calyxes except (chlorophyll (%) and protein (%) contents) in the leaves. The highest values (19.53%, 15.21%, 45.77 mg.g^{-1} , 117.02 mg.kg^{-1}, 93.28 mg.kg^{-1}, 20.81 mg.kg^{-1}, 3.61 mg.kg^{-1} and 11.87 mg.kg^{-1}) were obtained for (moisture content (%) in the stem and TSS (%) total flavonoids mg.kg^{-1}, anthocyanins mg.kg^{-1}, ascorbic acid mg.kg-1, genitein, hesperetin and myricetin mg.kg^{-1}) respectively, but for calyxes the highest values were (21.71 %15.59%, 21.22 mg.kg^{-1}, 819.24 mg.kg^{-1}, 17.63 mg.kg^{-1}, 32.30 mg.kg^{-1}, 5.69 mg.kg^{-1} and 13.81 mg.kg^{-1}) for (protein(%) TSS (%), total flavonoids mg.g-1, anthocyanins mg.kg^{-1}, ascorbic acid mg.kg^{-1}, genitein mg.kg^{-1}, hesperetin mg.kg^{-1} and myricetin mg.kg^{-1}) respectively, when 150 mg.l^{-1} BA applied. Similar results recorded by Aycock *et al.* (1999) reported that the yield of cotton plants treated with cytokinin has increased significantly, and with Abdel Latef *et al*., (2009) when they discovered that BA treatment showed noticeable stimulation of the soluble and total carbohydrate content of two Roselle cultivars tested. Moreover, Ramtin *et al.* (2015) revealed that the most water content is gained by spraying Carnation (*Dianthus caryophyllus* L.) plants by BA 50 μM (8.973%)

which was about two folds more than control (4.426%).

Table (4) Effect of BA on studied chemical components of *H. sabdariffa* L.

Chemical contents	BA mg.l^{-1}						p-Values		
	0			150					
	stem	leaves	calyxes	Stem	leaves	calyxes	Stem	leaves	calyxes
Moisture content (%)	16.70	-	-	19.53	-	-	0.030	-	-
Chlorophyll (Spad) (%)	-	59.96	-	-	57.07	-	-	0.597	-
Protein (%)	-	27.52	16.55	-	23.91	21.71	-	0.342	0.000
TSS (%)	-	12.66	13.97	-	15.21	15.59	-	0.000	0.000
Total flavonoids (mg.g^{-1})	-	31.22	16.83	-	45.77	21.22	-	0.001	0.000
Anthocyanin (mg.kg^{-1})	-	98.12	679.65	-	117.02	819.24	-	0.000	0.000
Ascorbic acid (mg.kg^{-1})	-	76.73	14.33	-	93.28	17.63	-	0.000	0.000
Genistein (mg.kg^{-1})	-	15.99	28.09	-	20.81	32.30	-	0.000	0.000
Hesperetin (mg.kg^{-1})	-	2.04	3.56	-	3.61	5.69	-	0.001	0.000
Myricetin (mg.kg^{-1})	-	9.87	10.47	-	11.87	13.81	-	0.000	0.000

* Means a statistically significant difference of $P<0.05$ according to "Levene's Test for Equality of Variances"

3.3 Effect of GA_3 on water content in the stem and chemical contents in the leaves and calyxes of (*H. sabdariffa* L.)

Table (5) shows that the maximum significant amount of moisture content (19.83%) has been registered with 100 mg.l^{-1} GA_3. However, GA_3 treatment caused significant highest values of protein (%), TSS (%), total flavonoids mg.g^{-1}, anthocyanin mg.kg^{-1}, ascorbic acid mg.kg^{-1}, genistein mg.kg^{-1}, hesperetin mg.kg^{-1}and myricetin mg.kg^{-1} in the leaves and calyxes, except protein content in the leaves. Analogous results observed by (Hayssam *et al*., 2011) they discovered that *H. sabdariffa* L. under non-saline condition, application of GA_3 enhanced growth characteristics (relative water content, anthocyanin and photosynthetic pigments (chlorophyll a, b and total chlorophyll). They showed that alleviating effects of GA_3 might be due to its role in the enhancement of carbonic anhydrase CA activity, the enzyme that catalyzes the hydration reversible CO_2 to HCO^{3-}.

Table (5) Effect of GA_3 on studied chemical components of *H. sabdariffa* L.

Chemical contents	GA_3 mg.l^{-1}						p-Values		
	0			150					
	stem	leaves	calyxes	Stem	leaves	calyxes	Stem	leaves	calyxes
Moisture content (%)	16.40	-	-	19.83	-	-	0.008	-	-
Chlorophyll (Spad) (%)	-	51.12	-	-	65.90	-	-	0.003	-
Protein (%)	-	27.77	16.98	-	23.66	21.29	-	0.280	0.005
TSS (%)	-	13.05	14.10	-	14.82	15.46	-	0.010	0.004
Total flavonoids (mg.g^{-1})	-	32.39	17.21	-	44.59	20.84	-	0.005	0.002
Anthocyanin (mg.kg^{-1})	-	100.95	693.21	-	114.19	805.68	-	0.008	0.003
Ascorbic acid (mg.kg^{-1})	-	78.95	14.74	-	91.07	17.22	-	0.008	0.004
Genistein (mg.kg^{-1})	-	16.48	28.47	-	20.32	31.93	-	0.006	0.003
Hesperetin (mg.kg^{-1})	-	2.16	3.75	-	3.49	5.50	-	0.008	0.003
Myricetin (mg.kg^{-1})	-	10.12	10.89	-	11.62	13.39	-	0.005	0.006

* Means a statistically significant difference of $P<0.05$ according to "Levene's Test for Equality of Variances"

3.4 Interaction effects of IAA, BA and GA_3

The impact of IAA, BA and GA_3 on water content in the stem and chemical contents in *H. sabdariffa* L. leaves and calyxes is displayed in table (6). It can be seen that there were significant differences in all chemical content parameters in the plant parts with spraying the three different plant growth regulators. The highest values of moisture content in the stem and chlorophyll (spad), TSS, total flavonoids, anthocyanin, ascorbic acid (vitamin C), genistein, hesperetin and myrecetin in the leaves were (24.97%, 77.13%, 16.20%, 59.67 mg.g^{-1}, 123.57 mg.kg^{-1}, 103.38 mg.kg^{-1}, 25.91 mg.kg^{-1}, 5.61 mg.kg^{-1}and 12.90 mg.kg^{-1} respectively) when sprayed with100 mg.l^{-1} IAA+150 mg.l^{-1} BA+150 mg.l^{-1} GA_3, by the way the highest value for protein (32.34%) was obtained in the leaves with the treatment 0 mg.l^{-1} IAA+150 mg.l^{-1} BA+150 mg.l^{-1} GA_3, also, this treatment gave the highest values in the calyxes for protein, TSS, total flavonoids, anthocyanin, ascorbic acid (vitamin C), genistein, hesperetin and myrecetin (25.10%, 16.31%,24.73 mg.g^{-1}, 896.41 mg.kg^{-1}, 19.36 mg.kg^{-1}, 35.71 mg.kg^{-1}, 7.05 and 15.89 mg.kg^{-1} respectively). As we noticed, chemical contents of calyxes were superior in comparison with leaves. The rise in phenol content can be due to the increase in carbohydrate synthesis by application BA and or GA_3 (Sadak, 2005). Similar results have been reported by Hassanein *et al*. (2005) showing that

by applying the similar concentration of GA_3 and/or BA on Roselle calyxes, the anthocyanin content would increase significantly when the maximal value was reported at 100 $mg.l^{-1}$ of both GA3 + BA, this result was referred to as an increase in the activity of phenylalanine ammonia lyase and tyrosine ammonia lyase in Roselle's shoot. Also, it is in agreement with Mukhtar (2008) when he found that total chlorophyll (%), vitamin C $mg.kg^{-1}$ and protein (%) content were increased with 100 $mg.l^{-1}$ IAA, 100 $mg.l^{-1}$ with 15% coconut milk. Moreover, our results are partially similar with those found by Hayssam *et al.* (2011) on chlorophyll *a, b,* total chlorophyll and anthocyanin the best results were obtained with GA_3 as compared to control. In comparison of our study other researches were obtained similar results, (Khandaker *et al.* 2018) best result of chlorophyll (spad) content obtained with 60 $mg.l^{-1}$ GA3, and highest TSS content (2.47% Brix) was in the 90 $mg.l^{-1}$ IAA treatment.

Table (6) Effect of IAA, BA and GA_3 on studied chemical components of *H. sabdariffa* L.

Treatments			Chlorophyll (Spad) (%)	Moisture content (%)	Chemical contents															
					Protein (%)		TSS (%)		Total Flavonoids ($mg.g^{-1}$)		Anthocyan-in ($mg.kg^{-1}$)		Ascorbic acid (Vitamin C) ($mg.kg^{-1}$)		Genistein ($mg.kg^{-1}$)		Hesperetin ($mg.kg^{-1}$		Myricetin mg.kg-1	
IAA $mg.l^{-1}$	BA $mg.l^{-1}$	GA_3 $mg.l^{-1}$			Leaves	Calyxes	Leaves	Calyxes	Leaves	Calyxes	Leaves	Calyxes	Leaves	Calyxes	Leaves	Calyxes	Leaves	Calyxes	Leaves	Calyxes
0	0	0	64.90 e	15.67 d	24.20 f	14.17 h	11.38 h	12.33 h	25.09 h	14.48 h	85.83 h	600.42 h	68.96 h	12.36 h	13.59 h	25.70 h	1.26 h	21.17 h	8.60 h	8.59 h
	150		52.43 f	19.87 b	28.00 d	15.78 f	12.39 f	14.28 f	30.67 f	17.59 f	100.16 f	702.38 f	76.21 f	14.93 f	16.59 f	28.42 f	2.18 g	3.79 f	10.13 f	10.61 f
	0	150	36.73 h	15.27 d	28.25 d	16.62 e	13.81 e	14.64 e	31.53 e	18.63 e	108.45 e	723.50 e	79.23 e	15.35 e	17.40 e	29.30 e	2.34 f	4.08 e	10.59 e	11.49 e
	150		70.17 b	18.93 c	32.34 a	23.36 b	15.81 b	15.95 b	47.69 b	21.36 b	119.77 b	840.31 b	97.10 b	18.23 b	20.35 b	32.80 b	3.60 c	6.07 b	12.09 b	14.24 b
100	0	0	58.60 e	15.73 d	27.10 e	15.34 g	11.99 g	13.97 g	28.77 g	15.58 g	93.25 g	632.18 g	74.20 g	13.66 g	15.36 g	27.49 g	2.14 g	3.18 g	9.38 g	9.89 g
	150		63.90 d	15.53 d	30.81 c	20.92 d	14.87 d	15.29 d	40.36 d	19.68 d	113.25 d	783.63 d	87.57 d	16.36 d	18.42 d	30.78 d	2.59 e	5.09 d	11.38 d	12.81 d
	0	150	44.23 g	18.93 c	31.54 b	21.78 c	15.03 c	15.47 c	44.19 c	20.16 c	116.28 c	816.74 c	93.42 c	17.59 c	19.58 c	31.31 c	2.89 d	5.56 c	11.81 c	13.61 c
	150		77.13 a	24.97 a	3.50 g	25.10 a	16.20 a	16.31 a	59.67 a	24.73 a	123.57 a	896.41 a	103.38 a	19.36 a	25.91 a	35.71 a	5.61 a	7.05 a	12.90 a	15.89 a

* Values within each column followed with the same letters are not significantly different from each other according to Duncan's Multiple Range Test at the (0.05) level.

4. CONCLUSIONS

It is concluded that the application of 100, 150 and 150 $mg.l^{-1}$ of IAA followed by BA and GA_3 individually or in combination increased the studied phytochemical contents in leaves and calyxes of Roselle plant.

References

ABDEL LATEF, A. A., SHADDAD, M. A. K., ISMAIL, A. M. & AHMAD, M. F. A. 2009. Benzyladenine can alleviate saline injury of two roselle (*Hibiscus sabdariffa*) cultivars via equilibration of cytosolutes including anthocyanins. *Int. J. Agric. Biol,* 11, 151-157.

AHMED, Y.M., E.A. SHALABY & N.T. SHANAN, 2011. The use of organic and inorganic cultures in improving vegetative growth, yield characters and antioxidant activity of Roselle plants *(Hibiscus sabdariffa L.). Afr. J. Biotech.*, 10, 1988-1996.

ALI, H.M., SIDDIQUI, M.H., BASALAH, M.O., AL-WHAIBI, M.H., SAKRAN, A.M. & AL-AMRI, A., 2012. Effects of gibberellic acid on growth and photosynthetic pigments of *Hibiscus sabdariffa* L. under salt stress. African Journal of Biotechnology, 11, 800-804.

AL-RAWI, K.M. & KHALAF-ALLA, A. 1980. *Agriculture Experimental Design and Analysis*. Dar Al-Kutub for printing and publishing. Mosul - Iraq. (In Arabic).

ANTONY E, CHOWDHURY S.R. & KAR, G. 2003. Variations in heat and radiation use efficiency of green gram as influenced by sowing dates and chemical sprays. *Journal of Agrometeorology*, 5, 58-61.

AYCOCK, B., DUGGER, P. & RICHTER, D. 1999. Super start, Sul-15, GS-48 and GS-70 plant growth regulators carried with foliar fertilizers for cotton production. Proceedings of the Belt-Wide Cotton Conference, (BWCC'99), *Orlando, Florida, USA, Jan*, 1,71-73.

BIDWELL, R. G. S. 1979. *Plant physiology*. Second Edition. MacMillan Publishing Co, Inc, New York.

CASANOVA, E., VALDES, A.E., FERNANDEZ, B., MOYSSET, L. & TRILLAS, M.I. 2004. Levels and immunolocalization of endogenous cytokinins in thidiazuron-induced shoot organogenesis in carnation. *Journal of Plant Physiology*, 161, 95-104.

CASTRO, N.E.A, PINTO, J.E, CARDOSO, M.G, MORAIS, A.R, BERTOLUCCI, S.K.V, SILVA, F.G. & DELU FILHO, N. 2004. Planting time for maximization of yield of vinegar plant calyx (*Hibiscus sabdariffa* L.). Ciênc agrotec, 28, 542-551.

CUI, X.H., CHAKRABARTY, D., LEE, E.J. & PAEK, K.Y. 2010. Production of adventitious roots and secondary metabolites by *Hypericum perforatum* L. in a bioreactor. *Bioresour. Technology,* 101, 4708-4716.

ESTEFAN, G., SOMMER, R. & RYAN, J. 2013. *Methods of soil, plant, and water analysis: A manual for the west, Asia and North Africa region*. 3rd ed. ICARDA, Beirut, Lebanon.

FASOYRO, S.B., ASHAYE, O.A., ADEOLA, A. & SAMUEL, F.O. 2005. Chemical and storability of fruit flavoured (*Hibiscus*

sabdariffa) drinks. *World J. Agric. Sci*, 1, 165-168.

FRIMIL, J. 2003. *Auxin transport—shaping the plant*. Current Opinion in Plant Biol, 6, 7–12.

GEBREMEDIN, B., 2015. Influence of Variety and Plant Spacing on Yield and Yield Attributes of Roselle (*Hibiscus sabdariffa* L.). *Science, Technology, and Arts Research Journal*, 4, 25-30.

GUEBEL, D.V., NUDEL, B.C. & GIULIETTI, A.M. 1991. A simple and rapid micro-Kjeldahl method for total nitrogen analysis. *Biotechnology Techniques*, 5, 427–430.

HASSANEIN, R.A., HEMMAT, K.I., KHATTAB, H.K.I. & SADAK, M.S. 2005. Increasing the Active Constituents of Sepals of Roselle (*Hibiscus Sabdariffa* L.) Plant by Applying Gibberellic Acid and Benzyladenine. *J. Appl. Sci. Res*, 1, 137-146.

JACOBS, M., & RUBERY, P. H. 1988. Naturally occurring auxin transport regulators. *Science*, 241, 346-349.

KADIRI, M., MUKHTAR, F. & AGBOOLA, D.A. 1997. Responses of some Nigerian vegetables to plant growth regulator treatments. *Rev. Biol. Trop*, 44 / 45, 23-28.

KHANDAKER, M. M., AZAM, H. M., ROSNAH, J., TAHIR, D. & NASHRIYAH, M. 2018. The effects of application of exogenous IAA and GA3 on the physiological activities and quality of Abelmoschus esculentus (Okra) var. Singa 979. *Pertanika Journal of Tropical Agricultural Science*, 41, 209-224.

KIM, D.O., JEONG, S. W. & LEE, C. Y. 2003. Antioxidant capacity of phenolic phytochemicals from various cultivars of plums. *Food Chem*, 81, 321-326.

MOSTAFA, G. G. & ABOU ALHAMD, M. F. 2011. Effect of Gibberellic Acid and Indole 3-acetic Acid on Improving Growth and Accumulation of Phytochemical Composition in Balanites aegyptiaca Plants. *American Journal of Plant Physiology*, 6, 36-43.

MUKHTAR, F.B. 2008. Effect of Some Plant Growth Regulators on the Growth and Nutritional Value of *Hibiscus sabdariffa* L. (Red sorrel). *Int. Jor. P. App. Scs*, 2, 70–75.

OBOUAYEBA, A.P., DJYH, B. N., SEKOU, D. & JOSEPH, D. 2014. Phytochemical and antioxidant activity of Roselle (*Hibiscus Sabdariffa* L.) petal extracts. Journal of Pharmaceutical, Biological and Chemical Sciences, 5, 1453-1465.

OSMAN, M., FARUQ, G., SABERI, S., ABDUL MAJID, N., NAGOOR, N. H. & ZULQARNAIN, M. 2011. Morpho-agronomic analysis of three roselle (*Hibiscus sabdariffa* L.) mutants in tropical Malaysia. Australian Journal of Crop Science, 5, 1150-1156

PULLAIAH, T., SUBBA RAO, M.V. & SREEDEVI, E. 2017. *Plant Tissue Culture: Theory & Practicals*, 2nd Ed. Jodhpur: Scientific Publishers.

RAMTIN, A., S. KALATEJARI, NADERI, R. & MATINIZADEH, M. 2015. Effect of Pre-Harvest Foliar Application of Benzyl Adenine and Salicylic Acid on Carnation Cv. Spray and Standard, *Biological Forum – An Int. J.*, 7, 955-958.

REV, B. 2004. Wepi wagner part.Wagner Electronicproducts, Inc. #500-60601-002. http://www.wagnermeters.com

RIAZ, G. & CHOPRA, K. 2018. A review on phytochemistry and therapeutic uses of *Hibiscus sabdariffa* L. Biomedicine and Pharmacotherapy,102, 575-586.

SADAK, M.S., 2005. *Physiological studies on the interaction effects of gibberellic acid and benzyladenine on Roselle (Hibiscus sabdariffa L.) plant*. Ph.D. Thesis, Faculty of Science, Ain Shams University, Egypt.

SHEKHANY, H.K.A. 2014. *Influence of magnetized w`sw2ater on the ability of nutrient uptake and the growth of two cultivars of Pistachio (Pistacia vera L.) seedlings*. M.Sc. thesis, University of Salahaddin.

SHINTANI, H., 2013. HPLC Analysis of Ascorbic Acid (Vitamin C). *Pharmaceutica Analytica Acta*, 4, 1000234.

SUTHARUT, J. & SUDARAT J. 2012. Total Anthocyanin Content and Antioxidant Activity of Germinated Colored Rise, *International Food Research Journal*, 19, 215-221.

ZANCO Journal of Pure and Applied Sciences
The official scientific journal of Salahaddin University-Erbil
https://zancojournals.su.edu.krd/index.php/JPAS

ISSN (print):2218-0230**, ISSN (online):** 2412-3986**, DOI: http://dx.doi.org/10.21271/zjpas**

RESEARCH PAPER

Effect of Commercial Baker's Yeast Supplementation (*Saccharomyces Cerevisiae*) in Diet and Drinking Water on Productive Performance, Carcass Traits, Haematology and Microbiological characteristics of Local Quails

Rebin A. Mirza[1], Sheren Dh. Muhammad[1] and Karwan Y. Kareem[1]

[1] Department of Animal Resource, College of Agricultural Engineering Sciences, Salahaddin University-Erbil, Kurdistan Region, Iraq

A B S T R A C T:

The research was conducted to assess the impact of supplementation of *Saccharomyces cerevisiae* (SC) on the quality of products, intestinal microbiota, haematology parameters and histology of local quail. A number of 99 days old quails were randomly assigned and divided into three treatments in triplicate which contained 33 birds in each treatment for 42 days experimental period. Design of the dietary treatments was formulated as followings; control (T1) basal diet, 1% of SC in basal diet (T2) and 1% of SC in drinking water (T3). The results of this study revealed that addition and supplementation of SC had positive impact on blood biochemical profile and products quality of local quails. The contents of beneficial bacteria (*Lactobacillus* spp.) in caecal digesta was increased in both treatment of adding SC in diet and drinking water, while the coliform bacteria significantly ($p<0.05$) decreased in comparison to the control group. Also, Supplementation of SC in diet and drinking water substantially increased number of lymphocyte and lowered H/L (Heterophil/Lymphocyte) ratio comparing to control treatment at the final stage of the study. No significant ($p>0.05$) differences was seen regarding carcass traits of the treated quails. To summarize, baker's yeast supplementation in the diet and drinking water of quails substantially improved production performance, gut microbiota and hematology parameters of local quails.

KEY WORDS: Quail, Yeast, Performance, Gut microbiota, Haematology
DOI: http://dx.doi.org/10.21271/ZJPAS.32.3.21
ZJPAS (2020) , 32(3);200-205 .

1.INTRODUCTION :

Japanese quails (Coturnix coturnix japonica) have been of great interest among academics and poultry breeders recently since it is small in size, comforting to handle, a high number can be breed in a limited area and possesses high ability in egg production.

Yeast and yeast product derivatives have being fed to farm animals for more than ten decades (Owens and McCracken, 2007). Baker's yeast "*Saccharomyces cerevisiae*" is one of the popular widely commercialized types of yeast (Rezaeipour *et al.*, 2012). Yeasts are most widely used natural growth promoters (Mohamed *et al.*, 2015) because of its natural digestibility improving traits; nutrients absorption ability and enteric pathogens infection control (Gao *et al.*, 2005). Yeasts are probiotics act by competitive exclusion, controlling gut pH, beneficially alter the inherent gut microbiota, lysozyme and peroxides, inhibit

* **Corresponding Author:**
Rebin A. Mirza
E-mail: rebin.mirza@su.edu.krd
Article History:
Received: 19/08/2019
Accepted: 13/01/2020
Published: 15/06 /2020

the effects of toxins and improve the immune system (Grashorn, 2010).

The composition of yeast cell wall sugar consist of 30-60% polysaccharides (15-30% of β-1,3/1,6-glucan and 15-30% of mannan sugar polymers), 15-30% proteins, 5-20% lipids. The Beta-1, 3/1, 6-glucans that present in yeast cell wall was commonly known for a its immune modulator substance in poultry and humans (Noppawat *et al*., 2017).

The objective of the research was to examine the influence of commercial baker's Yeast (*Sachharomyces Cerevisiae)* supplementation in diet and drinking water on productive performance, haematology and microbiological traits of local quails.

2. MATERIALS AND METHODS

2.1. Experimental design

This research was carried out in Salahaddin University, College of Agriculture, Kurdistan Region, Erbil. This experiment is designed to investigate the influence of supplementation Baker's yeast (*Saccharomyces Cerevisiae)* in drinking water and diet on productive performance, carcass traits, microbiological and haematology parameters of Japanese quails. Ninety nine quails at 1 week of age were randomly registered into three treatments in triplicates containing 11 quail each, as CON= Control no baker's yeast in feed and water, Diet= adding 1% baker's yeast in commercial broiler diet, and Water= adding 1% baker's yeast in drinking water, for 42 days. The quails were scaled and kept in floor pens (60 × 60 cm), on wood shavings. The quails also designed in away to have full access to drinking water and feed.

2.2 Growth performance

During the whole study period the basic productive performance indicators includes body weight, weight gain, feed intake and conversion ratio, and European production efficacy factor was measured. Also, dressing percentage, weight of breast and leg were measured.

2.3 Haematology parameters

At the final stage of the experiment three quails from each treatment were randomly selected and killed by cervical dislocation. The blood samples were kept in fully sterilized tubes with presence anticoagulant Di-Potassium ethylene diamine tetra acetic acid (K_2EDTA). All parameters related to blood (Hemoglobin, WBC, Lymphocyte, Heterophil and H/L ratio) were examined by Full-Auto Haematology Analyzer (MCL 3800, China). (Pelicano *et al*., 2005; Baurhoo *et al*., 2007).

2.4 Gut microbiota analysis

At the end of experimentally designed period, the quails were taken from treatments and their caecal digesta were fully aseptically separated to investigate the intestinal microorganisms (*Lactobacillus* spp. and total coliform bacteria). Subsequently, these suspensions were serially diluted from 10^{-1} to 10^{-9}. For each dilution, 0.1 ml from the dilution was plated onto sterile selective medium agar to count targeted bacteria groups as following; MacConkey agar (Sigma-Aldrich, UK) for total coliform and MRS (De Man, Rogosa and Sharpe) agar for *Lactobacillus* spp.. The colonies number of microbial was then counted to determine the colony forming units (CFU). CFU/gm for fresh caecal digesta were calculated and expressed as logarithms.

2.5 Statistical Analysis

The data obtained in the experiments were statistically analyzed using one-way ANOVA test, SPSS program (Statistical Package for Social Science) (SPSS 22, 2005). Descriptive statistics aided for the analysis of the data. Therefore, means and stander error were calculated. Duncan test utilized and aided to calculate significant differences at 0.05 levels among the various parameters (Duncan, 1995).

3. RESULTS

Growth performance data is presented in Table 1. There were no significant ($p>0.05$) differences observed among treatments in relation to total feed intake. While, Final

weight, FCR and EPEF were improved significantly ($p<0.05$) when SC added in water and diet compared to control group. Carcass traits are shown in Table 2. There was no significant ($p>0.05$) difference observed among treatments on carcass traits.

Table 3 shows the influence of SC supplementation in diet and drinking water on the composition of microflora in the caecum digesta at 42 days of age. Both administrations of SC supplementation noticeably ($p<0.01$) increased number of *Lactobacillus* spp. and lowered number of coliform bacteria in comparison to control group.

Table 4 shows the impact of commercial baker's yeast supplementation in diet and drinking water on haematological parameters at six weeks of age. Both administration of SC supplementation were significantly ($p<0.05$) increased the number of Lymphocyte and lowered the number of heterophil in comparison with control group. Also, the H/L ratio parameter was improved by both administration of SC supplementation compared to control group. While, no significant ($p>0.05$) differences was observed among treatments on haemoglobin and WBCs traits.

4. DISCUSSION

The current research might confirm the positive impact of yeast supplementation *Saccharomyces cerevisiae* (SC) as novel probiotic in feeding diet and drinking water on growth rate, intestinal microflora and haematology.

This positive influence could directly be attributed to improvements in performance of birds. To the researchers' best knowledge, dissimilar microbial species of probiotics have been utilized in poultry production (Mountzouris *et al*., 2010; Patterson and Burkholder, 2003). Regarding broiler nutrition, probiotic species *Streptococcus, Bacillus, Aspergillus, Lactobacillus, Enterococcus, Bifidobacterium ,Saccharomyces* and *Candida* have shown positive impact on broiler performance (Zulkifli *et al*., 2000; Kalavathy *et al*., 2003; Kabir *et al*., 2004; Gil De Los Santos *et al*., 2005). This might be attributed to modulation of intestinal microflora and pathogen inhibition (Pascual *et al*., 1999).

In the current study, the data showed in table 1, indicates that supplementation of SC significantly enhanced better body weight gain when SC added to diet only, feed conversion ratio and EPEF (European production efficacy factor). This positive enhancements in feed conversion efficiency has also been reported by previous researchers (Zeweil, 1997; Chumpawadee *et al*., 2009; Devarestti, 2016).

Supplementation of SC in both diet and drinking water has also led to higher lactobacilli and the lower coliform bacteria comparing to control. This might be related to increasing the production of short chain fatty acids and lowering pH value in the intestine since it possesses bacteriostatic and bactericidal properties (Fuller, 2001).

It has also been reported that SC can stimulate the immune system of the bird against pathogenic bacteria, especially *Salmonella*, *E. coli* and *Clostridiunz* (Ghadban, 2002) and reduces bird mortality chances (Kralik *et al*., 2004).

It has been studied that presence of stress could lead to stimulate the adrenal gland to excrete stress hormones which posses influential impact to analyze a lymphatic cell and then lead to a rise in H/L ratio (Gross and Siegel, 1983). Therefore, ratio of H/L can be taken as a sign for the wellbeing of animals and any rise in H/L automatically refers to presence of high stress (James and Stanley, 1989). In the current research, the H/L ratio at the end of experiment was decreased for both yeast supplementation in comparison with the control group. Low H/L ratio in the treatments might be associated with the yeast supplementation in both diet and drinking water which could diminish the nutritional stress or any stress which causes an increase in H/L ratio (Karoglu and Drudage, 2005).

Table 1: Effect of Commercial Baker's Yeast Supplementation in Diet and Drinking Water on growth performance of local quails at six weeks of age (Mean ±SE).

Growth performance	Treatment			P. value
	CON	Diet	Water	
Initial weight (g)	24.10±0.42 a	24.26±0.34 a	24.85±0.13 a	0.992
Final weight (g)	213.13±3.84 b	236.33±6.38 a	222.76±3.71 ab	0.026
Weight gain (g/bird)	189.03±0.54 b	211.97±4.19 a	197.91±1.67 b	0.002
Feed intake (g/bird)	498.62±12.71 a	500.10±8.04 a	467.56±5.84 a	0.083
Feed convention ratio	2.63±0.06 a	2.36±0.08 b	2.36±0.02 b	0.034
(EPEF) [1]	129.25±5.24 b	129.88±1.24 a	121.83±0.83 a	0.213

[ab] Data in the same row with different superscript are significantly different (P<0.05).
[1] EPEF = liveability (%) × live weight (kg) × 100/ age (d) × FCR.

Table 2: Effect of Commercial Baker's Yeast Supplementation in Diet and Drinking Water on dressing parameters of local quails at six weeks of age (Mean ±SD).

Parameters	Treatment			P. value
	CON	Diet	Water	
Dressing Percentage	72.74±0.37 a	73.45±0.60 a	73.08±0.25 a	0.55
Leg (%)	27.0±2.0 a	30.32±2.42 a	28.46±1.26 a	0.524
Brest (%)	46.04±1.72 a	49.05±1.82 a	48.96±1.34 a	0.398

[ab] Data in the same row with different superscript are significantly different (P<0.05).

Table 3: Effect of Commercial Baker's Yeast Supplementation in Diet and Drinking Water on caecal microbiota of local quails at six weeks of age (Mean ±SD).

Microbes	Treatment			P. value
	CON	Diet	Water	
Lactobacillus ssp.	8.72±0.15 b	9.43±0.16 a	9.30±0.13 a	0.033
Total Coliform	7.19±0.03 b	6.89±0.04 a	6.94±0.05 a	0.007

[ab] Data in the same row with different superscript are significantly different (P<0.05).

Table 4: Effect of Commercial Baker's Yeast Supplementation in Diet and Drinking Water on Haematological parameters of local quails at six weeks of age (Mean ±SE).

Parameters	Treatment			P. value
	CON	Diet	Water	
Haemoglobin (g/L)	135.80±13.29 a	170.06±9.91 a	150.46±2.02 a	0.115
WBC (No.×10^9/L)	3.76±0.84 a	6.5±1.21 a	5.7±0.72 a	0.183
Lymphocyte (%)	69.56±1.53 b	79.23±1.59 a	76.86±1.83 a	0.015
Heterophil (%)	23.33±0.88 c	13.66±0.17 a	16.66±0.66 b	<0.001
H/L ratio (%)	0.33±0.01 c	0.16±0.003 a	0.21±0.008 b	<0.001

[ab] Data in the same row with different superscript are significantly different (P<0.05).

5. CONCLUSIONS

Yeast supplementation could possess positive influence the gut microbiota and hence improve health and performance of quails. The current study confirms that the supplementation of baker's yeast (*Saccharomyces cerevisiae*) as a probiotic in diet and drinking water significantly improved the growth ratio and performance, gut microbiota and blood haematology parameters of local quails.

Conflict of Interest (1)

None

References

BAURHOO, B., PHILLIP L. & RUIZ-FERIA C. A. 2007. Effects of Purified Lignin and Mannan Oligosaccharides on Intestinal Integrity and Microbial Populations in the Ceca and Litter of Broiler Chickens. *Poultry Science*, 86:1070–1078.

CHUMPAWADEE S, CHANTIRATIKUL A. & SANTAWEESUK S. 2009. Effect of dietary inclusion of cassava yeast as probiotic source on egg production and egg quality of laying hens. *International Journal of Poultry Science*. 8:195-199.

DEVARESTTI, A. K. 2016. Effect of dietary yeast on the performance and biochemical profile in Japanese quails. *International Journal of Veterinary Sciences and Animal Husbandry*. 1(2): 27-29

DUNCAN, D. B. 1995. Multiple range and Multiple F test. Bometrics . 11:1-42.

FULLER, R. 2001. The chicken gut microflora and probiotic supplements. *Journal of Poultry Science*, 38: 189-196.

GAO, J, ZHANG HJ, YU SH, WU SG, YOON I, QUIGLEY J, GAO YP & QI GH. 2008. Effects of yeast culture in broiler diets on performance and immunomodulatory functions. *Poultry Science*, 87:1377-1384.

GHADBAN, G. S. 2002. Probiotics in broiler nutrition – a review. Arch. Geflugelk. 66:49-58.

GIL DE LOS SANTOS, J.R., STORCH O.B. & GIL-TURNES C. 2005. *Bacillus cereus* var. toyoii and *Saccharomyces boulardii* increased feed efficiency in broilers infected with Salmonella Enteritidis. *British Poultry Science*, 46, 494-497.

GRASHORN, M.A., 2010. Use of phytobiotics in broiler nutrition– an alternative to infeed antibiotics. *Journal of Animal and Feed Science*, 19, 338-347.

GROSS, W. B. & SIEGEL H. S. 1983. Evaluation of heterophile/lymphocyte ratio as a measure of stress in chickens. *Avian Disease*, 27: 972-979.

JAMES, M. & STANLEY E. C. 1989. Multiple Concurrent Stressors in Chicks.: 3. Effects on Plasma Corticosterone and the Heterophil:Lymphocyte Ratio. *Poultry Science*, 68:522-527.

KABIR, S.M.L., RAHMAN M.M., RAHMAN M.B., RAHMAN M.M. & AHMED S.U. 2004. The dynamics of probiotics on growth performance and immune response in broilers. *International Journal of Poultry Science*, 3:361–364.

KALAVATHY R, ABDULLAH N, JALALUDIN S. & HO Y.W. 2003. Effects of *Lactobacillus* cultures on growth performance, abdominal fat deposition, serum lipids and weight of organs of broiler chickens. *British Poultry Science*, 44: 139-144.

KAROGLU, M. & DURDAG H. 2005. The influence of dietary probiotic (*Sacchromyces cerviciae*) supplementation and different slaughter age on the performance, slaughter and carcass properties of broiler. *International Journal of Poultry Science*, 4:309-316

KRALIK, G., MILAKOVIC Z. & LVANKOVIC S. 2004. Effect of probiotics supplementation on the performance and the composition of the intestinal microflora in broilers. *Act Agraria Kaposvariensis*, 8: 23-31.

MOHAMED, E., TALHA E., MOJAHID A. & DAFAALLA E. 2015. Effect of Dietary Yeast (*Saccharomyces cerevisiae*) Supplementation on Performance, Carcass Characteristics and Some Metabolic Responses of Broilers. *Animal and Veterinary Sciences*, 3(5-1): 5-10.

MOUNTZOURIS, K. C., TSITRSIKOS P., PALAMIDI I., ARVANITI A., MOHNL M., SCHATZMAYR G. & FEGEROS K. 2010. Effects of probiotic inclusion levels in broiler nutrition on growth performance, nutrient digestibility, plasma immunoglobulins, and cecal microflora composition. *Poultry Science*, 89 (1): 58-67.

NOPPAWAT, P., BHAGAVATHI S., SASITHORN S., SARTJIN P., PERIYANAINA K., KHONTAROS C. & CHAIYAVAT C. 2017. Extraction of β-glucan from *Saccharomyces cerevisiae*: Comparison of different extraction

methods and in vivo assessment of immunomodulatory effect in mice. *Food Science and Technology*, 37(1): 124-130.

OWENS, B. & MCCRACKEN K. J. 2007. A comparison of the effects of different yeast products and antibiotic on broiler performance. *British Poultry Science*, 48: 49-54.

PASCUAL, M., HUGAS M., BADIOLA J.I., MONFORT J.M. & GARRIGA M. 1999. *Lactobacillus salivarius* CTC2197 prevents *Salmonella enteritidis* colonization in chickens. *Applied and Environmental Microbiology*, 65: 4981-4986.

PELICANO, E.R.L., SOUZA P.A., SOUZA H.B.A., FIGUEIREDO D.F., BOIAGO M.M., CARVALHO S.R. & BORDON V.F. 2005. Intestinal mucosa development in broiler chickens fed natural growth promoters. *Brazilian Journal of Poultry Science*, 7 (4): 221- 229.

PATTERSON, J.A. & BURKHOLDER, K.M. 2003. Application of prebiotics and probiotics in poultry production'. *Poultry Science*, 82:627-631.

REZAEIPOUR V, FONONI H. & IRANI M. 2012. Effects of dietary L-threonine and *Saccharomyces cerevisiae* on performance, intestinal morphology and immune response of broiler chickens. South African *Journal of Animal Science*, 42: 266-273.

ZEWEIL, H.S. 1997. Evaluation of using some feed additives in growing Japanese quail diets. *Journal of Agricultural Science*, (11):3611-3622.

ZULKIFLI, I., ABDULLAH N., AZRIN N.M. & HO Y.W. 2000. Growth performance and immune response of two commercial broiler strains fed diets containing *Lactobacillus* cultures and oxytetracycline under heat stress conditions. *British Poultry Science*, 41:593-597.

ZANCO Journal of Pure and Applied Sciences
The official scientific journal of Salahaddin University-Erbil
https://zancojournals.su.edu.krd/index.php/JPAS

RESEARCH PAPER

Bioremediation of Oily Wastewater by Using of Bacteria (*Bacillus subtilis)*

Shahd F. Hussein[1], Siraj M. A. Goran[2]

[1] Department of Environmental Sciences, College of Science, Salahaddin University-Erbil, Kurdistan Region, Iraq
[2] Department of Environmental Sciences, College of Science, Salahaddin University-Erbil, Kurdistan Region, Iraq

A B S T R A C T:

This paper is trying to arrange to develop the efficiency of the wastewater treatment system of a petroleum refinery (Namely KAR Refinery) by using bacterial (Bacillus subtile) bioremediation treatment. Wastewater samples have been collected from system output from October 2018 to March 2019. After the collection of the sample, the author treated the samples by adding different weights of powder bacteria (5,10, and 15gm) to 10 L of wastewater samples. Oily wastewater samples were examined before and afterward treatment for phosphate (PO_4), total hardness, ammonia (NH_4), chloride (CL^{-1}), and analysis for hydrocarbons by using GC-MS. The results indicated the effectiveness of 15 gm of powder bacteria's best use of wastewater bioremediation technique caused a decrease in the value of hydrocarbon affectedly.

Keywords: bioremediation, degradation, bacteria, hydrocarbons, oil wastewater.
DOI: http://dx.doi.org/10.21271/ZJPAS.32.3.22
ZJPAS (2020) , 32(3);206-223

1. INTRODUCTION

Crude oil has been defined as an extremely mixture of hydrocarbons, paraffin, and aliphatic compounds with oxygen, nitrogen, compounds containing variable amounts of sulfur and other substances including organic and inorganic minerals (Acuna-Arguelles *et al.*,2003). Crude oil consists of a group of hydrocarbon compounds that are chemically distinct and necessitate reactive mechanisms for initiation and consumption (Arafa, 2003).

* **Corresponding Author:**
Rebin A. Mirza
E-mail: rebin.mirza@su.edu.krd
Article History:
Received: 27/10/2019
Accepted: 13/02/2020
Published: 15/06 /2020

Beside fact of the negative side of petroleum caused yet oil still is an important factor in all the sectors of any country's economy input for sustainable development of the country. However. Those side effects from the process of refinement oil should not be ignored (Thabit, T.H. and Jasim, Y.A., 2016).

Oil has many disadvantages; such as Refining petroleum generates air contamination. Transforming crude oil into petrochemicals discharges toxins into the atmosphere that are dangerous for ecosystem and human health. Burning gasoline releases CO2 because of not complete combustion of oil during refining process (Bhargava, 2017).

Oil contamination can have a harmful effect on the water environment; it

extents over the surface in a thin layer that stops oxygen reaching to animals and plants that live in the water. Oil pollution avoids photosynthesis in plants and disturbs the food chain (Enujiugha, 2004).

Wastewaters one of the environmental harms through crude oil-processing and petrochemical industries since the presence of large amounts of crude oil products, polycyclic and aromatic hydrocarbons, phenols, metal derivatives, surface-active substances, sulfides, naphthenic acids and other chemicals (Suleimanov, 1995).

According to Beg, Al-Muzaini , 2003 the discharged wastewaters become acutely threatening, to the accumulation of toxic products in receipt of water bodies with potentially severe significances on the environment. These discharges contain different chemicals at different attentions, including sulfides, hydrocarbons, ammonia, phenol, and water. Other reports have shown a positive connection between pollutants from refinery effluent wastewater and the health of aquatic organisms. Former explanations done by Kuehn et al. (1995) who submitted a relationship between water contamination and sediments with aromatic hydrocarbons from refinery effluents, these big amounts of a chemical substance that appear with the oil will have a toxicity effect on the environment, thus, to protect the environment from the wastewater effect, it must be treating and reusing it for irrigation and industrial use (Aziz, S.Q., Saleh, S.M. and Omar, I.A., 2019).

Furthermore, refinery wastewaters are subjected to different physical, chemical, and biological treatment processes that considerably decrease total emissions, and they are also probable cause to adverse effects on our environment (ECETOC,2019). Numerous scientists have identified different types of organisms that have the potential to consume active hydrocarbons in a natural environment such as *Marinobacter, Pseudomonas, Alcanivorax, Sphinogomonas, Micrococcus, Gordonia Cellumonas.* In addition to fungi, yeasts, and algae (Atlas, 2005 and Collee, *et al.*, 1996).

The procedure of biological treatment is can be seen as one of the best ways to recover water or soil using other living organisms that decompose toxic hydrocarbons. It is a cost-effective and straightforward process that applies to large areas of pollution (Al-Jaff, 1998). Still no researches conducted on Bacteriological treatment of industrial wastewater in the Kurdistan Region.

The aim of this paper to control hydrocarbon in oily wastewater using powder Bacteria with different bacterial count as bioremediation and the physico-chemical properties of wastewater before and after bioremediation.

2.MATERIAL AND METHOD

2.1.Study area

The study area is located in the Khabat area, also known as Kawrkosek, 40 km west of Erbil city and it dominates a land of 2.5km² to the left of the Upper Zab River. KAR locates on 36. 3179° Latitude and 43.7573° Longitude. The Kawrkosek refinery, the fourth largest in Iraq and the most noteworthy private sector, in Kurdistan region of Iraq. The below (Figure 1 and Plate 1 shows the exact location of KAR refinery among the other in green dots). These products such as crude oil, gasoil, benzene, naphthalene, and etc. are stored and distributed in storage tanks and then transported through-loading stations by tankers. The water quality standard of discharged water according to national environment and World Bank, as shown in table (1):

Table (1): water quality standard of discharged water according to national environment and world bank.

Parameter	National environment standard	World bank
Chloride	500 mg/L	250 mg/L
PO4	5 mg/L	2.0 mg/L
Ammonia	10 mg/L	10 mg/L

Total hardness	500 mg/L	_

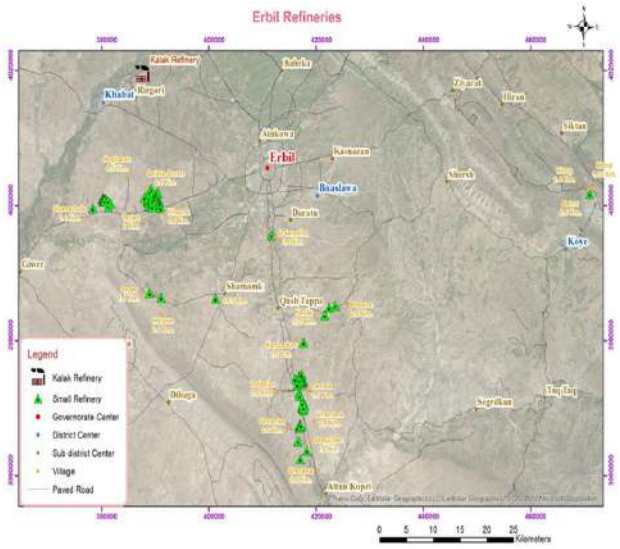

Figure (1): KAR group refinery- khabat (at Kawrgosk village).

Plate (1): discharge of contaminated wastewater after passing the wastewater treatment system (Sampling area).

2.2.Collection of Samples and analysis

Samples were obtained from the discharge point (output) of the treatment system in Kawrgosk refinery- Unit 1, which is the last point of contaminated water treatment after passes through physical, chemical, and biological therapy. This output will discharge to the Kalk River.

The phosphate (PO_4) was determined and defined by APHA (1998), Total hardness measured as $CaCO_3$ by using a test kit HACH, ammonia (NH3) was measured by a portable HANNA device named HI 700, chloride (CL^{-1}) was measured as described in (Bartram and Balance, 1996) and hydrocarbons measured by using GC-MS according to (Marriott, et.al., 2001) before and after treatment.

2.3.Bioremediation model

At the beginning, Broth bacillus bacteria prepared by adding few milligrams of powder bacteria to 10 ml of trypton soya broth media. The broth media incubated 3 – 4 hours at 30 ^{o}C to enrich the growth of Bacteria.

-0.1 ml broth bacteria progress to Petri dish and addition of 20 ml of Trypton Soya Agar on it. After that moving the Petri dishes in infinity shape to make the agar dry and distribution in equals volume, incubated at 18 to 24hours at 37 ^{o}C. Later count the growth colony counts (viable count).

- 2 ml of the growth broth media taken to measure turbidity at 625 nm compared to standard McFarland, 0.1) to count total bacterial cell count.

-After that, from powder Bacteria, the author took different weights (5 gm,10 gm, and 15gm) and added to 10L of oily wastewater at room temperature with aeration using an air pump. The research was carried out with inoculated pools that constituted the control. As shown in Plate (2) and Figure (2) down.

-All pools incubated at 25 ^{o}C for determined hydrocarbon residual for five weeks of adding Bacteria. Residual concentration of crude oil determined by gas chromatography.

-Samples took from oily wastewater analyzed by GC-2014 (SHIMADZU) to determine hydrocarbon depredation compering with oil samples.

Plate (2): preparing pools to full it by oily wastewater

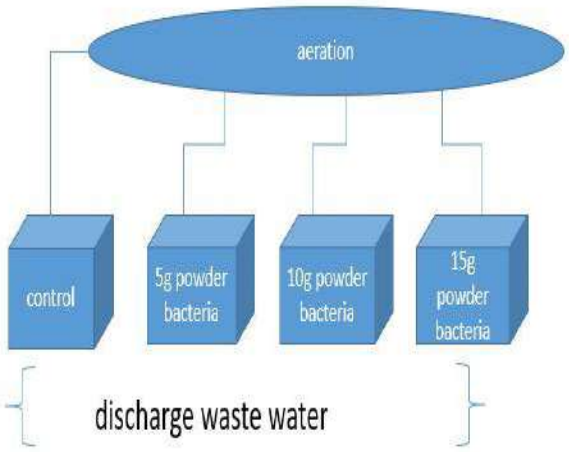

Figure (2): The design of pools

2.4.Gas chromatography analysis:

Remaining of crude oil after extraction at the end of each incubation period was measured chromatographically via tube gas chromatography using Agilent 6890 plus gas chromatograph equipped with split injector, and fused silica capillary column HP-1 of 30 m length, 0.25 µm internal diameter, and 0.5 µm film fatness. Both indicator and injector temperatures were sustained at 220°C. The column temperature was programmed to rise from 80°C to 260 °C with a rate of 5°C/min and the final time 40 min. Nitrogen/air used as a carrier gas at a flow rate of 3 mL/min.

3.RESULTS

As an outcome of total bacterial amount and viable count of triggered Bactria in broth media, the total bacterial count was 65.8 x 106 cell/ ml, whereas the viable bacterial cell was (540 cells per ml of broth media). Results of total hardness, ammonia, chloride, and phosphate are shown in Table 2.

Table (2): Results of analysis for oily wastewater before treatment by Bacteria.

Name of the parameters	Result
Total hardness	239.4 (mg $CaCO_3.l^{-1}$)
Ammonia	3.642 (ppm)
CL	636 (mg.l^{-1})
PO_4	5.05 (µgPO4-P.l^{-1})

Table (3) shows total hardness concentration for five weeks and ranged from a minimum value of 239.4 mg $CaCO_3.l^{-1}$ to a maximum amount of 256.5 mg $CaCO_3.l^{-1}$ in control containers. While in treatment pools, the value increased to 393.3 mg $CaCO_3.l^{-1}$ for 5 mg of bacteria with 10L of oily wastewater. Apparent variation was found between the first week of treatment and 5th week of treatment. Total hardness concentrations were shown in Figure (3) and Table (3).

Table (3): The results of total hardness (mg CaCO3.l^{-1}) from analyzing of oily wastewater treated by Bacteria and control.

Pool name	18 March 2019	25 March 2019	31 March 2019	7 April 2019	14 April 2019	Mean ±SD
Control	239.4	239.5	256.5	239.4	256.5	**246.26**
5 mg of bacteria with 10 L of oily wastewater	241.4	273.5	273.6	324.9	393.3	**301.34**
10 mg of bacteria with 10 L of oily wastewater	242.2	273.6	239.4	273.6	324.9	**270.74**
15 mg of bacteria with 10 L of oily wastewater	242.8	273.9	273.6	290.7	342	**284.6**

Mean ±SD	**241.45**	**265.125**	**260.775**	**282.15**	**329.175**	**1340.8075**

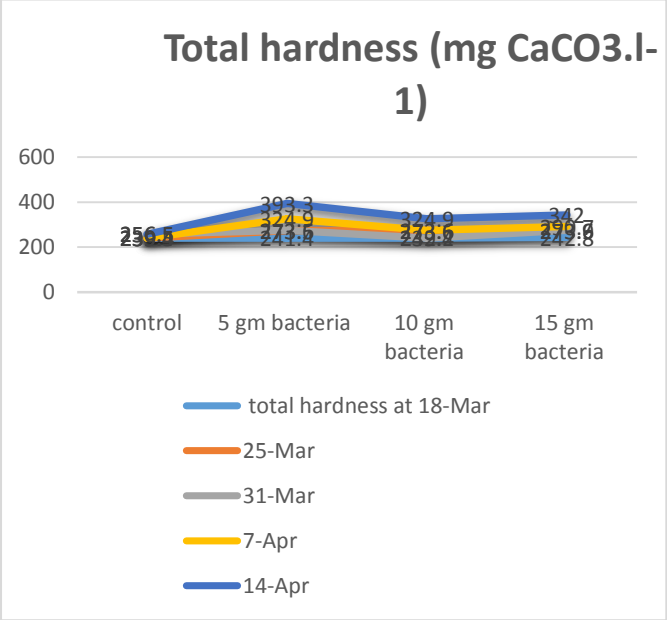

Figure (3): Total hardness in oily wastewater during the period of study

Table (4) represents the value of Ammonia in the current study; ammonia levels increased with an increase in the concentration of bacteria (Figure 4). The minimum amount of ammonia was 6.7 ppm at pools, which contains 5 mg of bacteria with 10 L of oily wastewater, while the maximum value was 10.465 ppm at pools with 15 mg of bacteria with 10 L of oily wastewater. Under the same condition with proceeding weeks, the amount of ammonia increased to a maximum value of 13.55 ppm for the pool with the highest concentration of bacteria (15 mg). This change happened only in pools that contain bacteria, while in control pools, there is no clear change. The increase in ammonia levels is continuous until the last week (5^{th}). The maximum value of 14.811 ppm was measured at pools that contain 15 gm of bacteria, while the minimum value 13.35 ppm was measured in the first pool, which contains 5 gm of bacteria.

Table (4): The results of Ammonia (ppm) from analyzing oily wastewater treated by Bacteria consist of control.

Pool name	18 March 2019	25 March 2019	31 March 2019	7 April 2019	14 April 2019	Mean±SD
Control	6.313	6.312	6.1	4.128	5.706	**5.7118**
5 mg of bacteria with 10 L of oily wastewater	6.7	8.9	18.938	15.418	13.35	**12.6612**
10 mg of bacteria with 10 L of oily wastewater	10.023	12.868	10.683	13.597	13.42	**12.1182**
15 mg of bacteria with 10 L of oily wastewater	10.465	13.55	14.811	17.7244	14.811	**14.27228**
Mean±SD	**8.37525**	**10.4075**	**12.633**	**12.71685**	**11.82175**	**50.358915**

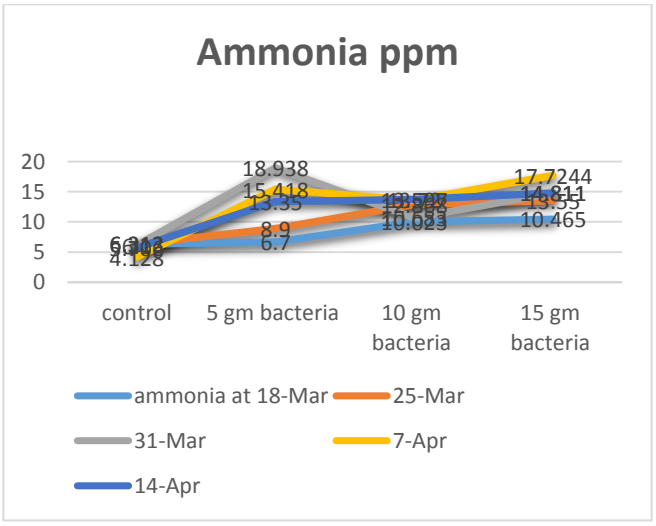

Figure (4): Ammonia levels in oily wastewater during the five weeks of bacteriological treatment.

Table (5) and Figure (5) show values of CL, which decrease along the treatment process, the same change happened to control pools. On the 14^{th} of April, which is the last week of the procedure. The lowest value (119 mg. l^{-1}) recorded in pools that contain 5mg of bacteria, while the highest value measured in pools which contain 15 gm.

Table (5): Results of Chloride (mg. l^{-1}) in control (Row wastewater) and treated pools by Bacteria.

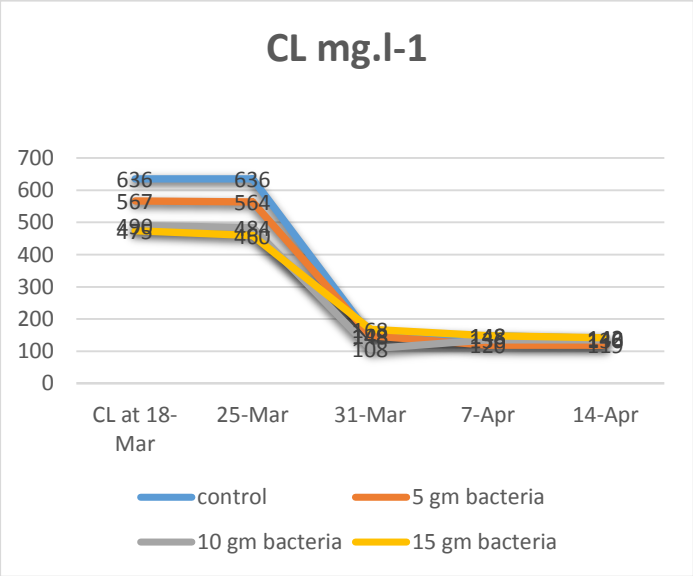

Figure (5): Chloride levels in oily wastewater during the five weeks of biological treatment.

Table (6) and Figure (6): presents PO_4 concentration, which increased during biological therapy. In the first week, the higher level of PO4 (10.5 µgPO_4-P. l^{-1}**)** presented in pools that contain 15 gm of bacteria while the lower value (7.2 µgPO_4-P. l^{-1}) was recorded in pools which contains 5 gm of bacteria. After five weeks of treatment, the amount of PO4 continuous in increasing. The highest value (54.95 µgPO_4-P. l^{-1}) measured at pools with a weight of 15 mg of bacteria. However, the control pool results decreased from 5.05 to 0.45µgPO_4-P. l^{-1}) throughout the periods of study.

Table (6): PO_4 (µgPO_4-P. l^{-1}) results for oily wastewater treated by Bacteria and control pools

Pool name	18 March 2019	25 March 2019	31 March 2019	7 April 2019	14 April 2019	Mean ±SD
control	5.05	5.04	1.7	0.8	0.45	**2.608**
5 mg of bacteria with 10 L of oily wastewater	7.2	19.9	26.2	25.3	41.55	**24.03**
10 mg of bacteria with 10 L of oily wastewater	7.8	19.75	31.4	35.15	44.35	**27.69**
15 mg of bacteria with 10 L of oily wastewater	10.5	31.55	48.9	44	54.95	**37.98**
Mean ±SD	**7.6375**	**19.06**	**27.05**	**26.3125**	**35.325**	**103.465**

Pool name	18 March 2019	25 March 2019	31 March 2019	7 April 2019	14 April 2019	Mean±SD
control	636	636	148	148	140	**341.6**
5 mg of bacteria with 10 L of oily wastewater	567	564	148	120	119	**303.6**
10 mg of bacteria with 10 L of oily wastewater	490	484	108	136	136	**1354**
15 mg of bacteria with 10 L of oily wastewater	475	460	168	148	142	**278.6**
Mean±SD	**542**	**536**	**143**	**138**	**134.25**	**1885.525**

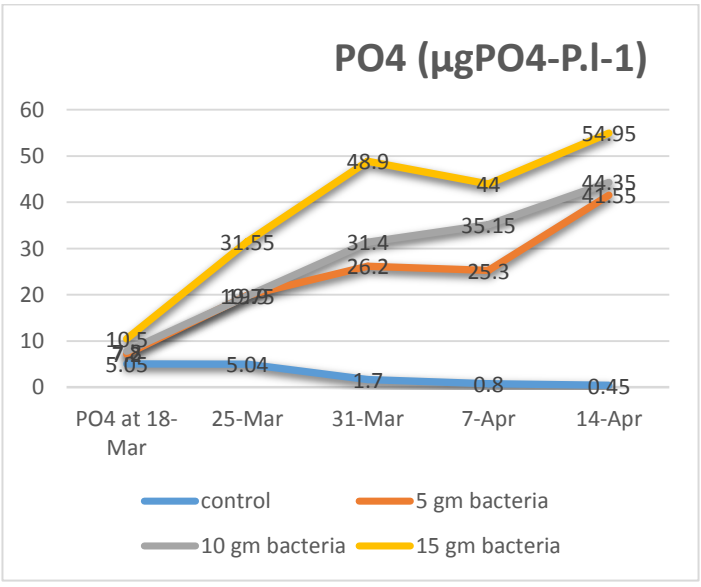

Figure (6): the amount of PO_4 in oily wastewater during the biological treatment.

Table (7): Forms and concentrations of hydrocarbon in oily wastewater of KAR oil refinery before disposal**.**

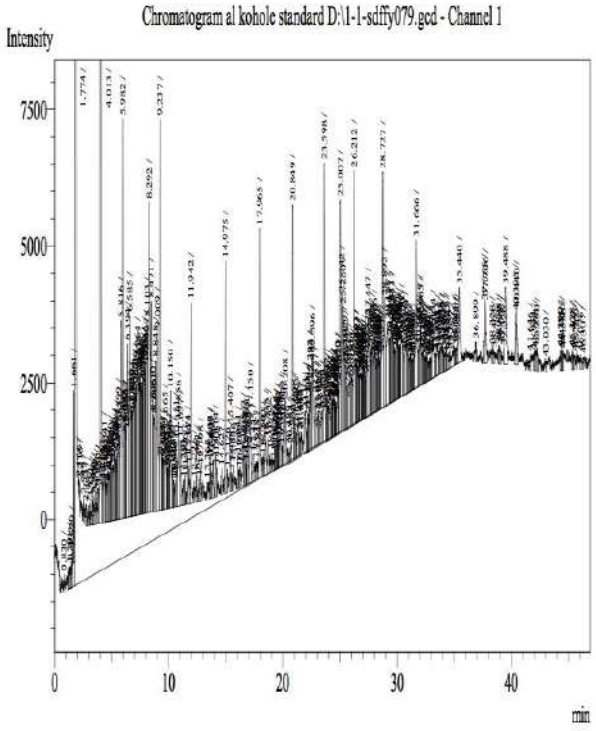

Figure (7): GC analysis graves of oily wastewater contamination without Bacteria

Figure (7) and Table (7) presents the analysis of crude wastewater with oil, and showing the oil comprised 19 hydrocarbon components plus hydrocarbon (C8, C9, C10, C11, C12, C14, C15, C16, C17, C18, and C19) which are (octane, nonane, decane, undecane, dodecane, tridecane, tetradecane, pentadecane, hexadecane, heptadecane, octadecane, and nonadecane) respectively according to normal standard GC analysis of hydrocarbons within the same contain (Teng, et.al. 1994).

Table (8): The types and concentrations of hydrocarbon in oily wastewater after adding 5 gm of powder Bacteria, after two weeks of treatment.

Hydrocarbon	Ret. Time	Area	Area %	µg/L
C8	4,324	42037	0.383	3830
C9	6.381	201659	1.835	18350
C10	9.009	457143	4.160	41600
C11	11.957	703764	6.405	64050
C12	14.994	554271	5.044	50440
C13	17.986	349275	3.179	31790
C14	20.869	233327	2.123	21230
C15	23.620	179851	1.637	16370
C16	26.233	168371	1.532	15320
C17	28.748	102491	0.933	9330
C18	31.685	75963	0.691	6910
C19	35.463	40537	0.369	3690
Total	64817.618	4108689	28.291	282910

Hydrocarbon	Ret. Time	Area of sample	Area%	µg/L
C9	6.368	31200	0.102	1020
C11	11.920	17131	0.056	560
C12	14.956	18799	0.061	610
C13	17.951	16040	0.052	520
C14	20.833	15650	0.051	510
C16	26.199	18073	0.059	590
C17	28.715	24606	0.080	800
C18	31.652	28222	0.092	920
C19	35.425	19775	0.064	640
Total	194.019	189496	0.617	6170

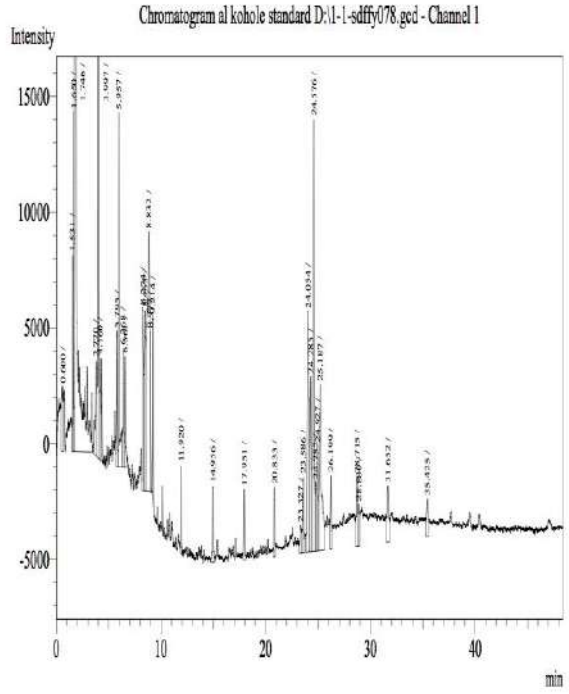

Figure (8): Sample (2) wastewater with 5gm of powder bacteria.

Figure (8): Demonstrates that the concentration of hydrocarbon after adding 5 gm of powder bacteria to 10 L of oil wastewater. Thus, the hydrocarbon declines because of the effect of bacteria to breakdown the carbon discovered in it. The hydrocarbons (C8, C10, and C15) concentration decreased to zero, while the hydrocarbon (C9, C11, C12, C13, C14, C16, C17, and C19) decrease (1020, 560, 610, 520, 510, 590, 800, 920, 640 µg/L). The remaining hydrocarbon measured by GC-MS under the same condition of standard analysis was (nonane, undecane, dodecane, tridecane, tetradecane, hexadecane, heptadecane, octadecane, nonadecane).

Table (9): The types and concentrations of hydrocarbon in oily wastewater after adding 10 gm of powder Bacteria. After two weeks of treatment.

Hydrocarbon	Ret. Time	Area	Area%	µg/L
C9	6.368	31200	0.102	1020
C11	11.920	17131	0.056	560
C12	14.956	18799	0.061	610
C13	17.951	16040	0.052	520
C14	20.833	15650	0.051	510
C16	26.199	18073	0.059	590
C17	28.715	24606	0.080	800
C18	31.652	28222	0.092	920
C19	35.425	19775	0.064	640
Total	194.019	189496	0.617	6170

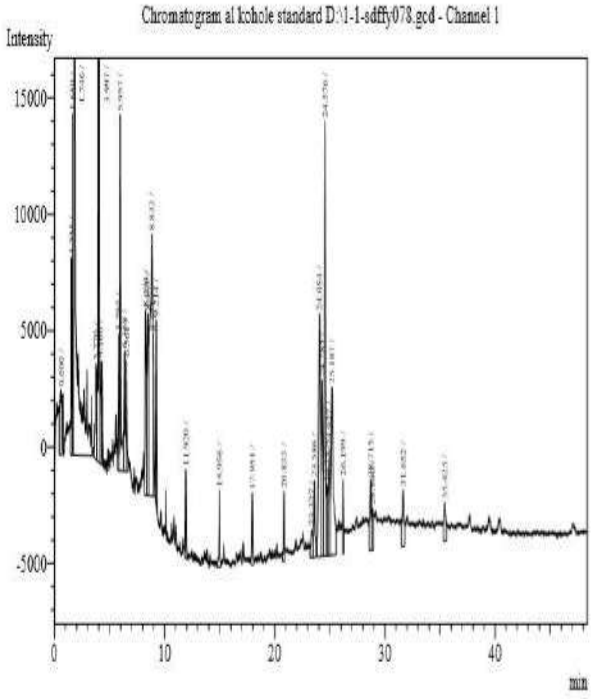

Figure (9): Sample (3) wastewater with 10 gm of powder Bacteria.

Figure 9: represents the concentration of hydrocarbon after adding 10 gm of powder bacteria to 10L of oily wastewater, the hydrocarbons (C8, C10, and C15) concentration decreased to zero, while the hydrocarbon (C9, C11, C12, C13, C14, C16, C17, and C19) decrease to (1020, 560, 610, 520, 510, 590, 800, 920, 640), which are (nonane, undecane, dodecane, tridecane, tetradecane, hexadecane, heptadecane, octadecane, nonadecane). Under the same measurement condition of standard analysis.

Table (10): The types and concentrations of hydrocarbon in oily wastewater after adding 15 gm of powder Bacteria. After two weeks of treatment**.**

Hydrocarbon	Ret. Time	Area	Area%	µg/L
C9	6.297	14815	0.120	1200
C10	9.003	233265	1.895	18950
C11	11.933	31125	0.253	2530
C12	14.968	31736	0.258	2580
C13	17.961	23883	0.194	1940
C14	20.842	22548	0.183	1830
C15	23.593	23194	0.188	1880
C16	26.208	17813	0.145	1450
C17	28.720	14637	0.119	1190
C18	31.668	13767	0.112	1120
C19	35.431	13352	0.108	1080
Total	226.624	1379255868	3.575	35750

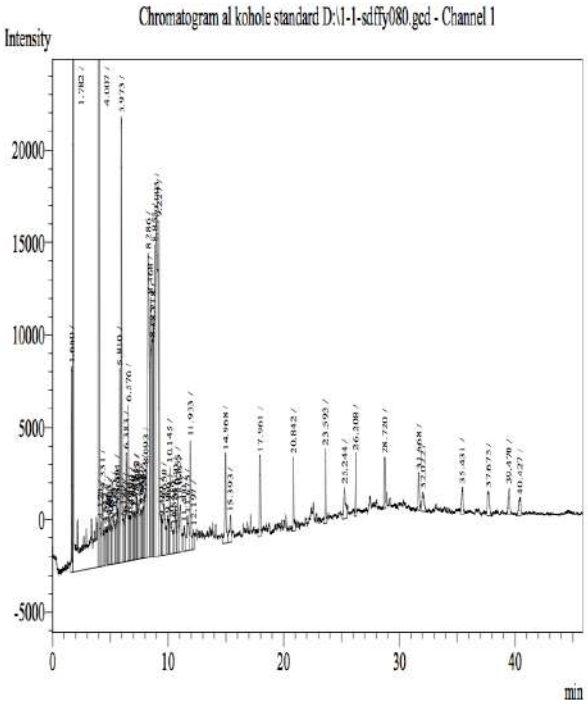

Figure (10): Sample (4) wastewater with 15gm of powder bacteria)

Figure 10: Shows the amount of hydrocarbon after adding 15 ml of broth bacteria to 200 ml of oily wastewater, the hydrocarbons (C8 and C9) concentration decreased to zero, while the hydrocarbon (C10, C11, C12, C13, C14, C15, C16, C17, C18, and C19) became (1200,18950, 2530, 2580, 1940, 1830, 1880, 1450, 1190, 1120, 1080 µg/L) which are (nonane, decane, undecane, dodecane, tridecane, tetradecane, pentadecane, hexadecane, heptadecane, octadecane, and nonadecane). Under the same measurement condition of standard analysis.

Table (11): Types and concentrations of hydrocarbon in oily wastewater for control containor, which is without bacteria.

Hydrocarbon	Ret. Time	Area	Area%	µg/L
C10	8.999	58546	0.272	2720
C11	11.934	66613	0.310	3100
C12	14.968	69515	0.323	3230
C13	17.958	57673	0.268	2680
C14	20.844	52667	0.245	2450
C16	26.211	50160	0.233	2330
C17	28.728	49710	0.231	2310

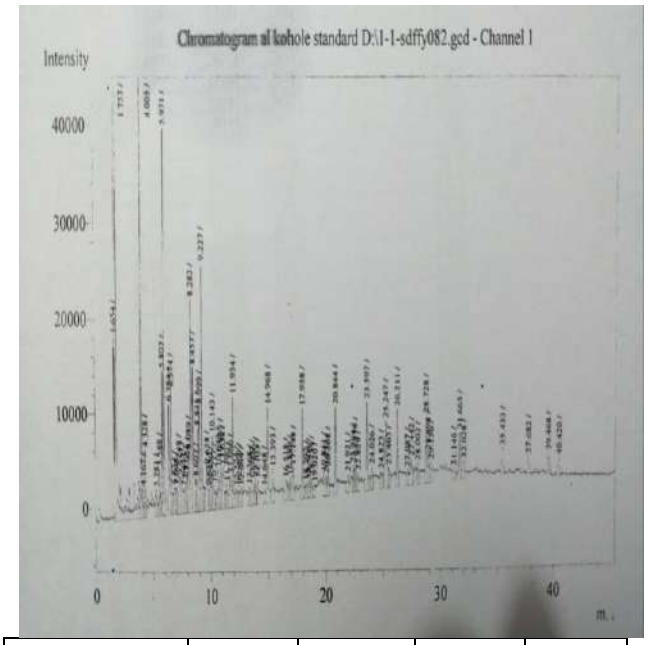

C18	31.665	38595	0.180	1800
C19	35.433	24137	0.112	1120
Total	196.74	467616	2.174	21740

Figure (11): Sample (5) is the control of oily wastewater without Bacteria only under aeration condition.

Figure (11): this figure represents control. Which is the oily wastewater without Bacteria only under aeration and the same temperature condition. After two weeks of leaving this wastewater, the result of GC-MS shows that the hydrocarbon (C8, C9, and C15) disappear just by aeration process. Still, other hydrocarbon value (C10, C11, C12, C13, C14, C16, C17,

C18, and C19) became (2720, 3100, 3230, 2680, 2450, 2330, 2310, 1800, 1120), which are (nonane, decane, undecane, dodecane, tridecane, tetradecane, hexadecane, heptadecane, octadecane, and nonadecane).

Table (12): The types and concentrations of hydrocarbon in oily wastewater after adding 5 gm bacteria after three weeks of treatment.

Hydrocarbon	Ret. Time	Area	Area%	µg/L
C9	5.996	28613	0.030	300
C13	17.479	1310	0.001	10
C17	28.545	24406	0.025	250
C18	31.570	8240	0.009	90
C19	35.242	22409	0.023	230
Total	118.832	84978	0.0799	880

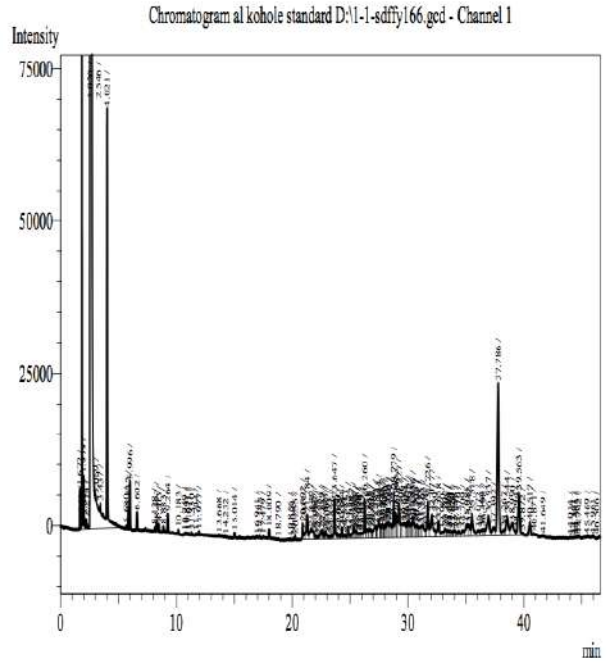

Figure (12): Sample (1) oily wastewater with 5 gm of Bacteria after 3 weeks of treating, under aeration condition.

Table (12) and Figure (12) shows the remaining hydrocarbons after three weeks of treating oily wastewater by 5 gm of bacteria under aeration and the same temperature condition. The results of GC-MS represent that hydrocarbon (C8, C10, C11, C12, C14, C15 andC16) disappear, while the remaining hydrocarbons (C9, C13, C17, C18 and C19) became (300, 10, 250, 90, 230) which are (nonane, heptadecane, octadecane, nonadecane).

Table (13): The types and concentrations of hydrocarbon in oily wastewater with 10 gm of bacteria after three weeks.

Hydrocarbon	Ret. Time	Area	Area%	µg/L
C11	11.702	4519	0.006	60
C13	17.473	4909	0.007	70
C17	28.517	15669	0.022	220
C18	31.561	1389	0.002	20
C19	35.225	13170	0.019	190
Total	124.478	39656	0.056	560

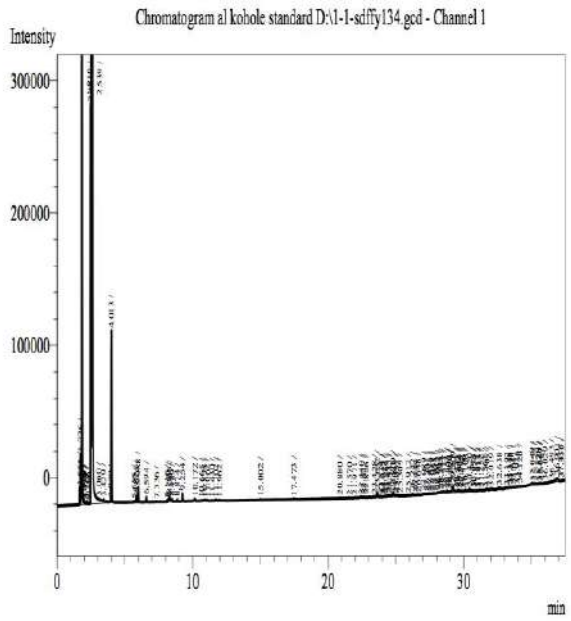

Figure (13): Sample (2) oily wastewater with 10 gm of Bacteria, under aeration condition.

Table (13) and figure (13) shows the remaining hydrocarbons after three weeks of treating oily wastewater by 10 gm of bacteria under aeration and the same temperature condition. The results of GC-MS represent that hydrocarbon (C8, C9, C10, C12, C14, C15, and C16) disappear, while the remaining hydrocarbons (C11, C13, C17, C18 and C19) became (60,70,220,20,190) which are (undecane, tridecane, heptadecane octadecane nonadecane).

Table (14): The types and concentrations of hydrocarbon in oily wastewater after three weeks of treating with 15 gm of bacteria under aeration condition.

Hydrocarbon	Ret. Time	Area	Area%	µg/L
C10	8.894	1648	0.002	20
C17	28.528	2382	0.002	20
C18	31.213	13650	0.013	130
C19	35.092	20301	0.020	200
Total	103.727	37981	0.037	370

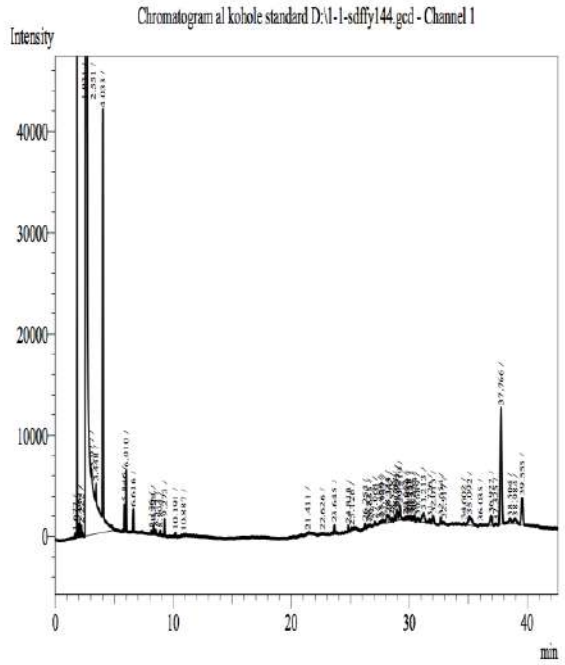

Figure (14): Sample (3) oily wastewater contains 15 gm of Bacteria after three weeks of treatment, under aeration condition.

Table (14) and Figure (14) shows the remaining hydrocarbons after three weeks of treating oily wastewater by 15 gm of bacteria under aeration and the same temperature condition. The results of GC-MS represent that hydrocarbon (C8, C9, C11, C12, C13, C14, C15, and C16) disappear, while the remaining hydrocarbons (C10, C17, C18 and C19) became (20, 20, 130, 200) which are (decane, heptadecane, octadecane, and nonadecane).

Table (15): The types and concentrations of hydrocarbon in oily wastewater (control) without bacteria, after three weeks of treating.

Hydrocarbon	Ret. Time	Area	Area %	µg/L
C11	11.715	1303	0.002	20
C13	17.485	1304	0.002	20
C16	26.035	4667	0.007	70
C17	28.533	8355	0.013	130
C18	31.241	2068	0.003	30
C19	35.215	5468	0.008	80
Total	150.224	23165	0.035	350

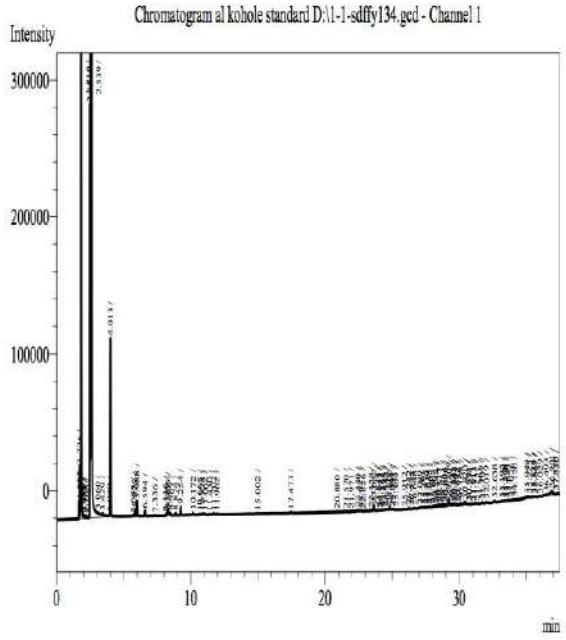

Figure (15): Sample (4) control of oily wastewater without Bacteria only under aeration condition.

Table (15) and Figure (15) shows the remaining hydrocarbons after three weeks of treating oily wastewater without bacteria under aeration and the same temperature condition. The results of GC-MS represent that hydrocarbon (C8, C9, C10, C12, C14, C15) disappear, while the remaining hydrocarbons (C11, C13, C16, C17, C18, C19) became (20,20,70,130,30,80) which are (undecane, tridecane, hexadecane, heptadecane octadecane nonadecane).

Table (16): The types and concentrations of hydrocarbon in oily wastewater with 5gm of bacteria after four weeks of treatment.

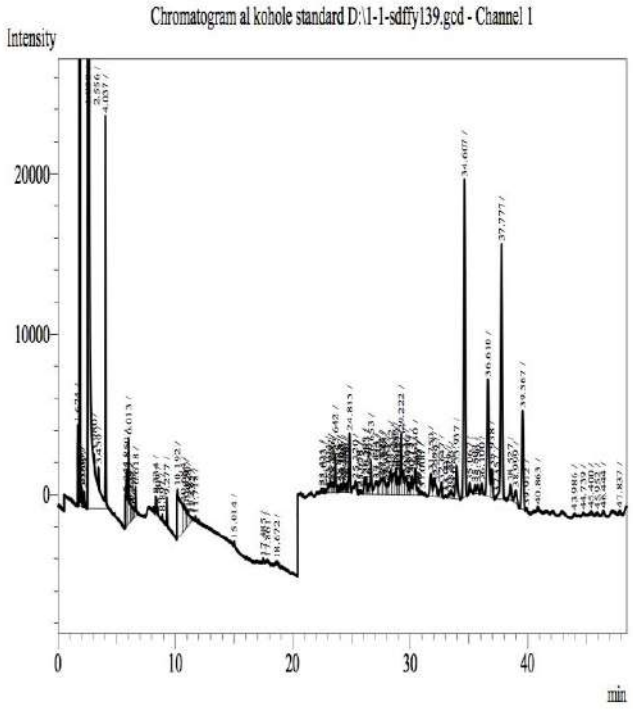

Figure (16): Sample (1) oily wastewater contains 5gm of Bacteria, after four weeks under aeration condition**.**

Table (16) and Figure (16) shows the remaining hydrocarbons after four weeks of treating oily wastewater with 5 gm bacteria under aeration and the same temperature condition. The results of GC-MS represent that hydrocarbon (C8, C10, C12, C14, C15, C16) disappear, while the remaining hydrocarbons (C9, C13, C17, C18, C19) became (110, 10, 210, 20, 40) which are (nonane, tridecane, heptadecane octadecane nonadecane).

Table (17): the types and concentrations of hydrocarbon in oily wastewater with 10 gm of bacteria, after four weeks from treatment.

Hydrocarbon	Ret. Time	Area	Area %	µg/L
C11	11.720	4957	0.005	50
C17	28.531	6980	0.007	70
C18	31.262	1544	0.001	10
C19	35.231	16503	0.016	160
Total	106.744	29984	0.029	290

Hydrocarbon	Ret. Time	Area	Area%	µg/L
C9	6.231	8385	0.011	110
C13	17.861	1114	0.001	10
C17	28.616	16539	0.021	210
C18	31.000	1649	0.002	20
C19	35.067	3495	0.004	40
Total	118.775	31182	0.039	390

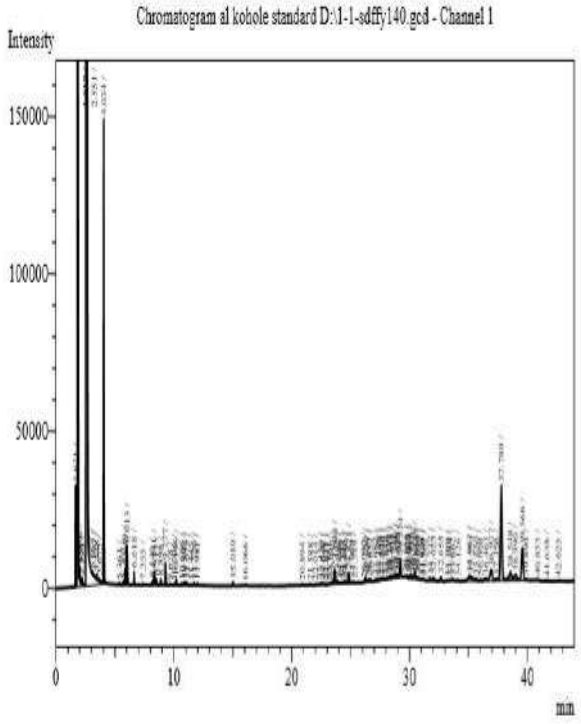

Figure (17): Sample (2) control of oily wastewater with 10 gm of Bacteria after 4 weeks of treatment.

Table (17) and Figure (17) shows the remaining hydrocarbons after four weeks of treating oily wastewater with 10 gm bacteria under aeration and the same temperature condition. The results of GC-MS represent that hydrocarbon (C8, C9, C10, C12, C13, C14, C15, C16) disappear, while the remaining hydrocarbons (C11, C17, C18, C19) became (50, 70, 10, 160) which are (undecane, heptadecane, octadecane, nonadecane).

Table (18): the types and concentrations of hydrocarbon in oily wastewater with 15 gm of bacteria, after four weeks of treatment.

Hydrocarbon	Ret. Time	Area	Area%	µg/L
C10	8.511	1042	0.001	10
C17	28.514	4058	0,004	40
C18	31.060	16447	0.014	140
C19	35.241	4463	0.004	40
Total	103.326	26010	0.023	230

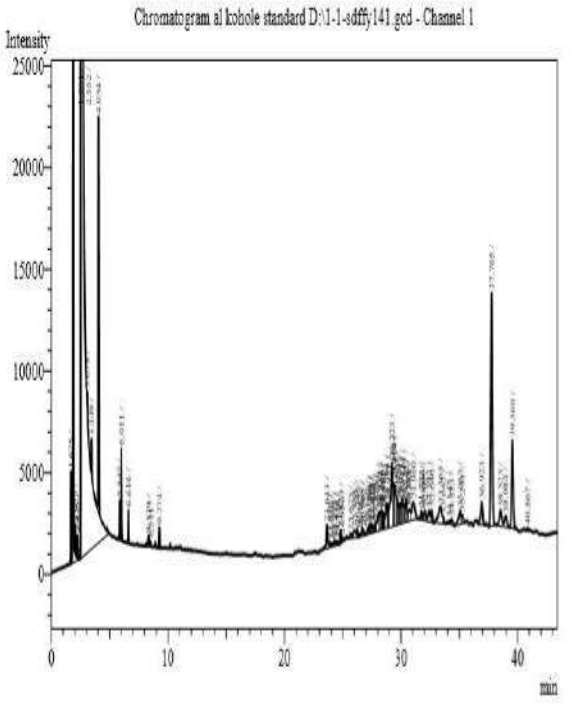

Figure (18): Sample (3) oily wastewater contains15 gm of Bacteria after four weeks of treatment, under aeration condition.

Table (18) and Figure (18) shows the remaining hydrocarbons after four weeks of treating oily wastewater with 15 gm bacteria under aeration and the same temperature condition. The results of GC-MS represent that hydrocarbon (C8, C9, C11, C12, C13, C14, C15, C16) disappear, while the remaining hydrocarbons (C10, C17, C18, C19) became (10, 40, 140, 40) which are (decane, heptadecane, octadecane, nonadecane).

Table (19): The types and concentrations of hydrocarbon in oily wastewater. In addition to the control, which is without bacteria.after four weeks.

Hydrocarbon	Ret. Time	Area	Area%	µg/L
C11	11.719	1649	0.002	20
C13	17.493	2310	0.002	20
C17	28.537	6809	0.007	70
C19	35.229	3629	0.004	40
Total	92.978	14397	0.015	150

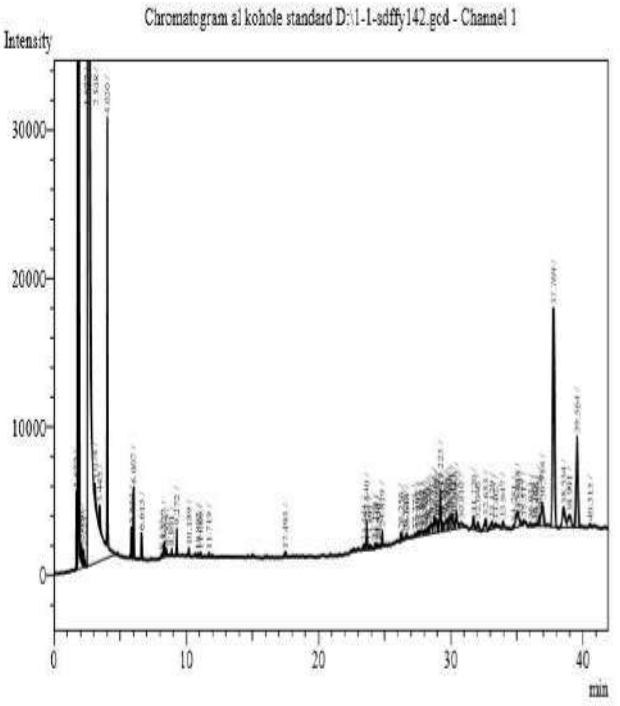

Figure (19): Sample (4) control of oily wastewater without Bacteria only under aeration condition. After four weeks of treatment.

Table (19) and Figure (19) shows the remaining hydrocarbons after four weeks of treating oily wastewater without bacteria under aeration and the same temperature condition. The results of GC-MS represent that hydrocarbon (C8, C9, C10, C12, C14, C15, C16) disappear, while the remaining hydrocarbons (C11, C13, C17, C19) became (20, 20, 70, 40) which are (undecane, tridecane, heptadecane, octadecane, nonadecane).

Table (20): The types and concentrations of hydrocarbon in oily wastewater with 5 gm of bacteria after five weeks.

Hydrocarbon	Ret. Time	Area	Area%	µg/L
C9	6.008	41179	0.119	1190
C17	28.522	6360	0.018	180
C19	35.245	14049	0.041	410
Total	69.775	61588	0.178	1780

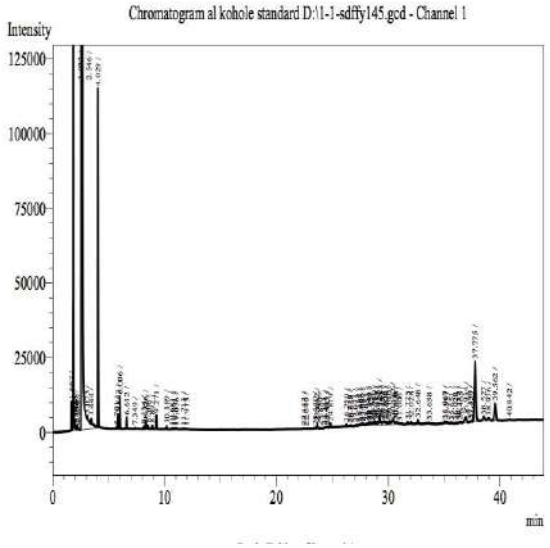

Figure (20): Sample (1) control of oily wastewater with 5 gm of Bacteria under aeration condition. After five weeks of treatment.

Table (20) and Figure (20) shows the remaining hydrocarbons after five weeks of treating oily wastewater with 5 gm bacteria under aeration and the same temperature condition. The results of GC-MS represent that hydrocarbon (C8, C10, C11, C12, C13, C14, C15, C16, C18) disappear, while the remaining hydrocarbons (C9, C17, C19) became (1190,180,410) which are (nonane, heptadecane, nonadecane).

Table (21): the types and concentrations of hydrocarbon in oily wastewater contain 10 gm of bacteria under aeration condition after five weeks of treatment.

Hydrocarbon	Ret. Time	Area	Area%	µg/L
C11	11.715	2742	0.002	20
C17	28.519	11816	0.010	100
C19	35.240	12588	0.011	110
Total	75.474	27146	0.023	230

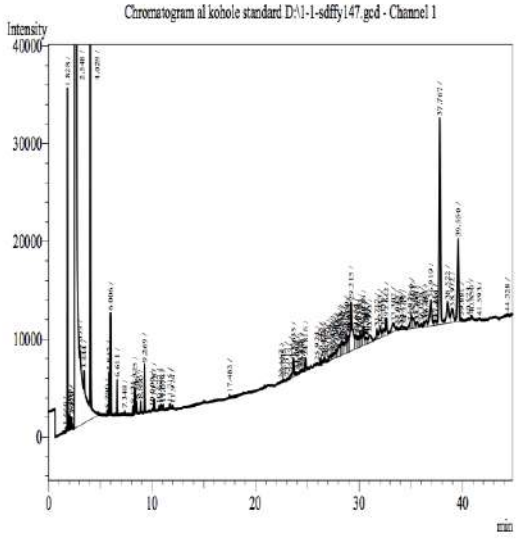

Figure (21): Sample (2) control of oily wastewater with 10 gm of Bacteria after five weeks of treatment.

Table (21) and Figure (21) shows the remaining hydrocarbons after five weeks of treating oily wastewater with 10 gm bacteria under aeration and the same temperature condition. The results of GC-MS represent that hydrocarbon (C8, C9, C10, C12, C13, C14, C15, C16, C18) disappear, while the remaining hydrocarbons (C11, C17, C19) became (20, 100, 110) which are (undecane, heptadecane, nonadecane).

Table (22): the types and concentrations of hydrocarbon in oily wastewater contain 15 gm of bacteria with aeration. After five weeks of treatment.

Hydrocarbon	Ret. Time	Area	Area%	µg/L
C19	35.076	1697	0.027	270

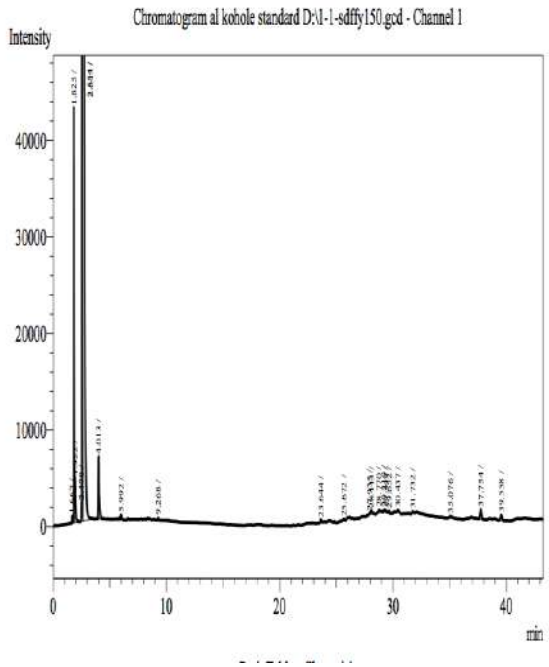

Figure (22): Sample (3) control of oily wastewater with 15 gm of Bacteria under aeration condition.

Table (22) and Figure (22) shows the remaining hydrocarbons after five weeks of treating oily wastewater with 10 gm bacteria under aeration and the same temperature condition. The results of GC-MS represent that hydrocarbon (C8, C9, C10, C11, C12, C13, C14, C15, C16, C18) disappear, while the remaining hydrocarbons (C19) became (270) which are (nonadecane).

Table (23): The types and concentrations of hydrocarbon in oily wastewater (control) without bacteria. After five weeks of treatment.

Hydrocarbon	Ret. Time	Area	Area%	µg/L
C11	17.483	1030	0.001	10
C18	31.552	1810	0.002	20
C19	35.224	5147	0.005	50
Total	84.259	7987	0.008	80

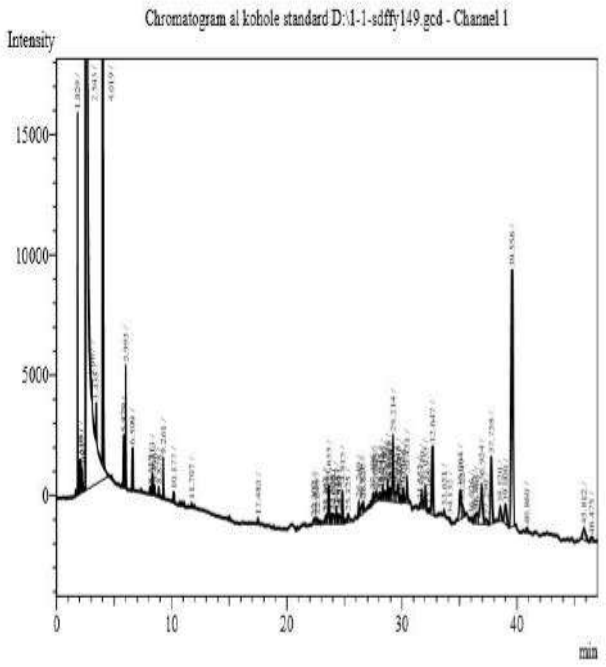

Figure (23): Sample (4) control of oily wastewater without Bacteria only under aeration condition. After five weeks of treatment.

Table (23) and Figure (23) shows the remaining hydrocarbons after five weeks of treating oily wastewater with 10 gm bacteria under aeration and the same temperature condition. The results of GC-MS represent that hydrocarbon (C8, C9, C10, C12, C13, C14, C15, C16, C17) disappear, while the remaining hydrocarbons (C11, C18, C19) became (10,20,50) which are (undecane, octadecane, nonadecane).

Discussion:

The GC- MS outcomes indicates that the hydrocarbon (C8, C9, C10, C11, C12, C14, C15, C16, C17, C18, and C19) in oil wastewater before bioremediation treatment with different highest peaks meaning types of hydrocarbons found as a result of a method of crude purification oil in the refiner. However, these hydrocarbons uncovered in complex wastewater products (Akpor *et.al.,* 2014)

Microorganisms are crucial to the degradation of petroleum hydrocarbons, and that they largely affect the transformation and fate of petroleum hydrocarbons in the environment. While some broad bacteria spectrum of petroleum hydrocarbon degradation ability (Xu. *et al.,* 2018). The degradation of petroleum hydrocarbons can be mediated by a specific enzyme system (Fritsche and Hofrichter, 2000). Other mechanisms involved are an attachment of microbial cells to the substrate and the production of biosurfactants. The uptake mechanism linked to the attachment of the cell to the oil droplet is still unknown, but the production of biosurfactant has been well studied (Das and Chandran, 2011). The enzyme involved in biodegradation of petroleum hydrocarbons have specialty such as soluble methane monooxygenases degrade C1-C8 (McDonald, *et al.,* 2006), alkB related Alkane hydroxylases substrate is C5-C16 (Jan, *et al.,* 2003), Dioxygenases substrate C10-C30 Alkanes (Jan, *et al.,* 1996). The difference in the results of upper carves as shown C8 and C9 remain mainly after bioremediation by bacteria due to the enzymes, which produce, by bacteria and their activity.

Although from the activity of bacteria to remove hydrocarbon, there is another chemical change that happened to the treated water.

According to Table (3) and Figure (3), the number of total hardness increases because of the rise of suspended particles of degraded drops of oil. As mentioned above, the enzyme produced by bacteria makes the coagulated drops of oil degraded and became particles easy to consume by bacteria. So this particle makes the reading of total hardness increase (Fakhru'l-Razi, et al., 2009).

The amount of ammonia changed with the time of treatment, as shown in Figure (4). The amount of ammonia in the first weeks increased; after that, with duration, we can see at the last week the ammonia decreased in all the pools of oily wastewater, which have different weights of bacteria. These changes are due to oxidizing ammonia by Bacillus bacteria as a source of energy for bacteria growth. This result then became the reason for choosing Bacillus to be used in the wastewater treatment system. Because it will not create pollution if the oily wastewater produced by this treatment discharging to the river, furthermore, Bacillus can be selected for industrial wastewater treatment system on a broad scale (Wardhani, 2017).

According to the chemical analysis, the amount of PO4 increased with increasing the amount of bacteria to the wastewater. This increase happened because some microorganisms like *Bacillus subtitles* bacteria release little P in their natural state. However, these microorganisms can increase the concentration of available P by secreting organic acids and various degrading enzymes (Phytase, nuclease, phosphatase, etc.) to decompose insoluble phosphate in the oily wastewater (Wu *et al.,* 2019). Also, this is like an indicator that shows that the bacteria are active, and there is an obvious effect in treatment.

Chloride for safety reasons, chloride in wastewater should not exceed 350 mg/L as directed and WHO Standard (WHO, 2006). In water bodies, elevated chloride levels can threaten the sustainability of ecological food sources, hence posing a risk to species survival, growth as well as reproduction. Bioaccumulation and persistence of chloride may affect aquatic organisms and water quality (Imo, 2017). The biological treatment by bacillus bacteria reduced the amount of chloride compared to the control because the CL is essential for the growth of bacteria (Roeßler, 2003).

The result of our study showed that 15 mg of Bacteria growth or bacterial number displaying more capabilities for the bioremediation of petroleum oil-contaminated water. In recent times, rapidly and achieved significant gains, microbial remediation technology has developed.

Conclusion:

To sum-up, petroleum hydrocarbons resulting in wastewater can be seen as one of the most dangerous pollutants due to their high toxicity and their effects on human comfort and environmental health. Bioremediation by petroleum hydrocarbon-degrading bacteria is generally regarded as an eco-friendly and efficient technology.

Reference:

Acuna-Arguelles, M.E.; Olguin-Lora, P. and Razo-Flores, E. (2003). Toxicity and kinetic parameters of the aerobic biodegradation of the phenol and alkylphenols by a mixed culture. Biotechnol. Lett. 25: 559-564. 2.

Akpor O.B., Okolomike U.F., Olaolu T.D. and Aderiye B.I., 2014. Remediation of Polluted Wastewater Effluents: Hydrocarbon Removal. Trends in Applied Sciences Research, 9: 160-173.

Al-Jaff, B.M.A. (1998) Microbiological and genetical study on local isolates of Bacillus cereus. PhD thesis, University of Baghdad, Iraq.

Arafa, M.A. (2003). Biodegradation of some aromatic hydrocarbons (BTEXs) by a bacterial consortium isolated from polluted site in Saudi Arabia. Pak. J. Biol. Sci. 6(17): 1482-1486.

Atlas, M.R. (2005). Handbook of media for Environmental Microbiology.2nd ed. Published by CRC press. Taylor and francis Group 6000 Broken sound parkway NW. Boca Raton, FL 33487- 2742.

Aziz, S.Q., Saleh, S.M. and Omar, I.A., 2019. Essential Treatment Processes for Industrial Wastewaters and Reusing for Irrigation. ZANCO Journal of Pure and Applied Sciences,31(s3), pp.269-275.

Beg, M.U., Al-Muzaini, S., Saeed, T., Jacob, P.G., Beg, K.R., Al-Bahloul, M., Al-Matrouk, K., Al-Obaid, T. & Kurian, A. (2001) Chemical contamination and toxicity of sediment from a coastal area receiving industrial effluents Kuwait. – Archives of Environmental Contamination and Toxicology 41: 289–297. [8].

Beg, M.U., Saeed, T., Al-Muzaini, S., Beg, K.R. & Al-Bahloul, M. (2003) Distribution of petroleum hydrocarbon in sediment from coastal area receiving industrial effluents in Kuwait. – Ecotoxicol Environ Saf. 54: 47–55.

Collee, J.G.; Fraser, A.G.; Marmion, B.P. and Simmons, A. (1996). Practical Medical Microbiology. 14th ed. The Churchill Livingstone. Inc. New York, USA.

Das, N. and Chandran, P., 2011. Microbial degradation of petroleum hydrocarbon contaminants: an overview. *Biotechnology research international*, *2011*.

ECETOC, (undated).'Technical report 125 RATIONALE FOR LEVEL OF IMPACTS OF OIL REFINERY DISCHARGE' <http://www.ecetoc.org/report-125/case-studies-step-3/case-study-1-oil-refinery-discharge-estuarine-environments/rationale-level-impacts-oil-refinery-discharge> access date 30/6/2019

Fakhru'l-Razi, A., Pendashteh, A., Abdullah, L.C., Biak, D.R.A., Madaeni, S.S. and Abidin, Z.Z., 2009. Review of technologies for oil and gas produced water treatment. Journal of hazardous materials, 170(2-3), pp.530-551.

Fritsche, W. and Hofrichter, M., 2000. Aerobic degradation by microorganisms. *Biotechnology. New York: John Wiley & Sons*, *11*, pp.146-164.

Imo, C.I.; Nwakuba, N.R.; Asoegwu, S.N.; Okereke, N.A.A. Impact of Brewery Effluents on Surface Water Quality in Nigeria: A Review. Chem. Res. J. 2017, 2, 101–113.

Jan, B., Sakai, Y., Tani, Y. and Kato, N., 1996. Isolation and characterization of a novel oxygenase that catalyzes the first step of n-alkane oxidation in Acinetobacter sp. strain M-1. *Journal of bacteriology*, *178*(13), pp.3695-3700.

Kuehn, R.L., Berlin, K.D., Hawkins, W.E. & Ostrander, G.K. (1995) Relationships among petroleum refining, water, and sediment contamination, and fish health. – Journal of Toxicology and Environmental Health 46: 101–116.

Marriott, P.J., Shellie, R. and Cornwell, C., 2001. Gas chromatographic technologies for the analysis of essential oils. *Journal of Chromatography A*, *936*(1-2), pp.1-22.

McDonald, I.R., Miguez, C.B., Rogge, G., Bourque, D., Wendlandt, K.D., Groleau, D. and Murrell, J.C., 2006. Diversity of soluble methane monooxygenase-containing methanotrophs isolated from polluted environments. *FEMS Microbiology Letters*, *255*(2), pp.225-232.

Roeßler, M., Sewald, X. and Müller, V., 2003. Chloride dependence of growth in bacteria. FEMS microbiology letters, 225(1), pp.161-165.

Suleimanov, R.A. (1995) Conditions of waste fluid accumulation at petrochemical and processing enterprises and prevention of their harm to water bodies. – Meditsina Truda i Promyshlennaia Ekologiia 12: 31–36.

Teng, S.T., Williams, A.D., and Urdal, K., 1994. Detailed hydrocarbon analysis of gasoline by GC-MS (SI-PIONA). *Journal of high-resolution chromatography*, *17*(6), pp.469-475.

Thabit, T.H. and Jasim, Y.A., 2016, April. The Role of Environmental Accounting Disclosure to Reduce Harmful Emissions of Oil Refining Companies. In The 3rd International Conference On Energy, Environment, And Applied Science, Ishik University, Erbil, Iraq.

Wardhani, S., 2017. Consortium of heterotrophic nitrification bacteria Bacillus sp. and its application on urea fertilizer industrial wastewater treatment. *Malaysian Journal of Microbiology*, *13*(3), pp.156-163.

World Health Organization. 2006. A Compendium of Standards for Wastewater Reuse in the Eastern. Mediterranean Region; Regional Office for the Eastern Mediterranean Regional Centre for Environmental Health Activities CEHA: Los Angeles, CA, USA; pp. 1–19.

Wu, F., Li, J., Chen, Y., Zhang, L., Zhang, Y., Wang, S., Shi, X., Li, L. and Liang, J., 2019. Effects of Phosphate Solubilizing Bacteria on the Growth, Photosynthesis, and Nutrient Uptake of Camellia oleifera Abel. *Forests*, *10*(4), p.348.

Xu X., Liu W., Tian S., Wang W., Qi O., Jiang P., Gao X., Li F., Li H. (2018). Petroleum Hydrocarbon-Degrading Bacteria for the Remediation of Oil Pollution Under Aerobic Conditions: A Perspective Analysis, Front. Microbiol., 9,2885.